Copy 76

VOYAGER

SPACECRAFT Phase B, Task D

FINAL REPORT

OCTOBER 1967

Prepared for

GEORGE C. MARSHALL SPACE FLIGHT CENTER

Huntsville, Alabama

Voyager Operations
Space Vehicles Division

TRW SYSTEMS GROUP

One Space Park, Redondo Beach, California

MODEL OF
TRW
RECOMMENDED
VOYAGER
SPACECRAFT

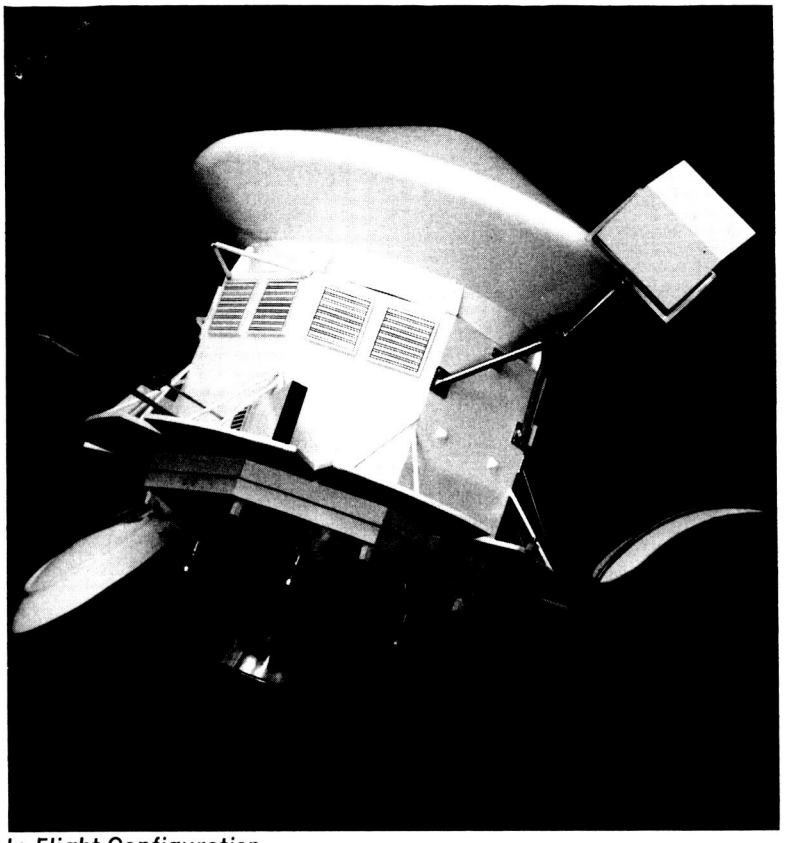

In-Flight Configuration

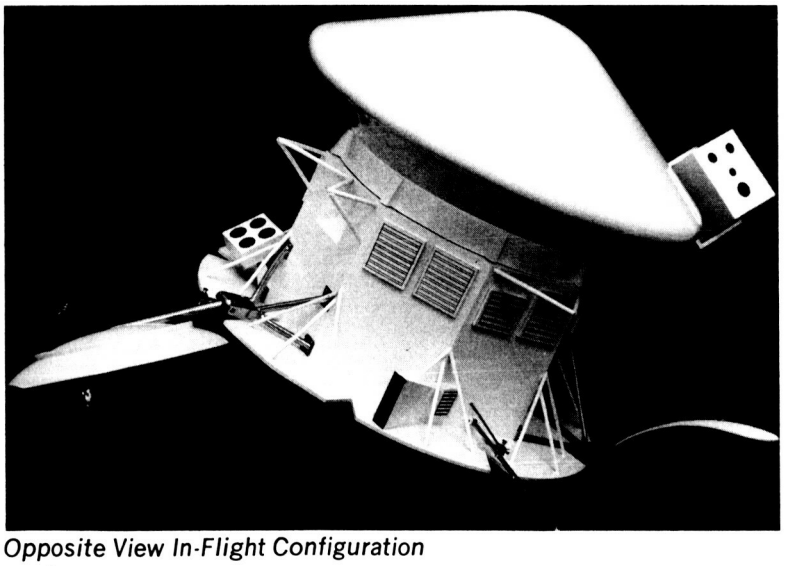

Opposite View In-Flight Configuration

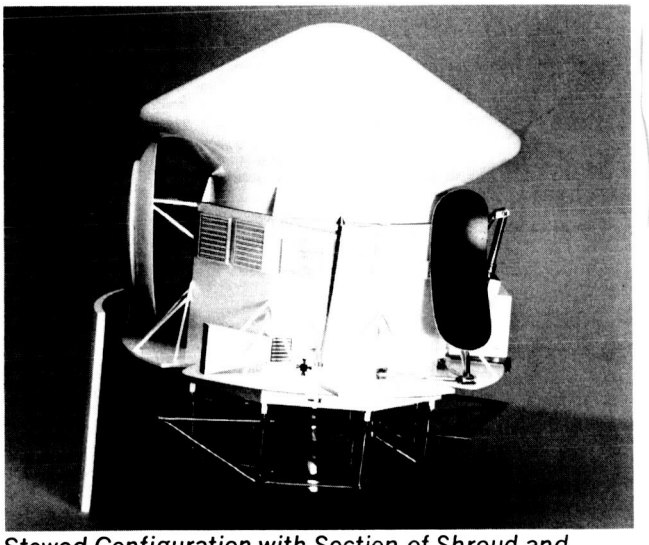

Stowed Configuration with Section of Shroud and Planetary Vehicle Adapter

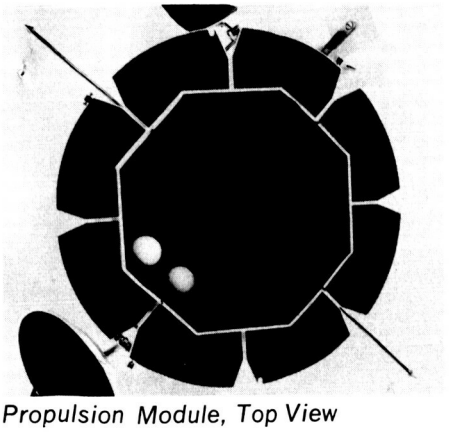

Propulsion Module, Top View

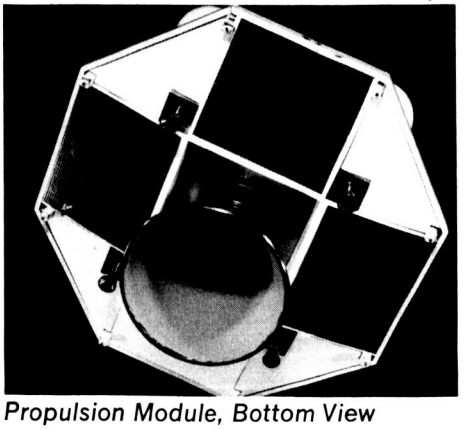

Propulsion Module, Bottom View

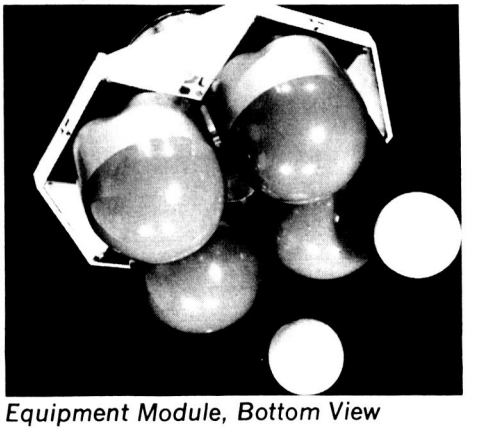

Equipment Module, Bottom View

Copy 16

VOYAGER

SPACECRAFT Phase B, Task D

FINAL REPORT

Annex to Volume 2. Spacecraft Design and Performance

OCTOBER 1967

Prepared for
GEORGE C. MARSHALL SPACE FLIGHT CENTER
Huntsville, Alabama

TRW
SYSTEMS GROUP

Voyager Operations
Space Vehicles Division

One Space Park, Redondo Beach, California

CONTENTS

SPACECRAFT MISSION DESCRIPTION

CONTENTS

APPENDIX A

SPACECRAFT MISSION DESCRIPTION

This appendix presents the sequence of phases and related mission events associated with the spacecraft for the general Voyager Mars mission. The mission operations begin with flight hardware acceptance review and shipment of the flight hardware to Cape Kennedy and continues until termination of the mission. Mission operation as defined here begins with the launch phase and primarily deals with spacecraft flight operations. Thus this description serves as a framework for the detailed flight sequence

As shown in Figure A-1, the mission has been divided into phases which are continuous periods of time arranged in order of occurrence and define the sequence in which the mission is conducted. Each phase is, in turn, made up of one or more periods; each such period of operation is in turn defined in terms of subsystem operating modes or functions. These operating modes are the functional building blocks for defining the mission and relate the mission functional requirements to subsystem design. Definition of operating modes is given in Appendix B as supporting data for the mission description. In presenting sequence tables for each mission phase, references are provided to the applicable mode description in Appendix B.

1. LAUNCH PHASE

The launch phase begins with the initiation of final countdown and terminates at the initiation of S-IVB stage second burn for injection into an interplanetary trajectory. Table A-1 gives a sequential list of operating modes and events for the launch phase.

1.1 Final Countdown

Confirmation of a Voyager mission readiness condition initiates the final countdown. The countdown will be conducted in two periods. During the first period all of the planetary vehicle components which will operate during launch will be turned on and will be monitored. Spacecraft system status and verification of planetary vehicle-launch vehicle interface status will be monitored via hard line and radio link

Table A-1. Operating Modes and Events for the Launch Phase

	Appendix B Reference
1. Launch phase	
1.1 Prelaunch	
Countdown initiated	
1.2 Space vehicle ascent flight	
S-IC stage ignition	
Holddown release and liftoff	
S-IC stage termination	
Vehicle coast	
S-IC stage jettison	
S-II stage ignition	
S-II stage termination	
Vehicle coast	
S-II stage jettison	
S-IVB stage ignition	
S-IVB stage shutdown	
1.3 Earth parking orbit	
Vehicle stabilize and coast	
Forward shroud elements jettison	9.1
Vehicle stabilize and coast	

while the launch vehicle undergoes preflight propulsion, mechanical, and electrical subsystem verification. During the second part of the countdown, the planetary vehicle will continue to be monitored, while the launch vehicle undergoes power transfer, final ordnance installation, and cryogenic propellant loading. Final safety and final status checks will be performed, the planetary vehicle will be transferred to internal power, and the automatic terminal countdown will be conducted. The terminal countdown ends when the space vehicle is released and lifts off.

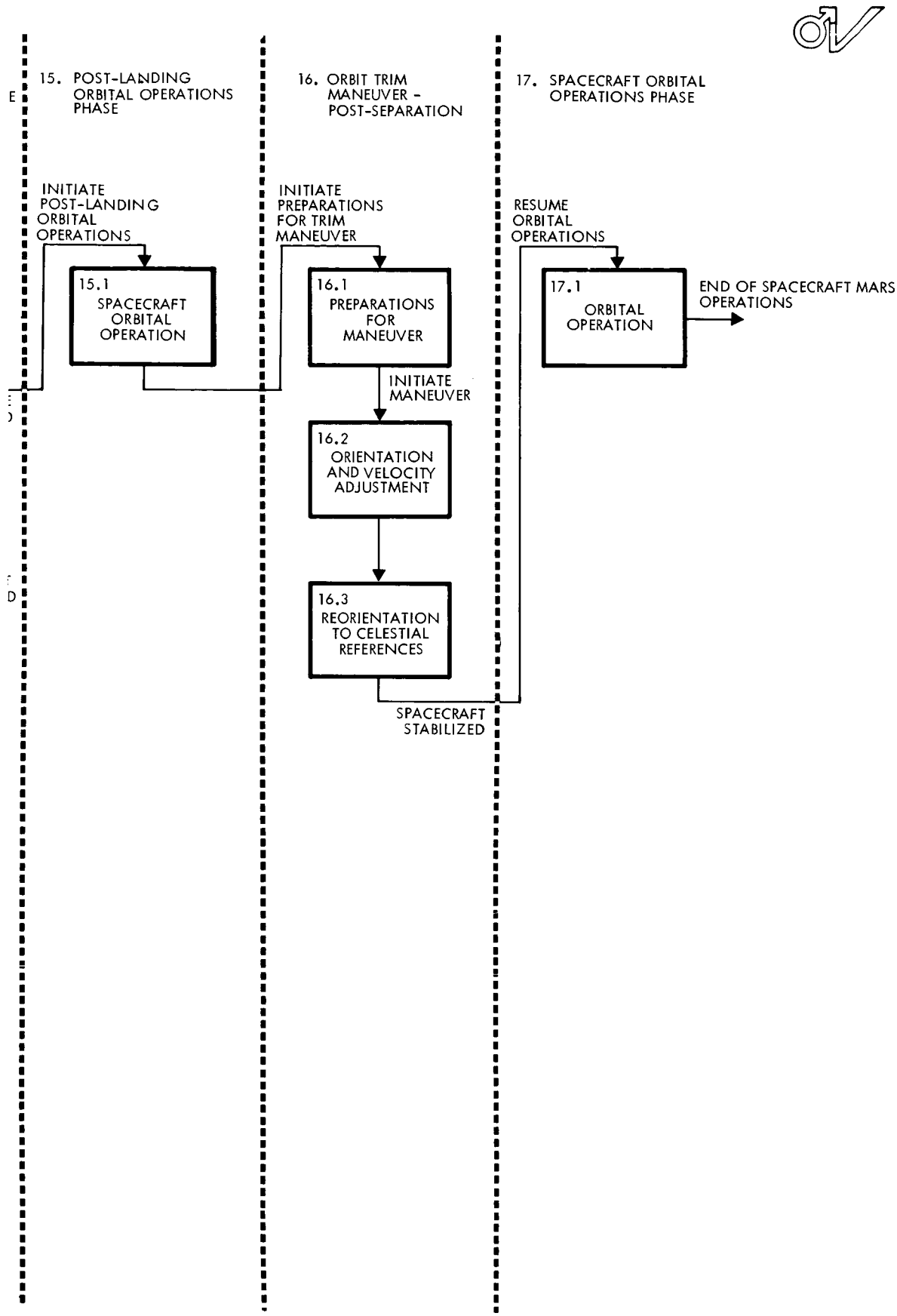

FOLDOUT FRAME 4

Figure A-1. Voyager Spacecraft Mission Phase Sequence

At liftoff the spacecraft has the following operating status:

Electrical Power. The spacecraft utilizes ground power until final status check. Prior to final status check electrical power is switched to internal battery power.

S-Band Radio. The up and down RF links are operative through the low-gain antennas. The radio transmission is on the low power transmitter and the high power transmitter is turned off.

UHF Capsule Relay Link. The UHF capsule relay link is nonoperative.

Command and Sequencing. The command and sequencing subsystem is on and operating. The mission clock is initiated late in the countdown prior to final status checks.

Data and Telemetry. The DS and T* is on and operating and onboard spacecraft data is processed for real-time relay to the ground station.

Guidance and Control. The gyros are turned on and operated in the rate mode.

Electrical Distribution and Pyrotechnic Control. The spacecraft will be coupled to the ground via umbilicals until late in the final countdown. After electrical power is switched to internal the shroud umbilicals for the planetary vehicle are disconnected. The pyrotechnic control assembly is in the prelaunch safe condition.

Configuration. The planetary vehicles are encapsulated in the shroud. All antennas, booms, and the PSP are stowed and latched for launch.

Thermal Control. The temperature control is operative during the countdown. Heaters will function automatically as required. Environmental control within the shroud compartment is provided by the launch vehicle system.

Propulsion. The propulsion system is unarmed and nonoperative.

Science Sensors. Science sensors are turned off.

*DS and T stands for data storage and telemetry

1.2 Space Vehicle Ascent Flight

Space vehicle ascent flight begins at Saturn V holddown release (liftoff) and continues until the S-IVB stage firing is terminated in earth parking orbit. During this period the Saturn V will automatically perform all functions and the spacecraft will be monitored via radio link transmitted through the shroud.

The first stage, S-IC, of the Saturn V will boost the space vehicle approximately 40 nautical miles and then separate. The second stage, S-II, will increase altitude and then be jettisoned. Finally, the third stage (S-IVB) will insert the remainder of the space vehicle including both planetary vehicles into a near-circular 100-nautical mile earth parking orbit. Figure A-2 shows pictorially the relationship between space vehicle elements and the earth during the launch phase.

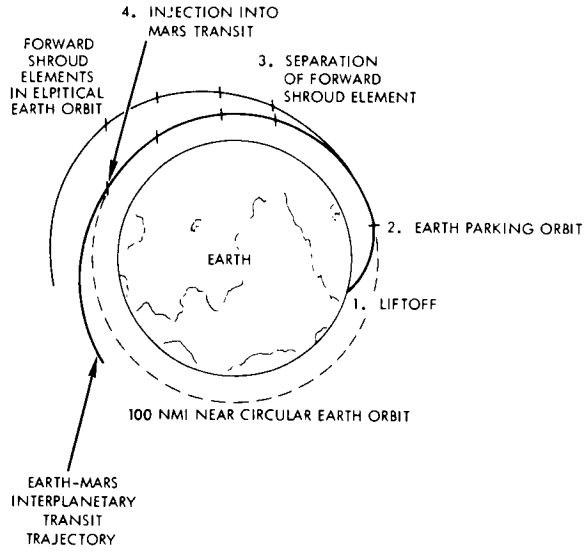

Figure A-2. Typical Launch Phase

1.3 Earth Parking Orbit Operations

During earth parking orbit operations, the nose fairing and shroud elements enclosing the forward planetary vehicle will be separated and the space vehicle will cruise until powered flight for injection into the interplanetary transfer trajectory is initiated. Separation will cause the

forward shroud elements to increase altitude and slow down with respect to the space vehicle.

2. INJECTION PHASE

The injection phase begins with the initiation of the S-IVB stage second burn and terminates when the aft planetary vehicle is separated from its planetary vehicle adapter. During this phase, the space vehicle is injected into an interplanetary transfer trajectory and the planetary vehicles are separated and prepared for interplanetary operations. Table A-2 gives a sequential list of subsystem operating modes employed during the injection phase. The major events are shown pictorially in Figure A-3.

Table A-2. Subsystem Operating Modes Employed During Injection Phase

	Appendix B Reference
2. Injection phase	
2.1 Injection	
S-IVB stage ignition	
S-IVB stage shutdown in earth-Mars transit trajectory	
Vehicle coast period	
2.2 Forward planetary vehicle separation sequence	9.2
IMU initiate separation sequence	
Planetary vehicle begins separation from shroud	
C and S start mission clock	
C and S assume control of planetary vehicle	
Pyrotechnic control pre-arm	8.5
2.3 Forward planetary vehicle post-separation sequence	
Planetary vehicle separated from shroud	
G and C switched to rate nulling mode	7.2

Table A-2. Subsystem Operating Modes Employed During Injection Phase (Continued)

		Appendix B Reference
	Temperature control appendage drive heaters turned on (if required)	11.2-11.5
	Radio uplink on low gain reception	2.1
	Radio downlink switched to low power and low-gain antenna	3.3
	Pyrotechnic control armed	8.4 and 8.7
	Cruise configuration established	10.1
	Boom mounted low-gain antennas deployed	10.1
	High-gain antennas released	10.1
	Medium-gain antennas released	10.1
	PSP deployed to cruise condition	10.1
	Temperature control in normal operating mode	11.1
	High-gain antenna pointed to earth	4.2
	Radio downlink switched to low power and high-gain antenna	3.1
	MOS verification of planetary vehicle cruise configuration	
	Planetary vehicle ready for acquisition phase	
2.4	Mid-shroud elements jettison	9.3
2.5	Aft planetary vehicle separation	9.2
	Sequence the same as 2.2	
2.6	Aft planetary vehicle post separation sequence	
	Sequence the same as 2.3	

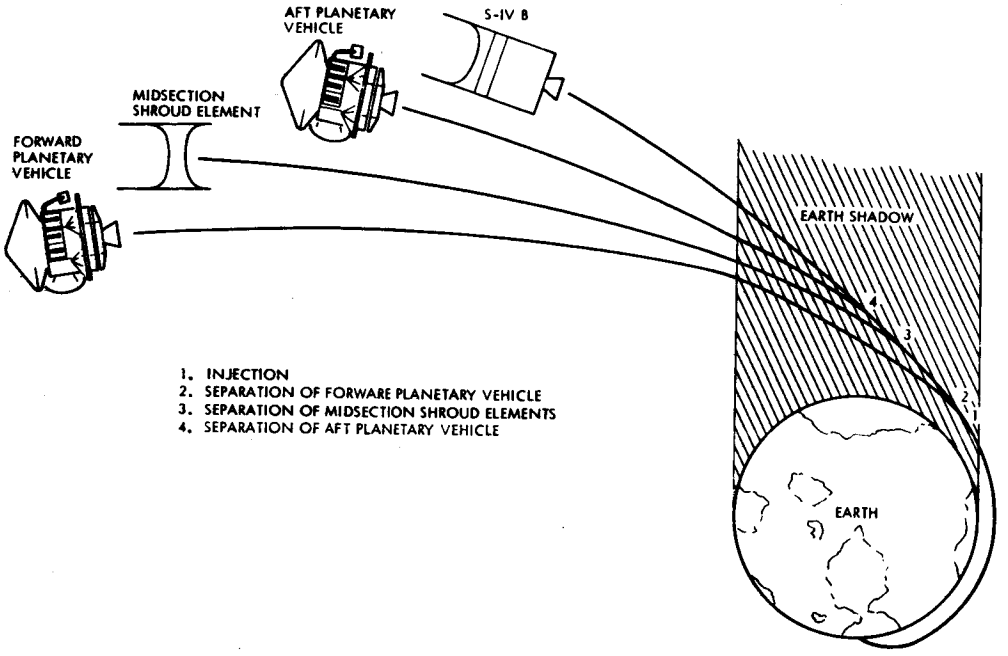

Figure A-3. Injection Phase

2.1 Injection into Interplanetary Transfer Trajectory

The injection into interplanetary transfer trajectory is accomplished by re-ignition of the S-IVB stage, which provides the velocity increment required to inject the planetary vehicles onto the specified interplanetary transit trajectory to Mars, biased to preclude dispersions from resulting in an inadvertent Martian impact.

2.2 Separation of Forward Planetary Vehicle

Separation of the forward planetary vehicle will be initiated automatically by the Saturn V with the transmission of a separation initiation signal from the instrument unit to the forward planetary vehicle after the space vehicle has stabilized from the shutdown transient. Separation will take place as soon as the spacecraft/DSN communication allows coverage of separation. The spacecraft of the forward planetary vehicle physically disconnects and separates with sufficient velocity to ensure that no interference occurs between it and any other elements of the space vehicle. During separation, uplink and downlink communication with the spacecraft is via the omnidirectional low-gain antenna.

2.3 Forward Planetary Vehicle Post-Separation Operations

The planetary vehicle post-separation operations begin when the planetary vehicle is separated from the space vehicle and continue until the initiation of celestial reference acquisition. During this period the planetary vehicle will be allowed to rotate at a low rate after the initial tipoff rates have been nulled to 0.01 deg/sec and will establish the cruise configuration. Appendages such as booms, antennas, and the PSP are released from the launch constraints and deployed to their cruise position. If required, appendage drive heaters may be turned on by ground command. All components and subsystems which operate during interplanetary transit phases will be turned on after separation has been completed. During post-separation operations the planetary vehicle will be in continuous communication, i.e., uplink command, downlink real-time telemetry, and tracking by the DSN. Command uplink lock-on is prerequisite to beginning celestial reference acquisition.

2.4 Coast Period and Jettison of Aft Shroud Elements

During the coast period, following separation of the forward planetary vehicle, the shroud elements forward of the aft planetary vehicle adapter will be separated. Jettison of the aft shroud elements will be initiated automatically by the Saturn V instrument unit.

2.5 Separation of Aft Planetary Vehicle

Separation of the aft planetary vehicle from its adapter will be executed in the same manner as the separation of the forward planetary vehicle.

2.6 Aft Planetary Vehicle Post-Separation Operations

The aft planetary vehicle post-separation operation is the same as forward planetary vehicle post-separation operations, Section 2.3.

3. ACQUISITION PHASE

The acquisition phase for each planetary vehicle begins after separation, and terminates when the vehicle attitude is stabilized on its celestial attitude references. Table A-3 gives a sequential list of subsystem operating modes employed during the acquisition phase. It

Table A-3. Subsystem Operating Modes Employed During Acquisition Phase

	Appendix B Reference
3. Acquisition phase	
DS and T switched to store engineering data	5.5
Radio uplink switched to low gain coverage	2.1
Radio downlink switched to low power and low-gain antenna	3.3
G and C begins sun acquisition	7.4
Electrical power switched to solar arrays	1.1
Batteries begin recharge	1.1
G and C begins Canopus acquisition	7.5

should be noted that from initiation of the acquisition phase through the end of the mission, each planetary vehicle will be considered separately. Mission operations activities, including tracking and telemetry data acquisition, will be coordinated but independent for each of the planetary vehicles throughout the remainder of the mission. The remaining phase descriptions are for one planetary vehicle. Each phase will be duplicated for each vehicle.

3.1 Orientation of Planetary Vehicle to Celestial Reference

During this period the planetary vehicle will automatically initiate and execute a maneuver to acquire the celestial referenced orientation. The gas reaction control system is used in conjunction with a coarse sun sensor to align the planetary vehicle aft roll axis with the sun. A fine sun sensor will be utilized to accurately maintain the sun orientation. The vehicle will then be oriented in roll by acquiring the star Canopus. Following the acquisition of the celestial references, the planetary vehicle will maintain a stabilized attitude for interplanetary cruise. Figure A-4 shows the orientation of the planetary vehicle at various times during the acquisition phase.

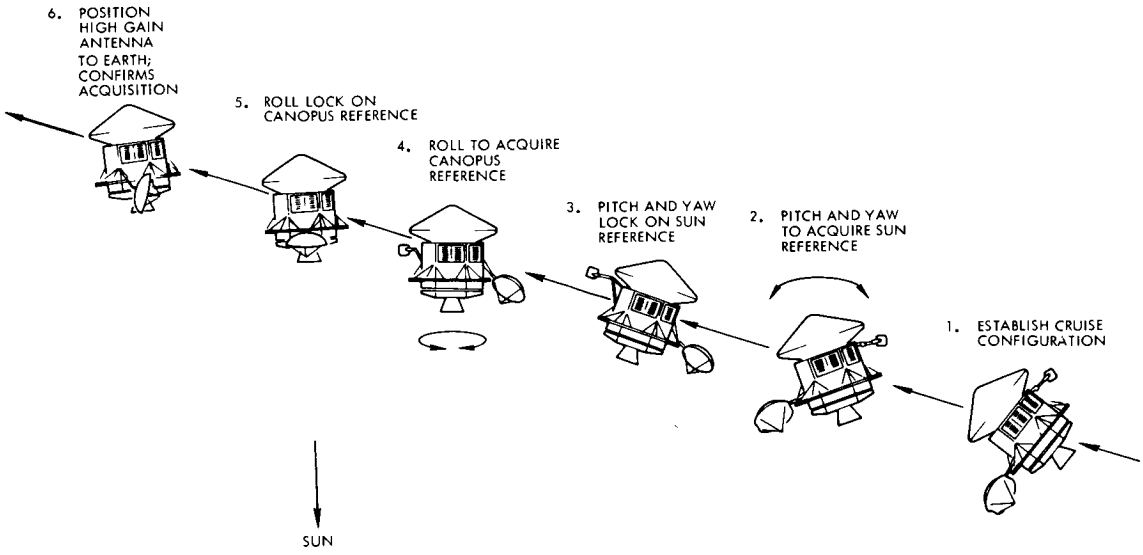

Figure A-4. Acquisition Phase

4. INITIAL INTERPLANETARY CRUISE PHASE

The interplanetary cruise phase for each planetary vehicle will be initiated after the vehicle is initially stabilized on its celestial attitude references. The initial interplanetary cruise phase for each planetary vehicle will be interrupted for an arrival date separation maneuver. Table A-4 gives a sequential list of operating modes employed during the initial interplanetary cruise phase.

Table A-4. Operating Modes Employed During Initial Interplanetary Cruise Phase

	Appendix B Reference
4. Initial interplanetary cruise	
G and C switched to cruise operation (coarse limit cycle)	7.6
DS and T switched to stored data readout	5.6
DS and T switched to real-time engineering data	5.1
High-gain antenna automatic reposition	4.1
Canopus sensor updated as required	7.1
Radio downlink switched to high power and low-gain antenna	3.6

During the initial interplanetary cruise the planetary vehicles remain oriented with respect to the celestial reference system (sun-Canopus) and are maintained attitude-stabilized by G and C cruise limit cycle. Continuous communications with the earth are maintained via the omnidirectional antenna. Any data stored during maneuvers or the reorientation period preceding the cruise phase are dumped. The high-gain antenna will be positioned to earth pointing and its position will be updated as the angle between the sun-spacecraft and earth-spacecraft lines change. In the event celestial reference is lost at any time, the G and C will automatically initiate inertial hold, and when possible will reacquire celestial references.

During interplanetary cruise, phase tracking data will be acquired by switching to range code transmission as required to collect sufficient metric data to calculate periodic trajectory corrections.

Figure A-5 shows the time and spatial relationship between earth, Mars, sun, and the two planetary vehicles during their interplanetary transit to Mars. In addition to the arrival date separation maneuver for each planetary vehicle the other maneuvers performed during transit are shown.

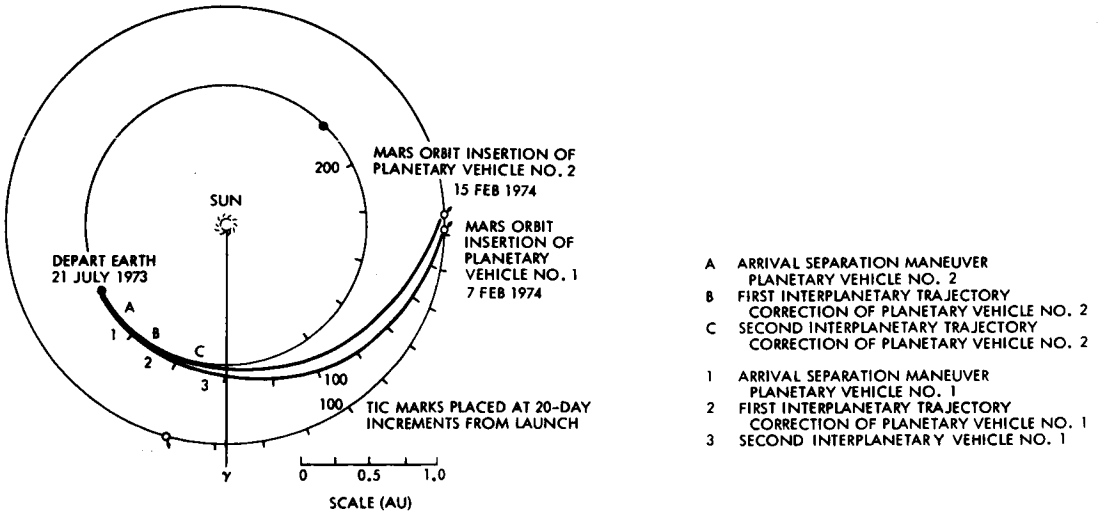

Figure A-5. Typical 1973 Voyager Mission Interplanetary Cruise and Maneuvers

5. ARRIVAL DATE SEPARATION MANEUVER

At preselected times, between 2 and 20 days after injection, each of the planetary vehicles will execute ground-commanded maneuvers designed to provide the time separation in planetary vehicle arrivals at Mars, and correct for the S-IVB aiming point bias and injection errors after sufficient tracking data has been acquired and the initial interplantary trajectory has been accurately determined. After the maneuver is completed, the spacecraft will automatically reacquire the cruise attitude.

The times selected for the maneuvers may be changed by ground command if necessary. Each subphase will be automatically sequenced on board; however, verification by the MOS of the status of the previous subphase will be required to enable the progression to events. Table A-5 gives a sequential list of subsystem operating modes employed to accomplish the arrival date separation maneuver. Figure A-6 shows a typical maneuver sequence.

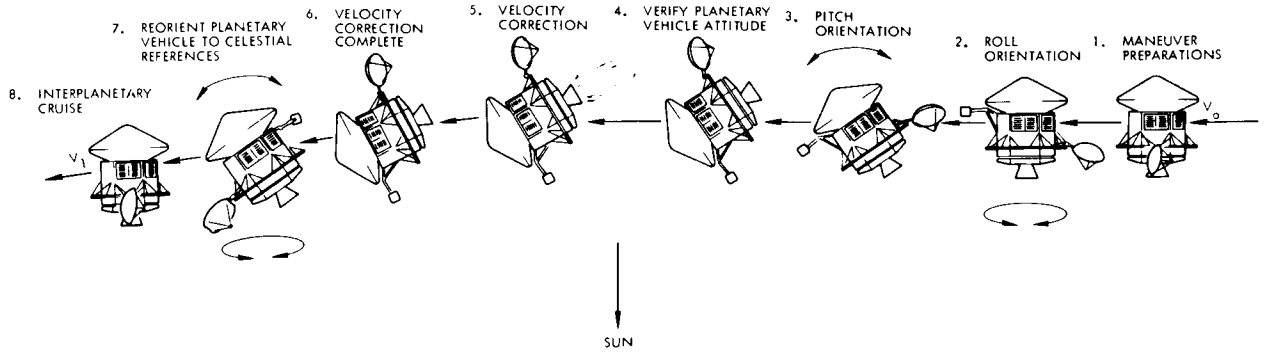

Figure A-6. Typical Maneuver Sequence

5.1 Preparation for Maneuver

During this period, maneuver preparations are carried out by the MOS, and the planetary vehicle will receive ground commands updating maneuver parameters stored in the C and S. Preparation for the arrival date separation maneuver includes G and C preparations, memory readout, and the selection of the appropriate data and transmission modes.

Table A-5. Subsystem Operating Modes Employed to Accomplish Arrival Date Separation Maneuver

	Appendix B Reference
5. Arrival date separation maneuver	
5.1 Preparation for maneuver	
MOS initiate update of maneuver parameters	
Radio uplink switched to maximum coverage reception	2.1
Radio downlink switched to high power and low-gain transmission	3.6
C and S memory (maneuver parameters) updated from ground	
G and C begins maneuver preparation	7.7
DS and T switched to C and S memory readout	5.2
MOS verification of C and S memory	
5.2 Orientation and velocity adjustment	
High-gain antenna command reposition (to be earth pointing after reorientation)	4.2
DS and T switched to spacecraft real-time engineering data	5.1
MOS verification of G and C maneuver preparation	
DS and T switched to engineering data storage	5.5
G and C begins attitude orientation	7.8
G and C switched to attitude hold (limit cycle)	7.3
Radio downlink switched to low power and high-gain transmission	3.1
DS and T switched to stored data readout	5.6
MOS verification of planetary vehicle attitude	
Pyrotechnic bus armed for propulsion operation	8.5
Propulsion system pressurized	12.1
Radio downlink switched to high power and low-gain transmission	3.6
DS and T switched to engineering data storage	5.1

Table A-5. Subsystem Operating Modes Employed to Accomplish Arrival Date Separation Maneuver (Continued)

	Appendix B Reference
G and C switched to engine operation control	7.9
Propulsion system begins low thrust operation	12.1
5.3 Reorientation to celestial references	
G and C switched to maneuver completion mode (to reacquire celestial references)	7.10
High-gain antenna command repositioned (to be earth pointing after celestial acquisition)	4.2
DS and T switched to engineering data storage	5.5
Electrical power on solar array (recharge batteries as required)	1.1

5.2 Orientation and Velocity Adjustment

During this period, the planetary vehicle thrust axis will be oriented for the maneuver and the high-gain antenna repositioned to be earth pointing after the proper maneuver orientation has been achieved. While the spacecraft is turning, communication will be maintained through the omnidirectional antennas (which provide spherical coverage from the spacecraft), the high-gain antenna will be repositioned, and the propulsion system will be pressurized. The maneuver data will be recorded on board as well as transmitted in real-time and, after orientation is complete, the attitude will be verified by switching to the high-gain antenna and stored data will be played back. After the MOS verifies the orientation, the engine will be ignited and operated to achieve the velocity vector required for Mars arrival time separation and to correct dispersions in the trajectory which may be determined from ground tracking data acquired prior to the maneuver.

5.3 Reorientation to Celestial References

After the maneuver is completed the planetary vehicle will automatically reacquire the celestial attitude references by turning through the same angles in a negative direction as those which were turned

during the orientation for the maneuver. Prior to reorienting, the communications will be switched to the low-gain antenna for omnidirectional transmission and the data switched to storage in addition to real-time transmission. When the reorientation is complete, the planetary vehicle will be aligned with the sun-Canopus references and cruise operations will be resumed.

6. INTERPLANETARY CRUISE PHASE

The interplanetary cruise phase for each planetary vehicle will be initiated when the vehicle is initially stabilized on its celestial attitude references after completion of the arrival date separation maneuver. Interplanetary cruise phase for each planetary vehicle will be interrupted subsequently for an interplanetary trajectory correction maneuver. Table A-6 gives a sequential list of operating modes employed during the initial interplanetary cruise phase.

Table A-6. Operating Modes Employed During Initial Interplanetary Cruise

	Appendix B Reference
6. Interplanetary cruise (resume 5)	
G and C switched to cruise operation (coarse limit cycle)	7.6
DS and T switched to stored data readout	5.6
DS and T switched to spacecraft real-time engineering data	5.1
High-gain antenna automatic reposition	4.1
Canopus sensor updated as required	7.11
Radio uplink switched to maximum gain	2.2
Radio downlink switched to low power high-gain transmission (for ranging)	3.1

6.1 Interplanetary Cruise

During the interplanetary cruise, the planetary vehicles remain oriented with respect to the celestial reference system (sun-Canopus)

and are maintained attitude stabilized by G and C cruise limit cycle. Continuous communications with earth are maintained via the omni-directional antenna as long as the gain margin at the ground reception station is sufficient to provide usable data. When the margin drops below this level, the spacecraft downlink antenna or power will be switched to main signal strength at the ground station. The high-gain antenna will be positioned to be earth pointing and position will be updated as the angle between the sun-spacecraft and earth-spacecraft lines changes.

The Canopus sensor has an adequate field of view so that no updating is required to compensate for the variation in Canopus position over the course of the Voyager mission.

Tracking data will be acquired immediately after cruise is established to collect sufficient metric data to assess the maneuver and calculate subsequent trajectory corrections.

7. INTERPLANETARY TRAJECTORY CORRECTION

At a time between 2 and 20 days after injection, each of the planetary vehicles will execute ground-commanded maneuvers designed to adjust the interplanetary transit trajectory such that the Mars flyby path will have the proper Mars-centered periapsis consistent with the position and arrival time requirements for Mars orbit insertion. After the maneuver is completed, the spacecraft will automatically reacquire the cruise attitude.

Each subphase will be automatically sequenced on-board; however, verification by the MOS of the status of the previous subphase generally will be required to enable propulsion firing. Table A-7 gives a sequential list of subsystem operating modes employed to accomplish the interplanetary trajectory correction.

The nominal mission requirements are for up to two interplanetary trajectories to be performed as required. The accuracy of the first will determine the requirements for a second. Each is conducted in the same manner. Table A-7a gives the sequence for the second correction.

Table A-7. Subsystem Operating Modes Employed to Accomplish Interplanetary Trajectory Correction

	Appendix B Reference
7. Interplanetary trajectory correction	
7.1 Preparation for maneuver	
MOS initiate update of maneuver parameters	
Radio uplink switched to maximum coverage reception	2.1
Radio downlink switched to high power and low-gain transmission	3.6
C and S memory (maneuver parameters) updated from ground	
G and C begins maneuver preparation	7.7
DS and T switched to C and S memory readout	5.2
MOS verification of C and S memory	
High-gain antenna command reposition (to be earth pointing after reorientation)	4.2
DS and T switched to spacecraft real-time engineering data	5.1
MOS verification of G and C maneuver preparation	
7.2 Orientation and velocity adjustment	
DS and T switched to engineering data storage	5.5
G and C begins attitude orientation	7.8
G and C switched to attitude hold (limit cycle)	7.3
Radio downlink switched to high power and high-gain transmission	3.1
DS and T switched to stored data readout	5.6
Pyrotechnic bus armed for propulsion operation	8.5
Radio downlink switched to high power and low-gain transmission	3.6
DS and T switched to engineering data storage	5.5
G and C switched to engine operation control	7.9
Propulsion system begins low thrust ullage blowdown operation	12.2

Table A-7. Subsystem Operating Modes Employed to Accomplish Interplanetary Trajectory Correction (Continued)

	Appendix B Reference
7.3 Reorientation for celestial references	
G and C switched to maneuver completion mode (to reacquire celestial references)	7.10
High-gain antenna command reposition (to be earth pointing after celestial acquisition)	4.2
DS and T switched to engineering data storage	5.5
Electrical power on solar array (recharge batteries as required)	1.1

Table A-7a. Subsystem Operating Modes Employed to Accomplish Second Interplanetary Trajectory Correction

	Appendix B Reference
7a. Interplanetary trajectory correction (second)	
7a.1 Preparation for maneuver	
MOS initiated update of maneuver parameters	
Radio uplink switched to maximum coverage reception	2.1
Radio downlink switched to high power and low-gain transmission	3.6
C and S memory (maneuver parameters) updated from ground	
G and C begins maneuver preparation	7.7
DS and T switched to C and S memory readout	5.2
MOS verification of C and S memory	
DS and T switched to spacecraft real-time engineering data	5.1
MOS verification of G and C maneuver preparation	

Table A-7a. Subsystem Operating Modes Employed to Accomplish Second Interplanetary Trajectory Correction (Continued)

	Appendix B Reference
7a.2 Orientation and velocity adjustment	
High-gain antenna command reposition (to be earth pointing after reorientation)	4.2
DS and T switched to engineering data storage	5.5
G and C begins attitude orientation	7.8
G and C switched to attitude hold (limit cycle)	7.3
Radio downlink switched to high power and high-gain transmission	3.1
DS and T switched to stored data readout	5.6
MOS verification of planetary vehicle attitude	
Pyrotechnic bus armed for propulsion operation	8.5
DS and T switched to engineering data storage	5.5
G and C switched to engine operation control	7.9
Propulsion system begins low thrust ullage blowdown operation	12.2
7a.3 Reorientation to celestial reference	
High-gain antenna command reposition (to be earth pointing after celestial acquisition)	4.2
DS and T switched to engineering data storage	5.5
G and C switched to maneuver completion mode (to reacquire celestial references)	7.10
Electrical power on solar array (recharge batteries as required)	1.1

7.1 Preparation for Maneuver

During this period, maneuver preparations will be initiated by the MOS. The planetary vehicle will receive ground commands to provide maneuver parameters for storage in the C and S memory. Preparation for the interplanetary trajectory correction includes G and C preparations, memory readout, and the selection of the appropriate data and transmission modes. After completion of this period and MOS verification, the spacecraft will proceed with orientation for velocity adjustment.

7.2 Orientation and Velocity Adjustment

During this period, the planetary vehicle thrust axis will be oriented for the maneuver and the high-gain antenna repositioned to be earth-pointing after the proper maneuver orientation has been achieved. While the spacecraft is turning, communication will be maintained through the low-gain antennas, which provide spherical coverage from the spacecraft, and the high-gain antenna will be repositioned. During the turn, in the event that this maneuver is performed beyond the range for adequate transmission link margin with the low-gain antenna, only tracking will be available in real-time. The maneuver data will be recorded on board as well as transmitted in real-time and, after the orientation is complete and the attitude verified by switching to the high-gain antenna, the stored data will be played back.

After the MOS verifies the spacecraft orientation, the engine will be ignited and operated in the low thrust mode to achieve the velocity vector required for the trajectory correction.

7.3 Reorientation to Celestial References

After the maneuver is completed, the planetary vehicle will reacquire the celestial attitude references by turning through the same angles in a negative direction as those which were turned during the orientation for the maneuver. Prior to reorienting, the communications will be switched to the low-gain antenna for omnidirectional transmission and the data switched to storage in addition to real-time transmission. When the reorientation is complete, the planetary vehicle will again be aligned with the sun-Canopus references and interplanetary cruise operations will be resumed. If an additional correction is required, it will be performed in a like manner.

8. FINAL INTERPLANETARY CRUISE PHASE

The interplanetary cruise phase for each planetary vehicle will be resumed when the vehicle is stabilized on its celestial attitude references following the interplanetary trajectory correction. The interplanetary cruise phase for each planetary vehicle will last at least 2 days and be finally terminated approximately 7 days prior to the actual

Mars orbit insertion, when the preparations for insertion begin by ground command from the MOS. Table A-8 gives a sequential list of operating modes employed during the final interplanetary cruise phase.

Table A-8. Operating Modes Employed During Final Interplanetary Cruise Phase

	Appendix B Reference
8. Final interplanetary cruise (resume 5)	
G and C switched to cruise operation (coarse limit cycle)	7.6
DS and T switched to stored data readout	5.6
DS and T switched to spacecraft real-time engineering data	5.1
High-gain antenna automatic reposition	4.1
Canopus sensor updated as required	7.11
Radio downlink switched to high power and high-gain antenna when required (approximately 1 ± 70 days)	3.4
Radio uplink switch to maximum gain	2.2

8.1 Final Interplanetary Cruise

During the final interplanetary cruise, the planetary vehicles remain oriented with respect to the celestial reference system and are maintained attitude stabilized by G and C cruise limit cycle. Continuous communications with the earth are maintained through the high-gain antenna until approximately 20 days prior to Mars orbit insertion when the spatial geometry will allow the medium-gain single-gimballed antenna to be earth pointed as a backup to the high-gain antenna. Any data stored during maneuver or reorientation period succeeding the cruise phase are dumped. The high-gain and medium-gain antennas will be positioned to be earth pointing and position will be updated as required.

The Canopus sensor has an adequate field of view so that no updating is required to compensate for the variation in the Canopus position over the course of the Voyager mission.

During interplanetary cruise phase, sufficient tracking data will be acquired to accurately calculate the maneuver parameters required for Mars orbit insertion.

9. MARS ORBIT INSERTION PHASE

The orbital insertion phase will be initiated at preselected times. This event will occur between several days after the final trajectory correction is completed and approximately 7 days prior to Mars encounter and will be terminated when the planetary vehicle is stabilized with respect to the celestial references in Mars orbit.

The time selected for the maneuver may be changed by ground command if necessary. The Mars orbit insertion phase will take place in full view of the earth. Each subphase will be automatically sequenced on board; however, verification by the MOS of the status of the previous subphase will be required to enable the progression to propulsion firing. Table A-9 gives a sequential list of subsystem operating modes employed to accomplish the arrival Mars orbit insertion maneuver. The sequence of events is shown in Figure A-7.

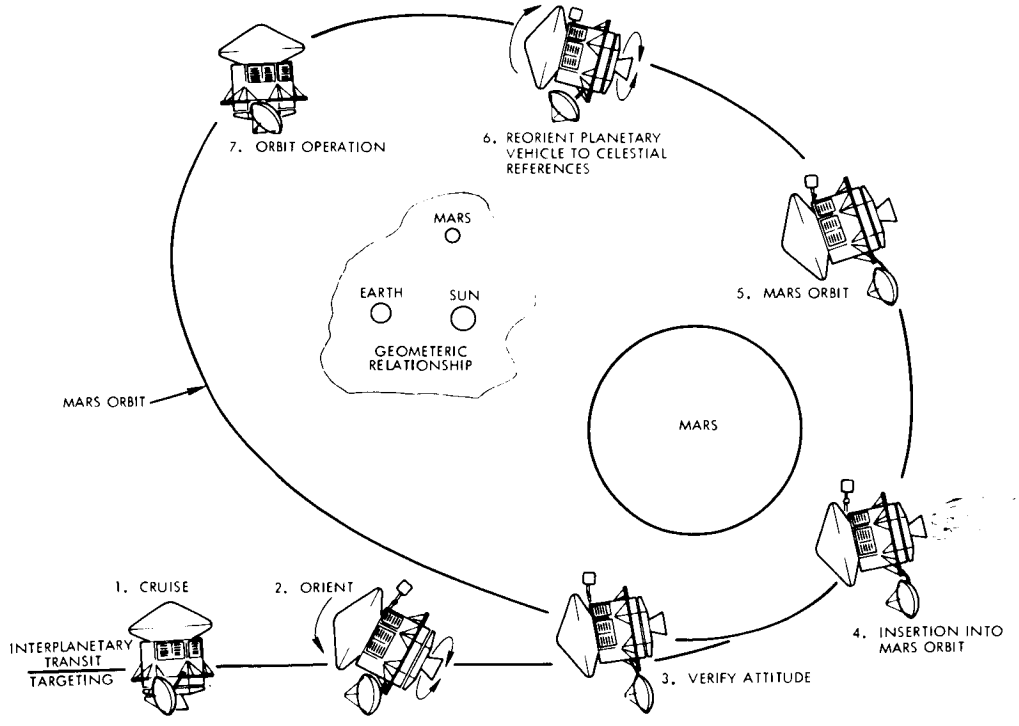

Figure A-7. Typical Mars Orbit Insertion Sequence

Table A-9. Subsystem Operating Modes Employed to Accomplish Mars Orbit Insertion

	Appendix B Reference
9. Mars orbit insertion	
9.1 Preparation for maneuver	
MOS initiated update of maneuver parameters	
Radio uplink switched to maximum coverage reception	2.1
Radio downlink switched to high power and medium-gain transmission	3.6
C and S memory (maneuver parameters) updated from ground	
G and C begins maneuver preparation	7.7
DS and T switched to C and S memory readout	5.2
MOS verification of C and S memory	
DS and T switched to spacecraft real-time engineering data	5.1
MOS verification of G and C maneuver preparation	
9.2 Orientation and Insertion	
High-gain antenna command reposition (to be earth pointing after reorientation)	4.2
DS and T switched to engineering data storage	5.5
Radio downlink switched to high power and low-gain transmission	3.6
G and C begins attitude orientation	7.8
Electrical power switched to batteries	1.2
G and C switched to attitude hold (limit cycle)	7.3
Radio downlink switched to high power and high-gain transmission	3.1
DS and T switched to stored data readout	5.6
MOS verification of planetary vehicle attitude	
Pyrotechnic bus armed for propulsion operation	8.5
DS and T switched to engineering data storage	5.5
G and C switched to engine operation control	7.9
Propulsion system begins high thrust operation	12.3

Table A-9. Subsystem Operating Modes Employed to Accomplish Mars Orbit Insertion (Continued)

	Appendix B Reference
9.3 Reorient to celestial references	
Radio downlink switched to high power and low-gain transmission (for tracking)	3.6
G and C switched to maneuver completion mode (to reacquire celestial references)	7.10
High-gain antenna command reposition (to be earth pointing after celestial acquisition)	4.2
Electrical power switched to solar array (recharge batteries as required)	1.1

9.1 Preparation for Maneuver

During this period, maneuver preparations will be initiated by the MOS. The planetary vehicle will receive ground commands updating insertion parameters stored in the C and S memory. Preparation for the Mars orbital insertion includes G and C preparations, memory readout, and the selection of the appropriate data and transmission modes. After verification by the MOS that preparations have been satisfactorily completed, the spacecraft is ready to proceed with the orientation for velocity adjustment. Updating of maneuver parameters may be accomplished if required up to the time orientation begins.

9.2 Orientation and Insertion

During this period, the planetary vehicle thrust axis will be oriented for insertion into Mars orbit. Initially, communications will be with the medium-gain antenna and later switched to the omnidirectional antenna, which will provide carrier tracking during the turn. The high-gain antenna will be repositioned to be earth pointing after the proper maneuver orientation has been achieved. The maneuver data will be recorded on board after the orientation is completed, the attitude will be verified by switching to the high-gain antenna, and stored data will be played back. After the MOS verifies the orientation, the engine will be ignited and operated in the high thrust mode, to achieve

the velocity vector required for Mars orbit insertion. The timing of the orbit insertion maneuver is the most critical of the maneuvers, since the time in which the insertion may take place will be limited. Therefore, the orientation will be performed as early as possible to allow for verification of the attitude and sufficient time for reorienting the planetary vehicle, if required, prior to engine operation. The constraint on starting the turn will be determined based on time allowable on battery power under the electrical loads developed during the maneuver. In the event of a malfunction of the main engine the C-1 engines are available to take over as a backup for propulsion operations. In the event that the main engine fails to provide thrust the C-1 engine will automatically take over as a backup for the orbit insertion propulsion operation.

9.3 Reorientation to Celestial References

After the maneuver is completed, the planetary vehicle will reacquire the celestial attitude references by turning through the angles required to reorient the planetary vehicle attitude with respect to the celestial references. Prior to reorienting, the communications will be switched to the low-gain antenna omnidirectional carrier tracking transmission and the data switched to storage of engineering measurements. When the reorientation is complete, the planetary vehicle will be aligned with the sun and Canopus references and cruise operations will be resumed.

10. POST-INSERTION PLANETARY VEHICLE ORBITAL OPERATION PHASE

The post-insertion orbital operation (pre-trim) is initiated after the planetary vehicle is stabilized following Mars orbit insertion and is interrupted for an orbital trim maneuver. Table A-10 gives a sequential list of subsystem operating modes employed during this phase.

10.1 Orbital Checkout

During this period, the planetary vehicle will be in orbital cruise around Mars. The medium- and high-gain antennas will be pointed to earth and data stored will be played back. Then the spacecraft will be

Table A-10. Subsystem Operating Modes Employed During Post-Insertion Planetary Vehicle Orbital Operation

	Appendix B Reference
10. Post-insertion orbital operation	
10.1 Orbital checkout	
G and C switched to cruise limit cycle	7.6
Radio uplink switched to maximum coverage reception	2.1
Radio downlink switched to high power and high-gain transmission	3.4
Medium-gain antenna automatically repositioned (to be earth pointing)	4.1
DS and T switched to stored data readout	5.6
DS and T switched to real-time engineering and science data	5.4
PSP switched to automatic ground tracking	13.3
G and C switched to fine limit cycle	7.3
Orbital science preparations	13.1
DS and T switched to real-time science and video data storage	5.4/5.5
DS and T switched to stored video data readout and science data storage	5.6/5.5
DS and T switched to real-time science data	5.4
MOS verification of science operation	
MOS update of science sequences (if required)	
C and S science sequences updating from ground	
DS and T switched to C and S memory readout	5.2
MOS verification of C and S memory	
10.2 Orbital operation (pre-separation)	
Orbital science operation initiated	13.2
DS and T switched to real-time science and video data storage	5.4/5.5

Table A-10. Subsystem Operating Modes Employed During Post-Insertion Planetary Vehicle Orbital Operation (Continued)

	Appendix B Reference
DS and T switched to stored video data readout and science data storage	5.6/5.5
DS and T switched to real-time science data	5.4
See Section 17 for more detailed sequence	

brought into the orbital configuration. The PSP will be turned on and will begin tracking the center of Mars. The science instruments will be turned on and calibrated (if required), sequence data will be taken and the instruments will be checked out, the limb and terminator sensors will be turned on, and the C and S will be switched to automatic science sequencing. After all subsystems, including the science package, have been checked out, the MOS can verify the orbital operations and, if required, update the science orbital sequencing by ground command and adjustment of science instruments. Following the updating, the spacecraft will begin pre-separation orbital operation.

10.2 Orbital Operation (Pre-Separation)

After the MOS has verified and updated the orbital operating parameters, if such updating is required, the spacecraft will begin orbital operations. The orbital operations will continue for the remainder of the mission; however, interruptions will occur as required for orbital trim maneuvers before and after separation, the spacecraft will begin orbital science operation by sequencing the appropriate sensors and by operating the PSP in automatic Mars tracking mode or by target pointing as required to obtain the desired data. The data acquired will be for support of the capsule operations, i.e., surveying landing areas and obtaining detailed information about the area finally chosen for capsule touchdown. Video and science data will be primarily gathered

during periods when the suborbital point on the Mars surface is in daylight between the dawn and evening terminators and near the orbit periapsis. Video data will be stored during the period of video data acquisition and transmitted to earth during the remainder of the orbital period. A more detailed description of orbital operations is found in Section 17, spacecraft orbital operation.

11. ORBIT TRIM MANEUVER

An orbit trim maneuver will be performed between orbital insertion and capsule separation. This maneuver will be initiated by ground command, and will be performed to correct errors in the initial Mars orbit or to improve the orbital characteristics to support the capsule landing. After the maneuver is completed, the spacecraft will automatically reacquire the celestial referenced attitude and resume orbital operations.

The times selected for the maneuver may be changed by ground command if necessary. Each subphase will be automatically sequenced on board; however, verification by the MOS of the status of the previous subphase will be required to enable the progression to events. Table A-11 gives a sequential list of subsystem operating modes employed to accomplish the orbit trim maneuver.

11.1 Preparation for Maneuver

During this period, maneuver preparations will be initiated by the MOS. The planetary vehicle will receive ground commands to enter maneuver parameters in the C and S memory. Preparation for the orbit trim maneuver includes G and C preparations, memory readout, and the selection of the approximate data and transmission modes.

11.2 Orientation and Velocity Adjustment

During this period, the planetary vehicle thrust axis will be oriented for the maneuver and the high-gain antenna repositioned to be earth pointing after the proper maneuver orientation has been achieved. The spacecraft is commanded initially on the medium-gain antenna; however, while the spacecraft is turning, communication will be obtained through the omnidirectional low-gain antennas, which provide carrier

Table A-11. Subsystem Operating Modes Employed to Accomplish Orbit Trim Maneuver

	Appendix B Reference
11. Pre-separation Mars orbit trim maneuver	
11.1 Preparations for maneuver	
MOS initiated update of maneuver parameters	
Radio uplink switched to maximum coverage reception	2.1
Radio downlink switched to high power and medium-gain transmission	3.5
C and S memory (maneuver parameters) updated from ground	
Orbital science operation inhibited	
G and C begins maneuver preparation	7.7
DS and T switched to C and S memory readout	5.2
MOS verification of C and S memory	
High-gain antenna command reposition (to be earth pointing after reorientation)	4.2
DS and T switched to spacecraft real-time engineering data	5.1
MOS verification of G and C maneuver preparation	
11.2 Orientation and velocity adjustment	
DS and T switched to engineering data storage	5.5
Radio downlink switched to high power and low-gain transmission (for tracking)	3.6
G and C begins attitude orientation	7.8
Electric power switched to batteries	1.2
G and C switched to attitude hold (limit cycle)	7.3
Radio downlink switched to high power and high-gain transmission	3.1
DS and T switched to stored data readout	5.6
MOS verification of planetary vehicle attitude	

Table A-11. Subsystem Operating Modes Employed to Accomplish Orbit Trim Maneuver (Continued)

		Appendix B Reference
	Pyrotechnic bus armed for propulsion operation	8.5
	DS and T switched to engineering data storage	5.5
	G and C switched to engine operation control	7.9
	Propulsion system begins low thrust ullage blowdown operation	12.2
11.3	Reorientation to celestial references	7.3
	DS and T switched to store spacecraft engineering data	5.5
	Radio downlink switched to high power and low-gain transmission (for tracking)	3.6
	G and C switched to maneuver completion mode (to reacquire celestial references)	7.10
	High-gain antenna command reposition (to be earth pointing after celestial acquisition)	4.2
	Electrical power switched to solar array (recharge batteries as required)	1.1

tracking of the spacecraft. The maneuver data will be recorded on-board and, after the orientation is complete, the attitude will be verified by switching to the high-gain antenna and playing back the stored data. After the MOS verifies the orientation, the engine will be ignited and operated in the low thrust mode to achieve the velocity vector required for the orbit trim.

11.3 Reorientation to Celestial References

After the maneuver is completed the planetary vehicle will reacquire the celestial attitude references by turning through the same angles in a negative direction as those which were turned during the orientation for the maneuver. Prior to reorienting, the communications will be switched to the low-gain antenna for omnidirectional carrier tracking and the data switched to storage. When the reorientation is complete, the planetary vehicle will be aligned with the sun-Canopus references and cruise operations will be resumed.

12. PRE-SEPARATION ORBITAL OPERATIONS PHASE (POST-TRIM)

The pre-separation orbital operations phase begins when orbital operations are resumed after the planetary vehicle is stabilized with respect to the celestial references following the planetary vehicle orbit trim maneuver, and will be terminated when the preparations for spacecraft-capsule separation are initiated. Table A-12 gives a sequential list of subsystem operating modes employed during this phase.

Table A-12. Subsystem Operating Modes Employed to Accomplish Pre-Separation Orbital Operations

	Appendix B Reference
12. Pre-separation orbital operation	
G and C switched to cruise limit cycle	7.6
Radio uplink switched to maximum gain reception	2.2
Radio downlink switched to high power and high-gain transmission	3.4
Medium-gain antenna automatically repositioned	4.1
High-gain antenna automatically repositioned	4.1
DS and T switched to stored data readout	5.6
DS and T switched to spacecraft real-time engineering and science data	5.4
PSP switched to automatic ground tracking	13.3
G and C switched to fine limit cycle	7.3
Orbital science operations initiated	13.2
DS and T switched to real-time science and video data storage	5.4/5.5
DS and T switched to stored video readout and science data storage	5.6/5.5
DS and T switched to real-time science data	5.4

12.1 Orbital Operation (Pre-Separation)

After the planetary vehicle orbit trim maneuver is completed, the spacecraft will begin orbital operations which will continue until capsule

support operations are initiated. During this period, which precedes capsule separation, the spacecraft will resume orbital science operation by sequencing the appropriate sensors and by operating the PSP in automatic Mars tracking mode or by target point as required to obtain the desired data. Additional data will be acquired to support the capsule landing operation. Additional details may be found in Section 11.2, orbital operation (pre-separation).

13. SPACECRAFT-CAPSULE SEPARATION PHASE

The spacecraft-capsule separation phase will begin at the time the capsule subsystems are activated for separation, and extend until the capsule thrust axis is oriented for the capsule deorbit maneuver after it has separated from the spacecraft. Insofar as spacecraft operations are concerned, this phase ends when the capsule (lander) is separated from the planetary vehicle. Table A-13 gives a sequential list of subsystem operating modes employed during the spacecraft-capsule separation phase. A pictorial representation of the sequence of capsule separation and support is shown in Figure A-8.

13.1 Preparation for Separation

During this period, the spacecraft separation sequence will be initiated. Nominal values for the separation initiation time and the capsule deorbit maneuver parameters, stored in the C and S memory prior to launch, will be updated by ground command from the MOS, if necessary. The capsule will be activated and checked out and separation will be enabled and initiated by the spacecraft.

13.2 Capsule Separation

The capsule separation will be initiated by verification of the capsule readiness by the MOS. The C and S will then send a separation signal to the capsule. After receipt of the separation signal, the capsule physically separates and moves away from the spacecraft. Nominal spacecraft-capsule separation requires no maneuvers by the spacecraft. However, a backup capability for spacecraft orientation of the capsule prior to separation is available.

Table A-13. Subsystem Operating Modes Employed During Spacecraft-Capsule Separation

	Appendix B Reference
13. Spacecraft-capsule separation	
13.1 Preparation for separation	
MOS initiated update of maneuver parameters	
Radio uplink switched to maximum gain reception	2.2
Radio downlink switched to high power and high-gain transmission	3.4
DS and T switched to real-time capsule data	5.3
C and S memory (maneuver parameters) updated from ground	
Orbital science operations inhibited	
DS and T switched to C and S memory readout	5.2
MOS verification of C and S memory	
Capsule lid jettisoned	Capsule
DS and T switched to real-time capsule engineering and science data	5.3
C and S initiate capsule separation sequence	
Capsule systems activated	
Capsule system checked out	
13.2 Capsule separation	
MOS verification capsule readiness	
C and S sent separation signal to capsule system	
Capsule separation from spacecraft	

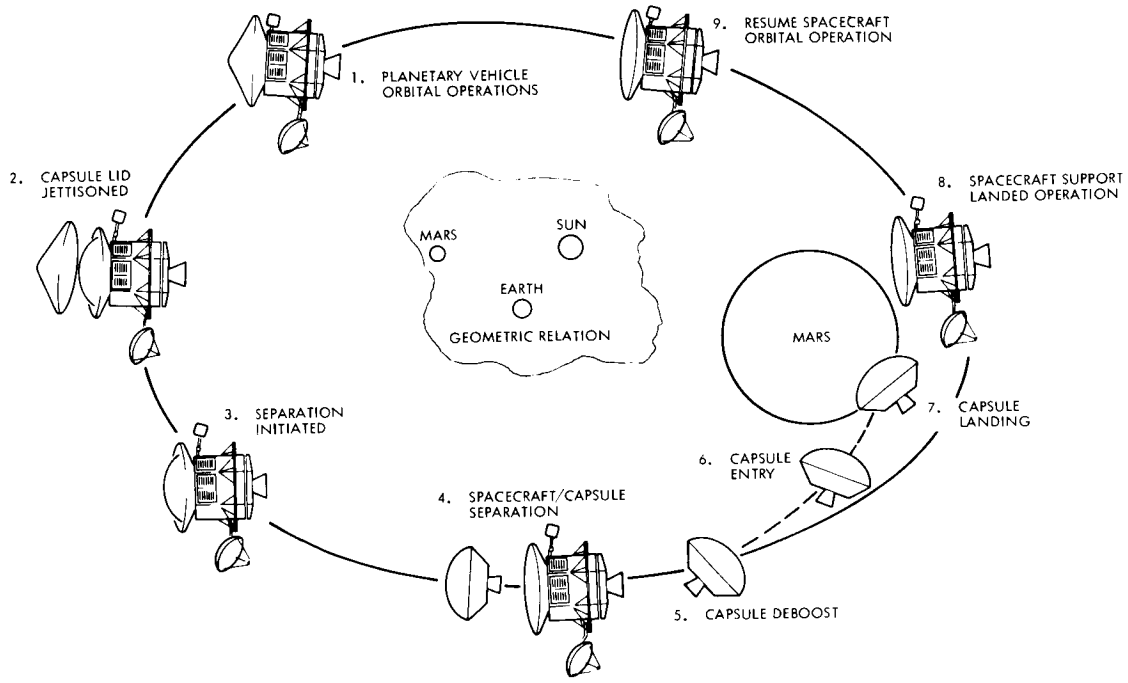

Figure A-8. Spacecraft-Capsule Separation and Support Sequence

14. POST-SEPARATION CAPSULE SUPPORT PHASE

The post-separation capsule flight phase will begin for the spacecraft when the flight capsule is separated, and continue until the capsule has landed on the Martian surface and completed landed operations. Table A-14 gives a sequential list of subsystem operating modes employed during the post-separation capsule support phase. The phase is shown in Figure A-9.

14.1 Post-Separation Orbital Operations

During this period, the spacecraft continues orbital operations and will support the capsule between separation and landing and (as required) until the end of operations on Mars by receiving capsule data for retransmission by the spacecraft to earth.

When the capsule enters the Mars atmosphere, the capsule will switch from low rate engineering data to both low rate engineering and higher rate science data. The data which is relayed to the spacecraft will be received by the UHF capsule link receiver and then transferred to the spacecraft data storage and telemetry subsystem for handling and

Table A-14. Subsystem Operating Modes Employed During Post-Separation Capsule Support

	Appendix B Reference
14. Capsule separation from spacecraft	
Capsule radio link receives capsule engineering data	
Capsule deorbit	Capsule
Capsule enters atmosphere (800, 000-ft altitude)	Capsule
Capsule radio link switched to high rate data	
Capsule video transmission begins	Capsule
DS and T switched to real-time capsule engineering and video data storage	5.3/5.5
Capsule landing	Capsule
Capsule out of spacecraft line of sight	
DS and T switched to stored data readout	5.6
Capsule within spacecraft line of sight	
DS and T switched to real-time capsule engineering and video data storage	5.3/5.5

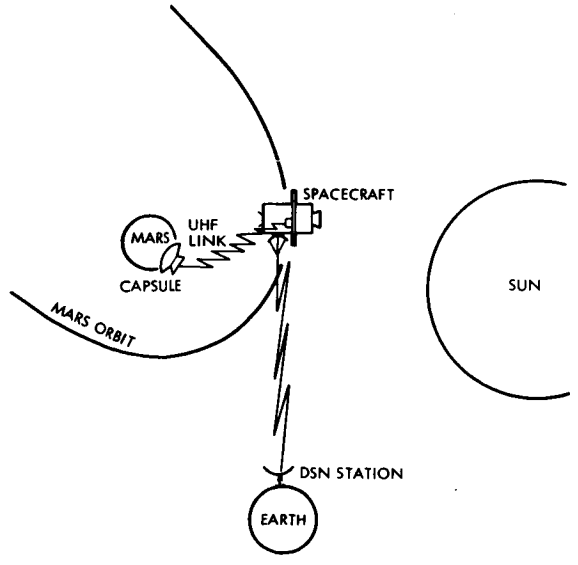

Figure A-9. Post-Separation Capsule Support Phase

retransmission to earth. Data storage will be provided for capsule data for both video and capsule engineering. The data storage mode will be used at times when the capsule relay link data rate exceeds the spacecraft transmission capability or for periods in which the downlinks between the spacecraft and the earth are ineffective or inoperative for any reason.

15. POST-LANDING ORBITAL OPERATIONS PHASE

Post-landing orbital operations will begin when the flight capsule has landed on Mars. The spacecraft will either support capsule landed operations or begin orbital experiments for the acquired scientific data for transmission to earth. This phase may be interrupted for a spacecraft orbit trim maneuver, if required, for adjustment of the orbit characteristics. See Table A-15 for a sequential list of subsystem operating modes.

Table A-15. Subsystem Operating Modes Employed During Post-Landing Orbital Operations

	Appendix B Reference
15. Post-landing orbital operations	
15.1 Orbital operations (post-separation)	
Pyrotechnic bus armed for PSP deployment	8.7
PSP deployed to post-separation final orbital configuration	10.2
Initiate orbital sequence	
See Table A-17 for detailed orbital sequence	

15.1 Spacecraft Orbital Operation

After the flight capsule has landed on Mars, the spacecraft will continue in orbit around Mars and accomplish orbital science operation and will support the flight capsule landed operations as required. Detailed descriptions of the operating characteristics of the spacecraft during this period are found in Section 14.1 for capsule support, and Sections 17.1, 17.2, 10.2, and 12.1 for orbital science operations. In addition, the

PSP is deployed to its fully extended position after the capsule has been separated from the spacecraft.

16. ORBIT TRIM MANEUVER—POST-SEPARATION

One or more trim maneuvers may be required subsequent to capsule separation if orbit adjustments are required to optimize spacecraft orbital operations. The maneuver will be initiated by ground command and be performed in a similar manner to the previous orbit trim (see Section 11). After the maneuver is completed, the spacecraft will automatically reacquire the celestial referenced attitude and resume orbital operations.

The times selected for the maneuver will be selected by ground, based on orbital science requirements and tracking data acquired after capsule separation. Each subphase will be automatically sequenced on-board; however, verification by the MOS of the status of the previous subphase will be required to enable the progression to events. Table A-16 gives a sequential list of subsystem operating modes employed to accomplish the orbit trim post-separation maneuver.

16.1 Preparation for Maneuver

During this period, maneuver preparations will be initiated by the MOS. The planetary vehicle will receive ground commands to enter maneuver parameters in the C and S memory. Preparation for the orbit trim maneuver includes G and C preparations, memory, readout, and the selection of the approximate data and transmission modes.

16.2 Orientation and Velocity Adjustment

During this period, the planetary vehicle thrust axis will be oriented for the maneuver and the high-gain antenna will be repositioned to be earth pointing after the proper maneuver orientation has been achieved. The spacecraft communication will initially be through the medium-gain antenna; however, while the spacecraft is turning, communications will be maintained through the omnidirectional low-gain antennas, which provide carrier tracking of the spacecraft. The maneuver data will be recorded on-board and, after the orientation is complete, the attitude will be verified by switching to the high-gain

Table A-16. Subsystem Operating Modes Employed to Accomplish Orbit Trim Post-Separation

	Appendix B Reference
16. Post-separation orbital trim maneuver	
16.1 Preparation for maneuver	
MOS initiated update of maneuver parameters	
Radio uplink switched to maximum coverage	2.1
Radio downlink switched to high power and medium-gain transmission	3.5
C and S memory (maneuver parameters) updated from ground	
Orbital science operation inhibited	
G and C begins maneuver preparation	7.7
DS and T switched to C and S memory readout	5.2
High-gain antenna command reposition (to be earth pointing after reorientation)	4.2
DS and T switched to spacecraft real-time engineering data	5.1
MOS verification of G and C maneuver preparation	
16.2 Orientation and velocity adjustment	
DS and T switched to engineering data storage	5.5
Radio downlink switched to high power and low-gain transmission	3.6
G and C begins attitude orientation	7.8
Electric power switched to batteries	1.2
G and C switched to attitude hold (limit cycle)	7.3
Radio downlink switched to high power and high-gain transmission	3.1
DS and T switched to stored data readout	5.6
MOS verification of planetary vehicle attitude	
Pyrotechnic bus armed for propulsion operation	8.5
DS and T switched to engineering data storage	5.5
G and C switched to engine operation control	7.9
Propulsion system begins low thrust ullage blowdown operation	12.2

Table A-16. Subsystem Operating Modes Employed to Accomplish Orbit Trim Post-Separation (Continued)

	Appendix B Reference
16.3 Reorientation to celestial references	
DS and T switched to engineering data storage	5.5
Radio downlink switched to high power and low-gain transmission (for tracking)	3.6
G and C switched to maneuver completion mode (to reacquire celestial references)	7.10
High-gain antenna command reposition (to be earth pointing after celestial acquisition)	4.2
Electrical power switched to solar array (recharge batteries as required)	1.1
G and C switched to limit cycle	7.3
Radio downlink switched to high power high-gain transmission	3.4
DS and T switched to stored data readout	5.6
DS and T switched to engineering data storage	5.5
Propellant tanks vented to ambient	12.4
DS and T switched to stored data readout	5.6

antenna and playing back the stored data. After the MOS verifies the orientation, the engine will be ignited and operated in the low thrust mode to achieve the velocity vector required for the spacecraft orbit trim.

16.3 Reorientation to Celestial References

After the maneuver is completed, the planetary vehicle will re-acquire the celestial attitude references by turning through the same angles in a negative direction as those which were turned during the orientation for the maneuver. Prior to reorienting, the communications will be switched to the low-gain antenna for omnidirectional carrier tracking and the data switched to storage. When the reorientation is complete, the planetary vehicle will be aligned with the sun-Canopus references and orbit cruise will be resumed. However, prior to entering

orbital operations after the final maneuver when it has been determined that all orbital requirements have been met, the propellant tanks will be vented to ambient. The tanks are vented one at a time by operating in the propulsion vent mode. After the tanks are completely vented, the spacecraft will resume the orbital operation phase and continue in this phase for the remainder of the spacecraft mission life.

17. SPACECRAFT ORBITAL OPERATIONS PHASE

Spacecraft orbital operations will be resumed after the spacecraft is established following the final spacecraft orbit trim maneuver and continue through the end of the mission. During this phase, the spacecraft will complete an orbit approximately every 14 hours. This phase can be subdivided into two types of periods. The first type corresponds to orbit periods in which the spacecraft is never in the shadow of Mars, and the second to those orbit periods in which the spacecraft passes through the shadow of Mars. Figure A-10a shows a typical orbit altitude versus time curve for the Mars orbit, the time is referenced in hours from periapsis, and markers indicate typical terminator crossings for dawn and evening. The terminator crossings will initiate the orbital sequences for the science instruments.

17.1 Orbital Operation (Noneclipse)

During the orbital operation phase when the spacecraft does not pass through the shadow of a Mars eclipse, the orbital operation sequence will be performed per the sequential list of subsystem operating modes presented in Table A-17. The radio communication to the ground will be through the high-power and high-gain antenna downlink as long as the spacecraft is in sight of a DSN station. If the spacecraft is not in sight of a DSN station, the science as well as engineering data will be stored on board and transmitted to ground at the earliest convenient time.

The orbital sequence will be initiated by the C and S each orbit by sensing the spacecraft crossing of the dawn terminator and refined by signals from the limb crossing sensor. The sensors will be turned on and warmed up if required, the G and C will be switched to fine limit cycle, science and the PSP will be switched to automatic Mars tracking.

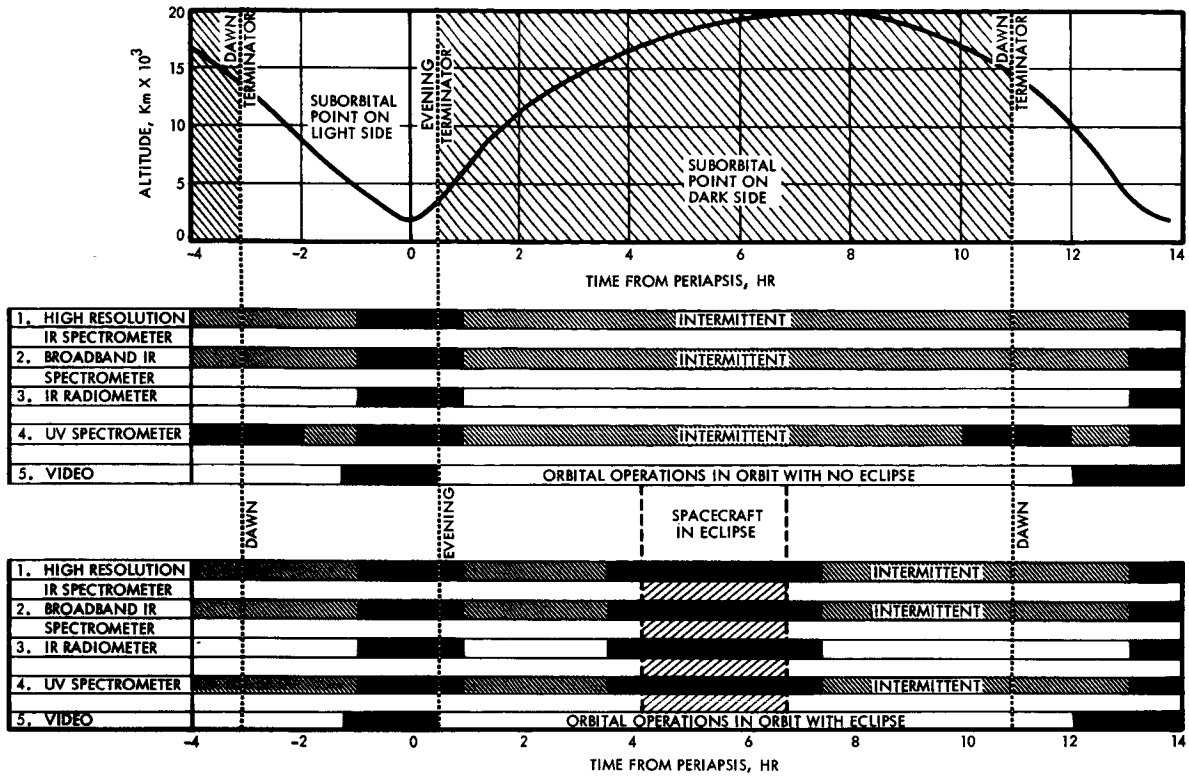

Figure A-10. Spacecraft Orbital Operations Phase

Table A-17. Subsystem Operating Modes During Orbital Operation

	Appendix B Reference
17. Spacecraft orbital operations	
17.1 Orbital operation (noneclipse)	
Electrical power on solar array	1.1
Radio uplink switched to maximum gain reception	2.2
Radio downlink switched to high power and high-gain transmission	3.4
DS and T switched to stored data readout	5.6
Spacecraft terminator crossing (down)	
C and S starts science sequence	13.2
Science sensors turned on	
DS and T switched to real-time science data	5.4

Table A-17. Subsystem Operating Modes During Orbital Operation (Continued)

		Appendix B Reference
	G and C switched to fine limit cycle	7.3
	PSP switched to automatic tracking	13.3
	Sensors switched to continuous data take	
	DS and T switched to real-time science and video data storage	5.4/5.5
	Photo-imaging switched to data take	14.1
	Science sensors switched to intermittent data take	
	Science sensors switched to continuous data take	
	Photo-imaging switched off	
	DS and T switched to real-time science	5.4
	Spacecraft terminator crossing (evening)	
	Electrical power switched to battery recondition (if required)	1.3
	Science sensors switched to intermittent data take	
	DS and T switched to real-time science and stored data readout	5.4/5.6
	DS and T switched to real-time science	5.4
	High-gain antenna automatic reposition (to be earth pointing)	4.1
	Canopus sensor updated (as required)	7.1
	C and S memory updated (as required)	
	(Repeat sequence)	
17.2	Orbital operation (eclipse)	
	Electrical power on solar array	1.1
	Radio uplink switched to maximum gain reception	1.1
	Radio downlink switched to high power and high-gain transmission	2.2
	DS and T switched to stored data readout	5.6
	Spacecraft terminator crossing (down)	
	C and S starts science sequence	13.2

Table A-17. Subsystem Operating Modes During Orbital Operation (Continued)

	Appendix B Reference
Science sensors turned on	
DS and T switched to real-time science data	5.4
G and C switched to fine limit cycle	7.3
PSP switched to automatic tracking	13.3
Sensors switched to continuous data take	
DS and T switched to real-time science and video data storage	5.4/5.5
Photo-imaging switched to data take	
Science sensors switched to intermittent data take	14.1
Science sensors switched to continuous data take	
Photo-imaging switched off	
DS and T switched to real-time science	5.4
Spacecraft sensors switched to intermittent data take	
DS and T switched to real-time science and stored data readout	5.4/5.6
DS and T switched to real-time science	5.4
High-gain antenna automatic reposition (to be earth pointing)	4.1
Canopus sensor updated (as required)	7.1
C and S memory updated (as required)	
Spacecraft enters eclipse	
Electrical power switched to batteries	1.2
G and C switched to inertial attitude hold	7.12
Science sensors switched to continuous data take	
Spacecraft emerges from eclipse	7.4
G and C reacquire sun	
Electric power switched to solar array (batteries recharged as required)	1.1

Table A-17. Subsystem Operating Modes During Orbital Operation (Continued)

	Appendix B Reference
G and C switched to coarse limit cycle	7.3
Science sensors switched to intermittent data take	
(Repeat sequence at dawn terminator crossing)	

After tracking is established, the appropriate sensors will begin continuous scanning of the planet, for a short period of time near the dawn terminator. As the spacecraft approaches periapsis, the photo-imaging subsystem will begin to view the surface. The data acquired by the video sensors are stored on board for transmission to the ground at a reduced playback speed at a later date as link capacity allows.

The science sensors are normally taking intermittent data; however, some sensors will take a continuous period of data shortly after passing the dawn terminator and again prior to passing the evening terminator. The timing between terminators will be detected on the previous orbit and updated each orbit. After passing the evening terminator, the suborbital point will be in darkness and the science sensors will again be switched to intermittent data. During the period when the suborbital point is in darkness, stored data will be dumped and antenna positioning, sensor update, C and S update, and any other required housekeeping functions will be performed as needed. A typical science sensor operations time line is shown in Figure A-10b for the orbital operations with no eclipse.

As the spacecraft approaches the dawn terminator, the orbital sequence will be repeated.

17.2 Orbital Operation (Eclipse)

The orbital operations in orbital periods which pass through the shadow of Mars are similar to the preceding sequence except for those

additional functions which result from the eclipse. A list of the sequential subsystem operating modes for an orbit period with an eclipse is given in Table A-17.

During the eclipse the spacecraft will be isolated from solar electric power and sun reference. Therefore, the electric power will be switched to the batteries and the G and C to attitude hold until the spacecraft emerges from the shadow. At that time, the G and C will reacquire celestial references and solar power will be regained. The batteries will automatically recharge after solar power is regained. As the mission progresses, the batteries will lose capacity due to the repeated duty cycle. When required, the batteries will be reconditioned by command from the MOS.

The science sequencing will also be modified for orbital periods in which eclipses occur. A typical science sensor operations time line is shown in Figure A-10c for the orbital operation with eclipses. During such periods, the science sensors will be switched to continuous data acquisition during the eclipse in addition to the continuous data acquisition during the lighted surface pass.

SPACECRAFT OPERATING MODES

CONTENTS

APPENDIX B

SPACECRAFT OPERATING MODES

This appendix supports the mission description given in Appendix A by discussing the subsystem operating modes referenced there. These operating modes represent building blocks for defining the mission and relate the corresponding functional requirements to the detail subsystem design as presented in Volumes 3, 4, and 5.

The modes for each subsystem are defined and a detailed sequence of events is given representing pertinent commands and conditions. The source of control and the active subsystem is given for each event along with comments to provide supplementary information. Prerequisites for the mode are also identified, corresponding to spacecraft generated conditions outside the subsystem concerned. This mode sequence data along with the general mission flow in Appendix A provides a complete detailed sequence for the mission. The associated discussion then provides a narrative mission description.

1. ELECTRICAL POWER

The electric power subsystem functions in the following operating modes: solar power, battery power, and battery reconditioning.

1.1 Solar Power Mode

The normal operating mode of the electric power subsystem is on solar arrays. During solar power operation the batteries are charged as required at a high rate until completely charged, then switched to a trickle charge rate and remain in this condition until a power load exceeding the solar power capability causes the batteries to discharge. The batteries continue supplying power on a load sharing basis with the solar array until the overload condition is relieved. Regulation of the main bus is provided by a combined boost/shunt regulation approach. While the array temperature is high and the output voltage is low, the boost regulator increases the voltage. The main bus voltage is maintained at 50 VDC $\pm$ 1 percent except during battery charging, when it drops to the charging voltage of the batteries. At Mars encounter, when boosting is

no longer required, the shunt element assembly automatically provides the main bus voltage limiting function. Table B-1 gives the mode sequence.

Table B-1. Solar Power Mode Sequence

Item	Event	Control Source	Active Subsystem	Comment
1	Presence of sun on solar panels			
2	On solar power with battery on trickle charge	Power	Power	*
3	Power overload		Power	Automatic
4	Load sharing with battery power	Power	Power	Automatic as required
5	Power overload relieved		Power	Automatic
6	Off battery power		Power	Automatic
7	Start charging battery at high rate		Power	*
8	Complete battery charged at high rate		Power	Automatic
9	Switch to trickle charge	Power	Power	*
10	Absence of sun on solar panels		Power	
11	On battery power	Power	Power	

*Automatic with battery charging subject to command override

1.2 Battery Power Mode

The spacecraft switches over automatically from solar power to obtain battery power, as required, in the absence of sufficient power from the solar panels to satisfy the loads. The main bus is maintained between 37 and 50 VDC. The spacecraft remains on battery power until the solar panels are again illuminated. The batteries are recharged when solar-generated power is available above load demand. Table B-2 gives the mode sequence.

Table B-2. Battery Power Mode Sequence

Item	Event	Control Source	Active Subsystem	Comment
1	Absence of sun on solar panels			
2	Drop in voltage output	Power	Power	Automatic
3	On battery power	Power	Power	Automatic
4	Presence of sun on solar panel			
5	On solar power	Power	Power	Automatic

1.3 Battery Reconditioning Mode

To regain full battery capacity after the irregular discharges occurring during maneuvers, reconditioning of the battery is planned prior to the start of the eclipse season. This occurs on command from the ground while the spacecraft is on solar power and no overload condition exists or is foreseen for at least 24 hours. One battery is switched to a dummy load and is completely discharged. After battery discharge is complete, the battery is then recharged. This sequence is repeated for each of the three batteries.

Battery reconditioning at the end of the eclipse season is also desirable. Table B-3 gives the mode sequence.

2. S-BAND RADIO UPLINK

The S-band radio uplink functions in the following operating modes: high-gain reception, medium-gain reception, and low-gain reception.

2.1 Low-Gain Reception Mode

Maximum coverage of reception from earth is obtained by the low-gain reception mode, which utilizes the two low-gain spacecraft antennas. If the low-gain antennas have been commanded for transmission they will also be selected for reception. They may also be selected for reception by direct command.

Table B-3. Battery Reconditioning Mode Sequence

Item	Event	Control Source	Active Subsystem	Comment
	Prerequisites • On solar power • Available power exceed load, to allow charging			
1	Enable battery reconditioning	MOS	C and S	Ground command
2	Switch battery charge regulator to dummy load	C and S	Power	
3	Begin battery discharge	Power	Power	Automatic
4	Complete battery discharge		Power	Automatic
5	Switch battery to charge	Power	Power	Automatic
6	Begin battery charge at high rate	Power	Power	Automatic
7	Complete charge at high rate		Power	Automatic
8	Switch to trickle charge	Power	Power	Automatic

As shown in Figure B-1, the detected low-gain receiver outputs are combined in the low-gain antenna selectors and fed to the receiver selector to serve as the selected uplink channel for coherent drive, range code, and command data. If the receivers for the low-gain antennas are below threshold the receiver selector will choose the output from the receiver connected to the high-gain antenna. If this is also below threshold, the output of the receiver connected to the medium-gain antenna will be selected. In any event that no coherent drive is available, the transmitters will operate in a noncoherent mode.

The low-gain reception mode sequence is given in Table B-4.

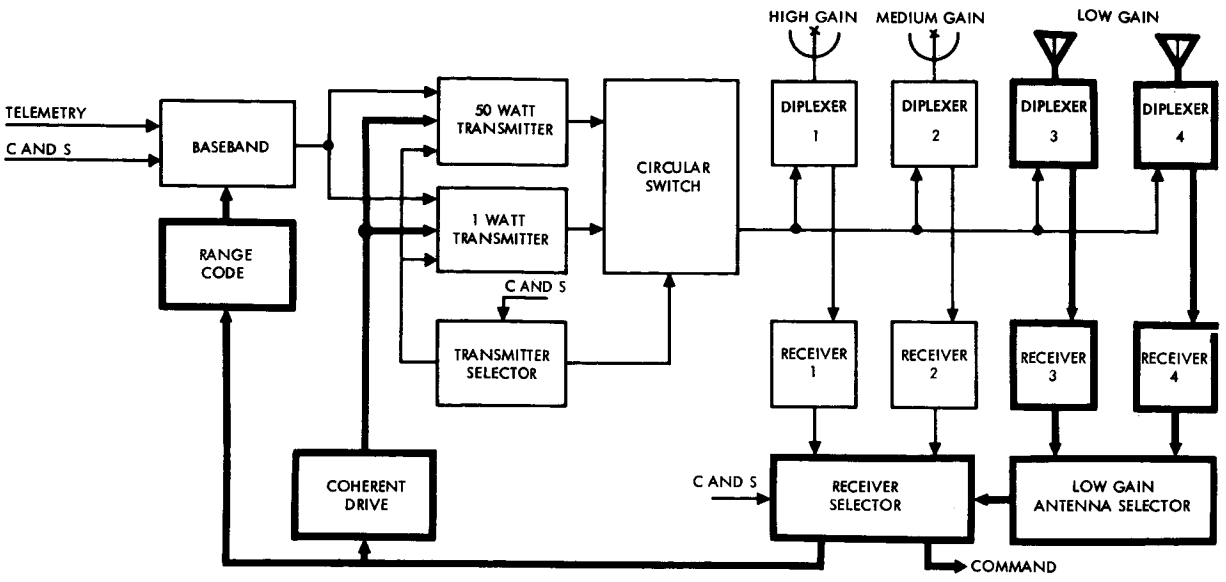

Figure B-1. Low-Gain Reception Mode Block Diagram

Table B-4. Low-Gain Reception Mode Sequence

Item	Event	Control Source	Active Subsystem	Comment
	Prerequisites			
	• Radio power supply on			Preflight
	• Receivers turned on			Preflight
	• Select transmission mode and antenna			
1	Receive uplink signal	TDAS	Radio	
2	Lock on low-gain antenna signal		Radio	Automatic if no lock, switch to noncoherent
3	Select receiver (low-gain)	Radio	Radio	Automatic
4	Provide coherent drive to transmitter		Radio	Automatic Override if desired
5	Provide signal to command subsystem		Radio	
6	Provide range code to transmitter		Radio	

2.2 High-Gain Reception Mode

Maximum gain reception from earth is obtained by the high-gain reception mode, which utilizes the high-gain antenna. If the high-gain antenna has been commanded for transmission, it will also be selected for reception. It may also be selected for reception by direct command.

The description and operating sequence of this mode is similar to the low-gain reception mode except the high-gain receiver feeds directly into the receiver selector, as shown in Figure B-2.

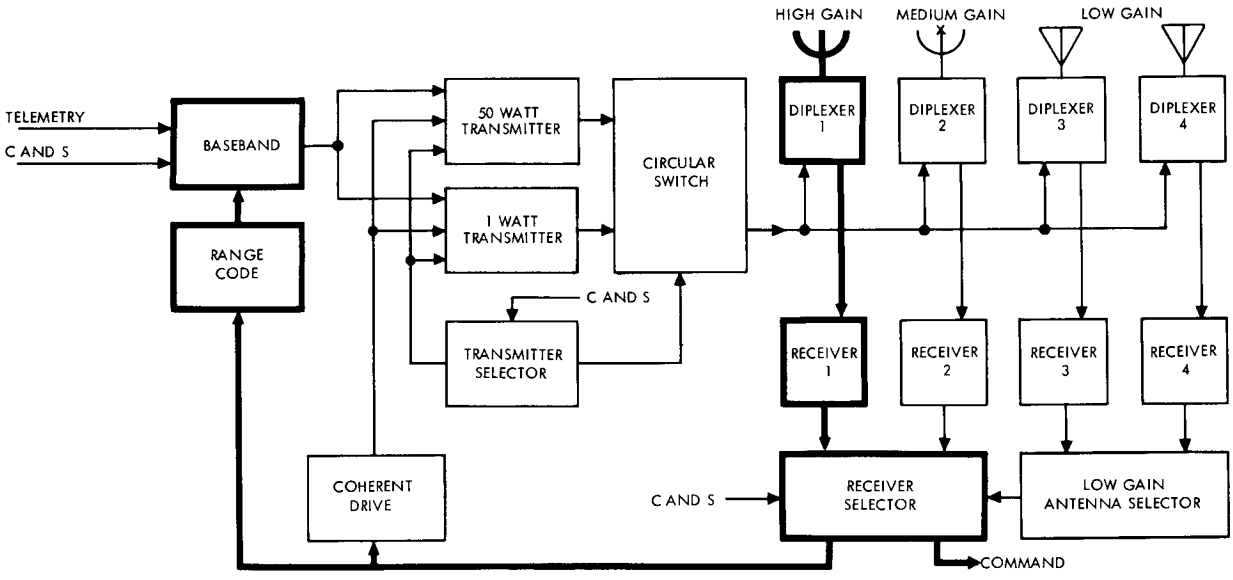

Figure B-2. High-Gain Reception Mode Block Diagram

2.3 Medium-Gain Reception Mode

For operations requiring reception of ground signals by the medium-gain antenna, the medium-gain reception mode may be selected in a manner similar to the high-gain reception mode of 2.2.

3. S-BAND RADIO DOWNLINK

The downlink radio functions in the following operating modes: low-power and high-gain transmission. low-power and medium gain transmission, low-power and low-gain transmission, high-power and high-gain transmission, high-power and medium-gain transmission, and high-power and low-gain transmission.

3.1 Low-Power and High-Gain Transmission Mode

The transmission mode sequence is initiated by the command for low-power and high-gain transmission mode selection. The appropriate exciter power supplies and amplifier power supplies are turned on and the low-power transmitter is selected. After an appropriate warmup period is completed, the high-gain antenna is selected which automatically switches transmission to the desired antenna and transmitter combination. In addition, an option for range code and coherence may be selected. Prerequisites for selecting transmission modes are the completion of antenna positioning, and selection of telemetry data rate and data mode. Low-power and high-gain transmission is utilized during interplanetary cruise when the geometry of the spacecraft-earth allows for high-gain antenna communication with earth and the data requirements are modest.

The associated block diagram is shown in Figure B-3 and the mode sequence is given in Table B-5.

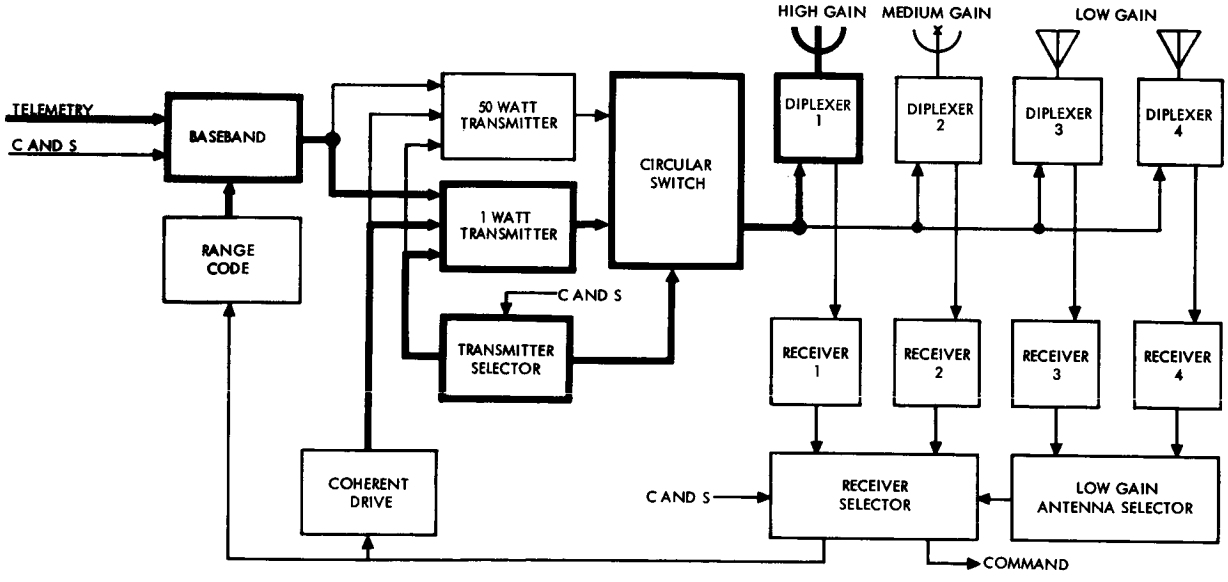

Figure B-3. Low-Power and High-Gain Transmission Mode Block Diagram

Table B-5. Low-Power and High-Gain Transmission Sequence

Item	Event	Control Source	Active Subsystem	Comment
	Prerequisites • Transmitter and amplifier power supply on • Antennas positioned			
1	Enable transmission mode selection	MOS		
2	Select transmission option for low-power and high-gain	C and S	Radio	
3	Select transmitter (low-power)	Radio	Radio	
4	Switch transmitter on	C and S	C and S	
5	Start warmup timer	C and S	C and S	
6	Switch amplifier exciter on	C and S	Radio	
7	Complete warmup		C and S	
8	Select antenna option		Radio	Will normally be in coherent operation if receiver is locked on
9	Switch to desired antenna (high-gain)		Radio	
10	Begin transmission		Radio	
11	Turn off previous transmitter		Radio	

3.2 Low-Power and Medium-Gain Transmission Mode

Near earth, when transmission power requirements are low and the spacecraft is being oriented, it may be possible to utilize the medium-gain antenna for transmission while the high-gain antenna is pointing away from earth (Figure B-4). This mode operation is similar to Mode 3.1 except for the selection of the medium-gain option with the low-power transmitter. This causes the transmitter selector to switch the antenna control to medium-gain.

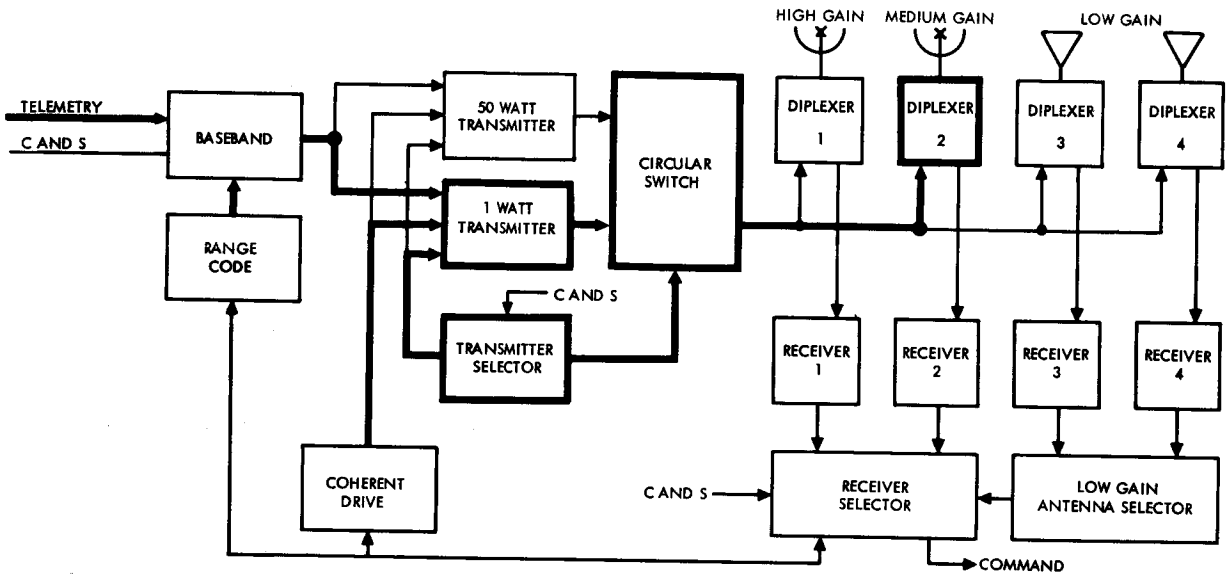

Figure B-4. Low-Power and Medium-Gain Transmission Mode Block Diagram

3.3 Low-Power and Low-Gain Transmission Mode

The low-power and low-gain transmission mode is used for initial acquisition of the spacecraft, or when neither of the directional antennas is pointing to earth, or if both are eclipsed by elements of the spacecraft. This mode of operation is similar to Mode 3.1 except for the selection of the low-gain antennas (Figure B-5).

3.4 High-Power and High-Gain Transmission Mode

This mode is similar to Mode 3.1 except the high power option is selected. The high-power and high-gain transmission mode is utilized when the spacecraft orientation and the volume of data being transmitted

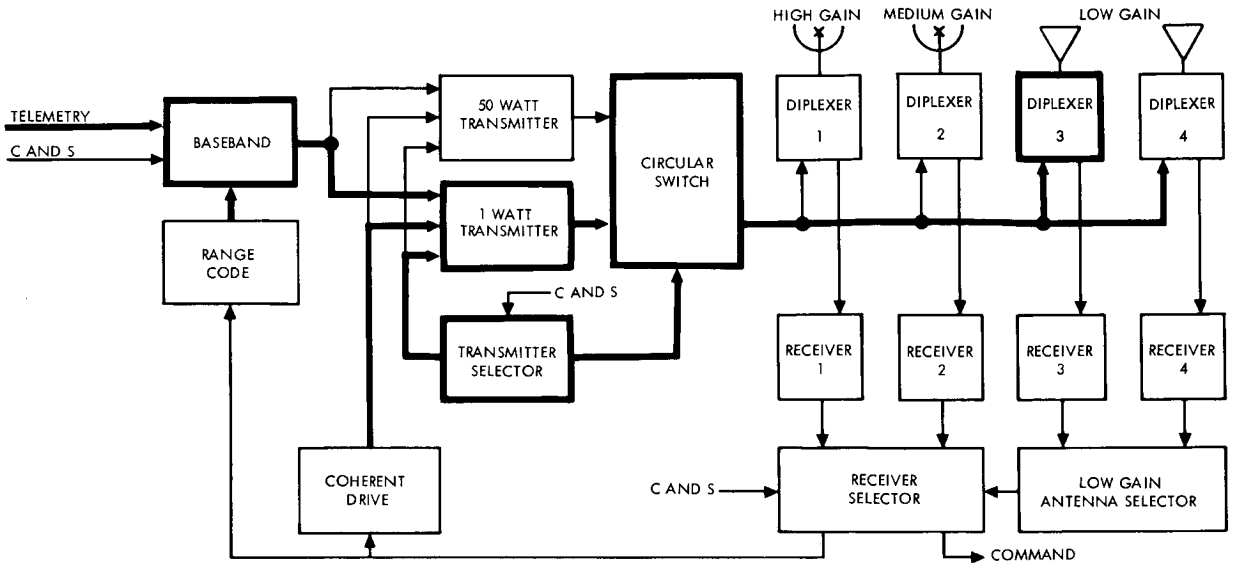

Figure B-5. Low-Power and Low-Gain Transmission Mode Block Diagram

require this mode. This mode allows for high data rates transmission and verification of spacecraft orientation. This mode operates similar to Mode 3.1 except selection of this mode causes the high power transmitter to be turned on a block diagram of the high-power and high-gain transmission mode is shown in Figure B-6.

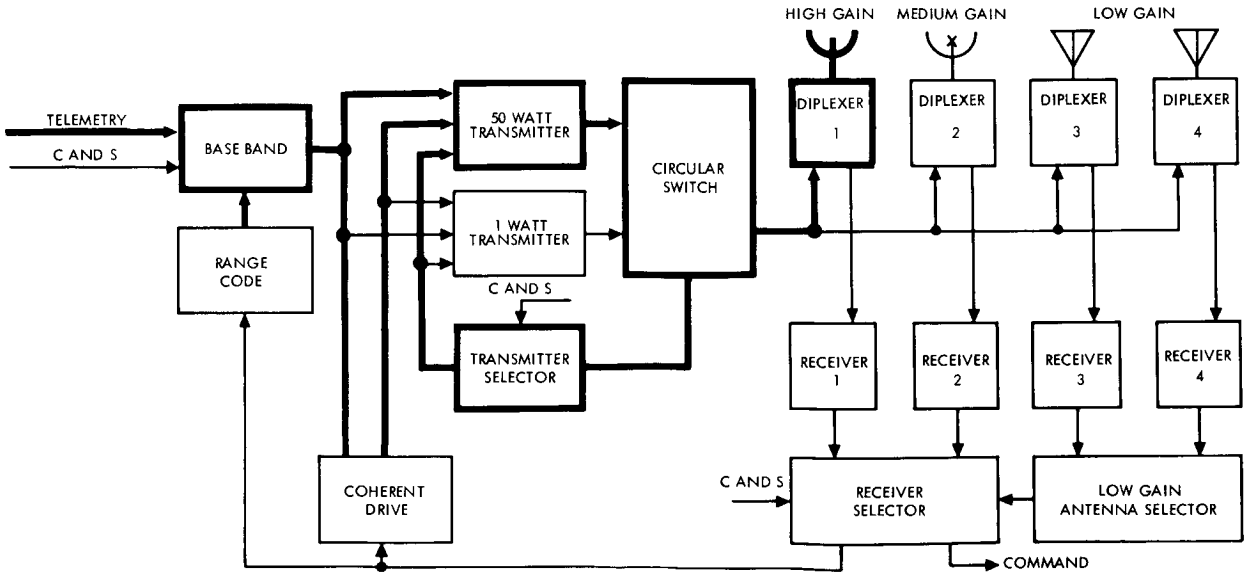

Figure B-6. High-Power and High-Gain Transmission Mode Block Diagram

3.5 High-Power and Medium-Gain Transmission Mode

This mode is similar to Mode 3.4 except the medium-gain antenna option is selected.

3.6 High-Power and Low-Gain Transmission Mode

This mode is utilized for normal operation when data rates are not excessive but the distance to earth requires high power. The mode operation is similar to Mode 3.4 except for the selection of the low-gain antenna option.

4. ANTENNA POINTING

The antenna pointing function involves the following operating modes (Figure B-7): automatic positioning, position high-gain antenna, and position medium-gain antenna.

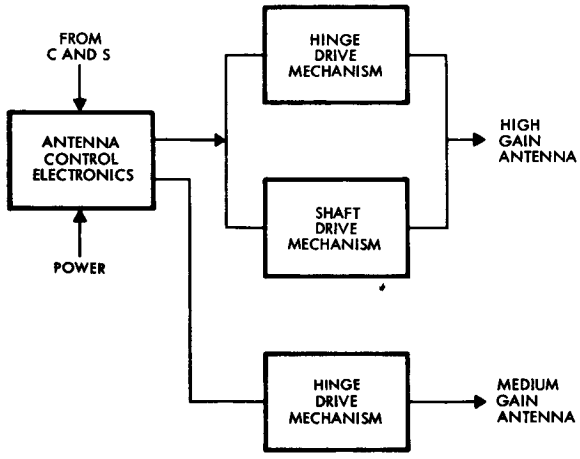

Figure B-7. Antenna Automatic Repositioning Mode Block Diagram

4.1 Antenna Automatic Positioning Mode

The high- and medium-gain antennas are automatically repositioned to point to earth. The pointing commands are provided by a function generator in the C and S to actuate the antenna gimbal driver.

4.2 High-Gain Antenna Command Reposition Mode

The high-gain antenna will be positioned upon command. The antenna drive power will be turned on and the antenna will start rotating

about the hinge axis until proper hinge orientation has been accomplished, the antenna will then begin to rotate about the shaft until the proper position has been achieved and the drive power turned off.

4.3 Medium-Gain Antenna Command Reposition Mode

The medium-gain antenna will be positioned upon command. The antenna drive power will be turned on and the antenna will begin rotating about the hinge axis until the desired orientation with respect to the spacecraft body attitude has been achieved.

5. ON-BOARD DATA HANDLING

The data handling functions correspond to the following operating modes: spacecraft real-time engineering data transmission, command and sequencer memory data readout, real-time capsule descent data transmission, real-time science data transmission, data storage, and spacecraft stored data playback.

5.1 Spacecraft Real-Time Engineering Data Mode

Spacecraft real-time engineering data (including hard wire capsule data) is continuously transmitted to the ground at 512 bits/sec by means of the S-band radio subcarrier, which is devoted exclusively to this function. The data is normally biorthogonal coded, but this coding may be switched out by command from the ground. The block diagram for this mode is given in Figure B-8. The mode sequence is given in Table B-6.

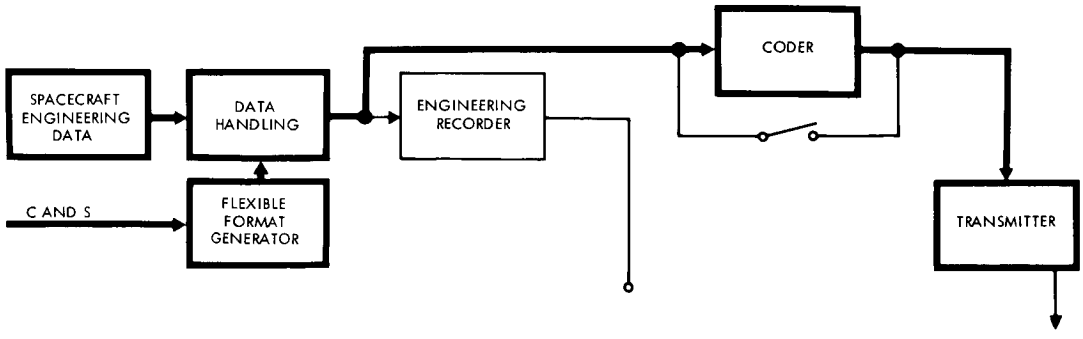

Figure B-8. Spacecraft Real-Time Engineering Data Mode Block Diagram

Table B-6. Spacecraft Real-Time Engineering Data Sequence

Item	Event	Control Source	Active Subsystem	Comment
	Prerequisites			
	• Turn on appropriate instruments and sensors			
	• Switch biorthogonal coder		Telemetry	Normally included
	• Position antennas, as required		Radio	
	• Select transmission mode		Radio	
1	Select data handling mode, spacecraft real-time engineering data	C and S	Data	
2	Begin transmission of data		Data	This mode is always in operation

5.2 Computer and Sequencer Memory Readout Mode

The computer and sequencer memory readout may be accomplished by selecting this mode. The memory data is transmitted over the main carrier simultaneously with the real-time engineering and low-rate science data which is transmitted over the subcarrier. After the data readout is complete, the data is verified by the MOS. The mode block diagram is given in Figure B-9 and the mode sequence in Table B-7.

5.3 Real-Time Capsule Data Mode

By selecting the real-time capsule data, the telemetry mode is switched to provide the output of the capsule (low rate) radio link to the spacecraft high-data-rate channel for modulation of the S-band radio main carrier. Real-time spacecraft engineering data will continue to be transmitted utilizing the subcarrier. The mode block diagram is given in Figure B-10 and the mode sequence in Table B-8.

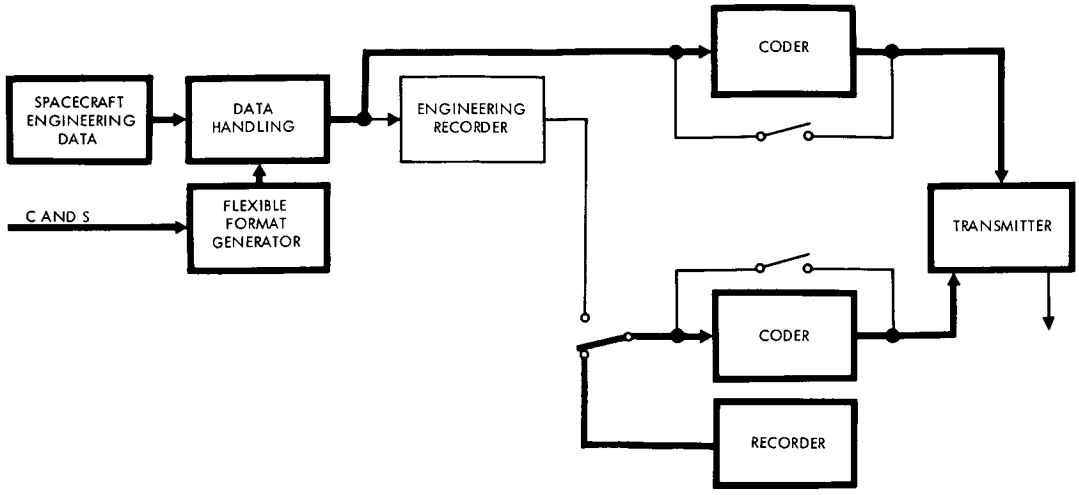

Figure B-9. Computer and Sequencer Memory Readout Mode Block Diagram

Table B-7. Computer and Sequencer Memory Readout Sequence

Item	Event	Control Source	Active Subsystem	Comment
	Prerequisites			
	• Turn on appropriate instruments and sensors			
	• Switch biorthogonal coder		Telemetry	Normally included
	• Position antennas, as required		Radio	
	• Select transmission mode		Radio	
1	Select data handling mode, computer and sequencer memory dump and verification	C and S	Data	
2	Switch C and S memory readout	C and S	Data	

Table B-7. Computer and Sequencer Memory Readout Sequence

Item	Event	Control Source	Active Subsystem	Comment
3	Begin transmission of data		Data	
4	Complete transmission of data	DATS	C and S	
5	Verify C and S memory data	MOS		
6	Select next data mode	C and S	DATS	

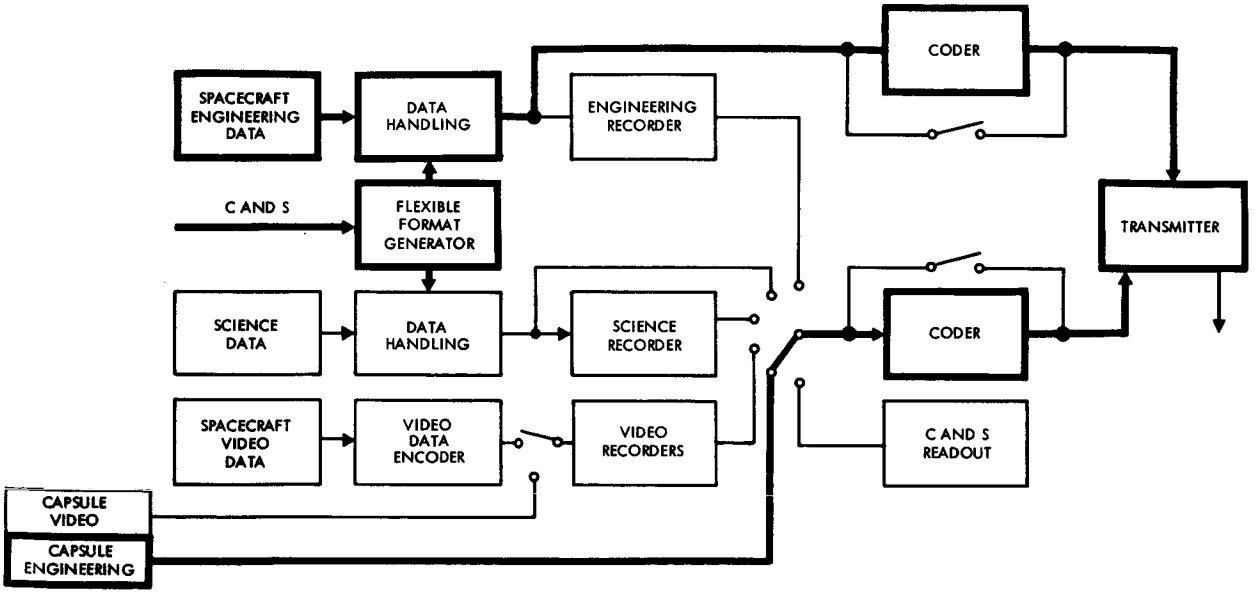

Figure B-10. Real-Time Capsule Engineering Data Mode Block Diagram

Table B-8. Real-Time Capsule Engineering Data Sequence

Item	Event	Control Source	Active Subsystem	Comment
	Prerequisites			
	• Separation of capsule			
	• Turn on appropriate instruments and sensors			
	• Switch biorthogonal coder		Telemetry	Normally included
	• Position antennas, as required		Radio	
	• Select transmission mode		Radio	
1	Select data handling mode, real-time capsule data	C and S	Data	
2	Switch to capsule engineering data	Data	Data	
3	Begin transmission of data	Data	Radio	
4	Complete transmission of data	Data	Radio	

5.4 Real-Time Science Data Mode

Real-time science data is transmitted in a manner similar to Mode 5.3 except the data mode selection is set at medium-rate science output. The mode block diagram is given in Figure B-11 and the mode sequence in Table B-9.

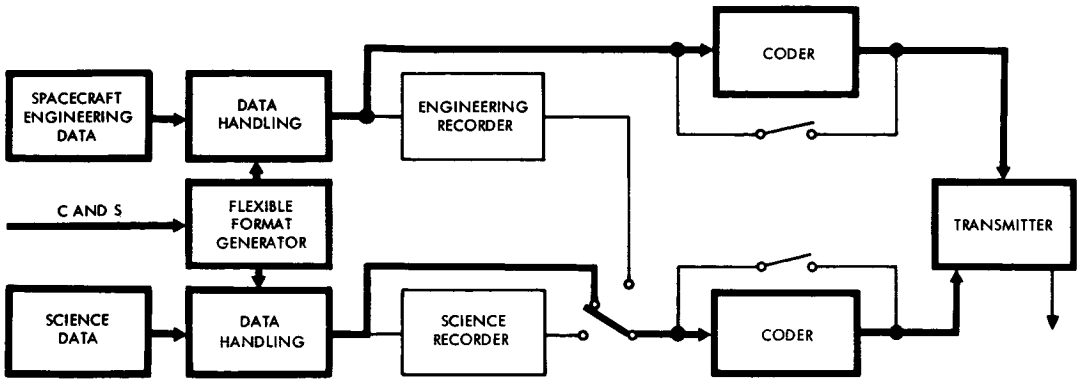

Figure B-11. Real-Time Science Data Mode Block Diagram

Table B-9. Real-Time Science Data Sequence

Item	Event	Control Source	Active Subsystem	Comment
	Prerequisites			
	• Turn on appropriate instruments and sensors			
	• Switch biorthogonal coder		Telemetry	Normally included
	• Position antennas, as required		Radio	
	• Select transmission mode		Radio	
1	Select data handling mode, real-time medium-rate science data	C and S	C and S	
2	Switch to medium-rate science data	C and S	Data	
3	Begin transmission of data	Data	Radio	
4	Complete transmission of data	Data	Radio	

5.5 Data Storage Mode

In addition to the transmission of spacecraft engineering data in real-time, additional data may be stored on one or more tape recorders for later transmission. The instruments, sensors, or TV having been turned on, the appropriate tape recorder is switched to record and turned on. Any or all of the recorders can record data simultaneously, while one of the data modes is operating to provide data transmission. The mode block diagram is given in Figure B-12 and the mode sequence in Table B-10.

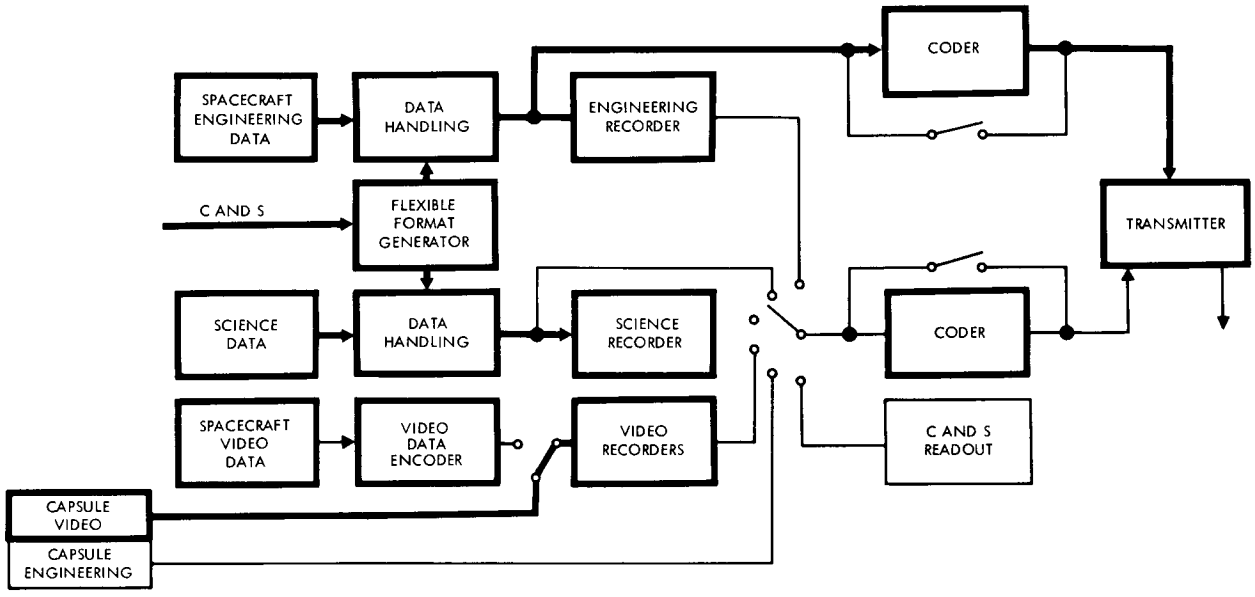

Figure B-12. Data Storage Mode Block Diagram

5.6 Stored Data Readout Mode

Stored data may be transmitted simultaneously with the real-time engineering data after selecting the stored data readout option, i.e., engineering, science or video option. The selected recorder output is switched in to the high data rate channel for transmission, the recorder is switched to playback and turned on. When the playback is completed, the recorder is turned off and the data select switch repositioned for the next data storage operation. The mode block diagram is given in Figure B-13 and the mode sequence is given in Table B-11.

Table B-10. Data Storage Sequence

Item	Event	Control Source	Active Subsystem	Comment
	Prerequisites • Data input available			
1	Select data handling mode, data storage	C and S	Data	
2	Select tape recorders (for record) Engineering Science Spacecraft television (4)	C and S	Data	Any combinations of recorders may be selected
3	Switch tape recorders to record	C and S	Data	
4	Switch tape recorder off	Data input	Data	

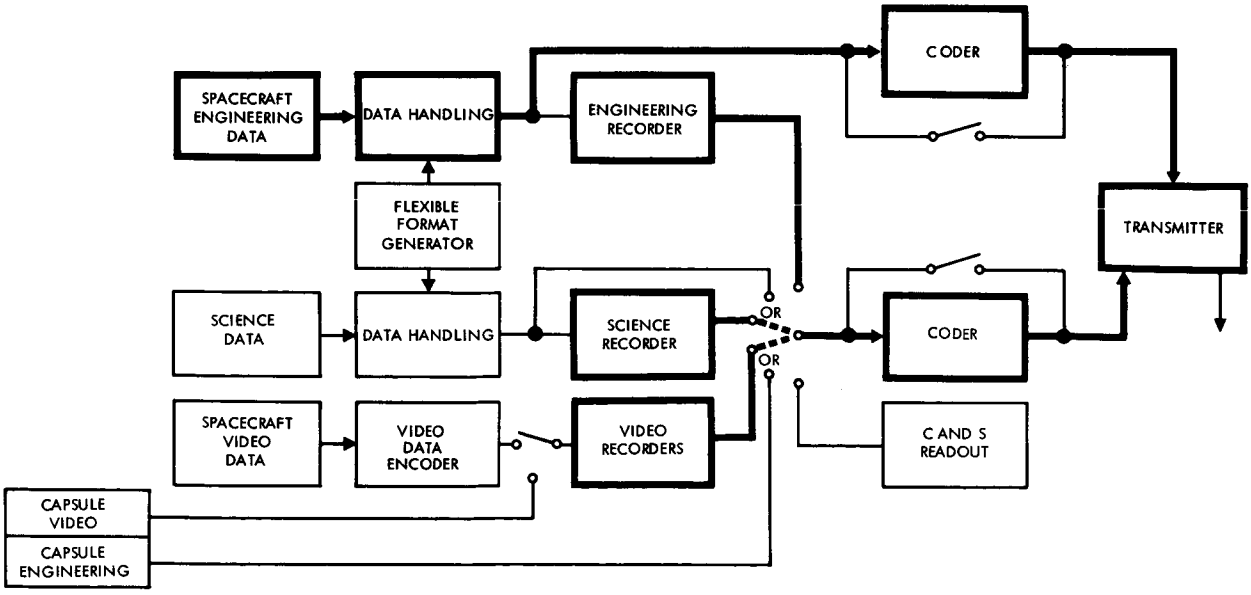

Figure B-13. Stored Data Readout Mode Block Diagram

Table B-11. Stored Data Readout

Item	Event	Control Source	Active Subsystem	Comment
	Prerequisites			
	• Turn on appropriate instruments and sensors			
	• Position antennas, as required		Radio	
	• Select transmission mode		Radio	
1	Select data handling mode, data storage readout	C and S	C and S	
2	Switch tape recorder Engineering Science Video	C and S	Data	Only one recorder selected for playback at a time
3	Switch tape recorder to playback	C and S	Data	
4	Turn on tape recorder power	C and S	Data	
5	Start recorder	C and S	Data	
6	Begin transmission of data	Data	Radio	
7	Complete transmission of data	Data	Radio	
8	Turn off tape recorder power	C and S	Data	
9	Rewind tape recorder	C and S	Data	

6. DATA RATE CONTROL

The telemetry high-data-rate channel functions in the various possible data rates under control of the computer and sequencer or by direct ground command. The following modes are used:

6.1	(51.2 kbits/sec data rate)
6.2	(25.6 kbits/sec data rate)
6.3	(12.8 kbits/sec data rate)
6.4	(6.4 kbits/sec data rate)
6.5	(3.2 kbits/sec data rate, emergency)

7. GUIDANCE AND CONTROL

The attitude control section of the guidance and control subsystem functions in the following modes: boost, rate nulling, limit cycle, sun acquisition, Canopus acquisition, cruise flight, maneuver preparations, attitude maneuver, engine operation, maneuver completion, Canopus sensor update, and inertial attitude mode.

7.1 Boost Mode

The boost mode is activated during prelaunch operations and continues through planetary vehicle separation. After the guidance and control subsystem has been turned on and the boost mode selected, the gyros are electrically caged until active control of the spacecraft is initiated by the guidance and control at planetary vehicle separation from the shroud. The mode block diagram is given by Figure B-14 and the mode sequence by Table B-12.

7.2 Rate Nulling Mode

The rate nulling mode is initiated at planetary vehicle separation. The reaction control system is activated and set at the 3-pound thrust level. The spacecraft begins nulling attitude rates until the rates are reduced to 0.01 deg/sec. The mode block diagram is given in Figure B-15 and the mode sequence in Table B-13.

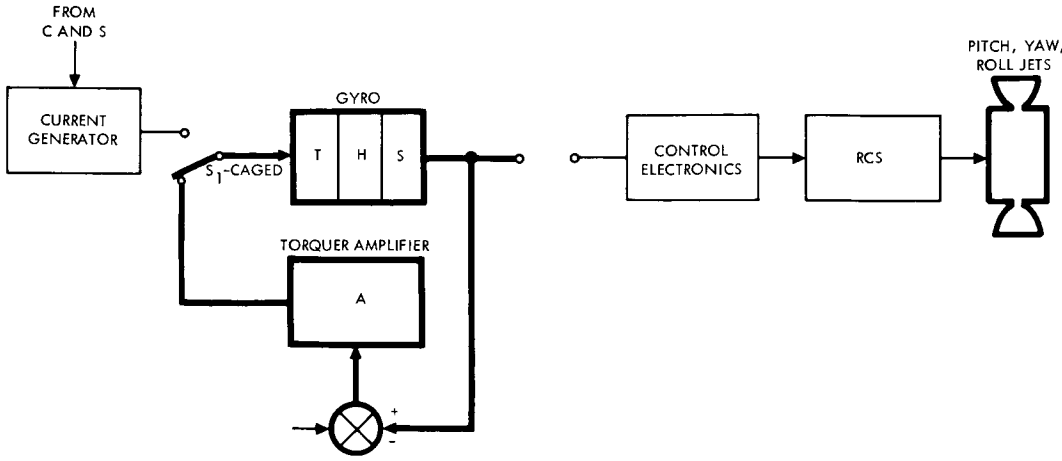

Figure B-14. Boost Mode Block Diagram

Table B-12. Boost Mode Sequence

Item	Event	Control Source	Active Subsystem	Comment
	Prerequisites • G and C turned on and checked out • Countdown initiated			
1	Gyro power on	C and S	G and C	
2	Enable boost mode	C and S	G and C	After warmup period
3	Switch gyros to caged	C and S	G and C	
4	Begin measuring attitude rates		G and C	
5	Liftoff		SI-C	
6	Planetary vehicle separation signal	IU	Mechanical	
7	Enable rate nulling mode	C and S	G and C	

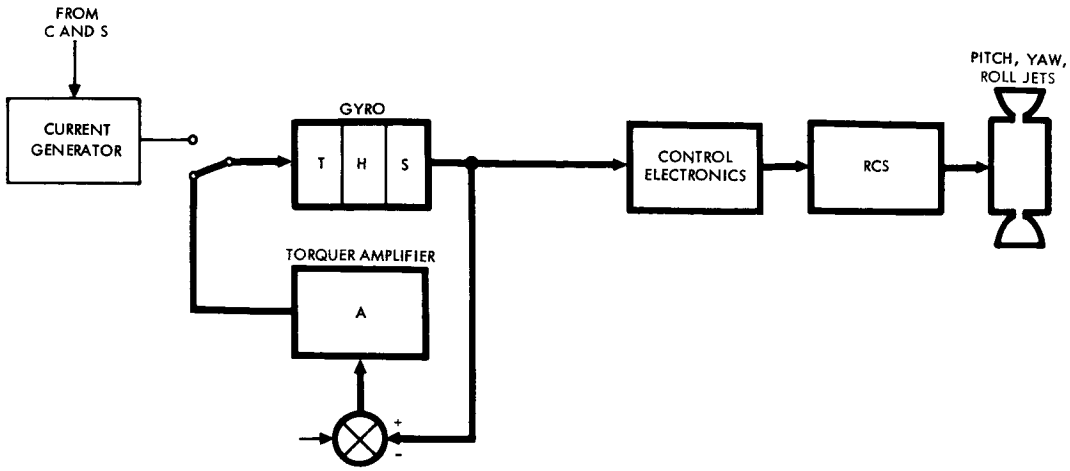

Figure B-16. Rate Nulling Mode Block Diagram

Table B-13. Rate Nulling Mode Sequence

Item	Event	Control Source	Active Subsystem	Comment
1	Set RCS to high thrust level (3 lb)	C and S	G and C	
2	Planetary vehicle separation signal	Mechanical	C and S	
3	Initiate separation timer	C and S	C and S	
4	Enable rate nulling mode	C and S	G and C	
5	Enable RCS solenoid valve	C and S	G and C	
6	Close control electronics switch	C and S	G and C	
7	Start rate-nulling		G and C	
8	Achieve rate-nulled condition		C and S	Rates reduced to 0.01 deg/sec
9	Timer initiated backup signal	C and S	C and S	

7.3 Limit Cycle Mode

The limit cycle operation is controlled by the switching amplifier in the control loop. The amplitude of the spacecraft limit cycle is governed by the deadband in the switching amplifier (±0.5 or ±0.25 degree according to control requirements). During the cruise flight (in earth-Mars or Mars orbit cruise) the amplitude of the limit cycle is ±0.5 degree which is required to meet the high-gain antenna pointing accuracy. For PSP imaging operation, a limit cycle rate of less than 10/deg hr is required in addition to ±0.25 degree limit cycle requirement. For capsule separation, the ±0.25 degree limit cycle is maintained to meet capsule attitude requirements.

7.4 Sun Acquisition Mode

When sun acquisition is enabled, the attitude control is switched to coarse sun sensor control with caged cyros and the spacecraft begins to pitch and yaw at controlled (0.2 deg/sec) until the sun is acquired in the field of view of the fine sun sensor. Control is then switched to the fine sun sensor and pitch and yaw rates are automatically reduced to limit cycle levels (less than 0.001 deg/sec). The spacecraft roll axis is aligned with the sun line within ±0.5 degree.

In the presence of a sun acquisition enable, the sun acquisition mode is automatically initiated at any time the alignment of the roll axis deviates from the sun, causing loss of the sun by the fine sun sensor. The mode block diagram is given in Figure B-16 and the mode sequence in Table B-14.

7.5 Canopus Acquisition Mode

The Canopus acquisition mode begins when Canopus acquisition enable is commanded after the sun acquisition gate has been activated. A bias roll rate (0.1 deg/sec) is initiated with the roll gyros caged to provide the spacecraft with roll damping. The roll rate continues until the star Canopus appears in the field of view of the Canopus sensor; roll attitude control is then switched to the Canopus sensor. When lock-on has occurred, the roll rate is nulled and roll control is switched to limit cycle operation for maintenance of the spacecraft orientation,

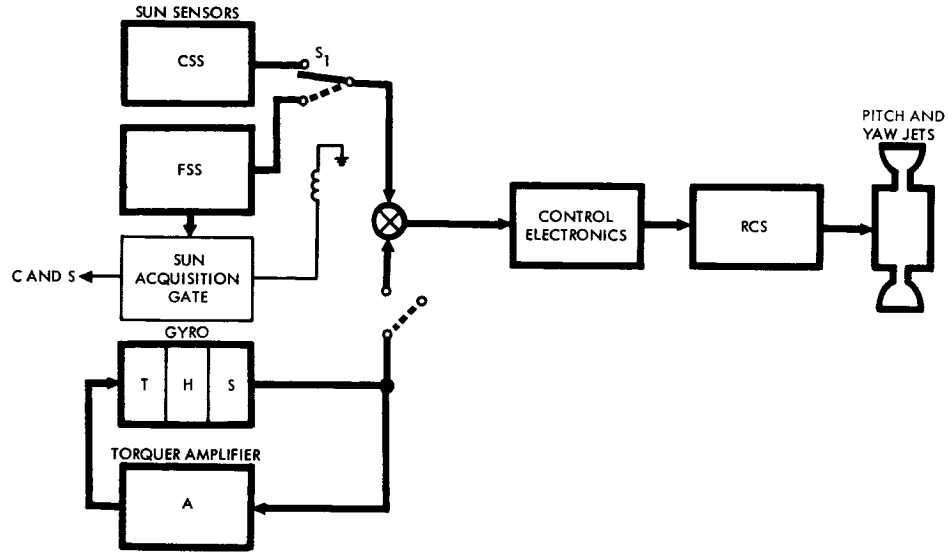

Figure B-16. Sun Acquisition Mode Block Diagram

Table B-14. Sun Acquisition Mode Sequence

Item	Event	Control Source	Active Subsystem	Comment
	Prerequisites			
	• Sun sensors on			Coarse and fine
1	Enable sun acquisition	C and S	G and C	
2	Gyros turned on and caged	C and S	G and C	Warmup required
3	Set RCS to high thrust level	C and S	G and C	
4	Switch control electronics to coarse limit cycle	C and S	G and C	±0.5 deg/sec
5	Switch control to coarse sun sensor	C and S	G and C	
6	Connect pitch and yaw gyros to control electronics	C and S	G and C	
7	Begin pitch and yaw at high rate		G and C	Both rates 0.2 deg/sec

Table B-14. Sun Acquisition Mode Sequence (Continued)

Item	Event	Control Source	Active Subsystem	Comment
8	Sun appears in field of view of fine sensor			±10 degrees of LOS
9	Switch control to fine sun sensor		G and C	Automatic
10	Rates reduced to limit cycle values		G and C	
11	Achieve roll axis alignment with sun		G and C	±0.5 degree of LOS
12	Signal sun acquisition	G and C	C and S	

i.e., hold Canopus sensor axis on the spacecraft-Canopus line (within 0.5 degree) and the Canopus acquisition gate closes. After verification of the spacecraft attitude from MOS, the gyros are disconnected and turned off, and the reaction control jet thrust level is switched to the low setting (0.2 pound). The mode block diagram is given by Figure B-17 and the mode sequence by Table B-15.

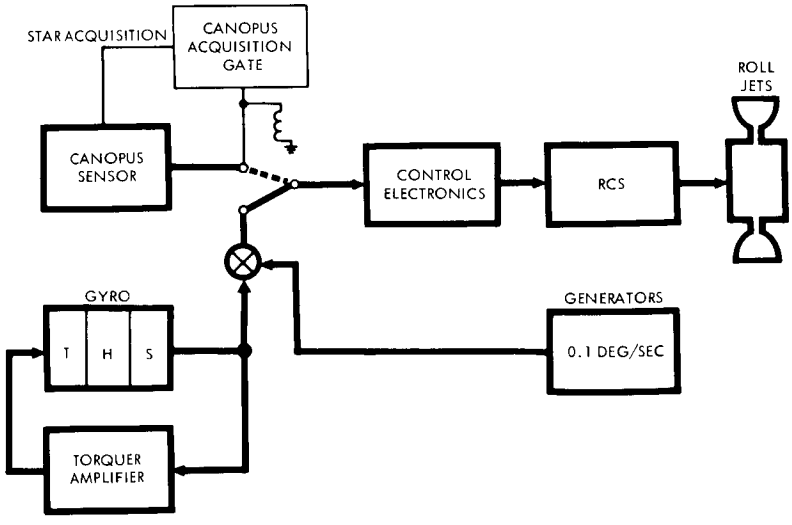

Figure B-17. Canopus Acquisition Mode Block Diagram

Table B-15. Canopus Acquisition Mode Sequence

Item	Event	Control Source	Active Subsystem	Comment
	Prerequisites			
	• Canopus sensor on			
	• Sun acquisition complete			
1	Enable Canopus acquisition	C and S	C and S	
2	Gyros turned on and caged	C and S	G and C	Warmup required if not previously on
3	Set RCS to high thrust level	C and S	G and C	
4	Switch control electronics to coarse limit cycle	C and S	G and C	
5	Switch roll bias generator to low rate	C and S	G and C	0.01 deg/sec
6	Switch roll bias rate on	C and S	G and C	
7	Canopus appears in field of view of sensors, and switch control to Canopus sensor		G and C	
8	Stop roll rate and converge to roll limit cycle		G and C	
9	Signal Canopus acquisition and switch gyros out	G and C	C and S	

7.6 Cruise Flight Mode

After completion of sun and Canopus acquisition, the roll axis and zero degree clock angle plane of the spacecraft are in the celestial reference system defined by the sun and Canopus lines of sight. Both sensor acquisition gates are closed, allowing the gyros to be turned off

to conserve electrical power. The reaction control jets are switched to the low thrust level (0.2 pound) by deactivating the high pressure regulator in the gas supply line. The G and C maintains the spacecraft attitude within a $\pm$0.5 degree limit cycle about the celestial reference axes during cruise flight mode. The mode block diagram is given in Figure B-18 and the mode sequence in Table B-16.

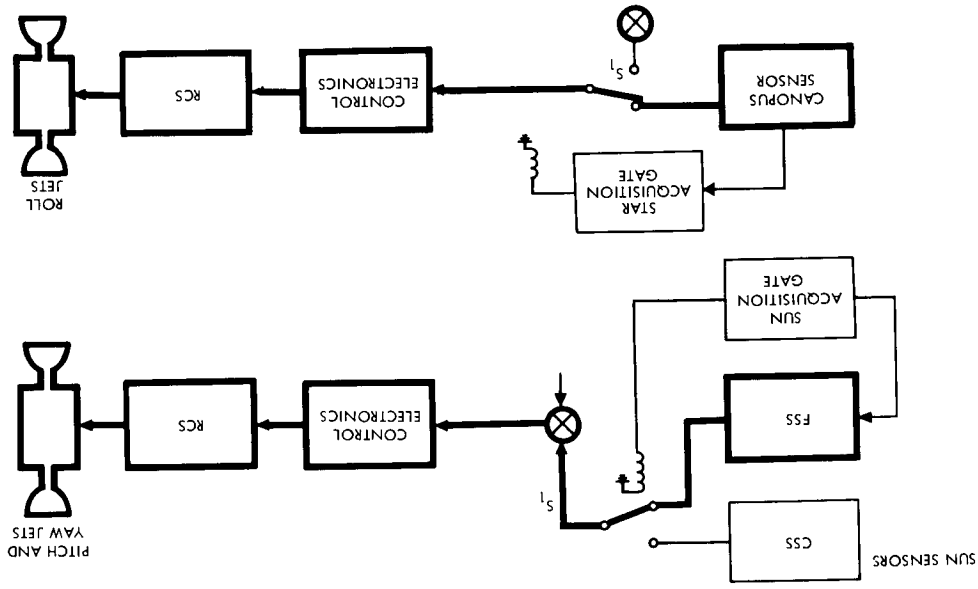

Figure B-18. Cruise Flight Mode Block Diagram

Table B-16. Cruise Flight Mode Sequence

Item	Event	Control Source	Active Subsystem	Comment
	Prerequisites • Sun acquisition complete • Canopus acquisition complete with gyros switched out			
1	Attitude reference verification	MOS		If required
2	Turn off gyro power	C and S	G and C	
3	Switch RCS to low thrust	C and S	G and C	0.2 pound

7.7 Maneuver Preparations Mode

Prior to any propulsive maneuver, the guidance and control system completes a set of premaneuver events. After the maneuver preparation has been initiated, the gyros are turned on and allowed to warm up, and the accelerometers and the TVC actuators are activated. After TVC power has been turned on, the gain is selected (high or low depending on thrust level of the maneuver), the TVC gimbal test is accomplished by actuating in pitch, then yaw, and returning the gimbal to center. Verification from the ground that the gyros, accelerometers, and TVC are ready, combined with a verification of antenna position, communication mode selection, and the C and S memory, allows the spacecraft to proceed to the attitude maneuver mode. The mode sequence is given in Table B-17.

7.8 Attitude Maneuver Mode

The attitude maneuver mode begins when the spacecraft attitude maneuver is enabled, inhibiting sun and star acquisition. The pitch, yaw and roll gyros are uncaged, and the reaction control thrust is regulated to the high setting (3 pounds). The control system is then switched to maneuver mode and commanded to rotate at 0.2 deg/sec in sequential yaw, pitch, and roll until the proper orientation has been established. The rates are nulled and the system converges to an inertial hold limit cycle operation. The communications are switched to the high-gain antenna and verification of spacecraft attitude by the MOS enables engine operation.

After engine operation has been enabled, the TVC and accelerometer are activated and pitch and yaw attitude control is switched to the TVC during the engine start signal. A backup timer is started at engine operation enable which automatically shuts down the engine in event of normal shutdown signal failure and returns control of pitch and yaw attitude to the RCS.

The mode block diagram is given in Figure B-19 and the mode sequence in Table B-18.

Table B-17. Maneuver Preparations Sequence

Item	Event	Control Source	Active Subsystem	Comment
1	Initiate maneuver preparations	C and S		Or by MOS command
2	Turn on gyro power	C and S	G and C	
3	Begin gyro warmup		G and C	
4	Turn on accelerometer power	C and S	G and C	
5	Turn on TVC actuator power	C and S	G and C	
6	Turn on TVC electronics	C and S	G and C	
7	Initiate gimbal test	C and S	G and C	
8	Actuate TVC (pitch)		G and C	
9	End TVC pitch		G and C	
10	Actuate TVC (yaw)		G and C	
11	End TVC yaw		G and C	
12	Return TVC to center		G and C	
13	Complete TVC centering		G and C	
14	Gyro warmup completed		G and C	
15	Initiate gyro test	C and S	G and C	
16	Complete gyro test	G and C	C and S	
17	Initiate accelerometer test	C and S	G and C	
18	Complete accelerometer test	G and C	C and S	
19	Verification of space-craft readiness	MOS		
20	Enable spacecraft attitude maneuver	MOS	C and S	

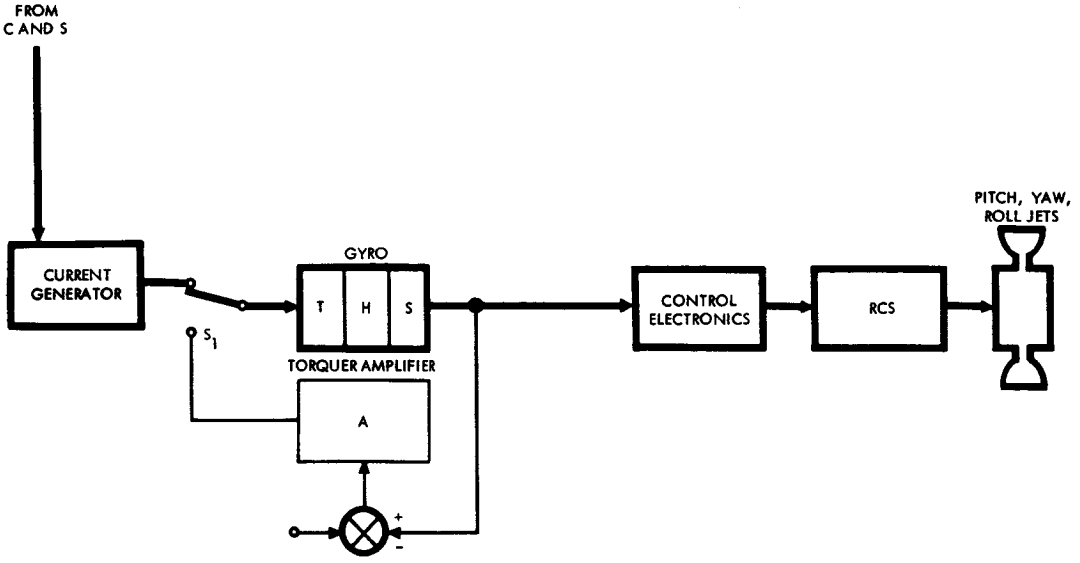

Figure B-19. Attitude Maneuver Mode Block Diagram

7.9 Guidance and Control Engine Operation Mode

During main engine operation, pitch and yaw control are switched from RCS to TVC and pitch, yaw, and roll gyros are uncaged. The control gains set during maneuver preparation allow for engine gimbal control under high or low engine thrust levels. The mode block diagram is given in Figure B-20 and the mode sequence in Table B-19.

7.10 Maneuver Completion Mode

The maneuver completion mode begins when an engine shutdown signal or engine shutdown backup signal is generated. The control system is switched to coarse limit cycle ($\pm$0.5 degree), and TVC and accelerometers are turned off. The comparator in the C and S which registers the angular position change commanded during the attitude maneuver mode commands a spacecraft maneuver equal in angular magnitude and of opposite polarity to the attitude maneuver to reacquire the sun-Canopus celestial attitude reference. The automatic sun-Canopus acquisition modes serve as a backup capability for celestial reference acquisition.

Table B-18. Attitude Maneuver Mode Sequence

Item	Event	Control Source	Active Subsystem	Comment
	Prerequisites			
	• Communication mode			
	• Gyros uncaged			
1	Initiate spacecraft attitude maneuver	C and S		
2	Switch control electronics to fine limit cycle	C and S	G and C	
3	Set RCS to high thrust level	C and S	G and C	3 pounds
4	Switch spacecraft control to gyros	C and S	G and C	
5	Inhibit sun sensor	C and S	G and C	
6	Inhibit Canopus sensor	C and S	G and C	
7	Start yaw at 0.2 deg/sec		G and C	
8	Stop yaw and converge to limit cycle		G and C	
9	Start pitch at 0.2 deg/sec		G and C	$\pm$0.25 degree, automatic
10	Stop pitch and converge to limit cycle		G and C	
11	Start roll at 0.2 deg/sec		G and C	
12	Stop roll and converge to limit cycle		G and C	
13	Verify maneuver complete	MOS		
14	Enable engine operation	MOS	C and S	

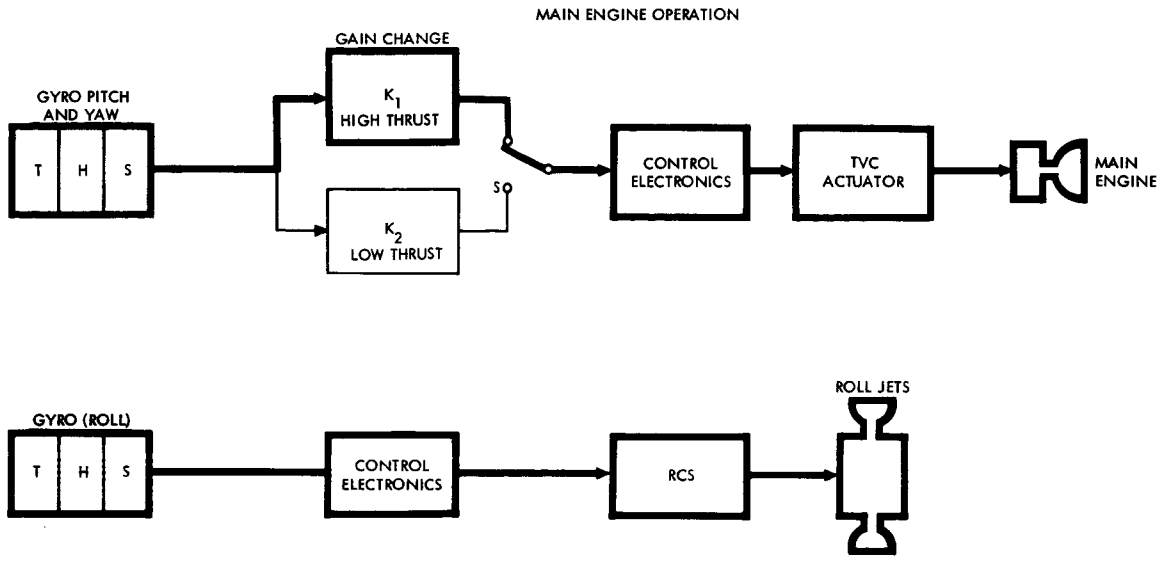

Figure B-20. Engine Operation Mode Block Diagram

Table B-19. Engine Operation Mode Sequence

Item	Event	Control Source	Active Subsystem	Comment
	Prerequisites			
	o Enable by MOS			
1	Initiate G and C engine operation	C and S	G and C	
2	Switch gyros to uncaged	C and S	G and C	All gyros
3	Switch pitch and yaw RCS off	C and S	G and C	
4	Engine start	C and S	Propulsion	
5	Engine shutdown	C and S	Propulsion	
6	Switch pitch and yaw RCS on	C and S	G and C	
7	Switch TVC off	C and S	G and C	
8	Initiate G and C maneuver completion mode	C and S	G and C	

7.11 Inertial Attitude Hold Mode

Inertial attitude hold is also required to hold the spacecraft on inertial references any time the celestial references are lost. Gyros are uncaged and switched to position hold. The spacecraft will maintain a limit cycle operation within ± 0.5 or ± 0.25 degree as was the case prior to loss of the celestial references. The celestial references are re-established whenever this is possible.

8. PYROTECHNIC CONTROL

The electrical distribution subsystem functions in the following operating modes: prelaunch, launch, planetary vehicle adapter-spacecraft separation, antenna deployment, propulsion system operation for maneuvers and orbit injection, tank venting, and experiment package deployment.

8.1 Prelaunch Mode

During prelaunch, the pyrotechnic control assembly is normally in the "safe" condition because the separation switches are held open by the planetary vehicle adapter. A command override for this interlock is provided to allow testing. Reset of the interlock is accomplished by applying a control signal through the system test connector from ground test equipment. This cannot be accomplished after launch.

The distribution control unit allows individual on/off control of each spacecraft primary power bus through the systems test connectors from ground test equipment. A single decoder command is available for use after launch to step all relays to the On position, in case some disturbance causes one or more to move to the Off position.

8.2 Launch Mode

As part of the countdown for launch, the external umbilical cable from the launch complex to the shroud is disconnected.

8.3 Pre-Arm Mode

As part of the preparation for separation, the ordnance-operated umbilical connector between each spacecraft and its planetary vehicle adapter is ejected following receipt of firing signals from the launch vehicle.

Separation between the spacecraft and planetary vehicle adapter occurs as a result of pyrotechnic action controlled by the launch vehicle. Separation is sensed by the planetary vehicle adapter-spacecraft interface microswitches which send a signal to the pyrotechnic control assembly and the computer and sequencer. In the pyrotechnic control unit, this signal is used to operate the master or "pre-arm" arming relay, causing it to make electrical power available to the arming and firing circuits. In case of failure to accomplish this function, a backup command is provided.

8.4 Arm Antenna Deployment Mode

For this operation, the pyrotechnic control unit receives signals from the computer sequence or decoder and, in response, delivers firing signals to appropriate pyrotechnic devices.

8.5 Arm Propulsion System Operation Mode

For propulsion operation, the pyrotechnic control unit and the distribution control unit receive command signals from the computer sequence or decoder and, in response, deliver firing signals to appropriate pyrotechnic devices. For the second midcourse maneuver, signals are received only from the distribution control unit.

8.6 Arm Tank Venting Mode

Following all propulsion firings, firing signals are obtained from the pyrotechnic control unit to accomplish venting of the propulsion subsystem tanks.

8.7 PSP Deployment Mode

For this operation, the pyrotechnic control unit receives command signals from the computer sequence or decoder, and in response, delivers firing signals to appropriate pyrotechnic devices.

9. PLANETARY VEHICLE SEPARATION

Separation of the two planetary vehicles involves the following operating modes: nose fairing jettison, planetary vehicle separation, and aft shroud jettison.

9.1 Forward Shroud Elements Mode

The shroud nose fairing and forward section is jettisoned in earth parking orbit. The signal to jettison the fairing is generated by the S-IVB stage. Firing the initiators on the circumferential splice ordnance opens the forward splice, and allows the spring mechanism to release. The springs cause the nose fairing section of the shroud to separate from the space vehicle at a predetermined relative velocity. The jettisoned element will increase in altitude and slow down so as not to interfere with the remaining vehicle.

9.2 Planetary Vehicle Separation Mode

The planetary vehicles are separated shortly after Mars transfer trajectory is achieved. The separation sequence is initiated by a separation signal resulting from either second S-IVB shutdown (for the forward planetary vehicle) or by confirmation of aft shroud elements jettison (for the aft planetary vehicle). Initiation of the separation sequence causes the S-IVB to be properly oriented and attitude-stabilized for the separation event. Once S-IVB attitude hold has been achieved, the planetary vehicle is separated by firing explosive holddown bolts between the planetary vehicle and the planetary vehicle adapter; once released, the spring separation mechanism imparts a prescribed velocity difference to the planetary vehicle to separate it from its adapter.

9.3 Mid-Section Elements Jettison Mode

Aft elements of the shroud, forward of the second (aft) planetary vehicle, are jettisoned in Mars transfer trajectory after the first planetary vehicle has been separated. The S-IVB is attitude-stabilized and the aft shroud jettison signal fires the initiators which open the aft circumferential splice, allowing the spring mechanism to separate the shroud elements in a manner similar to Mode 9.1.

10. CONFIGURATION

Changes in configuration will occur by means of the following operating modes: establish cruise configuration and orbital operation.

10.1 Establish Cruise Configuration Mode

After separation of the planetary vehicle from the shroud, the cruise configuration is established by deploying stowed antennas and booms, and extending the planetary scan platform to its intermediate position. All of the appendages and articulated elements are released and deployed as soon as possible after the planetary vehicle becomes stabilized to enhance the probability of mission success.

10.2 Orbital Operation Mode

After capsule-spacecraft separation during the Mars orbital operation, the planetary scan platform is rotated to its fully deployed position. It remains in this configuration for the remainder of the mission.

11. THERMAL CONTROL

The temperature control subsystem functions in the following operating modes: normal operation, activation of high-gain antenna shaft drive heater, activation of high-gain antenna hinge drive heater, activation of high-gain antenna shaft drive heater, and activation of medium-gain antenna hinge drive heater.

11.1 Normal Operation Mode

During the mission and subsequent to separation from the shroud, the temperature control subsystem provides automatic control of the thermal environment by use of bimetallic louvers and thermostatically controlled heaters.

11.2 Activation of High-Gain Antenna Shaft Drive Heater Mode

Upon ground command, the high-gain antenna shaft drive heater is actuated for a prescribed period of time and turned off. The remainder of the temperature control system functions automatically.

11.3 Activation of High Gain Antenna Hinge Drive Heaters Mode

Upon ground command, the high-gain antenna hinge drive heater is activated for a prescribed period of time and turned off. The remainder of the temperature control system functions automatically. Sequential operation is the same as Mode 11.2.

11.4 Actuation of Medium-Gain Antenna Hinge Drive Heater Mode

Upon ground command, the medium-gain antenna hinge drive heater is actuated for a prescribed period of time and turned off. The remainder of the temperature control system functions automatically. Sequential operation is the same as Mode 11.2.

11.5 Actuation of Gimbal Platform Drive Heater Mode

Upon ground command, the planetary science package gimbal platform drive is actuated for a prescribed period of time and turned off. The remainder of the temperature control system functions automatically. Sequential operation is the same as Mode 11.2.

12. PROPULSION

The propulsion system operates in the following modes: low thrust, active pressurization; low thrust; ullage blowdown; high thrust; and propellant tank venting.

12.1 Low Thrust, Active Pressurization Mode

This firing mode is used only for the arrival date separation firing. All subsequent midcourse corrections, if required, and the orbit trim maneuvers are conducted using low thrust, ullage blowdown operation (Mode 12.2). The pressurization system is activated, pressurizing the propellant tanks, by firing open the normally-closed electro-explosive pressurant, fuel tank, and oxidizer tank isolation valves. With the propellant tanks pressurized, engine firing is accomplished by opening the start tank (with the pintle commanded to the low thrust position), then the engine quad bipropellant solenoid valves. After four seconds of engine operation to allow propellant settling in the main tanks, the main prevalves are opened and the start tank valves closed, so as to retain propellant for subsequent starts. The mode sequence is given in Table B-20.

12.2 Low Thrust, Ullage Blowdown Mode

This firing mode is used for all firings except the arrival date separation and orbit insertion firings. The engine operation sequence is the same as for Mode 12.1; however, the pressurization system is not

Table B-20. Low Thrust, Active Pressurization Sequence

Item	Event	Control Source	Active Subsystem	Comment
	Prerequisites			
	• Accelerometers on			
	• TVC on			
	• MOS verification and enable			
	• Pyrotechnic valves armed			
	• Attitude maneuver completed			
	• Communications mode selected			
	• Data and telemetry mode selected			
1	Enable engine low thrust mode	MOS	C and S	
2	Open first leg pressurization NC isolation valves	C and S	Pyrotechnic	3 valves
3	Tank pressure rise to 235 psia		Propulsion	
4	Pintle actuator to low thrust position		Propulsion	
5	Open start tank quad bipropellant solenoid valve	C and S	Propulsion	
6	Open engine low thrust quad bipropellant solenoid valve	C and S	Propulsion	
7	Engine starts		Propulsion	
8	Start integrating accelerometer		C and S	

Table B-20. Low Thrust, Active Pressurization Sequence (Continued)

Item	Event	Control Source	Active Subsystem	Comment
9	Start engine operation timer	C and S	C and S	
10	Switch pitch-yaw attitude control to TVC	C and S	G and C	
11	Open main propellant tank prevalves	C and S	Propulsion	
12	Close start tank quad bipropellant solenoid valves	Propul-sion	Propulsion	Signaled by pre-valve open limit switch
13	Timer commands start tank valves closed	C and S	Propulsion	Backup signal
14	Sense required level of integrated acceleration		C and S	
15	Close low thrust sole-noid valve	C and S	Propulsion	
16	Timer commands low thrust solenoid closed	C and S	Propulsion	Backup signal
17	Engine shutdown		Propulsion	
18	Switch attitude control to RCS	C and S	G and C	
19	Close main propellant tank prevalves	C and S	Propulsion	
20	Close first leg pressuri-zation NO isolation valves	C and S	Pyrotechnic	3 valves

activated prior to engine operation and the propellant expulsion is accomplished by allowing the ullage gas already in the propellant tanks to expand. The mode sequence is shown in Table B-21.

Table B-21. Low Thrust, Ullage Blowdown Sequence

Item	Event	Control Source	Active Subsystem	Comment
	Prerequisites • Accelerometers on • TVC on • MOS verification and enable • Pyrotechnic valves armed • Attitude maneuver completed • Communications mode selected • Data and telemetry mode selected			
1	Enable engine low thrust mode	MOS	C and S	
2	Pintle actuator to low thrust position		Propulsion	
3	Open start tank quad solenoid valve	C and S	Propulsion	
4	Open engine low thrust quad bipropellant solenoid valve	C and S	Propulsion	
5	Engine starts		Propulsion	
6	Start integrating accelerometer	C and S	C and S	
7	Start engine operation timer	C and S	C and S	
8	Switch pitch-yaw attitude control to TVC	C and S	G and C	

Table B-21. Low Thrust, Ullage Blowdown Sequence (Continued)

Item	Event	Control Source	Active Subsystem	Comment
9	Open main propellant tank prevalves	C and S	Propulsion	
10	Close start tank quad solenoid valves	Propulsion	Propulsion	Signaled by prevalve open limit switch
11	Timer commands start tank valves closed	C and S	Propulsion	Backup signal
12	Sense required level of integrated acceleration		C and S	
13	Close low thrust solenoid valve	C and S	Propulsion	
14	Timer commands low thrust solenoid closed	C and S	Propulsion	Backup signal
15	Engine shutdown		Propulsion	
16	Switch attitude control to RCS.	C and S	G and C	
17	Close main propellant tank prevalves	C and S	Propulsion	

12.3 High Thrust Mode

The high thrust firing mode is used only for the orbit insertion firing. The operation is essentially the same as Mode 12.1, except that after the engine has started, the main shutoff ball valves are open, the quad bipropellant solenoid valves are closed, and the pintle commanded to the high thrust position. The mode squence is shown in Table B-22.

12.4 Propellant Tank Venting Mode

After all propulsion system operations are completed, the system is vented and residual propellants depleted. The tanks remain vented open during the orbit operations. Venting is accomplished by opening

Table B-22. High Thrust Sequence

Item	Event	Control Source	Active Subsystem	Comment
	Prerequisites • Accelerometers on • TVC on • MOS verification and enable • Pyrotechnic valves armed • Attitude maneuver completed • Communications mode selected • Data and telemetry mode selected			
1	Enable engine low thrust mode	MOS	C and S	
2	Open first leg pressurization NC isolation valves	C and S	Pyrotechnic	3 valves
3	Tank pressure rise to 235 psia		Propulsion	
4	Pintle actuator to low thrust position		Propulsion	
5	Open start tank quad bipropellant solenoid valve	C and S	Propulsion	
6	Open engine low thrust quad bipropellant solenoid valve	C and S	Propulsion	
7	Engine starts		Propulsion	
8	Start integrating accelerometer		C and S	

Table B-22. High Thrust Sequence (Continued)

Item	Event	Control Source	Active Subsystem	Comment
9	Start engine operation timer	C and S	C and S	
10	Switch pitch-yaw attitude control to TVC	C and S	G and C	
11	Open main propellant tank prevalves	C and S	Propulsion	
12	Close start tank quad bipropellant solenoid valves	Propulsion	Propulsion	Signaled by prevalve open limit switch
13	Timer commands start tank valves closed	C and S	Propulsion	Backup signal
14	Command main ball valves open	C and S	Propulsion	
15	Shuttle pintle to high thrust position		Propulsion	
16	Close low thrust solenoid valves	C and S	Propulsion	
17	Sense required level of integrated acceleration	C and S	Propulsion	
18	Close low thrust solenoid valve	C and S	Propulsion	
19	Timer commands low thrust solenoid closed	C and S	Propulsion	Backup signal
20	Engine shutdown	Propulsion	C and S	
21	Switch attitude control to RCS	C and S	G and C	
22	Close main propellant tank prevalves	C and S	Propulsion	
23	Close first leg pressurization NO isolation valves	C and S	Pyrotechnic	

the normally closed explosive vent valves. The pressure in the oxidizer tank is vented first, and after a suitable delay the fuel and pressurant tanks are vented. The mode sequence is given in Table B-23.

13. PSP CONTROL

The PSP control system functions in the following operational modes: orbital science preparation, orbital science operation, and automatic tracking.

13.1 Orbital Science Preparation Mode

The spacecraft will orbit for several days prior to the orbit trim maneuver. During the initial period for applicable orbits, the terminator and limb crossing sensors are turned on and the crossing signals are utilized by the C and S to establish the science orbital program. For other orbits the stored orbital experiment preparation sequence is activated by the C and S, following celestial acquisition. The PSP is also turned on as required and the acquisition angles are supplied by the C and S so that the PSP can begin tracking Mars. The science experiments will be turned on and, following a warmup period, will be calibrated. The science subsystem will then acquire data and telemeter it to earth for verification of the planetary experiments operation. The mode sequence is given in Table B-24.

13.2 Orbital Science Operation Mode

During a six-month period following insertion into Mars orbit, the spacecraft will perform a prescribed automatic controlled science program. The automatic science program sequence will be stored in the C and S and turned on when the spacecraft is not supporting orbit trim maneuvers or capsule operations. The orbital sequence will be initiated for each orbit by a timer which is set and updated twice each orbit at the dawn and evening terminator. A description of the use of the terminator crossings for automatic sequencing of science operations was given in the TRW Phase 1A Task B Final Technical Report, Volume 1, of 17 January 1966.

The orbital sequence will automatically turn on each instrument, start and stop measurements, switch data modes, turn on and off tape recorders, and switch transmission modes as required.

Table B-23. Propellant Tank Venting Sequence

Item	Event	Control Source	Active Subsystem	Comment
	Prerequisites			
	• All engine operations completed		Pyrotechnic	
	• Pyrotechnic valves armed		Pyrotechnic	
	• Pressurization system locked up			All pressure lines valves closed
1	Enable oxidizer tank	C and S	C and S	
2	Open normally closed oxidizer tank explosive vent valve	C and S	Pyrotechnic	
3	Oxidizer tank pressure reduced to zero		Propulsion	
4	Oxidizer tanks empty		Propulsion	
5	Enable fuel tank venting	C and S	C and S	
6	Open normally closed fuel tank explosive vent valve	C and S	Pyrotechnic	
7	Fuel tank pressure reduced to zero		Propulsion	
8	Fuel tanks empty		Propulsion	
9	Enable pressurant tank			
10	Open NC pressurant tank vent valve	C and S	Pyrotechnic	
11	Pressurant tank pressure reduced to zero		Propulsion	

Table B-24. Orbital Science Preparation Sequence

Item	Event	Control Source	Active Subsystem	Comment
1	Turn on limb detection	C and S	G and C	
2	Turn on terminator detector	C and S	G and C	
3	Initiate orbital science preparation	C and S	C and S	
4	Start mode timers	C and S	C and S	
5	Turn on planetary science power			
6	Turn on photo-imaging	C and S	Photo	See photo-imaging sequence
7	Turn on broadband IR spectrometer	C and S	Science	
8	Turn on high resolution IR spectrometer	C and S	Science	
9	Turn on IR radiometer	C and S	Science	
10	Turn on UV spectrometer	C and S	Science	
11	Turn on Mars sensor	C and S	G and C	
12	Begin high-gain antenna positioning	C and S	G and C	
13	Complete high-gain antenna positioning	G and C	C and S	
14	Begin medium-gain antenna positioning	C and S	G and C	
15	Complete medium-gain antenna positioning	G and C	C and S	
16	Complete science subsystem warmup	C and S	C and S	
17	Switch high resolution IR spectrometer to calibrate	C and S	Science	

Table B-24. Orbital Science Preparation Sequence (Continued)

Item	Event	Control Source	Active Subsystem	Comment
18	Switch G and C to fine limit cycle	C and S	G and C	
19	Switch PSP to automatic control	C and S	G and C	
20	Enable science experiments	C and S	C and S	
21	Switch to data Mode 4	C and S	Data	
22	Begin data readout	Data	Science	
23	Complete data readout	Data	C and S	
24	Switch to data Mode 1	C and S	Data	
25	Switch G and C to coarse limit cycle	C and S	G and C	
26	Verification of science operation	MOS	C and S	
27	Initiate orbital science sequence	C and S	Science	

During Mars orbit, the high-gain and medium-gain antennas will be repositioned every nine hours and the Canopus sensor will be updated as required. During periods of long eclipses, operation of some of the science experiments will be reduced automatically if required for conservation of electrical power.

The orbital science operations sequence will be optimized for the entire mission although emphasis and priority will be placed on the early acquisition of data. The orbital science operations can be updated and revised by ground command after verification of initial orbital operations success criteria have been met. The flexibility of ground update of the sequence after initial period of orbital operation has been evaluated and will allow for maximum utilization of the spacecraft science sensors for satisfaction of the program objectives.

13.3 Automatic Mars Tracking Mode

The PSP will accept angle and angle rate commands from the Mars sensors, and will be capable of operating in an automatic tracking mode so as to point its boresight axis toward the center of Mars.

The PSP will be capable of aligning the boresight axis of the platform to the center of the planet Mars. While tracking, the random angular motion of the PSP will be limited so that it will be compatible with the operation of the mounted science equipment.

The mode sequence is given in Table B-25.

Table B-25. Automatic Mars Tracking Sequence

Item	Event	Control Source	Active Subsystem	Comment
	Prerequisites			
	• Stabilized in Mars Orbit		G and C	
	• Terminator and limb crossing sensors on		G and C	
1	Enable PSP Mars tracking	C and S	PSP	
2	Turn on PSP power	C and S	PSP	
3	Turn Mars sensor	C and S	PSP	
4	Switch Mars sensor to PSP drive electronics	C and S	PSP	
5	Set Mars acquisition angles	C and S	PSP	
6	Begin tracking Mars	C and S	PSP	
7	Enable PSP science experiments	C and S	PSP	

14. SPACECRAFT SCIENCE

The spacecraft science subsystem functions in the following operating mode: photo-imaging sequence.

14.1 Photo-Imaging Sequence Mode

The photo-imaging sequence is the same for all photo-imaging devices, and is given in Table B-26.

Table B-26. Photo-Imaging Sequence

Item	Event	Control Source	Active Subsystem	Comment
1	Initiate photo-imaging sequence	C and S		Sequence timed from termination crossing or by command
2	Turn on photo-imaging electronics	C and S	Photo	
3	Set color filter	C and S	Photo	
4	Set shutter speed	C and S	Photo	
5	Select image motion compensation rates (if required)	C and S	Photo	
6	Signal photo-imaging system warmup complete	Photo	C and S	
7	Switch G and C to fine limit cycle	C and S	G and C	
8	Switch PSP control option Automatic control Command pointing	C and S	PSP	Only one PSP mode See PSP control modes
9	Enable science experiments	G and C	C and S	
10	Actuate image motion compensation	C and S	Photo	
11	Actuate shutter	C and S	Photo	
12	Acquire photo image	Photo	Photo	
13	Switch to data mode	C and S	Data	

Table B-26. Photo-Imaging Sequence

Item	Event	Control Source	Active Subsystem	Comment
14	Begin reading camera data	Data	C and S	
15	Complete reading camera data	Data	C and S	Repeat 10 through 15 until photo sequence is completed
16	Complete photo sequence	C and S	C and S	
17	Switch to data mode	C and S	Data	
18	Switch PSP off	C and S	PSP	
19	Switch G and C to coarse limit cycle	C and S	G and C	
20	Turn off photo-imaging electronics	C and S	PSP	

SELECTED MARS ORBIT DATA FOR THE 1973 MISSION

APPENDIX C

SELECTED MARS ORBIT DATA FOR THE 1973 MISSION

Seven representative earth-Mars trajectories have been selected for the 1973 Mars opportunity and calculation for a number of related orbits at Mars have been carried out and presented here. The appropriate launch-arrival dates and hyperbolic excess speeds (V_∞) at Mars encounter are presented in Table C-1, along with an identification number for each trajectory.

Table C-1. Mars Encounter Data

Trajectory No.	Earth Launch Date	Mars Arrival Date	V_∞ (km/sec)
1	21 July 1973	7 February 1974	3.017
2	12 August 1973	7 February 1974	3.044
3	3 September 1973	7 February 1974	3.231
4	8 August 1973	21 March 1974	2.580
5	5 September 1973	21 March 1974	2.494
6	22 August 1973	25 April 1974	2.669
7	11 September 1973	25 April 1974	2.586

All data contained in this appendix are presented for various combinations of the following Mars orbit parameters.

Orbit size (h_p x h_a): periapsis altitude and apoapsis altitude, measured with respect to a spherical Mars (radius 3395 km).

Inclination (i): measured with respect to the Mars equator; inclination is designated either S or N, depending on whether the initial target point in the R-T plane is south or north of the T-axis.

Apsidal orientation angle (Ψ): locates the orbital line of apsides with respect to the approach asymptote vector ($\vec{s}$); it is measured from the negative approach asymptote vector ($\vec{-s}$) to the ellipse radius vector ($\vec{r}_p$) in the direction of orbital motion.

Time: measured from the impulsive orbit injection point (also commonly referred to as "insertion" or "encounter").

Three different orbit sizes are considered in the analysis, 1,000 x 10,000, 1,000 x 15,000, and 1,000 x 20,000 km. Time plots of attitude and true anomaly for these orbits are presented in Figures C-1 through C-3.

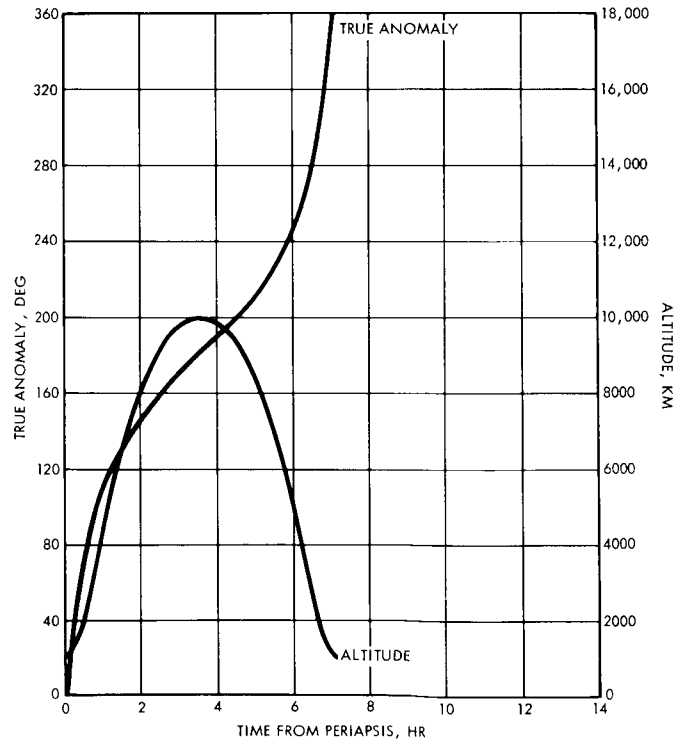

Figure C-1. True Anomaly and Altitude for 1000 x 10,000 km Orbit

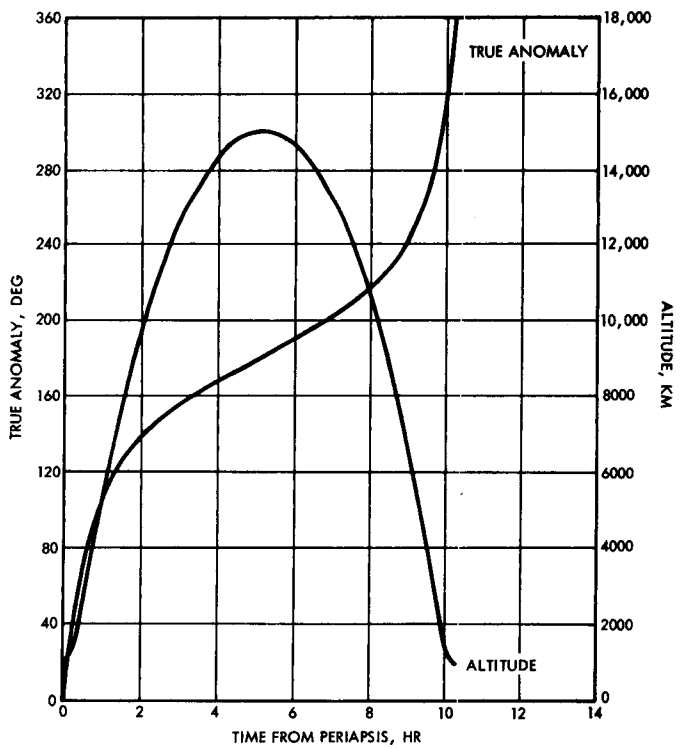

Figure C-2. True Anomaly and Altitude for 1000 x 15, 000 km Orbit

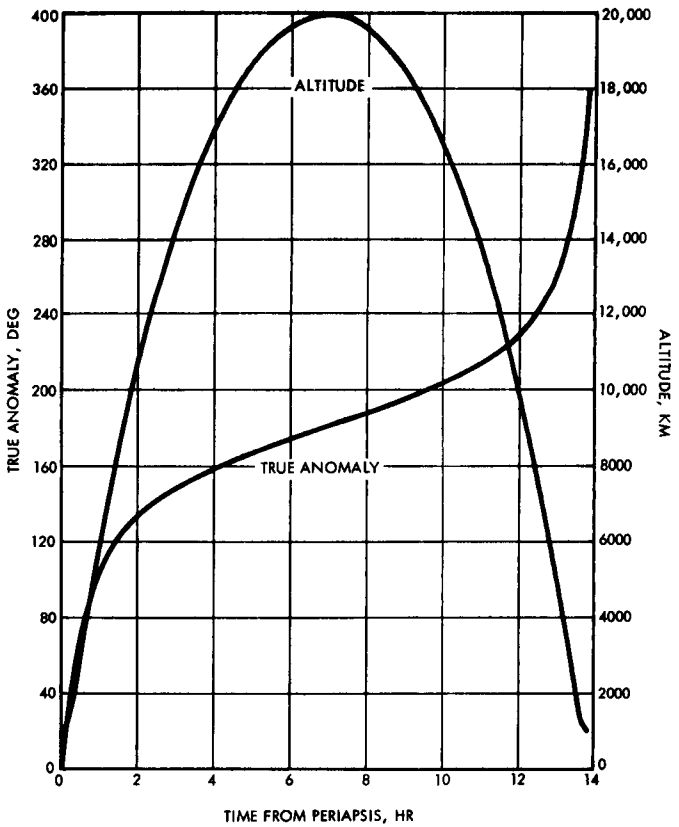

Figure C-3. True Anomaly and Altitude for 1000 x 20, 000 km Orbit

Pertinent Mars orbit insertion data for each of the seven 1973 - 74 earth-Mars trajectories are presented in Tables C-2 and C-3. The apsidal orientation angles and ΔV requirements for optimum cotangential, impulsive transfers into three different Mars orbits are presented in Table C-2. For comparison, the ΔV requirements for apsidal orientation angles of 60, 90, and 150 degrees are presented in Table C-3. Also included in this table are the transfer point true anomalies on the approach hyperbola (ν_H) and the elliptical capture orbit (ν_E), for the optimum transfers, $\nu_H = \nu_E = 0$ deg.

Table C-2. ΔV Requirements for Optimum Cotangential Periapsis Transfers into Mars Orbits

Trajectory No.	Ψ (deg)	Orbit Size (km)	ΔV (km/sec)
1	121.131	1000 x 10,000	1.516
		1000 x 15,000	1.381
		1000 x 20,000	1.297
2	120.834	1000 x 10,000	1.532
		1000 x 15,000	1.396
		1000 x 20,000	1.312
3	118.871	1000 x 10,000	1.640
		1000 x 15,000	1.504
		1000 x 20,000	1.420
4	126.453	1000 x 10,000	1.282
		1000 x 15,000	1.147
		1000 x 20,000	1.063
5	127.625	1000 x 10,000	1.239
		1000 x 15,000	1.104
		1000 x 20,000	1.019
6	125.289	1000 x 10,000	1.328
		1000 x 15,000	1.192
		1000 x 20,000	1.108
7	126.375	1000 x 10,000	1.285
		1000 x 15,000	1.150
		1000 x 20,000	1.066

Table C-3. ΔV Requirements and Geometry for Transfers into Rotated Mars Orbits

Trajectory No.	Orbit Size (km)	Apsidal Orientation Angle - Ψ (Deg)								
		60 Degrees			90 Degrees			150 Degrees		
		ΔV (km/sec)	ν_H (deg)	ν_E (deg)	ΔV (km/sec)	ν_H (deg)	ν_H (deg)	ΔV (km/sec)	ν_H (deg)	ν_E (deg)
1	1000 x 10,000	1.849	-28.757	-85.332	1.624	-19.693	-49.424	1.628	19.634	49.951
	1000 x 15,000	1.780	-34.694	-90.098	1.518	-24.475	-53.701	1.533	24.896	55.859
	1000 x 20,000	1.735	-39.149	-93.906	1.448	-28.405	-57.500	1.468	28.910	60.078
2	1000 x 10,000	1.863	-28.537	-84.873	1.637	-19.411	-48.877	1.645	19.648	50.283
	1000 x 15,000	1.794	-34.459	-89.639	1.532	-24.126	-53.096	1.551	24.867	56.152
	1000 x 20,000	1.748	-38.873	-93.418	1.461	-28.000	-56.846	1.487	28.858	60.352
3	1000 x 10,000	1.961	-27.101	-81.855	1.735	-17.582	-45.283	1.770	19.621	52.354
	1000 x 15,000	1.892	-32.706	-86.406	1.627	-21.819	-49.082	1.680	24.663	58.066
	1000 x 20,000	1.845	-36.927	-90.068	1.554	-25.319	-52.500	1.617	28.468	62.100
4	1000 x 10,000	1.640	-32.394	-93.252	1.420	-24.738	-59.170	1.356	18.864	43.467
	1000 x 15,000	1.573	-39.080	-98.477	1.320	-30.831	-64.580	1.251	24.519	49.678
	1000 x 20,000	1.529	-44.027	-102.559	1.256	-35.721	-69.199	1.180	28.895	54.180
5	1000 x 10,000	1.603	-33.139	-94.941	1.384	-25.845	-61.299	1.306	18.546	41.895
	1000 x 15,000	1.536	-39.967	-100.244	1.286	-32.215	-66.943	1.199	24.246	48.125
	1000 x 20,000	1.492	-45.023	-104.385	1.222	-37.316	-71.738	1.127	28.653	52.637
6	1000 x 10,000	1.680	-31.635	-91.553	1.459	-23.631	-57.041	1.409	19.144	45.000
	1000 x 15,000	1.613	-38.159	-96.680	1.358	-29.439	-62.207	1.307	24.718	51.152
	1000 x 20,000	1.568	-43.007	-100.713	1.292	-34.120	-66.650	1.237	29.055	55.635
7	1000 x 10,000	1.643	-32.352	-93.145	1.423	-24.661	-59.023	1.360	18.924	43.613
	1000 x 15,000	1.576	-39.013	-98.350	1.323	-30.732	-64.414	1.255	24.529	49.775
	1000 x 20,000	1.531	-43.956	-102.432	1.258	-35.610	-69.023	1.184	28.904	54.277

This appendix is divided into seven sections, one for each earth-Mars trajectory considered. For the combinations of orbit size, inclination, and apsidal orientation specified in Table C-4, the following parameters are presented as a function of time from orbit injection.

- Orbital inclination with respect to the Mars ecliptic
- Latitude of the sub-periapsis point
- Angle from periapsis to the terminator plane; + (-) indicates that the sub-periapsis point is on the light (dark) side of Mars
- True anomaly at entrance into, and duration of sun, earth, and reference star* (Canopus) occultations
- Angles between the normal to the orbit and the Mars-sun and Mars-earth lines
- Cone and clock angles of the normal to the orbit (see Figure C-4); tick marks designate 30 day intervals

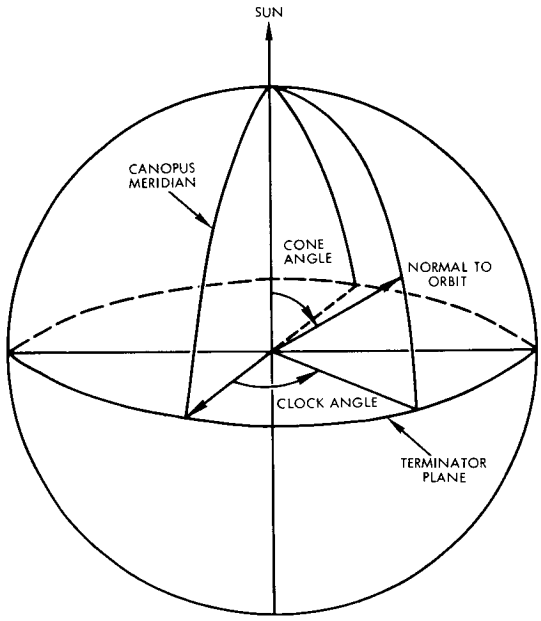

Figure C-4. Cone and Clock Angle Definition

* Data for Canopus occultation is included only for the 6 non-zero cases (6, 15, 21, 26, 32, 37).

Table C-4. Index to Data

Trajectory No.	Orbit Size $h_p \times h_a$ (km)	Inclination, i	Apsidal Orientation, Ψ (deg)	Case No.
1	1000 x 15,000	20°S	121.131	1
	↓	20°N	↓	2
		40°S		3
		40°N		4
		60°S		5
		60°N		6
	1000 x 10,000	40°S		7
	1000 x 20,000	↓	↓	8
	1000 x 15,000		60	9
	↓		90	10
			150	11
2	1000 x 15,000	40°S	120.834	12
	↓	40°N	↓	13
3	1000 x 15,000	40°S	118.871	14
	↓	40°N		15
4	1000 x 15,000	20°S	126.453	16
	↓	20°N	↓	17
		40°S		18
		40°N		19
		60°S		20
		60°N		21
		40°S	60	22
		↓	90	23
			150	24
5	1000 x 15,000	40°S	127.625	25
	↓	40°N	↓	26
6	1000 x 15,000	20°S	125.289	27
	↓	20°N	↓	28
		40°S		29
		40°N		30
		60°S		31
		60°N		32
		40°S	60	33
		↓	90	34
			150	35
7	1000 x 15,000	40°S	126.375	36
	↓	40°N	↓	37

In addition, for cases 1-6, 16-21, and 27-32, orbit displays are presented on a uniform latitude, longitude grid at three different points in time: injection, 90 days after injection, and 180 days after injection. Latitude is measured from the Mars equator, and longitude is referenced to the meridian containing the Mars-sun line. The following characteristics are indicated on each display.

- The Mars ecliptic
- The locations of the sun, earth, and Canopus
- The terminator plane
- The suborbital track
- Location of the periapsis radius vector
- Location of the approach asymptote vector (at encounter)
- Designation of intervals corresponding to sun, earth, or Canopus occultations
- Tick marks on the suborbital track designating variations in altitude, and time from periapsis. Time ticks are presented along the top of the track, and altitude ticks along the bottom as illustrated in Figure C-5.

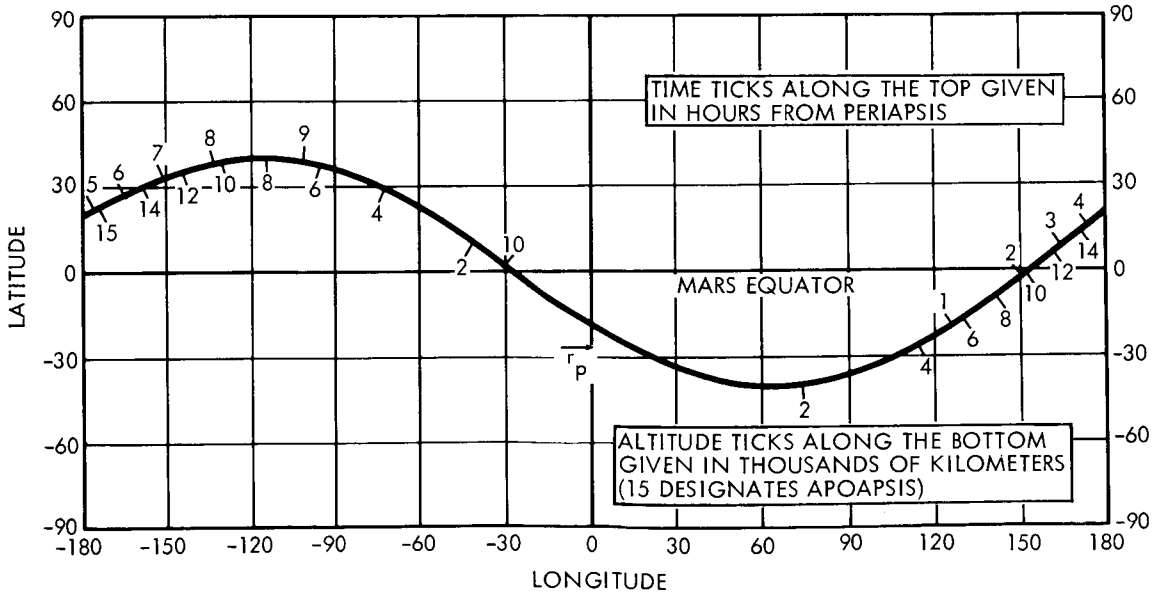

Figure C-5. Sample Orbit Track

CASE NO. 1

1000 x 15,000 km

$i = 20^{\circ}S$

$\Psi = 121.131$ deg

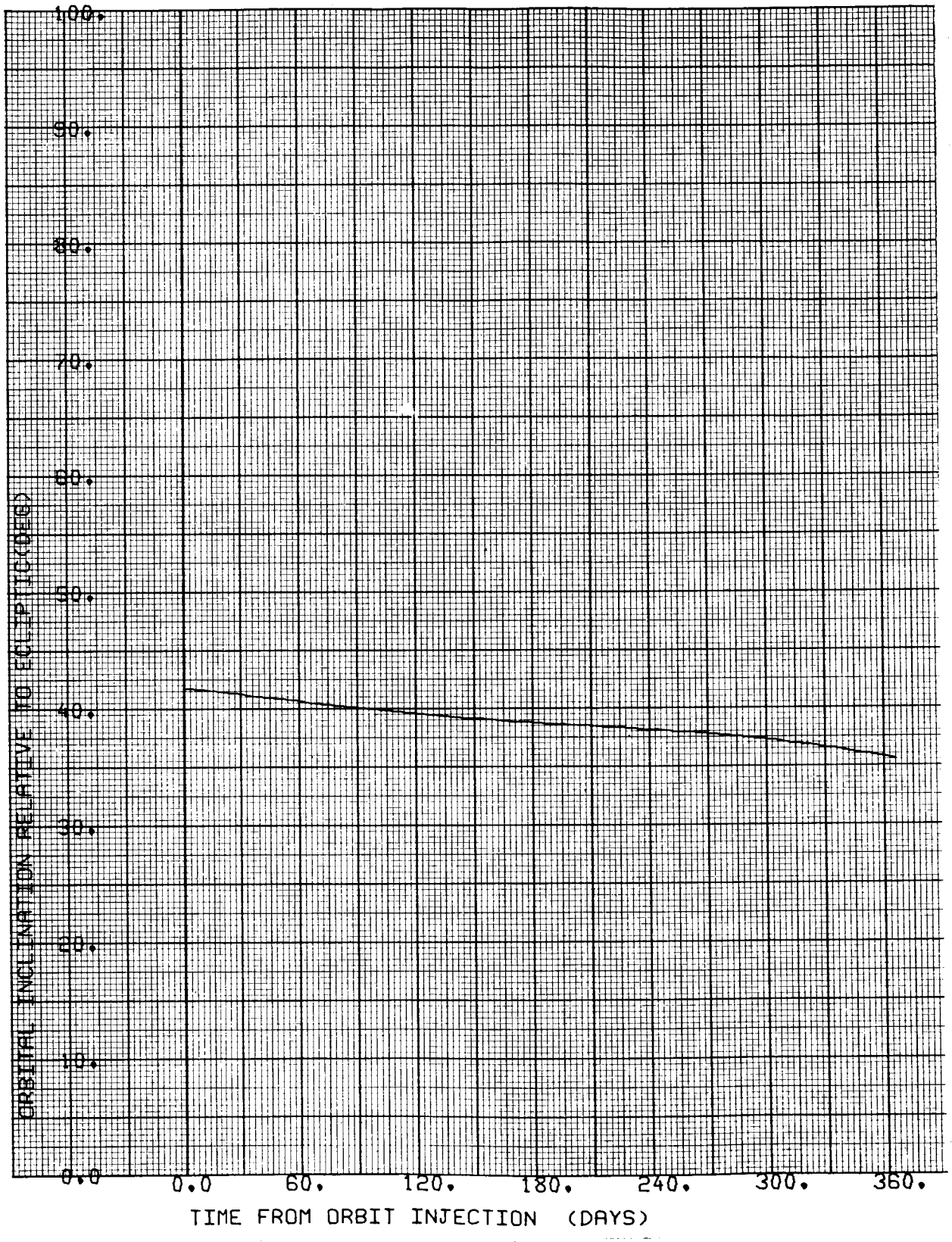
100.
90.
80.
70.
60.
50.
40.
30.
20.
10.
0.0
ORBITAL INCLINATION RELATIVE TO ECLIPTIC(DEG)
0.0
60.
120.
180.
240.
300.
360.
TIME FROM ORBIT INJECTION (DAYS)

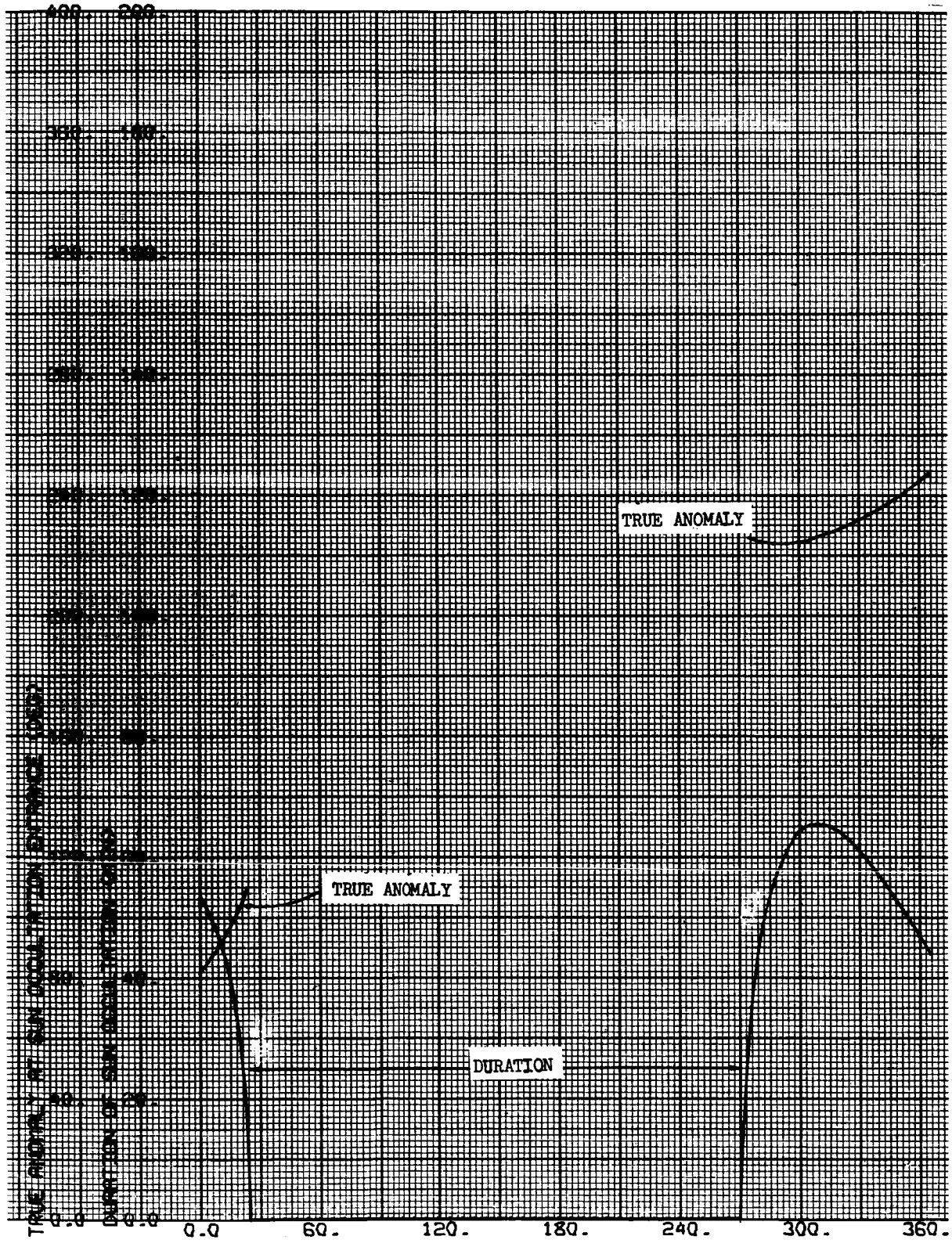
TRUE ANOMALY
TRUE ANOMALY
DURATION
0.0
60.
120.
180.
240.
300.
360.
TIME FROM INJECTION (DAYS)

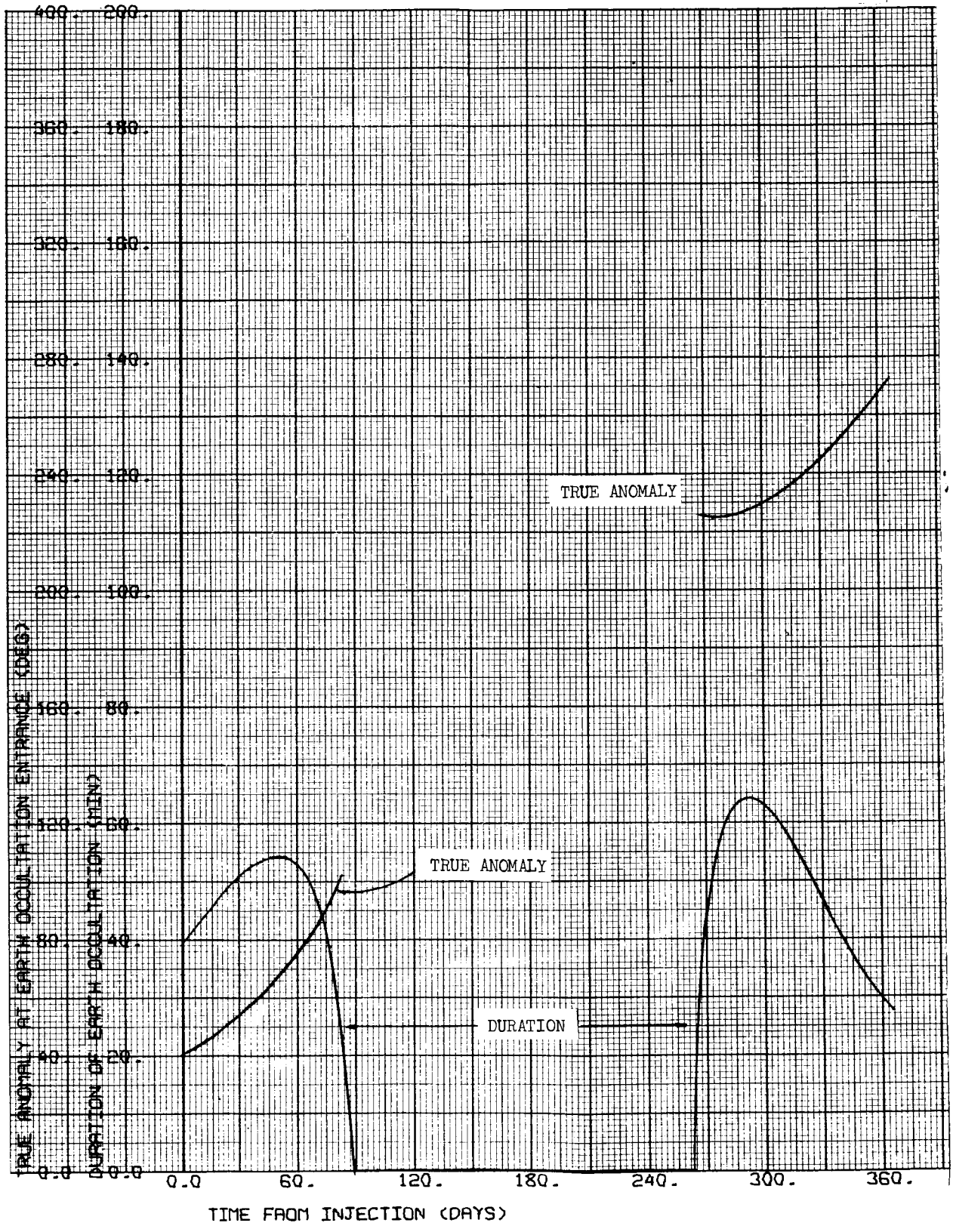
TRUE ANOMALY AT EARTH OCCULTATION ENTRANCE (DEG)
DURATION OF EARTH OCCULTATION (MIN)
TIME FROM INJECTION (DAYS)
TRUE ANOMALY
TRUE ANOMALY
DURATION
400.
360.
320.
280.
240.
200.
160.
120.
80.
40.
0.0
200.
180.
160.
140.
120.
100.
80.
60.
40.
20.
0.0
0.0
60.
120.
180.
240.
300.
360.

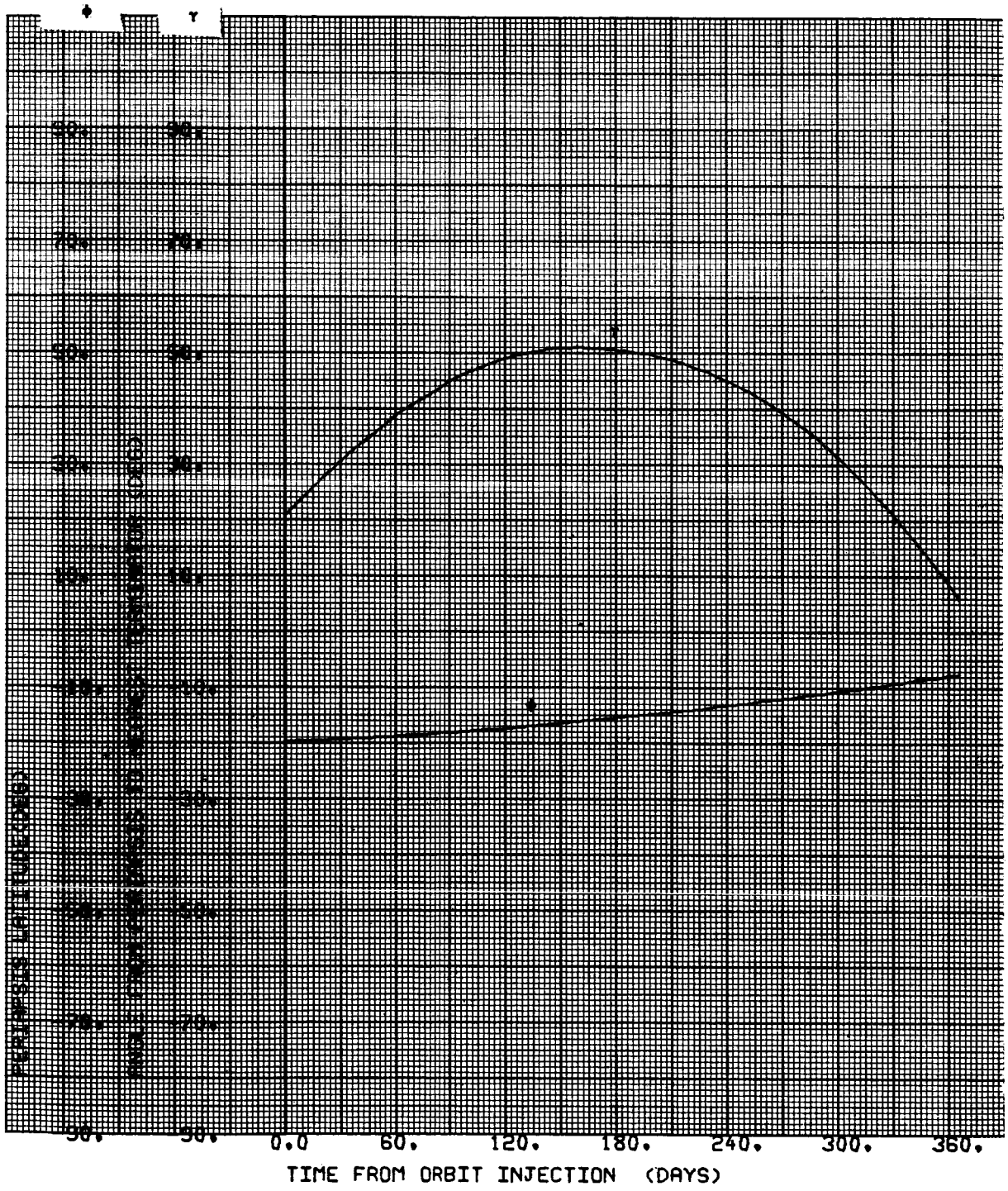
90.
80.
70.
60.
50.
40.
30.
20.
10.
0.0
60.
120.
180.
240.
300.
360.
TIME FROM ORBIT INJECTION (DAYS)

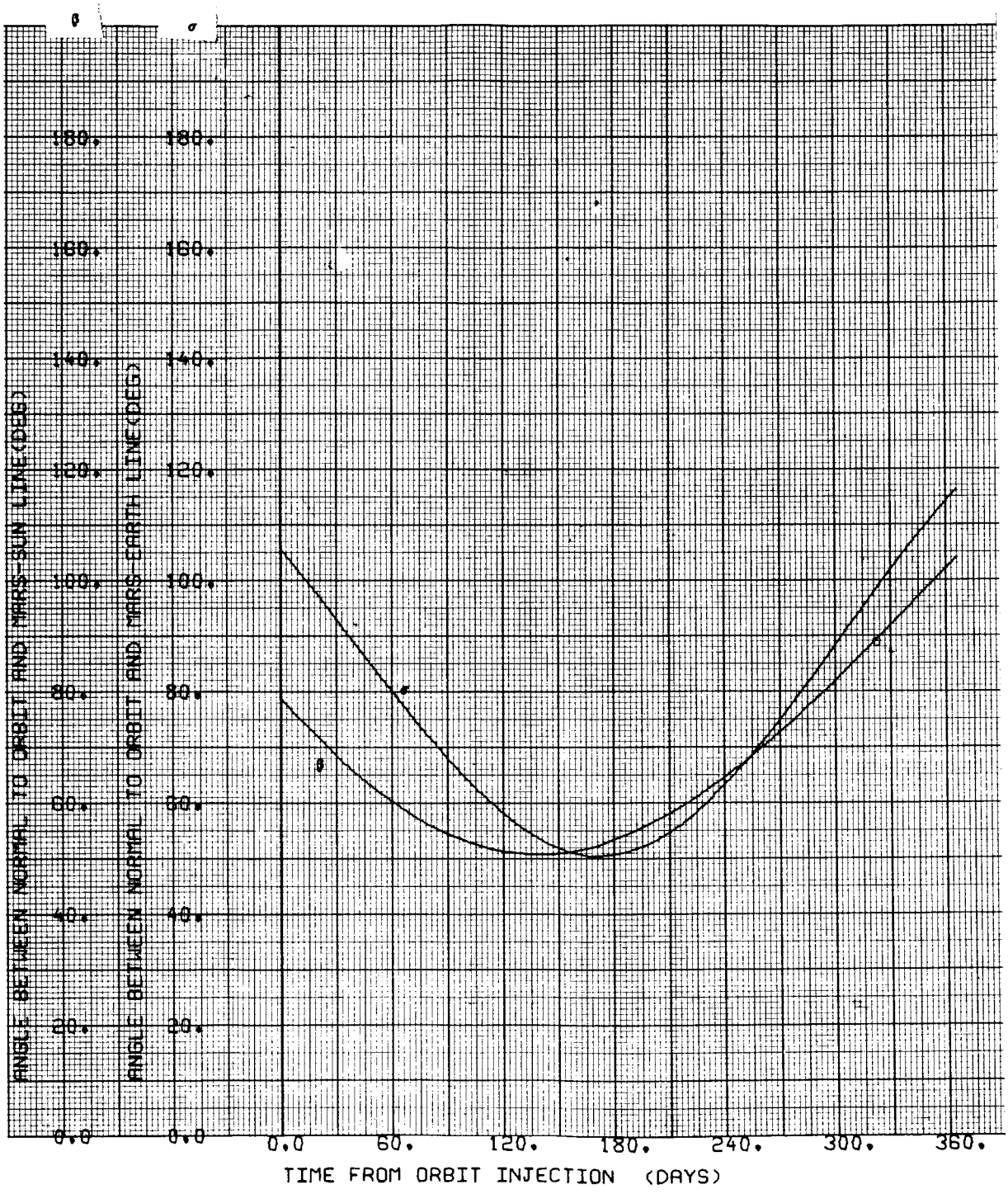
β
σ
180.
160.
140.
120.
100.
80.
60.
40.
20.
0.0
ANGLE BETWEEN NORMAL TO ORBIT AND MARS-SUN LINE (DEG)
ANGLE BETWEEN NORMAL TO ORBIT AND MARS-EARTH LINE (DEG)
0.0
60.
120.
180.
240.
300.
360.
TIME FROM ORBIT INJECTION (DAYS)

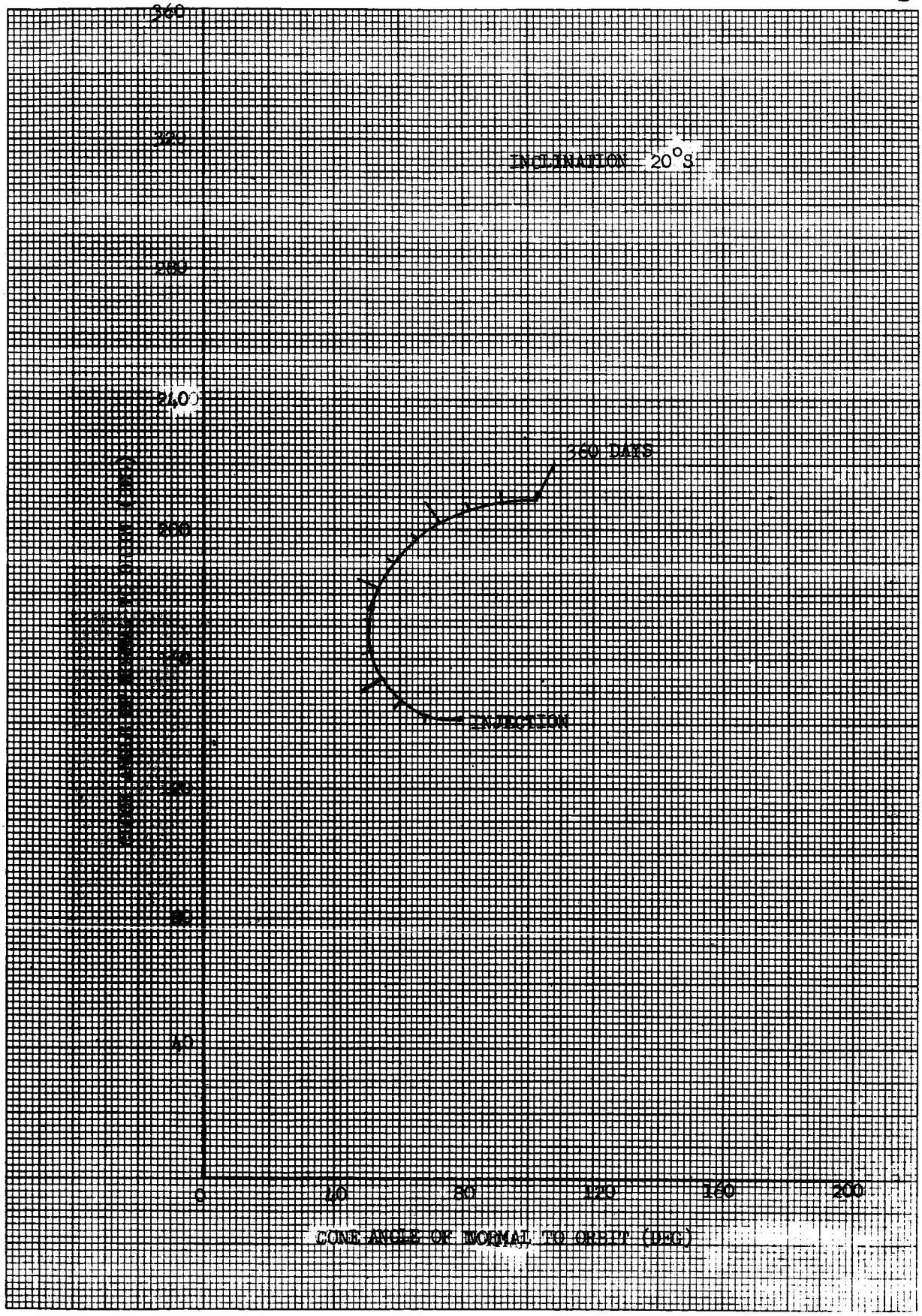
INCLINATION 20°S
360
320
280
240
200
160
120
80
40
0
40
80
120
160
200
260 DAYS
INJECTION
CONE ANGLE OF NORMAL TO ORBIT (DEG)

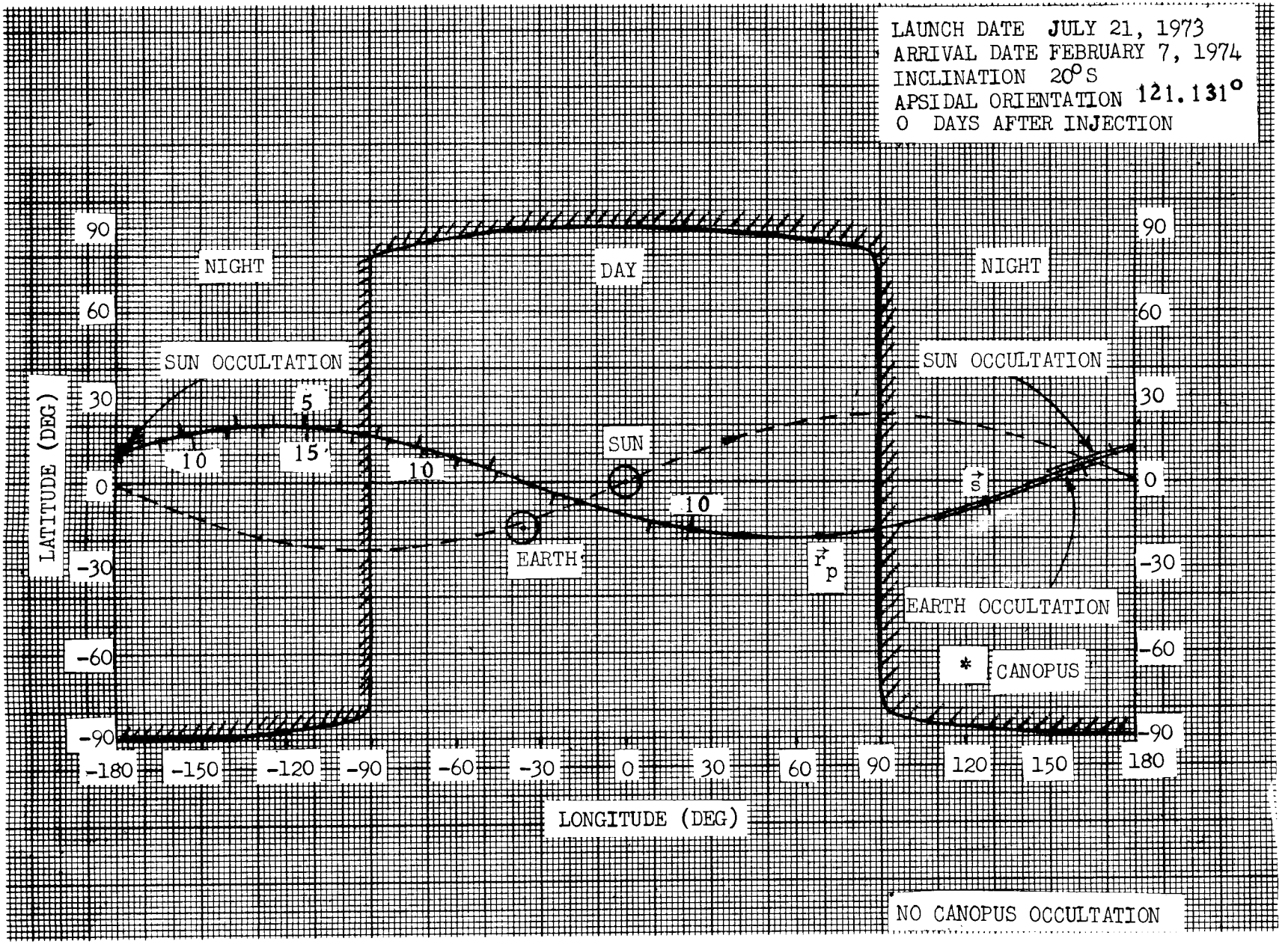
LAUNCH DATE JULY 21, 1973
ARRIVAL DATE FEBRUARY 7, 1974
INCLINATION 20° S
APSIDAL ORIENTATION 121.131°
0 DAYS AFTER INJECTION
NIGHT
DAY
NIGHT
SUN OCCULTATION
SUN OCCULTATION
SUN
EARTH
EARTH OCCULTATION
CANOPUS
NO CANOPUS OCCULTATION
LATITUDE (DEG)
LONGITUDE (DEG)
90
60
30
0
-30
-60
-90
-180
-150
-120
-90
-60
-30
0
30
60
90
120
150
180
10
5
15
10
10

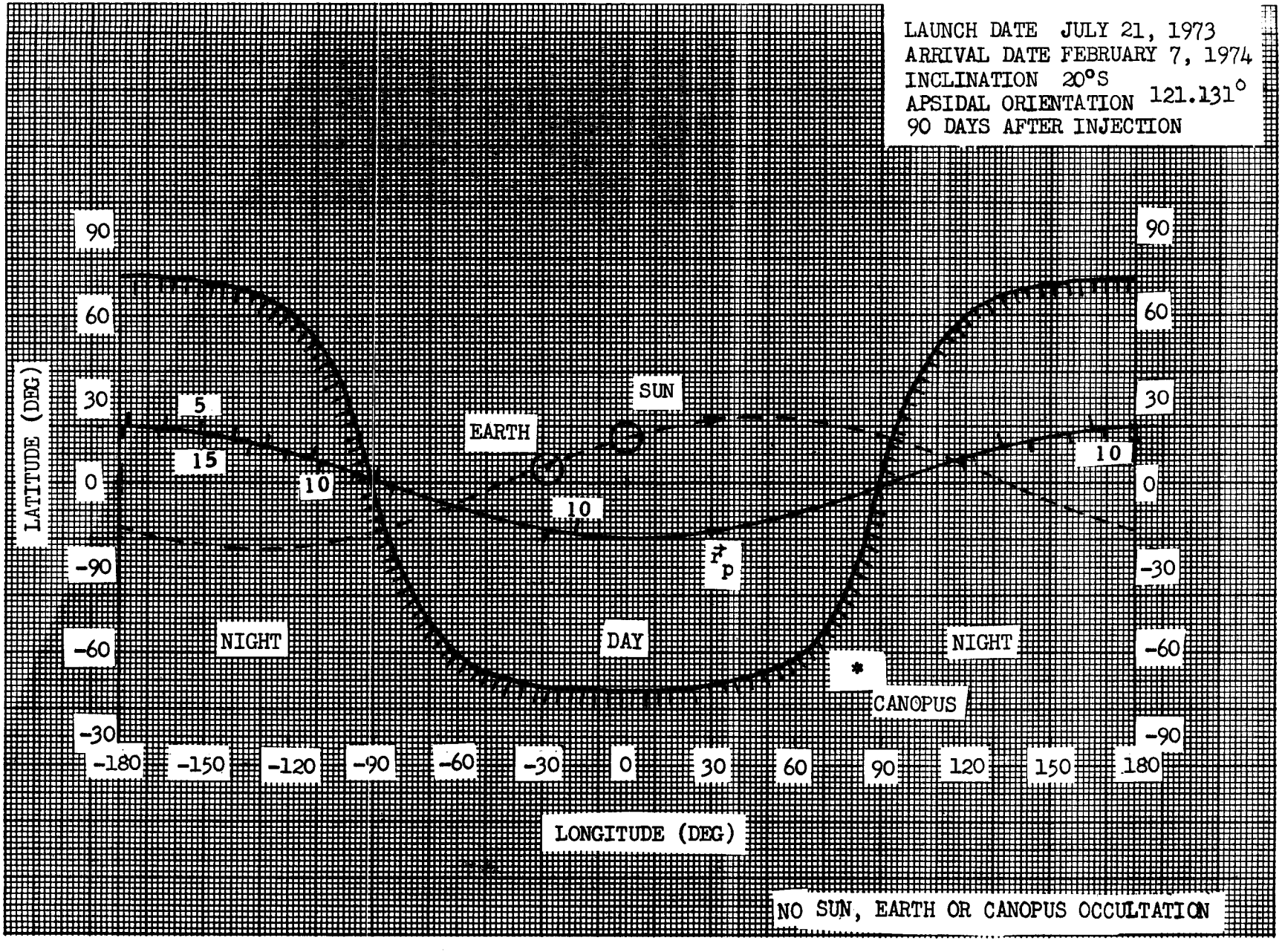
LAUNCH DATE JULY 21, 1973
ARRIVAL DATE FEBRUARY 7, 1974
INCLINATION 20°S
APSIDAL ORIENTATION 121.131°
90 DAYS AFTER INJECTION
LATITUDE (DEG)
90
60
30
0
-30
-60
-90
5
15
10
10
SUN
EARTH
r_p
NIGHT
DAY
NIGHT
CANOPUS
-180
-150
-120
-90
-60
-30
0
30
60
90
120
150
180
LONGITUDE (DEG)
NO SUN, EARTH OR CANOPUS OCCULTATION

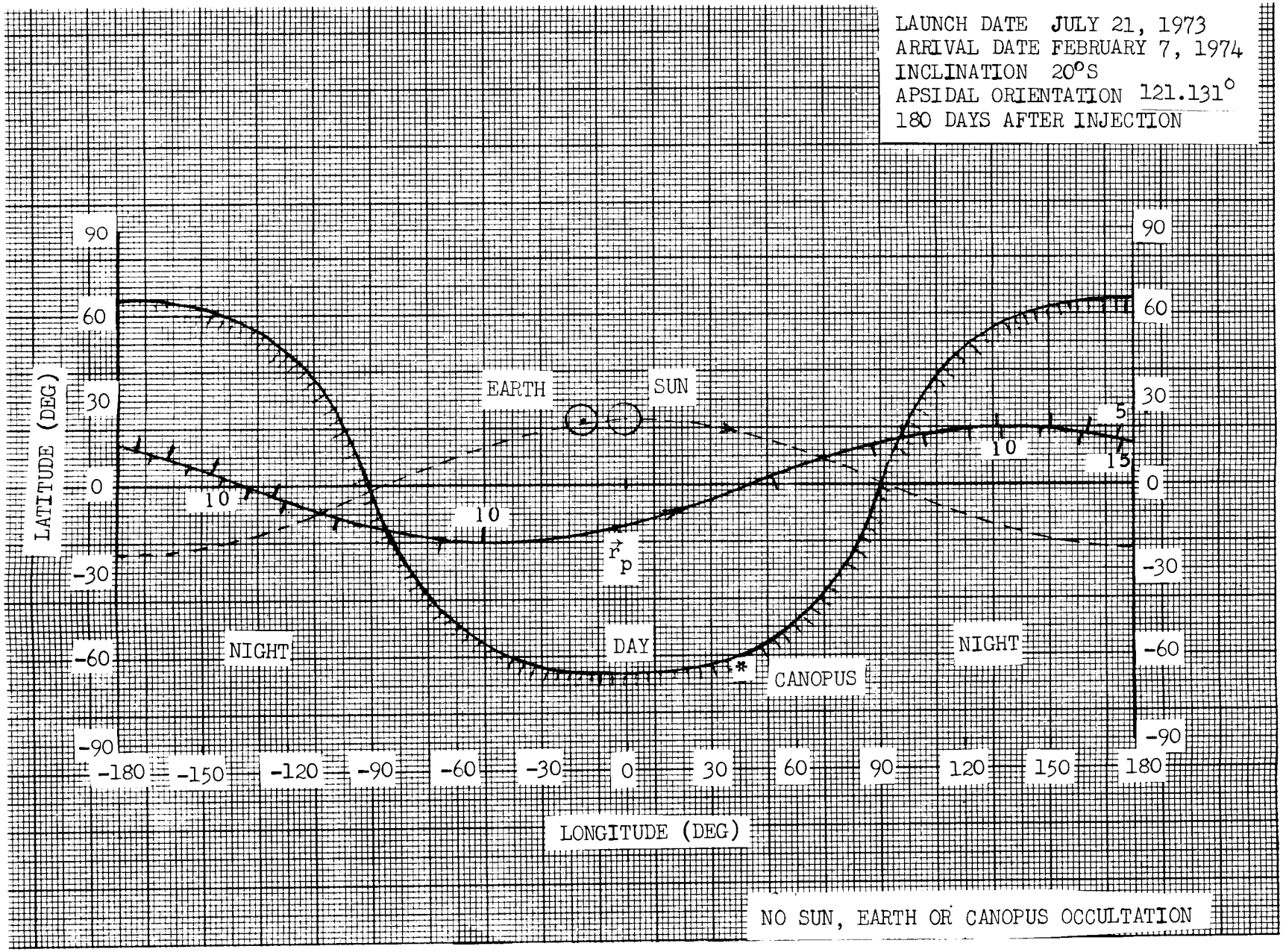
LAUNCH DATE JULY 21, 1973
ARRIVAL DATE FEBRUARY 7, 1974
INCLINATION 20°S
APSIDAL ORIENTATION 121.131°
180 DAYS AFTER INJECTION
LATITUDE (DEG)
90
60
30
0
-30
-60
-90
EARTH
SUN
10
10
5
10
15
$\vec{r}_p$
NIGHT
DAY
NIGHT
CANOPUS
-180
-150
-120
-90
-60
-30
0
30
60
90
120
150
180
LONGITUDE (DEG)
NO SUN, EARTH OR CANOPUS OCCULTATION

CASE NO. 2

1000 x 15, 000 km

$i = 20^{\circ}N$

$\Psi = 121.131$ deg

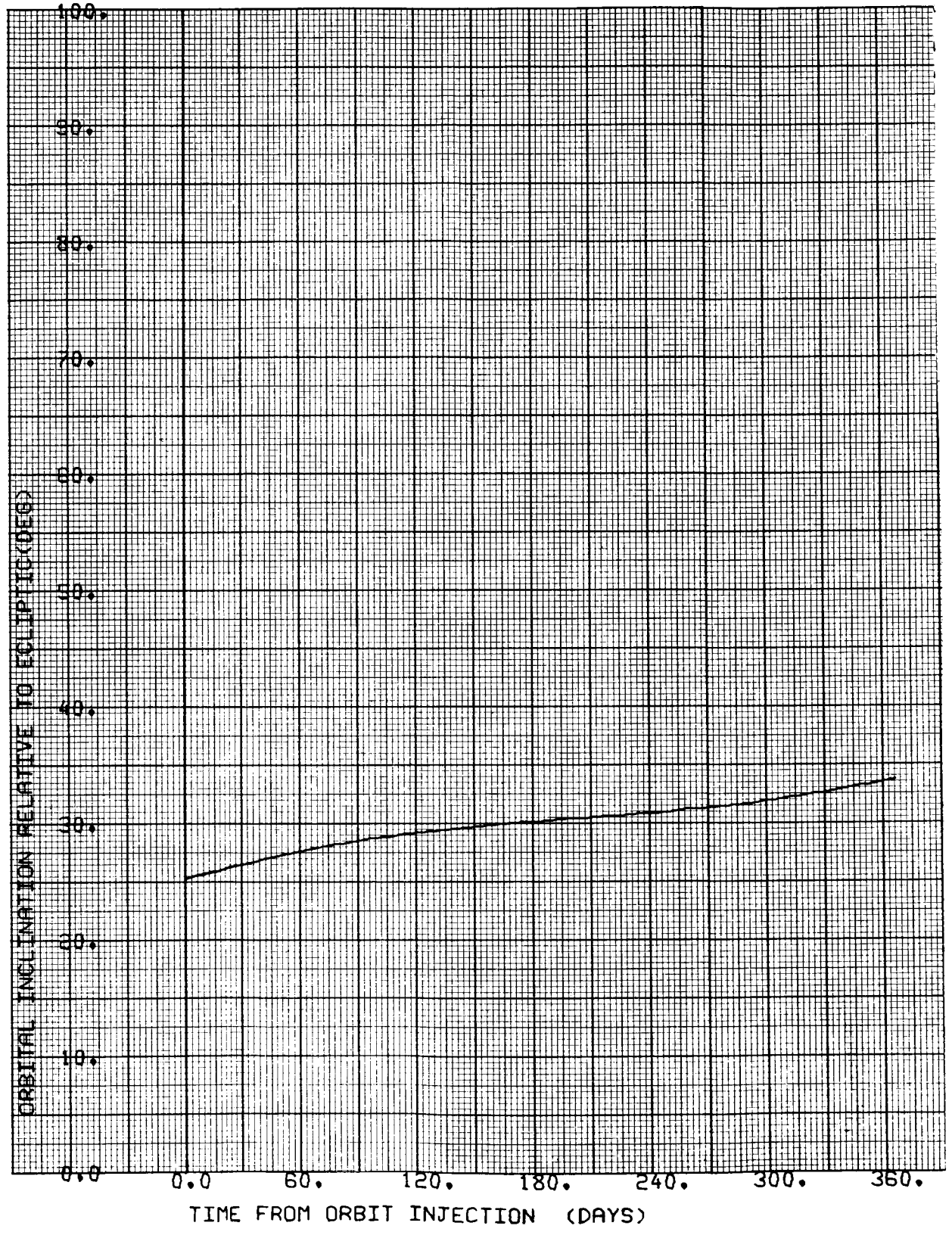
100.
90.
80.
70.
60.
50.
40.
30.
20.
10.
0.0
ORBITAL INCLINATION RELATIVE TO ECLIPTIC(DEG)
0.0
60.
120.
180.
240.
300.
360.
TIME FROM ORBIT INJECTION (DAYS)

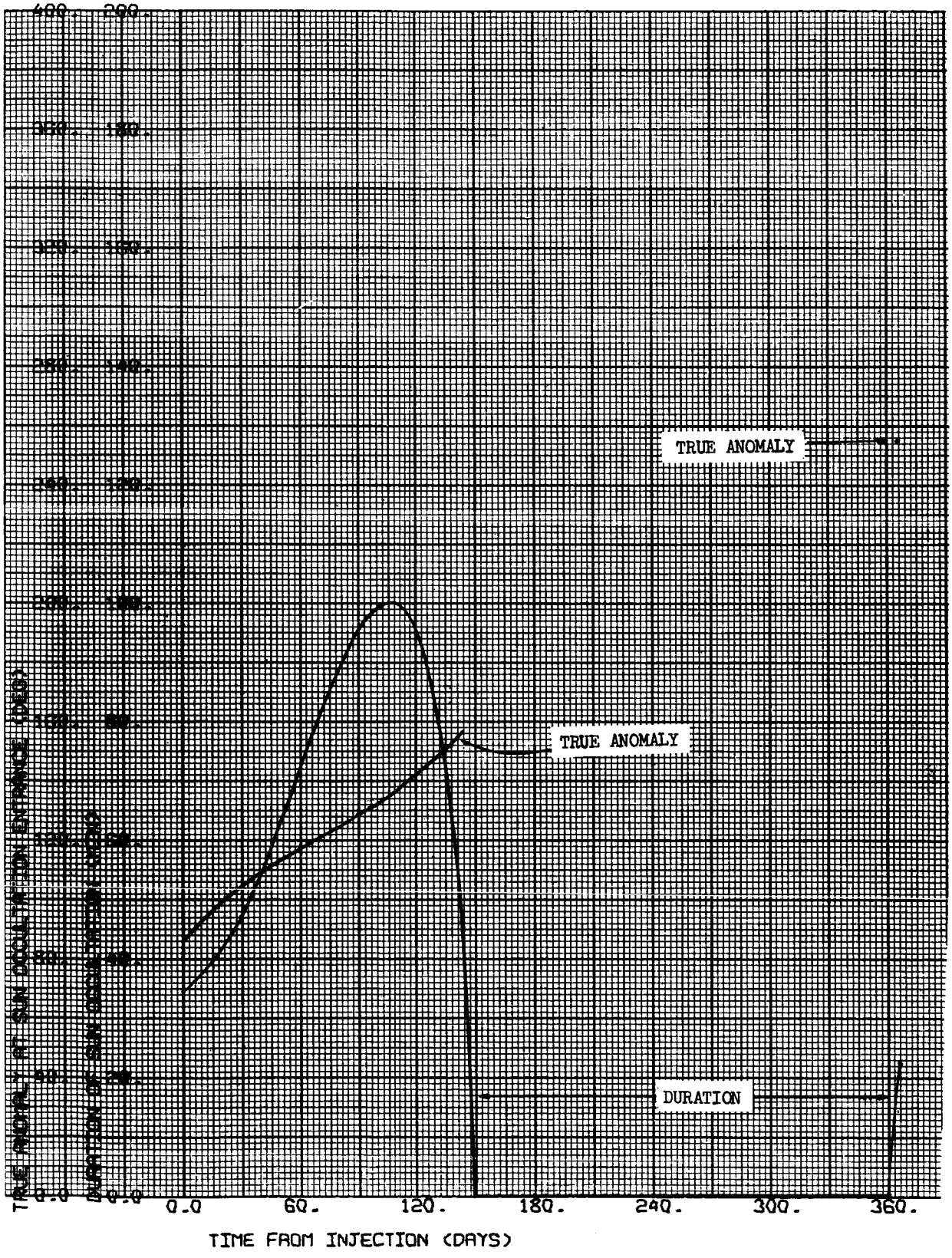
TRUE ANOMALY
TRUE ANOMALY
DURATION
0.0
60.
120.
180.
240.
300.
360.
TIME FROM INJECTION (DAYS)

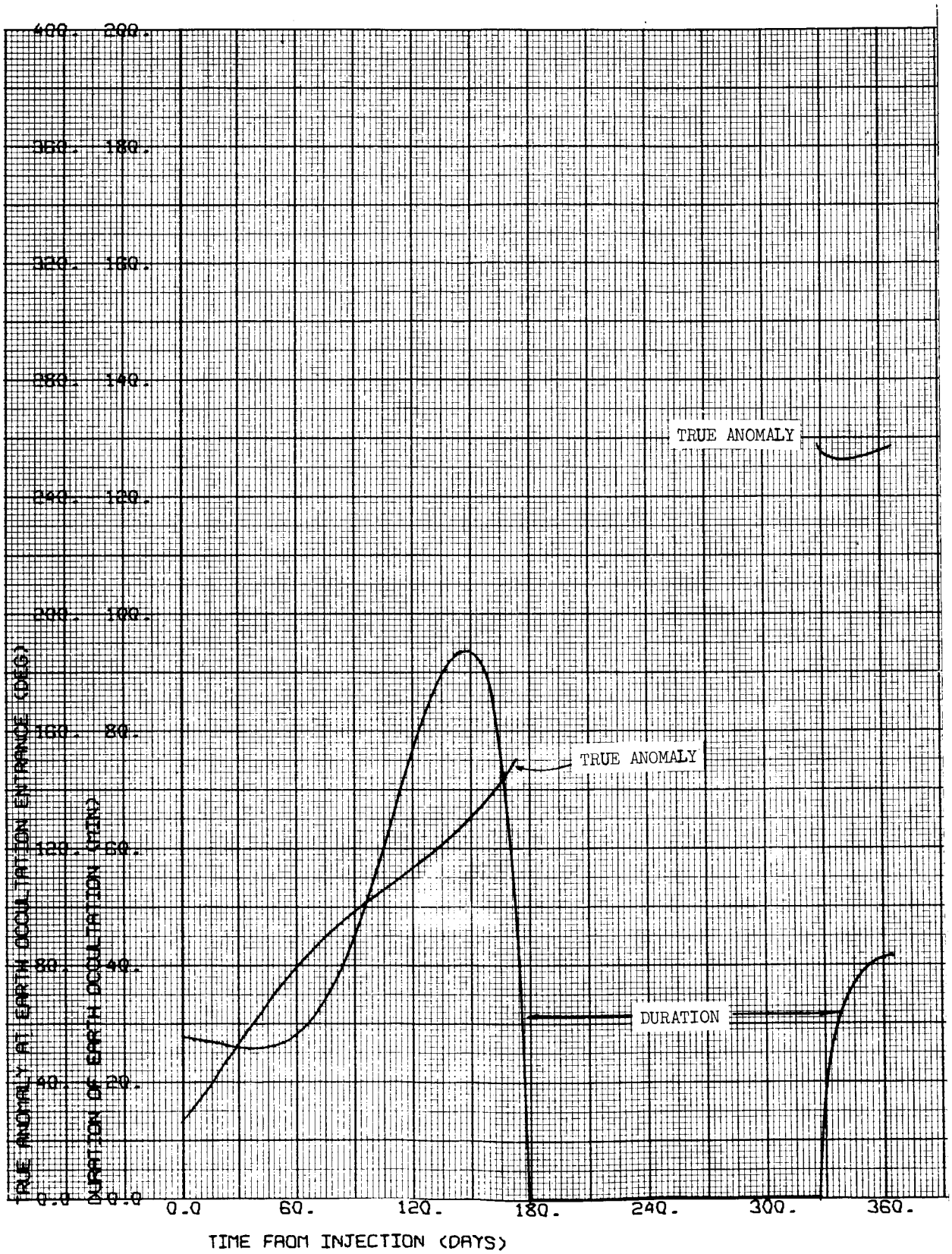
TRUE ANOMALY AT EARTH OCCULTATION ENTRANCE (DEG)
DURATION OF EARTH OCCULTATION (MIN)
TIME FROM INJECTION (DAYS)
TRUE ANOMALY
TRUE ANOMALY
DURATION
0.0
60.
120.
180.
240.
300.
360.
400.
360.
320.
280.
240.
200.
160.
120.
80.
40.
200.
180.
160.
140.
120.
100.
80.
60.
40.
20.
0.0

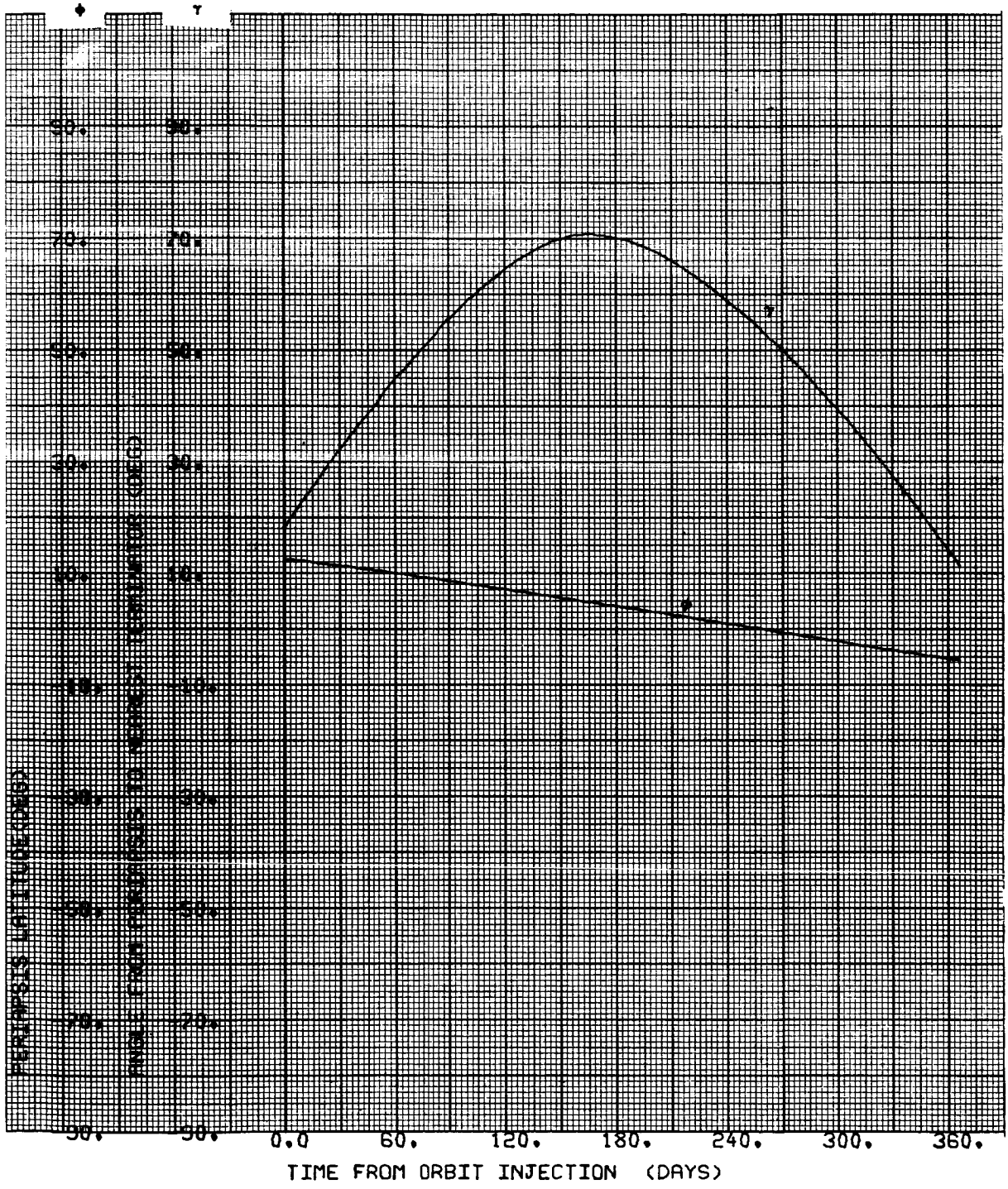
90.
70.
50.
30.
10.
-10.
-30.
-50.
-70.
-90.
0.0
60.
120.
180.
240.
300.
360.
TIME FROM ORBIT INJECTION (DAYS)
PERIAPSIS LATITUDE (DEG)
APOAPSIS LATITUDE (DEG)

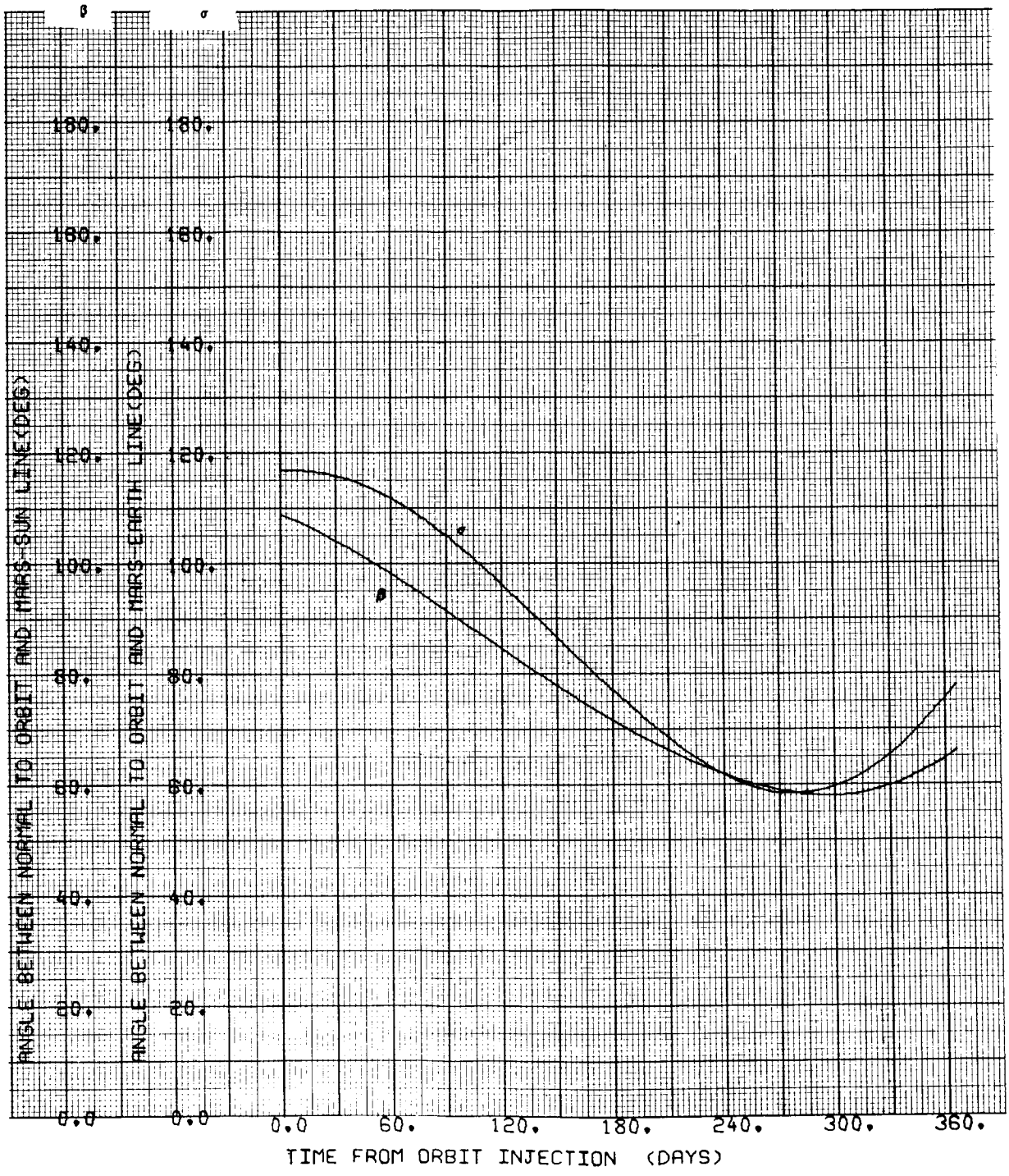
β
σ
180.
180.
140.
120.
100.
80.
60.
40.
20.
0.0
0.0
60.
120.
180.
240.
300.
360.
ANGLE BETWEEN NORMAL TO ORBIT AND MARS-SUN LINE(DEG)
ANGLE BETWEEN NORMAL TO ORBIT AND MARS-EARTH LINE(DEG)
TIME FROM ORBIT INJECTION (DAYS)

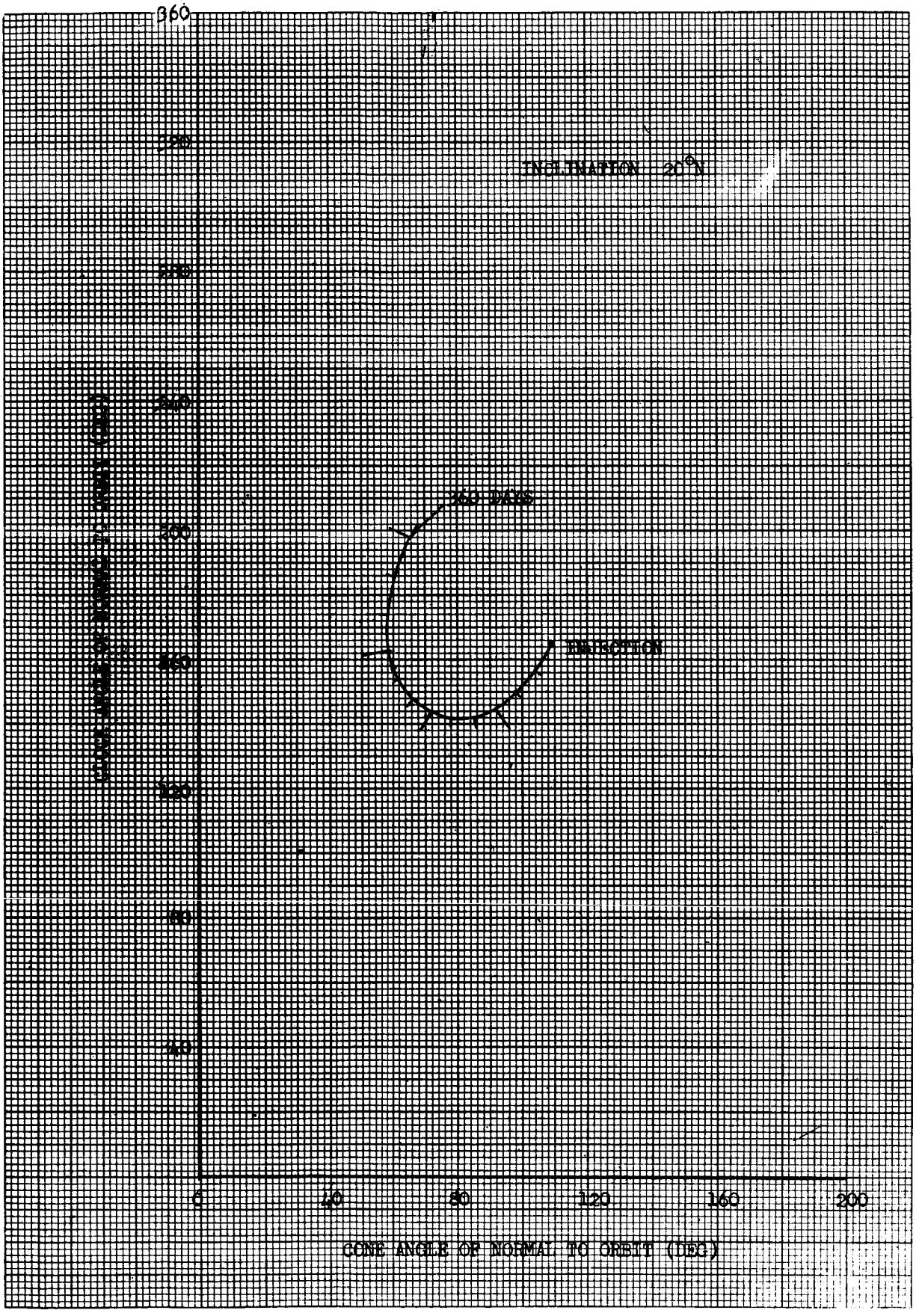
INCLINATION 20°N
360 DAYS
INJECTION
360
280
240
200
160
120
80
40
0
40
80
120
160
200
CONE ANGLE OF NORMAL TO ORBIT (DEG)

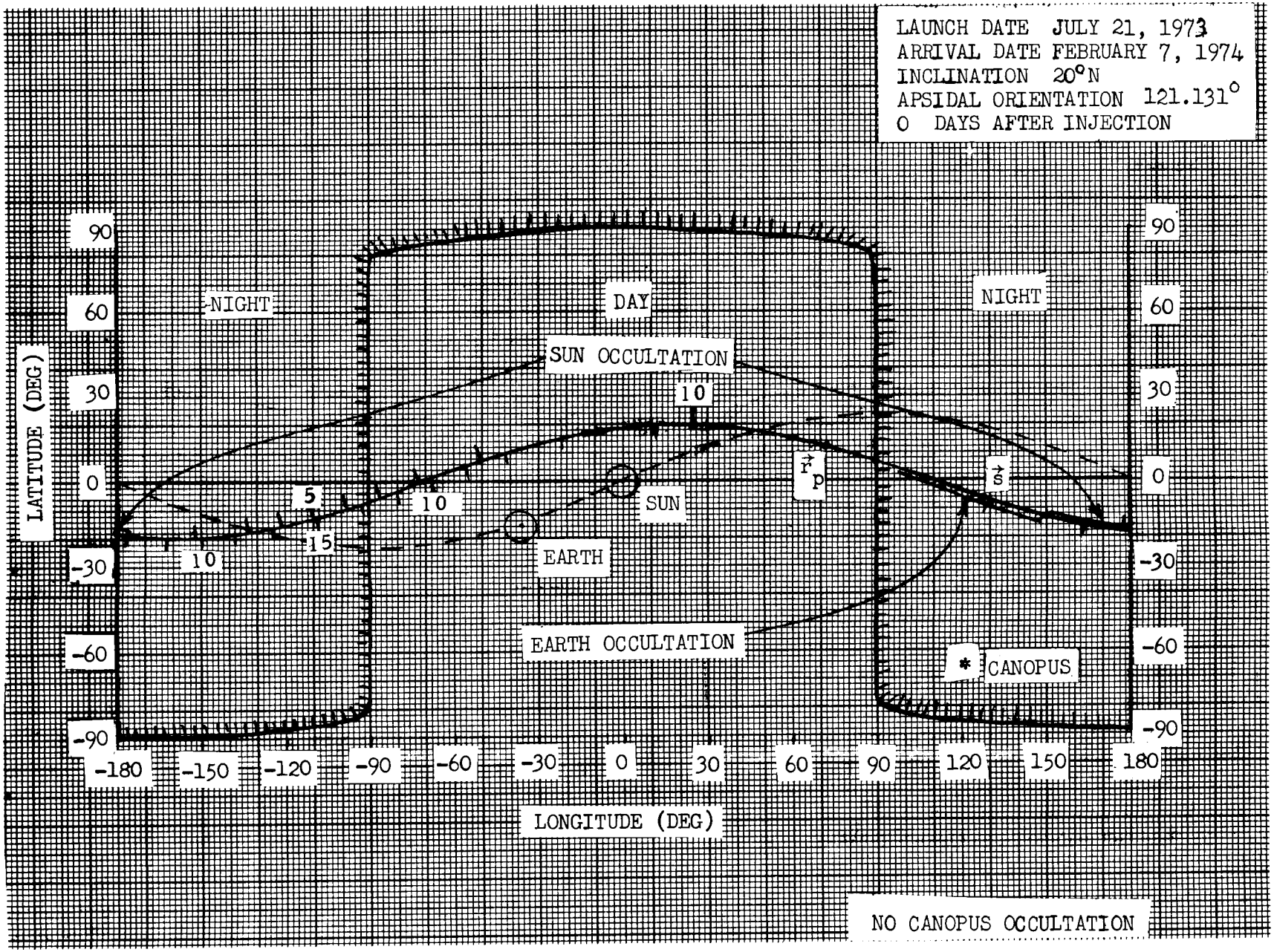
LAUNCH DATE JULY 21, 1973
ARRIVAL DATE FEBRUARY 7, 1974
INCLINATION 20°N
APSIDAL ORIENTATION 121.131°
0 DAYS AFTER INJECTION
NIGHT
DAY
NIGHT
SUN OCCULTATION
10
5
10
15
10
SUN
EARTH
EARTH OCCULTATION
CANOPUS
NO CANOPUS OCCULTATION
LATITUDE (DEG)
LONGITUDE (DEG)
90
60
30
0
-30
-60
-90
-180
-150
-120
-90
-60
-30
0
30
60
90
120
150
180

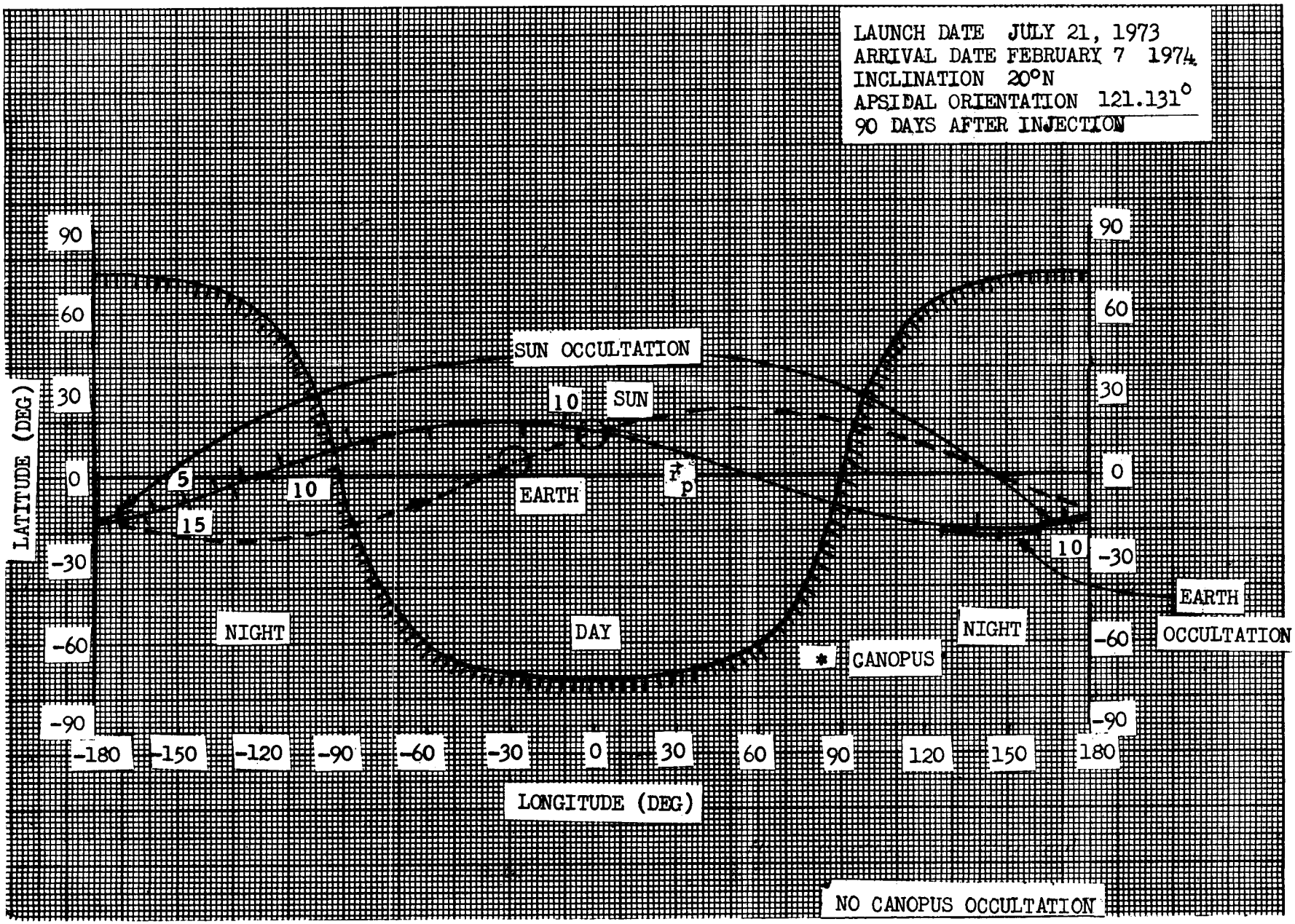
LAUNCH DATE JULY 21, 1973
ARRIVAL DATE FEBRUARY 7 1974
INCLINATION 20°N
APSIDAL ORIENTATION 121.131°
90 DAYS AFTER INJECTION
LATITUDE (DEG)
90
60
30
0
-30
-60
-90
SUN OCCULTATION
10
SUN
5
10
15
EARTH
NIGHT
DAY
NIGHT
CANOPUS
EARTH
OCCULTATION
-180
-150
-120
-90
-60
-30
0
30
60
90
120
150
180
LONGITUDE (DEG)
NO CANOPUS OCCULTATION

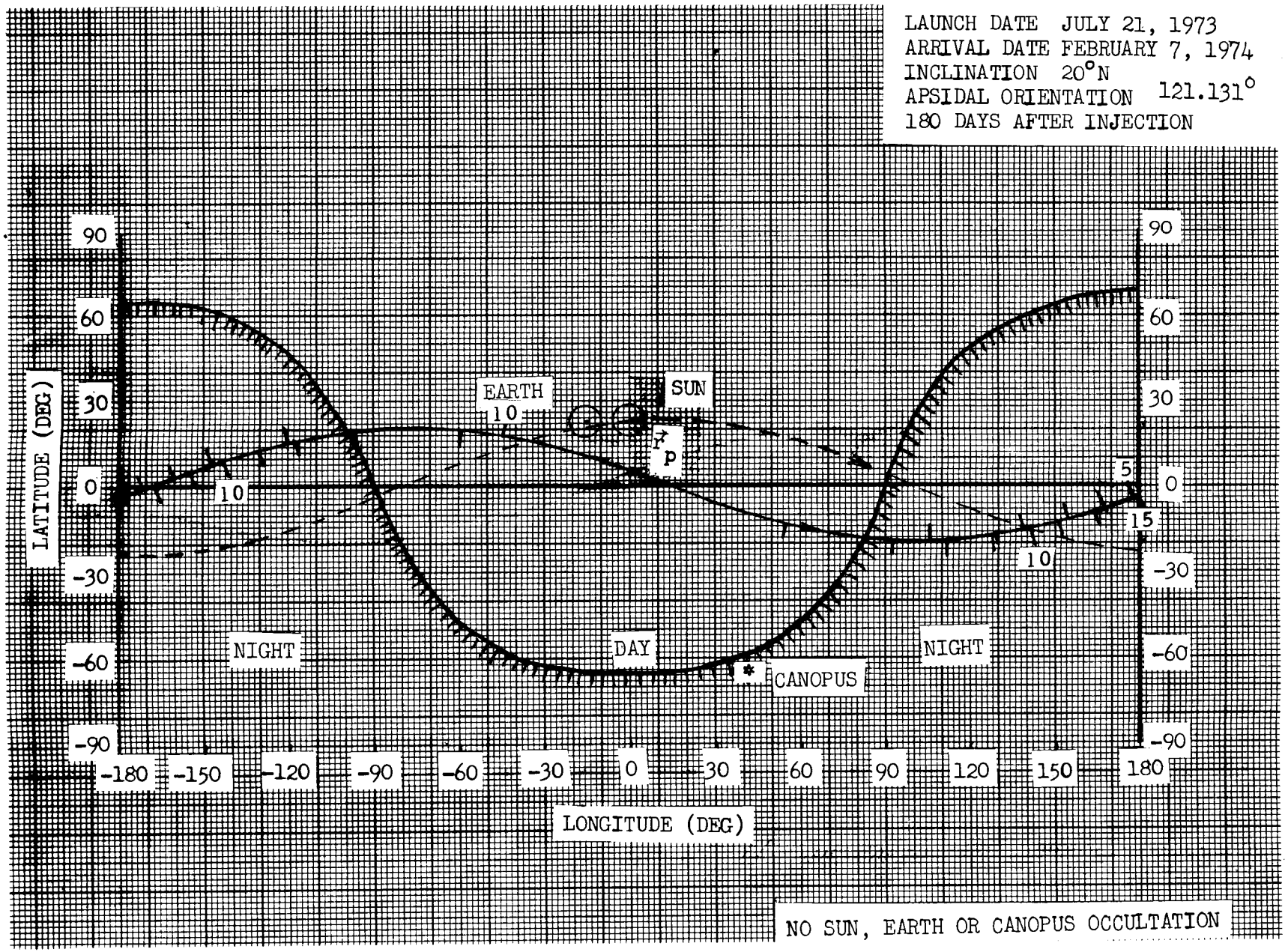
LAUNCH DATE JULY 21, 1973
ARRIVAL DATE FEBRUARY 7, 1974
INCLINATION 20°N
APSIDAL ORIENTATION 121.131°
180 DAYS AFTER INJECTION
LATITUDE (DEG)
90
60
30
0
-30
-60
-90
EARTH
SUN
10
10
5
15
10
NIGHT
DAY
NIGHT
CANOPUS
-180
-150
-120
-90
-60
-30
0
30
60
90
120
150
180
LONGITUDE (DEG)
NO SUN, EARTH OR CANOPUS OCCULTATION

CASE NO. 3

1000 x 15,000 km

$i = 40^{\circ}S$

$\Psi = 121.131$ deg

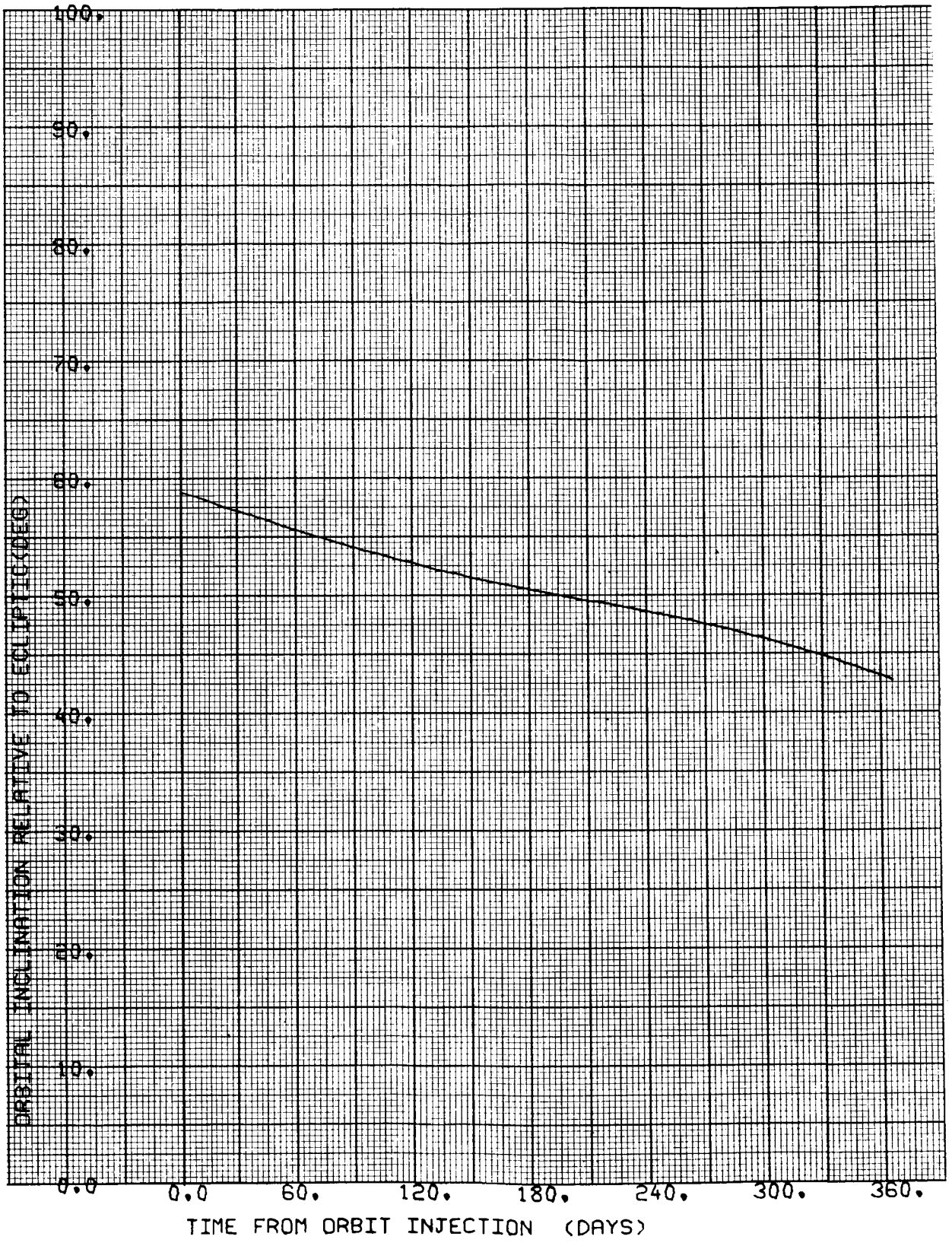
100.
90.
80.
70.
60.
50.
40.
30.
20.
10.
0.0
ORBITAL INCLINATION RELATIVE TO ECLIPTIC(DEG)
0.0
60.
120.
180.
240.
300.
360.
TIME FROM ORBIT INJECTION (DAYS)

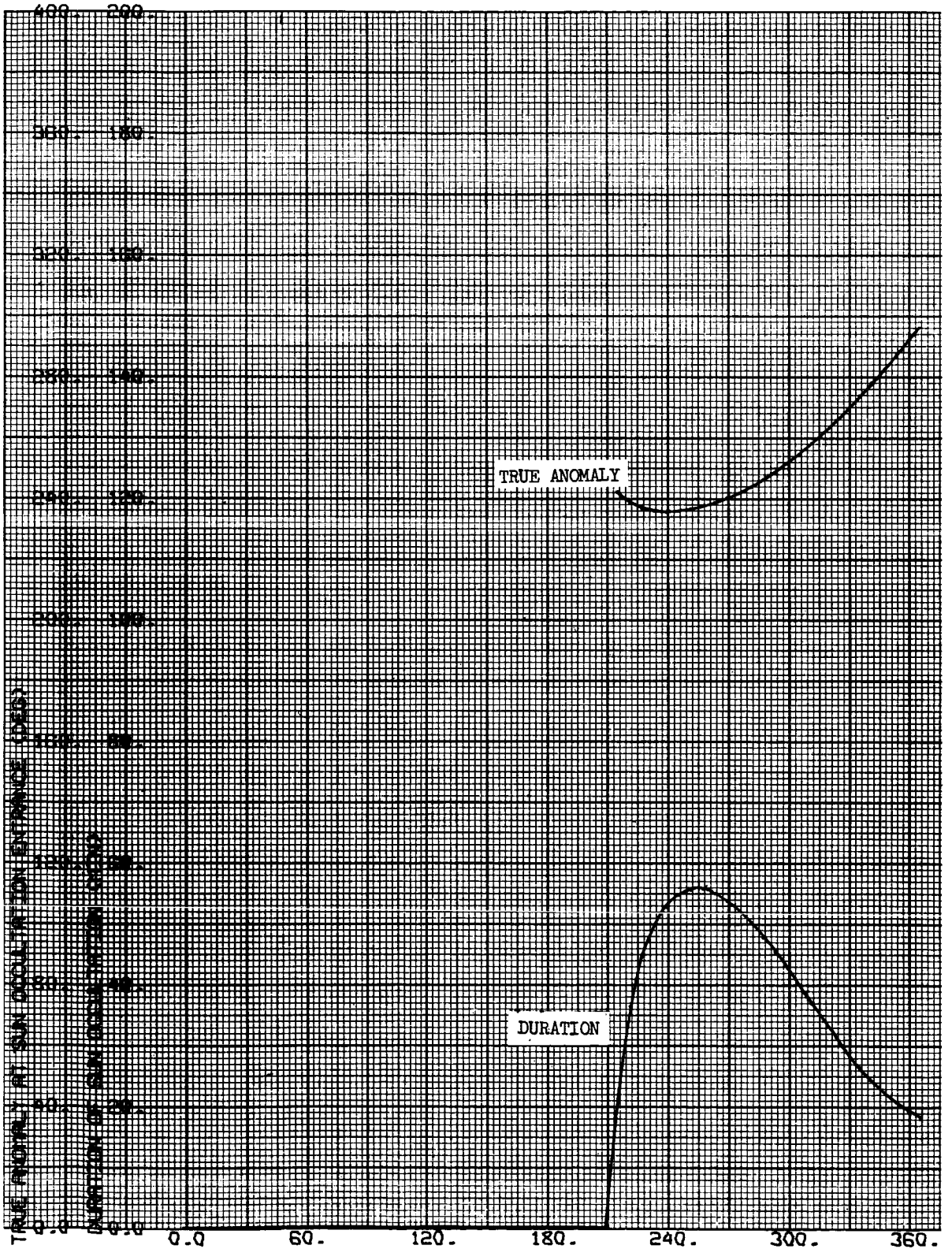
TRUE ANOMALY
DURATION
TRUE ANOMALY AT SUN OCCULTATION ENTRANCE (DEG)
DURATION OF OCCULTATION (DAYS)
0.0
60.
120.
180.
240.
300.
360.
TIME FROM INJECTION (DAYS)

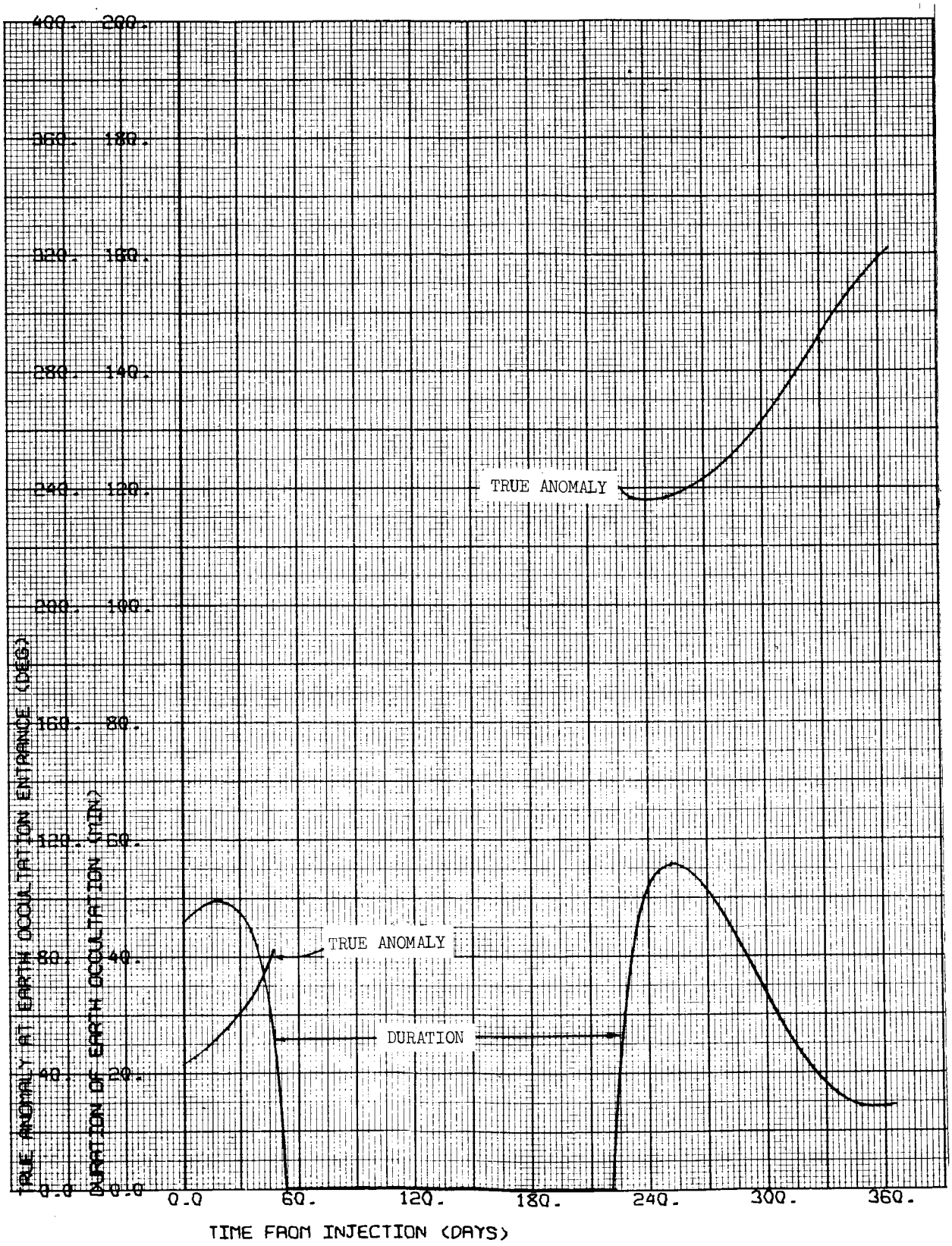
TRUE ANOMALY
TRUE ANOMALY
DURATION
TRUE ANOMALY AT EARTH OCCULTATION ENTRANCE (DEG)
DURATION OF EARTH OCCULTATION (MIN)
TIME FROM INJECTION (DAYS)
0.0
60.
120.
180.
240.
300.
360.
400.
360.
320.
280.
240.
200.
160.
120.
80.
40.
0.0
200.
180.
160.
140.
120.
100.
80.
60.
40.
20.
0.0

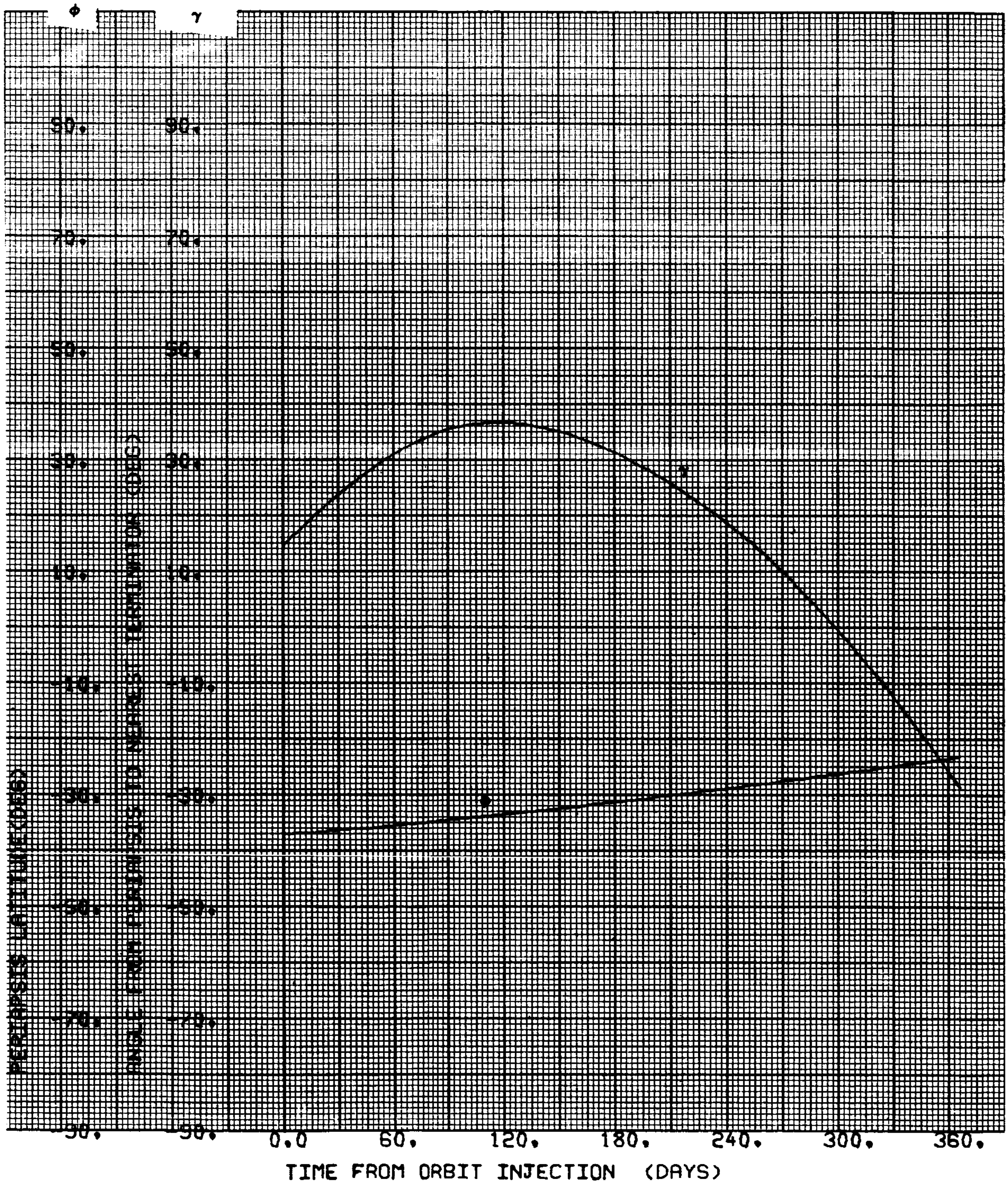

φ
γ
90.
90.
70.
70.
50.
50.
30.
30.
10.
10.
-10.
-10.
-30.
-30.
-50.
-50.
-70.
-70.
-90.
-90.
PERIAPSIS LATITUDE (DEG)
ANGLE FROM PERIAPSIS TO NEAREST TERMINATOR (DEG)
0.0
60.
120.
180.
240.
300.
360.
TIME FROM ORBIT INJECTION (DAYS)

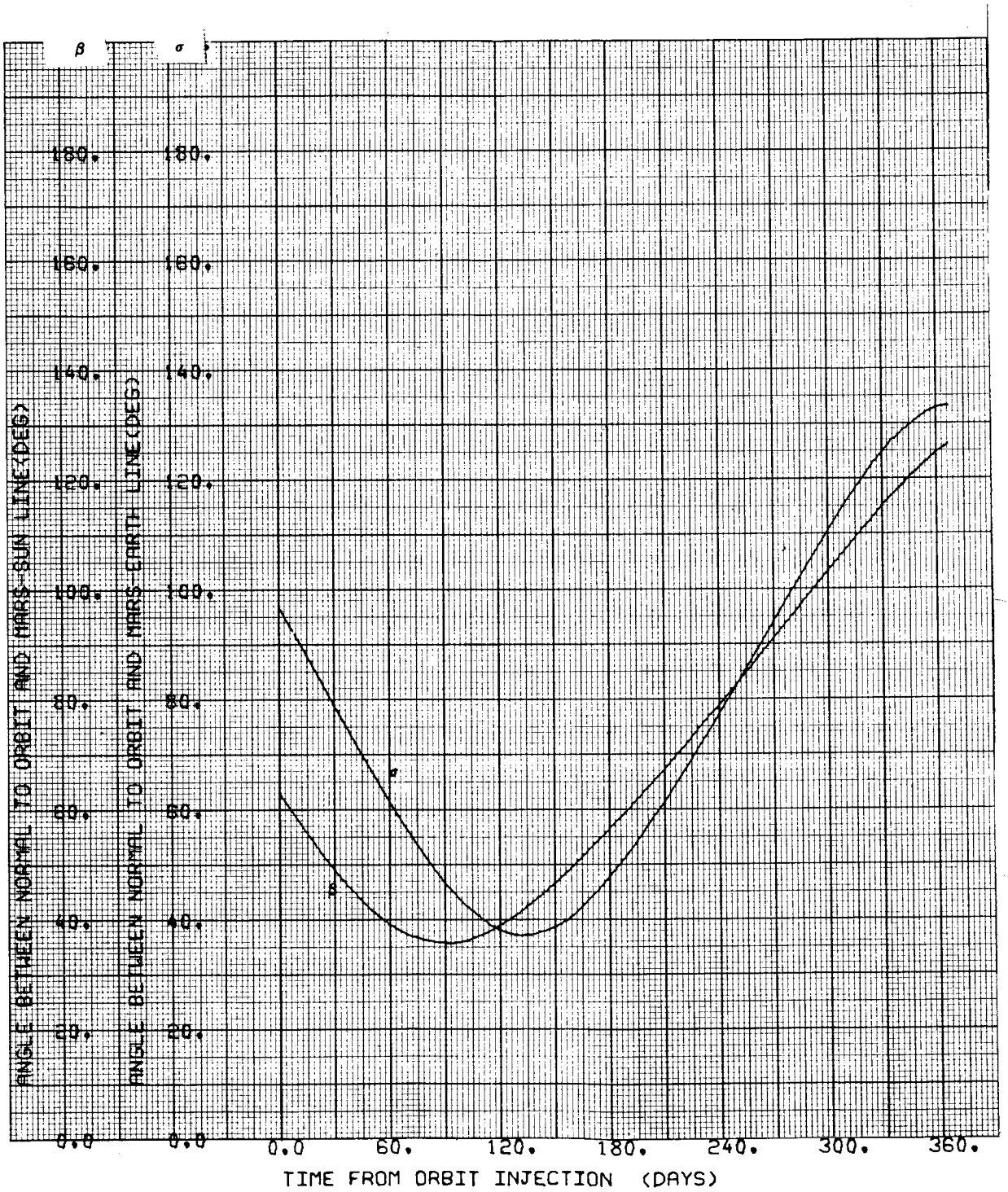
β
σ
180.
160.
140.
120.
100.
80.
60.
40.
20.
0.0
ANGLE BETWEEN NORMAL TO ORBIT AND MARS-SUN LINE(DEG)
ANGLE BETWEEN NORMAL TO ORBIT AND MARS-EARTH LINE(DEG)
0.0
60.
120.
180.
240.
300.
360.
TIME FROM ORBIT INJECTION (DAYS)

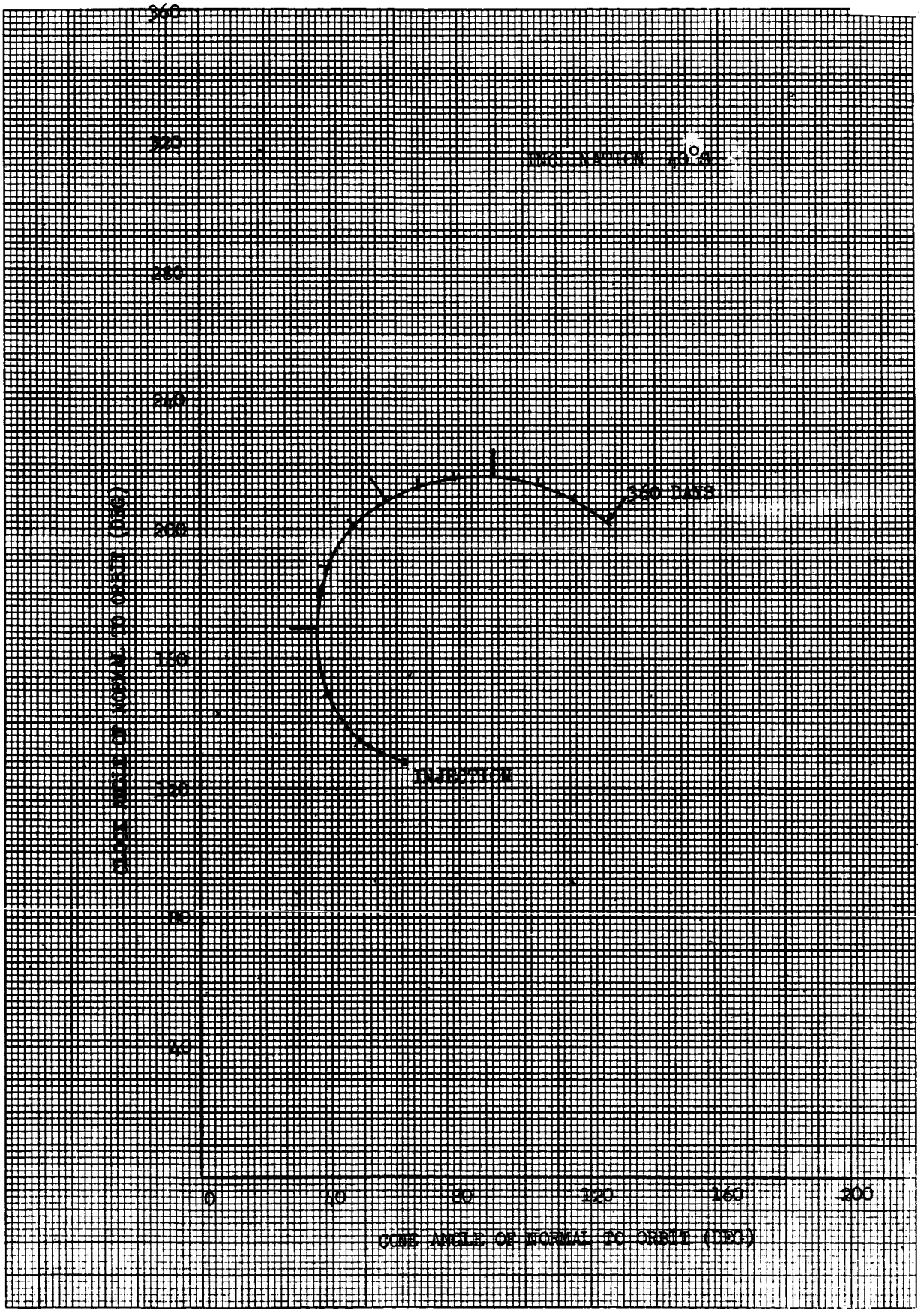
360
320
280
240
200
160
120
80
40
TMC DURATION 40 S
320 DAYS
DURATION
0
40
80
120
160
200
CONE ANGLE OF NORMAL TO ORBIT (DEG)

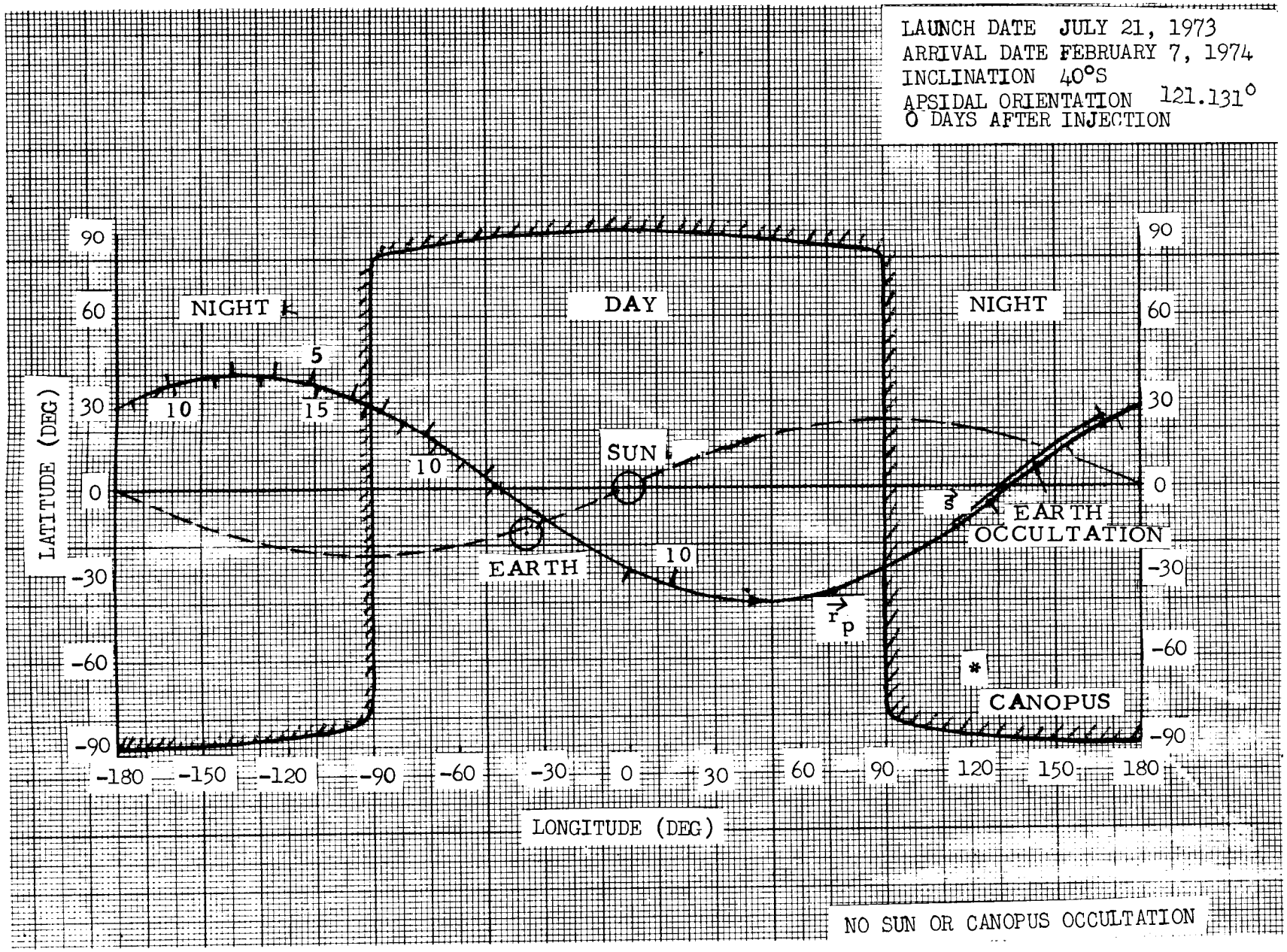
LAUNCH DATE JULY 21, 1973
ARRIVAL DATE FEBRUARY 7, 1974
INCLINATION 40°S
APSIDAL ORIENTATION 121.131°
0 DAYS AFTER INJECTION
NIGHT
DAY
NIGHT
SUN
EARTH
EARTH OCCULTATION
CANOPUS
LATITUDE (DEG)
LONGITUDE (DEG)
90
60
30
0
-30
-60
-90
-180
-150
-120
-90
-60
-30
0
30
60
90
120
150
180
5
10
15
10
10
NO SUN OR CANOPUS OCCULTATION

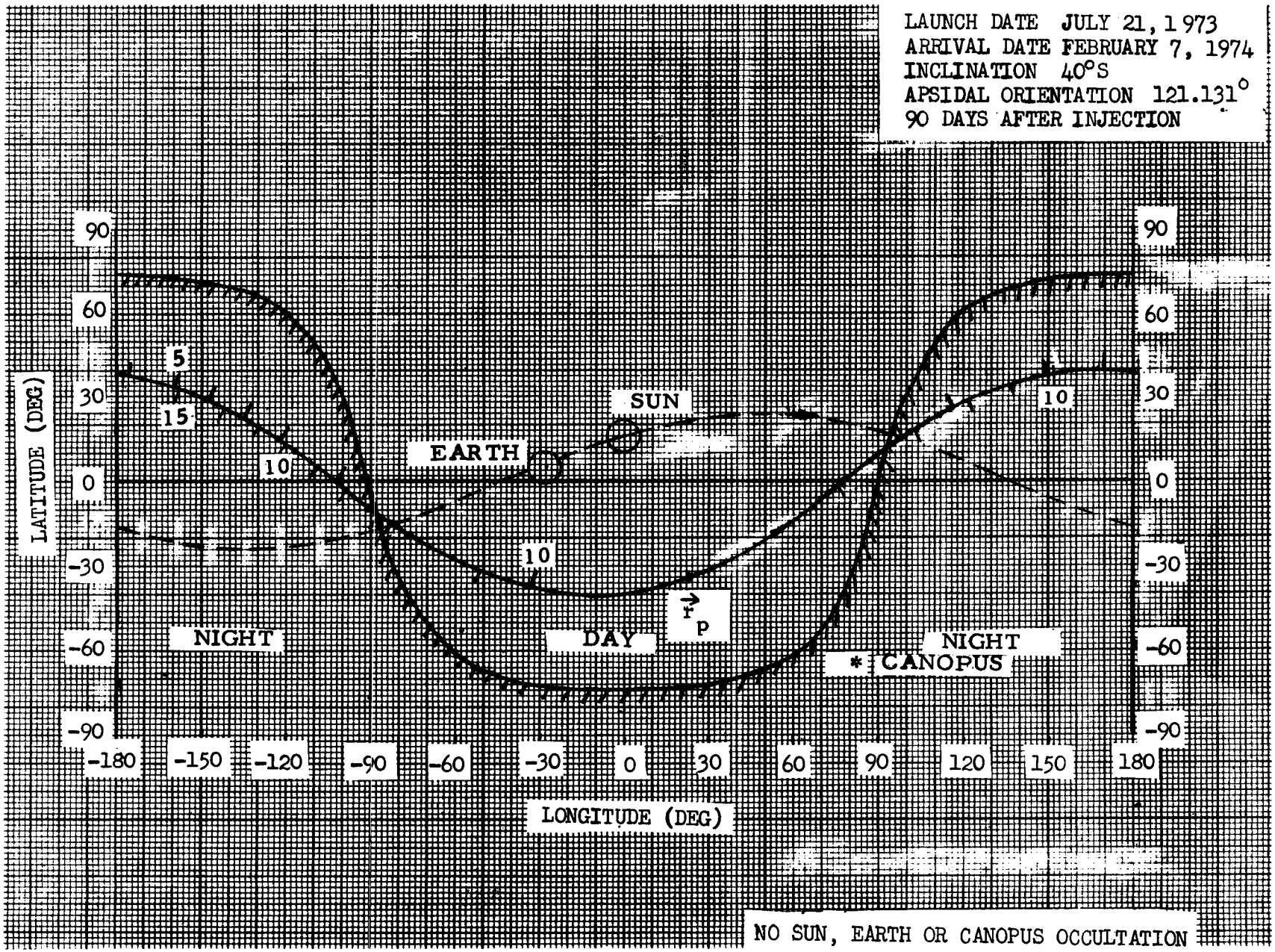
LAUNCH DATE JULY 21, 1973
ARRIVAL DATE FEBRUARY 7, 1974
INCLINATION 40°S
APSIDAL ORIENTATION 121.131°
90 DAYS AFTER INJECTION
LATITUDE (DEG)
90
60
30
0
-30
-60
-90
5
15
10
10
10
SUN
EARTH
NIGHT
DAY
r_p
NIGHT
* CANOPUS
-180
-150
-120
-90
-60
-30
0
30
60
90
120
150
180
LONGITUDE (DEG)
NO SUN, EARTH OR CANOPUS OCCULTATION

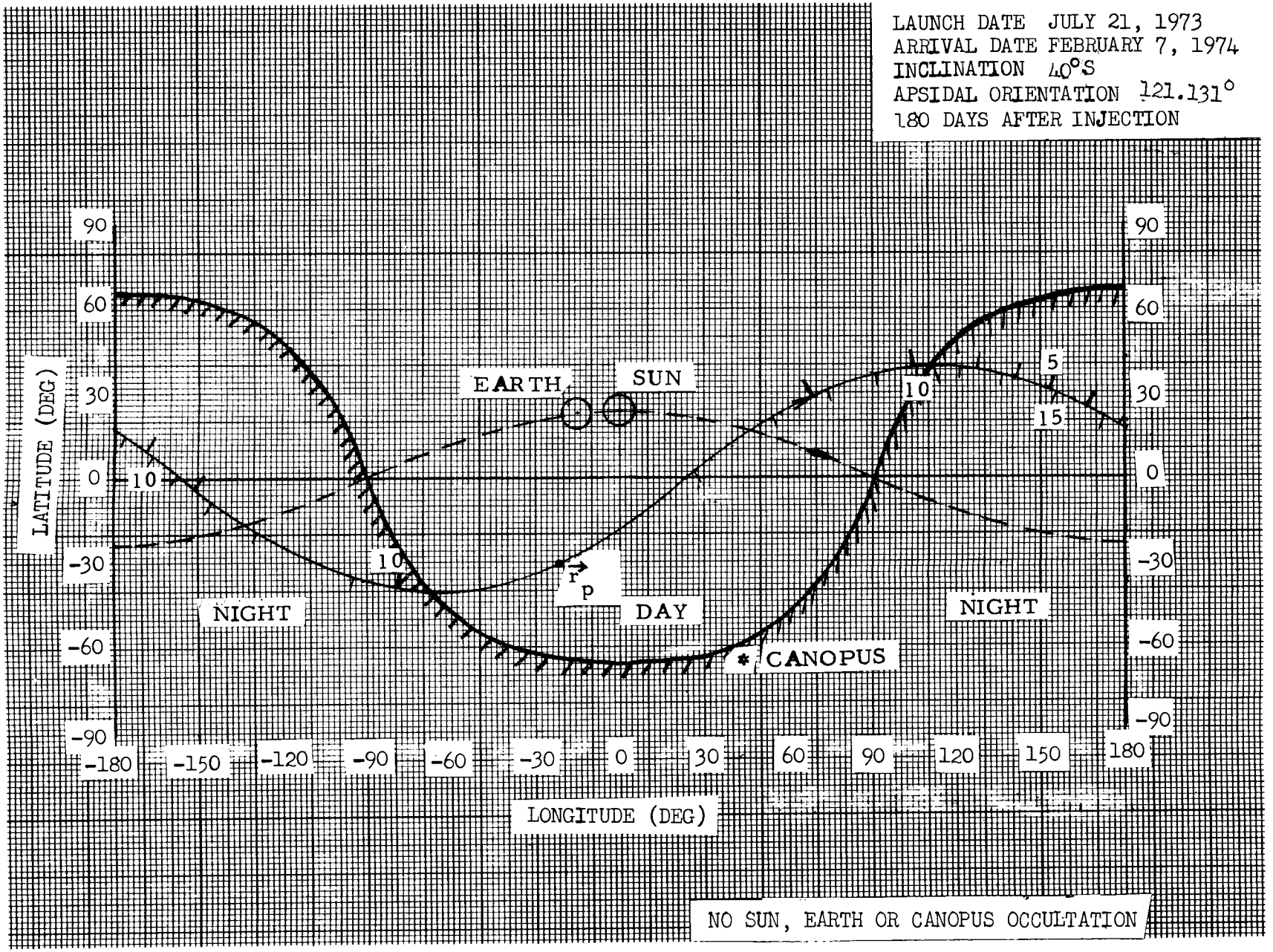
LAUNCH DATE JULY 21, 1973
ARRIVAL DATE FEBRUARY 7, 1974
INCLINATION 40°S
APSIDAL ORIENTATION 121.131°
180 DAYS AFTER INJECTION
LATITUDE (DEG)
90
60
30
0
-30
-60
-90
EARTH
SUN
10
5
15
10
10
$\vec{r}_p$
NIGHT
DAY
NIGHT
CANOPUS
-180
-150
-120
-90
-60
-30
0
30
60
90
120
150
180
LONGITUDE (DEG)
NO SUN, EARTH OR CANOPUS OCCULTATION

CASE NO. 4

1000 x 15, 000 km

$i = 40^{o}N$

$\Psi = 121.131$ deg

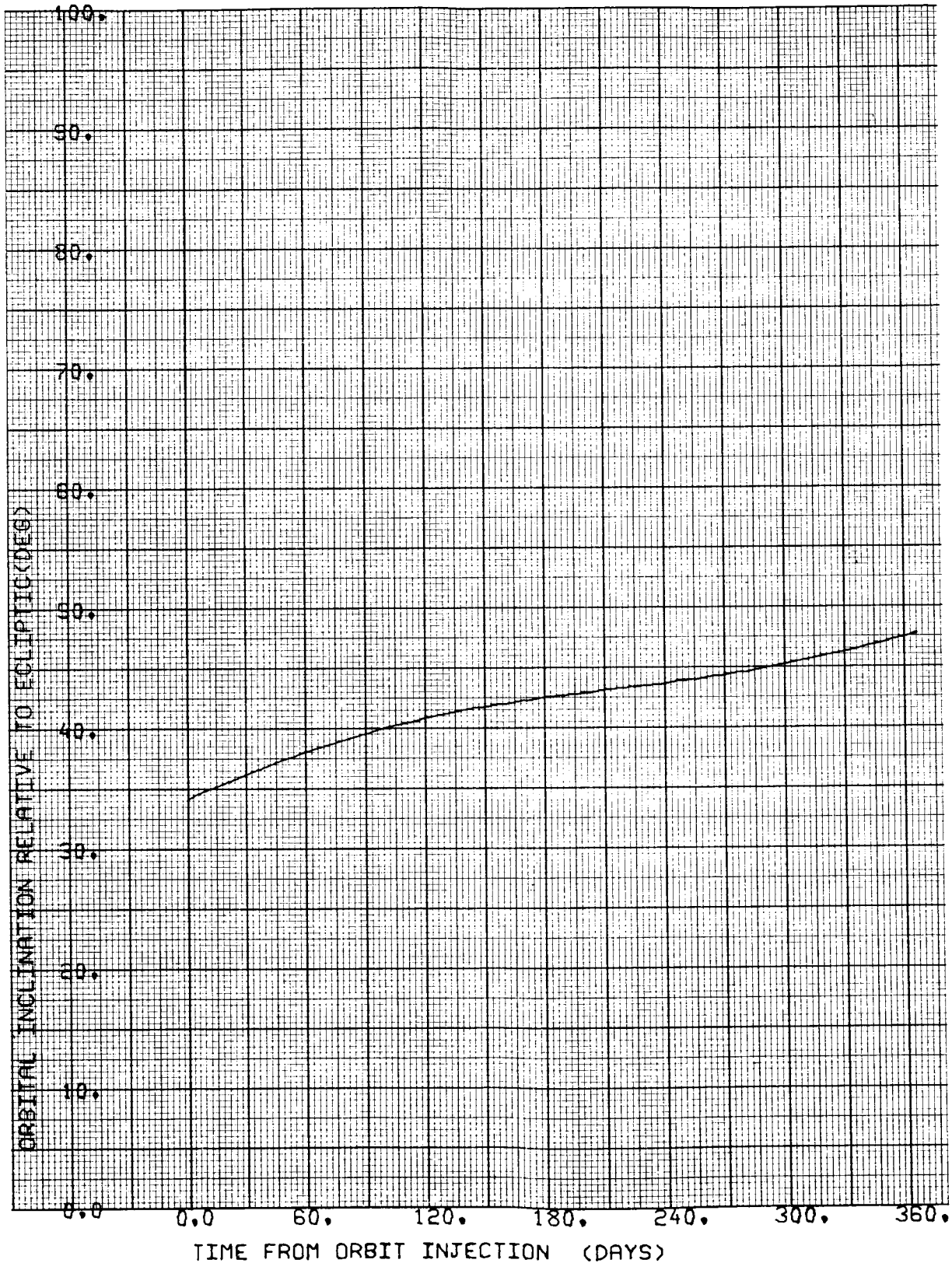
100.
90.
80.
70.
60.
50.
40.
30.
20.
10.
0.0
ORBITAL INCLINATION RELATIVE TO ECLIPTIC(DEG)
0.0
60.
120.
180.
240.
300.
360.
TIME FROM ORBIT INJECTION (DAYS)

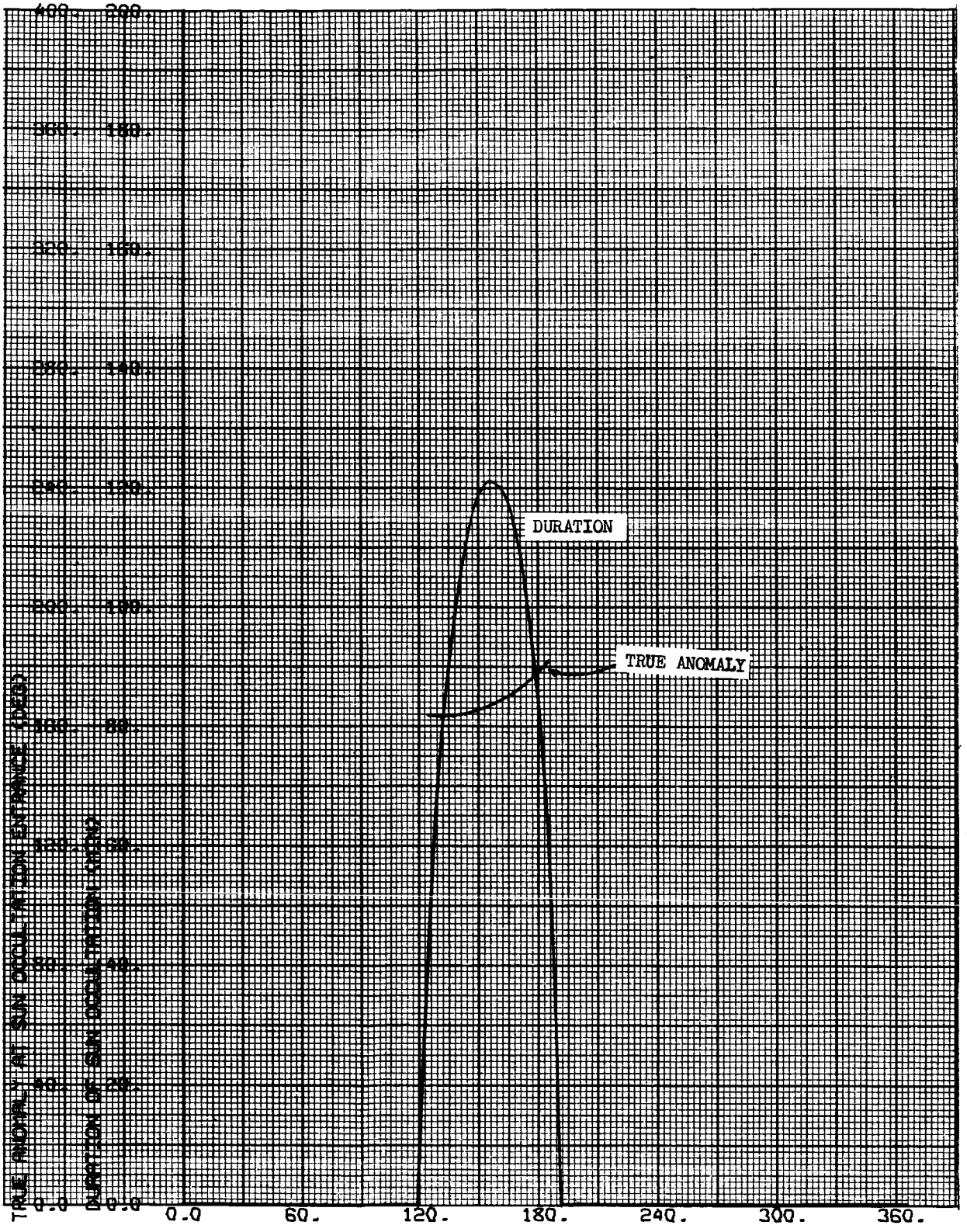
DURATION
TRUE ANOMALY
TRUE ANOMALY AT SUN OCCULTATION ENTRANCE (DEG)
DURATION OF SUN OCCULTATION (DEG)
0.0
60.
120.
180.
240.
300.
360.
TIME FROM INJECTION (DAYS)

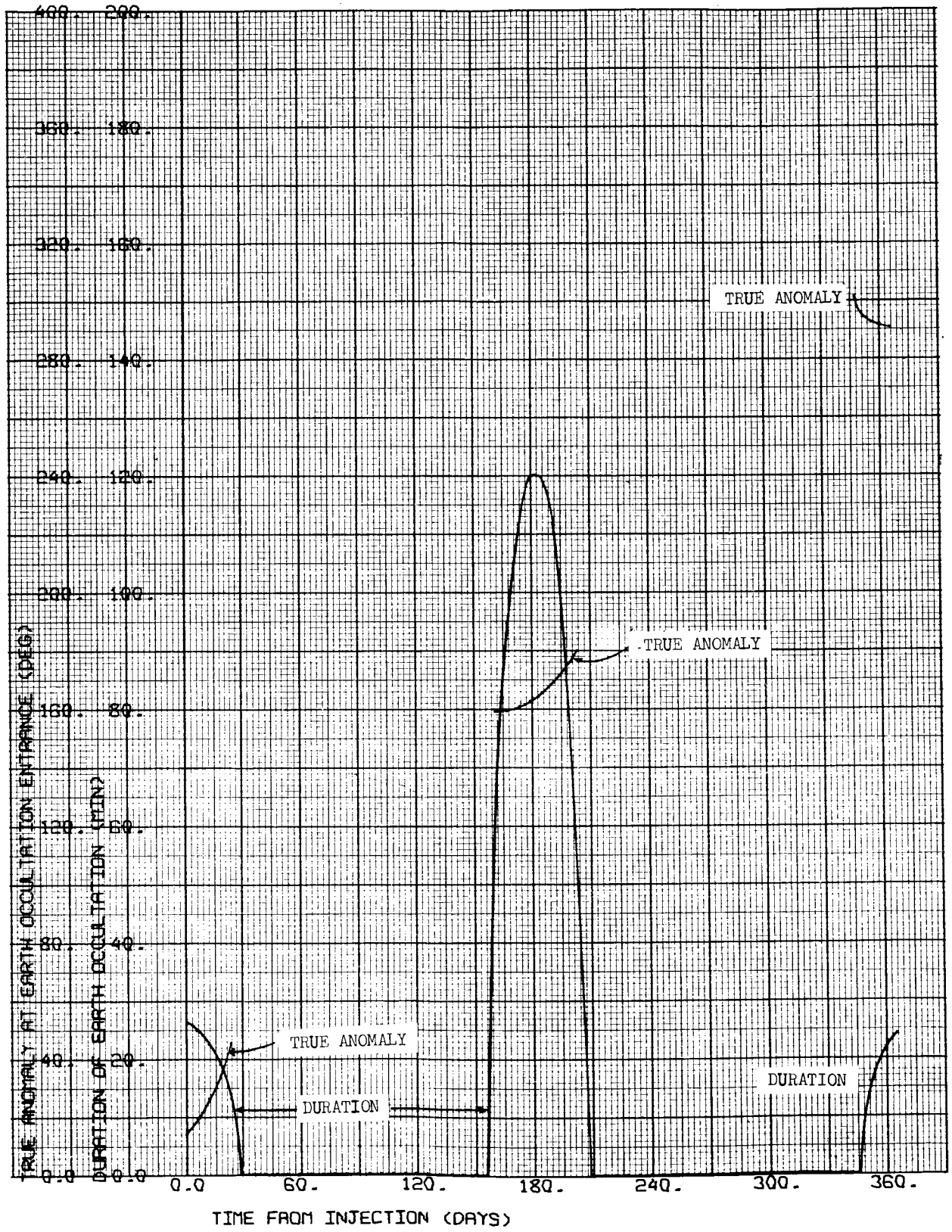
TRUE ANOMALY AT EARTH OCCULTATION ENTRANCE (DEG)
DURATION OF EARTH OCCULTATION (MIN)
TIME FROM INJECTION (DAYS)
TRUE ANOMALY
TRUE ANOMALY
TRUE ANOMALY
DURATION
DURATION
400.
360.
320.
280.
240.
200.
160.
120.
80.
40.
0.0
200.
180.
160.
140.
120.
100.
80.
60.
40.
20.
0.0
0.0
60.
120.
180.
240.
300.
360.

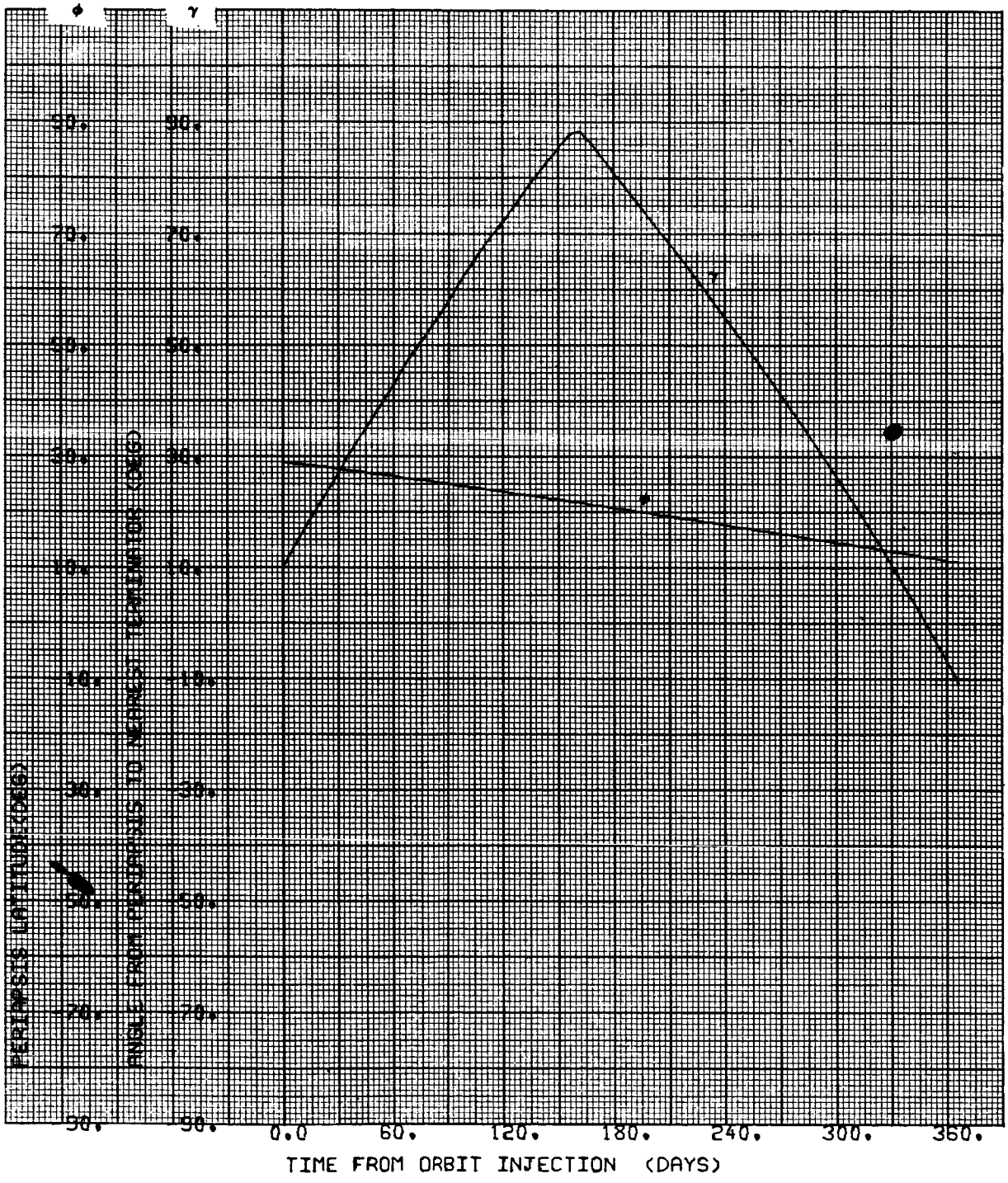
ϕ
γ
90.
70.
50.
30.
10.
-10.
-30.
-50.
-70.
-90.
0.0
60.
120.
180.
240.
300.
360.
PERIGEE LATITUDE (DEG)
ANGLE FROM PERIGEE TO VEHICLE TRAJECTORY (DEG)
TIME FROM ORBIT INJECTION (DAYS)

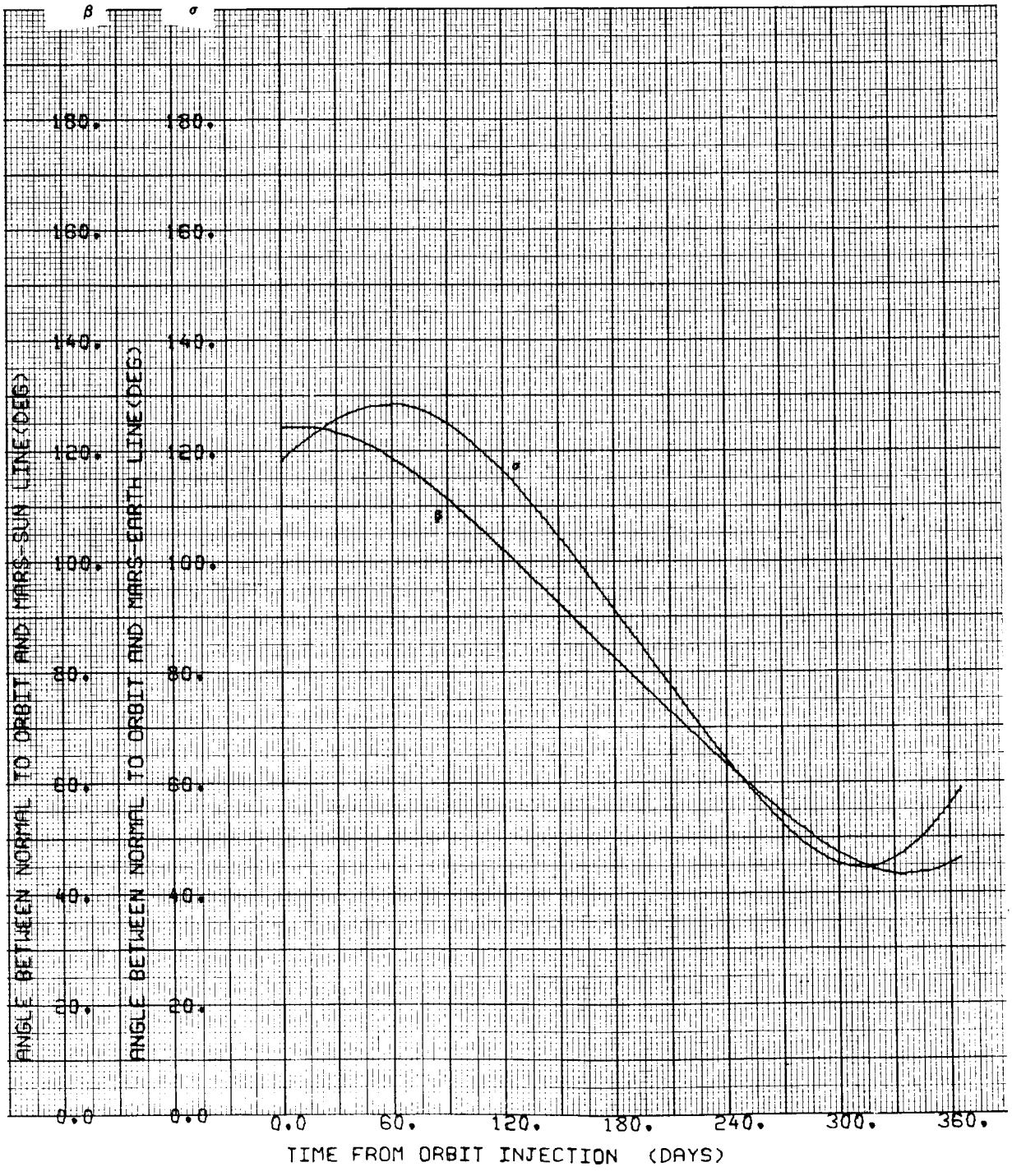
β
σ
180.
160.
140.
120.
100.
80.
60.
40.
20.
0.0
ANGLE BETWEEN NORMAL TO ORBIT AND MARS-SUN LINE(DEG)
ANGLE BETWEEN NORMAL TO ORBIT AND MARS-EARTH LINE(DEG)
0.0
60.
120.
180.
240.
300.
360.
TIME FROM ORBIT INJECTION (DAYS)

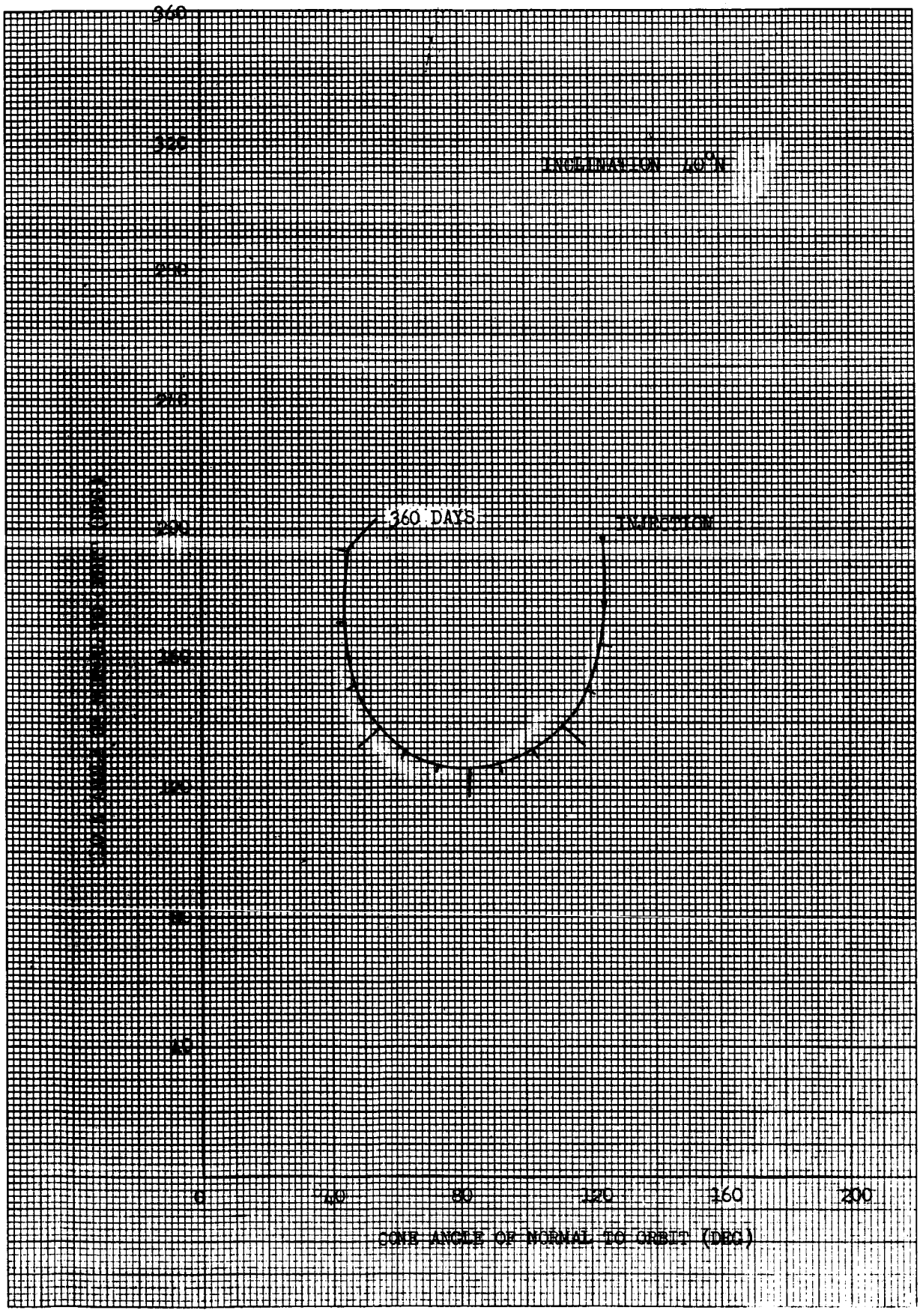
360
320
280
240
200
160
120
80
40
0
INCLINATION 40°N
360 DAYS
INJECTION
0
40
80
120
160
200
CONE ANGLE OF NORMAL TO ORBIT (DEG)

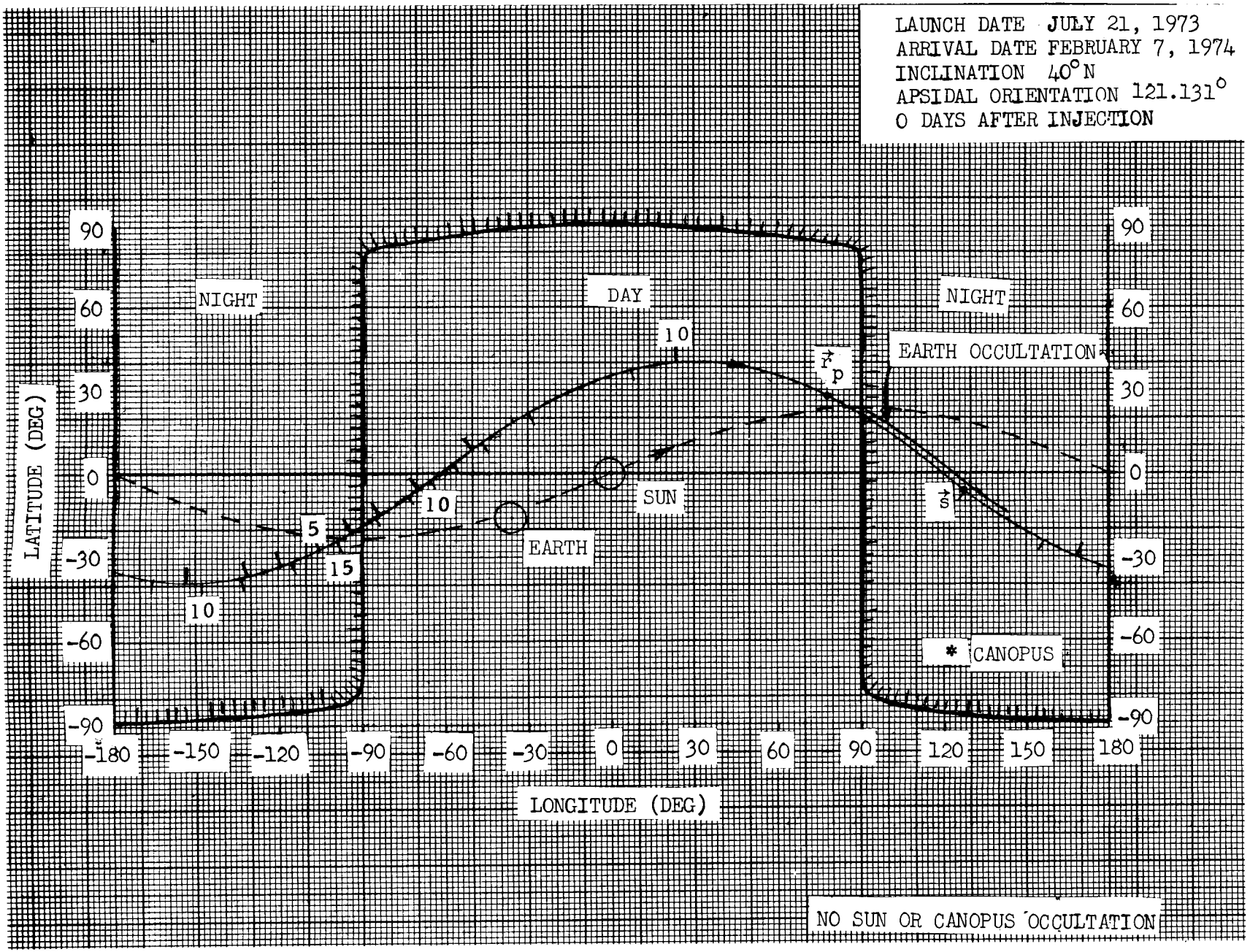
LAUNCH DATE JULY 21, 1973
ARRIVAL DATE FEBRUARY 7, 1974
INCLINATION 40°N
APSIDAL ORIENTATION 121.131°
0 DAYS AFTER INJECTION
NIGHT
DAY
NIGHT
EARTH OCCULTATION
SUN
EARTH
CANOPUS
LATITUDE (DEG)
LONGITUDE (DEG)
90
60
30
0
-30
-60
-90
-180
-150
-120
-90
-60
-30
0
30
60
90
120
150
180
10
10
5
15
10
NO SUN OR CANOPUS OCCULTATION

LAUNCH DATE JULY 21, 1973
ARRIVAL DATE FEBRUARY 7, 1974
INCLINATION 40° N
APSIDAL ORIENTATION 121.131°
90 DAYS AFTER INJECTION
LATITUDE (DEG)
LONGITUDE (DEG)
90
60
30
0
-30
-60
-90
-120
-150
-180
120
150
180
10
5
15
SUN
EARTH
CANOPUS
DAY
NIGHT
NIGHT
NO SUN, EARTH OR CANOPUS OCCULTATION

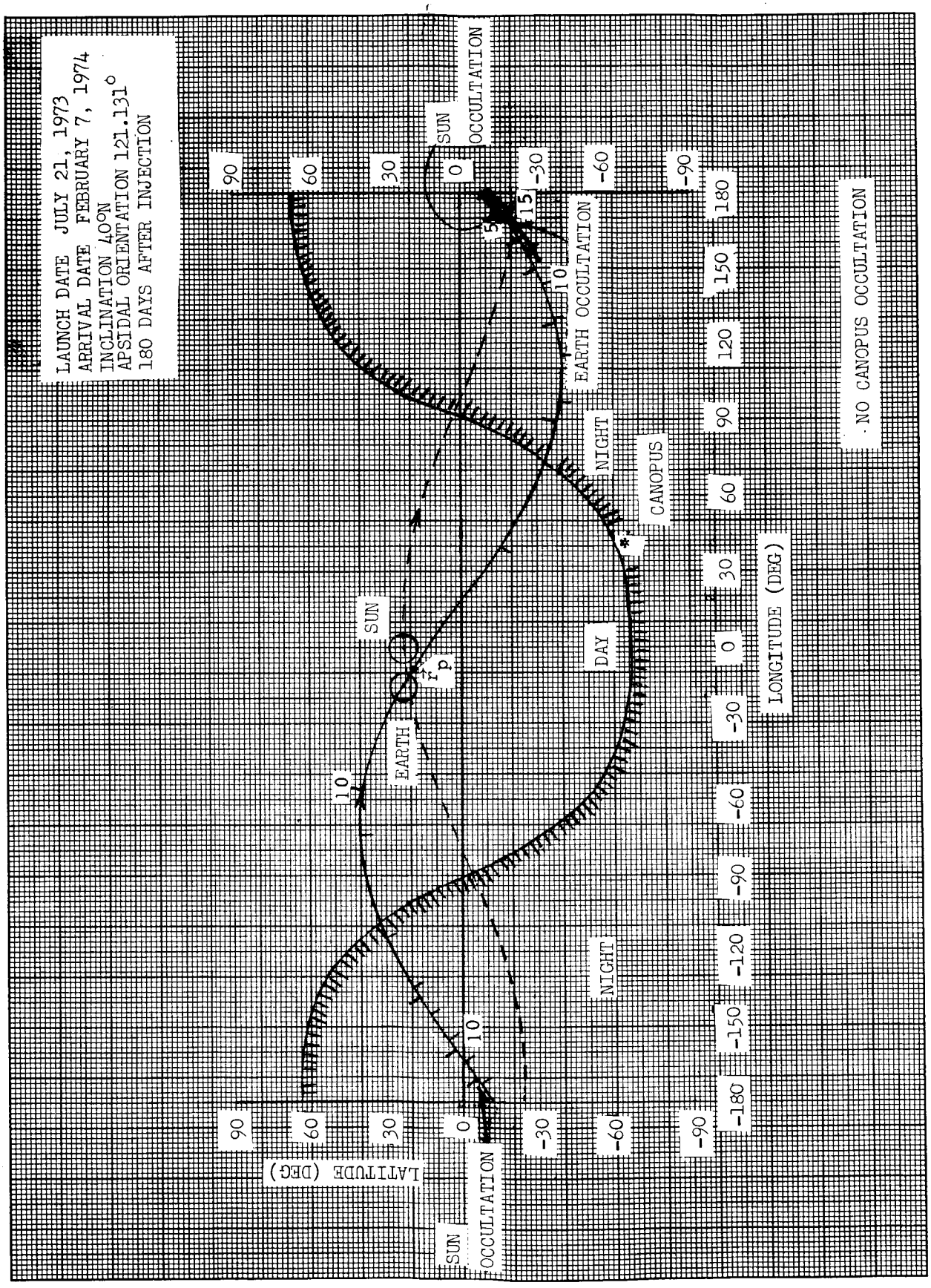
LAUNCH DATE JULY 21, 1973
ARRIVAL DATE FEBRUARY 7, 1974
INCLINATION 40°N
APSIDAL ORIENTATION 121.131°
180 DAYS AFTER INJECTION
LATITUDE (DEG)
90
60
30
0
-30
-60
-90
-180
-150
-120
-90
-60
-30
0
30
60
90
120
150
180
LONGITUDE (DEG)
SUN
OCCULTATION
EARTH
SUN
EARTH OCCULTATION
DAY
NIGHT
CANOPUS
NIGHT
NO CANOPUS OCCULTATION

CASE NO. 5

1000 x 15, 000 km

$i = 60^{\circ}S$

$\Psi = 121.131$ deg

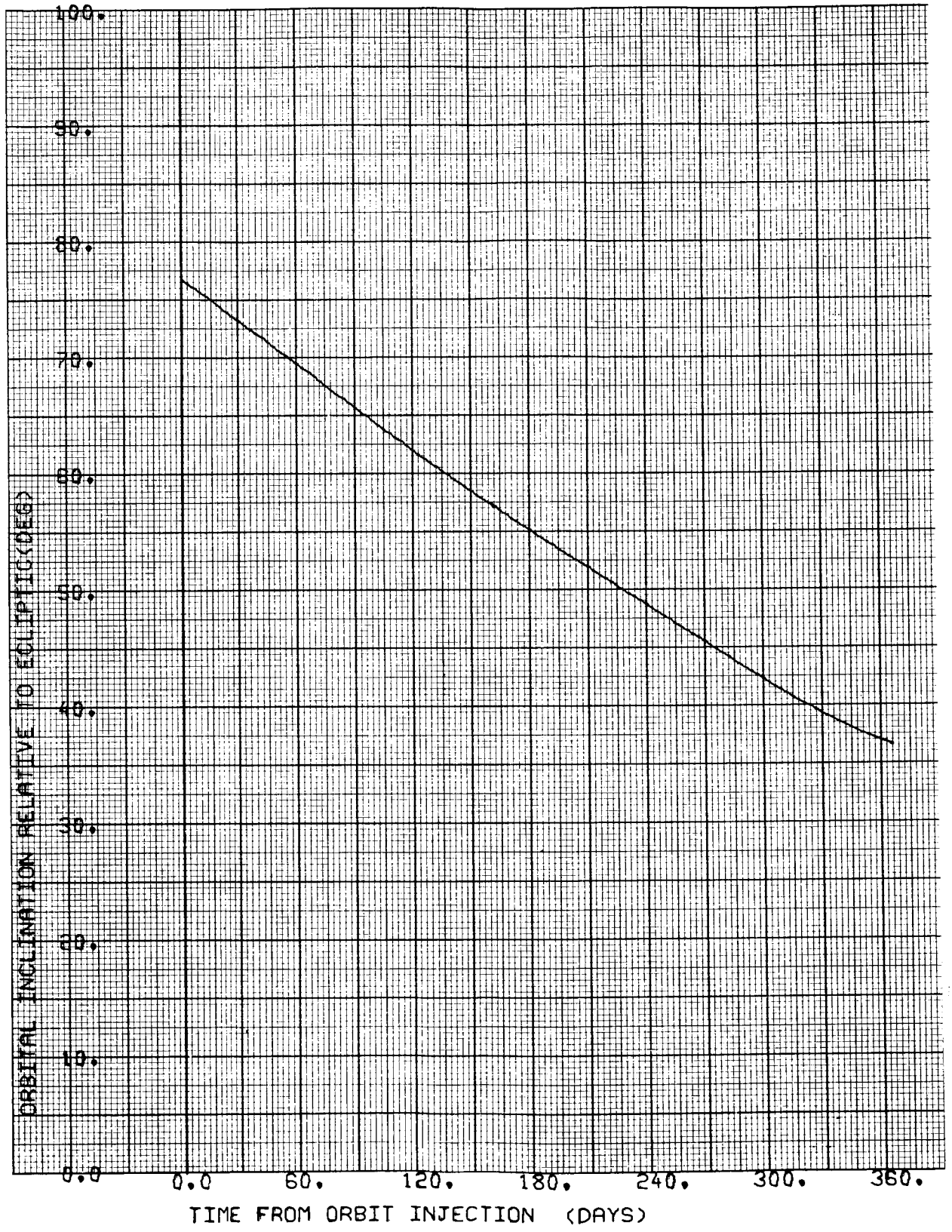
100.
90.
80.
70.
60.
50.
40.
30.
20.
10.
0.0
ORBITAL INCLINATION RELATIVE TO ECLIPTIC(DEG)
0.0
60.
120.
180.
240.
300.
360.
TIME FROM ORBIT INJECTION (DAYS)

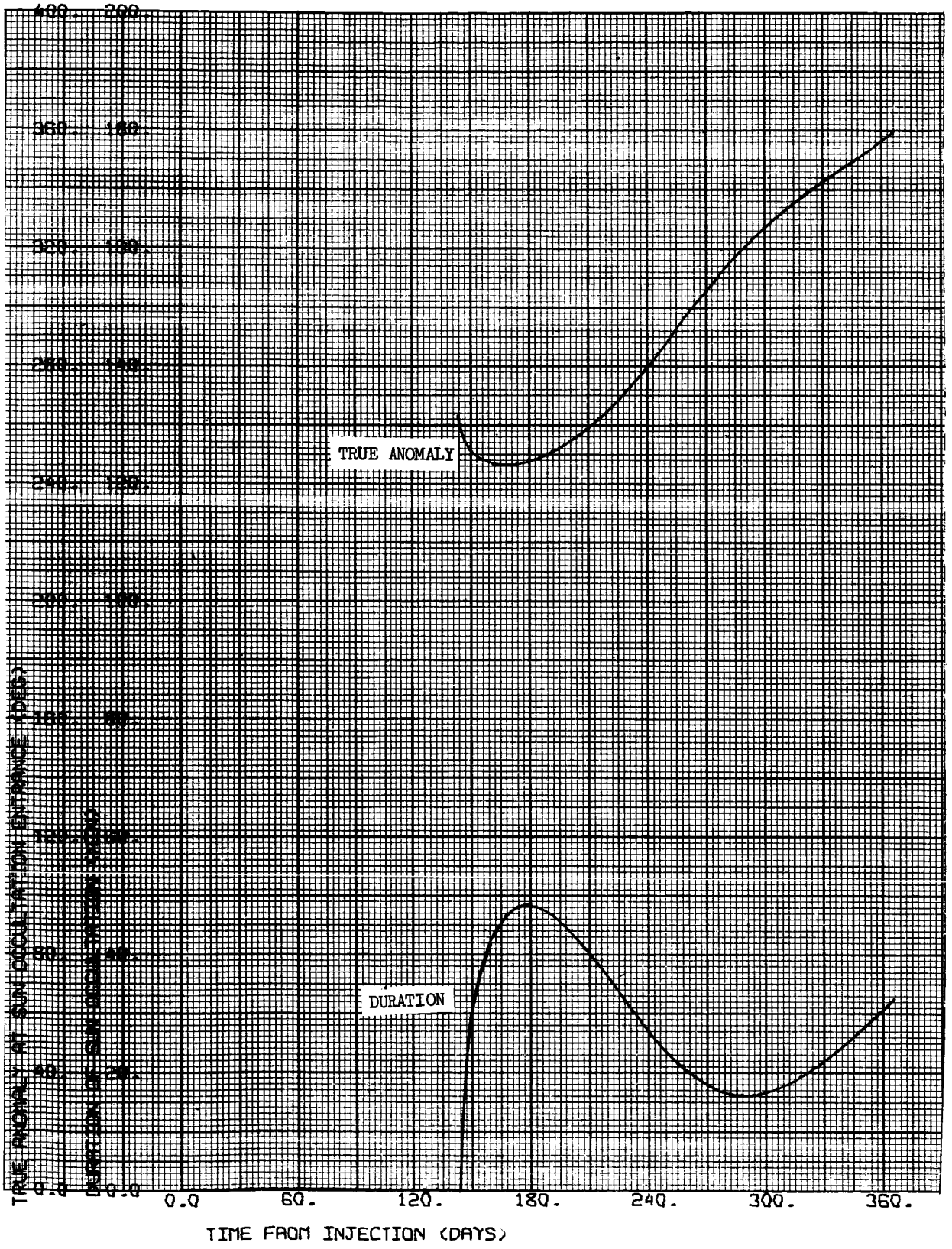
TRUE ANOMALY
DURATION
TRUE ANOMALY AT SUN OCCULTATION ENTRANCE (DEG)
DURATION OF SUN OCCULTATION (DAYS)
0.0
60.
120.
180.
240.
300.
360.
TIME FROM INJECTION (DAYS)

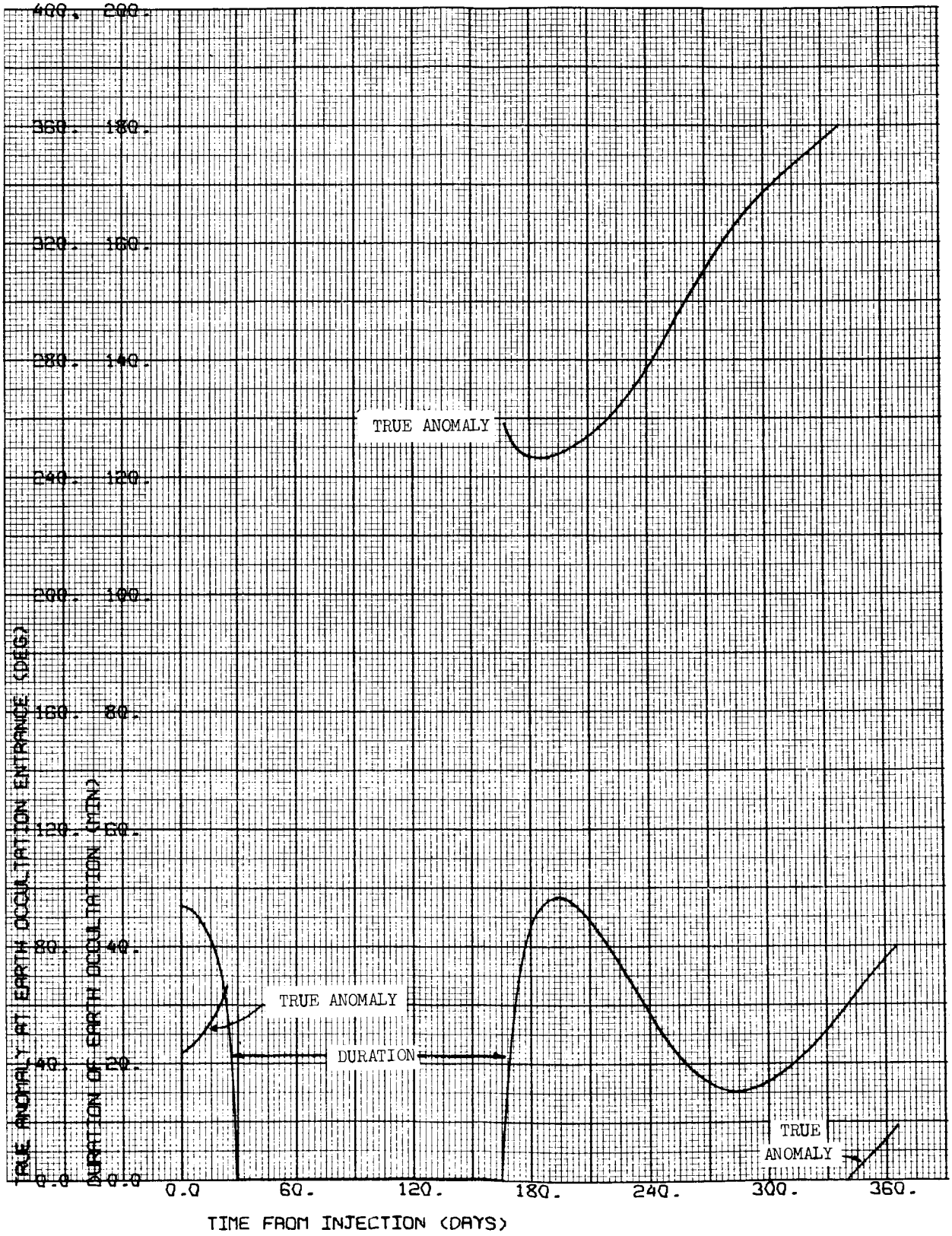
TRUE ANOMALY AT EARTH OCCULTATION ENTRANCE (DEG)
DURATION OF EARTH OCCULTATION (MIN)
TIME FROM INJECTION (DAYS)
TRUE ANOMALY
TRUE ANOMALY
DURATION
TRUE ANOMALY
400.
360.
320.
280.
240.
200.
160.
120.
80.
40.
0.0
200.
180.
160.
140.
120.
100.
80.
60.
40.
20.
0.0
0.0
60.
120.
180.
240.
300.
360.

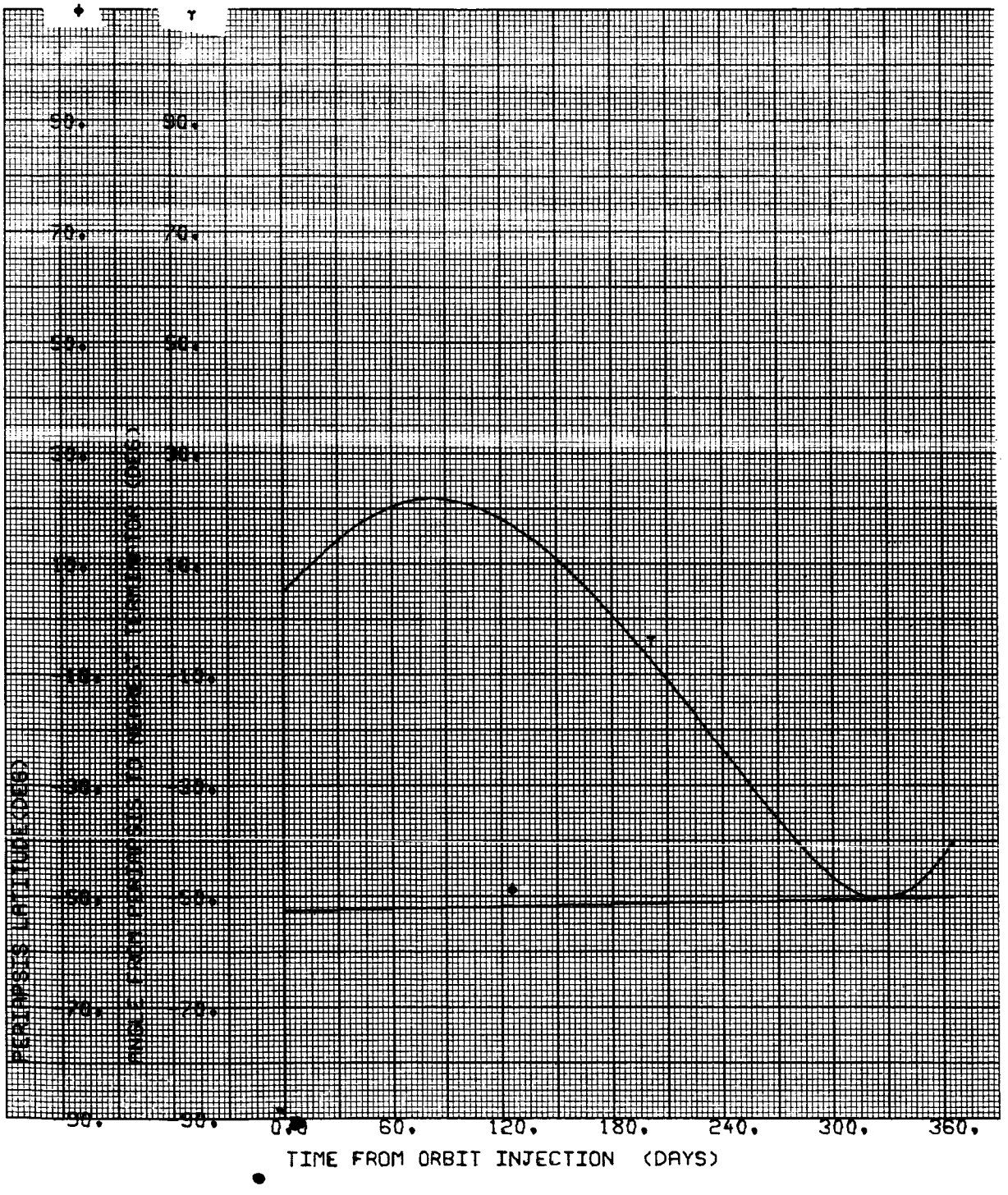
90.
70.
50.
30.
10.
-10.
-30.
-50.
-70.
-90.
0.0
60.
120.
180.
240.
300.
360.
PERIAPSIS LATITUDE (DEG)
TIME FROM ORBIT INJECTION (DAYS)

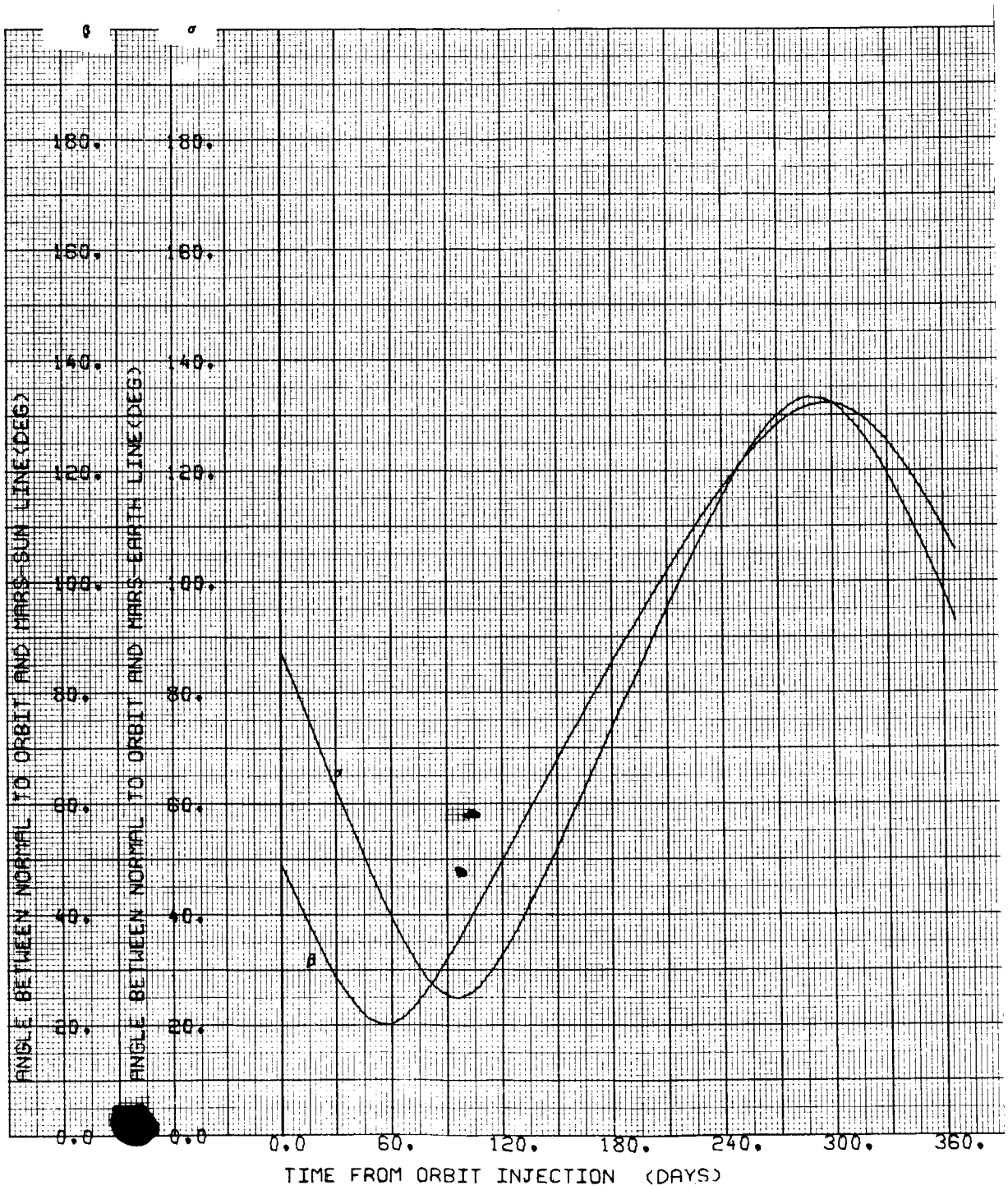
β
σ
180.
160.
140.
120.
100.
80.
60.
40.
20.
0.0
ANGLE BETWEEN NORMAL TO ORBIT AND MARS SUN LINE(DEG)
ANGLE BETWEEN NORMAL TO ORBIT AND MARS EARTH LINE(DEG)
0.0
60.
120.
180.
240.
300.
360.
TIME FROM ORBIT INJECTION (DAYS)

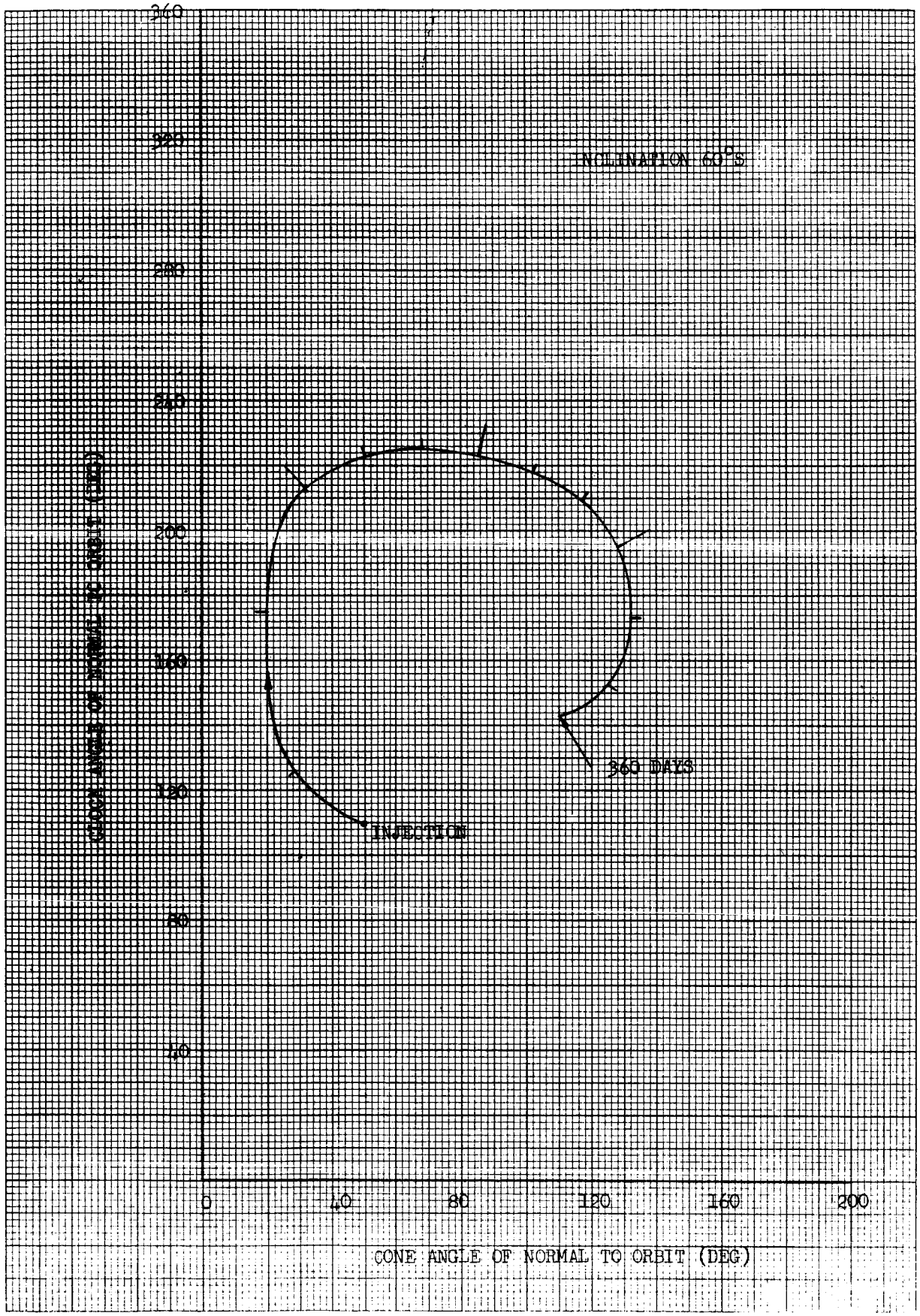
INCLINATION 60°S
360 DAYS
INJECTION
ALTITUDE (N MI)
CONE ANGLE OF NORMAL TO ORBIT (DEG)
360
320
280
240
200
160
120
80
40
0
40
80
120
160
200

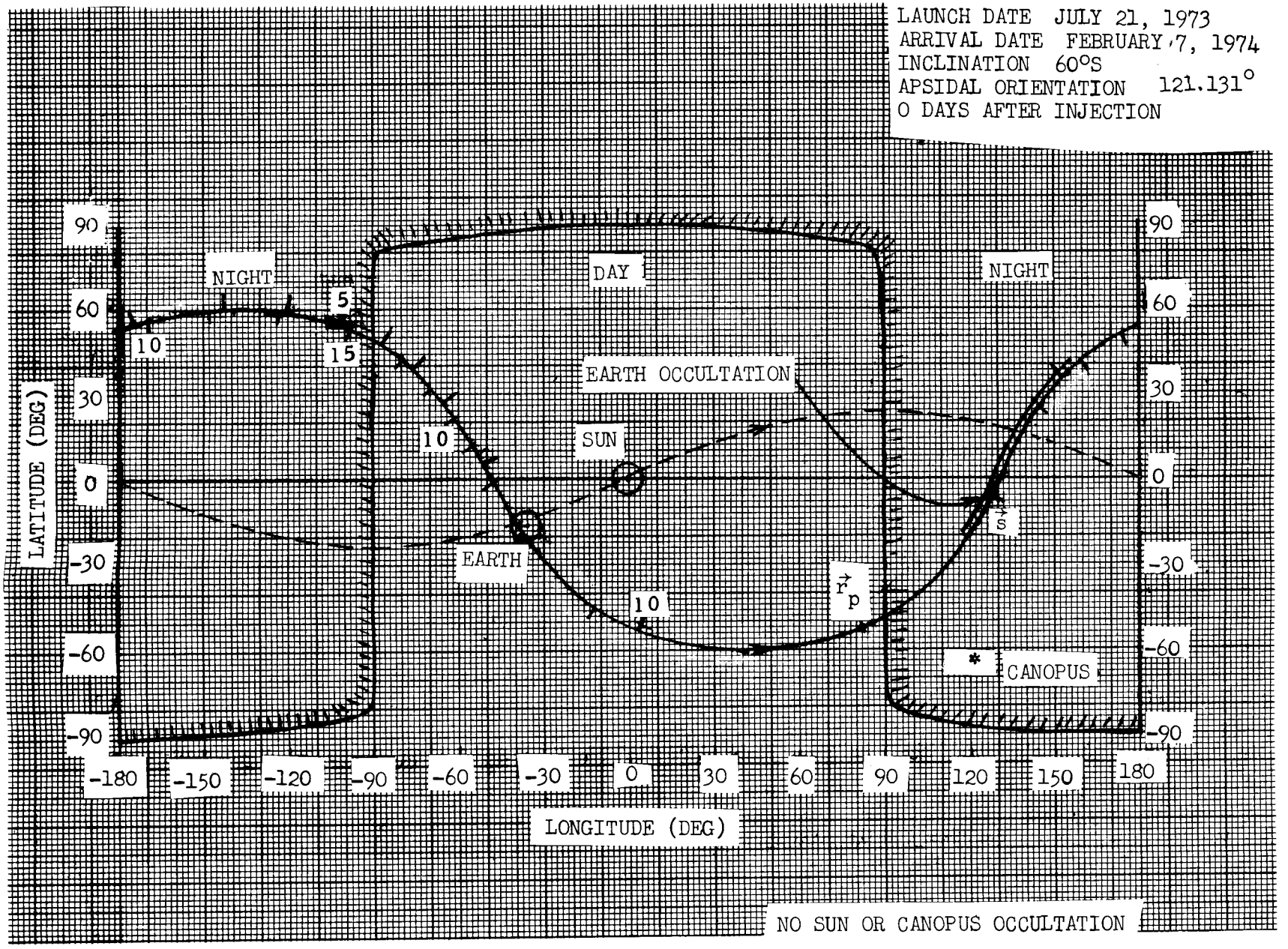
LAUNCH DATE JULY 21, 1973
ARRIVAL DATE FEBRUARY 7, 1974
INCLINATION 60°S
APSIDAL ORIENTATION 121.131°
0 DAYS AFTER INJECTION
NIGHT
DAY
NIGHT
EARTH OCCULTATION
SUN
EARTH
CANOPUS
LATITUDE (DEG)
LONGITUDE (DEG)
90
60
30
0
-30
-60
-90
-180
-150
-120
-90
-60
-30
0
30
60
90
120
150
180
5
10
15
10
10
NO SUN OR CANOPUS OCCULTATION

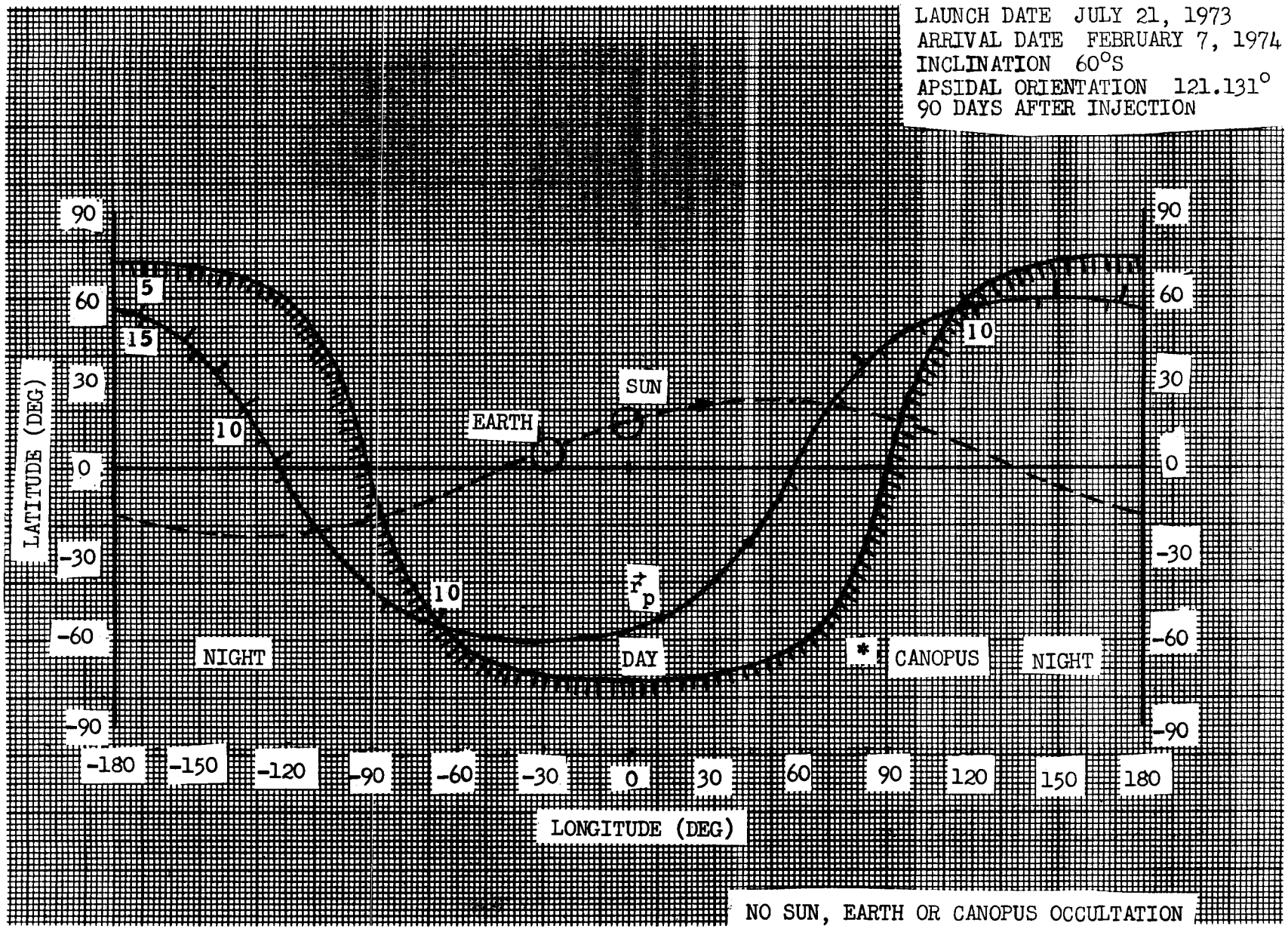
LAUNCH DATE JULY 21, 1973
ARRIVAL DATE FEBRUARY 7, 1974
INCLINATION 60°S
APSIDAL ORIENTATION 121.131°
90 DAYS AFTER INJECTION
LATITUDE (DEG)
90
60
30
0
-30
-60
-90
5
15
10
10
10
SUN
EARTH
NIGHT
DAY
CANOPUS
NIGHT
-180
-150
-120
-90
-60
-30
0
30
60
90
120
150
180
LONGITUDE (DEG)
NO SUN, EARTH OR CANOPUS OCCULTATION

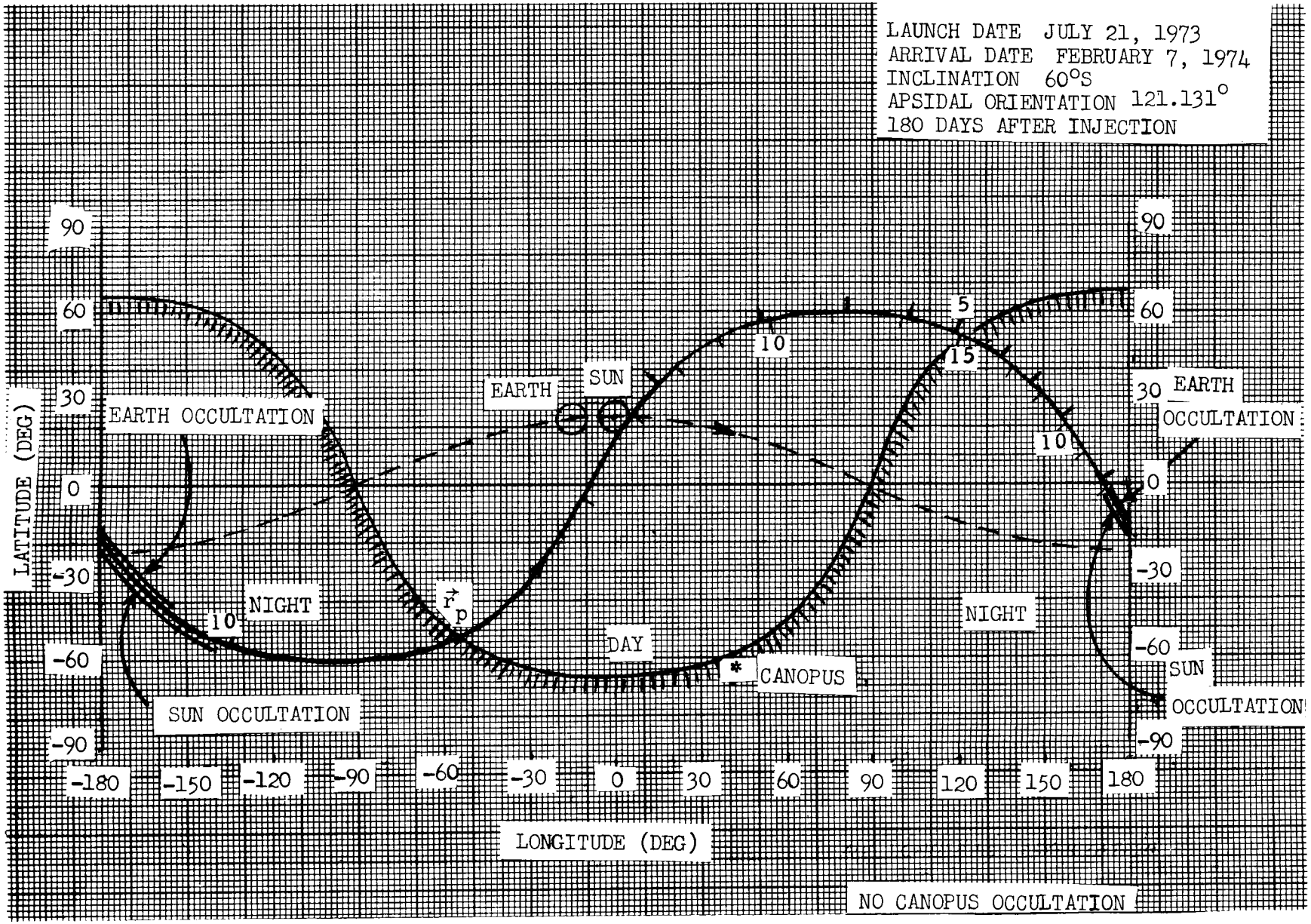
LAUNCH DATE JULY 21, 1973
ARRIVAL DATE FEBRUARY 7, 1974
INCLINATION 60°S
APSIDAL ORIENTATION 121.131°
180 DAYS AFTER INJECTION
LATITUDE (DEG)
90
60
30
0
-30
-60
-90
EARTH OCCULTATION
SUN OCCULTATION
NIGHT
DAY
EARTH
SUN
CANOPUS
r_p
10
5
15
-180
-150
-120
-90
-60
-30
0
30
60
90
120
150
180
LONGITUDE (DEG)
NO CANOPUS OCCULTATION

CASE NO. 6

1000 x 15, 000 km

$i = 60^{\circ}N$

$\Psi = 121.131$ deg

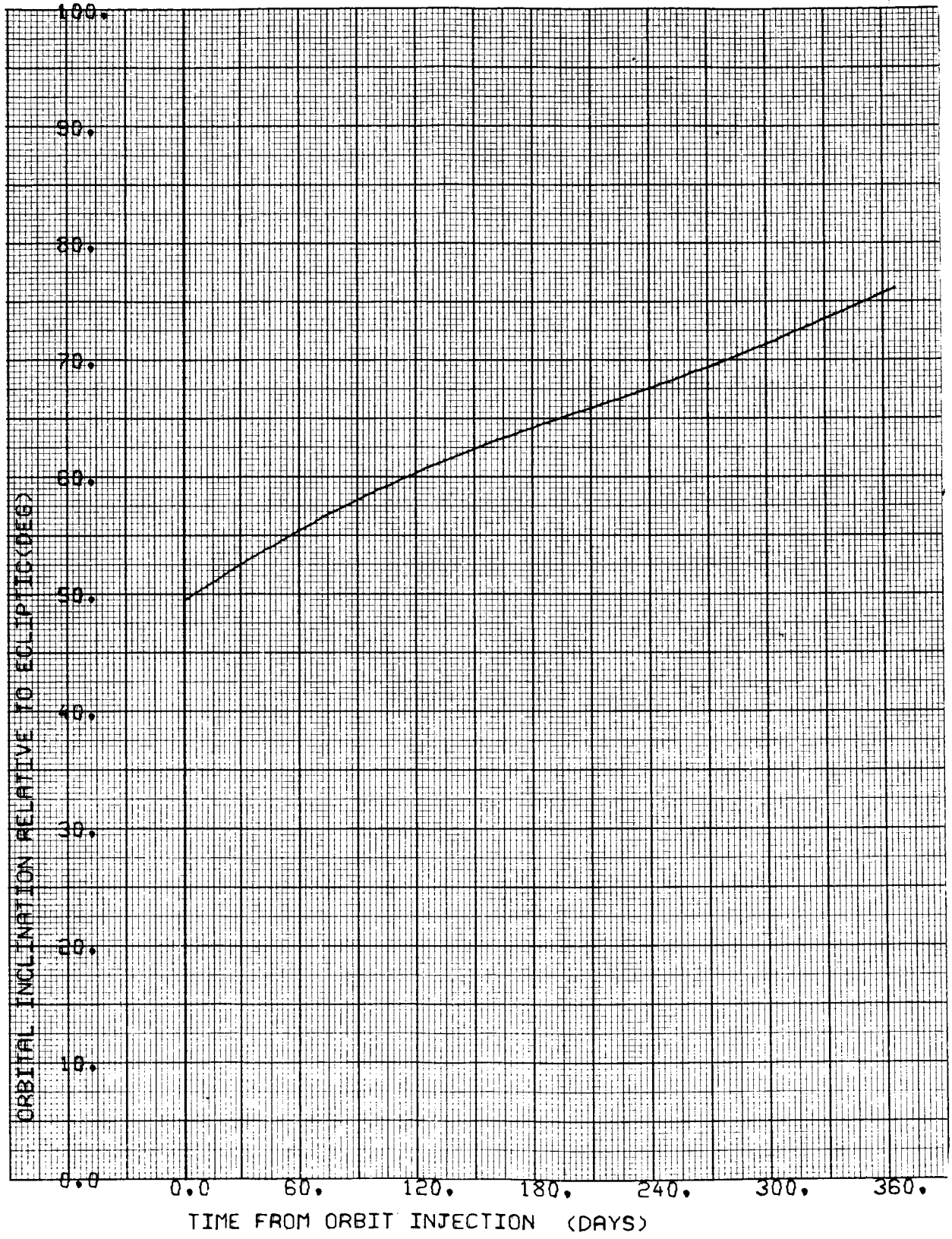
100.
90.
80.
70.
60.
50.
40.
30.
20.
10.
0.0
ORBITAL INCLINATION RELATIVE TO ECLIPTIC(DEG)
0.0
60.
120.
180.
240.
300.
360.
TIME FROM ORBIT INJECTION (DAYS)

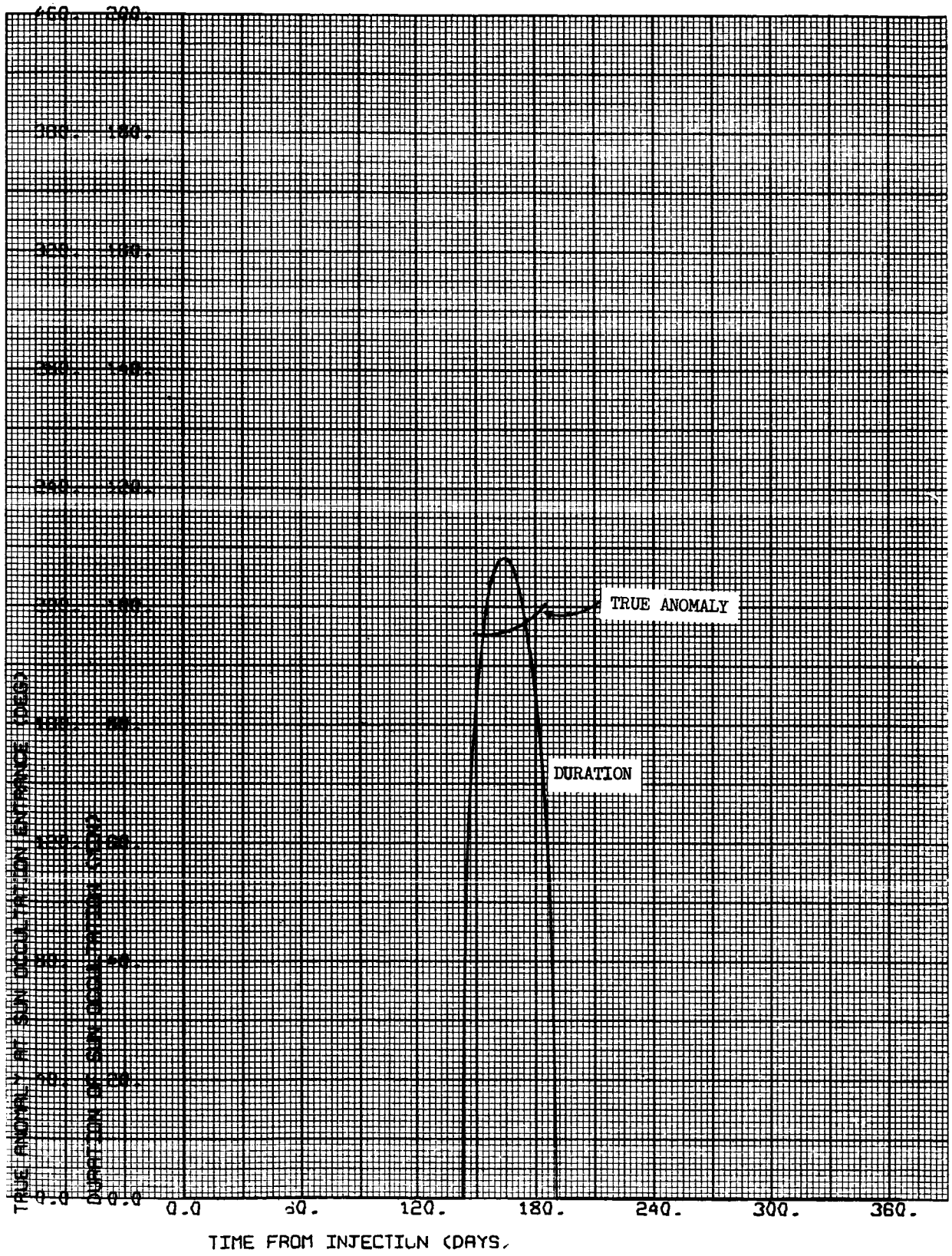
TRUE ANOMALY
DURATION
TRUE ANOMALY AT SUN OCCULTATION ENTRANCE (DEG)
DURATION OF SUN OCCULTATION (DEG)
0.0
60.
120.
180.
240.
300.
360.
TIME FROM INJECTION (DAYS)

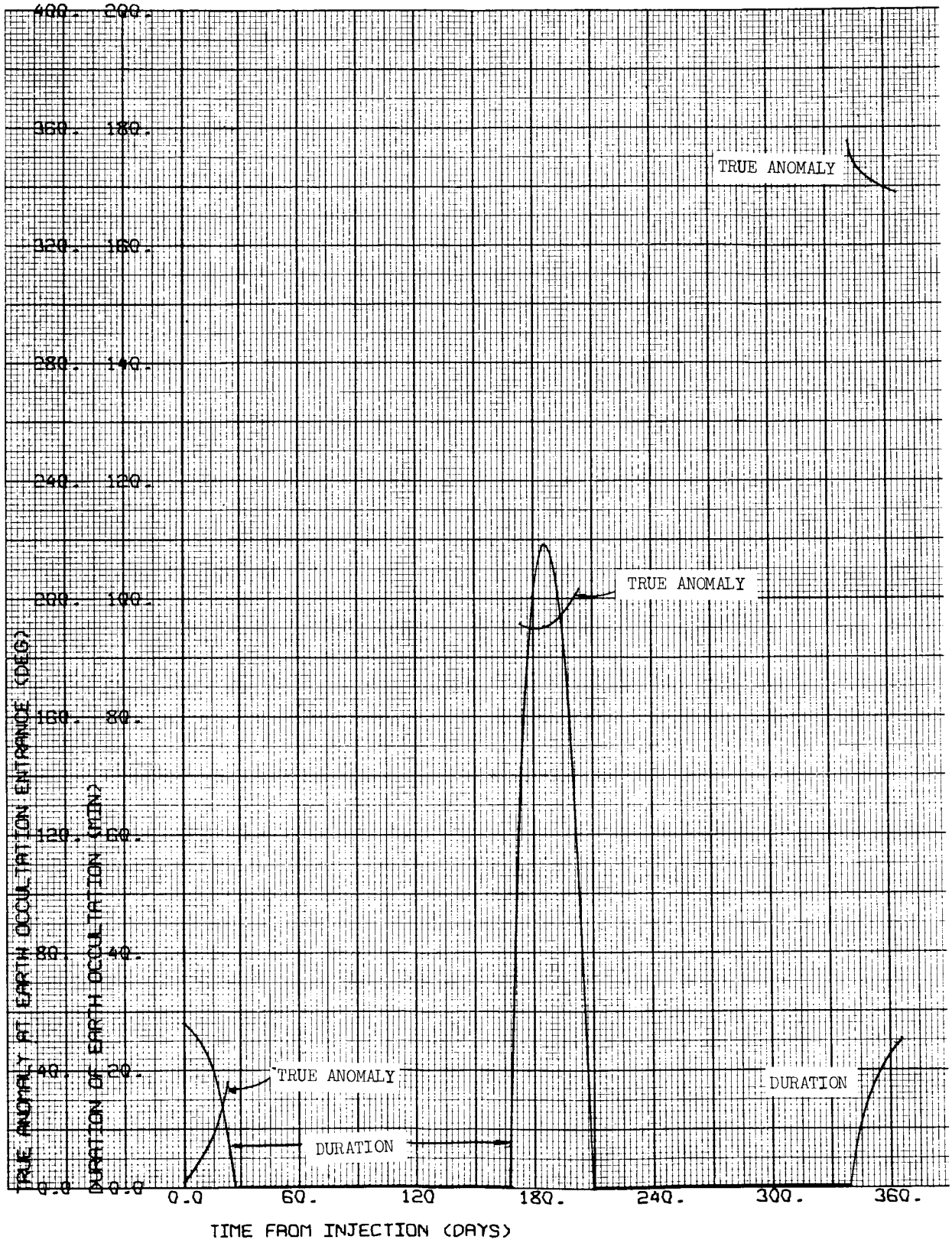
TRUE ANOMALY AT EARTH OCCULTATION ENTRANCE (DEG)
DURATION OF EARTH OCCULTATION (MIN)
TIME FROM INJECTION (DAYS)
400.
360.
320.
280.
240.
200.
160.
120.
80.
40.
0.0
200.
180.
160.
140.
120.
100.
80.
60.
40.
20.
0.0
0.0
60.
120
180.
240.
300.
360.
TRUE ANOMALY
TRUE ANOMALY
TRUE ANOMALY
DURATION
DURATION
DURATION

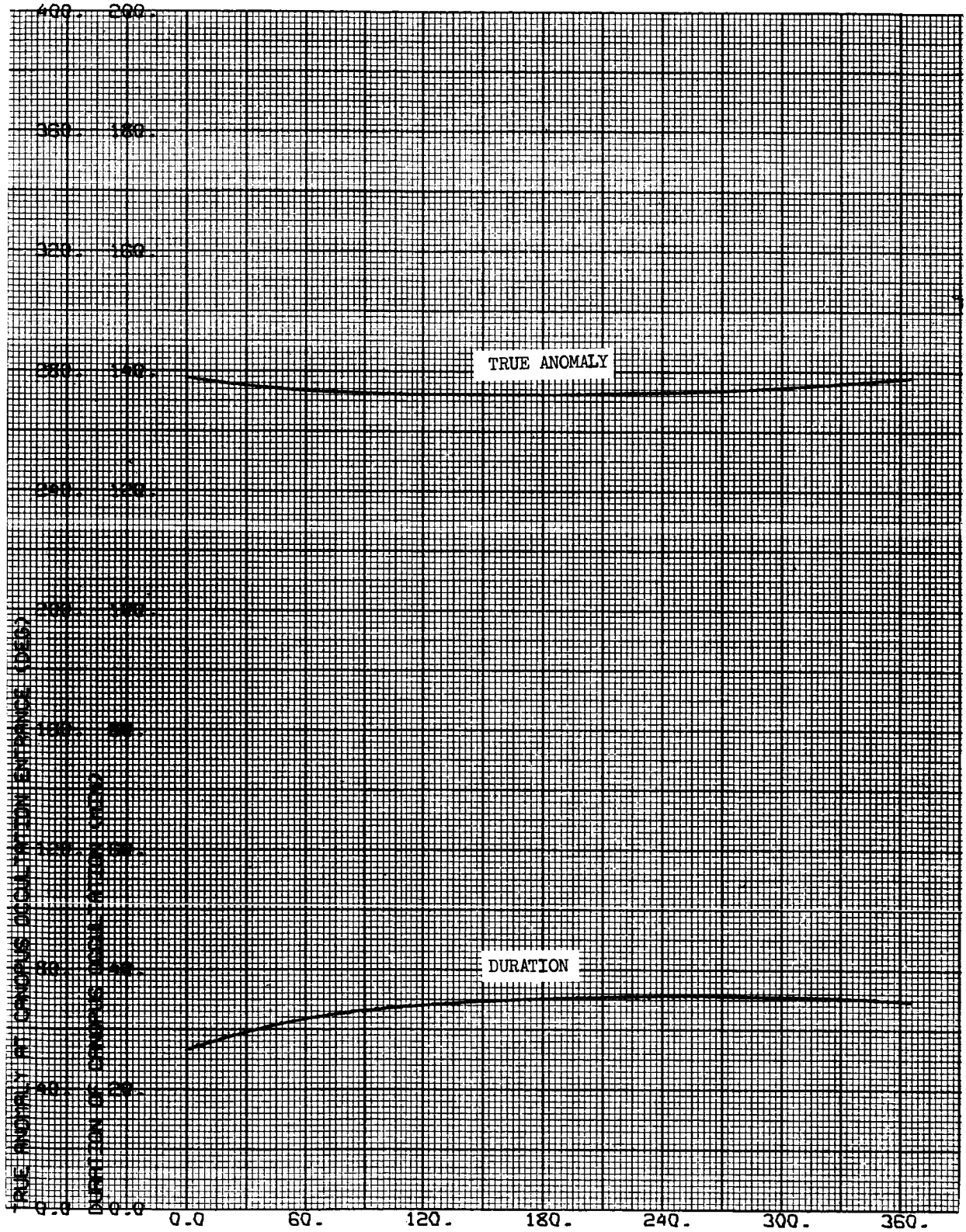
TRUE ANOMALY
DURATION
TRUE ANOMALY AT INJECTION (DEG)
DURATION (DAYS)
TIME FROM INJECTION (DAYS)
0.0
60.
120.
180.
240.
300.
360.

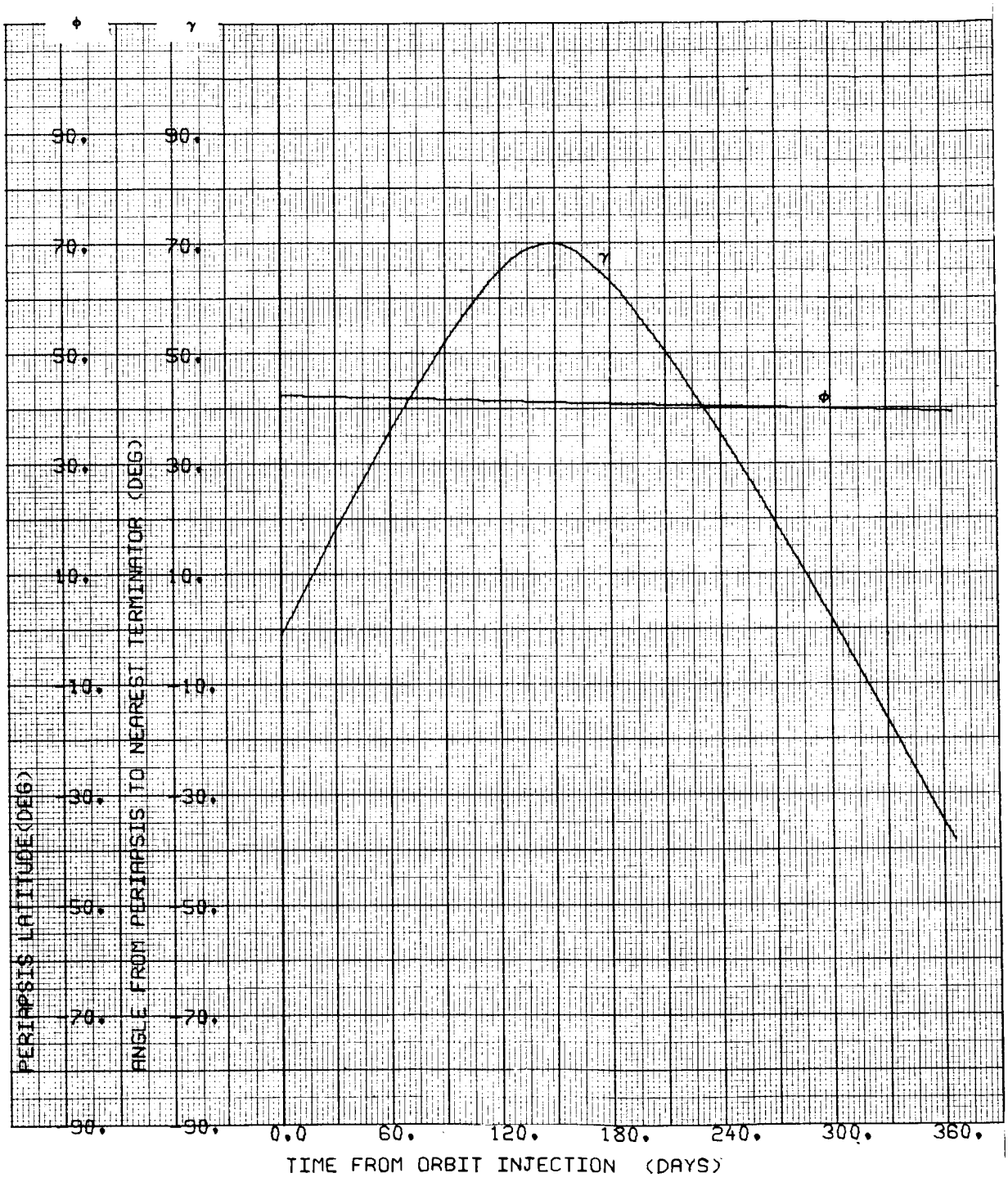
ϕ
γ
90.
70.
50.
30.
10.
-10.
-30.
-50.
-70.
-90.
0.0
60.
120.
180.
240.
300.
360.
γ
ϕ
PERIAPSIS LATITUDE (DEG)
ANGLE FROM PERIAPSIS TO NEAREST TERMINATOR (DEG)
TIME FROM ORBIT INJECTION (DAYS)

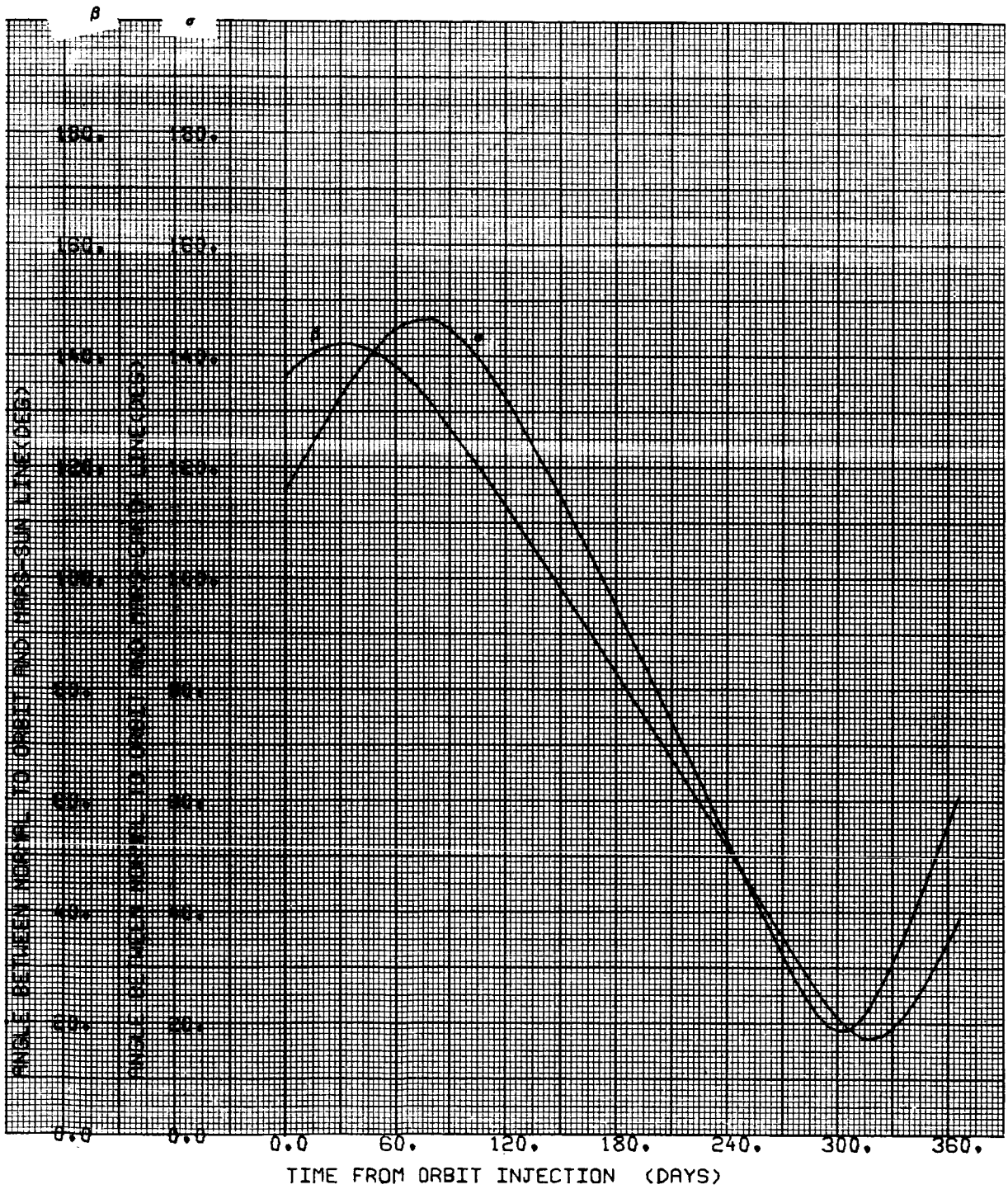
β
σ
180.
160.
140.
120.
100.
80.
60.
40.
20.
0.0
ANGLE BETWEEN NORTH, TO ORBIT AND HARS-SUN LINE (DEG)
0.0
60.
120.
180.
240.
300.
360.
TIME FROM ORBIT INJECTION (DAYS)

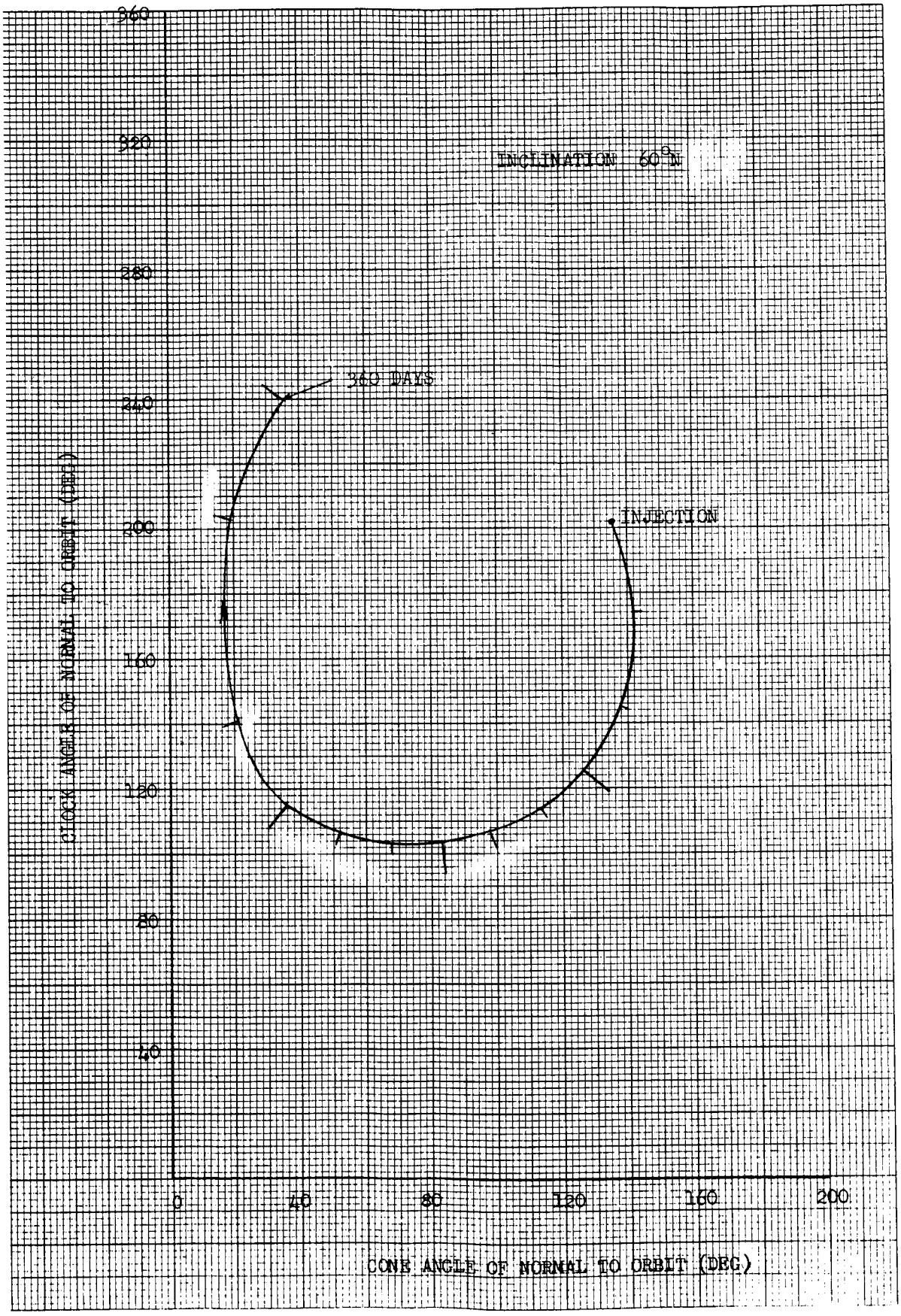
INCLINATION 60° N
360 DAYS
INJECTION
CLOCK ANGLE OF NORMAL TO ORBIT (DEG)
CONE ANGLE OF NORMAL TO ORBIT (DEG)
360
320
280
240
200
160
120
80
40
0
40
80
120
160
200

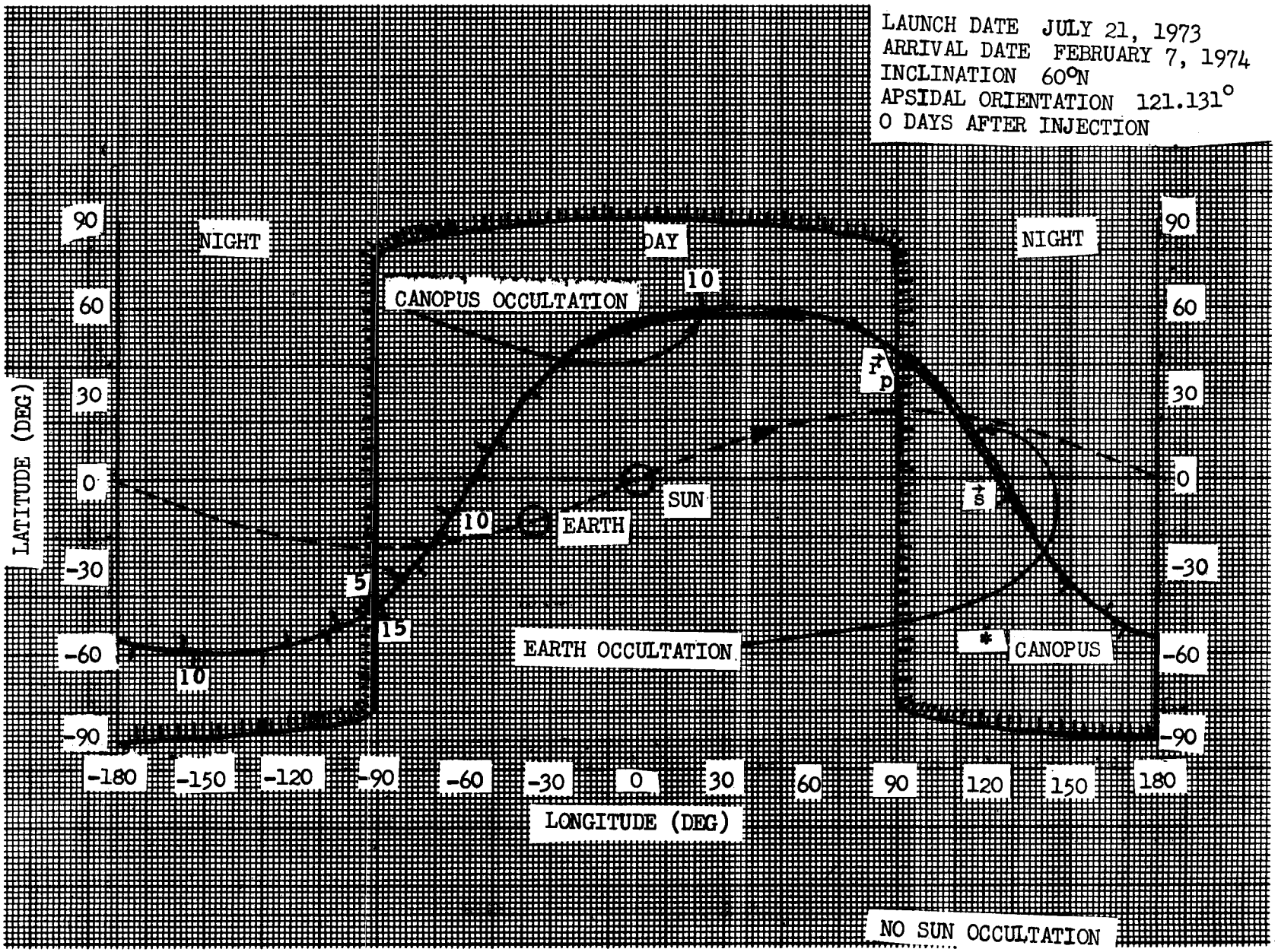
LAUNCH DATE JULY 21, 1973
ARRIVAL DATE FEBRUARY 7, 1974
INCLINATION 60°N
APSIDAL ORIENTATION 121.131°
0 DAYS AFTER INJECTION
NIGHT
DAY
NIGHT
CANOPUS OCCULTATION
10
5
15
10
SUN
EARTH
EARTH OCCULTATION
CANOPUS
NO SUN OCCULTATION
LATITUDE (DEG)
LONGITUDE (DEG)
90
60
30
0
-30
-60
-90
-180
-150
-120
-90
-60
-30
0
30
60
90
120
150
180

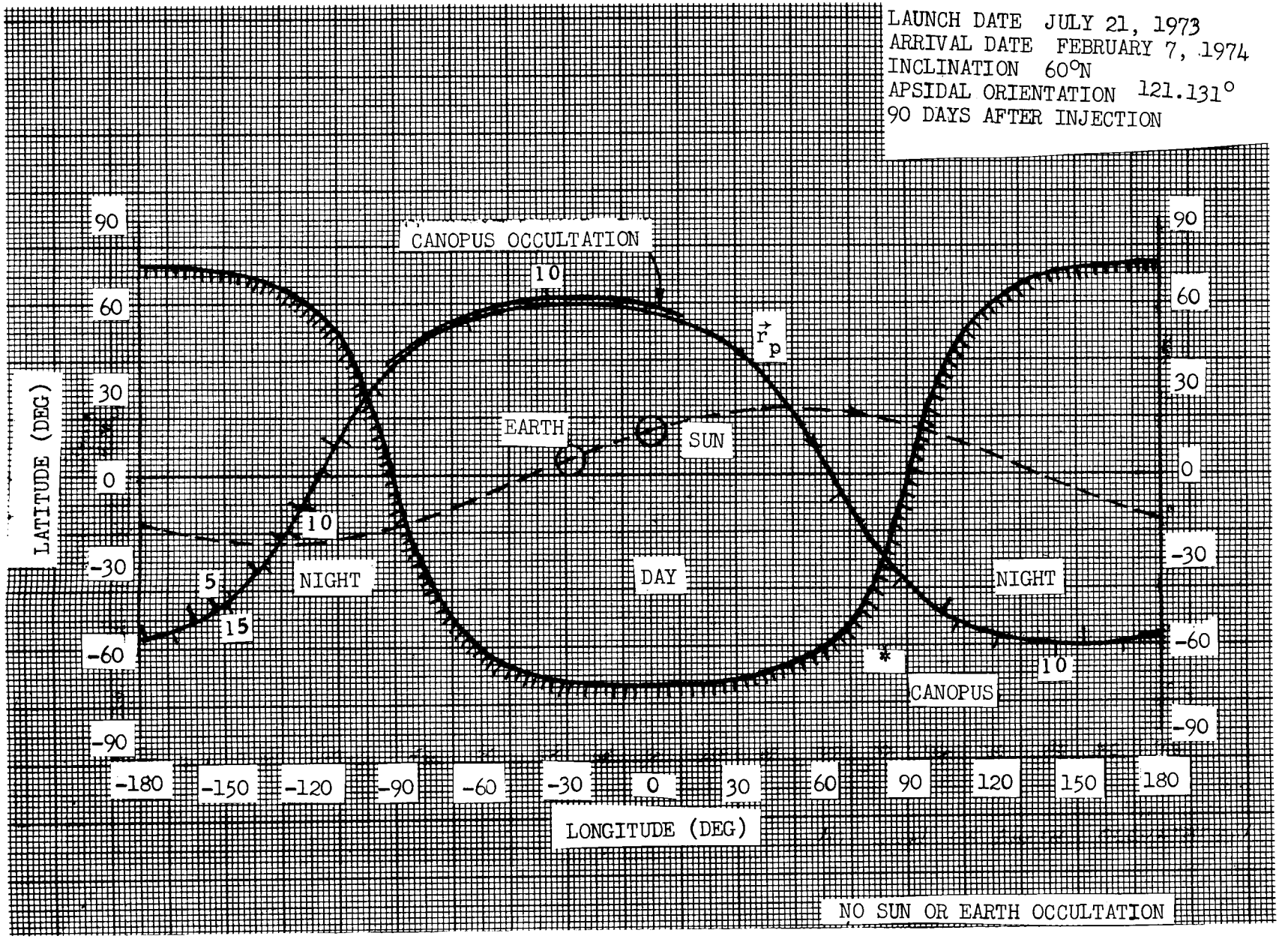
LAUNCH DATE JULY 21, 1973
ARRIVAL DATE FEBRUARY 7, 1974
INCLINATION 60°N
APSIDAL ORIENTATION 121.131°
90 DAYS AFTER INJECTION
CANOPUS OCCULTATION
10
$\vec{r}_p$
EARTH
SUN
NIGHT
DAY
NIGHT
10
5
15
CANOPUS
LATITUDE (DEG)
LONGITUDE (DEG)
90
60
30
0
-30
-60
-90
-180
-150
-120
-90
-60
-30
0
30
60
90
120
150
180
NO SUN OR EARTH OCCULTATION

LAUNCH DATE JULY 21, 1973
ARRIVAL DATE FEBRUARY 7, 1974
INCLINATION 60° N
APSIDAL ORIENTATION 121.131°
180 DAYS AFTER INJECTION
CANOPUS OCCULTATION
EARTH
SUN
DAY
NIGHT
EARTH OCCULTATION
CANOPUS
SUN OCCULTATION
NIGHT
LATITUDE (DEG)
LONGITUDE (DEG)
90
60
30
0
-30
-60
-90
-180
-150
-120
-90
-60
-30
0
30
60
90
120
150
180
5
10
15

CASE NO. 7

1000 x 10,000 km

$i = 40^{\circ}S$

$\Psi = 121.131$ deg

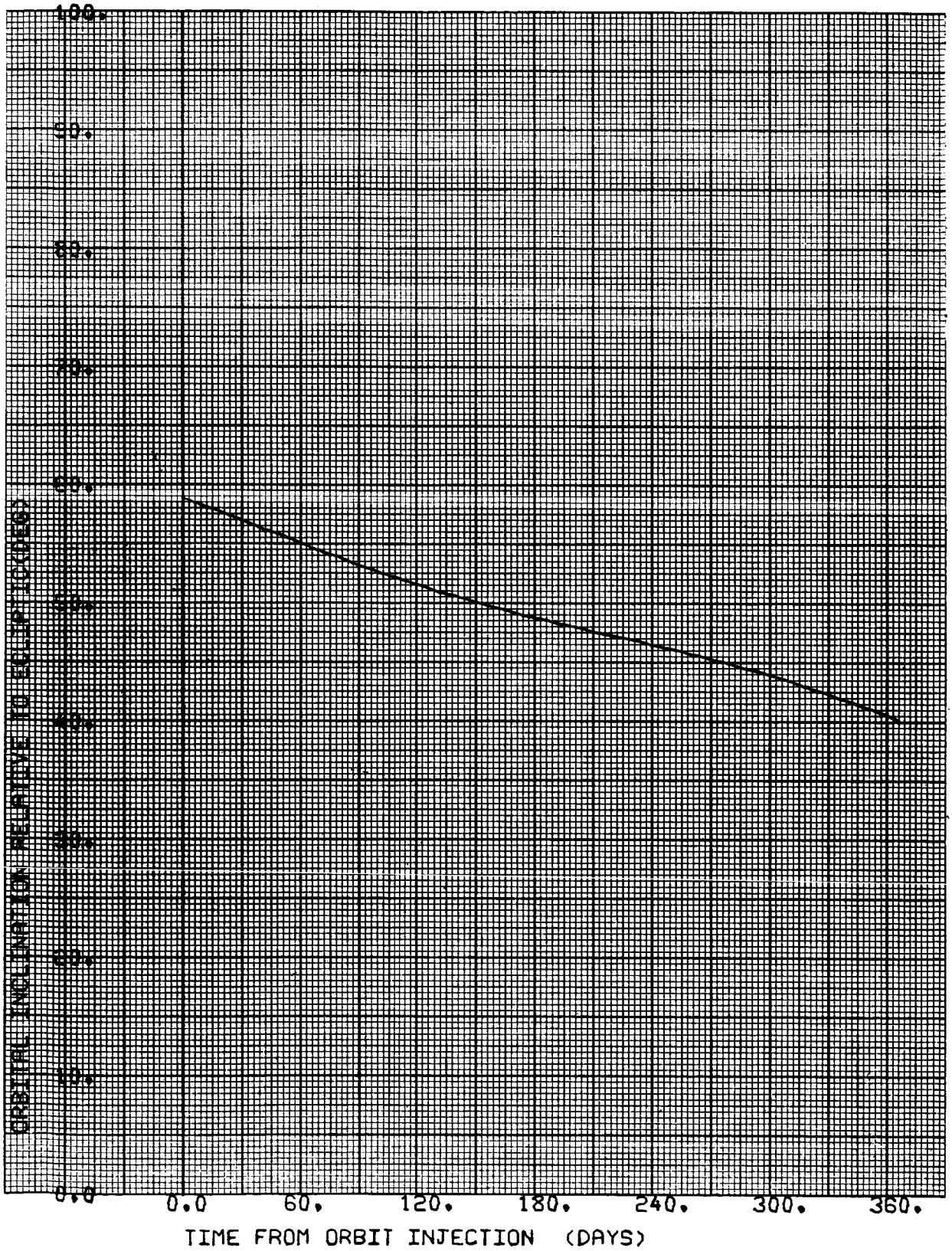
100.
80.
60.
40.
20.
0.0
ORBITAL INCLINATION RELATIVE TO EQUATOR (DEGREES)
0.0
60.
120.
180.
240.
300.
360.
TIME FROM ORBIT INJECTION (DAYS)

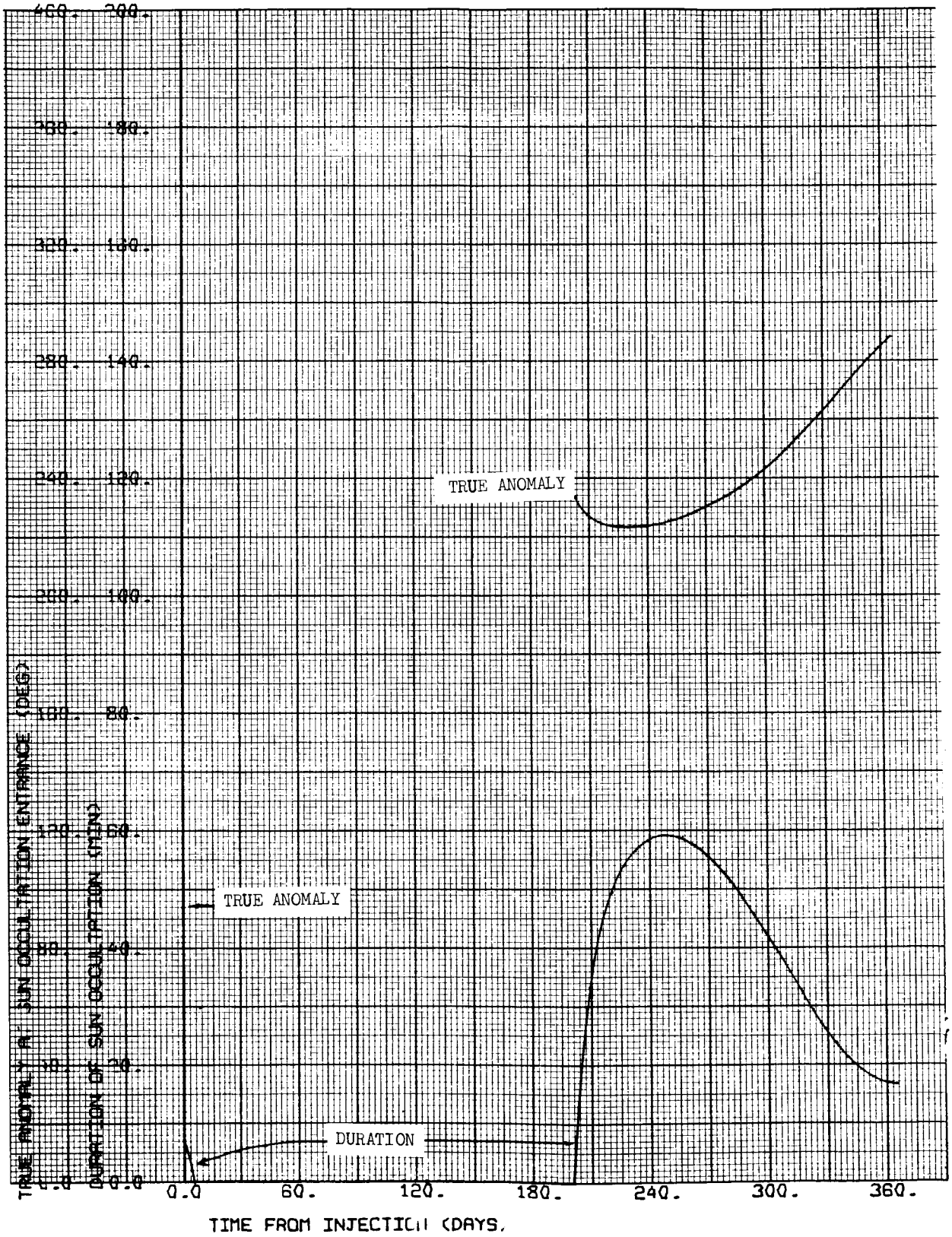
TRUE ANOMALY
TRUE ANOMALY
DURATION
TRUE ANOMALY @ SUN OCCULTATION ENTRANCE (DEG)
DURATION OF SUN OCCULTATION (MIN)
TIME FROM INJECTION (DAYS)
0.0
60.
120.
180.
240.
300.
360.
460.
420.
380.
340.
300.
260.
220.
180.
140.
100.
60.
20.
200.
180.
160.
140.
120.
100.
80.
60.
40.
20.
0.0

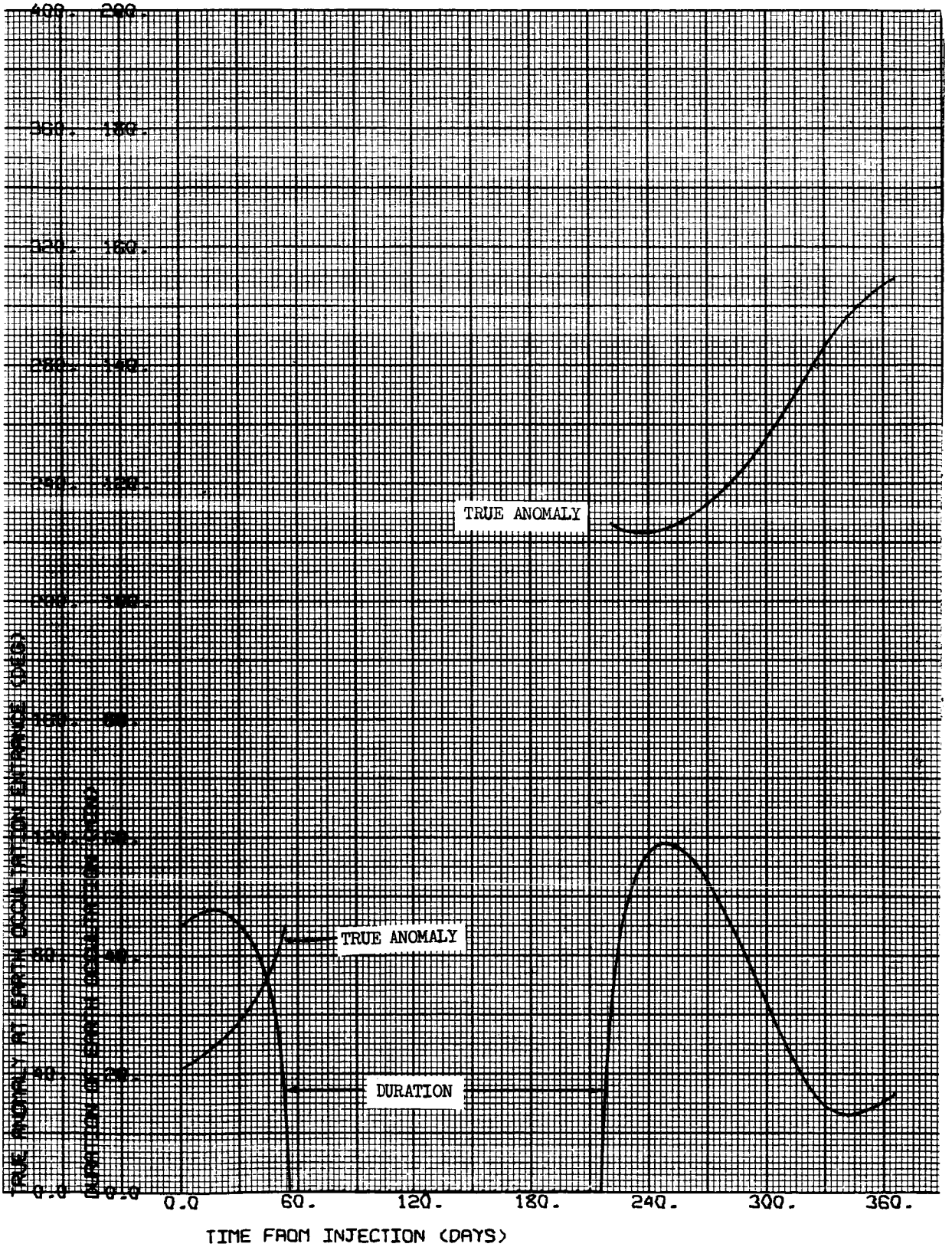
TRUE ANOMALY
TRUE ANOMALY
DURATION
0.0
60.
120.
180.
240.
300.
360.
TIME FROM INJECTION (DAYS)

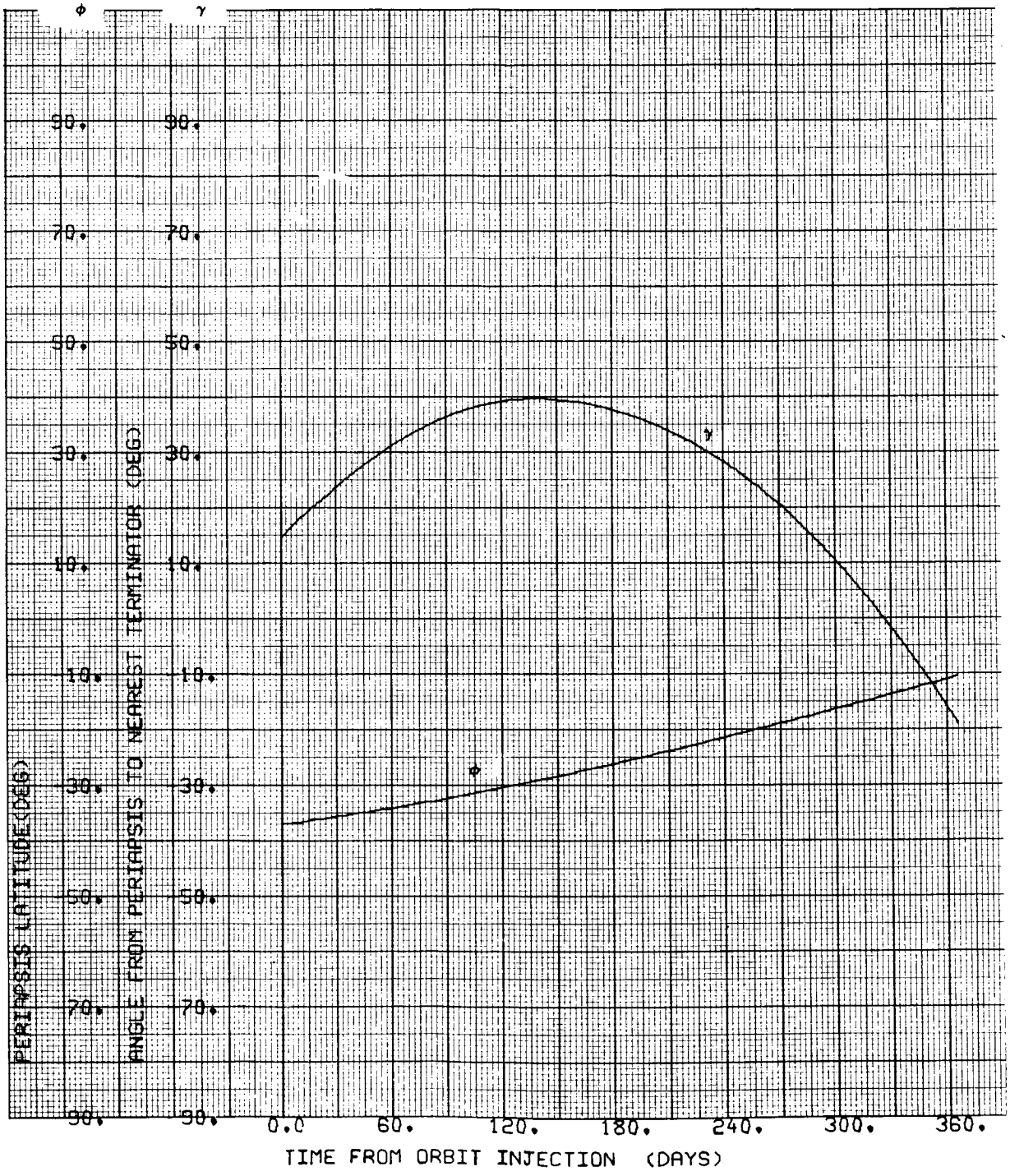
Φ
γ
90.
70.
50.
30.
10.
-10.
-30.
-50.
-70.
-90.
PERIAPSIS LATITUDE(DEG)
ANGLE FROM PERIAPSIS TO NEAREST TERMINATOR (DEG)
0.0
60.
120.
180.
240.
300.
360.
TIME FROM ORBIT INJECTION (DAYS)

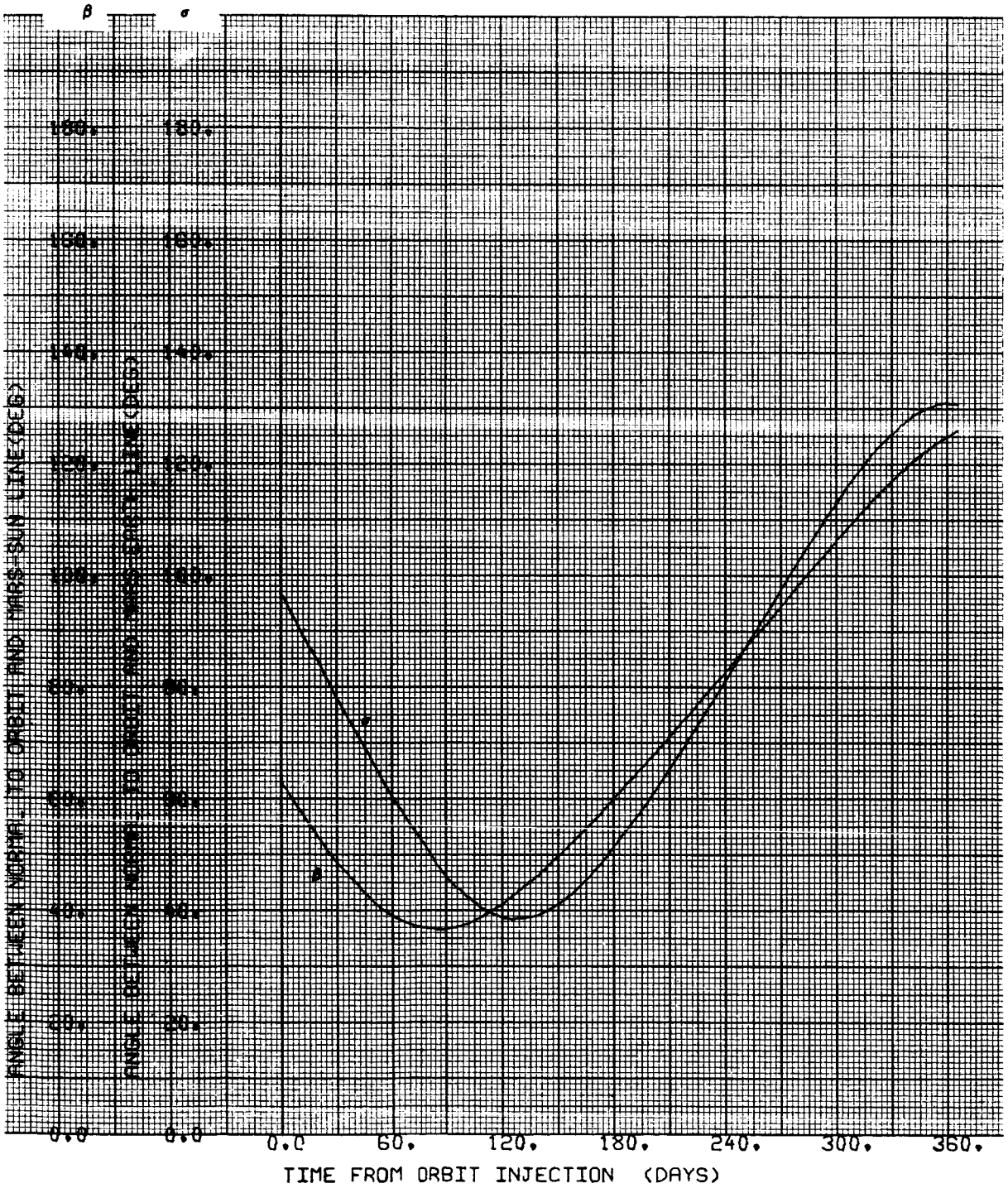
β
σ
180.
160.
140.
120.
100.
80.
60.
40.
20.
0.0
0.0
0.0
60.
120.
180.
240.
300.
360.
ANGLE BETWEEN NORMAL TO ORBIT AND MARS-SUN LINE (DEG)
TIME FROM ORBIT INJECTION (DAYS)

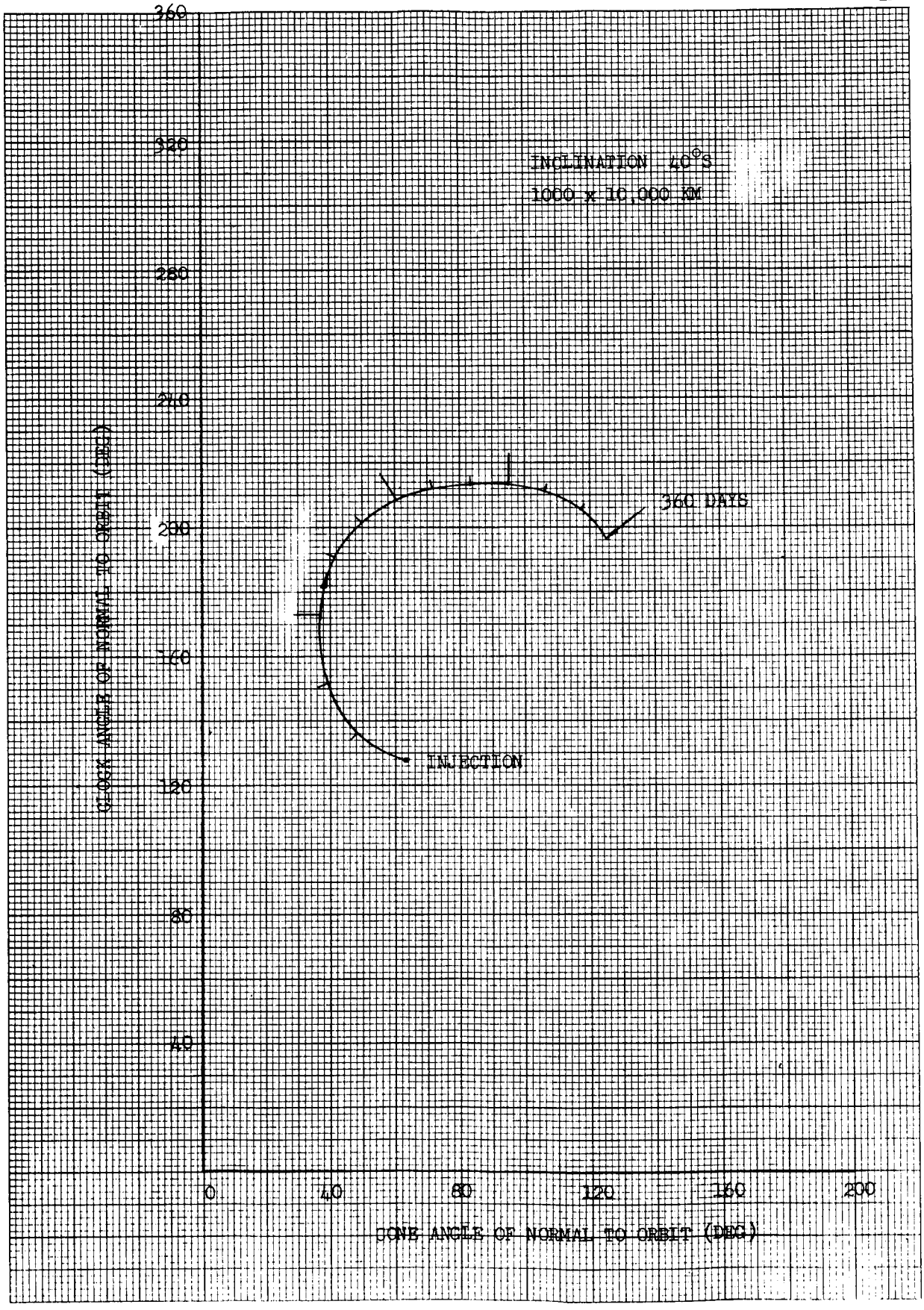
INCLINATION 40°S
1000 x 10,000 KM
360 DAYS
INJECTION
CLOCK ANGLE OF NORMAL TO ORBIT (DEG)
CONE ANGLE OF NORMAL TO ORBIT (DEG)
360
320
280
240
200
160
120
80
40
0
40
80
120
160
200

CASE NO. 8

1000 x 20,000 km

$i = 40^{\circ}S$

$\Psi = 121.131$ deg

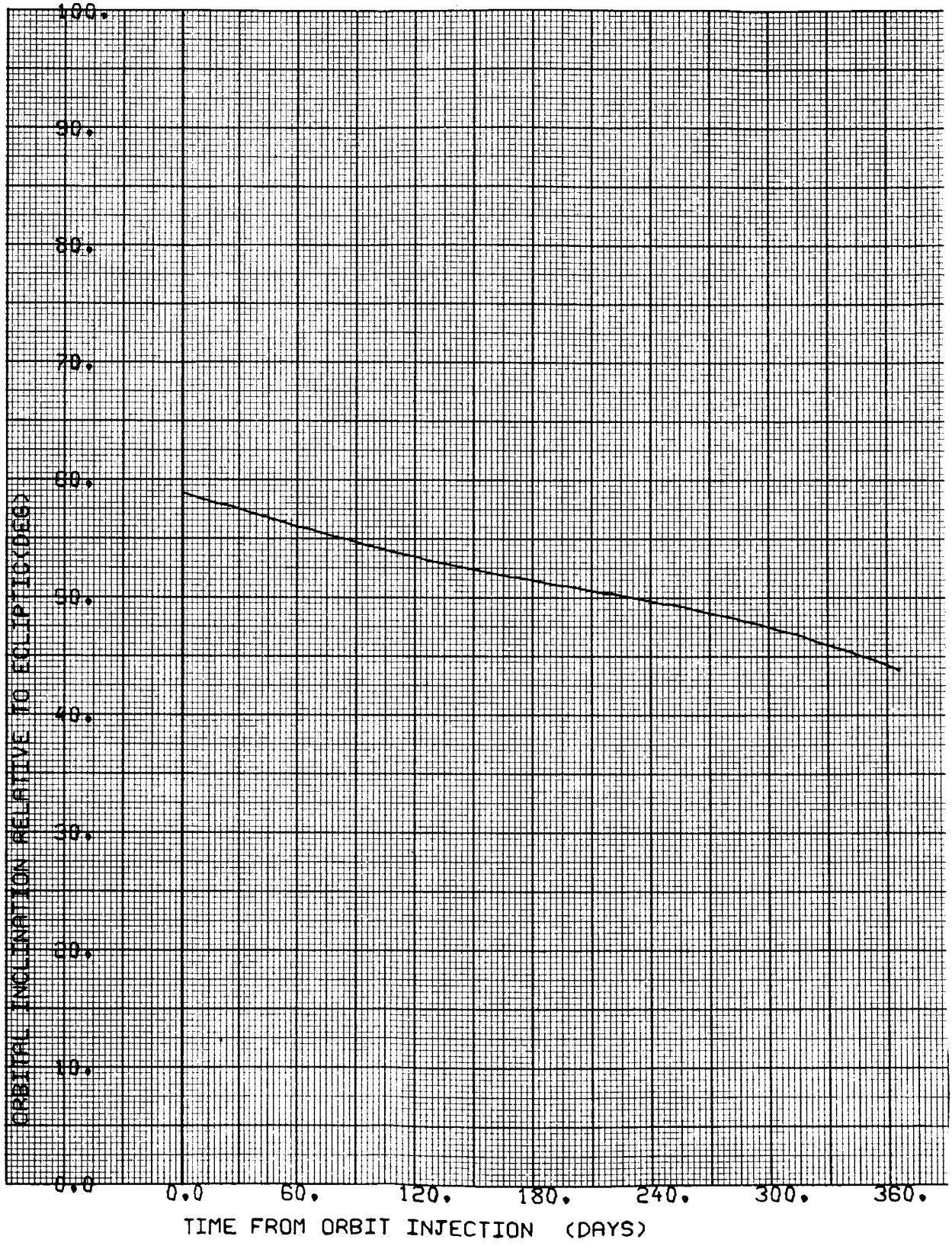
100.
90.
80.
70.
60.
50.
40.
30.
20.
10.
0.0
ORBITAL INCLINATION RELATIVE TO ECLIPTIC(DEG)
0.0
60.
120.
180.
240.
300.
360.
TIME FROM ORBIT INJECTION (DAYS)

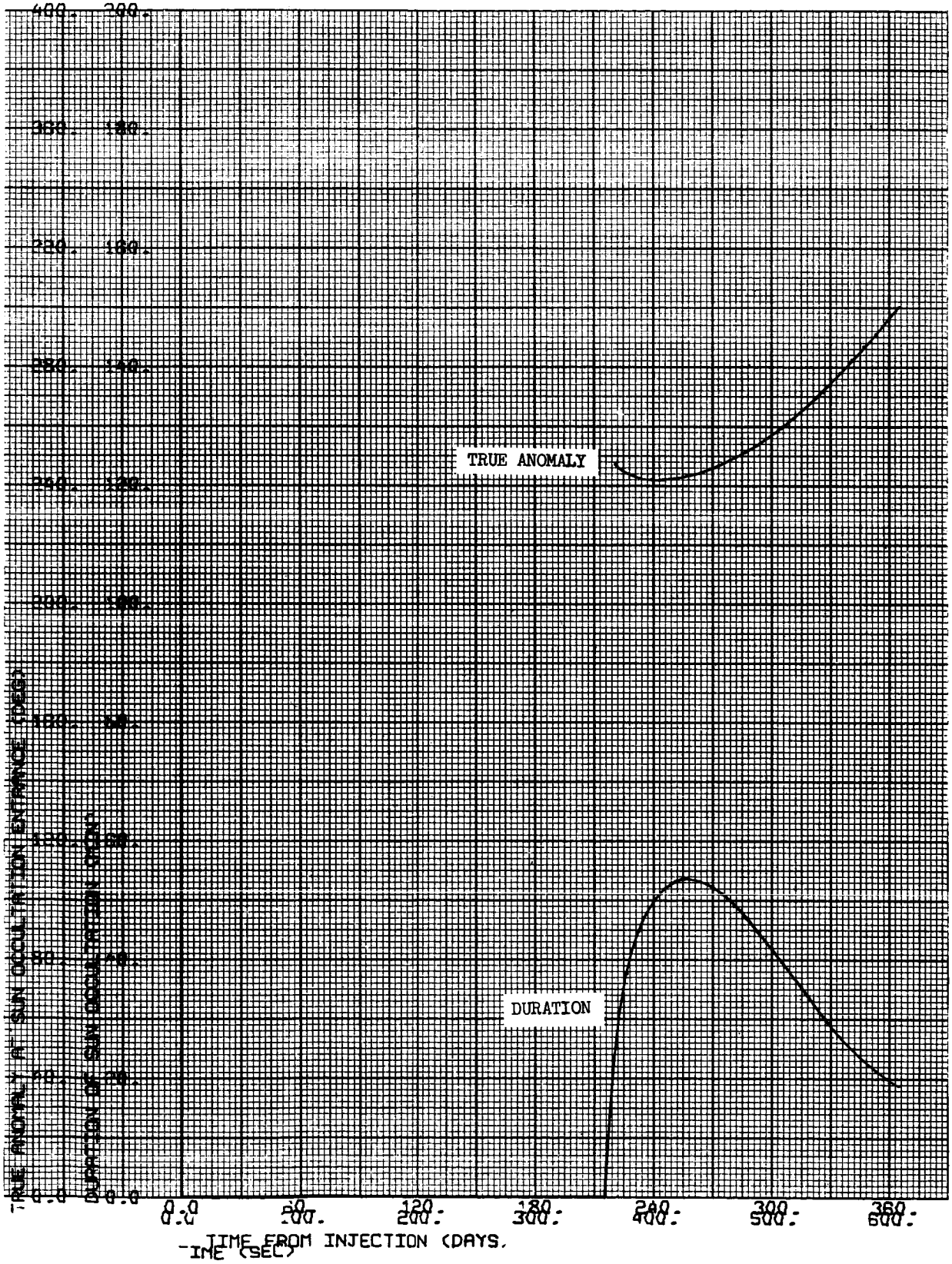
TRUE ANOMALY
DURATION
TRUE ANOMALY AT SUN OCCULTATION ENTRANCE (DEG)
DURATION OF SUN OCCULTATION (DAYS)
TIME FROM INJECTION (DAYS)
TIME (SEC)

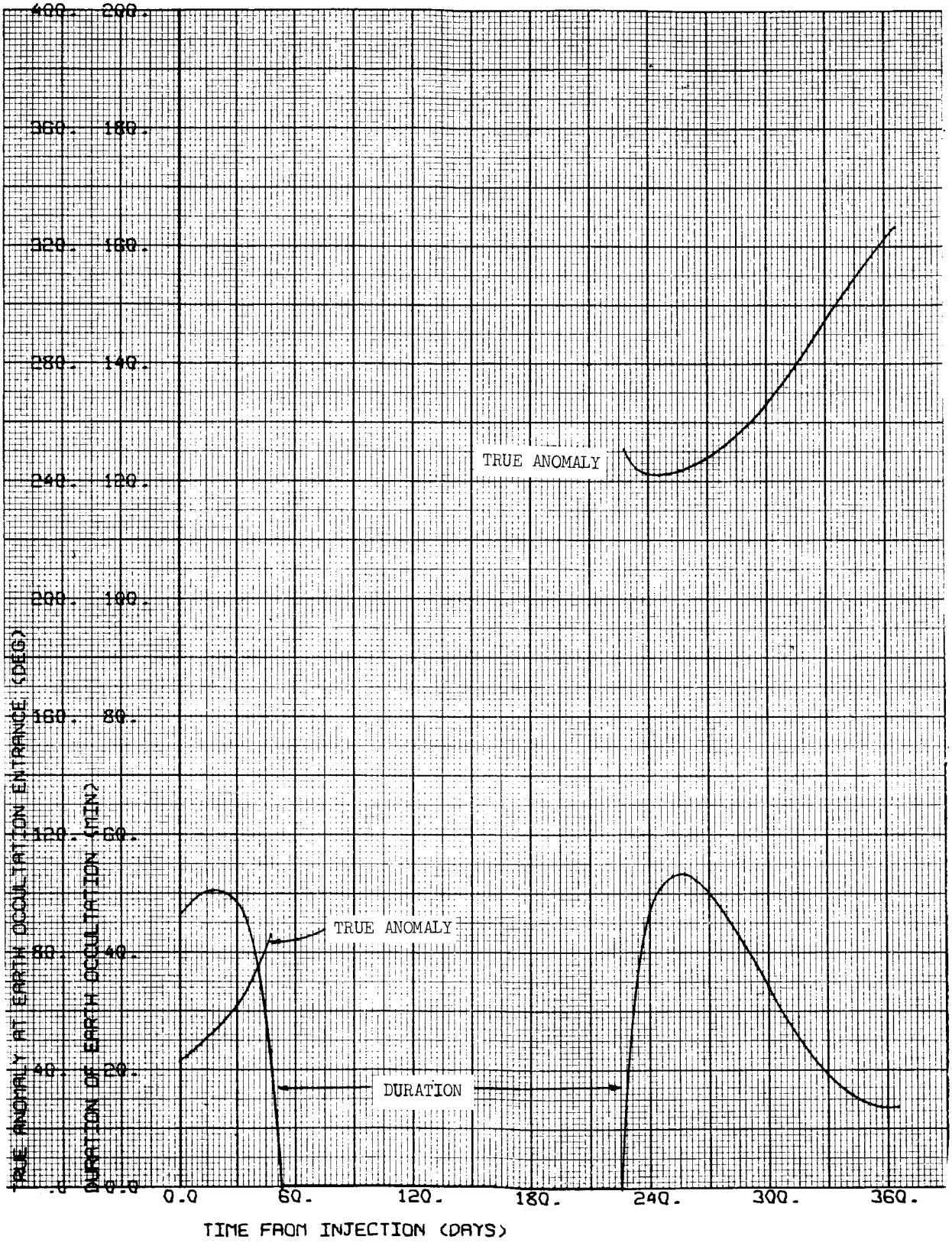
TRUE ANOMALY AT EARTH OCCULTATION ENTRANCE (DEG)
DURATION OF EARTH OCCULTATION (MIN.)
400.
360.
320.
280.
240.
200.
160.
120.
80.
40.
0.0
200.
180.
160.
140.
120.
100.
80.
60.
40.
20.
0.0
TRUE ANOMALY
TRUE ANOMALY
DURATION
0.0
60.
120.
180.
240.
300.
360.
TIME FROM INJECTION (DAYS)

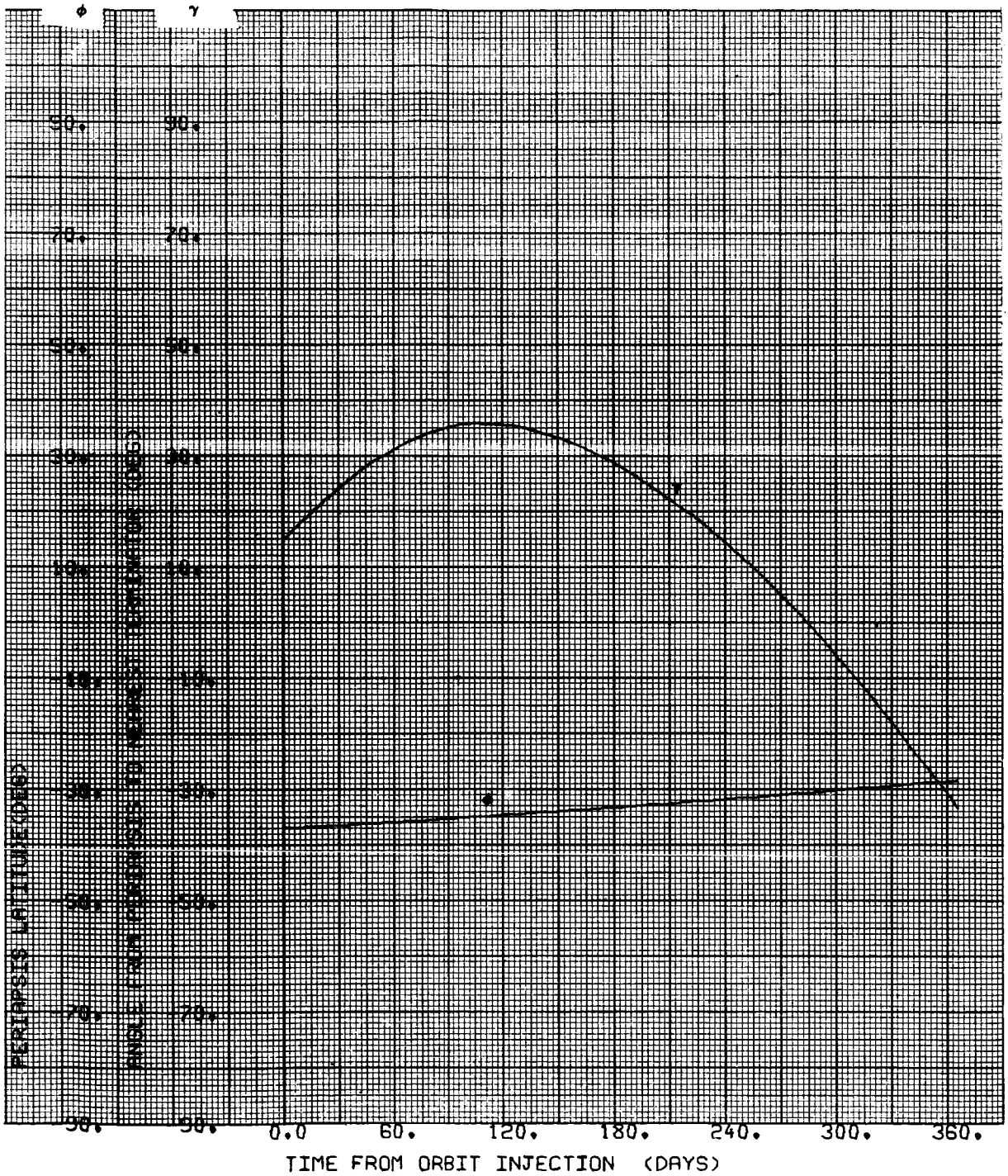
ϕ
γ
90.
70.
50.
30.
10.
-10.
-30.
-50.
-70.
-90.
ECLIPSE LATITUDE (DEG)
0.0
60.
120.
180.
240.
300.
360.
TIME FROM ORBIT INJECTION (DAYS)

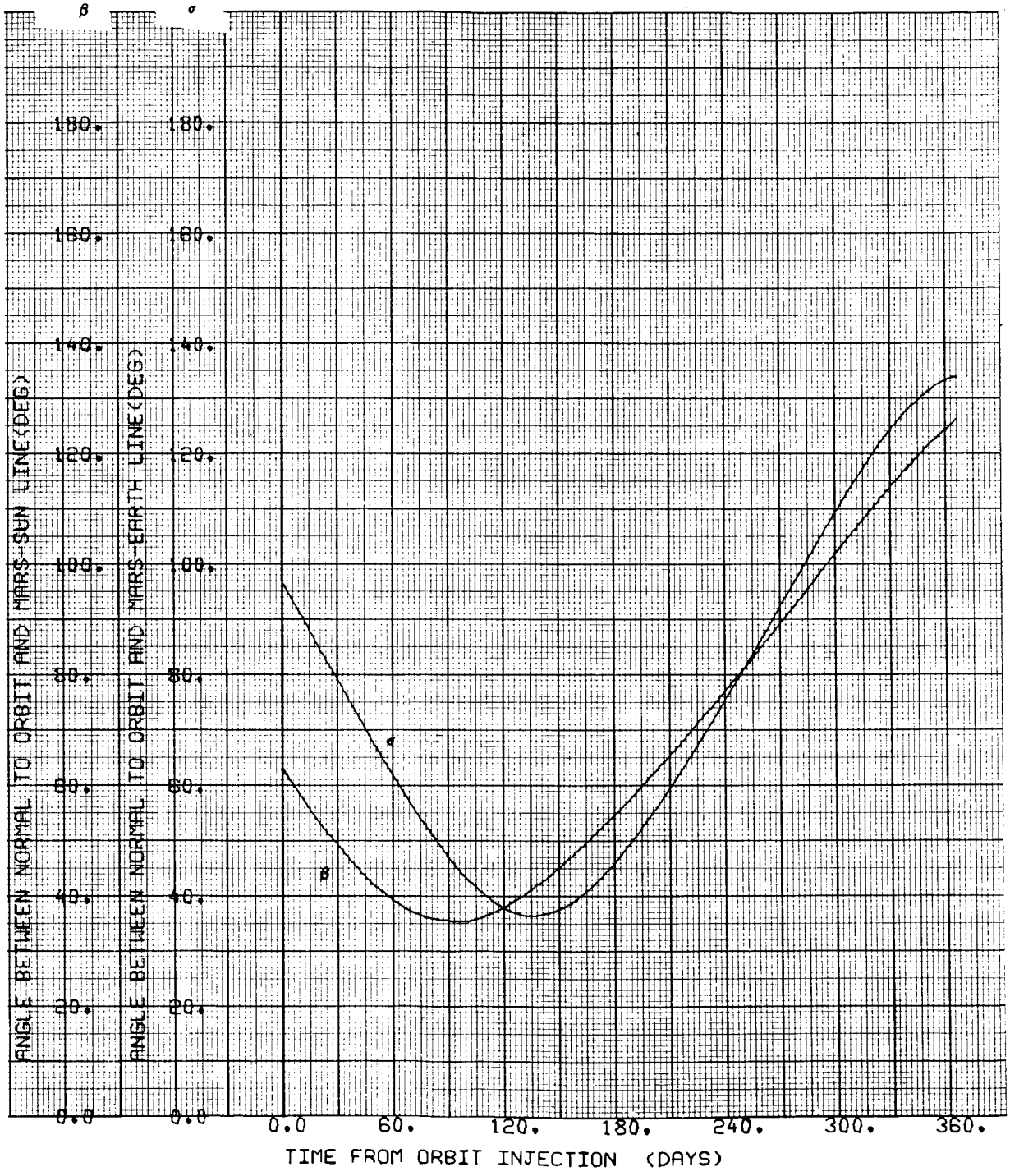
β
σ
180.
160.
140.
120.
100.
80.
60.
40.
20.
0.0
ANGLE BETWEEN NORMAL TO ORBIT AND MARS-SUN LINE(DEG)
ANGLE BETWEEN NORMAL TO ORBIT AND MARS-EARTH LINE(DEG)
0.0
60.
120.
180.
240.
300.
360.
TIME FROM ORBIT INJECTION (DAYS)

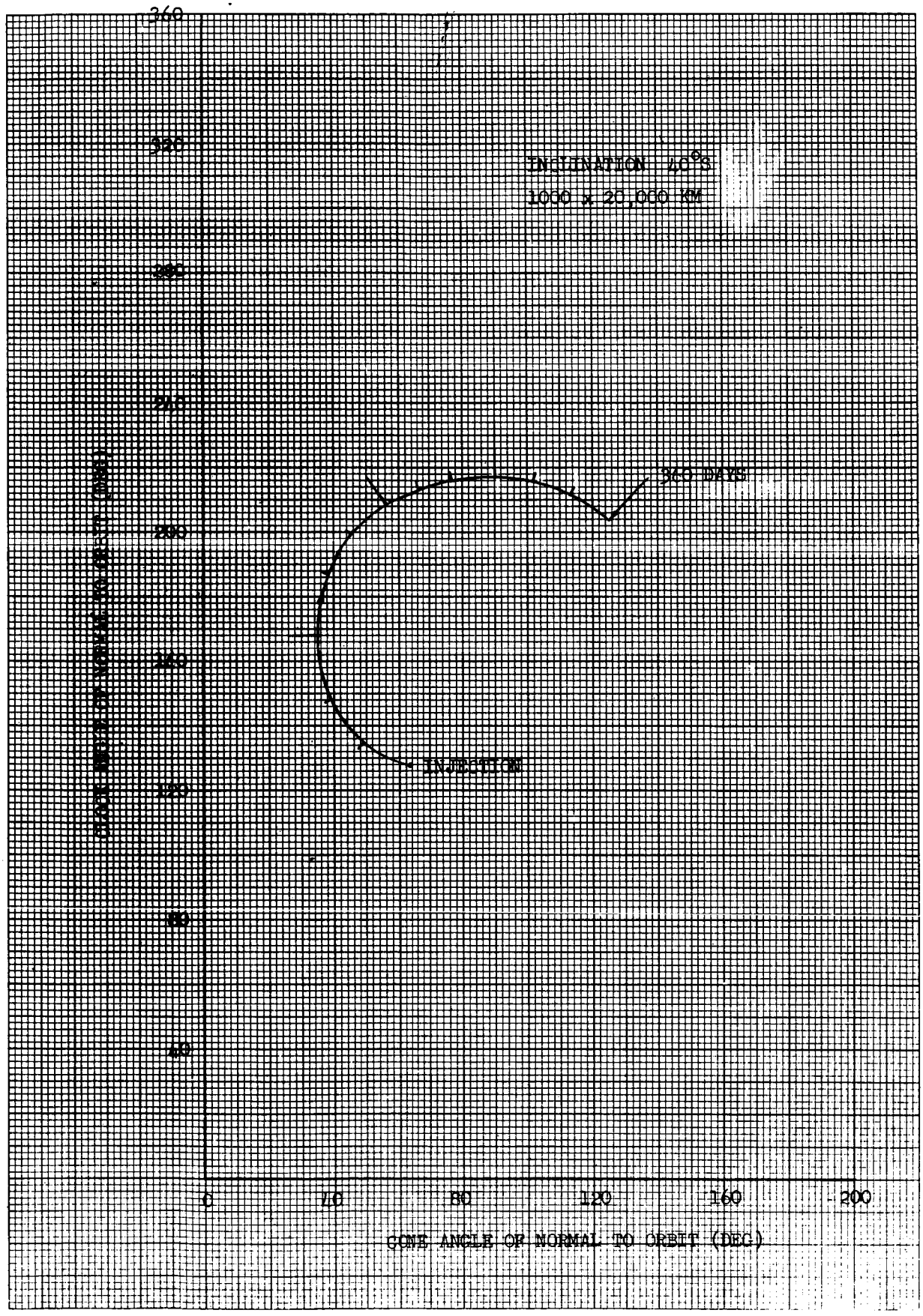
INCLINATION 40°S
1000 x 20,000 KM
360 DAYS
INJECTION
360
320
280
240
200
160
120
80
40
0
40
80
120
160
200
CONE ANGLE OF NORMAL TO ORBIT (DEG.)

CASE NO. 9

1000 x 15, 000 km

$i = 40^{o}S$

$\Psi = 60$ deg

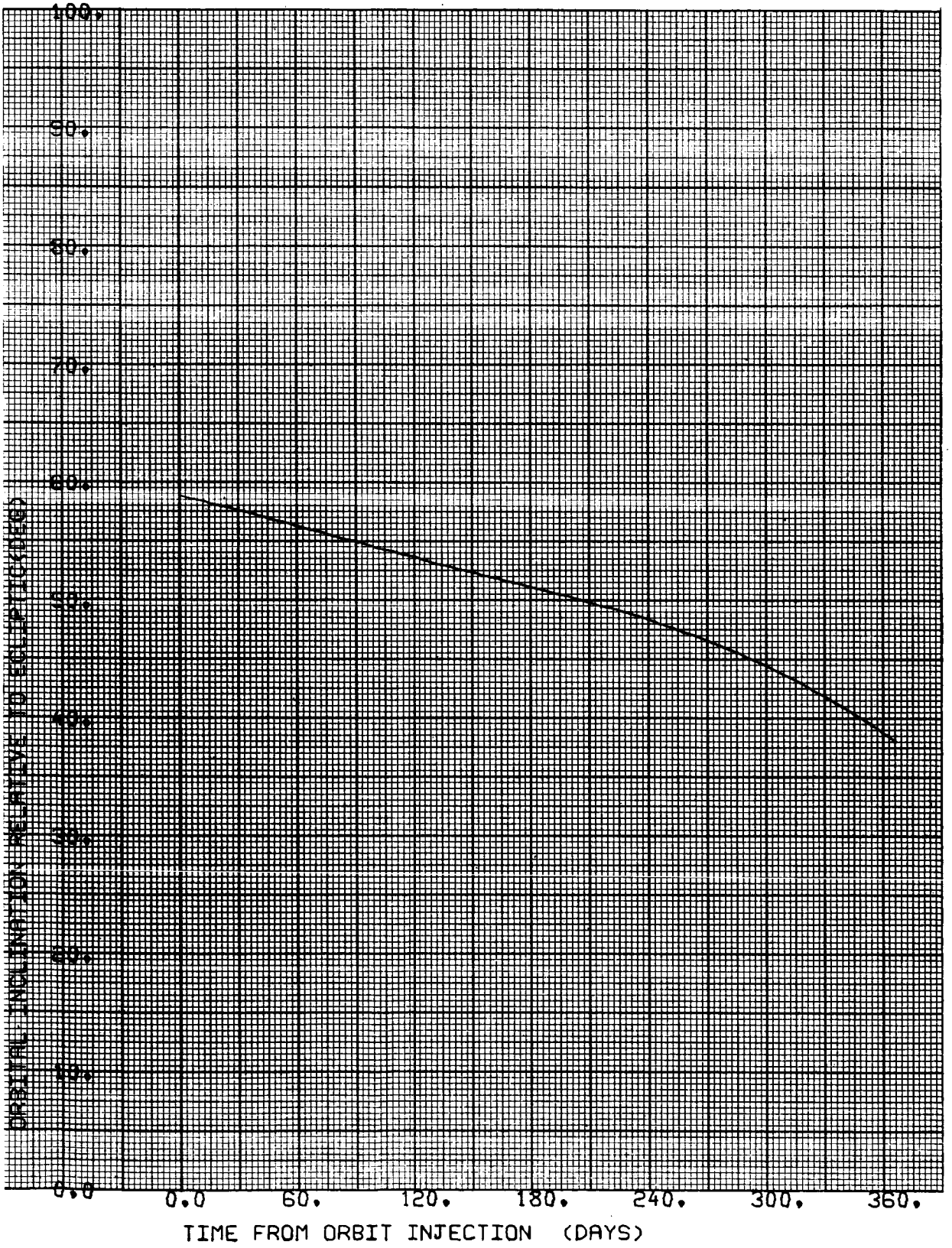
100.
90.
80.
70.
60.
50.
40.
30.
20.
10.
0.0
ORBITAL INCLINATION RELATIVE TO ECLIPTIC (DEG)
0.0
60.
120.
180.
240.
300.
360.
TIME FROM ORBIT INJECTION (DAYS)

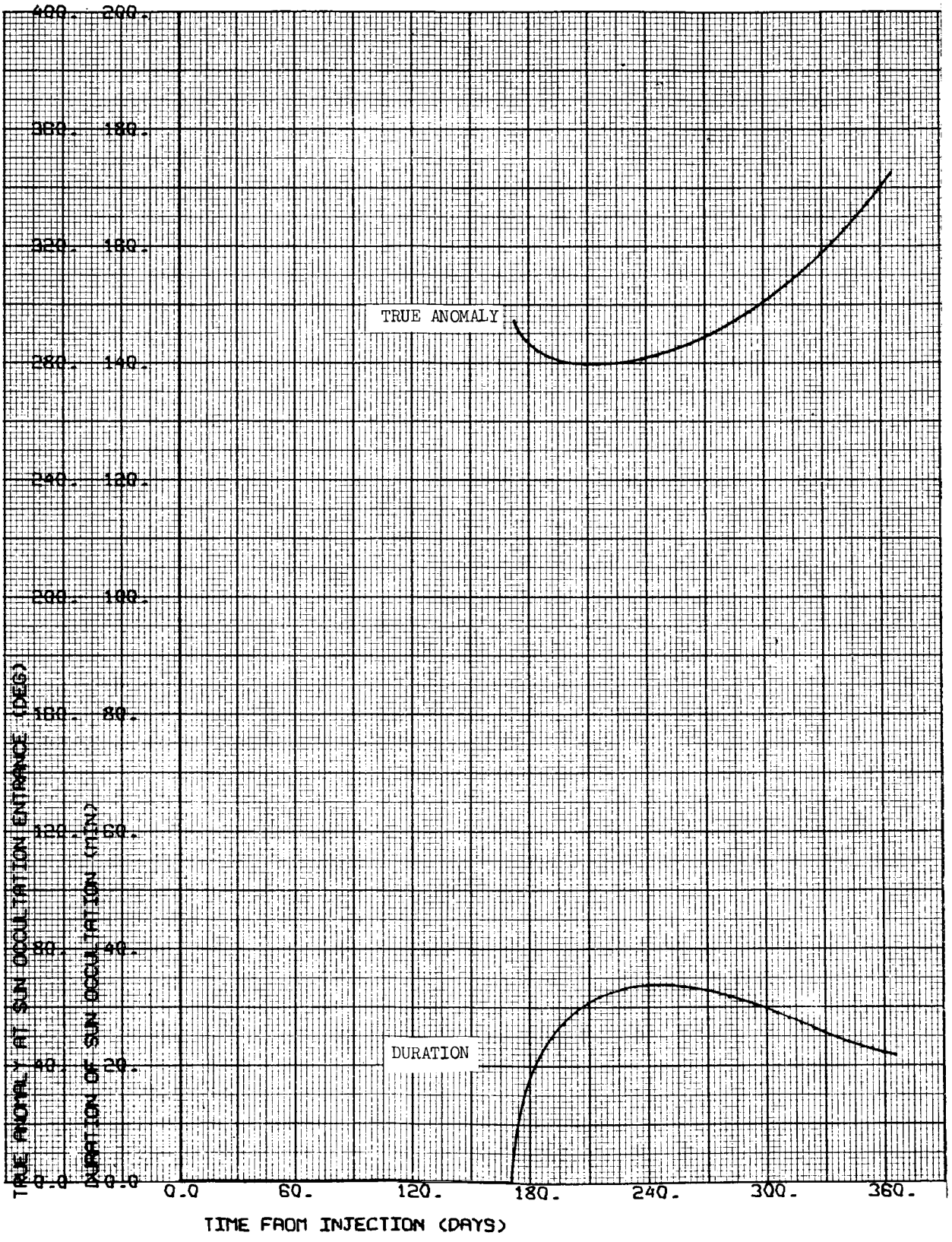
TRUE ANOMALY
DURATION
TRUE ANOMALY AT SUN OCCULTATION ENTRANCE (DEG)
DURATION OF SUN OCCULTATION (MIN)
TIME FROM INJECTION (DAYS)
400.
380.
320.
280.
240.
200.
160.
120.
80.
40.
0.0
200.
180.
160.
140.
120.
100.
80.
60.
40.
20.
0.0
0.0
60.
120.
180.
240.
300.
360.

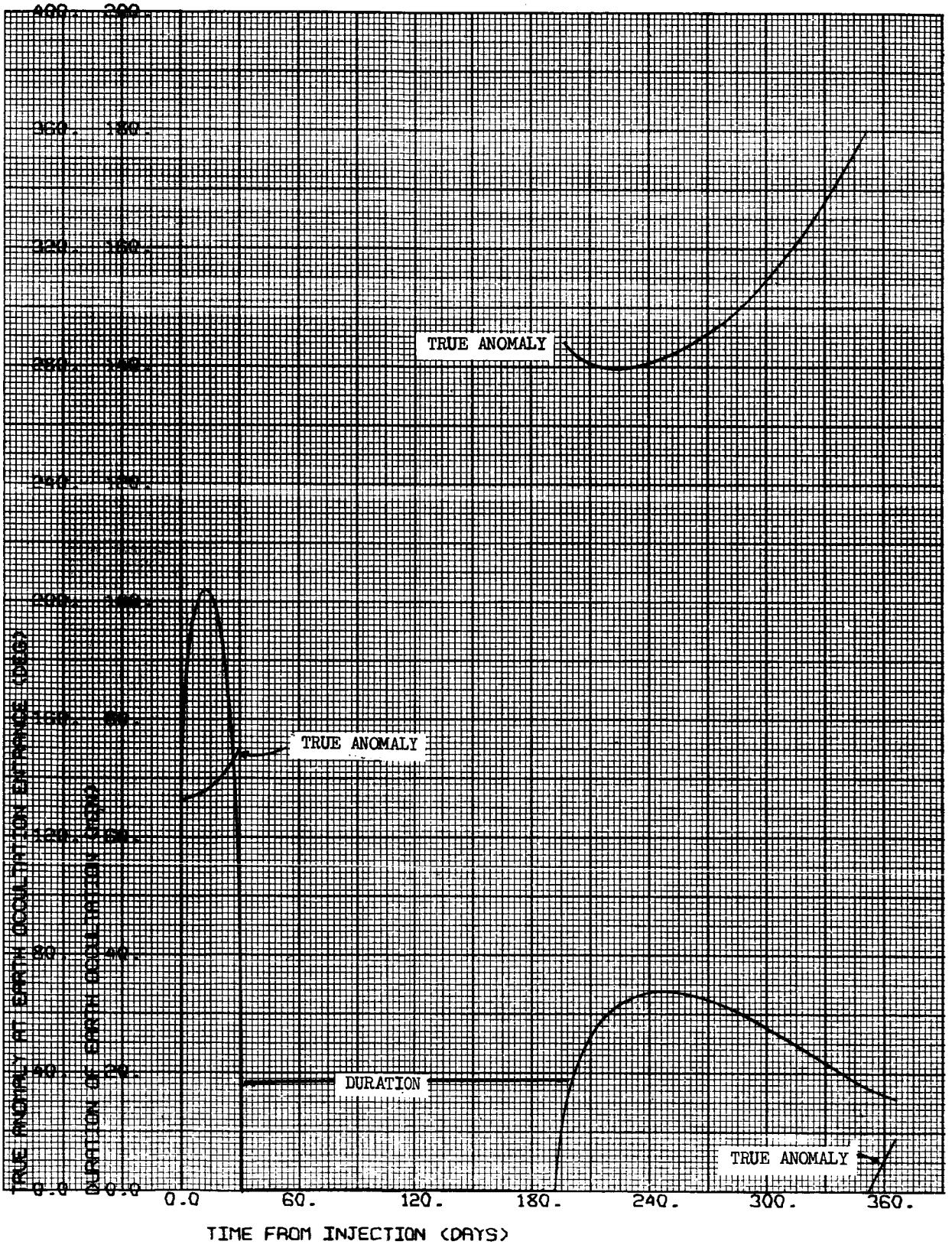
TRUE ANOMALY
TRUE ANOMALY
DURATION
TRUE ANOMALY
TRUE ANOMALY AT EARTH OCCULTATION ENTRANCE (DEG)
DURATION OF EARTH OCCULTATION (DAYS)
0.0
60.
120.
180.
240.
300.
360.
TIME FROM INJECTION (DAYS)

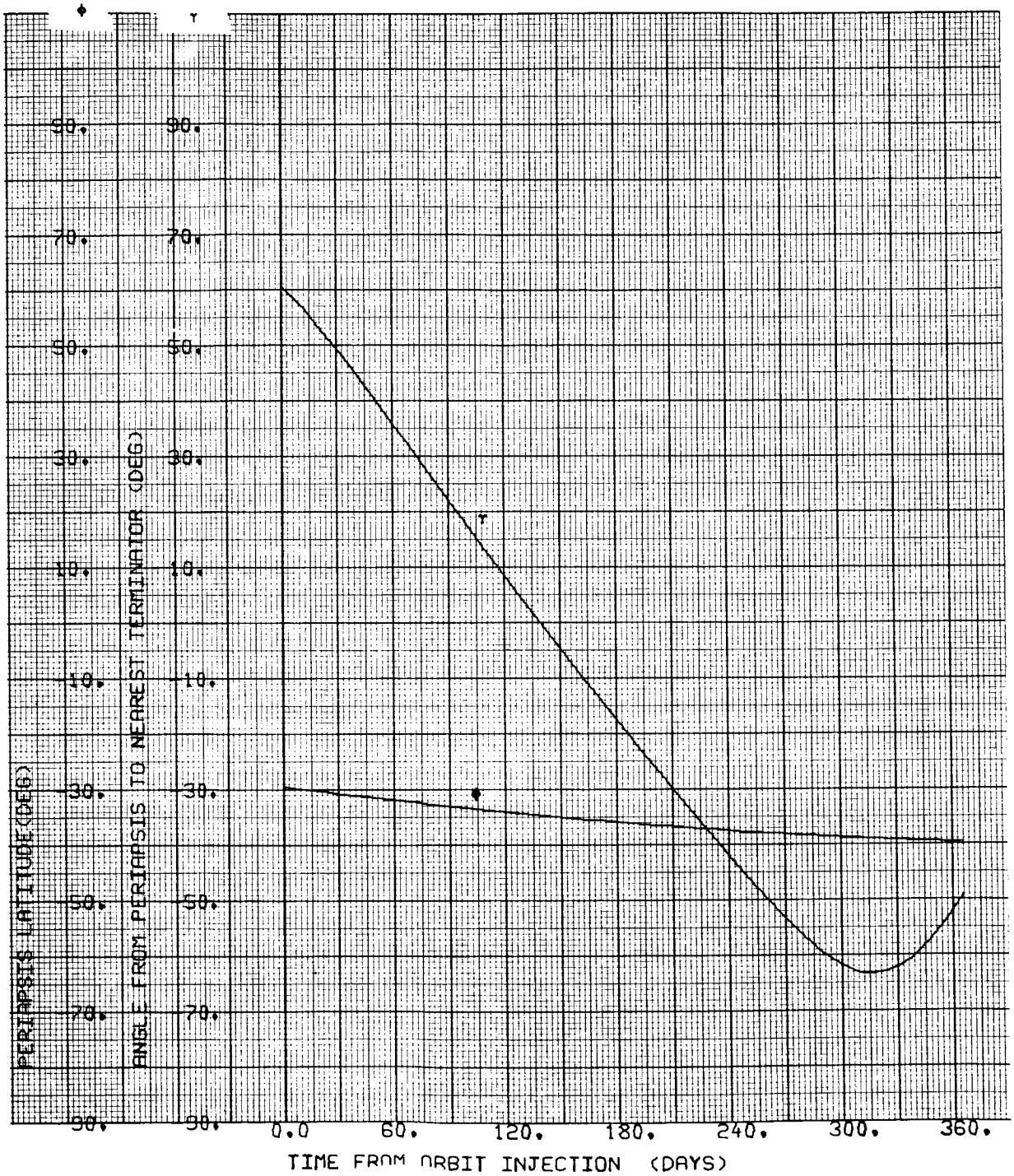
PERIAPSIS LATITUDE (DEG)
ANGLE FROM PERIAPSIS TO NEAREST TERMINATOR (DEG)
90.
70.
50.
30.
10.
-10.
-30.
-50.
-70.
-90.
0.0
60.
120.
180.
240.
300.
360.
TIME FROM ORBIT INJECTION (DAYS)

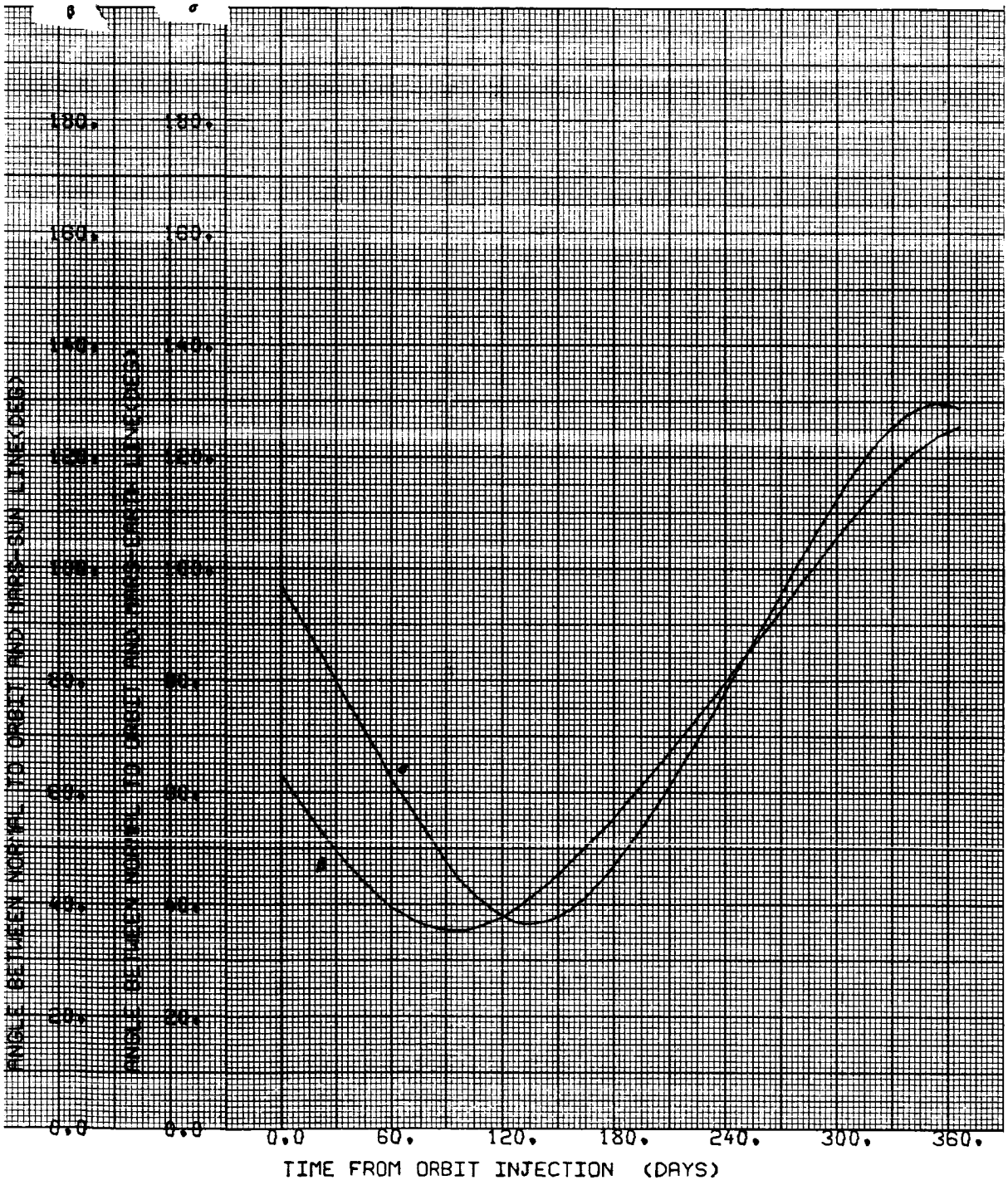
ANGLE BETWEEN VORTEX ORBIT AND THE SUN LINE (DEG)
ANGLE BETWEEN VORTEX ORBIT AND EARTH-SUN LINE (DEG)
180.
160.
140.
120.
100.
80.
60.
40.
20.
0.0
0.0
60.
120.
180.
240.
300.
360.
TIME FROM ORBIT INJECTION (DAYS)

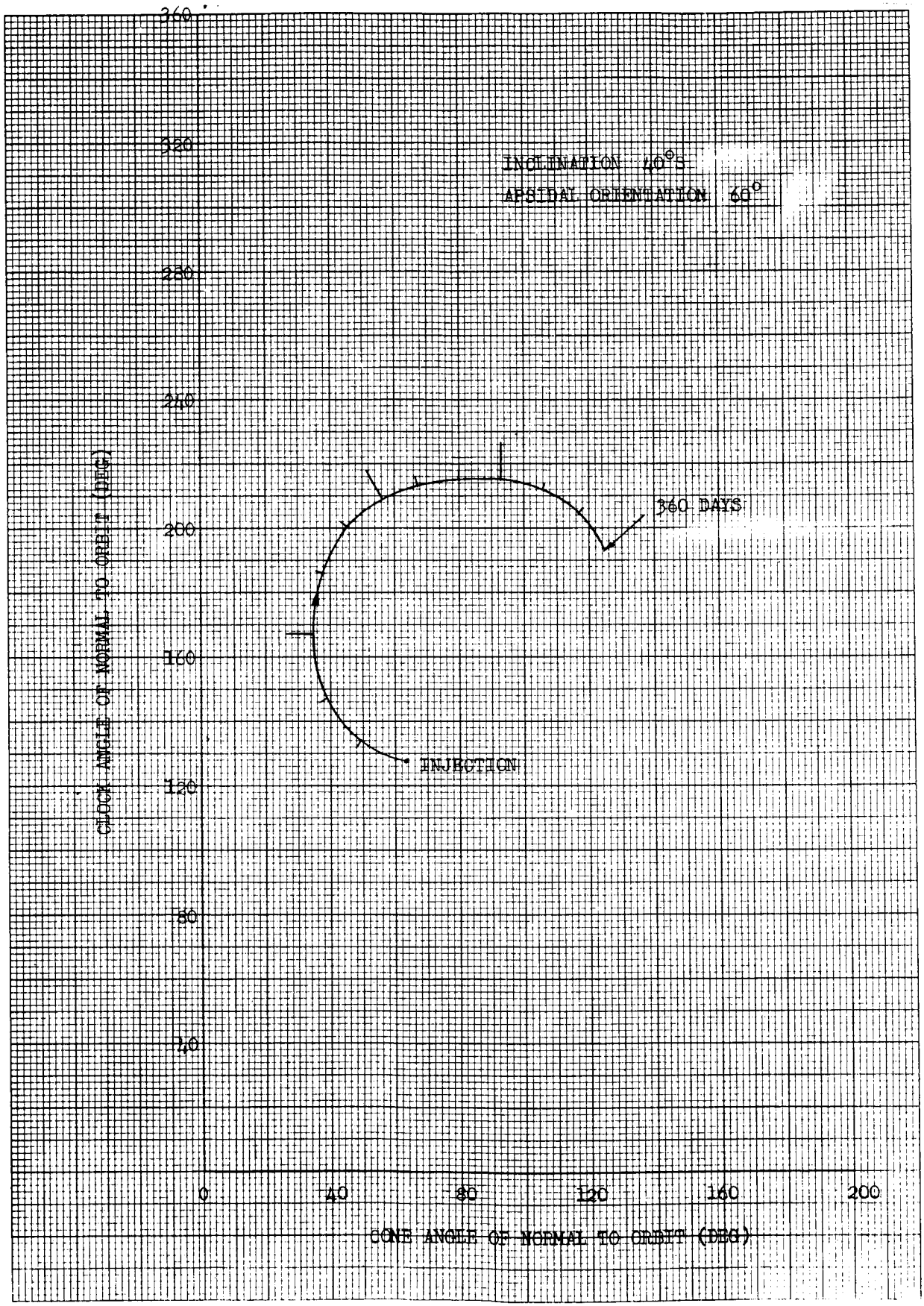
INCLINATION 40°S
APSIDAL ORIENTATION 60°
360 DAYS
INJECTION
CLOCK ANGLE OF NORMAL TO ORBIT (DEG)
CONE ANGLE OF NORMAL TO ORBIT (DEG)
360
320
280
240
200
160
120
80
40
0
40
80
120
160
200

CASE NO. 10

1000 x 15, 000 km

$i = 40^{o}S$

$\Psi = 90$ deg

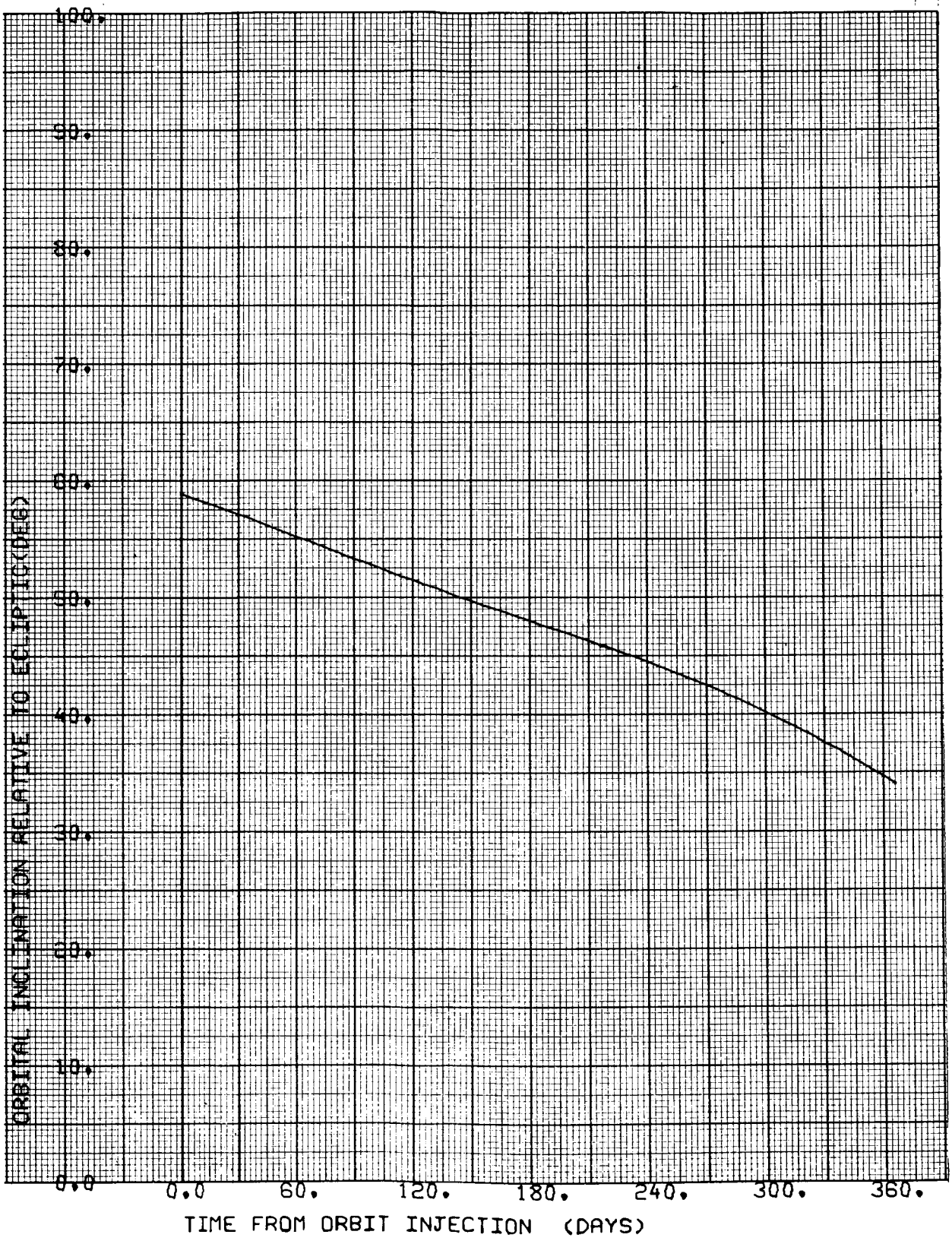
100.
90.
80.
70.
60.
50.
40.
30.
20.
10.
0.0
ORBITAL INCLINATION RELATIVE TO ECLIPTIC(DEG)
0.0
60.
120.
180.
240.
300.
360.
TIME FROM ORBIT INJECTION (DAYS)

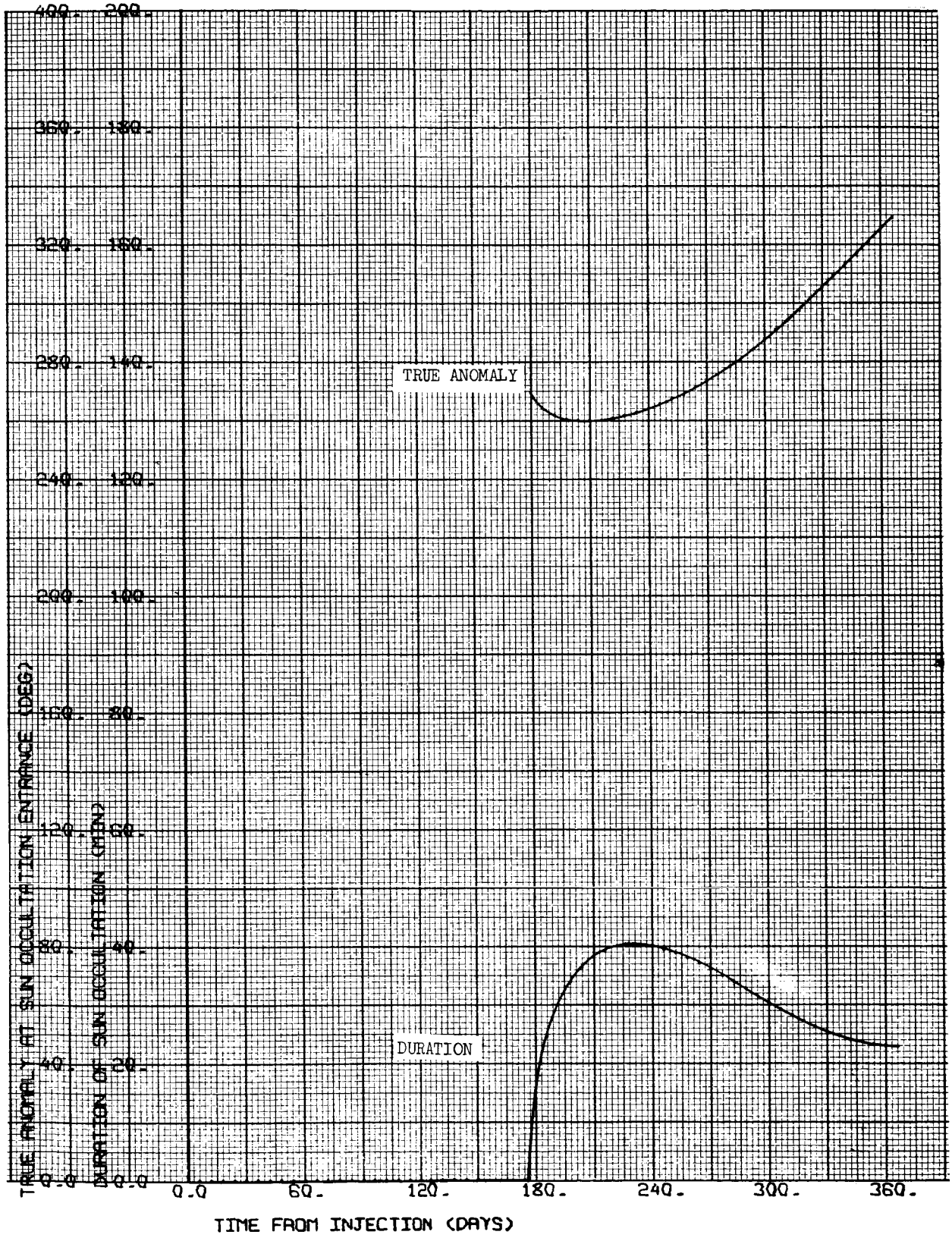
TRUE ANOMALY
DURATION
TRUE ANOMALY AT SUN OCCULTATION ENTRANCE (DEG)
DURATION OF SUN OCCULTATION (MIN)
TIME FROM INJECTION (DAYS)
0.0
60.
120.
180.
240.
300.
360.
400.
360.
320.
280.
240.
200.
160.
120.
80.
40.
0.0
200.
180.
160.
140.
120.
100.
80.
60.
40.
20.
0.0

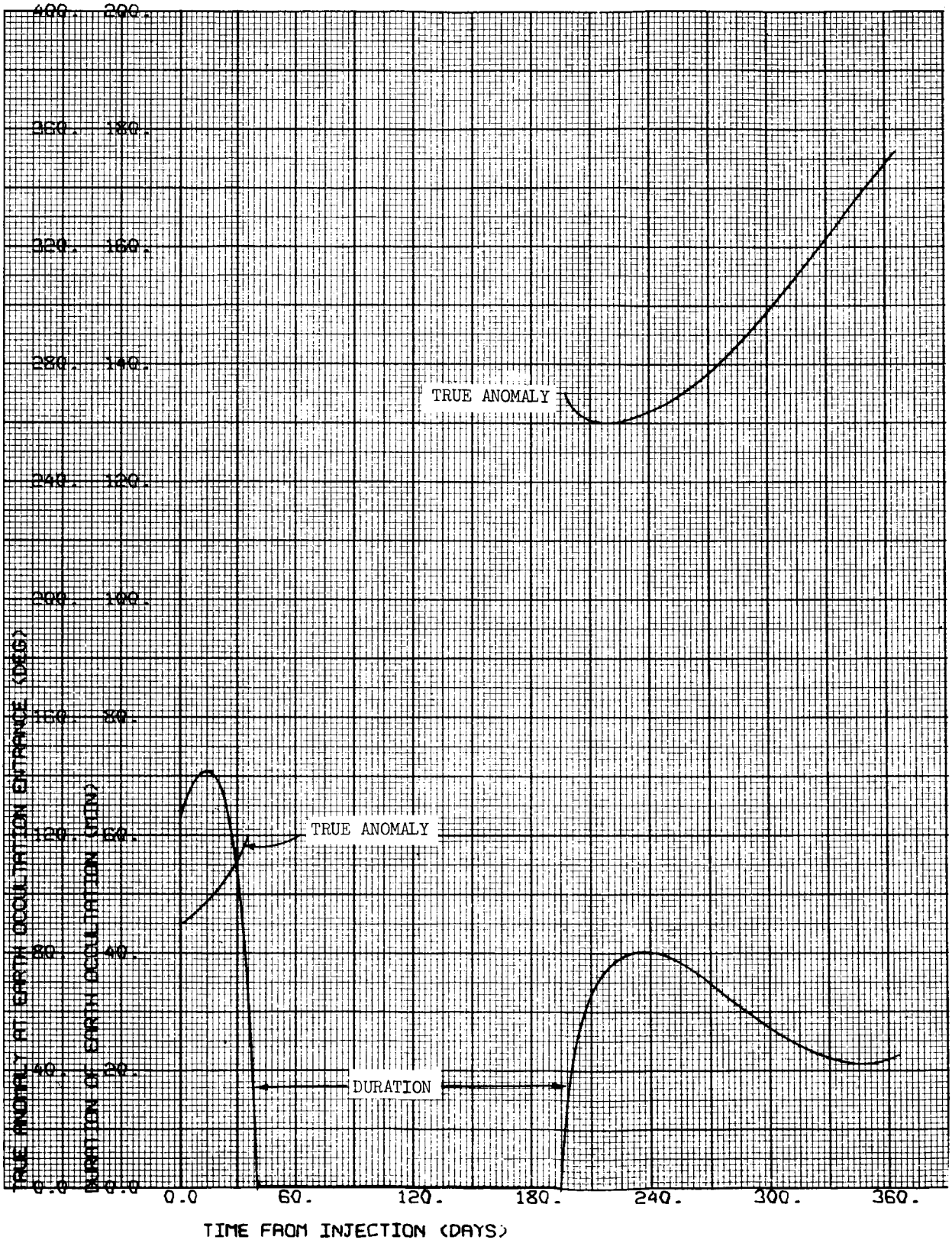
TRUE ANOMALY
TRUE ANOMALY
DURATION
TRUE ANOMALY AT EARTH OCCULTATION ENTRANCE (DEG)
DURATION OF EARTH OCCULTATION (MIN)
400.
360.
320.
280.
240.
200.
160.
120.
80.
40.
0.0
200.
180.
160.
140.
120.
100.
80.
60.
40.
20.
0.0
0.0
60.
120.
180.
240.
300.
360.
TIME FROM INJECTION (DAYS)

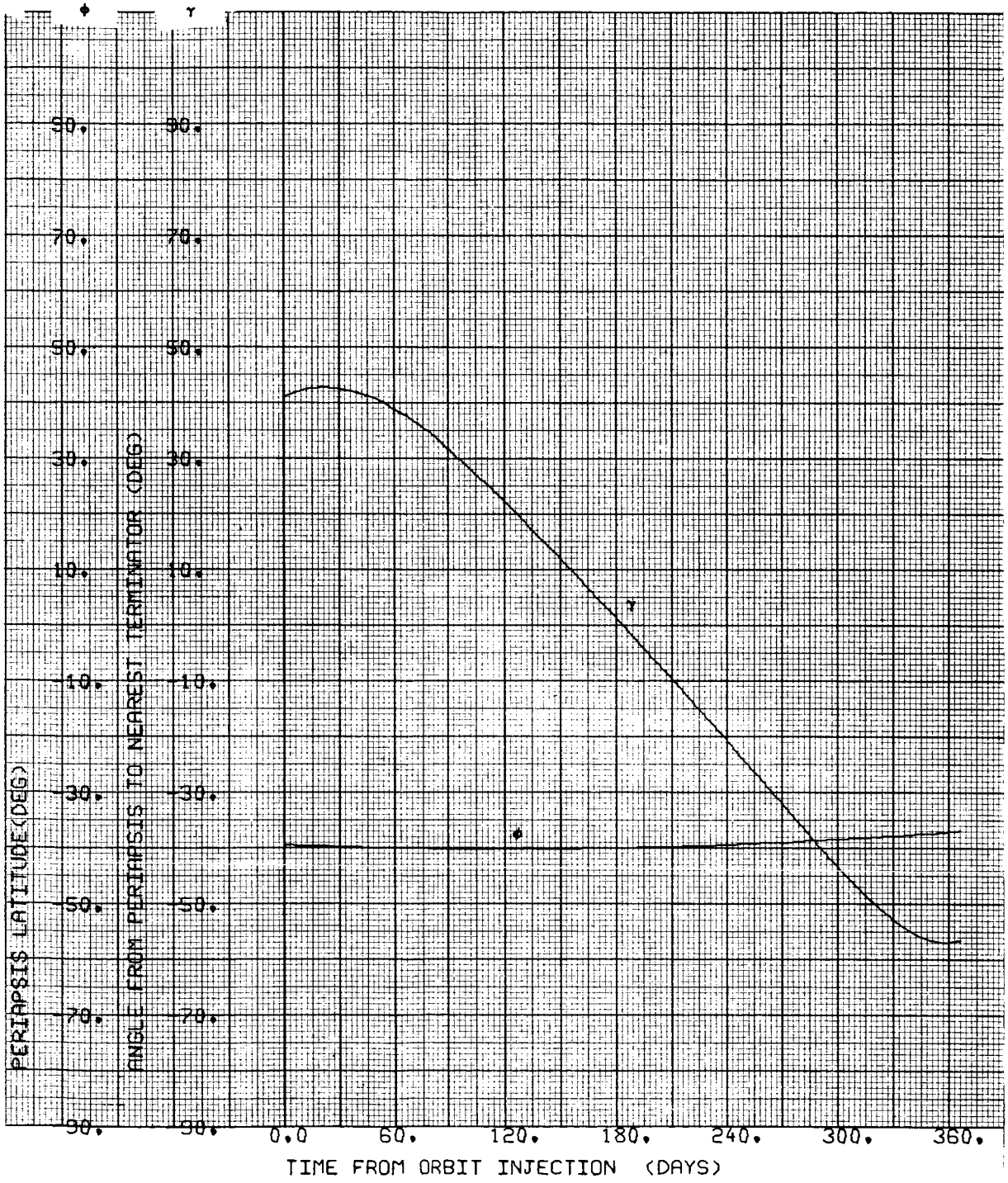
Φ
γ
90.
70.
50.
30.
10.
-10.
-30.
-50.
-70.
-90.
PERIAPSIS LATITUDE(DEG)
ANGLE FROM PERIAPSIS TO NEAREST TERMINATOR (DEG)
0.0
60.
120.
180.
240.
300.
360.
TIME FROM ORBIT INJECTION (DAYS)

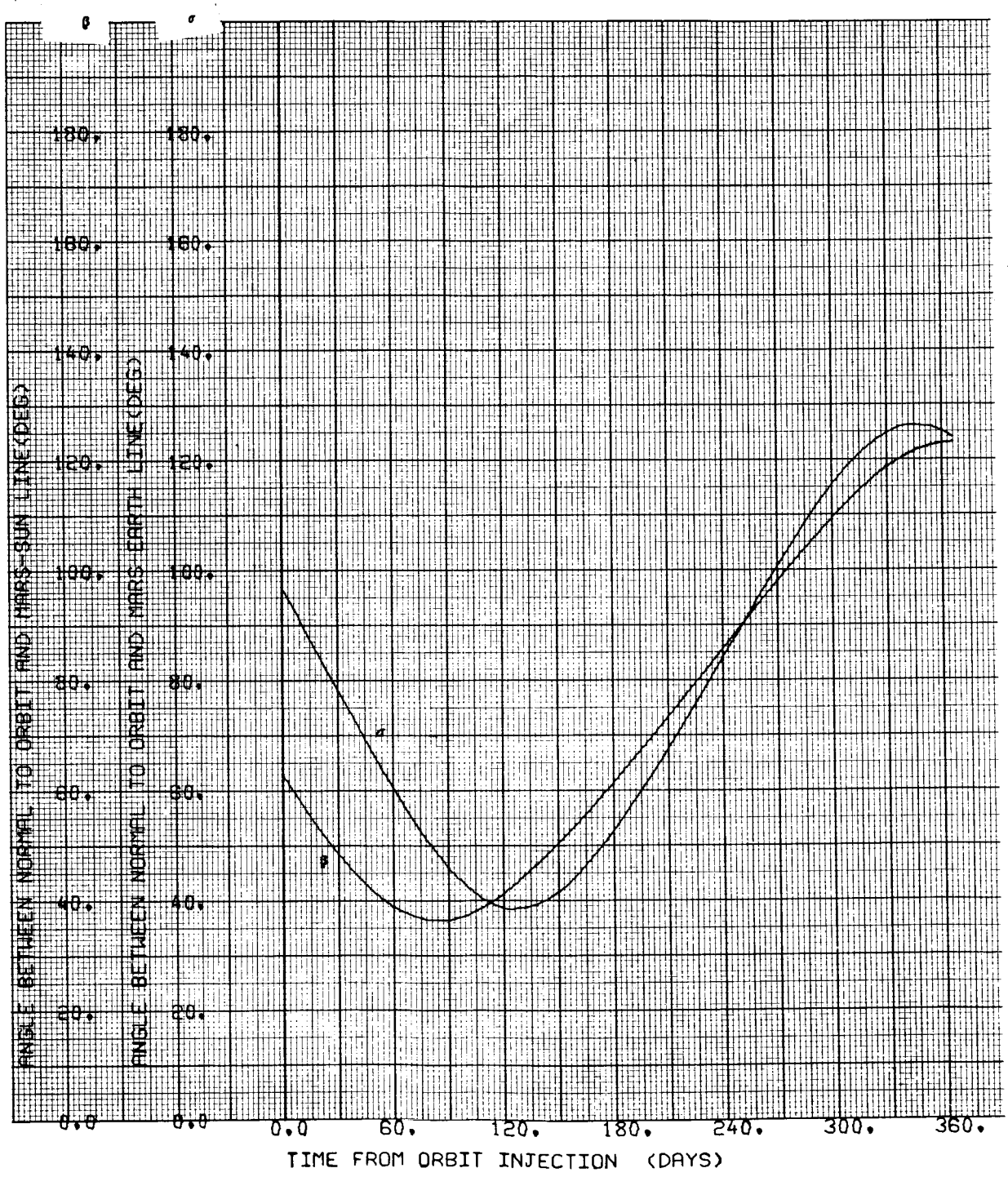
β
σ
180.
160.
140.
120.
100.
80.
60.
40.
20.
0.0
ANGLE BETWEEN NORMAL TO ORBIT AND MARS-SUN LINE (DEG)
ANGLE BETWEEN NORMAL TO ORBIT AND MARS-EARTH LINE (DEG)
0.0
60.
120.
180.
240.
300.
360.
TIME FROM ORBIT INJECTION (DAYS)

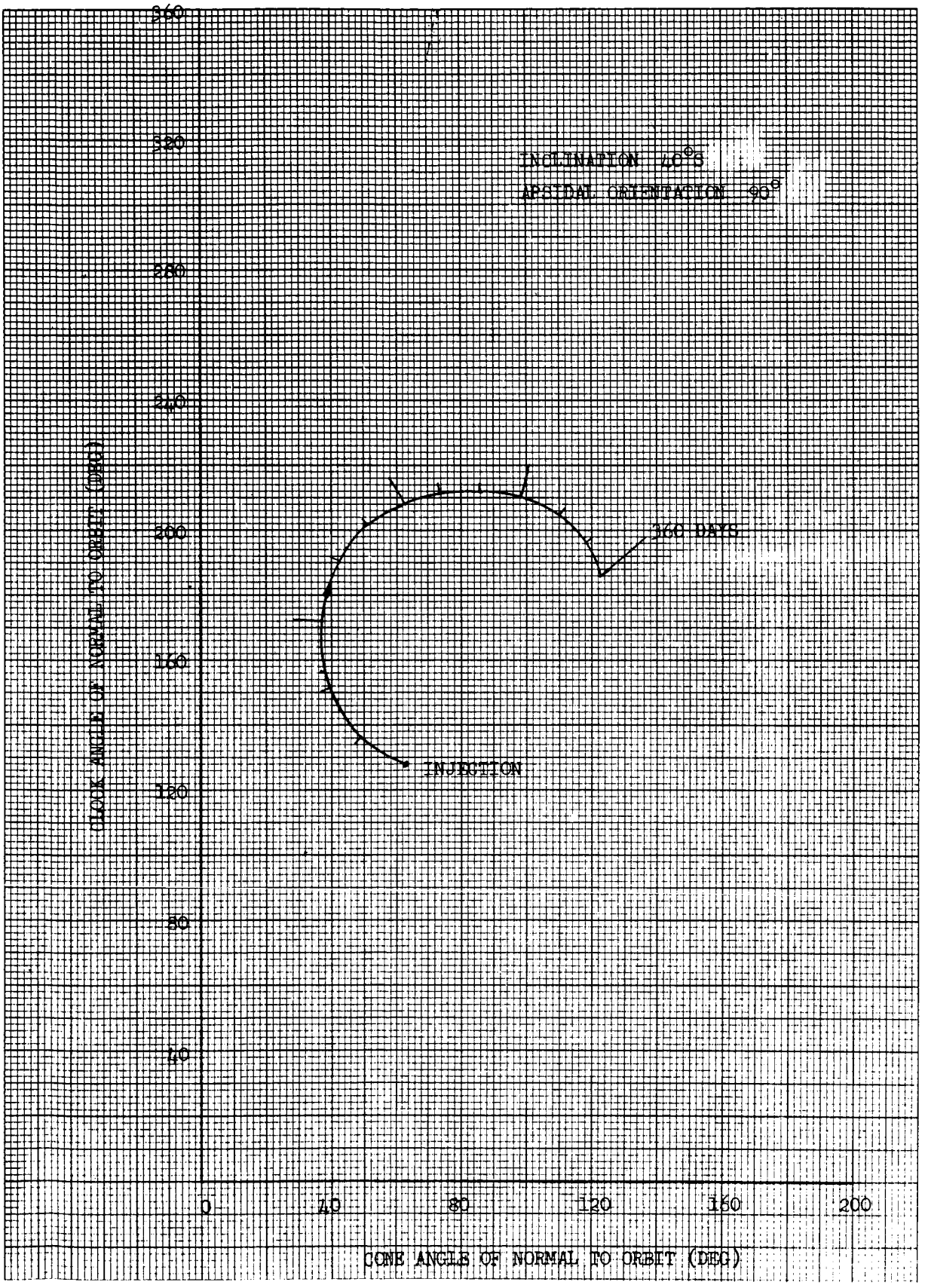
INCLINATION 40°S
APSIDAL ORIENTATION 90°
360 DAYS
INJECTION
CLOCK ANGLE OF NORMAL TO ORBIT (DEG)
360
320
280
240
200
160
120
80
40
0
40
80
120
160
200
CONE ANGLE OF NORMAL TO ORBIT (DEG)

CASE NO. 11

1000 x 15, 000 km

$i = 40^{o}S$

$\Psi = 150$ deg

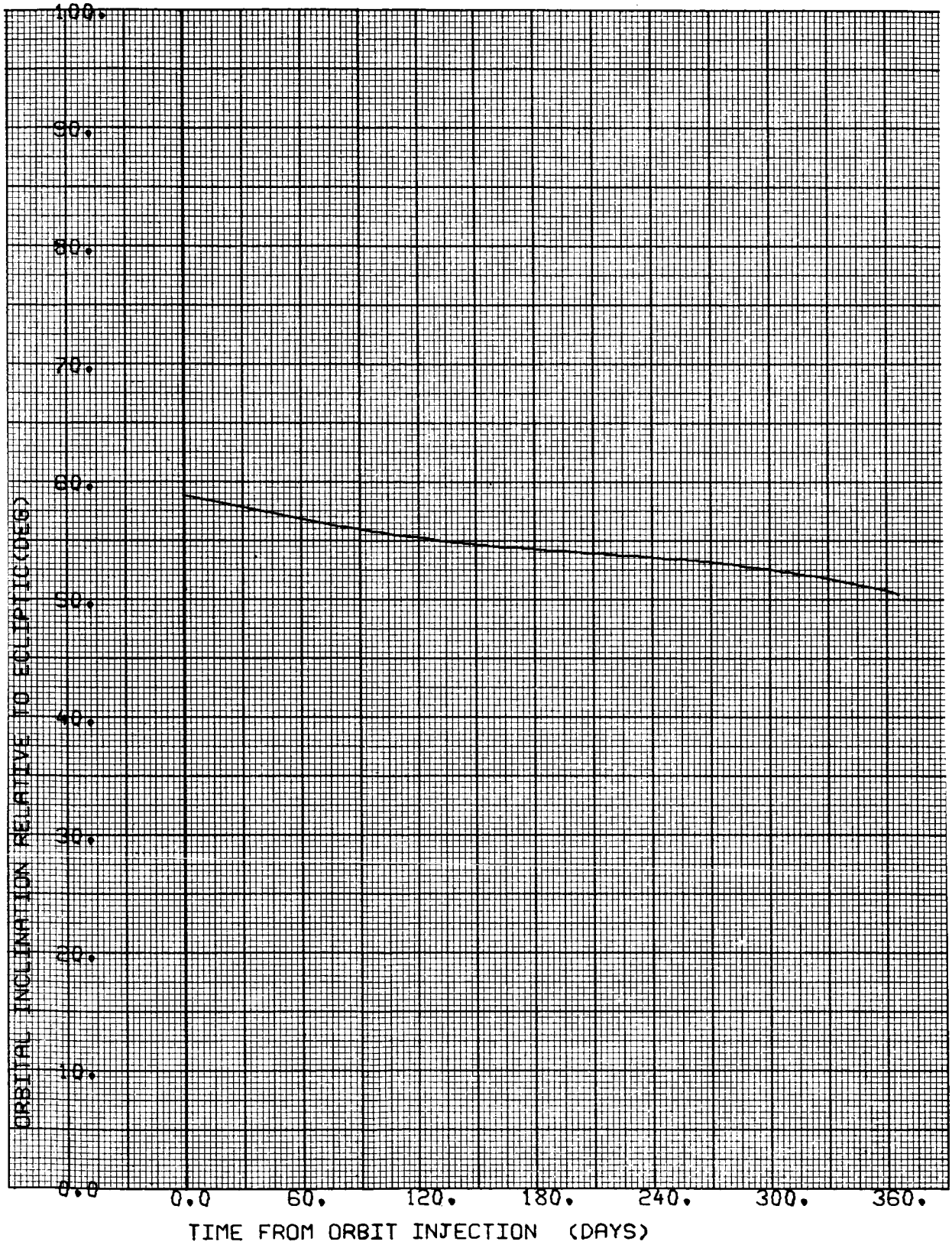
100.
90.
80.
70.
60.
50.
40.
30.
20.
10.
0.0
ORBITAL INCLINATION RELATIVE TO ECLIPTIC(DEG)
0.0
60.
120.
180.
240.
300.
360.
TIME FROM ORBIT INJECTION (DAYS)

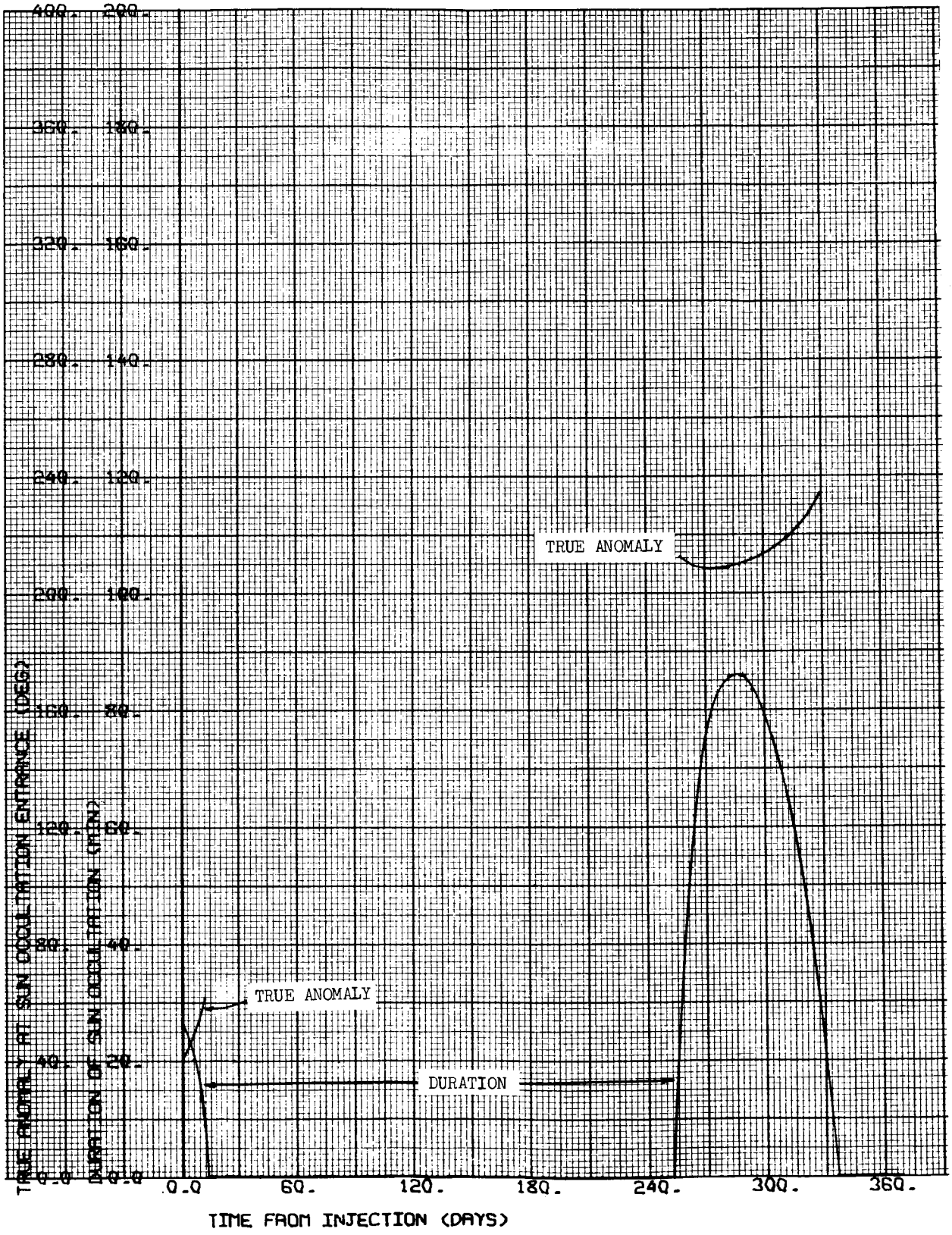
TRUE ANOMALY
TRUE ANOMALY
DURATION
TIME FROM INJECTION (DAYS)
TRUE ANOMALY AT SUN OCCULTATION ENTRANCE (DEG)
DURATION OF SUN OCCULTATION (MIN)
0.0
60.
120.
180.
240.
300.
360.
400.
360.
320.
280.
240.
200.
160.
120.
80.
40.
0.0
200.
180.
160.
140.
120.
100.
80.
60.
40.
20.
0.0

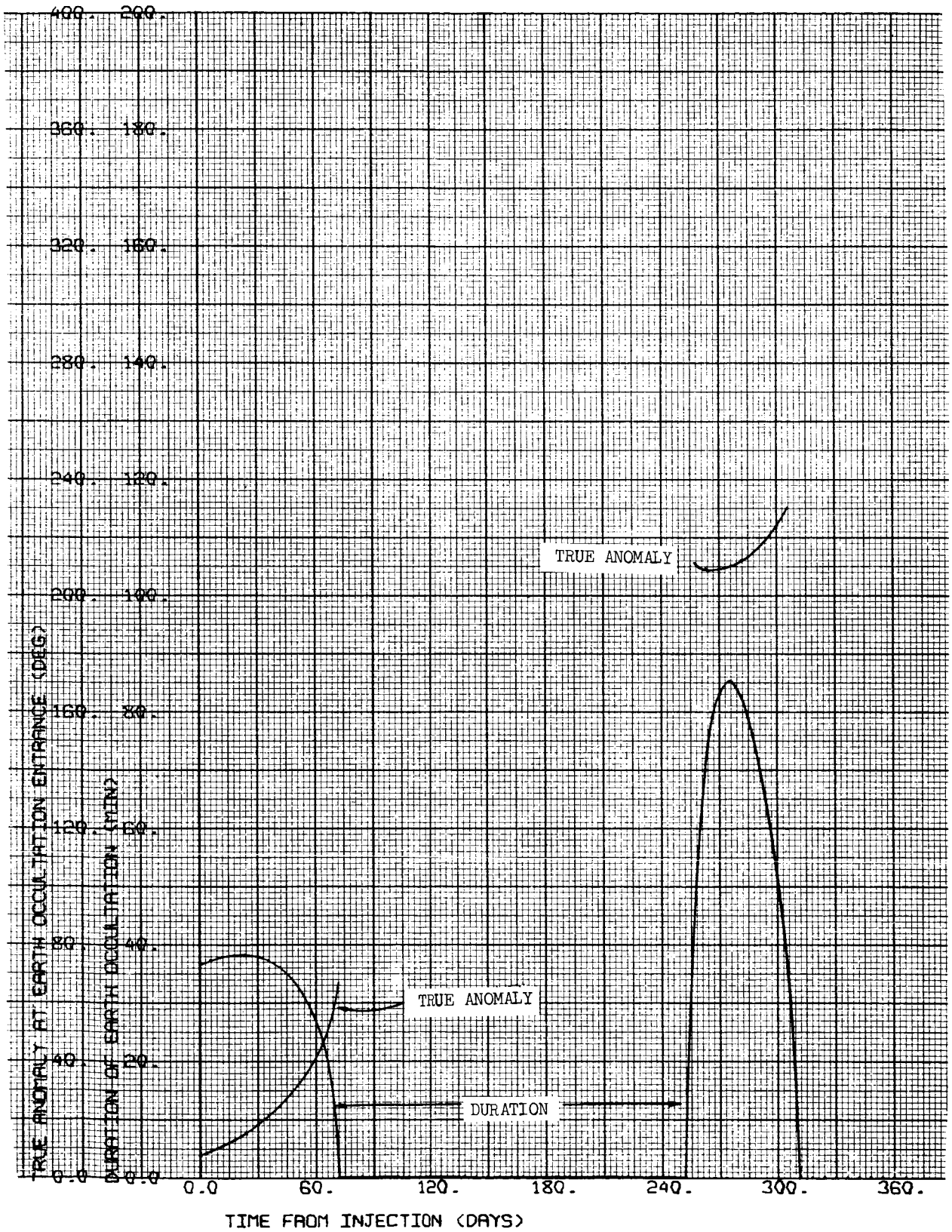
TRUE ANOMALY AT EARTH OCCULTATION ENTRANCE (DEG)
DURATION OF EARTH OCCULTATION (MIN)
TIME FROM INJECTION (DAYS)
TRUE ANOMALY
TRUE ANOMALY
DURATION
0.0
60.
120.
180.
240.
300.
360.
400.
360.
320.
280.
240.
200.
160.
120.
80.
40.
0.0
200.
180.
160.
140.
120.
100.
80.
60.
40.
20.
0.0

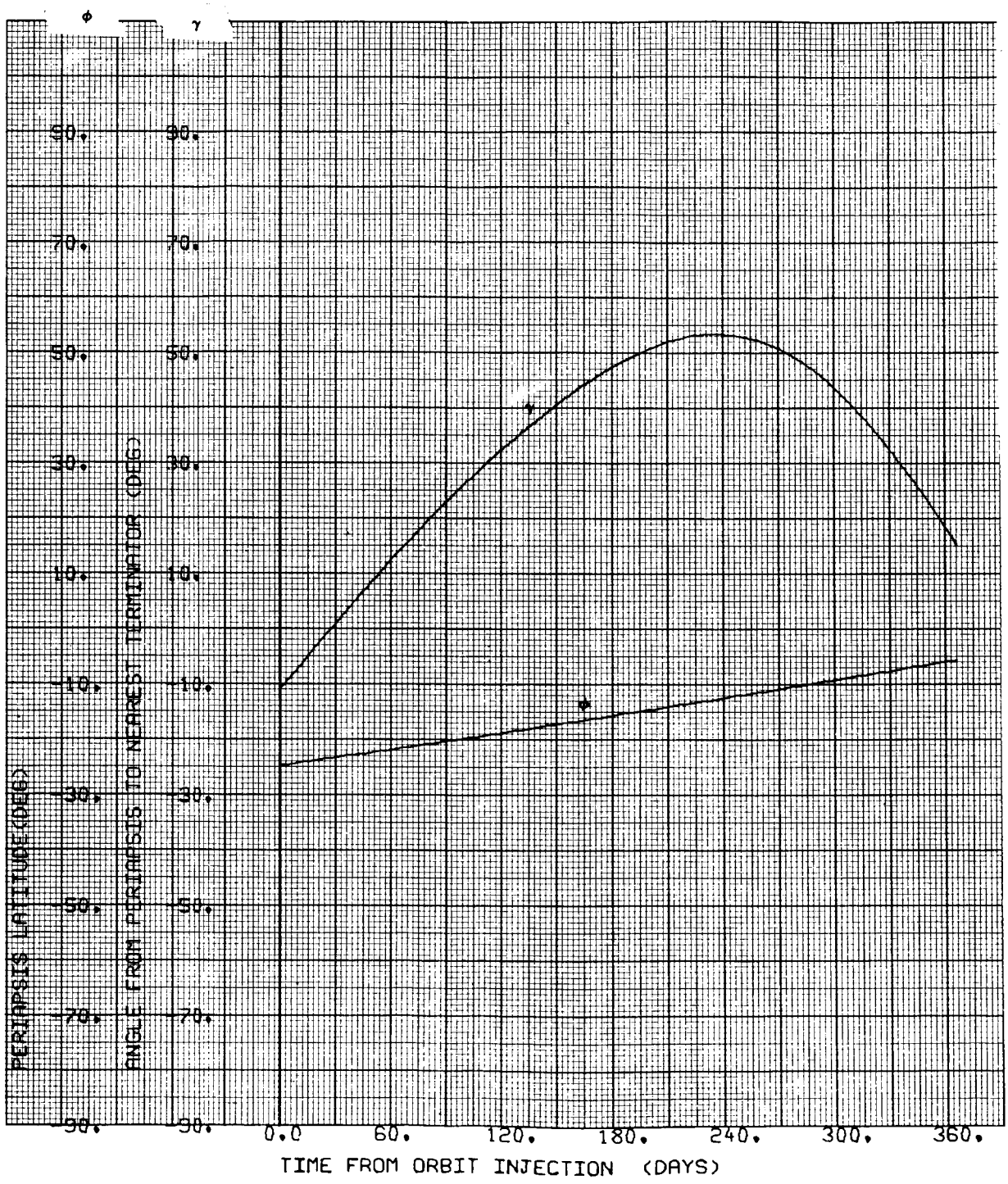
φ
γ
90.
70.
50.
30.
10.
-10.
-30.
-50.
-70.
-90.
PERIAPSIS LATITUDE (DEG)
ANGLE FROM PERIAPSIS TO NEAREST TERMINATOR (DEG)
0.0
60.
120.
180.
240.
300.
360.
TIME FROM ORBIT INJECTION (DAYS)

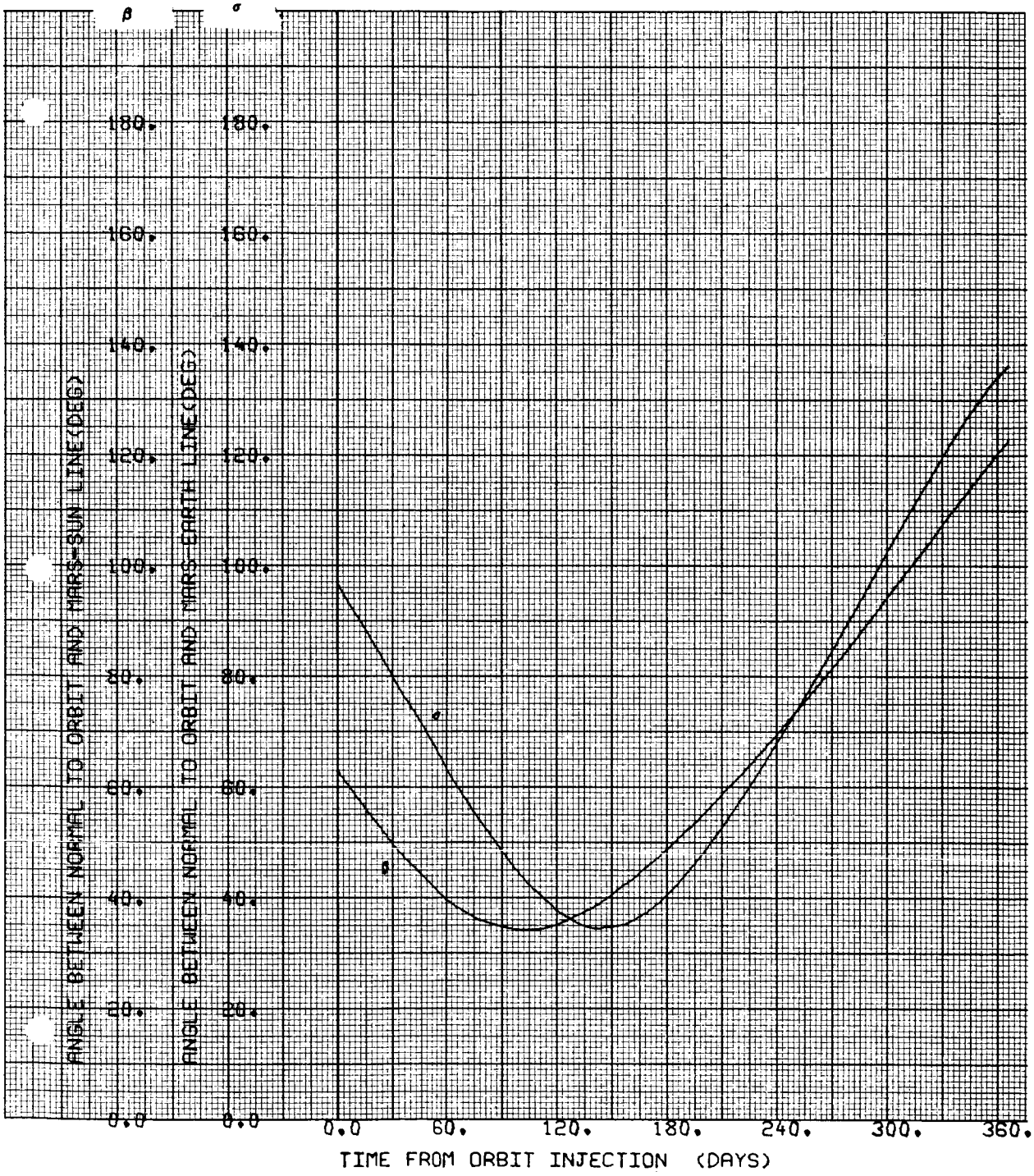
β
σ
180.
160.
140.
120.
100.
80.
60.
40.
20.
0.0
ANGLE BETWEEN NORMAL TO ORBIT AND MARS-SUN LINE(DEG)
ANGLE BETWEEN NORMAL TO ORBIT AND MARS-EARTH LINE(DEG)
0.0
60.
120.
180.
240.
300.
360.
TIME FROM ORBIT INJECTION (DAYS)

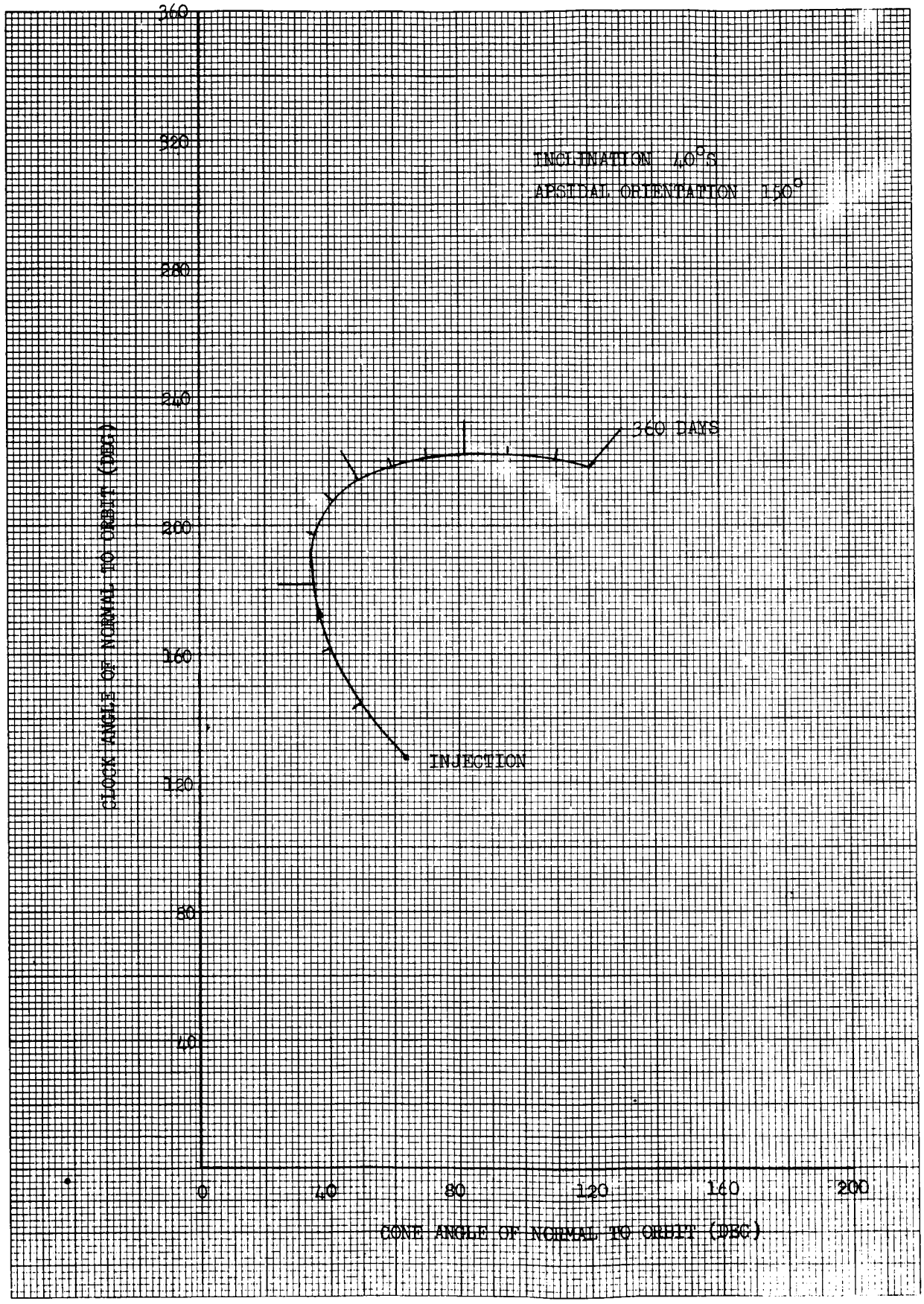
INCLINATION 40°S
APSIDAL ORIENTATION 150°
360 DAYS
INJECTION
CLOCK ANGLE OF NORMAL TO ORBIT (DEG)
CONE ANGLE OF NORMAL TO ORBIT (DEG)
360
320
280
240
200
160
120
80
40
0
40
80
120
160
200

CASE NO. 12

1000 x 15,000 km

$i = 40^{\circ}S$

$\Psi = 120.834$ deg

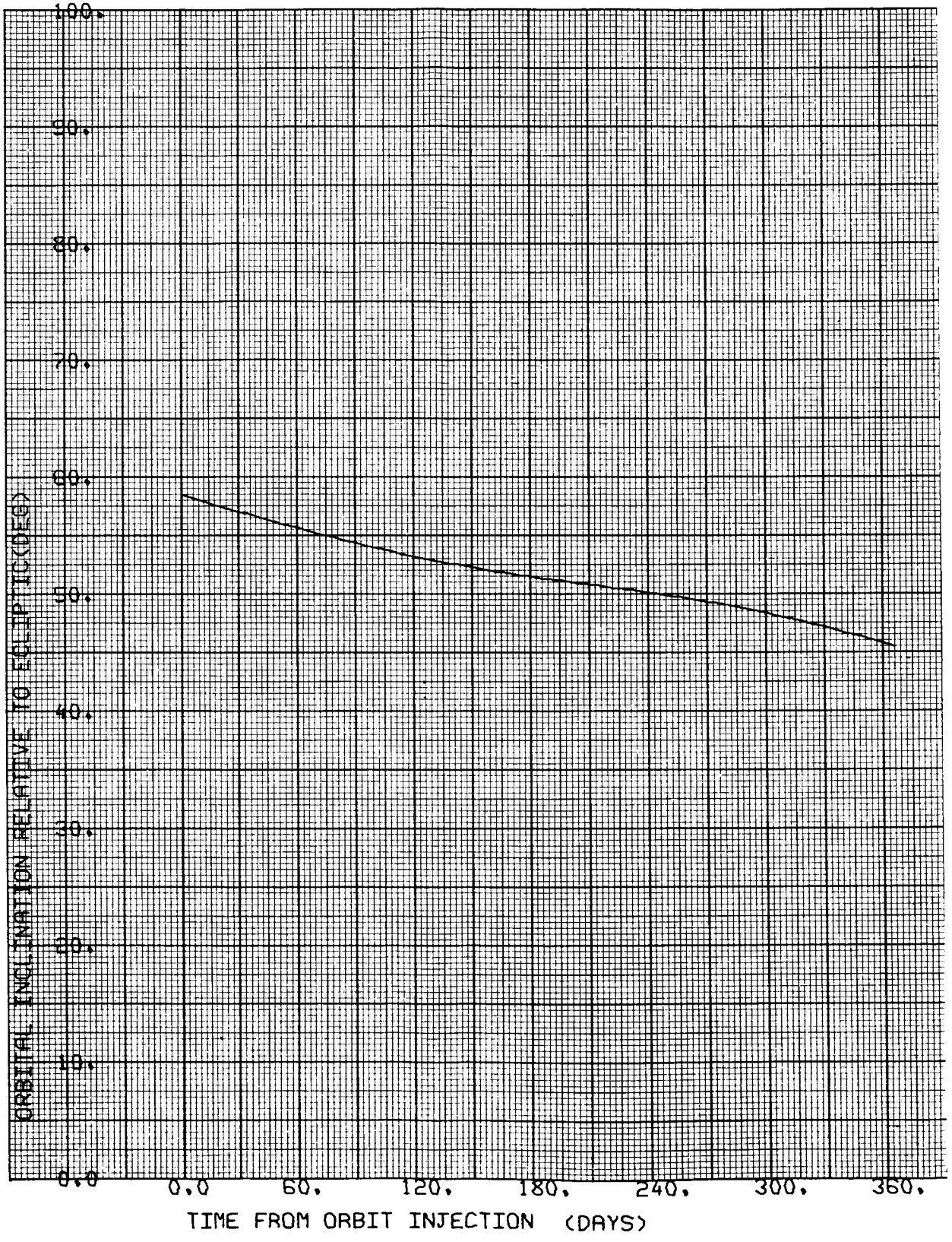
100.
90.
80.
70.
60.
50.
40.
30.
20.
10.
0.0
ORBITAL INCLINATION RELATIVE TO ECLIPTIC(DEG)
0.0
60.
120.
180.
240.
300.
360.
TIME FROM ORBIT INJECTION (DAYS)

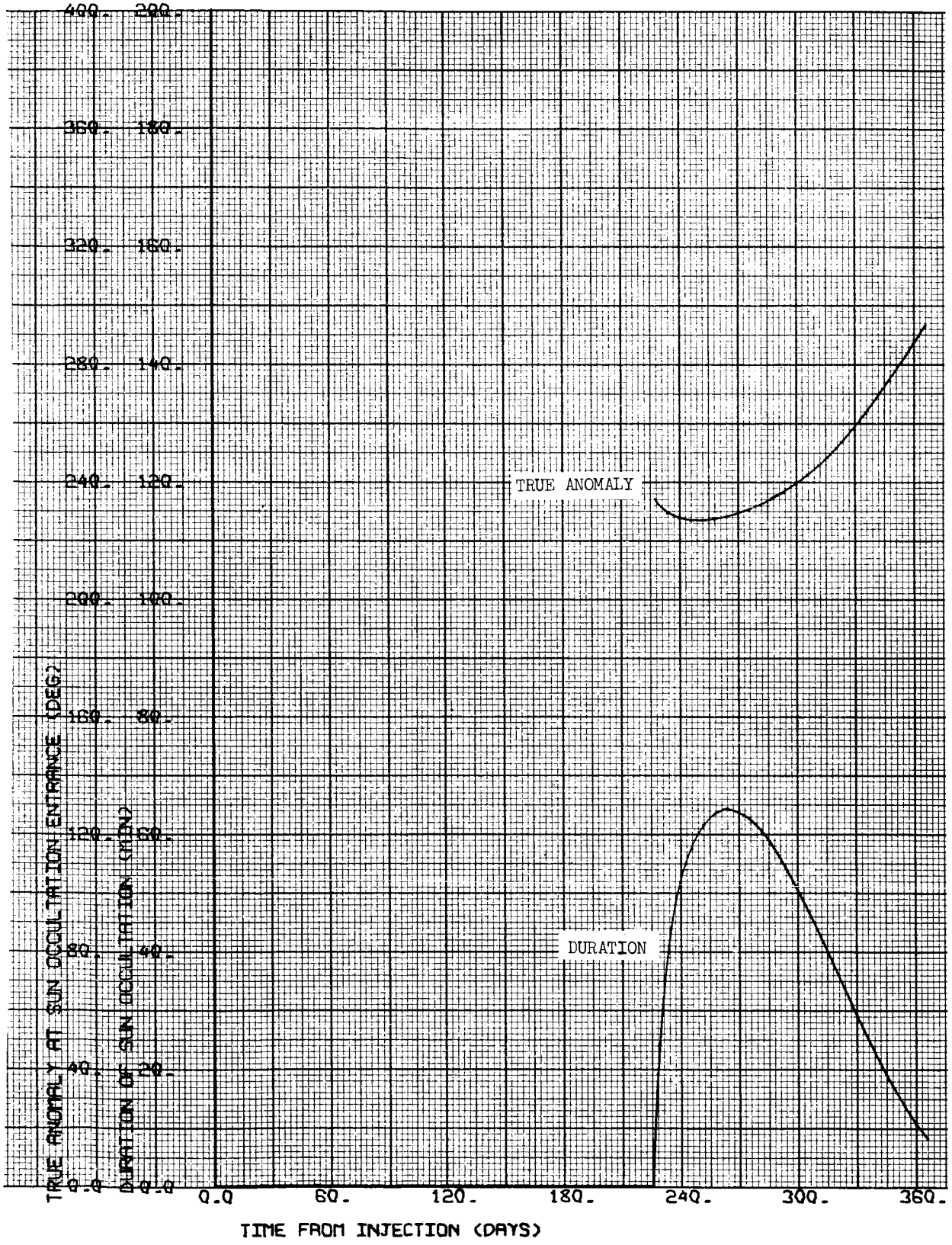
TRUE ANOMALY
DURATION
TRUE ANOMALY AT SUN OCCULTATION ENTRANCE (DEG)
DURATION OF SUN OCCULTATION (MIN)
TIME FROM INJECTION (DAYS)
0.0
60.
120.
180.
240.
300.
360.
400.
360.
320.
280.
240.
200.
160.
120.
80.
40.
0.0
200.
180.
160.
140.
120.
100.
80.
60.
40.
20.
0.0

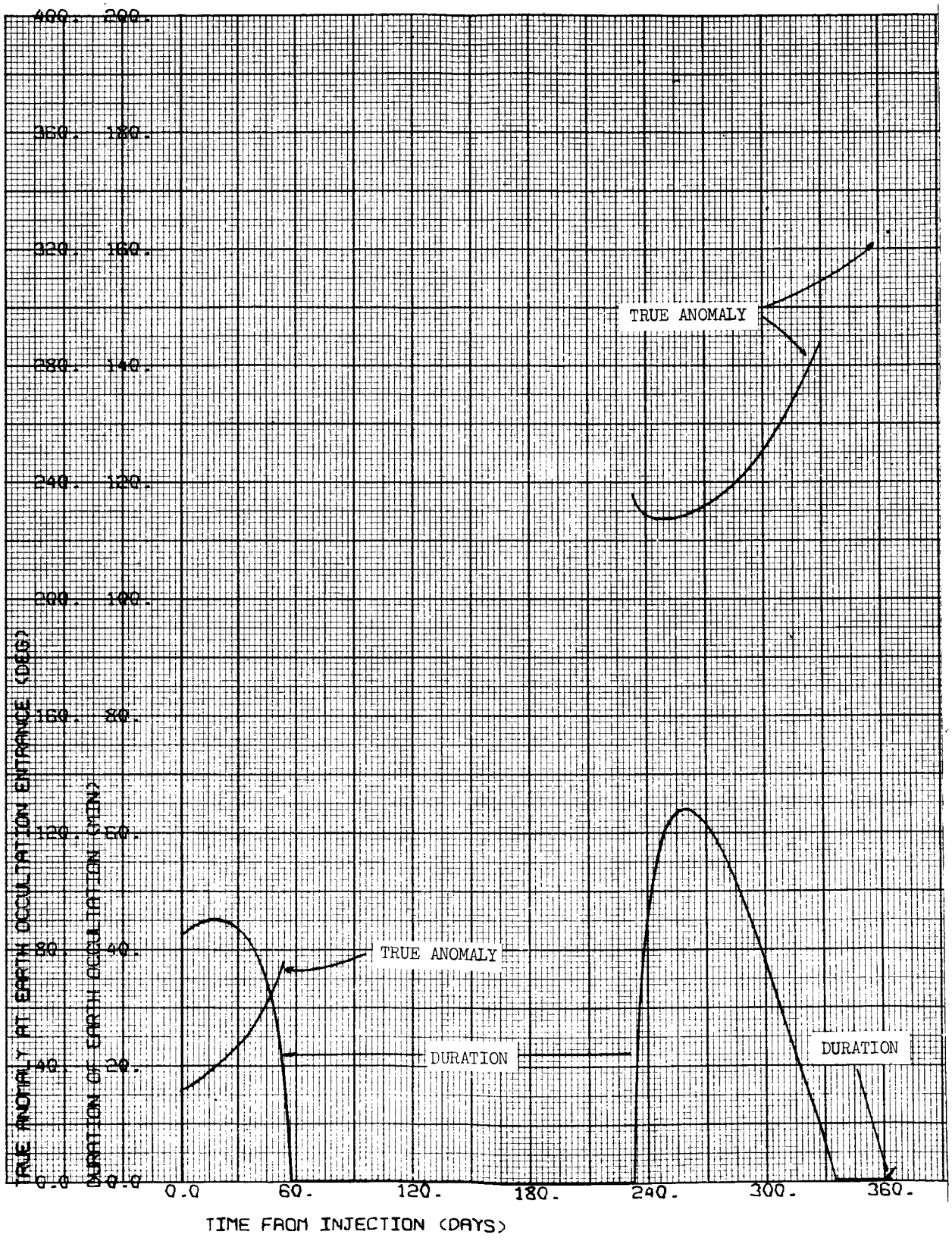
TRUE ANOMALY
TRUE ANOMALY
DURATION
DURATION
TRUE ANOMALY AT EARTH OCCULTATION ENTRANCE (DEG)
DURATION OF EARTH OCCULTATION (MIN)
TIME FROM INJECTION (DAYS)
0.0
60.
120.
180.
240.
300.
360.
400.
360.
320.
280.
240.
200.
160.
120.
80.
40.
0.0
200.
180.
160.
140.
120.
100.
80.
60.
40.
20.
0.0

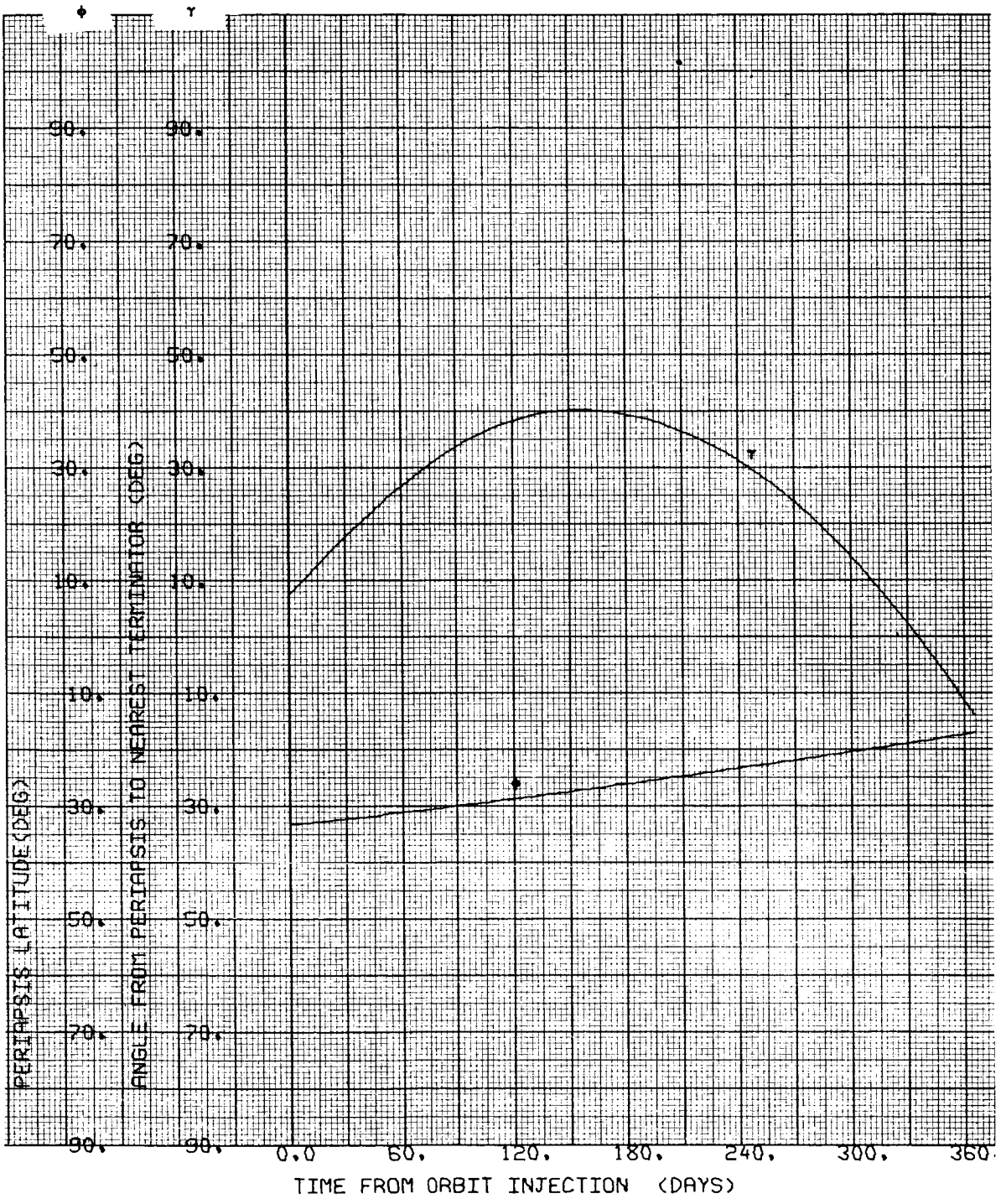
PERIAPSIS LATITUDE(DEG)
ANGLE FROM PERIAPSIS TO NEAREST TERMINATOR (DEG)
90.
70.
50.
30.
10.
0.0
60.
120.
180.
240.
300.
360.
TIME FROM ORBIT INJECTION (DAYS)

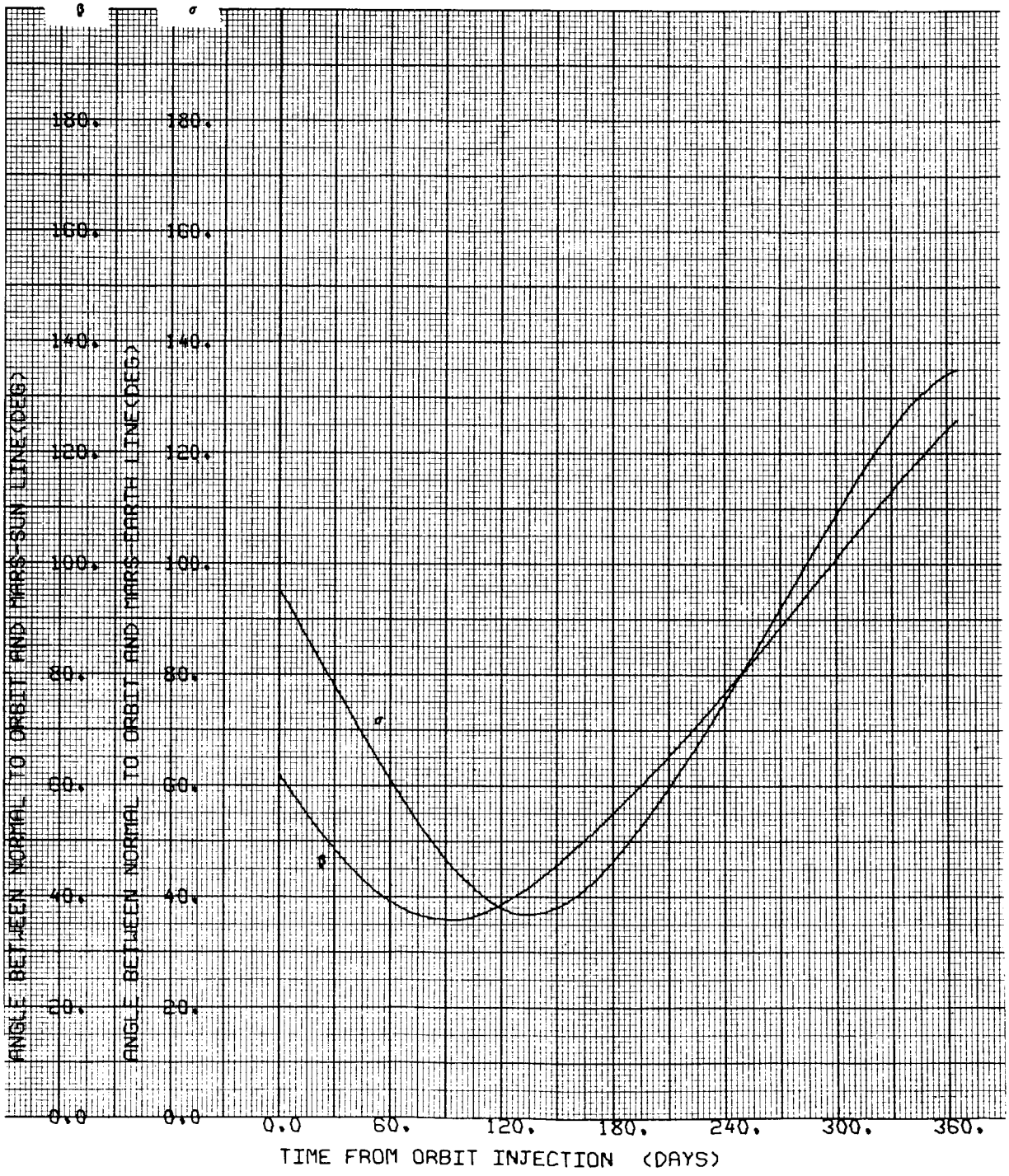
β
σ
180.
160.
140.
120.
100.
80.
60.
40.
20.
0.0
ANGLE BETWEEN NORMAL TO ORBIT AND MARS-SUN LINE(DEG)
ANGLE BETWEEN NORMAL TO ORBIT AND MARS-EARTH LINE(DEG)
0.0
60.
120.
180.
240.
300.
360.
TIME FROM ORBIT INJECTION (DAYS)

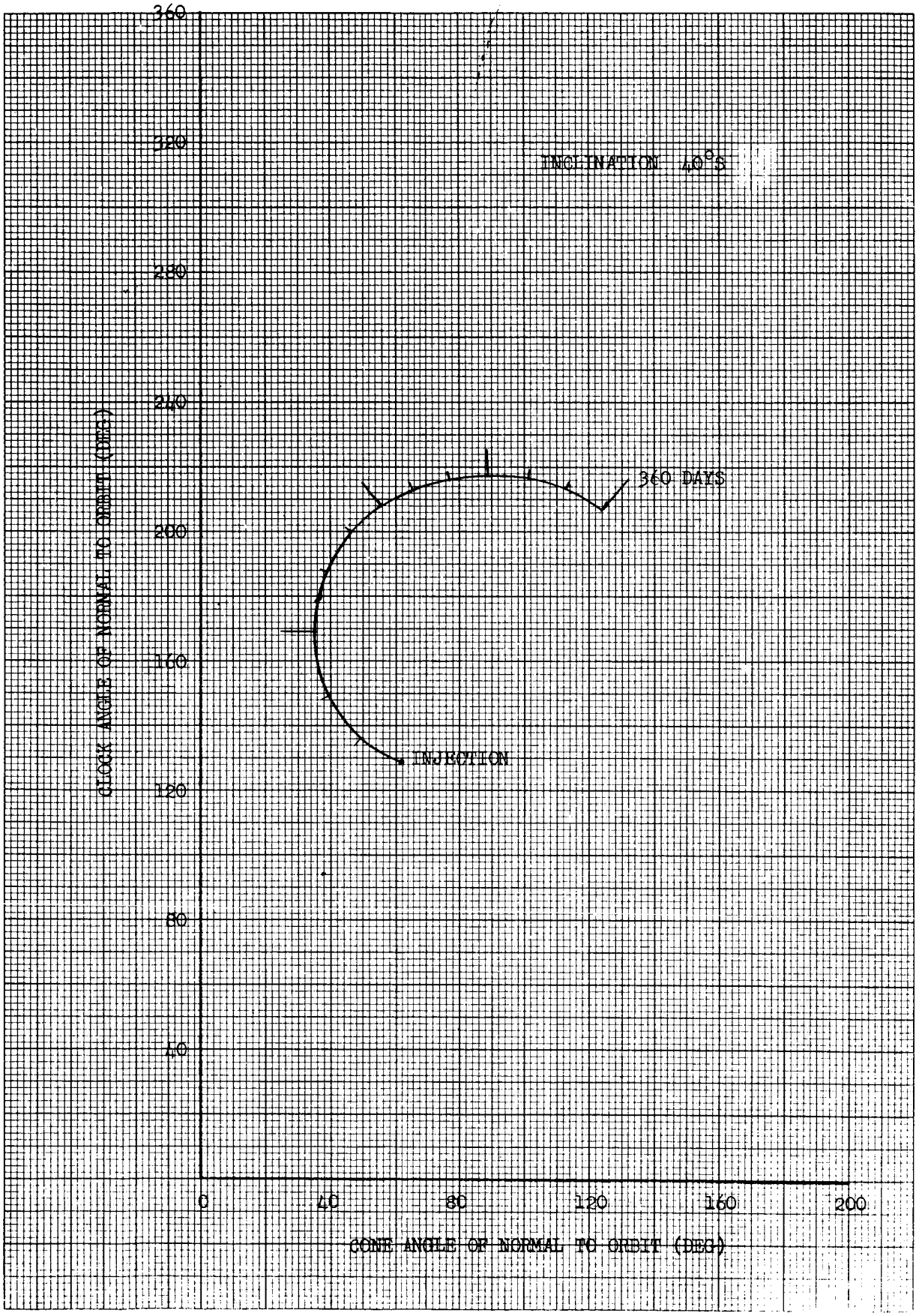
INCLINATION 40°S
360 DAYS
INJECTION
CLOCK ANGLE OF NORMAL TO ORBIT (DEG)
CONE ANGLE OF NORMAL TO ORBIT (DEG)
360
320
280
240
200
160
120
80
40
0
40
80
120
160
200

CASE NO. 13

1000 x 15,000 km

$i = 40^{\circ}N$

$\Psi = 120.834$ deg

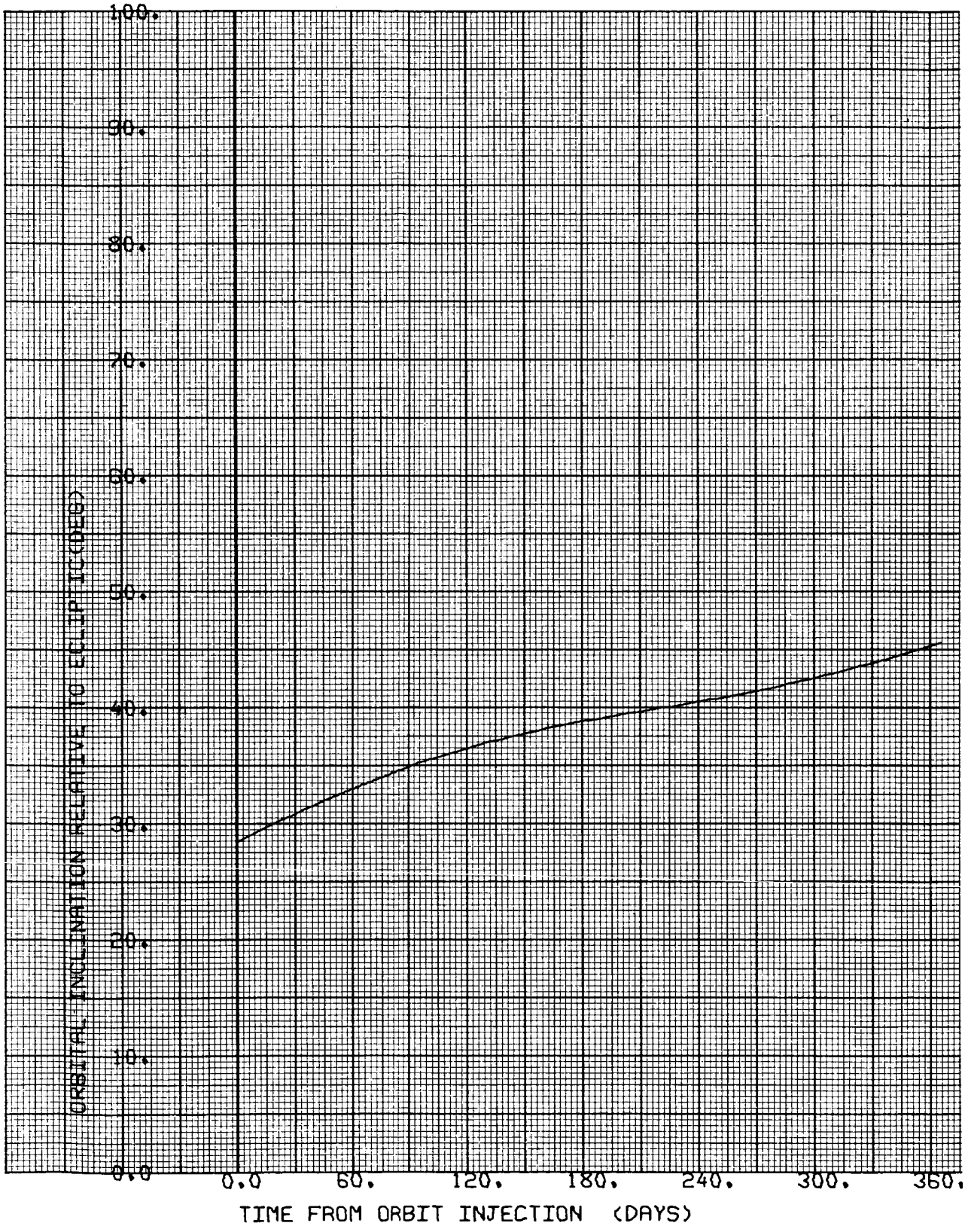
100.
90.
80.
70.
60.
50.
40.
30.
20.
10.
0.0
ORBITAL INCLINATION RELATIVE TO ECLIPTIC (DEG)
0.0
60.
120.
180.
240.
300.
360.
TIME FROM ORBIT INJECTION (DAYS)

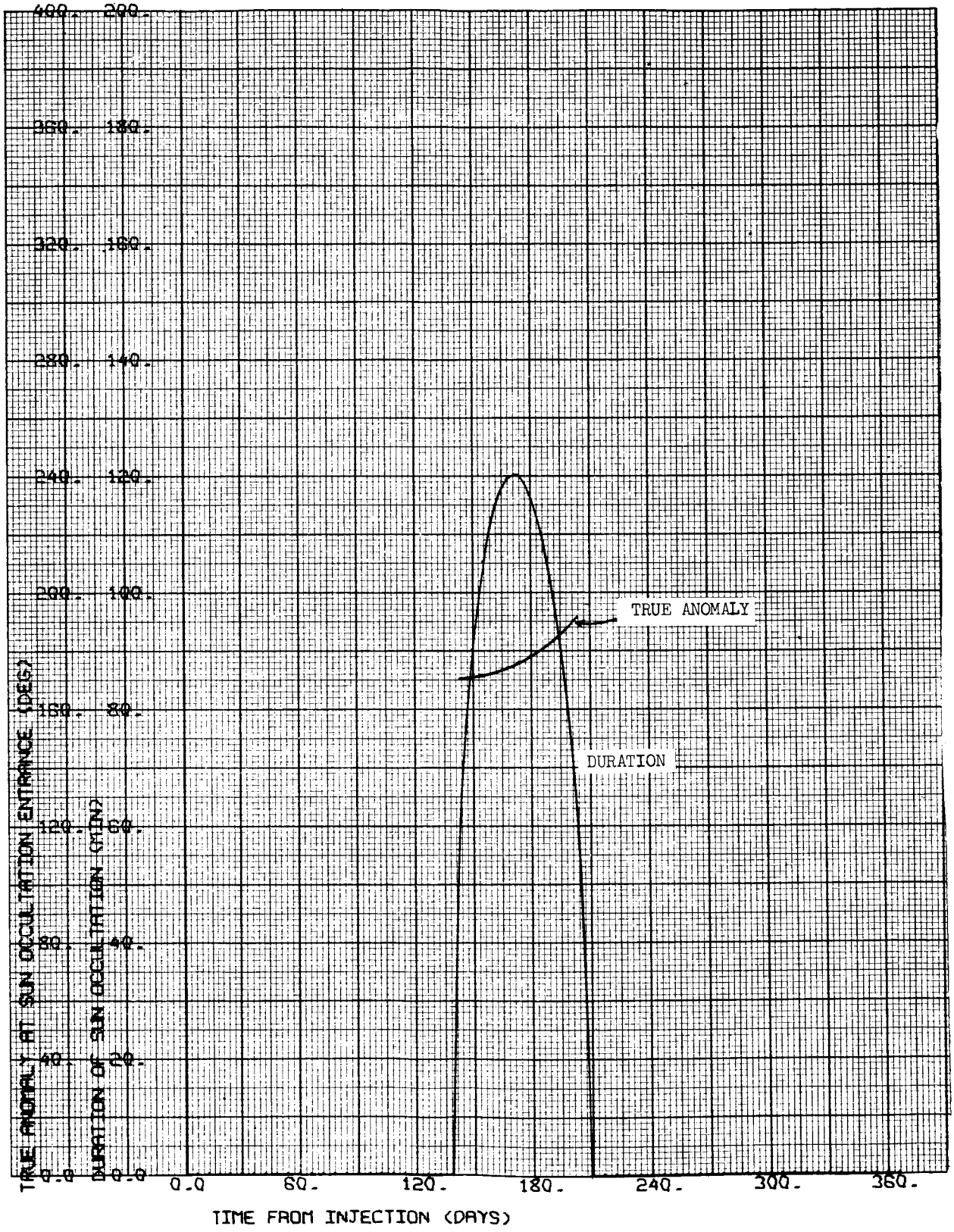
TRUE ANOMALY
DURATION
TRUE ANOMALY AT SUN OCCULTATION ENTRANCE (DEG)
DURATION OF SUN OCCULTATION (MIN)
TIME FROM INJECTION (DAYS)
0.0
60.
120.
180.
240.
300.
360.
400.
360.
320.
280.
240.
200.
160.
120.
80.
40.
0.0
200.
180.
160.
140.
120.
100.
80.
60.
40.
20.
0.0

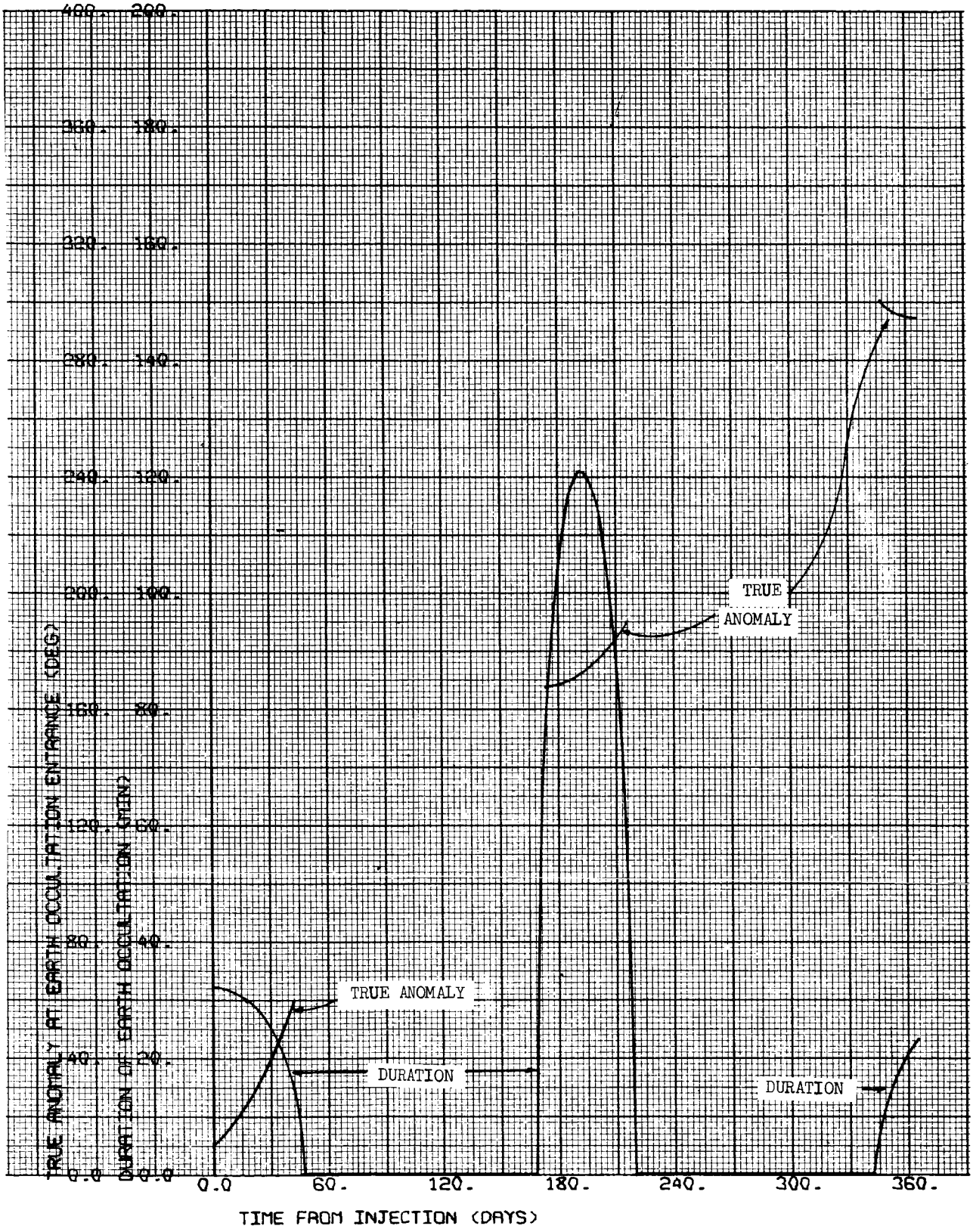
TRUE ANOMALY AT EARTH OCCULTATION ENTRANCE (DEG)
DURATION OF EARTH OCCULTATION (MIN)
TIME FROM INJECTION (DAYS)
TRUE ANOMALY
DURATION
TRUE ANOMALY
DURATION
0.0
60.
120.
180.
240.
300.
360.

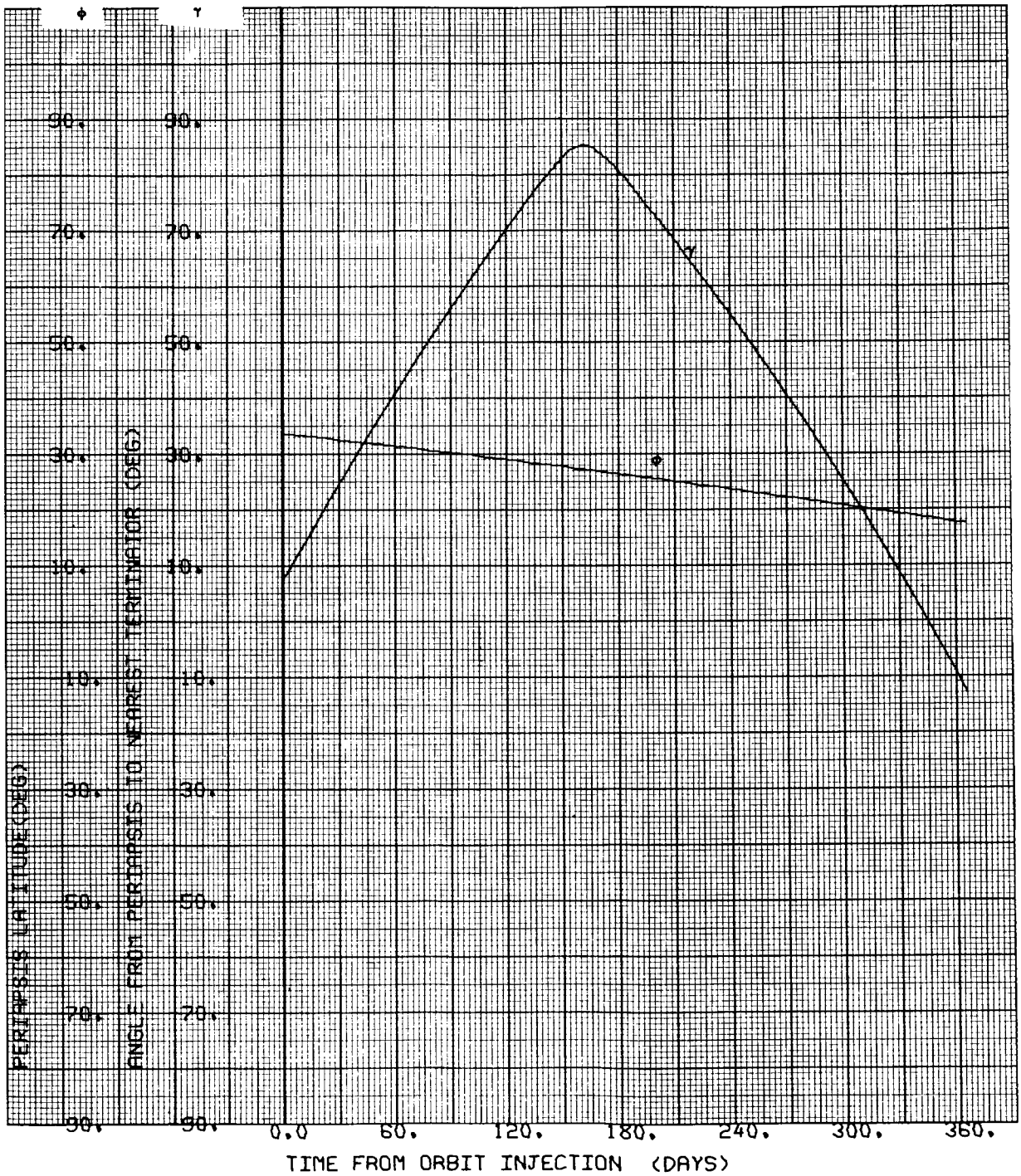
φ
γ
90.
70.
50.
30.
10.
10.
30.
50.
70.
90.
0.0
60.
120.
180.
240.
300.
360.
PERIAPSIS LATITUDE (DEG)
ANGLE FROM PERIAPSIS TO NEAREST TERMINATOR (DEG)
TIME FROM ORBIT INJECTION (DAYS)

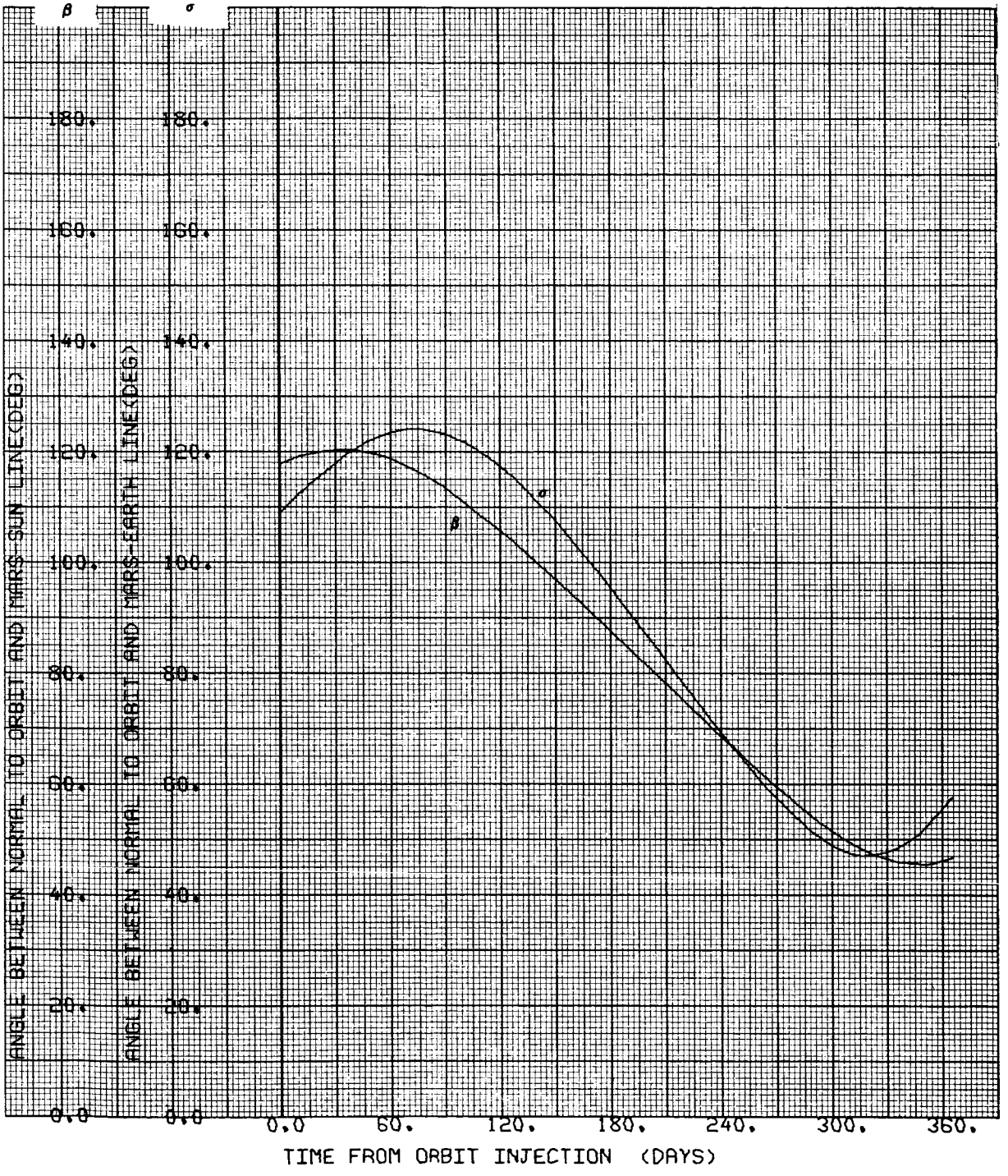
β
σ
180.
160.
140.
120.
100.
80.
60.
40.
20.
0.0
ANGLE BETWEEN NORMAL TO ORBIT AND MARS-SUN LINE(DEG)
ANGLE BETWEEN NORMAL TO ORBIT AND MARS-EARTH LINE(DEG)
0.0
60.
120.
180.
240.
300.
360.
TIME FROM ORBIT INJECTION (DAYS)

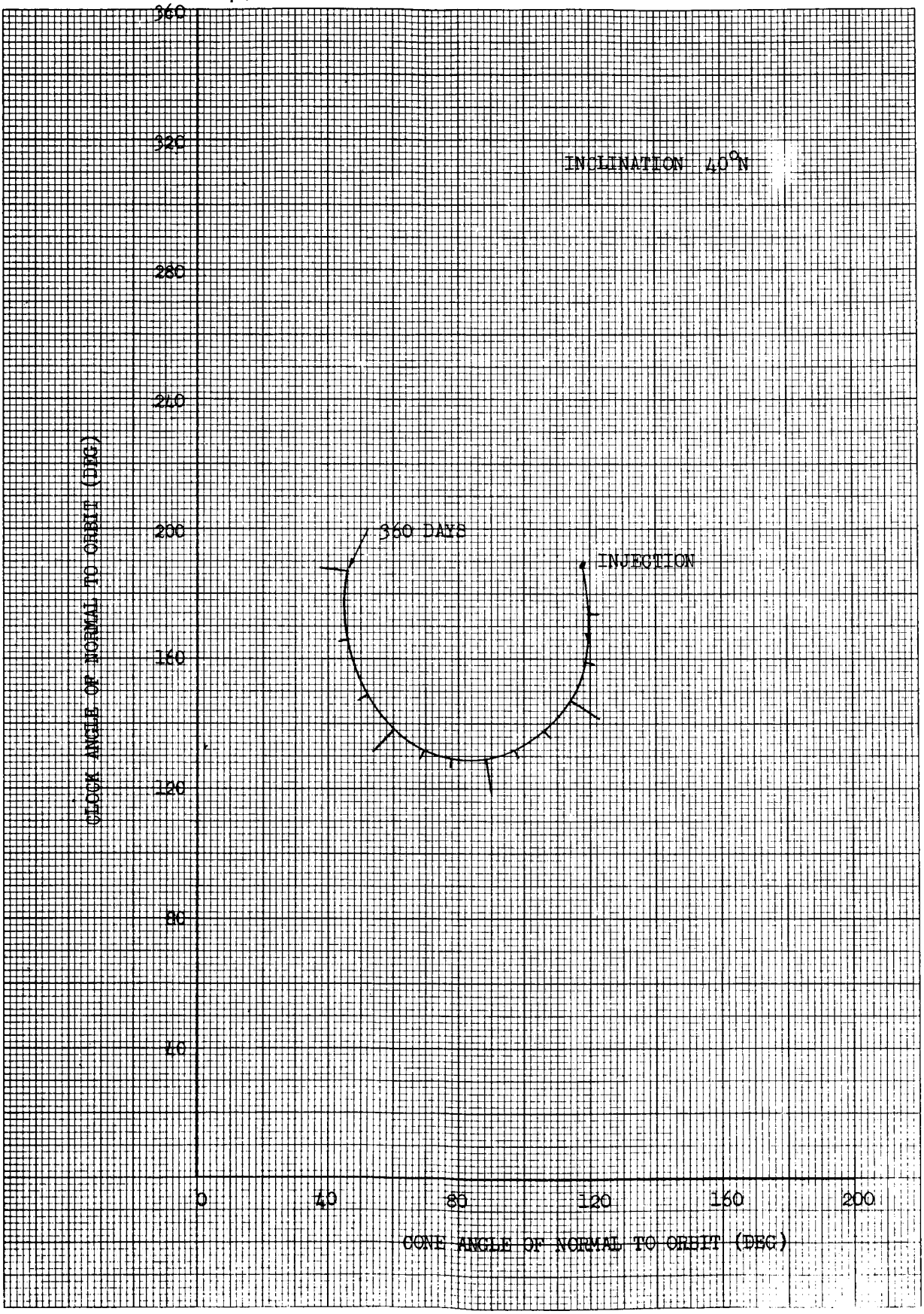
INCLINATION 40°N
360 DAYS
INJECTION
CLOCK ANGLE OF NORMAL TO ORBIT (DEG)
CONE ANGLE OF NORMAL TO ORBIT (DEG)
360
320
280
240
200
160
120
80
40
0
40
80
120
160
200

CASE NO. 14

1000 x 15,000 km

$i = 40^{\circ}S$

$\Psi = 118.871$ deg

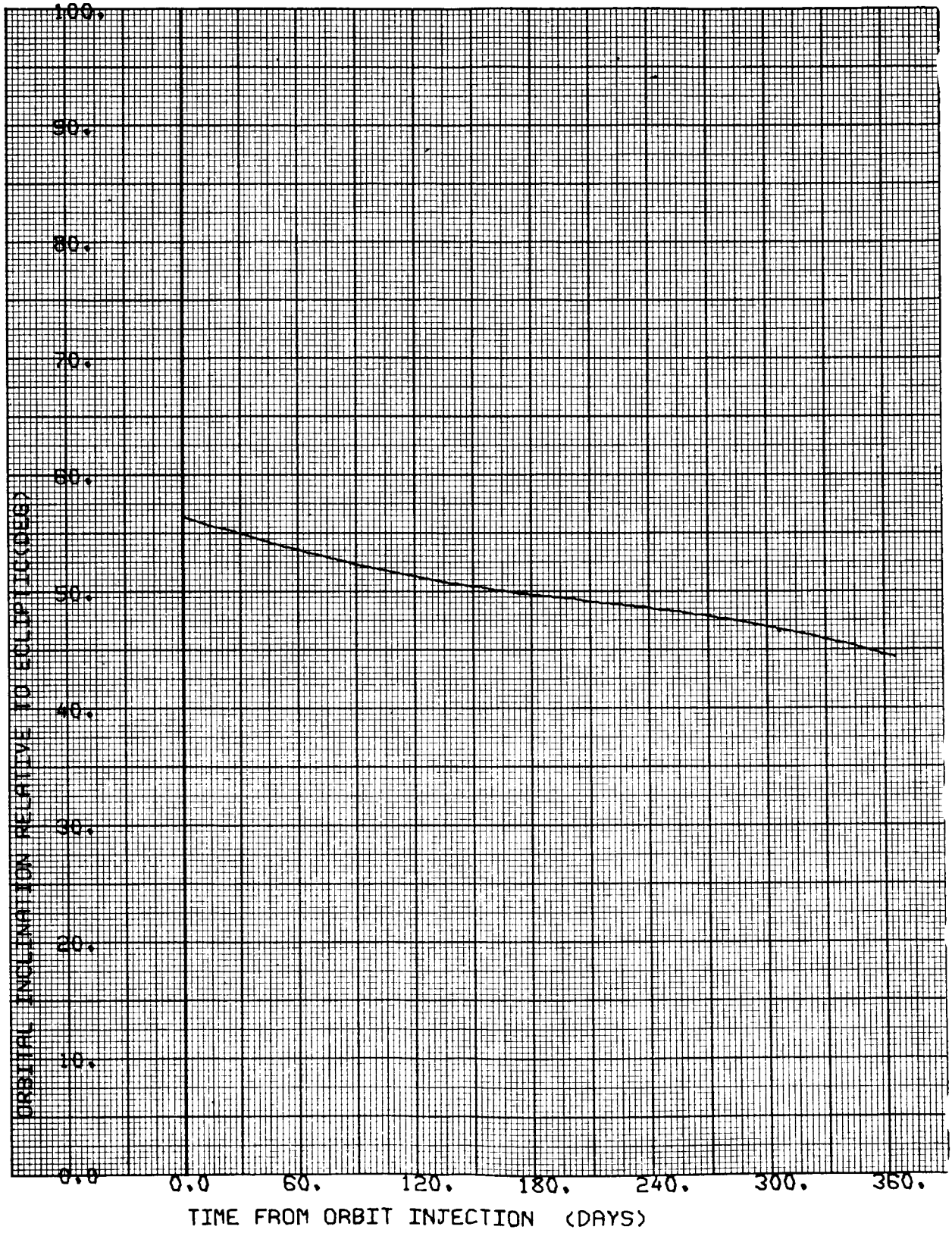
100.
90.
80.
70.
60.
50.
40.
30.
20.
10.
0.0
ORBITAL INCLINATION RELATIVE TO ECLIPTIC (DEG)
0.0
60.
120.
180.
240.
300.
360.
TIME FROM ORBIT INJECTION (DAYS)

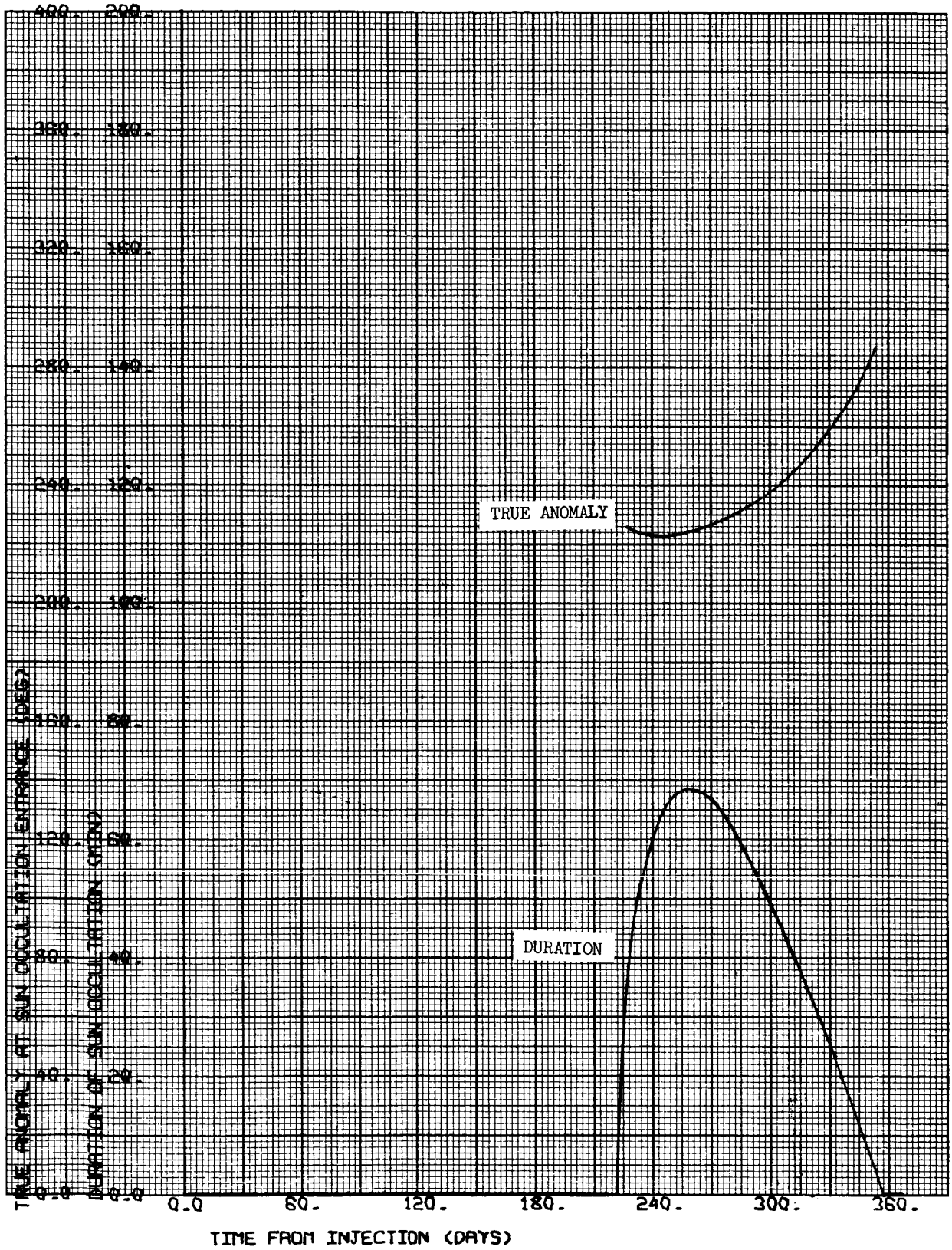
TRUE ANOMALY
DURATION
TRUE ANOMALY AT SUN OCCULTATION ENTRANCE (DEG)
DURATION OF SUN OCCULTATION (MIN)
TIME FROM INJECTION (DAYS)
0.0
60.
120.
180.
240.
300.
360.
400.
360.
320.
280.
240.
200.
160.
120.
80.
40.
0.0
200.
180.
160.
140.
120.
100.
80.
60.
40.
20.
0.0

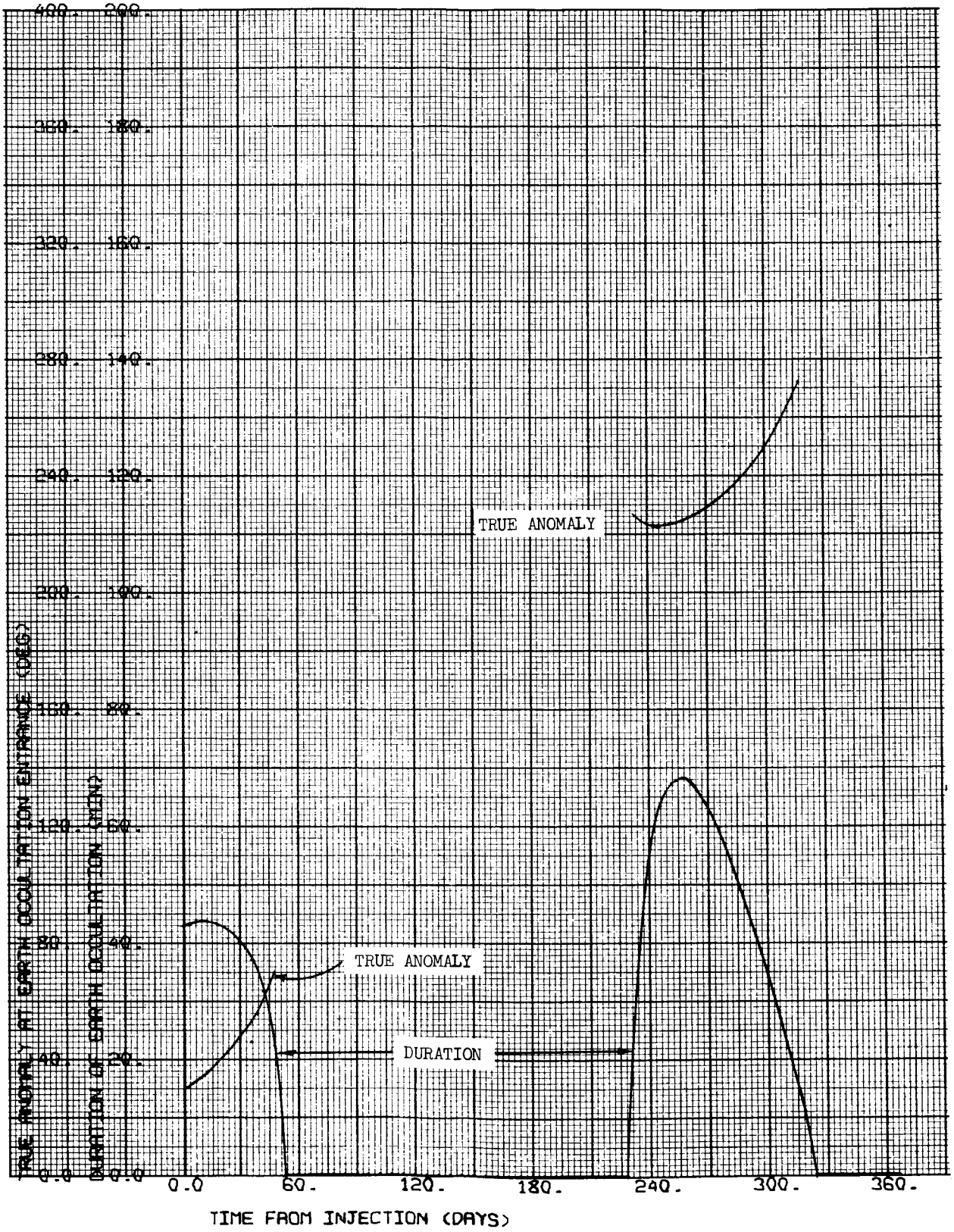
TRUE ANOMALY
TRUE ANOMALY
DURATION
TRUE ANOMALY AT EARTH OCCULTATION ENTRANCE (DEG)
DURATION OF EARTH OCCULTATION (DEG)
TIME FROM INJECTION (DAYS)
0.0
60.
120.
180.
240.
300.
360.
400.
360.
320.
280.
240.
200.
160.
120.
80.
40.
0.0
200.
180.
160.
140.
120.
100.
80.
60.
40.
20.
0.0

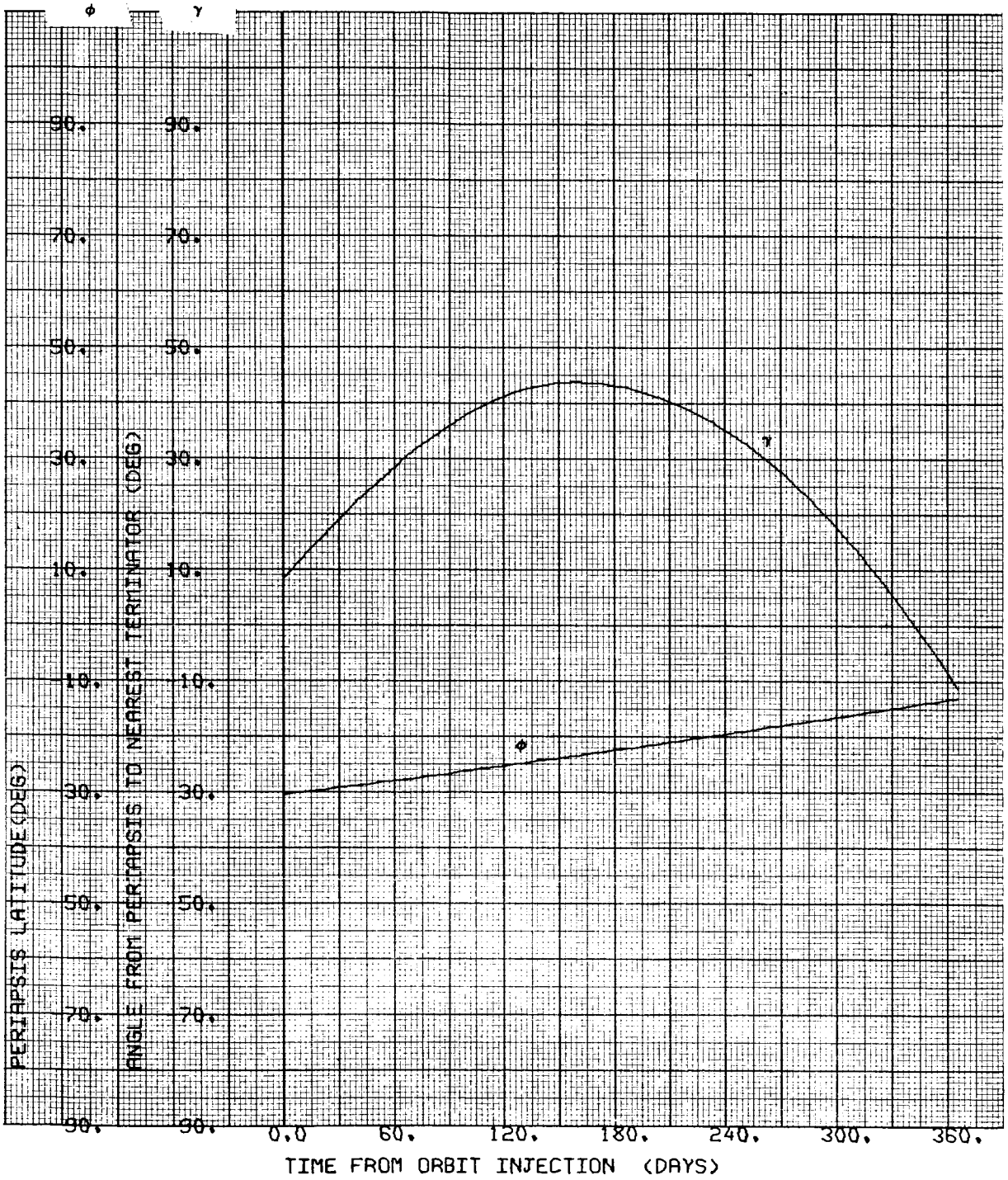
φ
γ
90.
70.
50.
30.
10.
-10.
-30.
-50.
-70.
-90.
PERIAPSIS LATITUDE (DEG)
ANGLE FROM PERIAPSIS TO NEAREST TERMINATOR (DEG)
0.0
60.
120.
180.
240.
300.
360.
TIME FROM ORBIT INJECTION (DAYS)

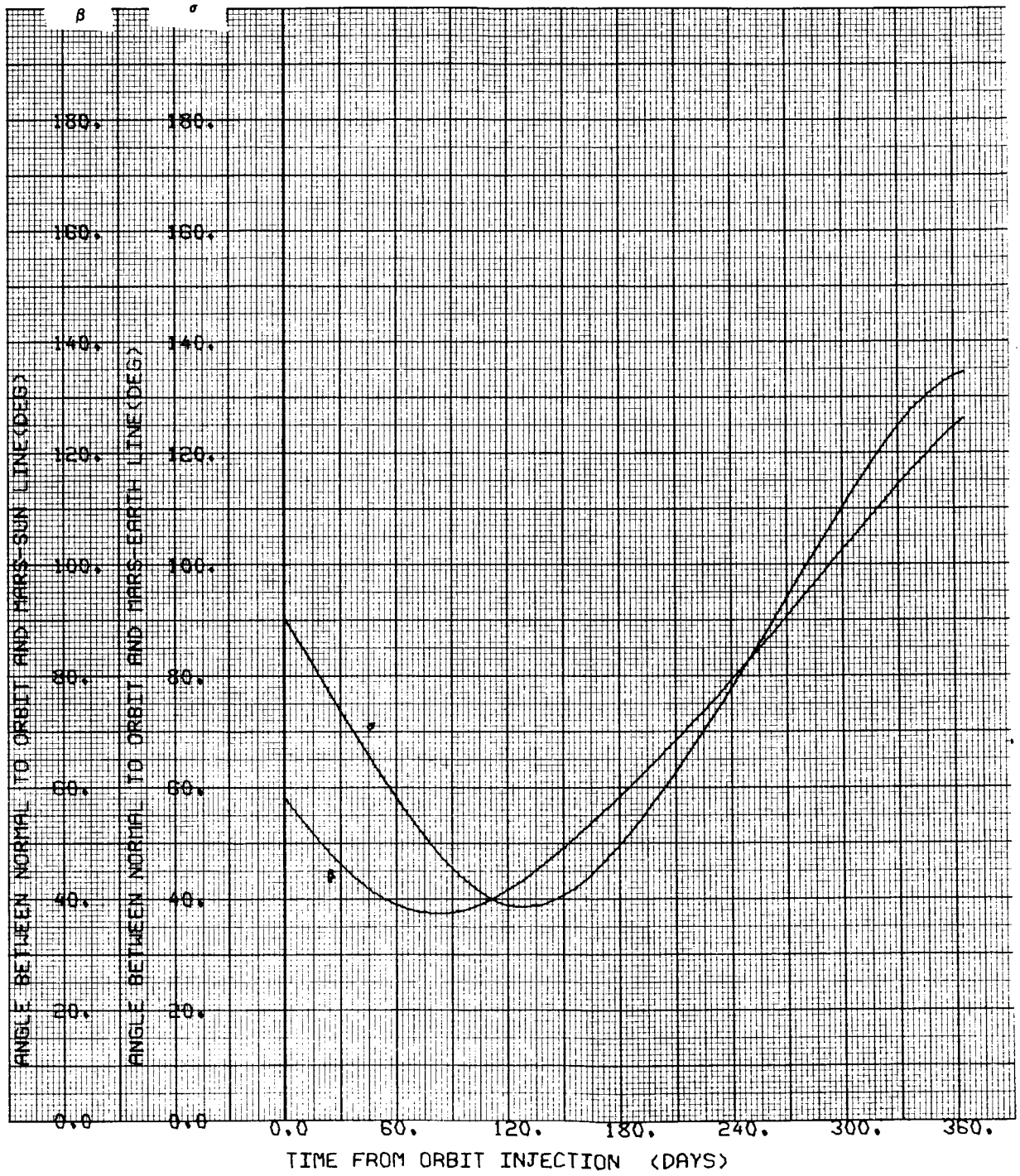
β
σ
180.
160.
140.
120.
100.
80.
60.
40.
20.
0.0
ANGLE BETWEEN NORMAL TO ORBIT AND MARS-SUN LINE(DEG)
ANGLE BETWEEN NORMAL TO ORBIT AND MARS-EARTH LINE(DEG)
0.0
60.
120.
180.
240.
300.
360.
TIME FROM ORBIT INJECTION (DAYS)

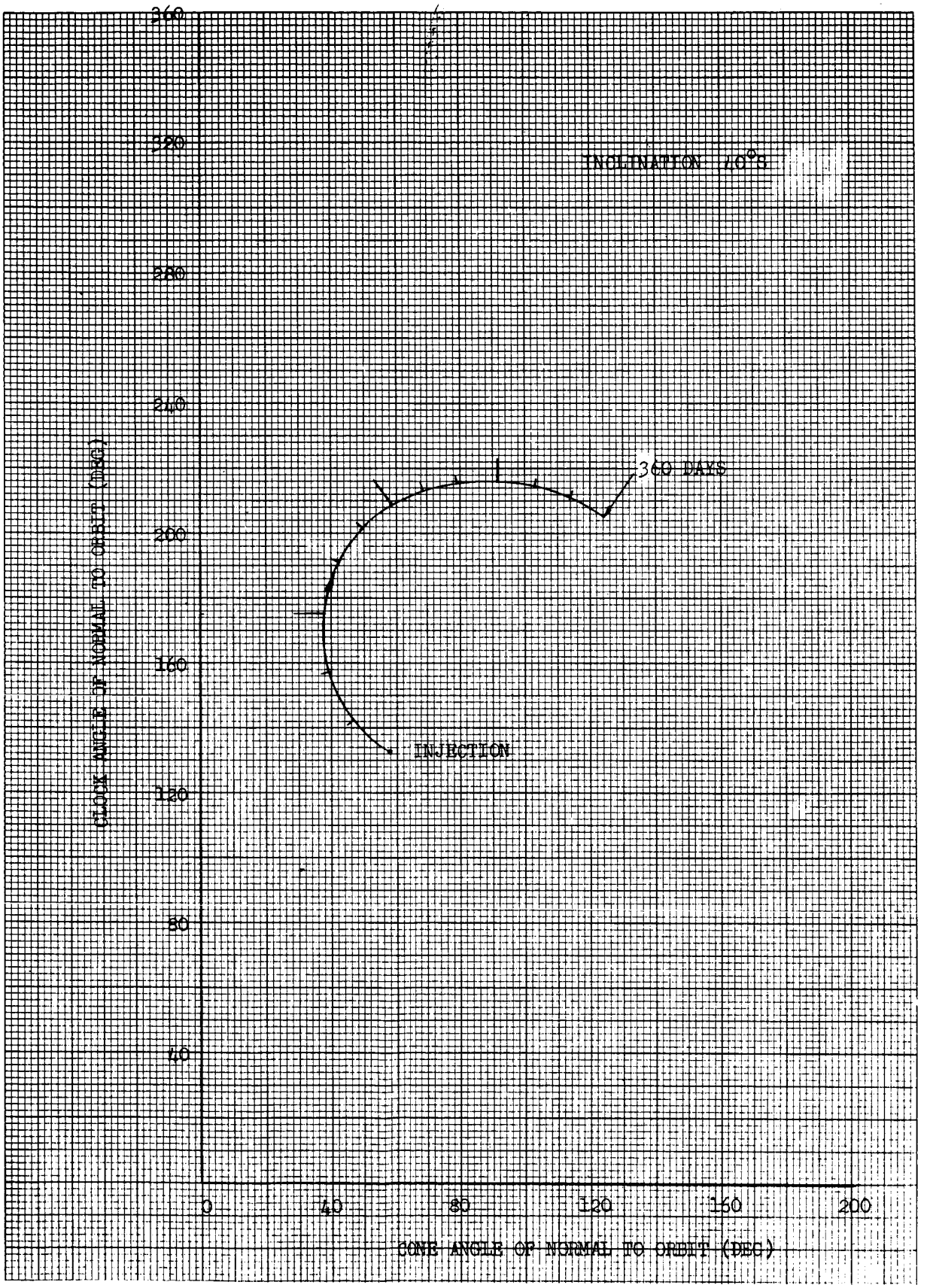
INCLINATION 40°S
360 DAYS
INJECTION
CLOCK ANGLE OF NORMAL TO ORBIT (DEG)
CONE ANGLE OF NORMAL TO ORBIT (DEG)
360
320
280
240
200
160
120
80
40
0
40
80
120
160
200

CASE NO. 15

1000 x 15, 000 km

$i = 40^{o}N$

$\Psi = 118.871$ deg

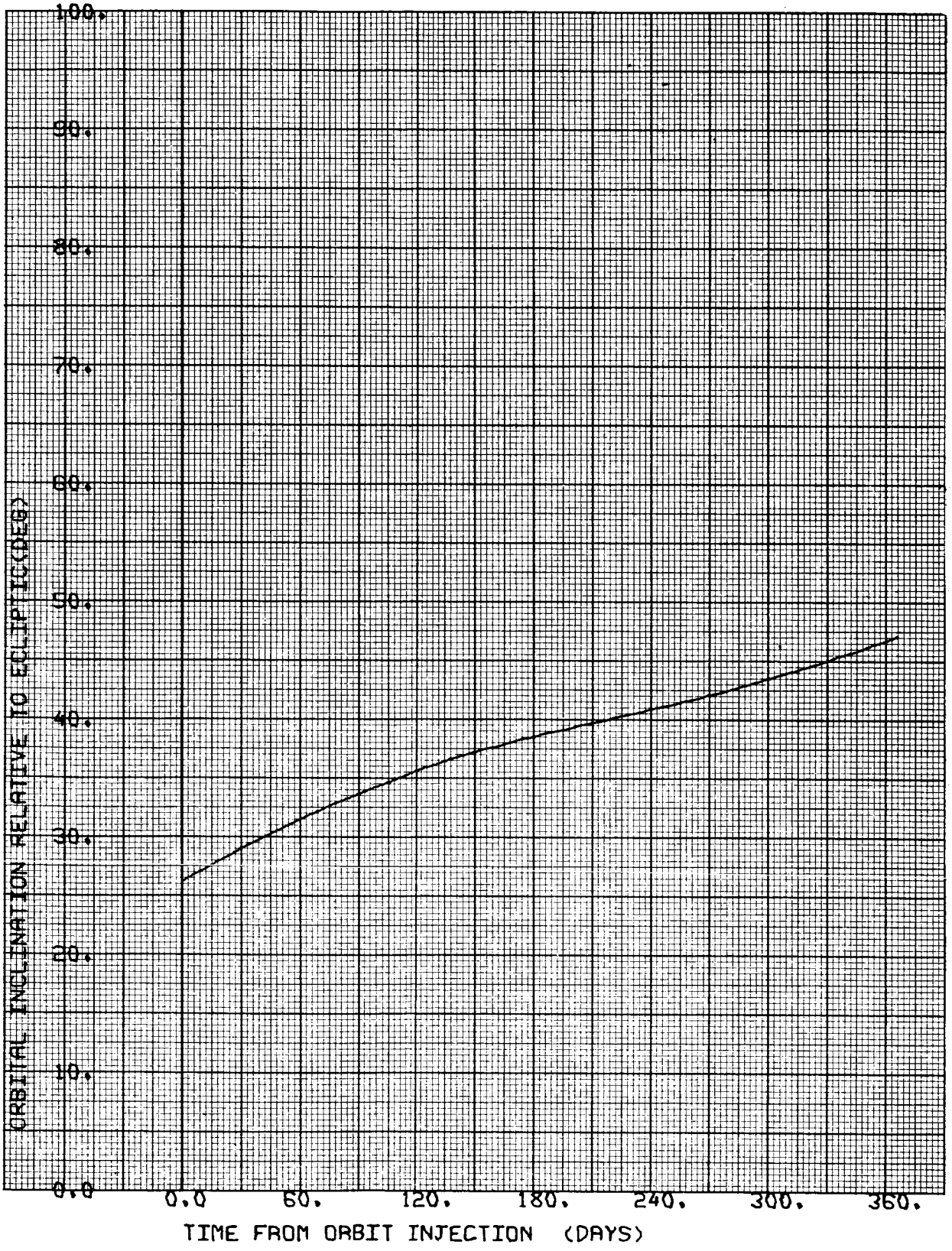
100.
90.
80.
70.
60.
50.
40.
30.
20.
10.
0.0
ORBITAL INCLINATION RELATIVE TO ECLIPTIC(DEG)
0.0
60.
120.
180.
240.
300.
360.
TIME FROM ORBIT INJECTION (DAYS)

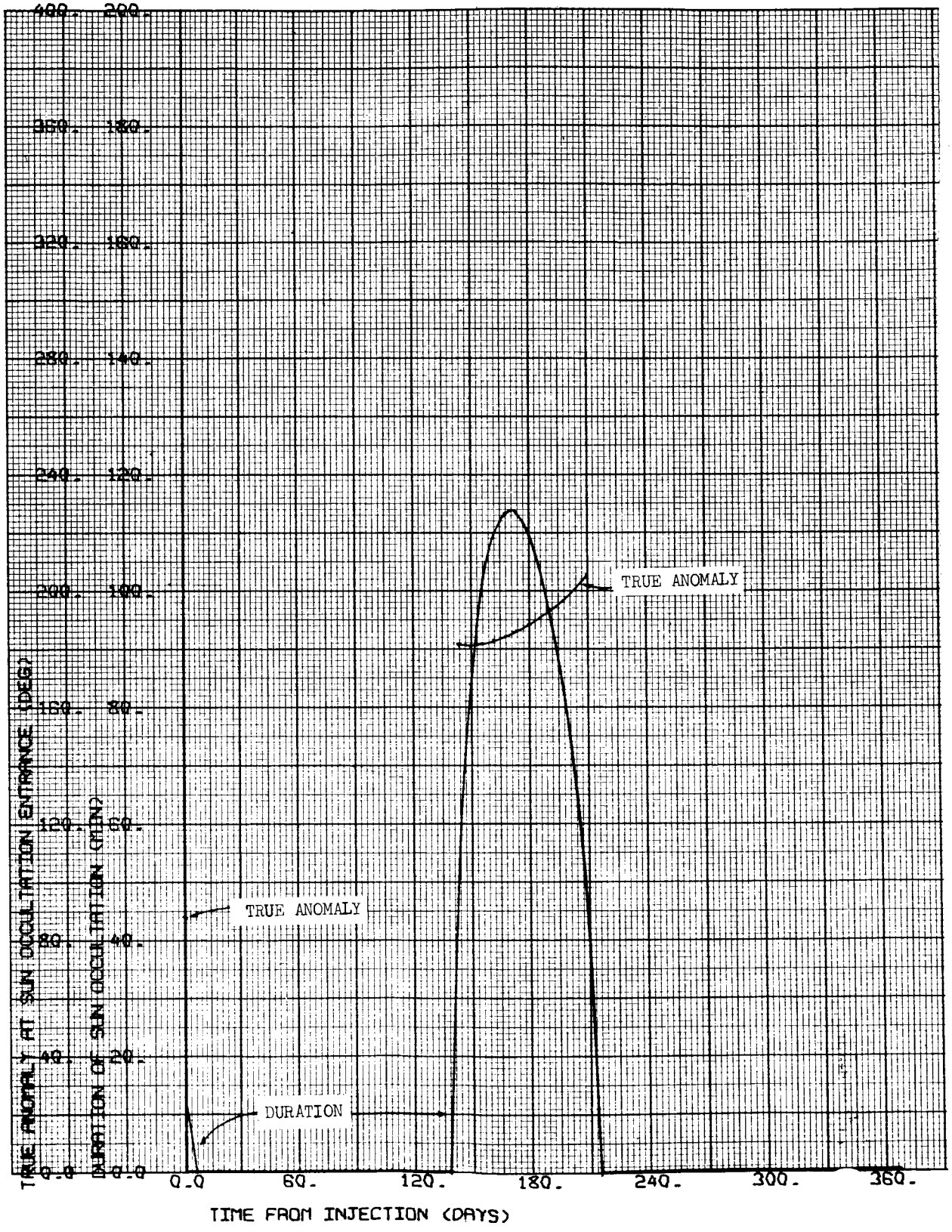
TRUE ANOMALY AT SUN OCCULTATION ENTRANCE (DEG)
DURATION OF SUN OCCULTATION (MIN)
400.
360.
320.
280.
240.
200.
160.
120.
80.
40.
0.0
200.
180.
160.
140.
120.
100.
80.
60.
40.
20.
0.0
TRUE ANOMALY
TRUE ANOMALY
DURATION
0.0
60.
120.
180.
240.
300.
360.
TIME FROM INJECTION (DAYS)

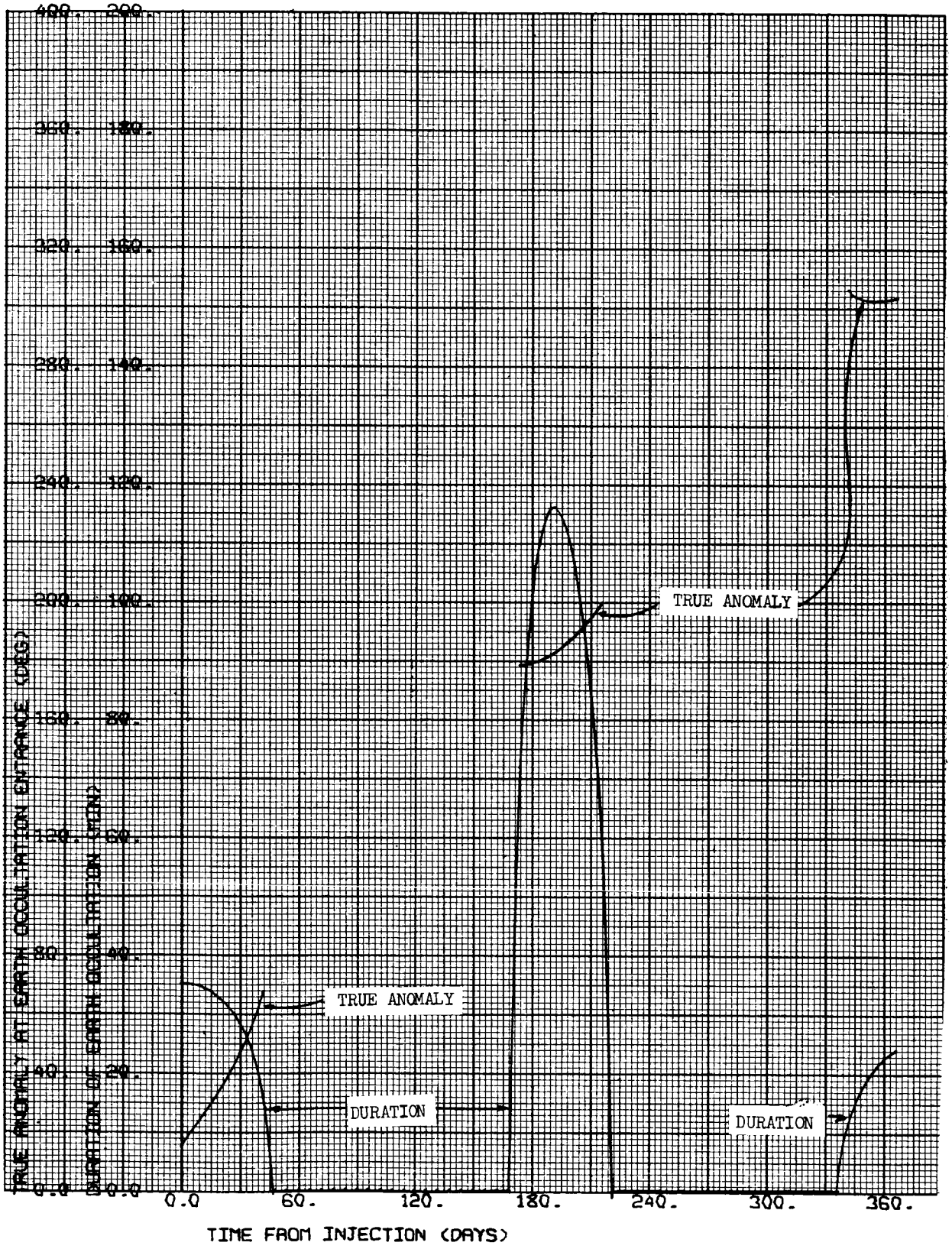
TRUE ANOMALY AT EARTH OCCULTATION ENTRANCE (DEG)
DURATION OF EARTH OCCULTATION (MIN)
TIME FROM INJECTION (DAYS)
TRUE ANOMALY
TRUE ANOMALY
DURATION
DURATION
0.0
60.
120.
180.
240.
300.
360.

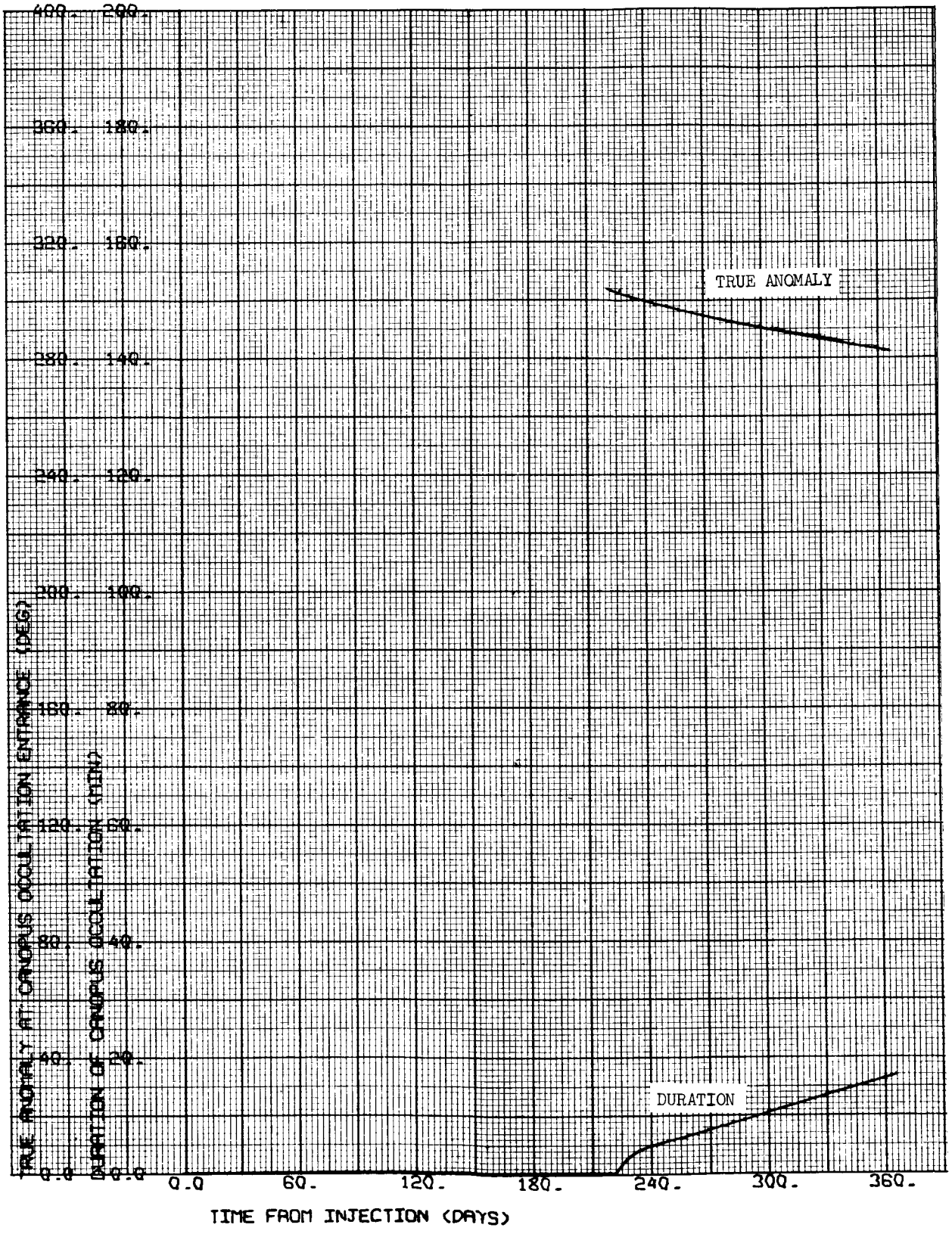
TRUE ANOMALY
DURATION
TRUE ANOMALY AT CANOPUS OCCULTATION ENTRANCE (DEG)
DURATION OF CANOPUS OCCULTATION (MIN)
TIME FROM INJECTION (DAYS)
0.0
60.
120.
180.
240.
300.
360.
400.
360.
320.
280.
240.
200.
160.
120.
80.
40.
0.0
200.
180.
160.
140.
120.
100.
80.
60.
40.
20.
0.0

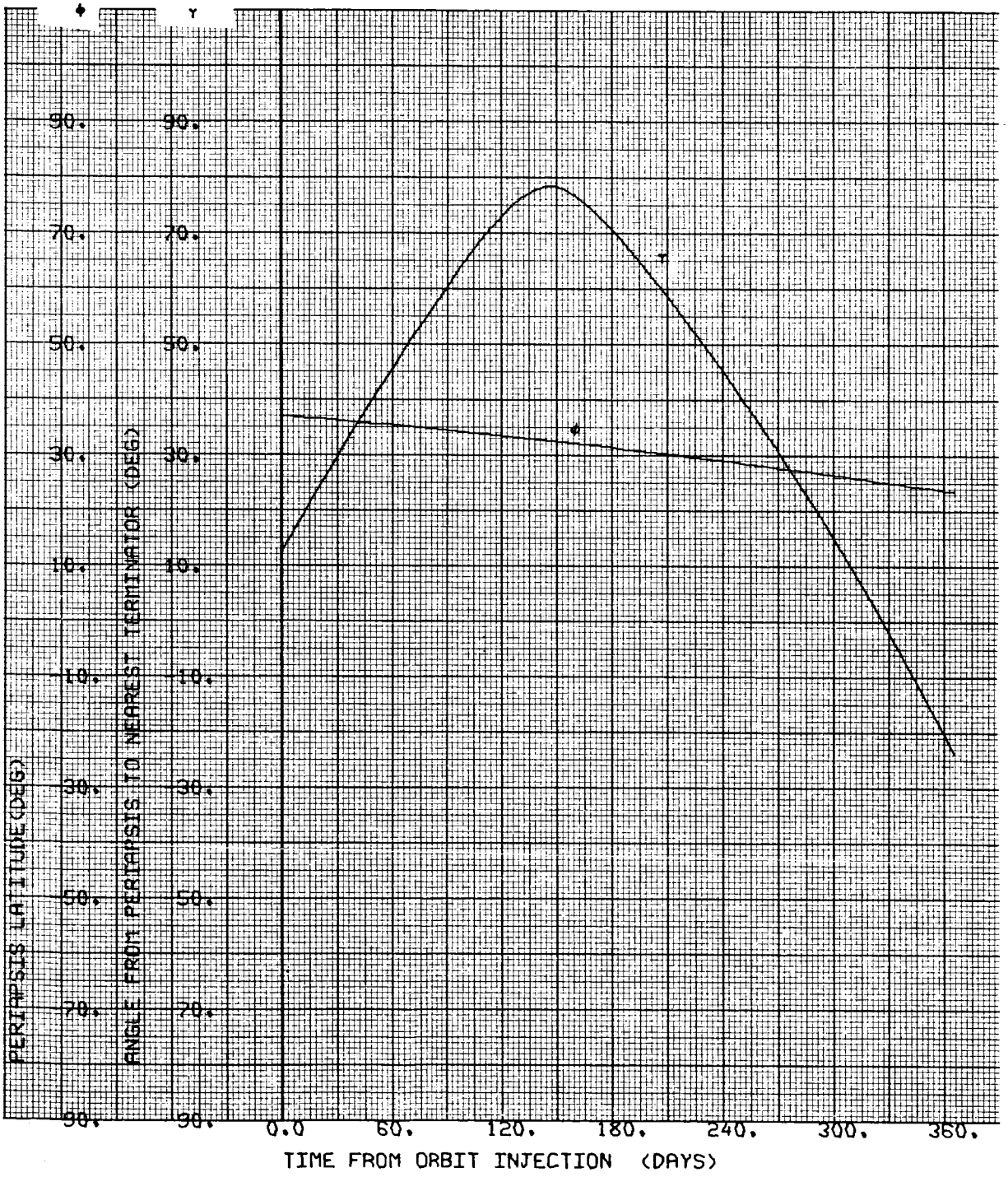
φ
γ
90.
70.
50.
30.
10.
-10.
-30.
-50.
-70.
-90.
0.0
60.
120.
180.
240.
300.
360.
PERIAPSIS LATITUDE (DEG)
ANGLE FROM PERIAPSIS TO NEAREST TERMINATOR (DEG)
TIME FROM ORBIT INJECTION (DAYS)

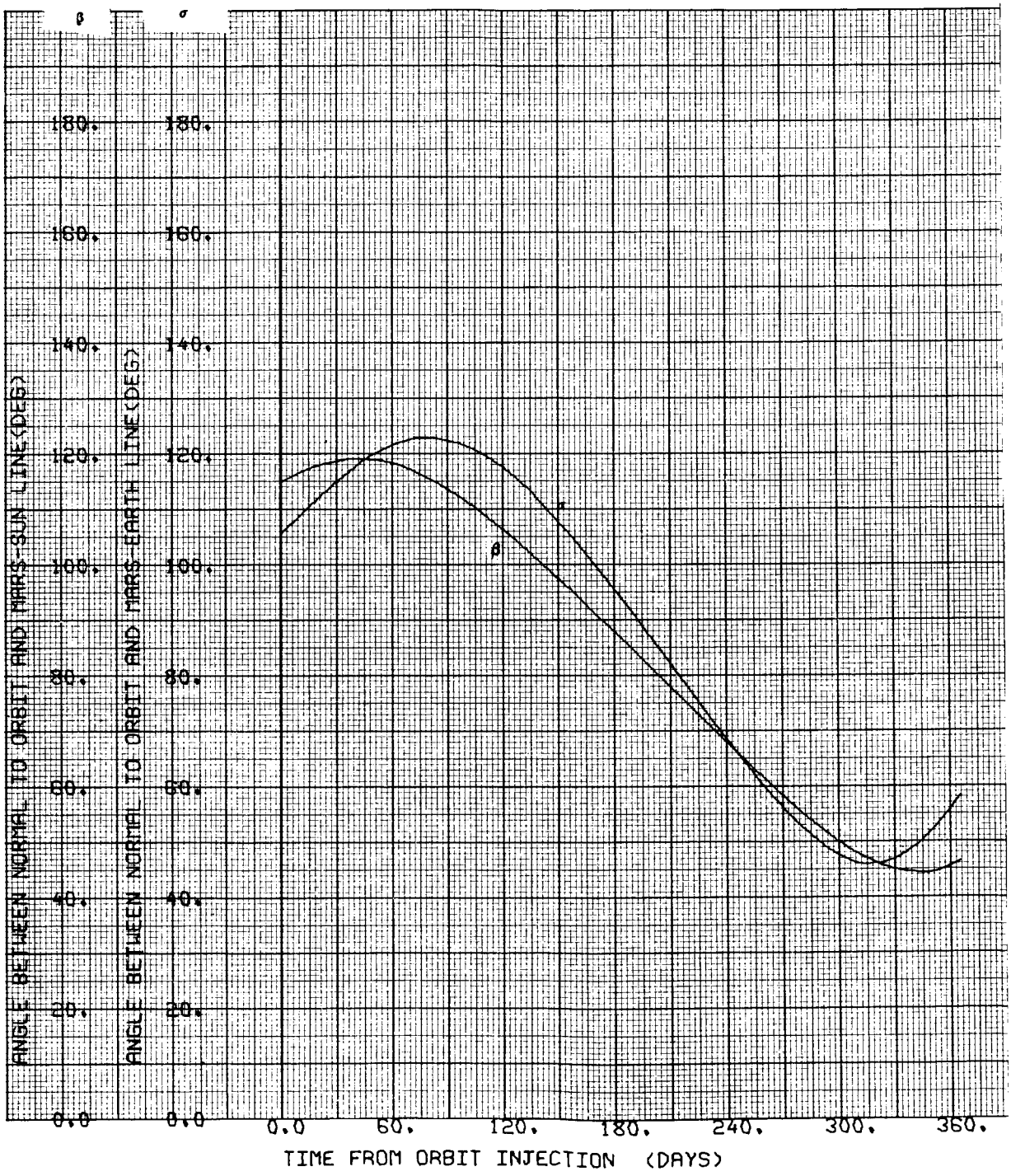
β
σ
180.
160.
140.
120.
100.
80.
60.
40.
20.
0.0
ANGLE BETWEEN NORMAL TO ORBIT AND MARS-SUN LINE(DEG)
ANGLE BETWEEN NORMAL TO ORBIT AND MARS-EARTH LINE(DEG)
0.0
60.
120.
180.
240.
300.
360.
TIME FROM ORBIT INJECTION (DAYS)

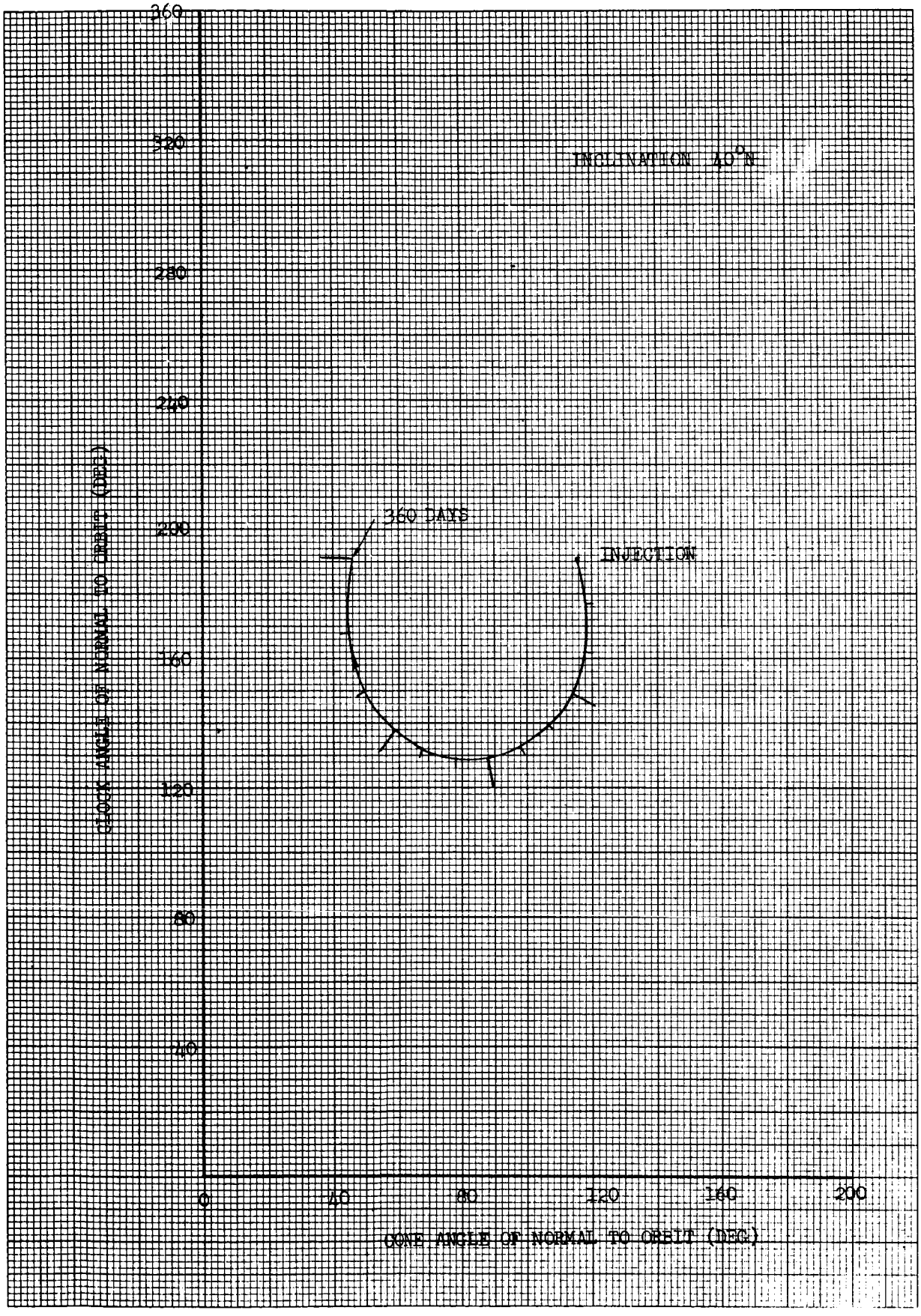
INCLINATION 40°N
360 DAYS
INJECTION
CLOCK ANGLE OF NORMAL TO ORBIT (DEG)
CONE ANGLE OF NORMAL TO ORBIT (DEG)
360
320
280
240
200
160
120
80
40
0
40
80
120
160
200

CASE NO. 16

1000 x 15,000 km

$i = 20^{\circ}S$

$\Psi = 126.453$ deg

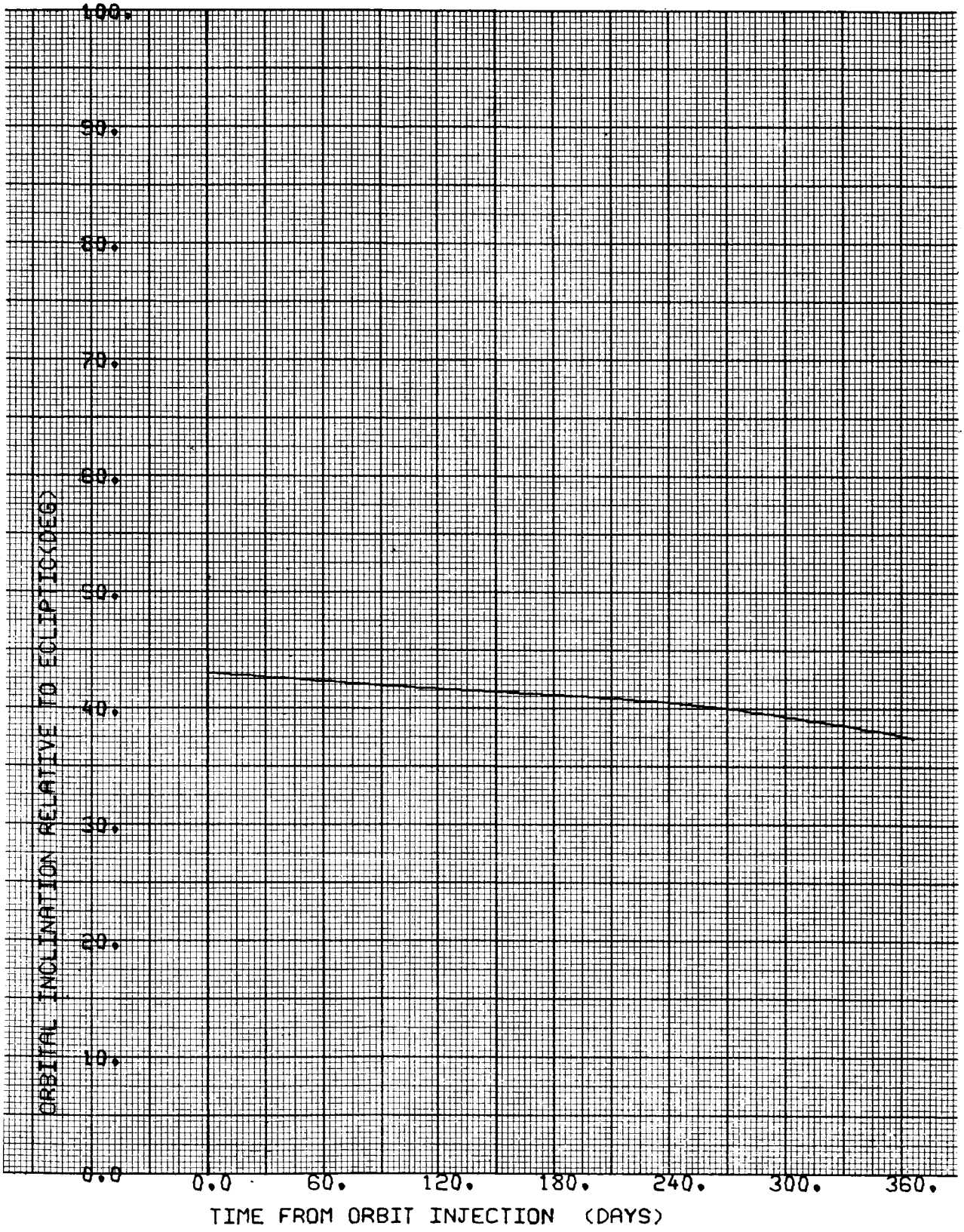
100.
90.
80.
70.
60.
50.
40.
30.
20.
10.
0.0
ORBITAL INCLINATION RELATIVE TO ECLIPTIC(DEG)
0.0
60.
120.
180.
240.
300.
360.
TIME FROM ORBIT INJECTION (DAYS)

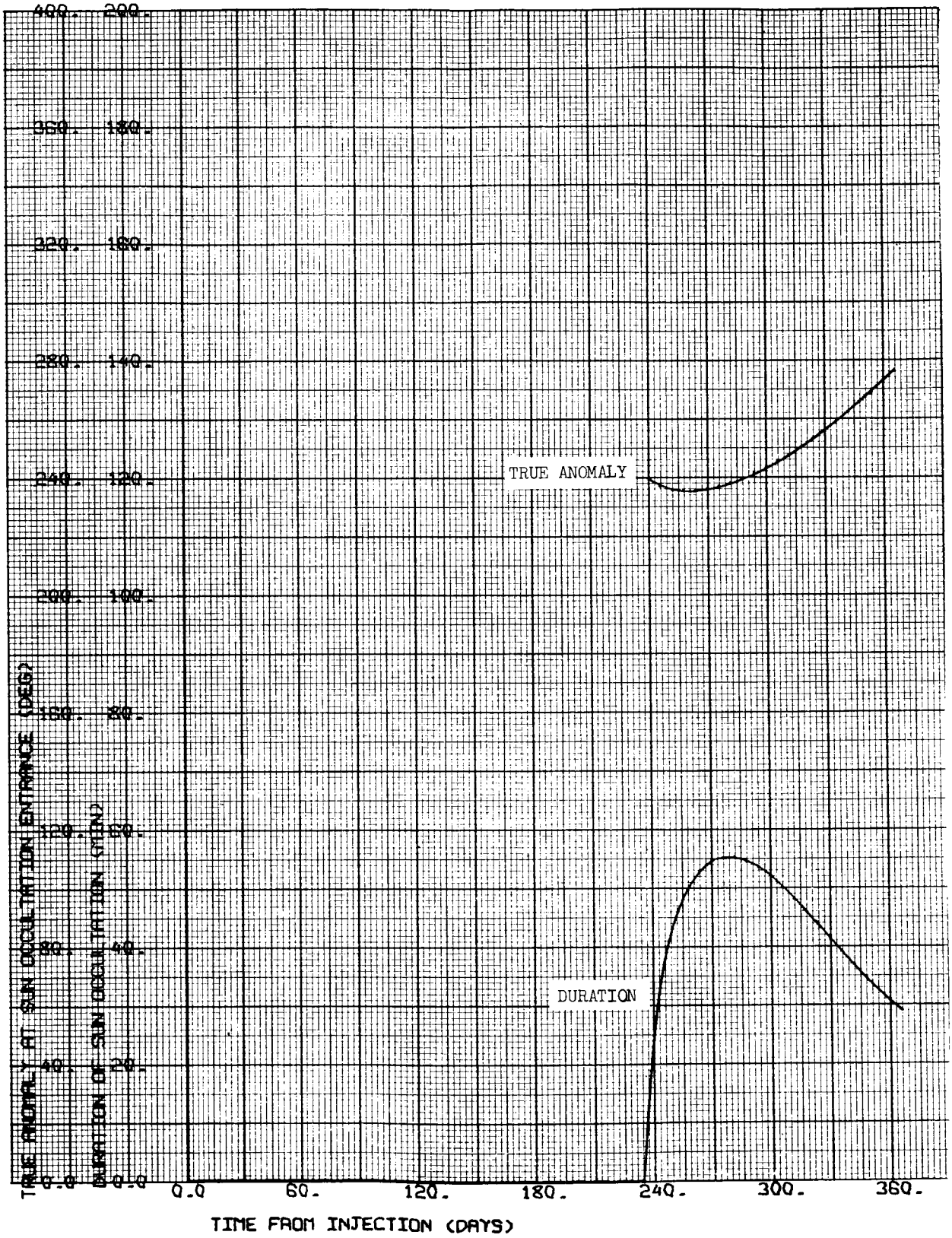
TRUE ANOMALY
DURATION
TRUE ANOMALY AT SUN OCCULTATION ENTRANCE (DEG)
DURATION OF SUN OCCULTATION (MIN)
TIME FROM INJECTION (DAYS)
0.0
60.
120.
180.
240.
300.
360.
400.
360.
320.
280.
240.
200.
160.
120.
80.
40.
0.0
200.
180.
160.
140.
120.
100.
80.
60.
40.
20.
0.0

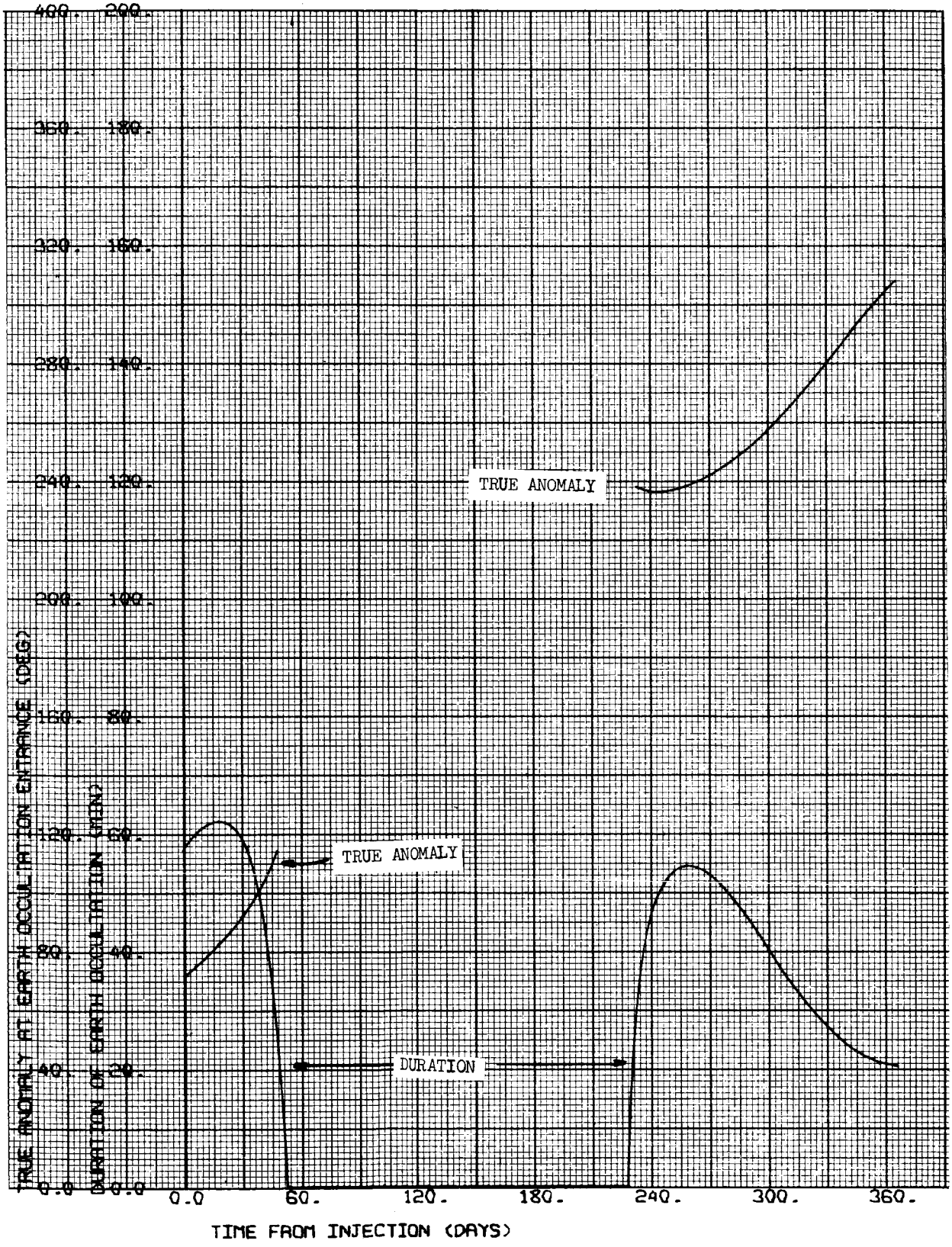
TRUE ANOMALY AT EARTH OCCULTATION ENTRANCE (DEG)
DURATION OF EARTH OCCULTATION (MIN)
TIME FROM INJECTION (DAYS)
TRUE ANOMALY
TRUE ANOMALY
DURATION
0.0
60.
120.
180.
240.
300.
360.
400.
360.
320.
280.
240.
200.
160.
120.
80.
40.
0.0
200.
180.
160.
140.
120.
100.
80.
60.
40.
20.
0.0

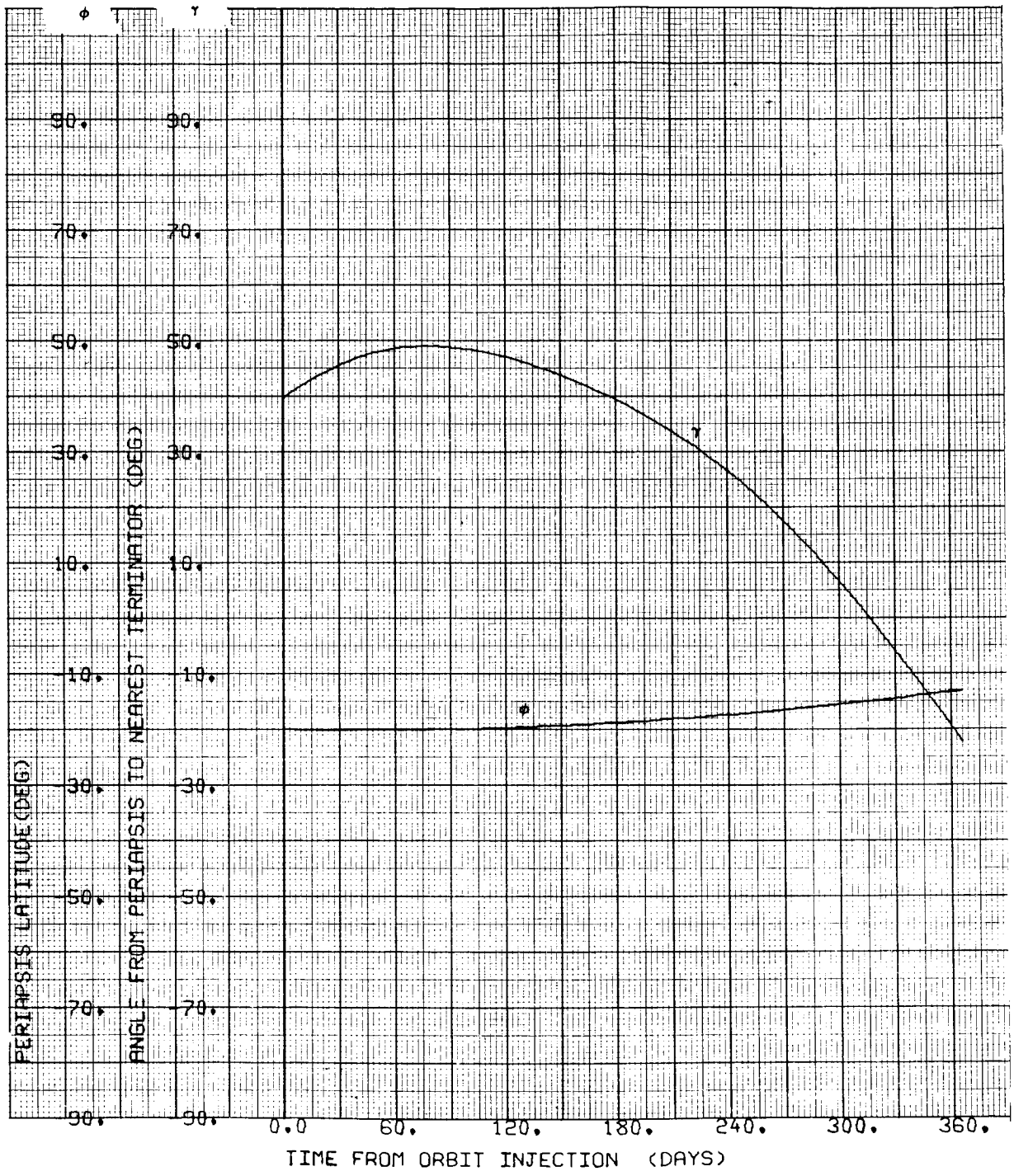
φ
γ
90.
70.
50.
30.
10.
-10.
-30.
-50.
-70.
-90.
PERIAPSIS LATITUDE (DEG)
ANGLE FROM PERIAPSIS TO NEAREST TERMINATOR (DEG)
0.0
60.
120.
180.
240.
300.
360.
TIME FROM ORBIT INJECTION (DAYS)

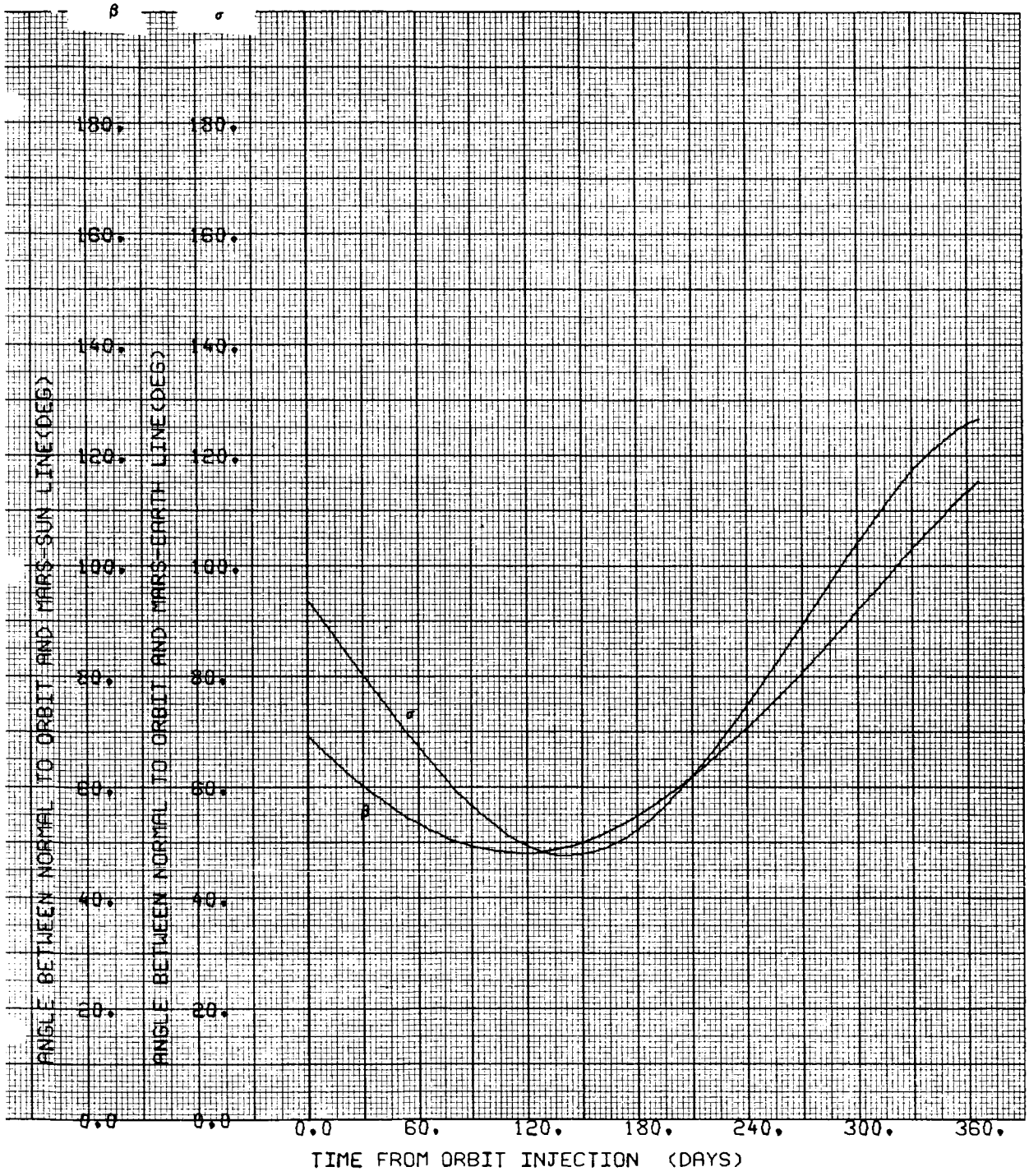
β
σ
180.
160.
140.
120.
100.
80.
60.
40.
20.
0.0
ANGLE BETWEEN NORMAL TO ORBIT AND MARS-SUN LINE(DEG)
ANGLE BETWEEN NORMAL TO ORBIT AND MARS-EARTH LINE(DEG)
0.0
60.
120.
180.
240.
300.
360.
TIME FROM ORBIT INJECTION (DAYS)

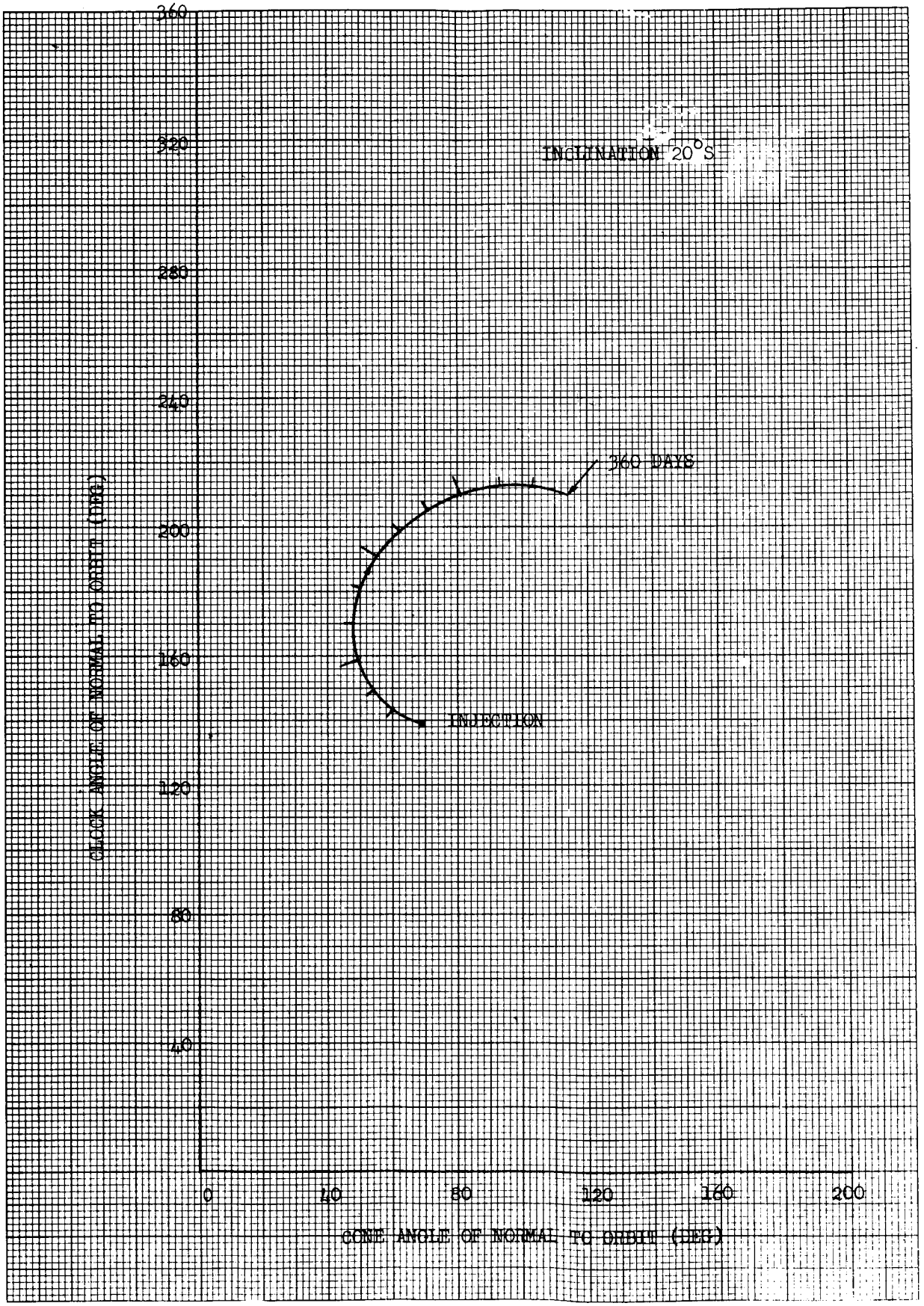
INCLINATION 20°S
360 DAYS
INJECTION
CLOCK ANGLE OF NORMAL TO ORBIT (DEG)
CONE ANGLE OF NORMAL TO ORBIT (DEG)
360
320
280
240
200
160
120
80
40
0
40
80
120
160
200

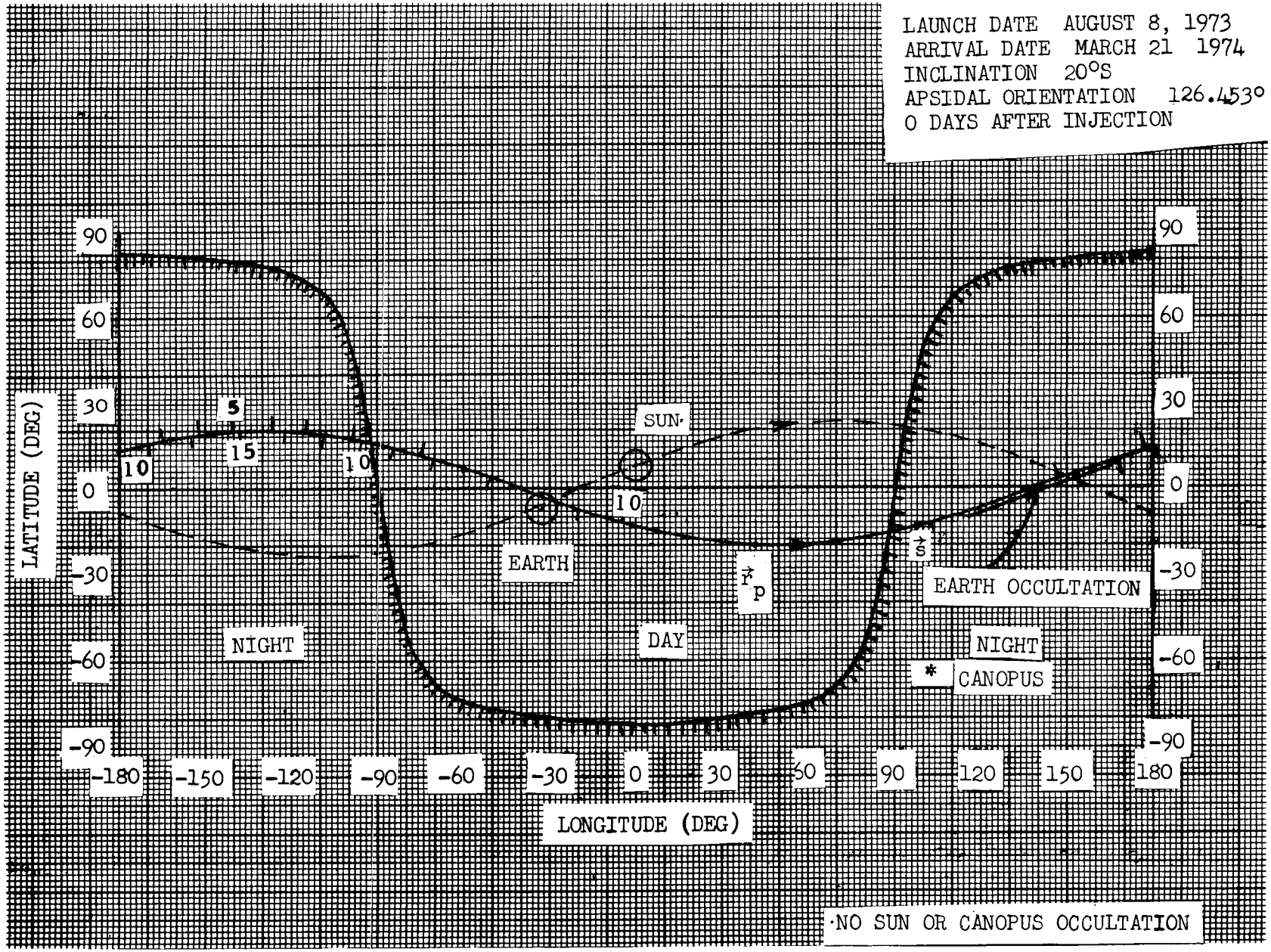
LAUNCH DATE AUGUST 8, 1973
ARRIVAL DATE MARCH 21 1974
INCLINATION 20°S
APSIDAL ORIENTATION 126.453°
0 DAYS AFTER INJECTION
LATITUDE (DEG)
90
60
30
0
-30
-60
-90
-180
-150
-120
-90
-60
-30
0
30
60
90
120
150
180
LONGITUDE (DEG)
5
10
15
10
10
SUN
EARTH
NIGHT
DAY
EARTH OCCULTATION
NIGHT
CANOPUS
NO SUN OR CANOPUS OCCULTATION

LAUNCH DATE AUGUST 8, 1973
ARRIVAL DATE MARCH 21, 1974
INCLINATION 20°S
APSIDAL ORIENTATION 126.453°
90 DAYS AFTER INJECTION
LATITUDE (DEG)
LONGITUDE (DEG)
90
60
30
0
-30
-60
-90
-180
-150
-120
-90
-60
-30
0
30
60
90
120
150
180
5
10
15
10
10
EARTH
SUN
NIGHT
DAY
NIGHT
CANOPUS
NO SUN, EARTH OR CANOPUS OCCULTATION

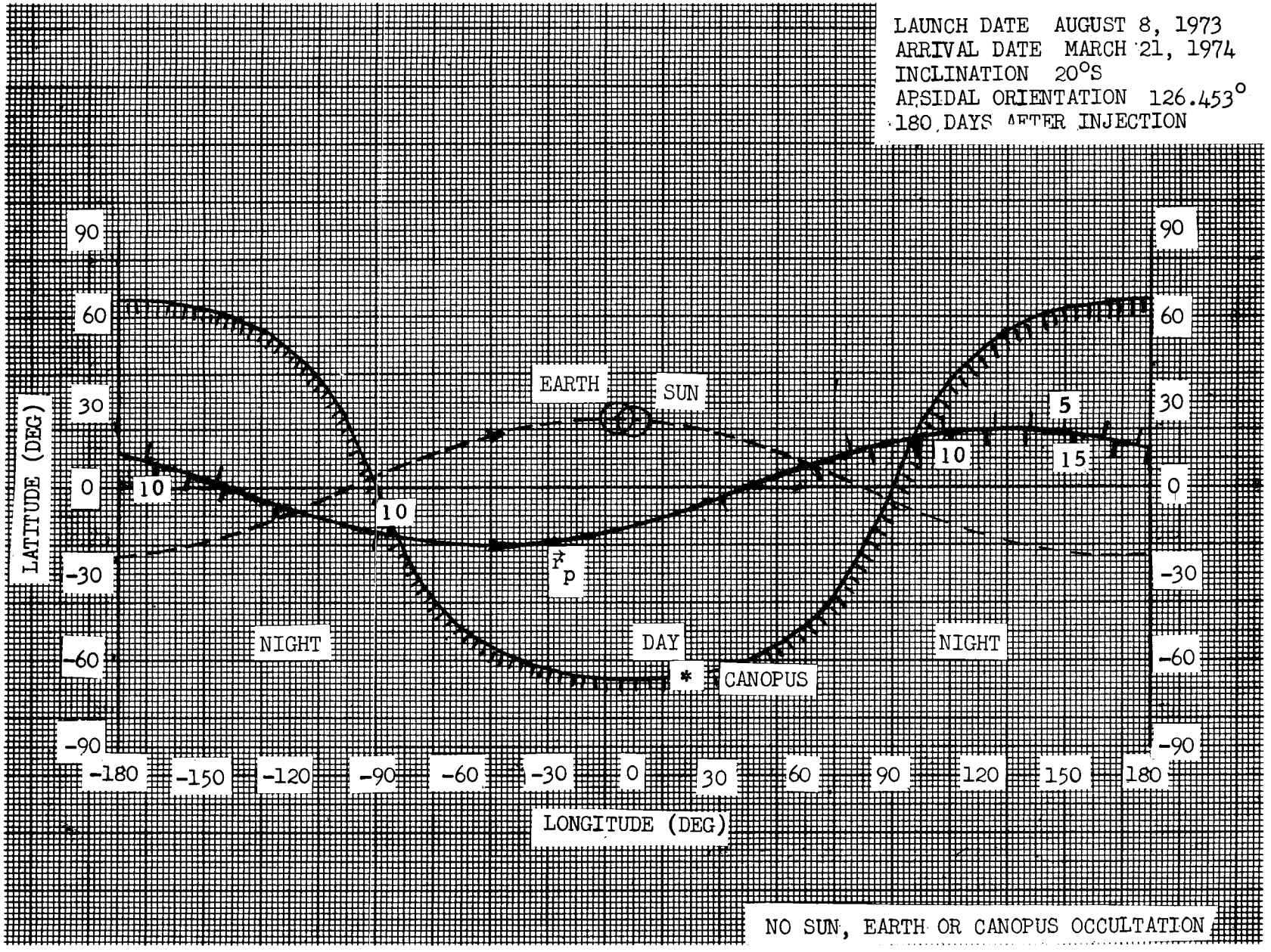
LAUNCH DATE AUGUST 8, 1973
ARRIVAL DATE MARCH 21, 1974
INCLINATION 20°S
APSIDAL ORIENTATION 126.453°
180 DAYS AFTER INJECTION
LATITUDE (DEG)
90
60
30
0
-30
-60
-90
EARTH
SUN
5
10
15
10
10
$\vec{r}_p$
NIGHT
DAY
NIGHT
CANOPUS
-180
-150
-120
-90
-60
-30
0
30
60
90
120
150
180
LONGITUDE (DEG)
NO SUN, EARTH OR CANOPUS OCCULTATION

CASE NO. 17

1000 x 15, 000 km

$i = 20^{o}N$

$\Psi = 126.453$ deg

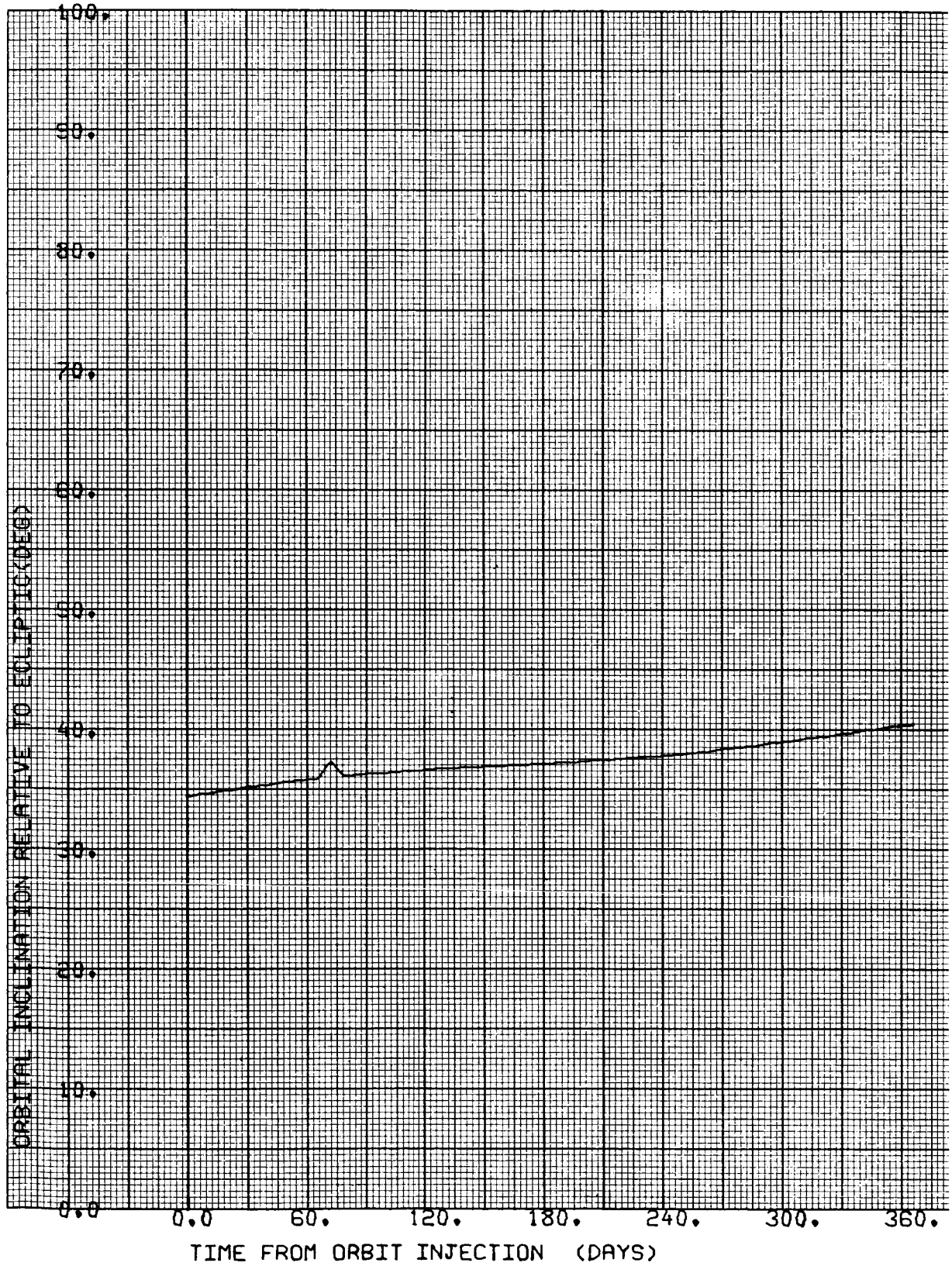
100.
90.
80.
70.
60.
50.
40.
30.
20.
10.
0.0
ORBITAL INCLINATION RELATIVE TO ECLIPTIC(DEG)
0.0
60.
120.
180.
240.
300.
360.
TIME FROM ORBIT INJECTION (DAYS)

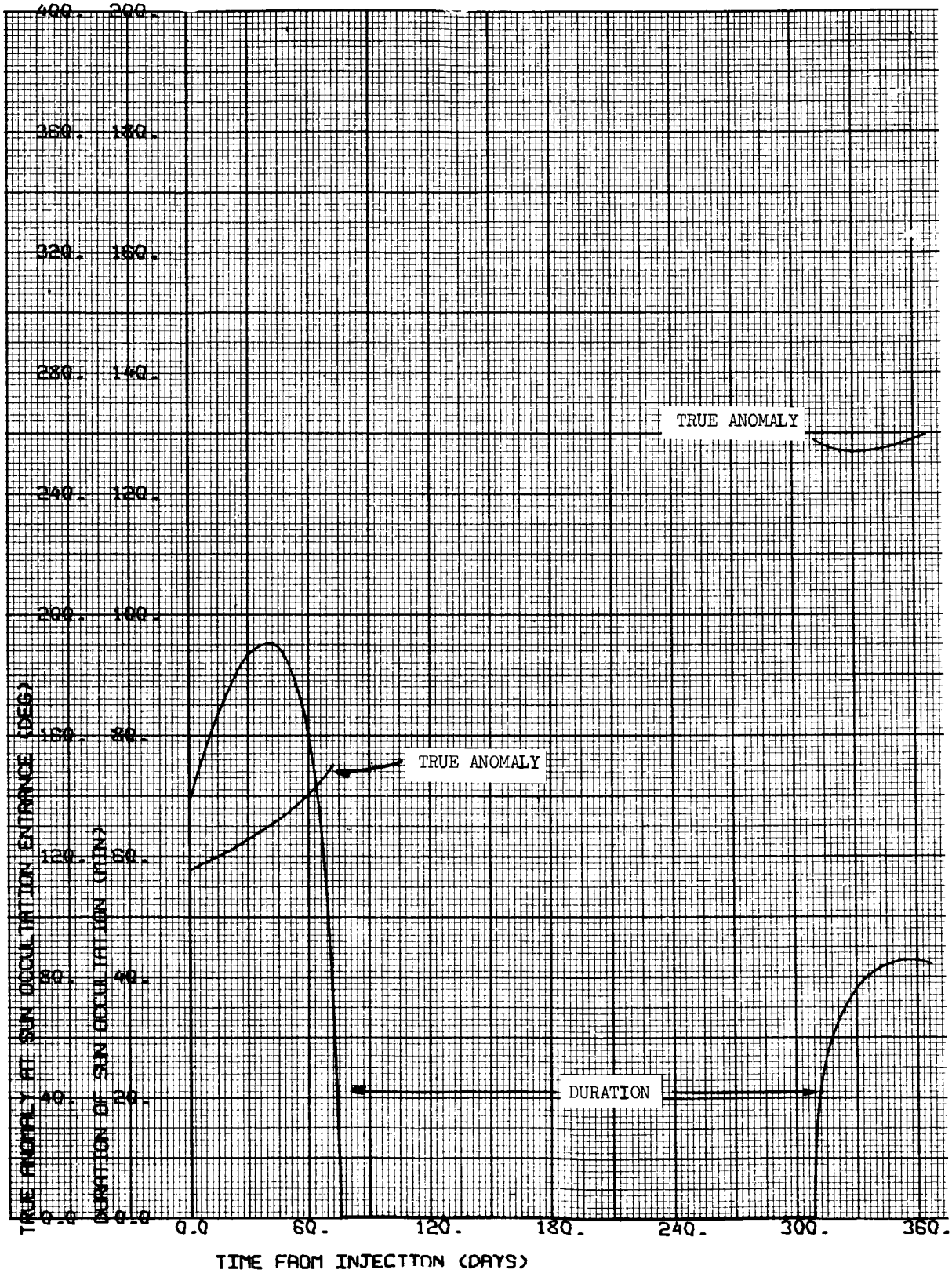
TRUE ANOMALY
TRUE ANOMALY
DURATION
TRUE ANOMALY AT SUN OCCULTATION ENTRANCE (DEG)
DURATION OF SUN OCCULTATION (MIN)
TIME FROM INJECTION (DAYS)
0.0
60.
120.
180.
240.
300.
360.
400.
360.
320.
280.
240.
200.
160.
120.
80.
40.
0.0
200.
180.
160.
140.
120.
100.
80.
60.
40.
20.
0.0

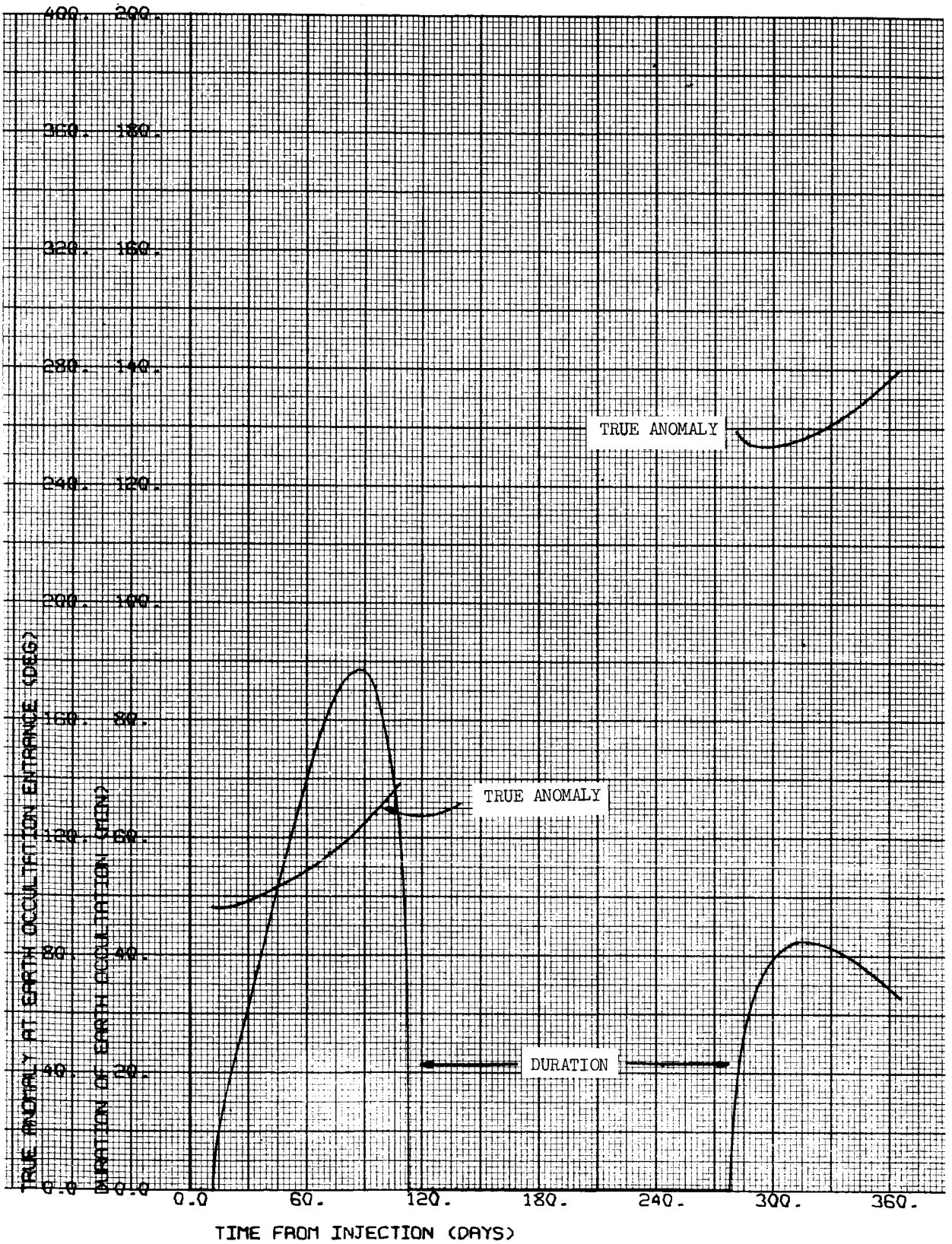
TRUE ANOMALY
TRUE ANOMALY
DURATION
TRUE ANOMALY AT EARTH OCCULTATION ENTRANCE (DEG)
DURATION OF EARTH OCCULTATION (MIN)
0.0
60.
120.
180.
240.
300.
360.
TIME FROM INJECTION (DAYS)

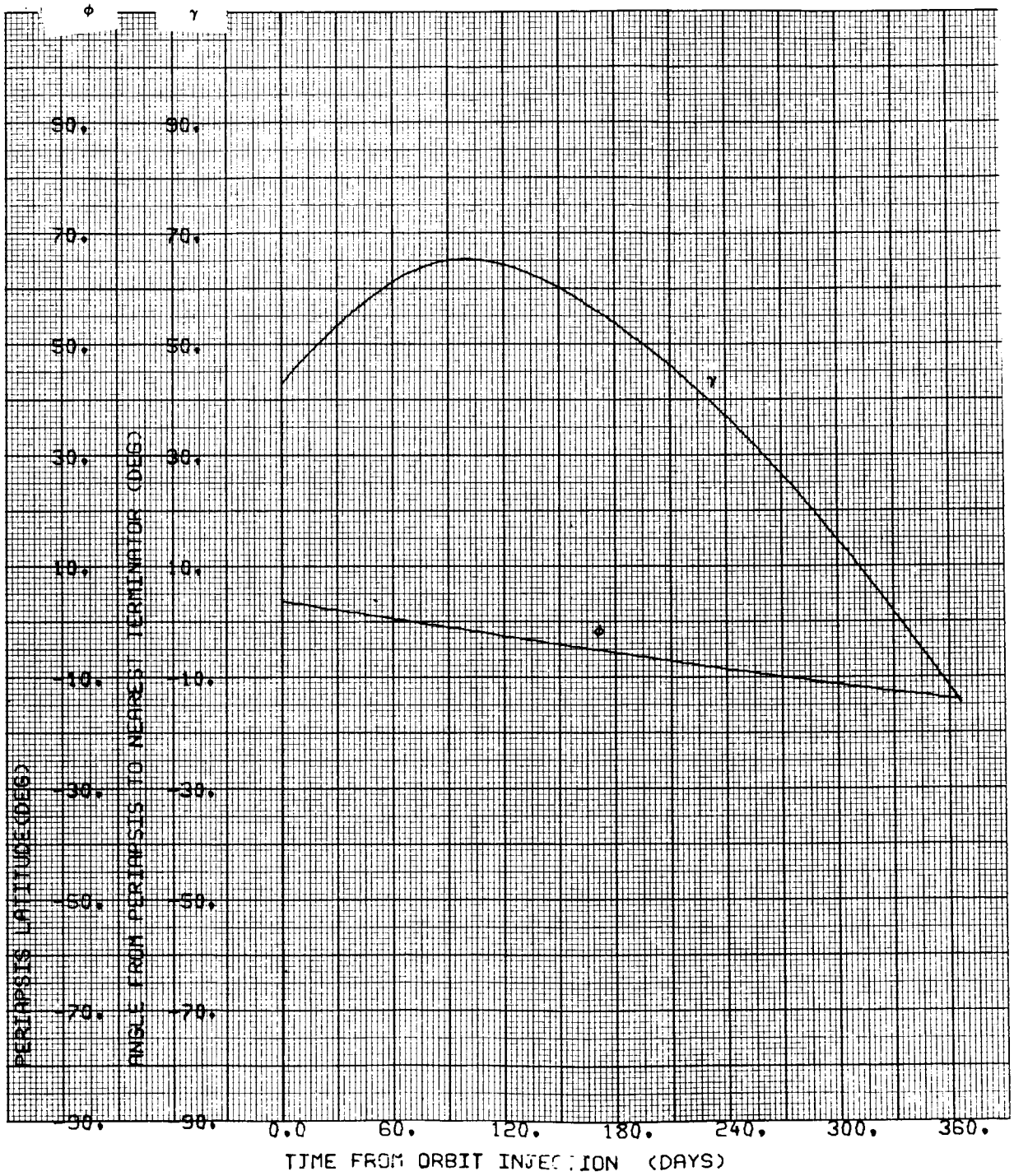
φ
γ
90.
70.
50.
30.
10.
-10.
-30.
-50.
-70.
-90.
0.0
60.
120.
180.
240.
300.
360.
PERIAPSIS LATITUDE (DEG)
ANGLE FROM PERIAPSIS TO NEAREST TERMINATOR (DEG)
TIME FROM ORBIT INJECTION (DAYS)

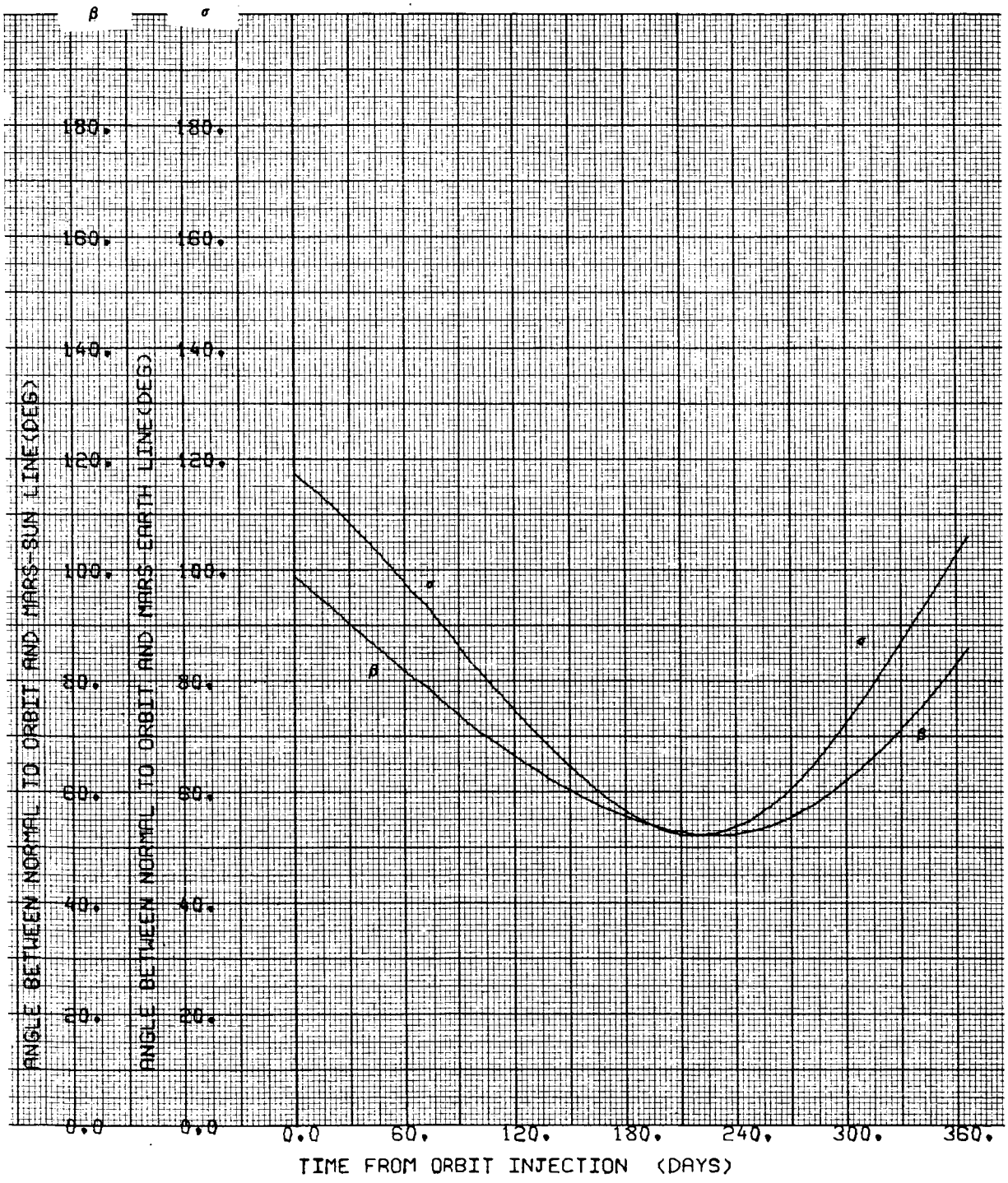
β
σ
180.
160.
140.
120.
100.
80.
60.
40.
20.
0.0
ANGLE BETWEEN NORMAL TO ORBIT AND MARS-SUN LINE(DEG)
ANGLE BETWEEN NORMAL TO ORBIT AND MARS EARTH LINE(DEG)
0.0
60.
120.
180.
240.
300.
360.
TIME FROM ORBIT INJECTION (DAYS)

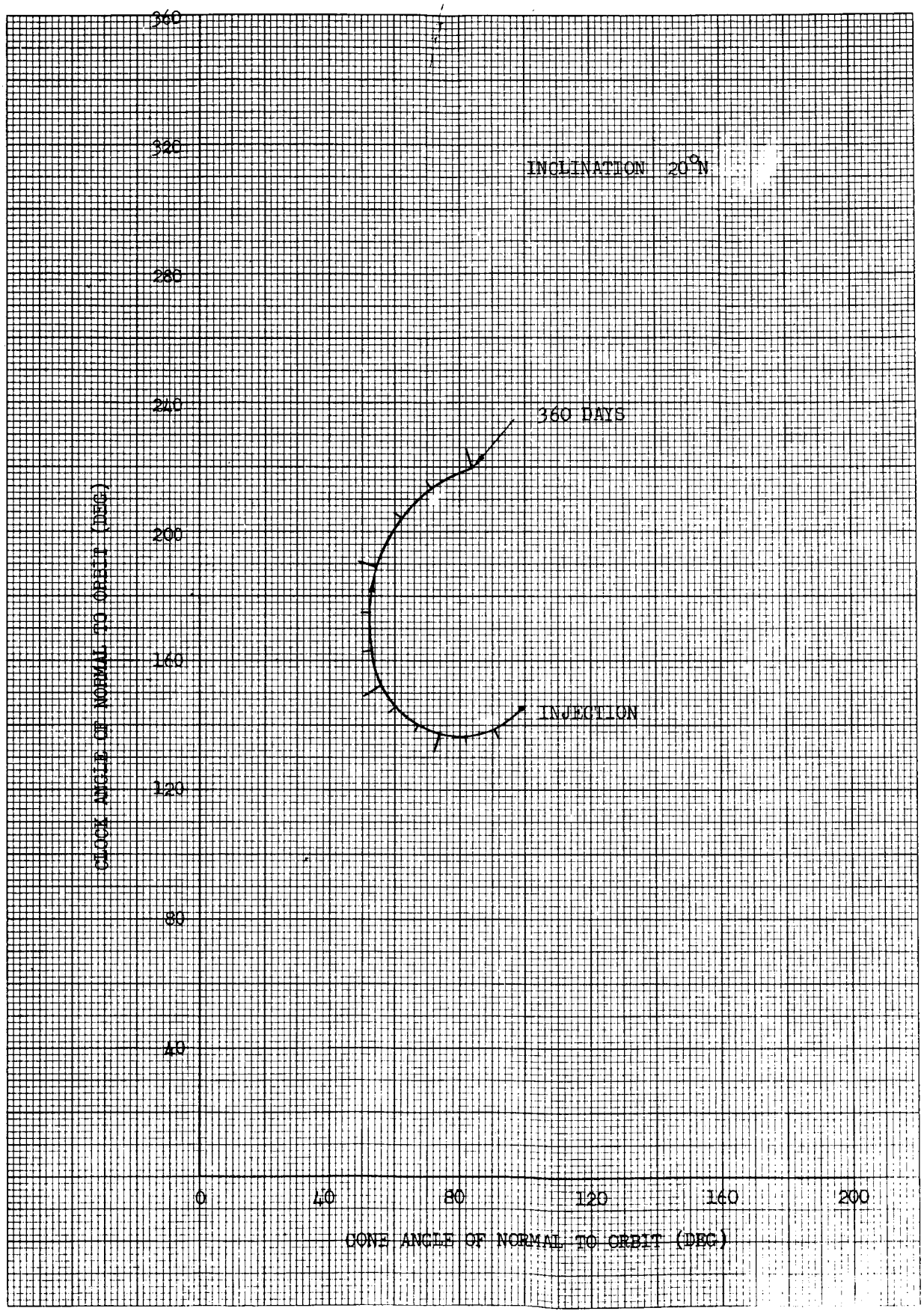
INCLINATION 20°N
360 DAYS
INJECTION
CLOCK ANGLE OF NORMAL TO ORBIT (DEG.)
CONE ANGLE OF NORMAL TO ORBIT (DEG.)
360
320
280
240
200
160
120
80
40
0
40
80
120
160
200

LAUNCH DATE AUGUST 8, 1973
ARRIVAL DATE MARCH 21, 1974
INCLINATION 20°N
APSIDAL ORIENTATION 126.453°
0 DAYS AFTER INJECTION
NO EARTH OR CANOPUS OCCULTATION
LATITUDE (DEG)
LONGITUDE (DEG)
90
60
30
0
-30
-60
-90
-180
-150
-120
-90
-60
-30
0
30
60
90
120
150
180
SUN
EARTH
SUN OCCULTATION
DAY
NIGHT
NIGHT
CANOPUS
5
10
15
10
10

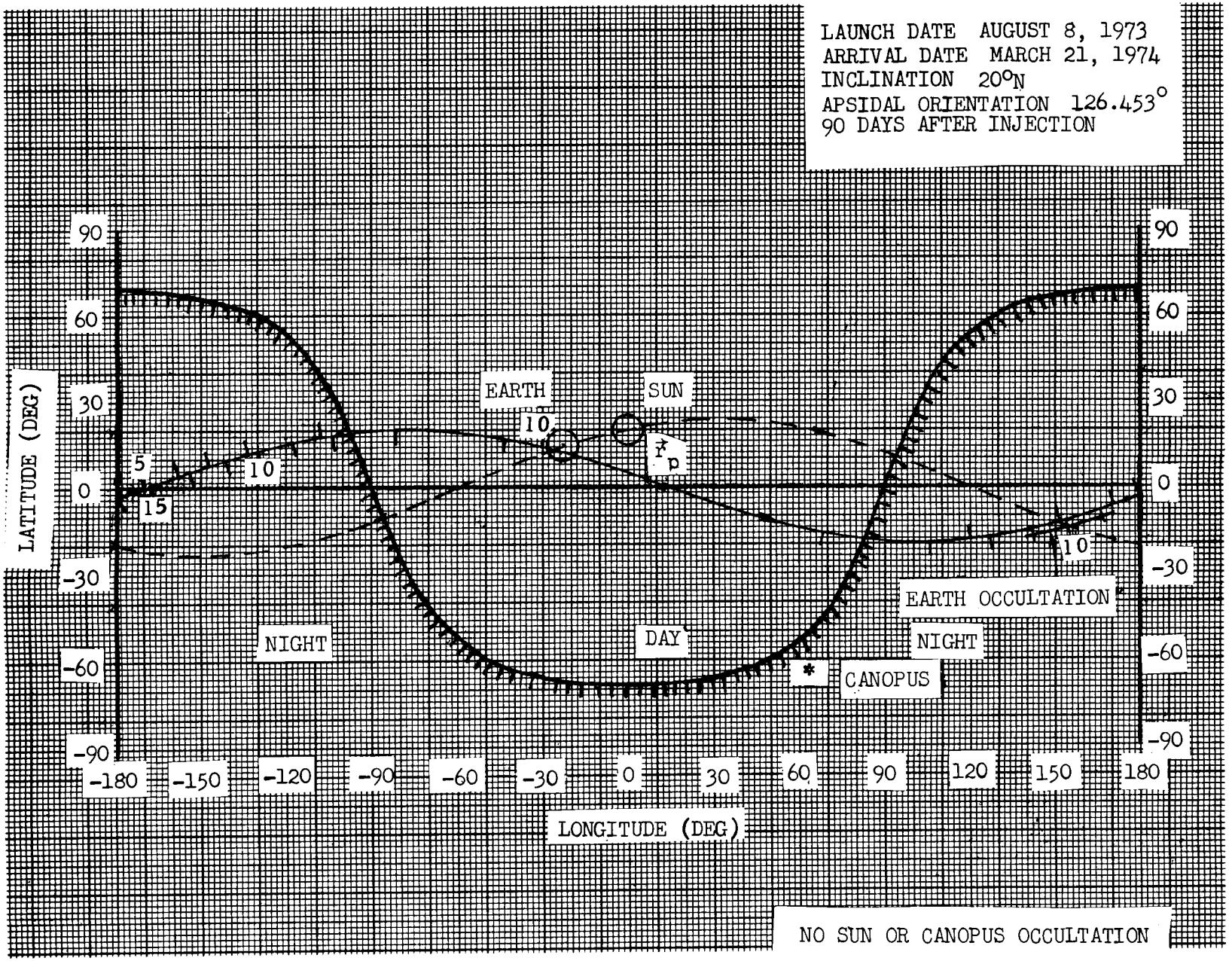
LAUNCH DATE AUGUST 8, 1973
ARRIVAL DATE MARCH 21, 1974
INCLINATION 20°N
APSIDAL ORIENTATION 126.453°
90 DAYS AFTER INJECTION
LATITUDE (DEG)
90
60
30
0
-30
-60
-90
EARTH
SUN
10
5
10
15
10
r_p
EARTH OCCULTATION
NIGHT
DAY
NIGHT
CANOPUS
-180
-150
-120
-90
-60
-30
0
30
60
90
120
150
180
LONGITUDE (DEG)
NO SUN OR CANOPUS OCCULTATION

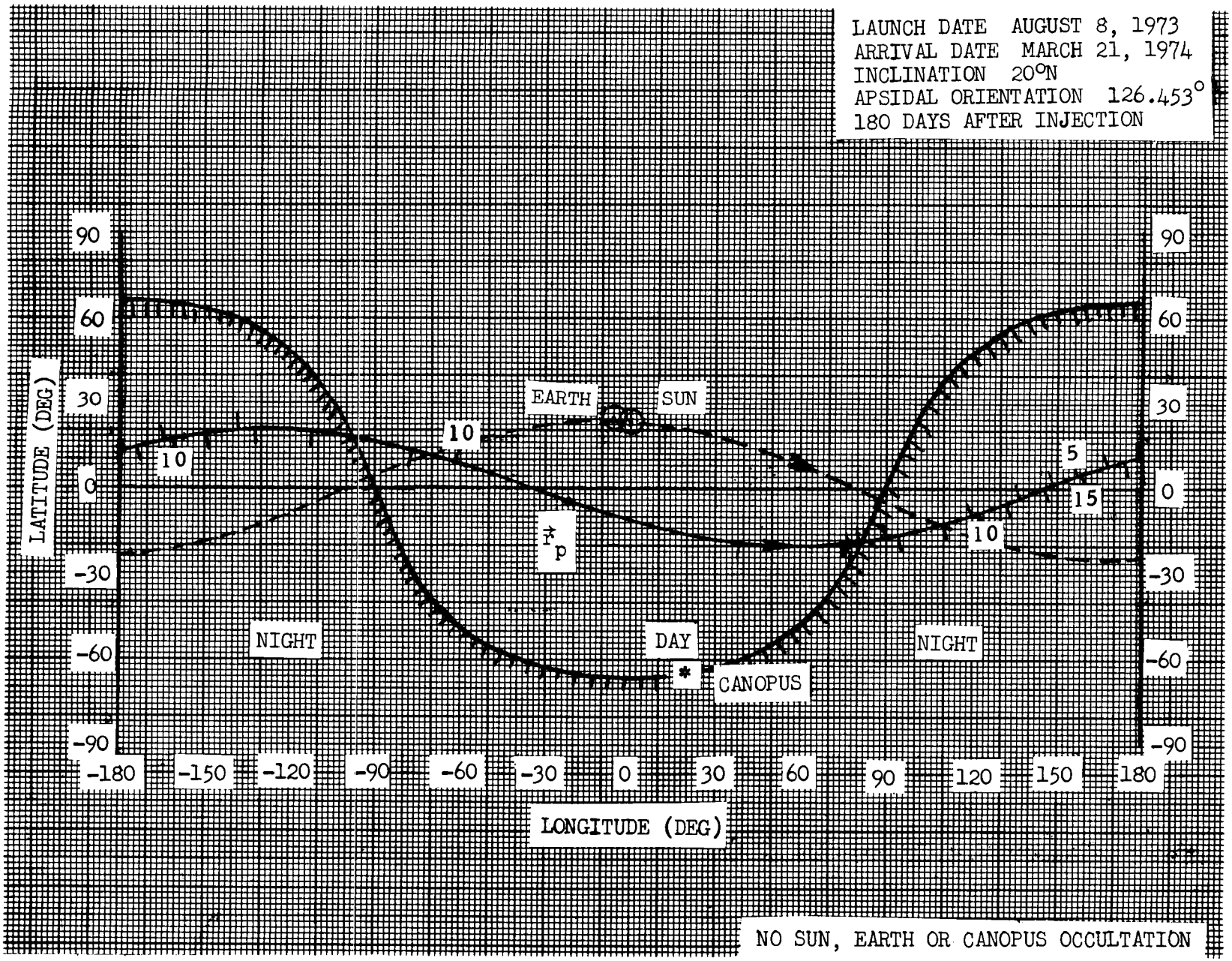
LAUNCH DATE AUGUST 8, 1973
ARRIVAL DATE MARCH 21, 1974
INCLINATION 20°N
APSIDAL ORIENTATION 126.453°
180 DAYS AFTER INJECTION
LATITUDE (DEG)
90
60
30
0
-30
-60
-90
EARTH
SUN
10
10
5
15
10
r_p
NIGHT
DAY
NIGHT
CANOPUS
-180
-150
-120
-90
-60
-30
0
30
60
90
120
150
180
LONGITUDE (DEG)
NO SUN, EARTH OR CANOPUS OCCULTATION

CASE NO. 18

1000 x 15, 000 km

$i = 40^{\circ}S$

$\Psi = 126.453$ deg

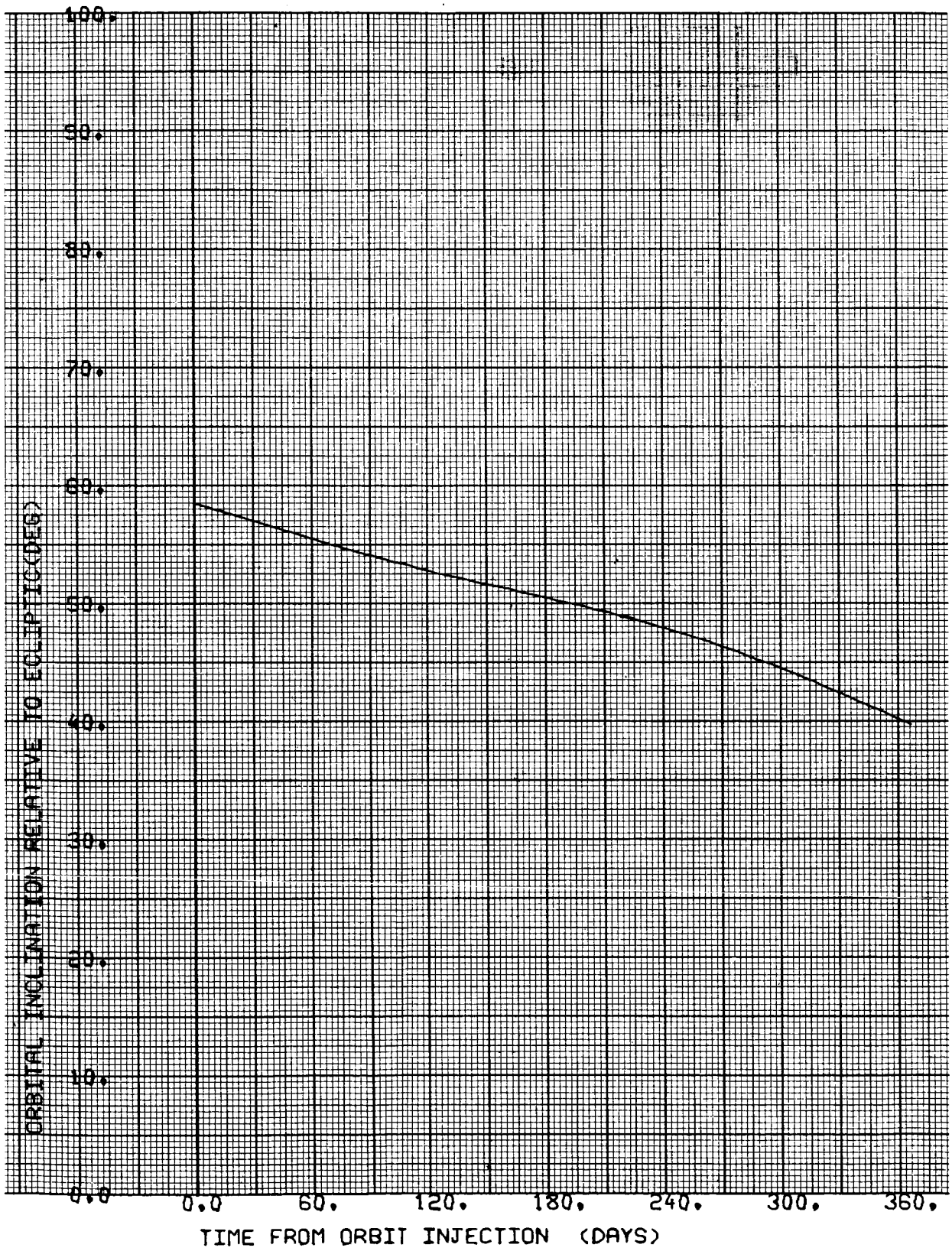
100.
90.
80.
70.
60.
50.
40.
30.
20.
10.
0.0
ORBITAL INCLINATION RELATIVE TO ECLIPTIC(DEG)
0.0
60.
120.
180.
240.
300.
360.
TIME FROM ORBIT INJECTION (DAYS)

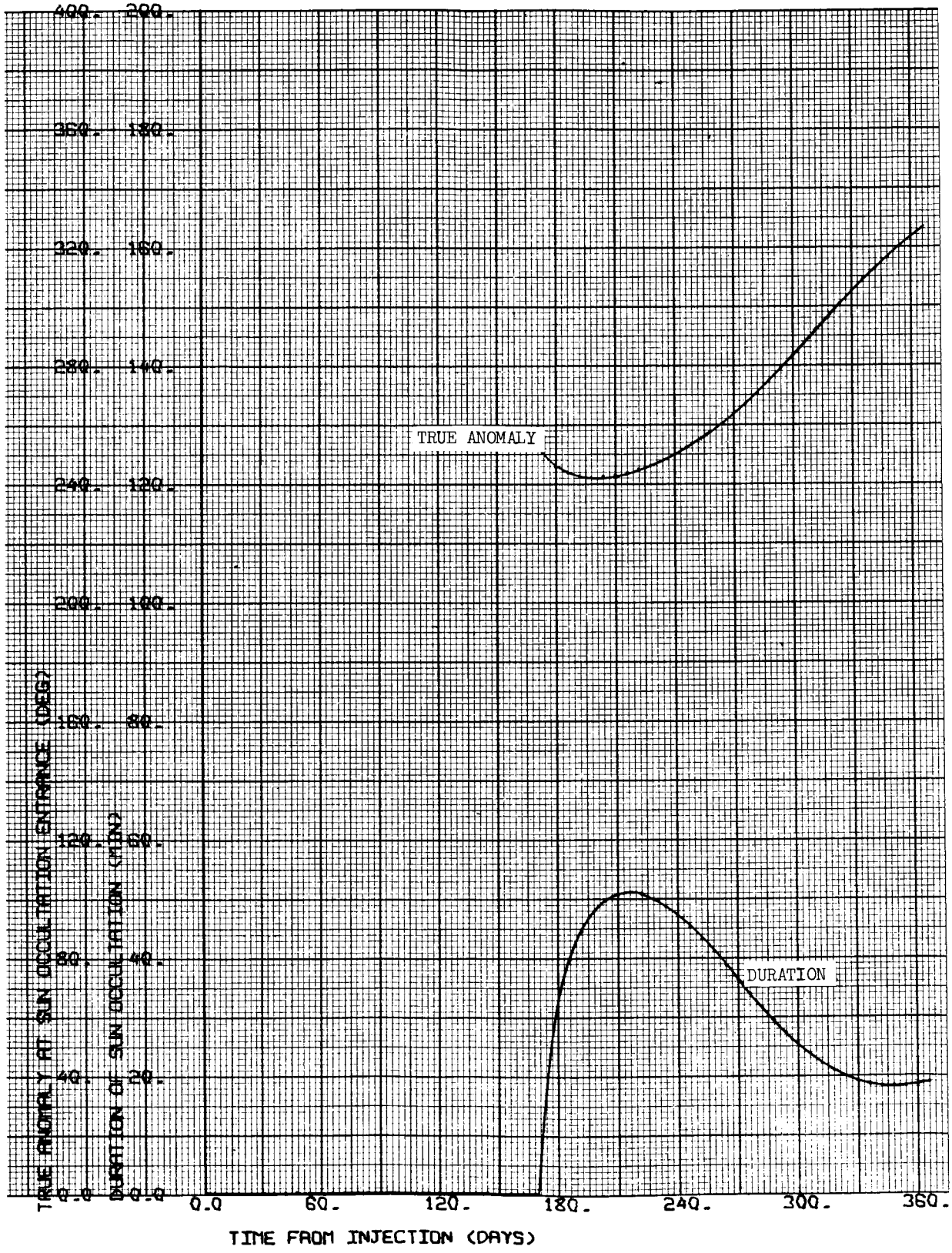
TRUE ANOMALY
DURATION
TRUE ANOMALY AT SUN OCCULTATION ENTRANCE (DEG)
DURATION OF SUN OCCULTATION (MIN)
TIME FROM INJECTION (DAYS)
0.0
60.
120.
180.
240.
300.
360.
400.
360.
320.
280.
240.
200.
160.
120.
80.
40.
0.0
280.
240.
200.
160.
120.
80.
40.
0.0

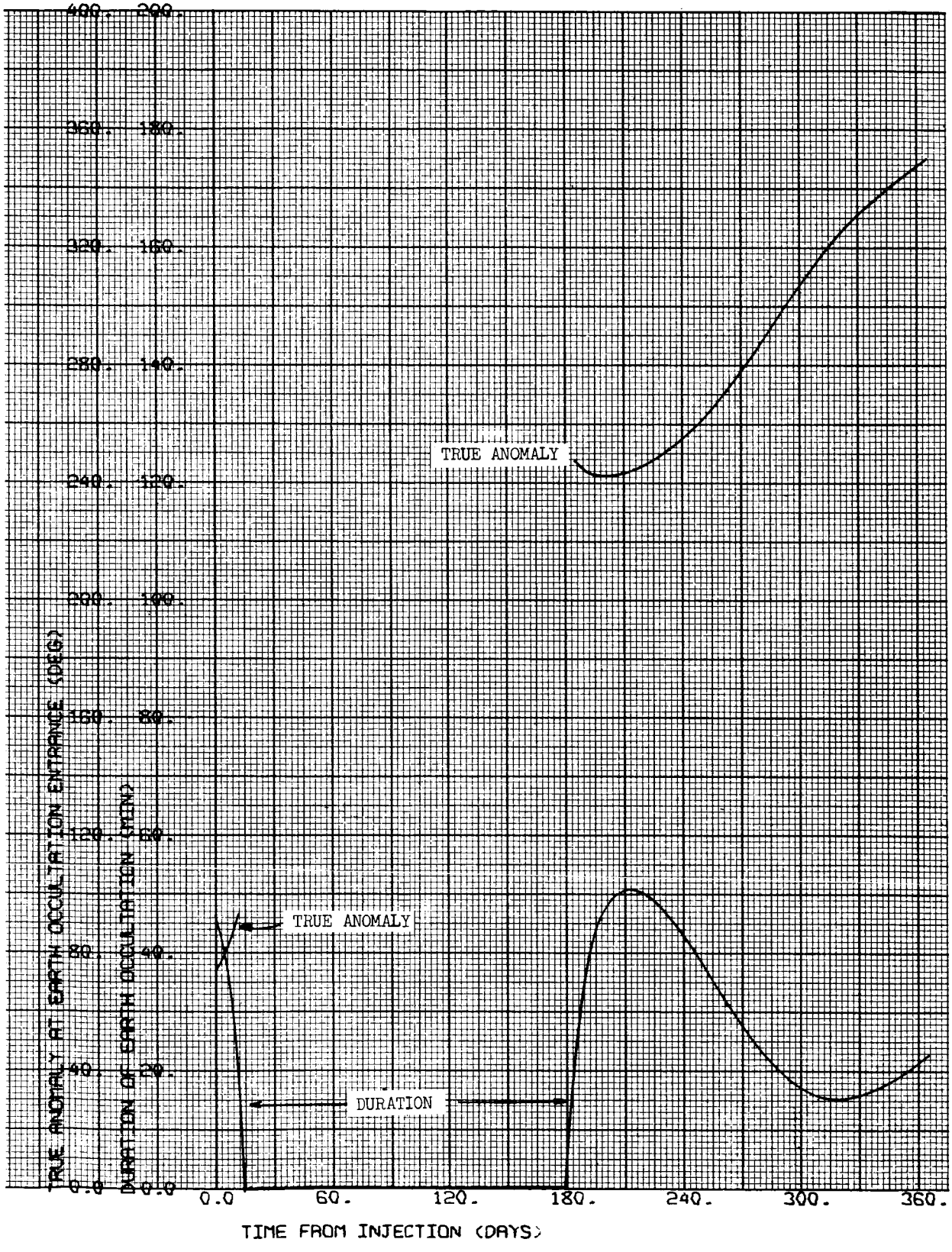
TRUE ANOMALY AT EARTH OCCULTATION ENTRANCE (DEG)
DURATION OF EARTH OCCULTATION (MIN)
TRUE ANOMALY
TRUE ANOMALY
DURATION
0.0
60.
120.
180.
240.
300.
360.
TIME FROM INJECTION (DAYS)

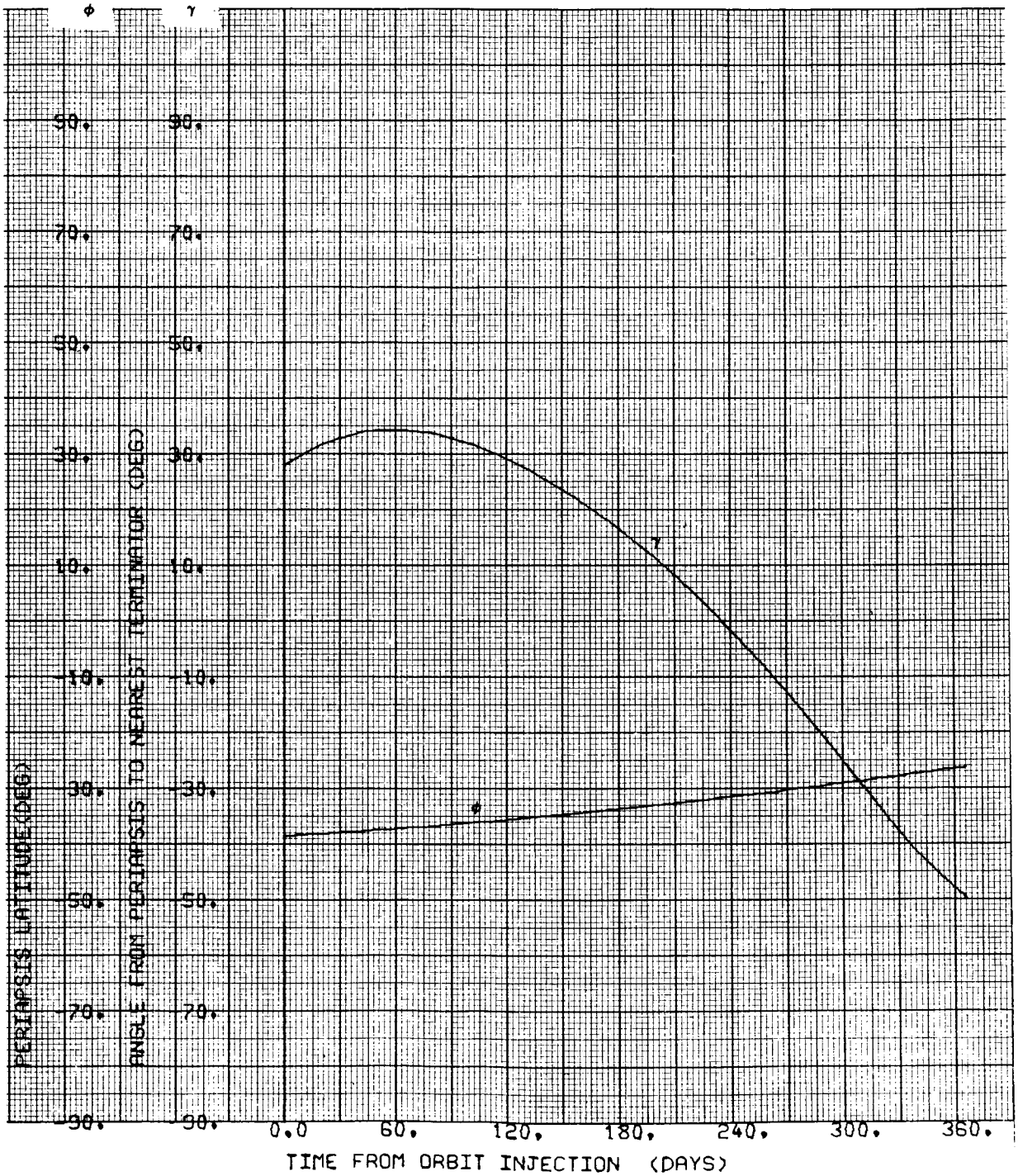
φ
γ
90.
70.
50.
30.
10.
-10.
-30.
-50.
-70.
-90.
0.0
60.
120.
180.
240.
300.
360.
PERIAPSIS LATITUDE(DEG)
ANGLE FROM PERIAPSIS TO NEAREST TERMINATOR (DEG)
TIME FROM ORBIT INJECTION (DAYS)

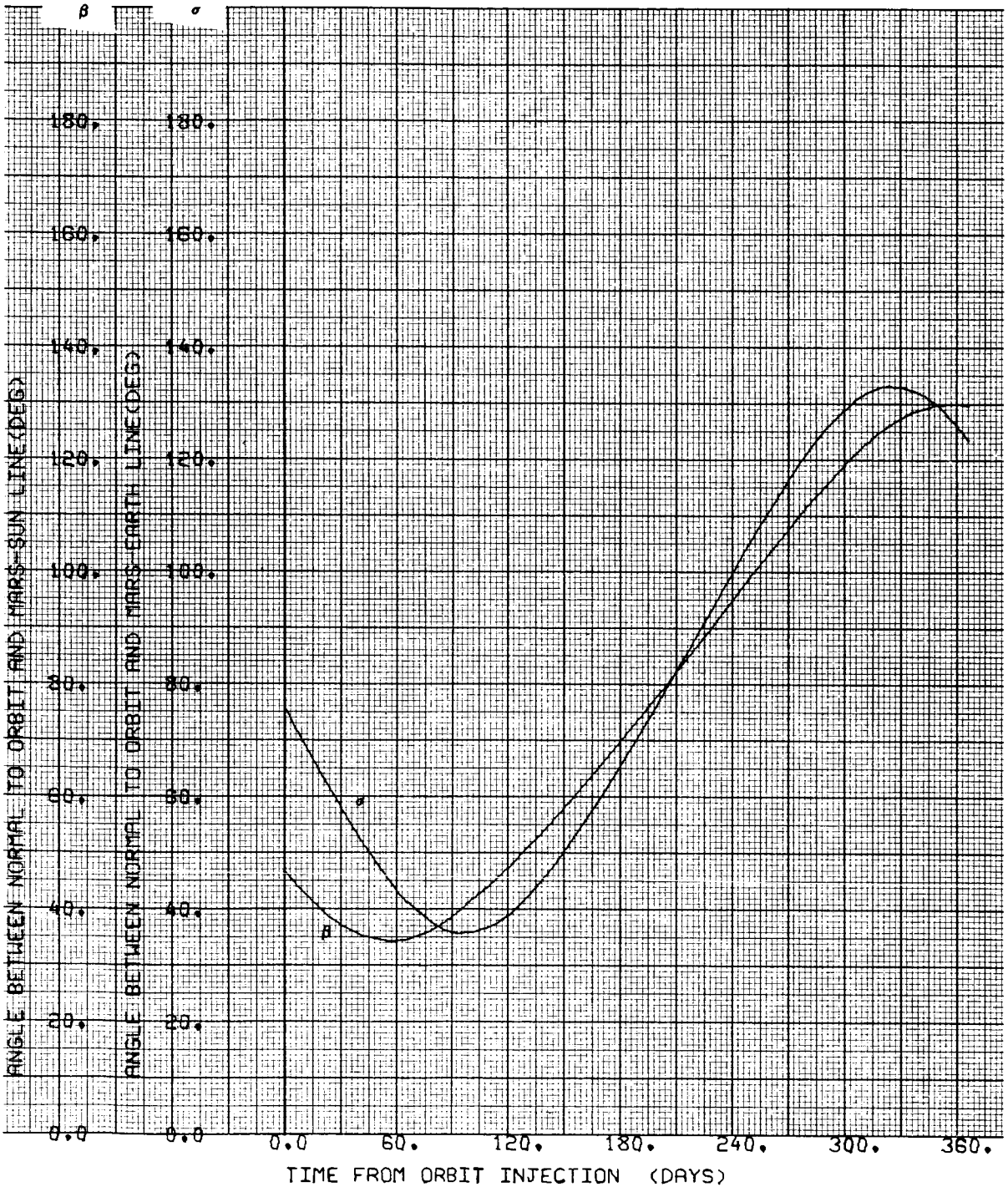
β
σ
180.
160.
140.
120.
100.
80.
60.
40.
20.
0.0
ANGLE BETWEEN NORMAL TO ORBIT AND MARS-SUN LINE(DEG)
ANGLE BETWEEN NORMAL TO ORBIT AND MARS-EARTH LINE(DEG)
0.0
60.
120.
180.
240.
300.
360.
TIME FROM ORBIT INJECTION (DAYS)

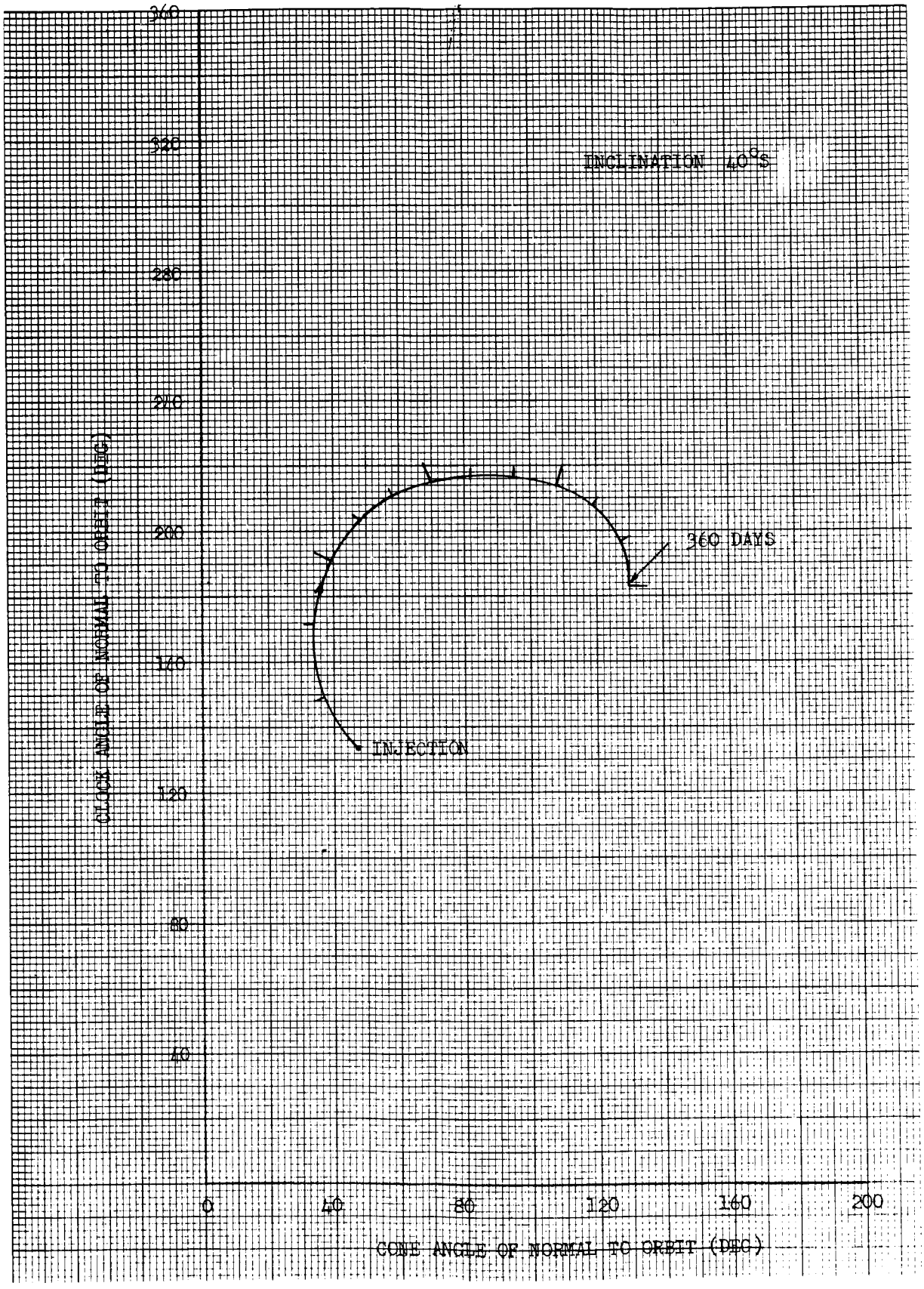
INCLINATION 40°S
360 DAYS
INJECTION
CLOCK ANGLE OF NORMAL TO ORBIT (DEG)
CONE ANGLE OF NORMAL TO ORBIT (DEG)
360
320
280
240
200
160
120
80
40
0
40
80
120
160
200

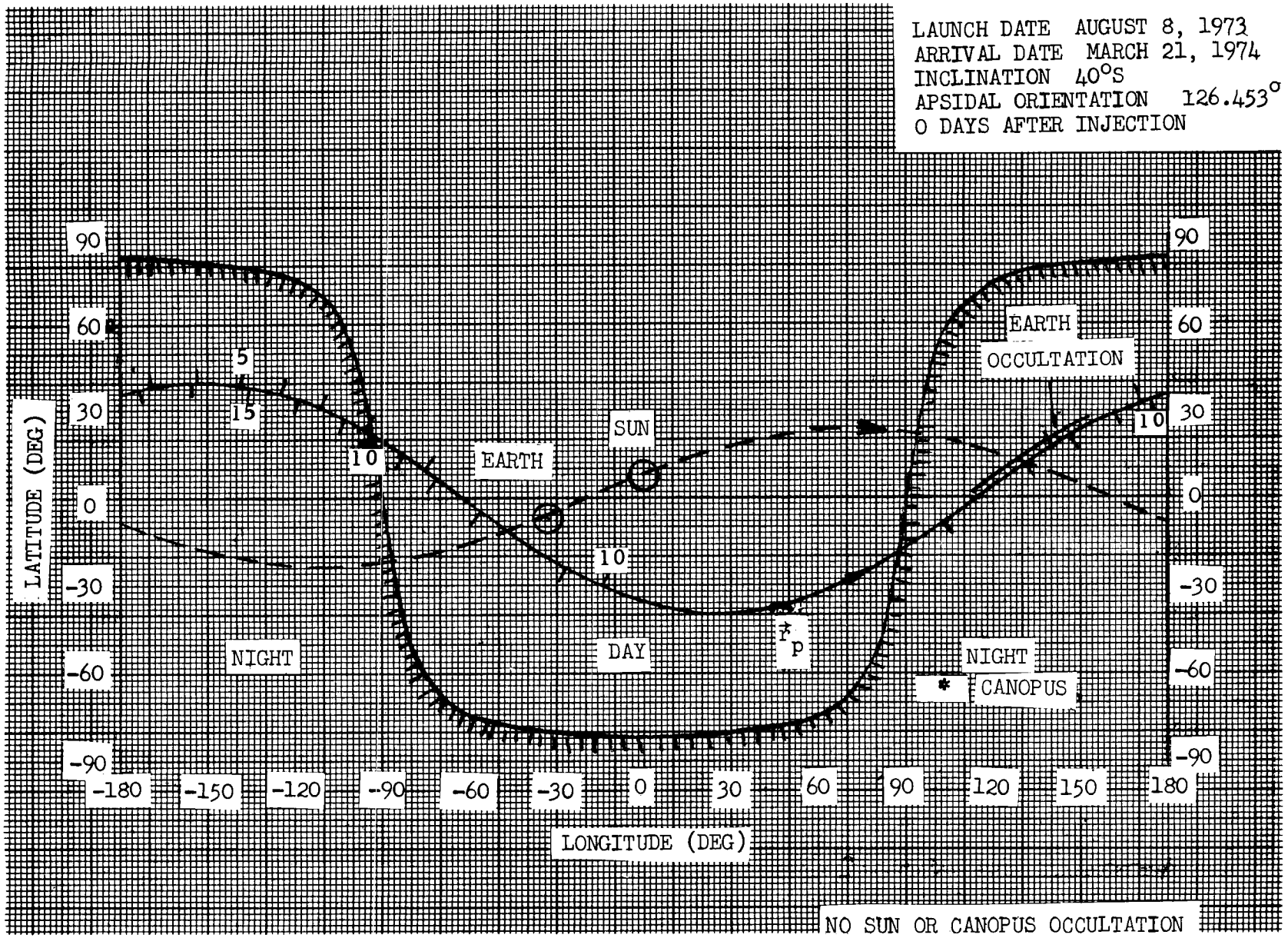
LAUNCH DATE AUGUST 8, 1973
ARRIVAL DATE MARCH 21, 1974
INCLINATION 40°S
APSIDAL ORIENTATION 126.453°
0 DAYS AFTER INJECTION
LATITUDE (DEG)
90
60
30
0
-30
-60
-90
5
15
10
EARTH
SUN
10
NIGHT
DAY
NIGHT
EARTH
OCCULTATION
10
CANOPUS
-180
-150
-120
-90
-60
-30
0
30
60
90
120
150
180
LONGITUDE (DEG)
NO SUN OR CANOPUS OCCULTATION

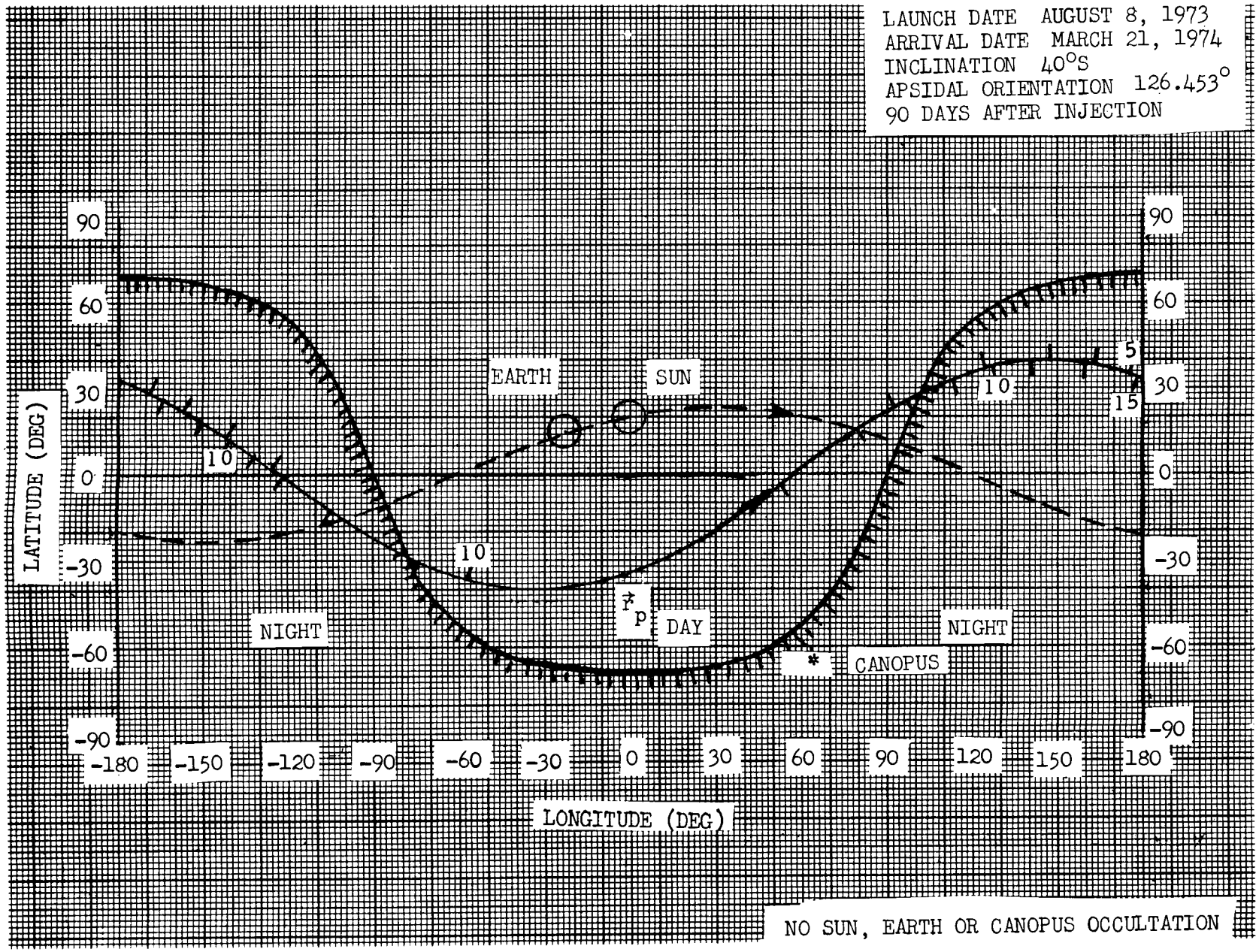
LAUNCH DATE AUGUST 8, 1973
ARRIVAL DATE MARCH 21, 1974
INCLINATION 40°S
APSIDAL ORIENTATION 126.453°
90 DAYS AFTER INJECTION
LATITUDE (DEG)
90
60
30
0
-30
-60
-90
EARTH
SUN
NIGHT
DAY
NIGHT
CANOPUS
10
10
10
5
15
-180
-150
-120
-90
-60
-30
0
30
60
90
120
150
180
LONGITUDE (DEG)
NO SUN, EARTH OR CANOPUS OCCULTATION

LAUNCH DATE AUGUST 8, 1973
ARRIVAL DATE MARCH 21, 1974
INCLINATION 40°S
APSIDAL ORIENTATION 126.453°
180 DAYS AFTER INJECTION
LATITUDE (DEG)
LONGITUDE (DEG)
90
60
30
0
-30
-60
-90
-150
-180
-120
150
120
NIGHT
DAY
SUN
EARTH
CANOPUS
SUN OCCULTATION
NO EARTH OR CANOPUS OCCULTATION

CASE NO. 19

1000 x 15,000 km

$i = 40^{\circ}N$

$\Psi = 126.453$ deg

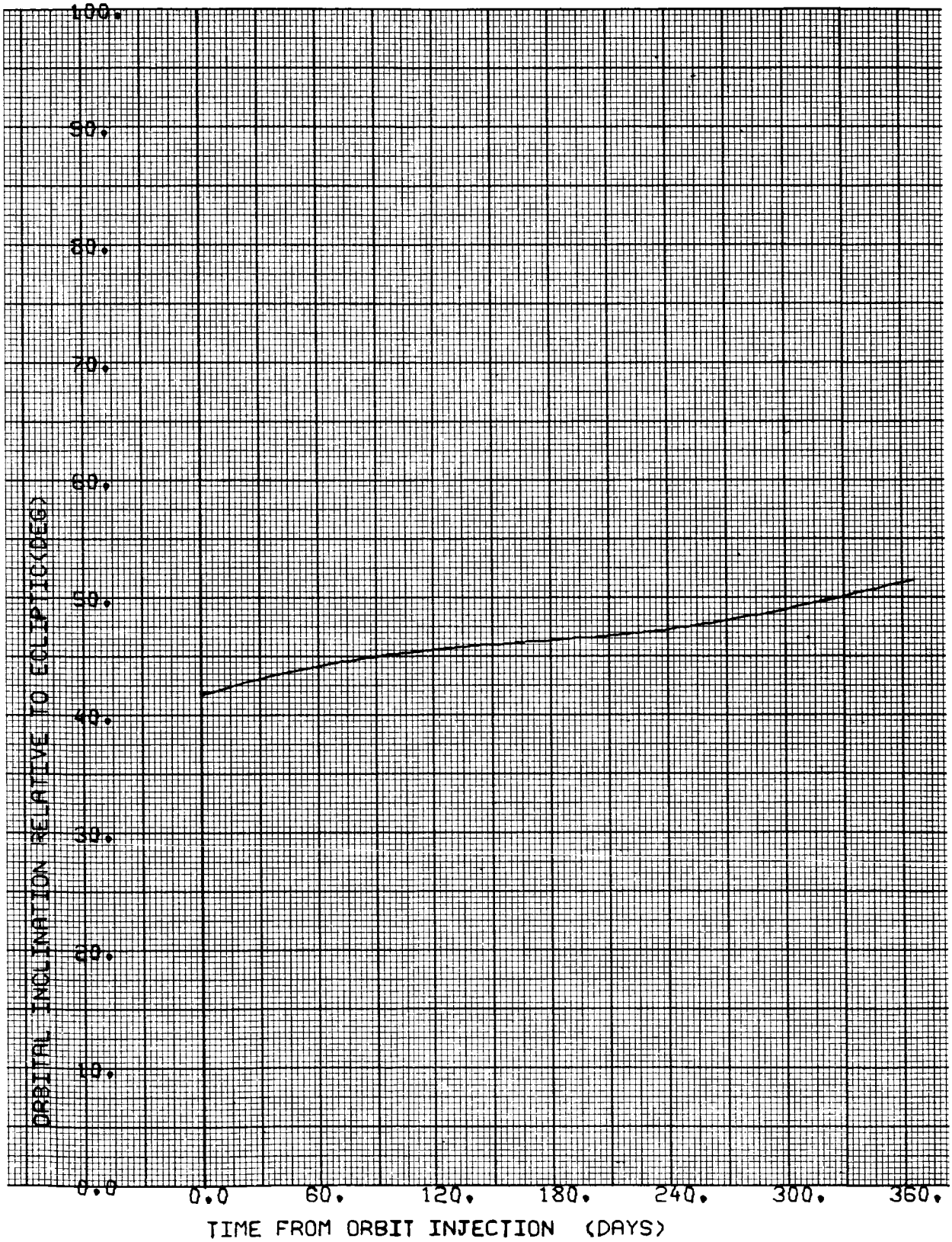
100.
90.
80.
70.
60.
50.
40.
30.
20.
10.
0.0
ORBITAL INCLINATION RELATIVE TO ECLIPTIC(DEG)
0.0
60.
120.
180.
240.
300.
360.
TIME FROM ORBIT INJECTION (DAYS)

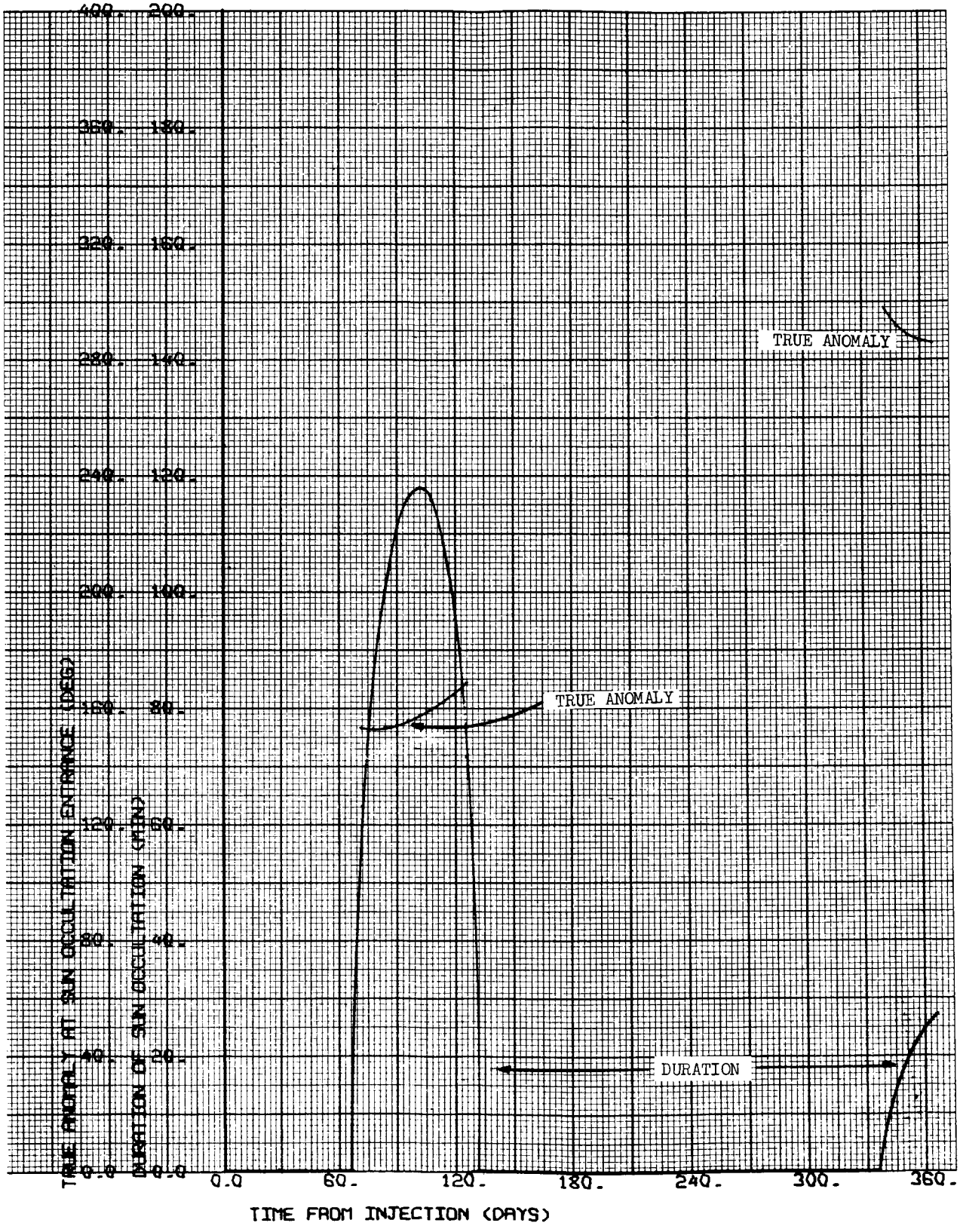
TRUE ANOMALY
TRUE ANOMALY
DURATION
TRUE ANOMALY AT SUN OCCULTATION ENTRANCE (DEG)
DURATION OF SUN OCCULTATION (MIN)
TIME FROM INJECTION (DAYS)
0.0
60.
120.
180.
240.
300.
360.
400.
360.
320.
280.
240.
200.
160.
120.
80.
40.
0.0
200.
180.
160.
140.
120.
100.
80.
60.
40.
20.
0.0

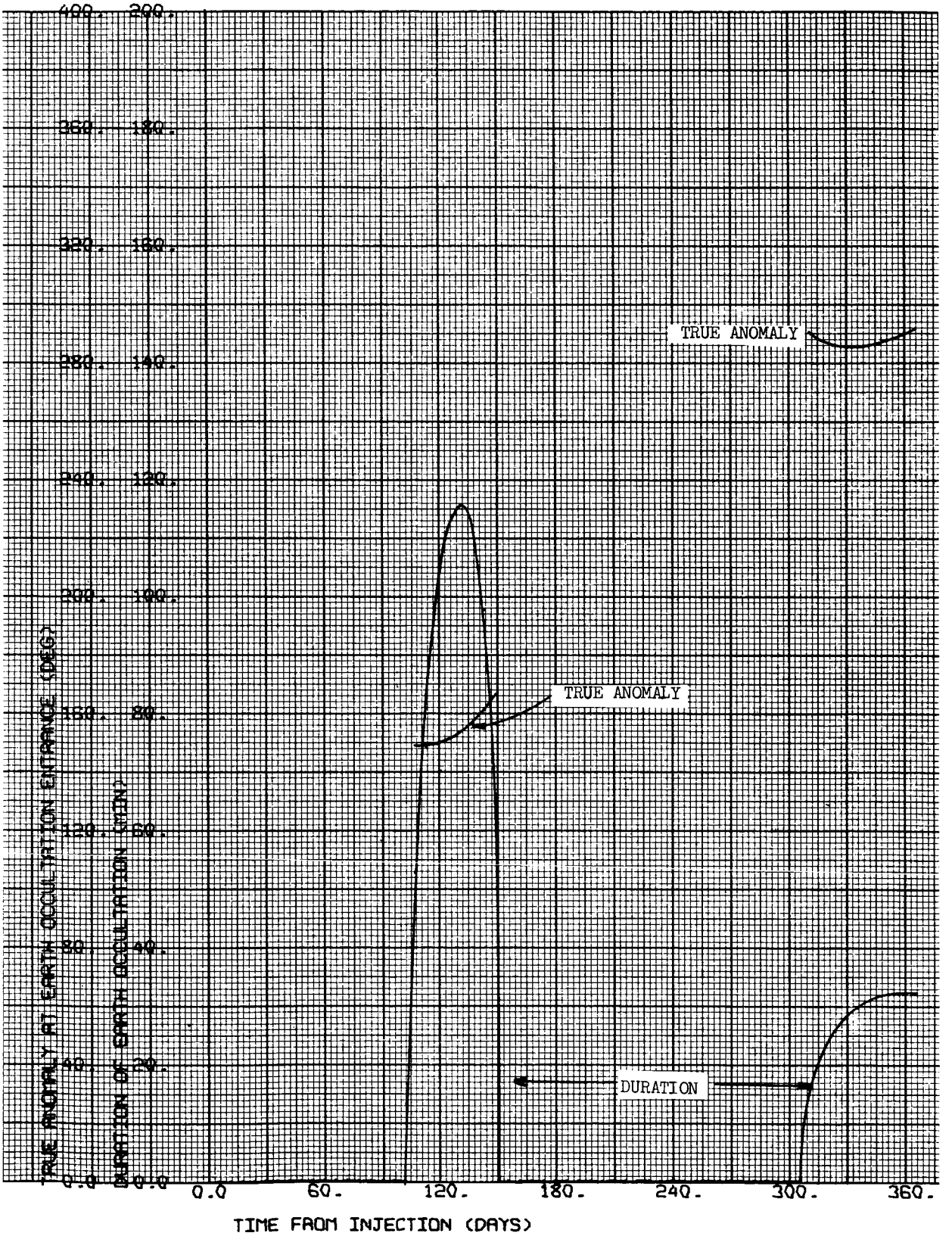
TRUE ANOMALY AT EARTH OCCULTATION ENTRANCE (DEG)
DURATION OF EARTH OCCULTATION (MIN)
TIME FROM INJECTION (DAYS)
TRUE ANOMALY
TRUE ANOMALY
DURATION
400.
360.
320.
280.
240.
200.
160.
120.
80.
40.
0.0
200.
180.
160.
140.
120.
100.
80.
60.
40.
20.
0.0
0.0
60.
120.
180.
240.
300.
360.

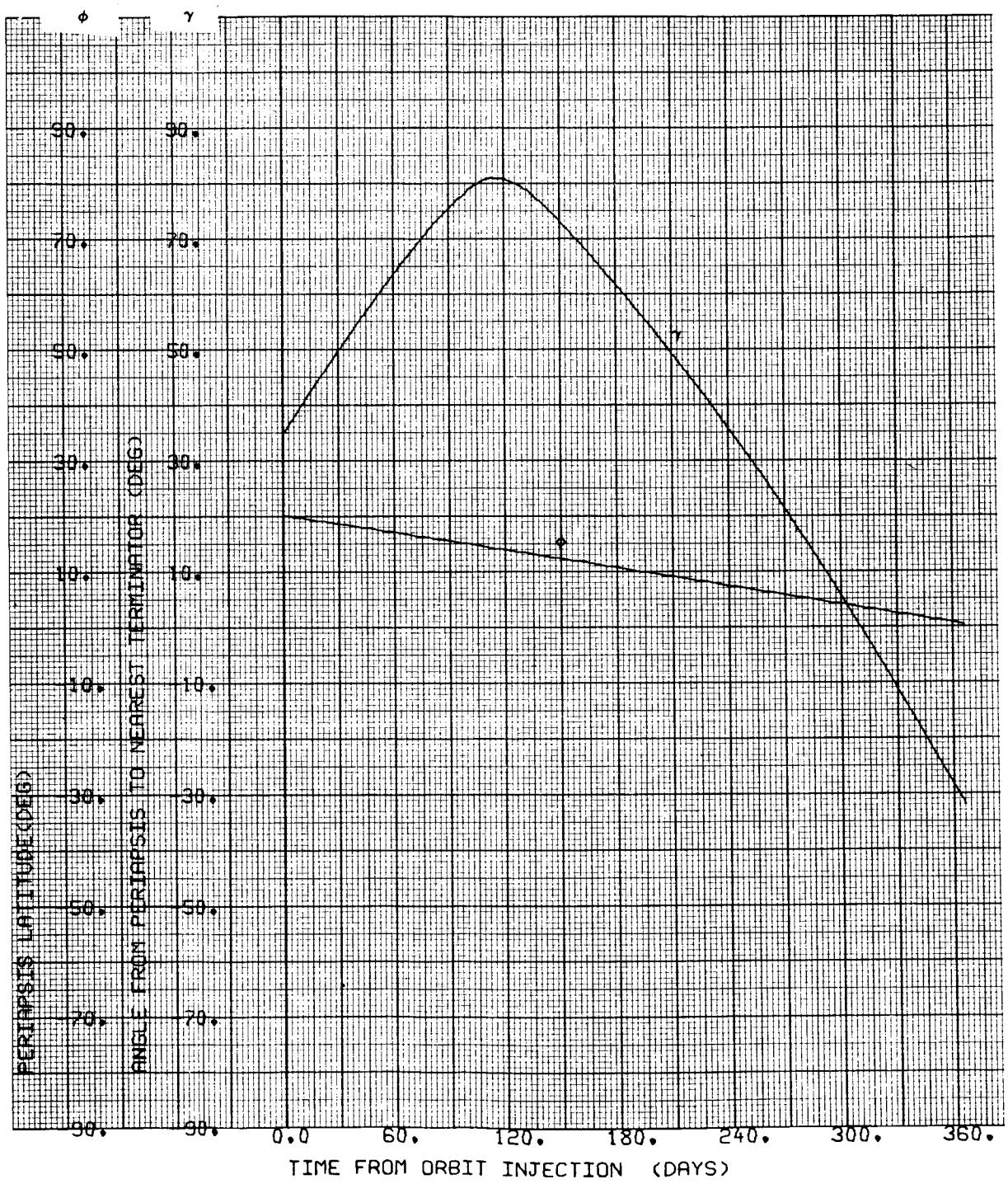
ϕ
γ
90.
70.
50.
30.
10.
10.
30.
50.
70.
90.
PERIAPSIS LATITUDE (DEG)
ANGLE FROM PERIAPSIS TO NEAREST TERMINATOR (DEG)
γ
ϕ
0.0
60.
120.
180.
240.
300.
360.
TIME FROM ORBIT INJECTION (DAYS)

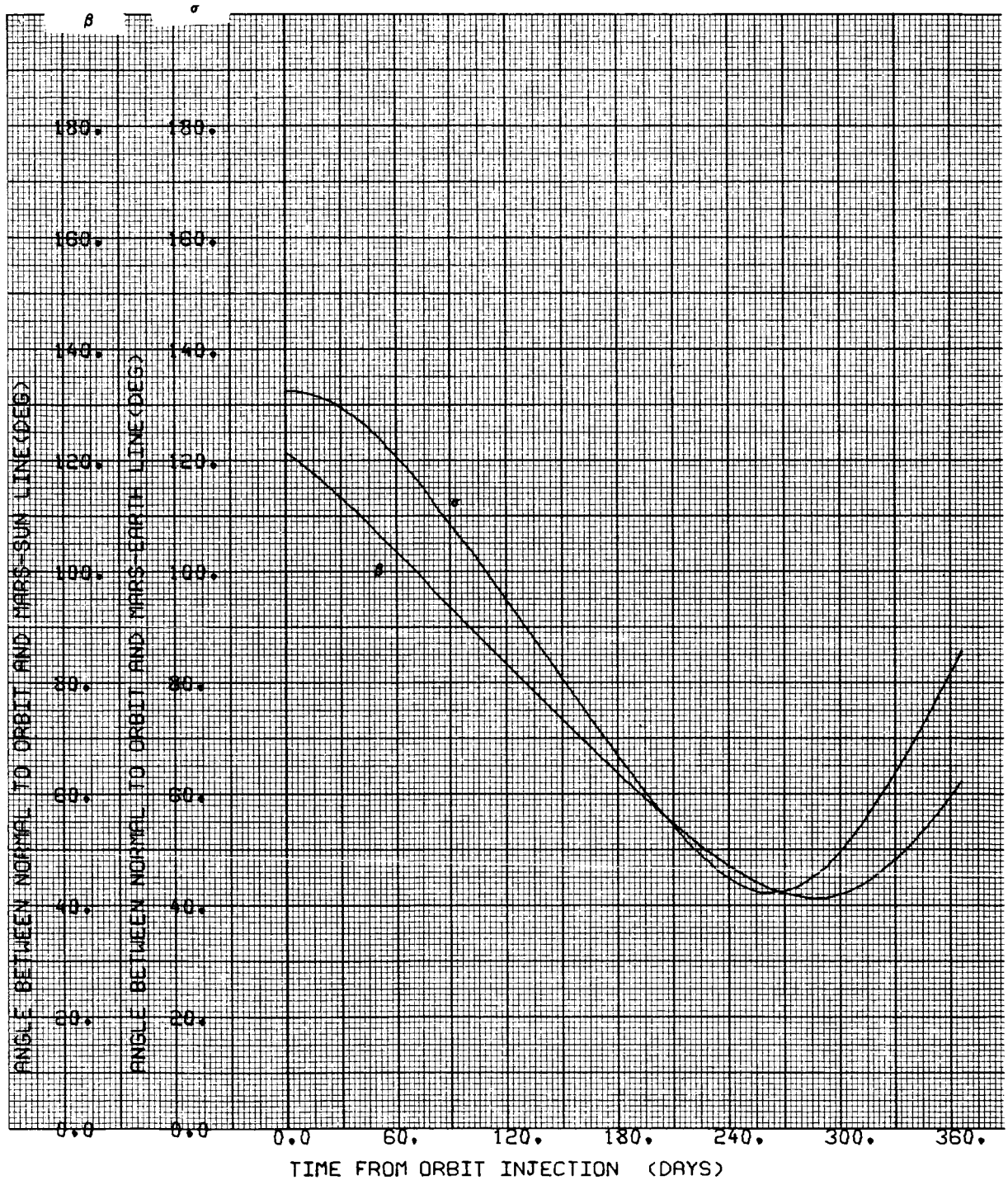
β
σ
180.
160.
140.
120.
100.
80.
60.
40.
20.
0.0
ANGLE BETWEEN NORMAL TO ORBIT AND MARS-SUN LINE(DEG)
ANGLE BETWEEN NORMAL TO ORBIT AND MARS-EARTH LINE(DEG)
0.0
60.
120.
180.
240.
300.
360.
TIME FROM ORBIT INJECTION (DAYS)

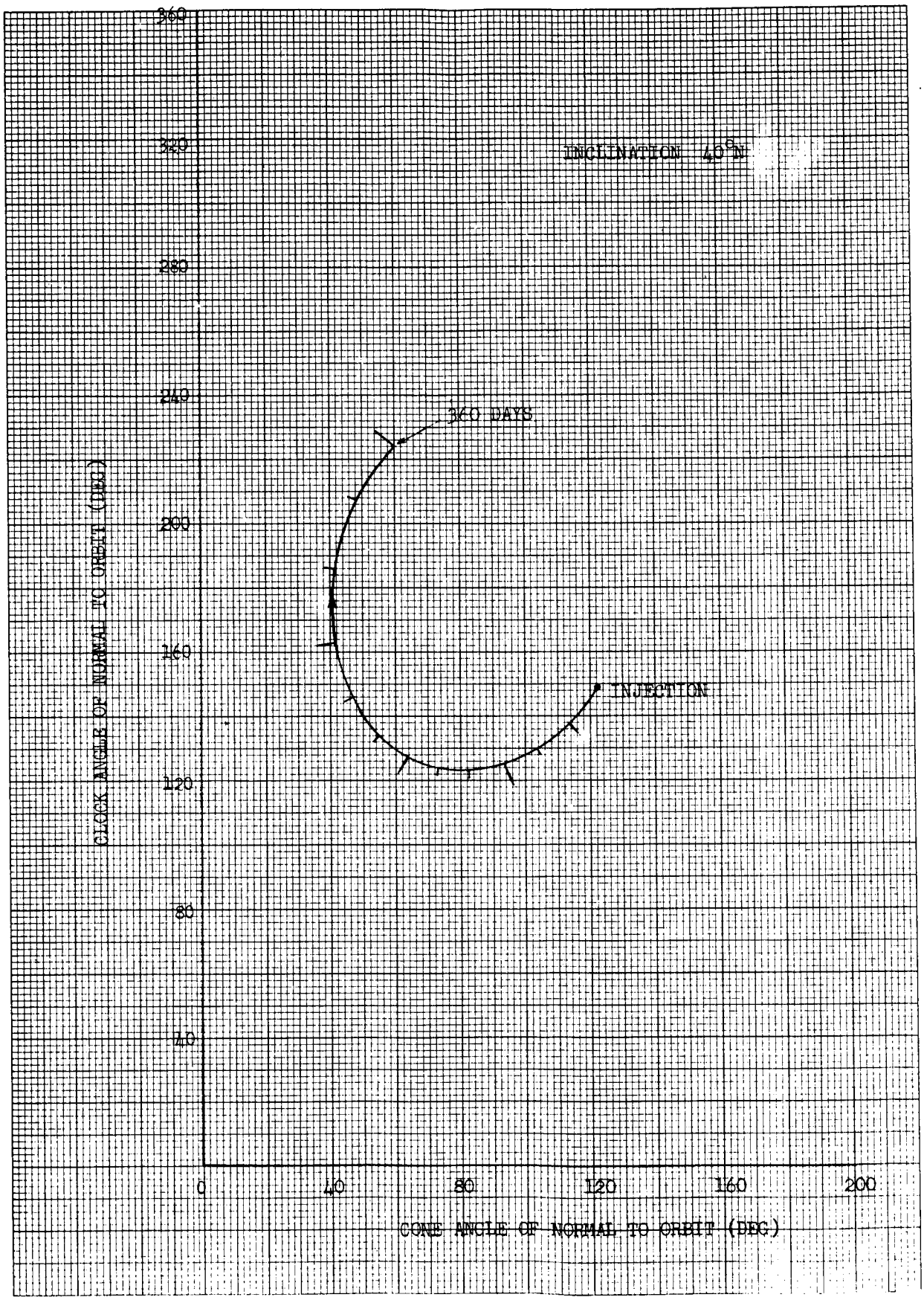
INCLINATION 46° N
360 DAYS
INJECTION
CLOCK ANGLE OF NORMAL TO ORBIT (DEG)
CONE ANGLE OF NORMAL TO ORBIT (DEG)
360
320
280
240
200
160
120
80
40
0
40
80
120
160
200

LAUNCH DATE AUGUST 8, 1973
ARRIVAL DATE MARCH 21, 1974
INCLINATION 40°N
APSIDAL ORIENTATION 126.453°
0 DAYS AFTER INJECTION
LATITUDE (DEG)
LONGITUDE (DEG)
90
60
30
0
-30
-60
-90
-180
-150
-120
-90
-60
-30
0
30
60
90
120
150
180
SUN
EARTH
DAY
NIGHT
NIGHT
CANOPUS
NO SUN, EARTH OR CANOPUS OCCULTATION

LAUNCH DATE AUGUST 8, 1973
ARRIVAL DATE MARCH 21, 1974
INCLINATION 40°N
APSIDAL ORIENTATION 126.453°
90 DAYS AFTER INJECTION
LATITUDE (DEG)
LONGITUDE (DEG)
90
60
30
0
-30
-60
-90
-120
-150
-180
150
120
90
60
30
0
-30
-60
-90
-90
-180
5
10
15
10
10
SUN
EARTH
NIGHT
DAY
NIGHT
SUN OCCULTATION
CANOPUS
NO EARTH OR CANOPUS OCCULTATION

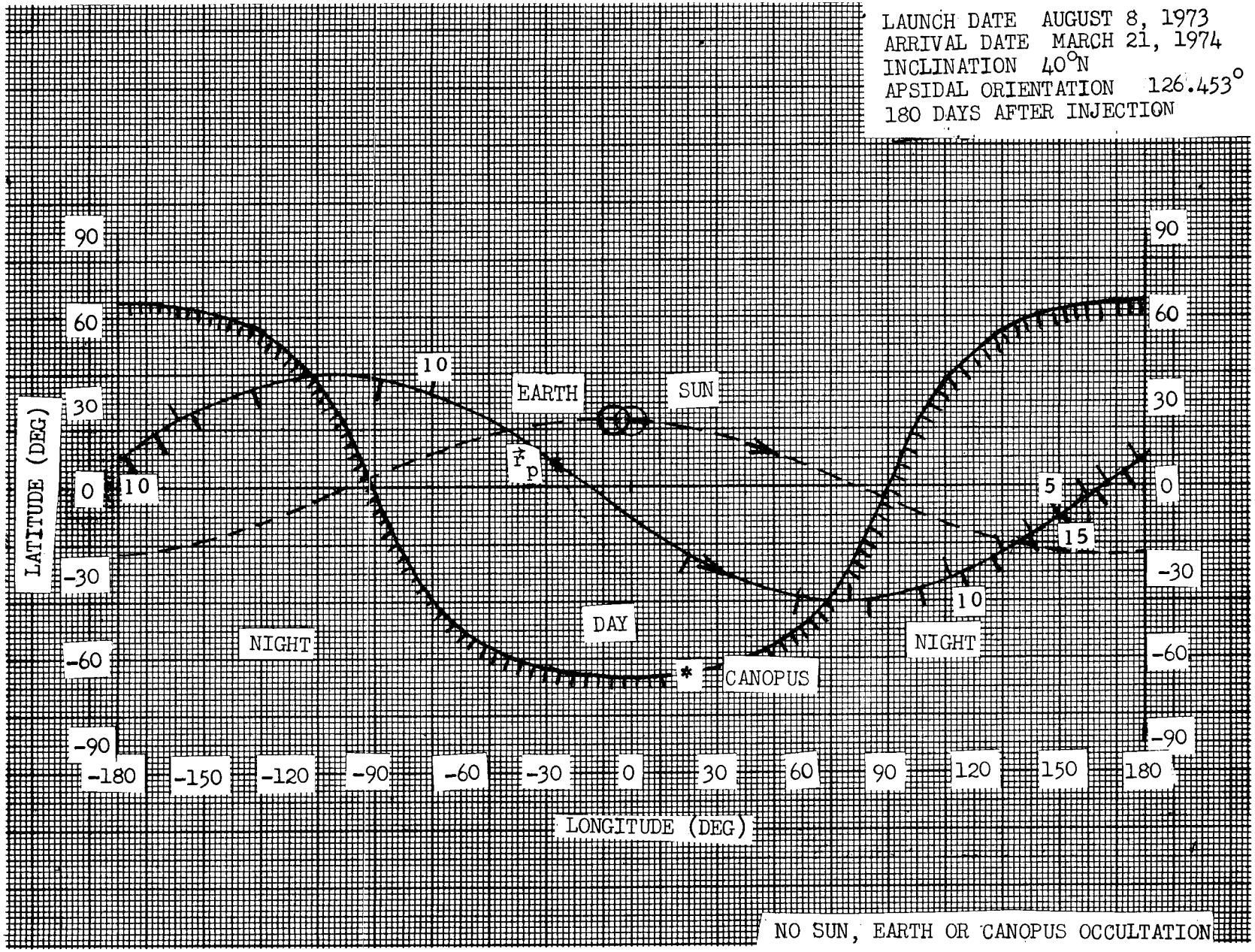
LAUNCH DATE AUGUST 8, 1973
ARRIVAL DATE MARCH 21, 1974
INCLINATION 40°N
APSIDAL ORIENTATION 126.453°
180 DAYS AFTER INJECTION
LATITUDE (DEG)
90
60
30
0
-30
-60
-90
10
10
EARTH
SUN
r_p
DAY
NIGHT
NIGHT
CANOPUS
5
15
10
-180
-150
-120
-90
-60
-30
0
30
60
90
120
150
180
LONGITUDE (DEG)
NO SUN, EARTH OR CANOPUS OCCULTATION

CASE NO. 20

1000 x 15,000 km

$i = 60^{\circ}S$

$\Psi = 126.453$ deg

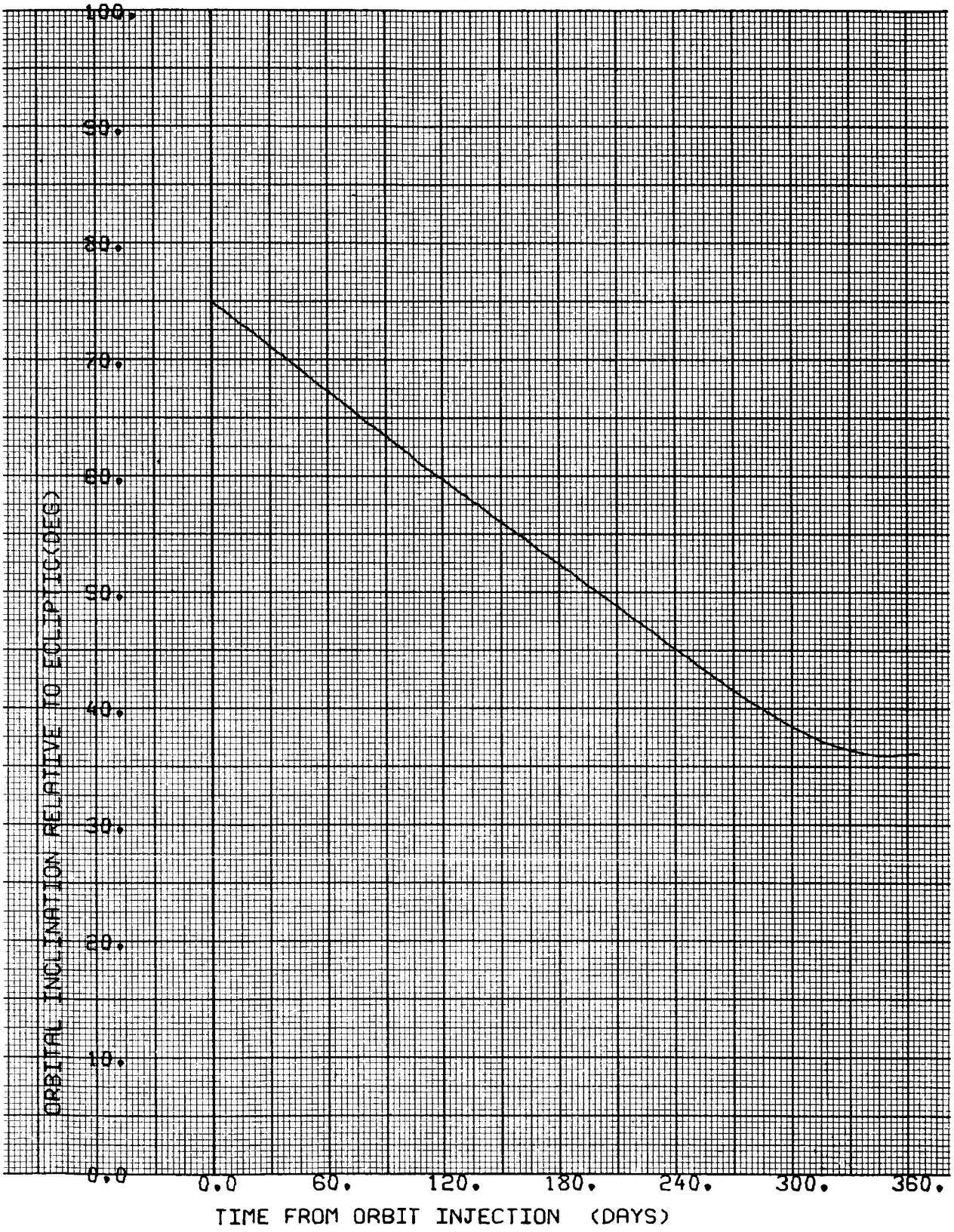
100.
90.
80.
70.
60.
50.
40.
30.
20.
10.
0.0
ORBITAL INCLINATION RELATIVE TO ECLIPTIC(DEG)
0.0
60.
120.
180.
240.
300.
360.
TIME FROM ORBIT INJECTION (DAYS)

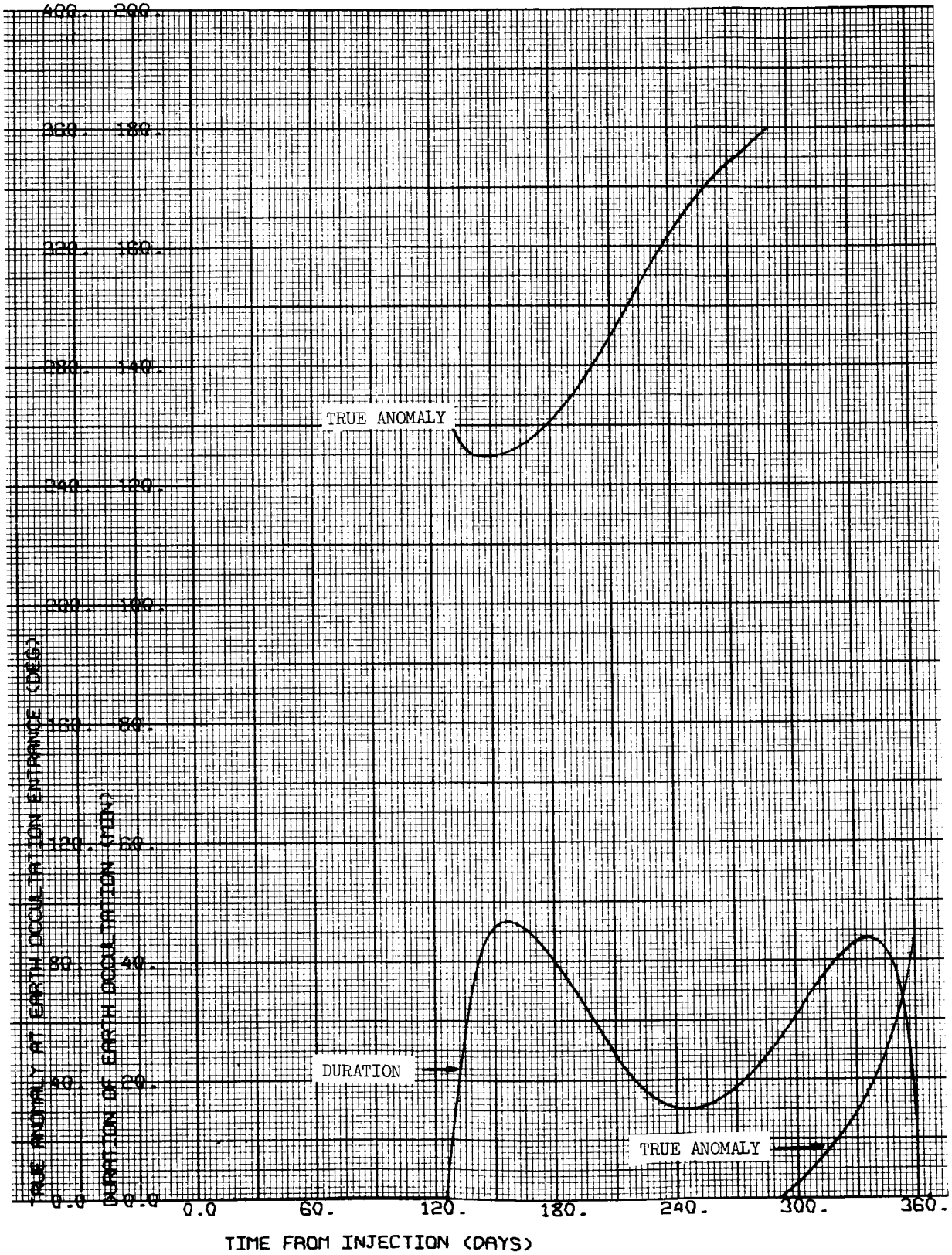
TRUE ANOMALY AT EARTH OCCULTATION ENTRANCE (DEG)
DURATION OF EARTH OCCULTATION (MIN)
TIME FROM INJECTION (DAYS)
TRUE ANOMALY
DURATION
TRUE ANOMALY
0.0
60.
120.
180.
240.
300.
360.

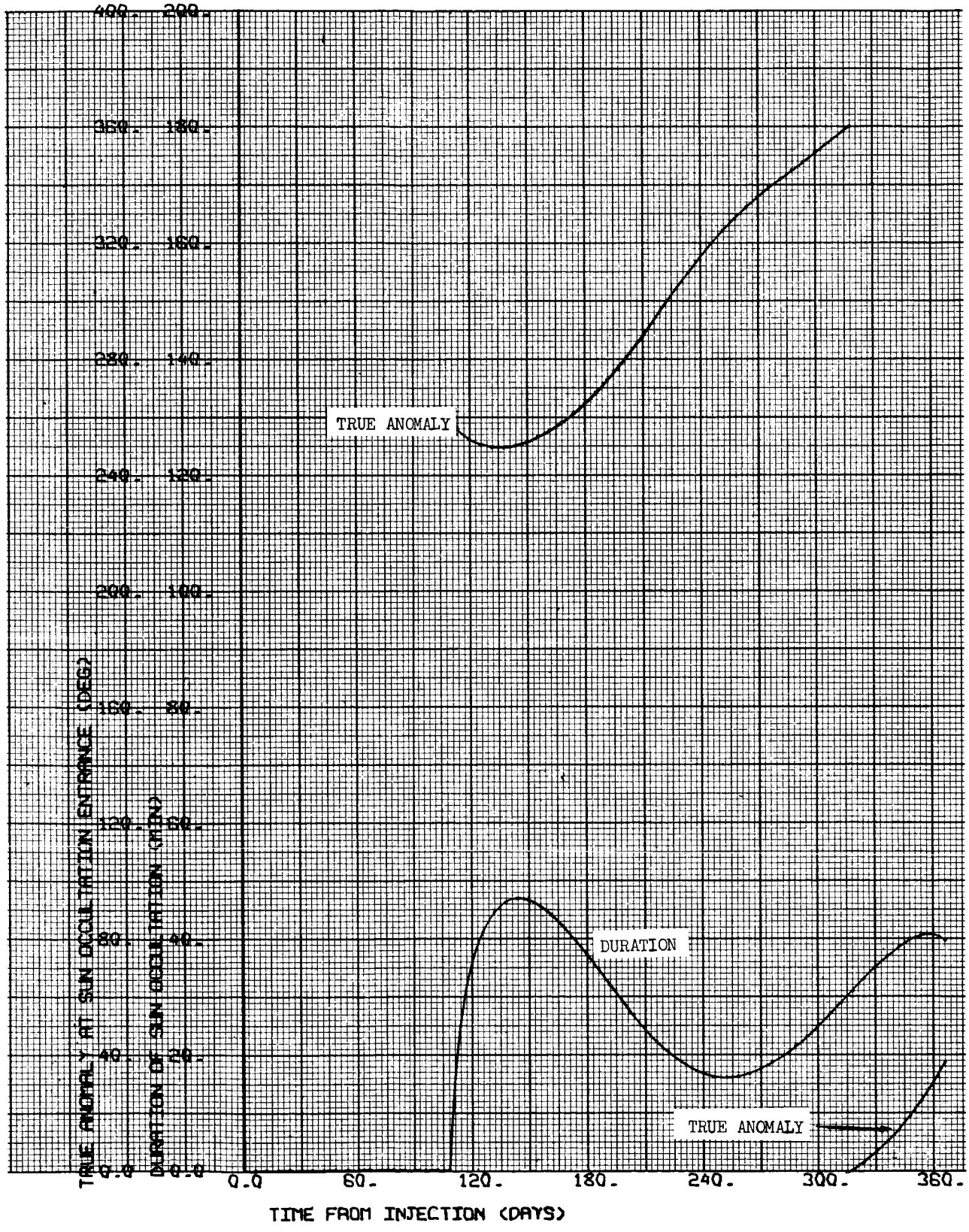
TRUE ANOMALY AT SUN OCCULTATION ENTRANCE (DEG)
DURATION OF SUN OCCULTATION (MIN)
TIME FROM INJECTION (DAYS)
TRUE ANOMALY
DURATION
TRUE ANOMALY
0.0
60.
120.
180.
240.
300.
360.
400.
360.
320.
280.
240.
200.
160.
120.
80.
40.
200.
180.
160.
140.
120.
100.
80.
60.
40.
20.
0.0

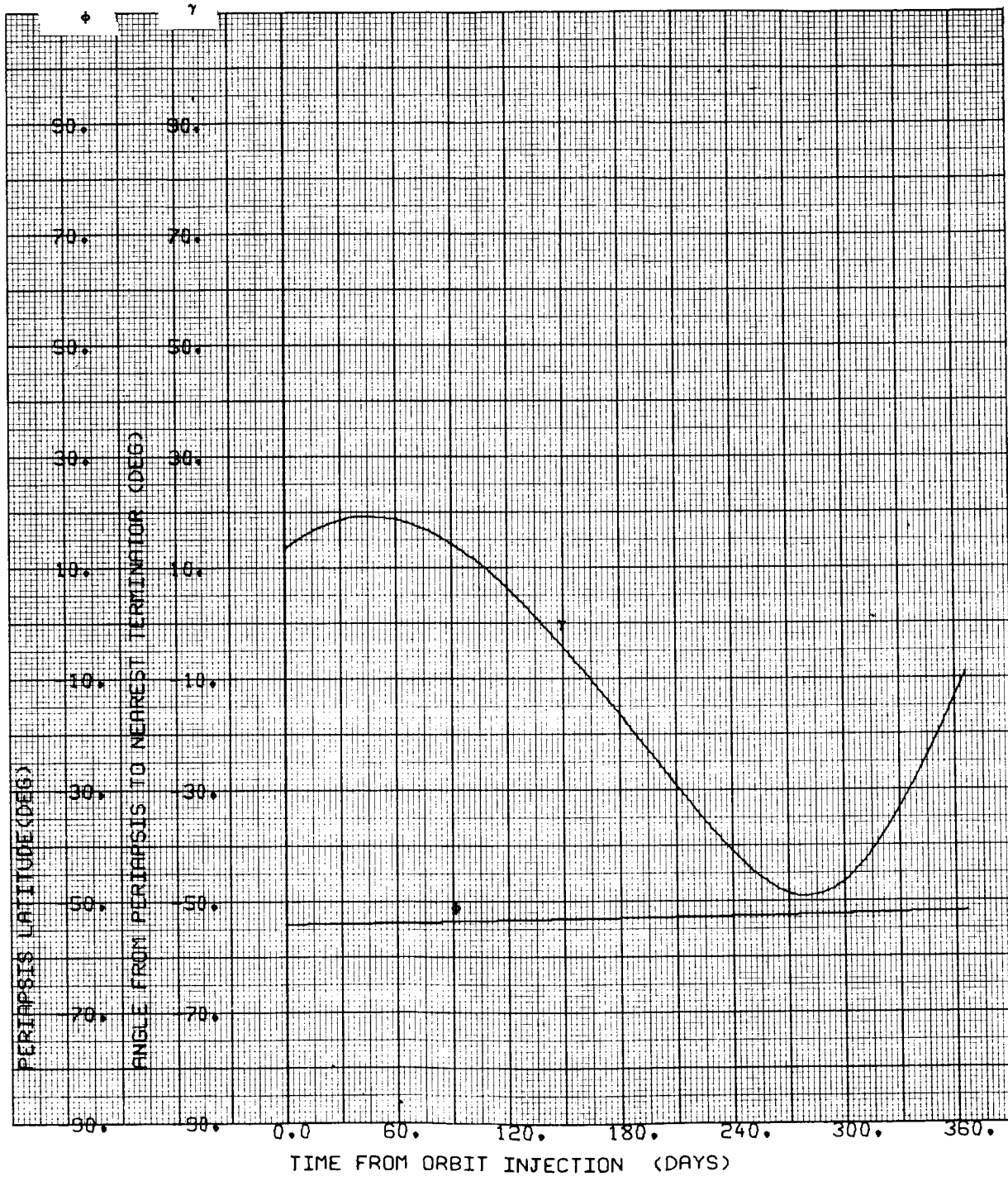
φ
γ
90.
70.
50.
30.
10.
-10.
-30.
-50.
-70.
-90.
PERIAPSIS LATITUDE(DEG)
ANGLE FROM PERIAPSIS TO NEAREST TERMINATOR (DEG)
0.0
60.
120.
180.
240.
300.
360.
TIME FROM ORBIT INJECTION (DAYS)

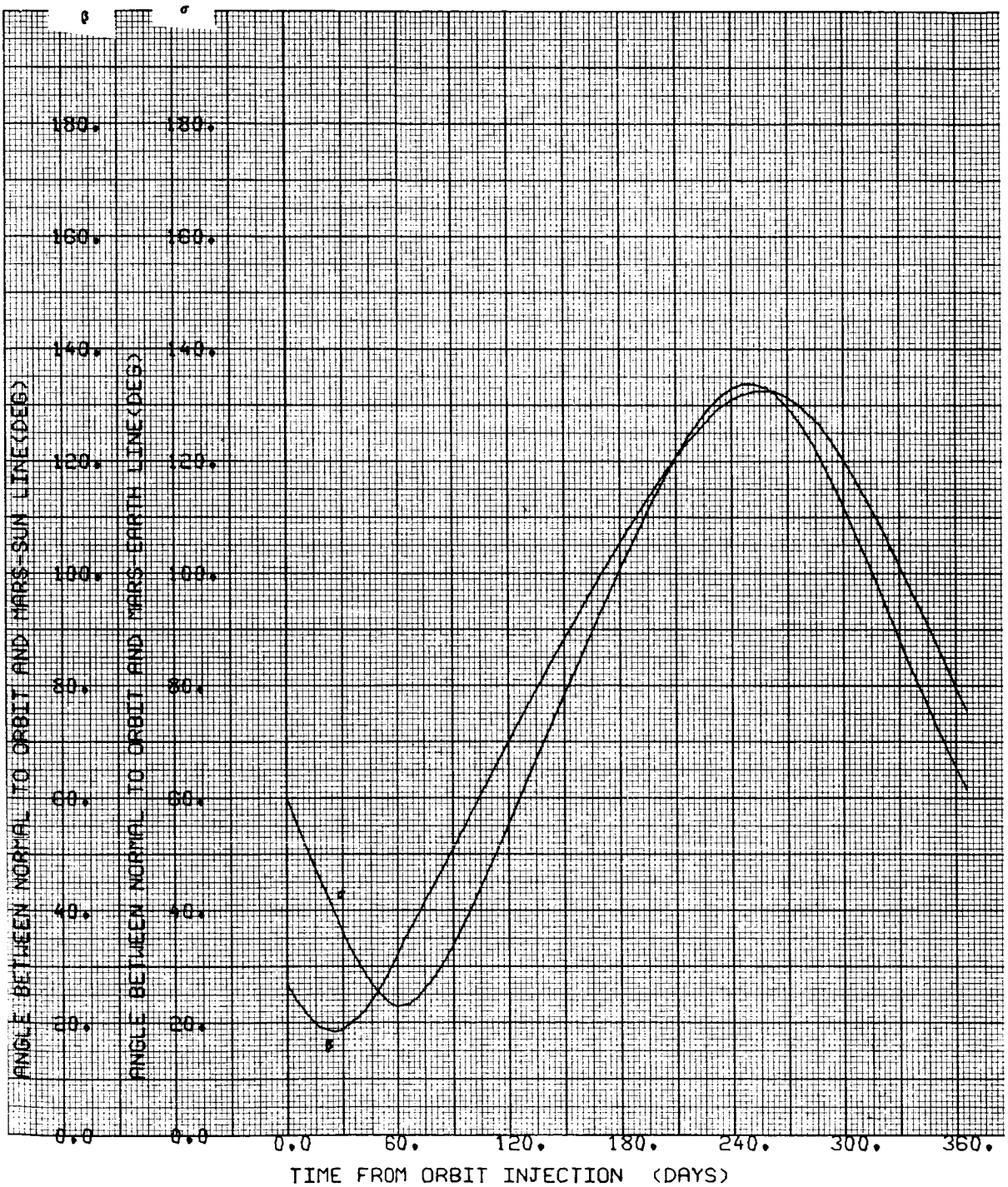
β
σ
180.
160.
140.
120.
100.
80.
60.
40.
20.
0.0
ANGLE BETWEEN NORMAL TO ORBIT AND MARS-SUN LINE(DEG)
ANGLE BETWEEN NORMAL TO ORBIT AND MARS-EARTH LINE(DEG)
0.0
60.
120.
180.
240.
300.
360.
TIME FROM ORBIT INJECTION (DAYS)

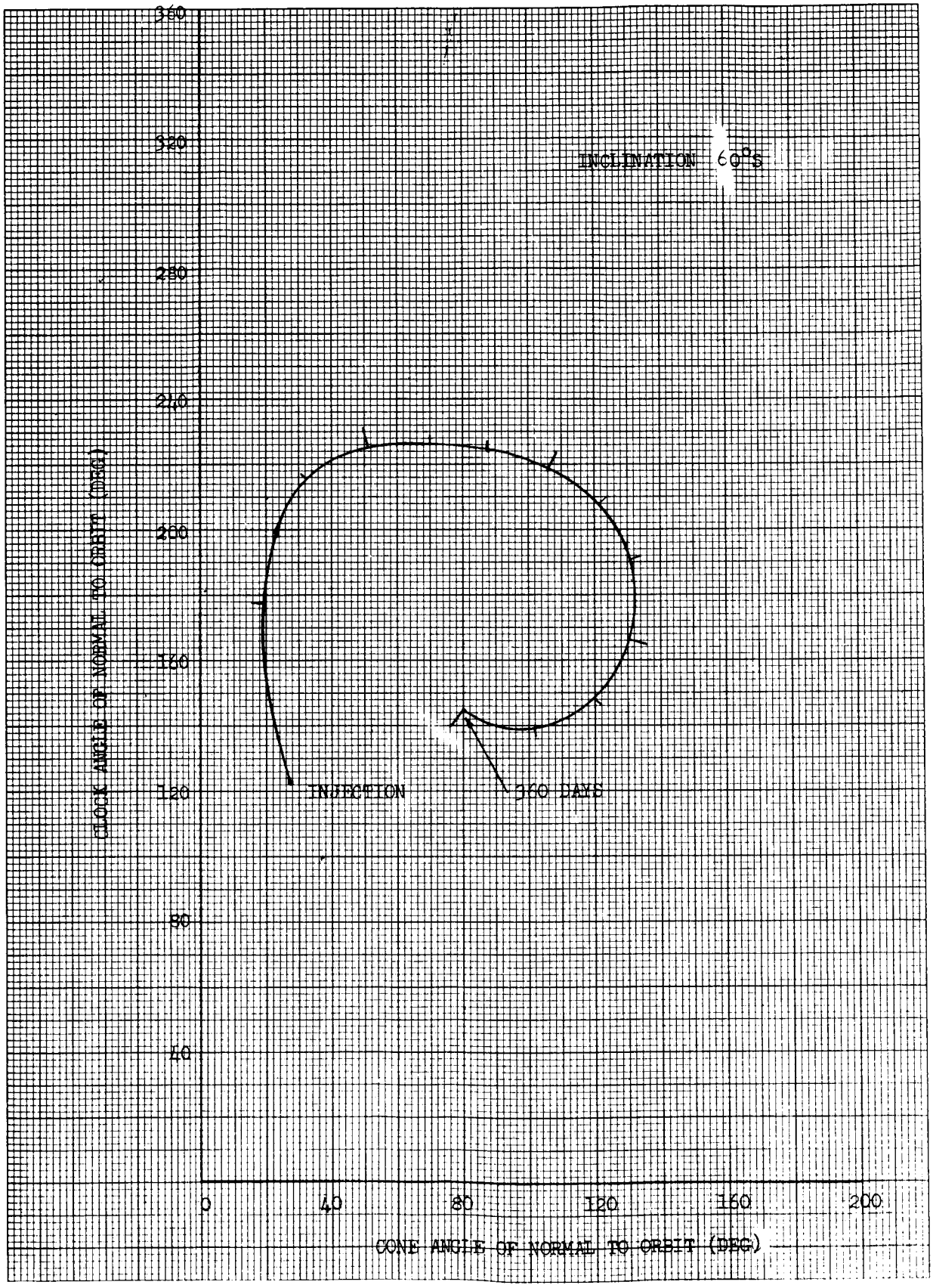
INCLINATION 60°S
CLOCK ANGLE OF NORMAL TO ORBIT (DEG)
CONE ANGLE OF NORMAL TO ORBIT (DEG)
INJECTION
360 DAYS
0
40
80
120
160
200
240
280
320
360

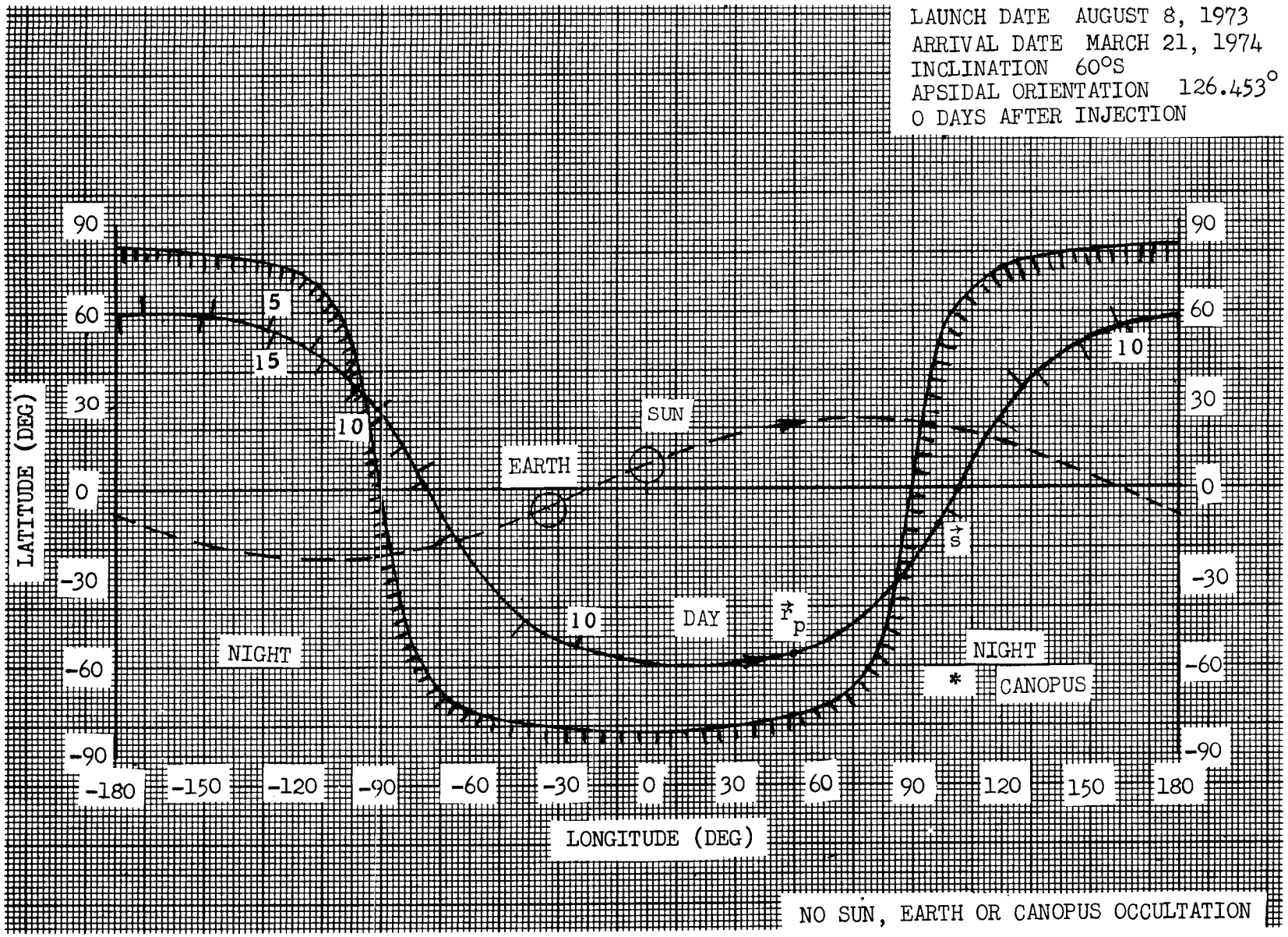
LAUNCH DATE AUGUST 8, 1973
ARRIVAL DATE MARCH 21, 1974
INCLINATION 60°S
APSIDAL ORIENTATION 126.453°
0 DAYS AFTER INJECTION
LATITUDE (DEG)
90
60
30
0
-30
-60
-90
5
15
10
10
10
SUN
EARTH
DAY
NIGHT
NIGHT
CANOPUS
$\vec{r}_p$
$\vec{r}_s$
-180
-150
-120
-90
-60
-30
0
30
60
90
120
150
180
LONGITUDE (DEG)
NO SUN, EARTH OR CANOPUS OCCULTATION

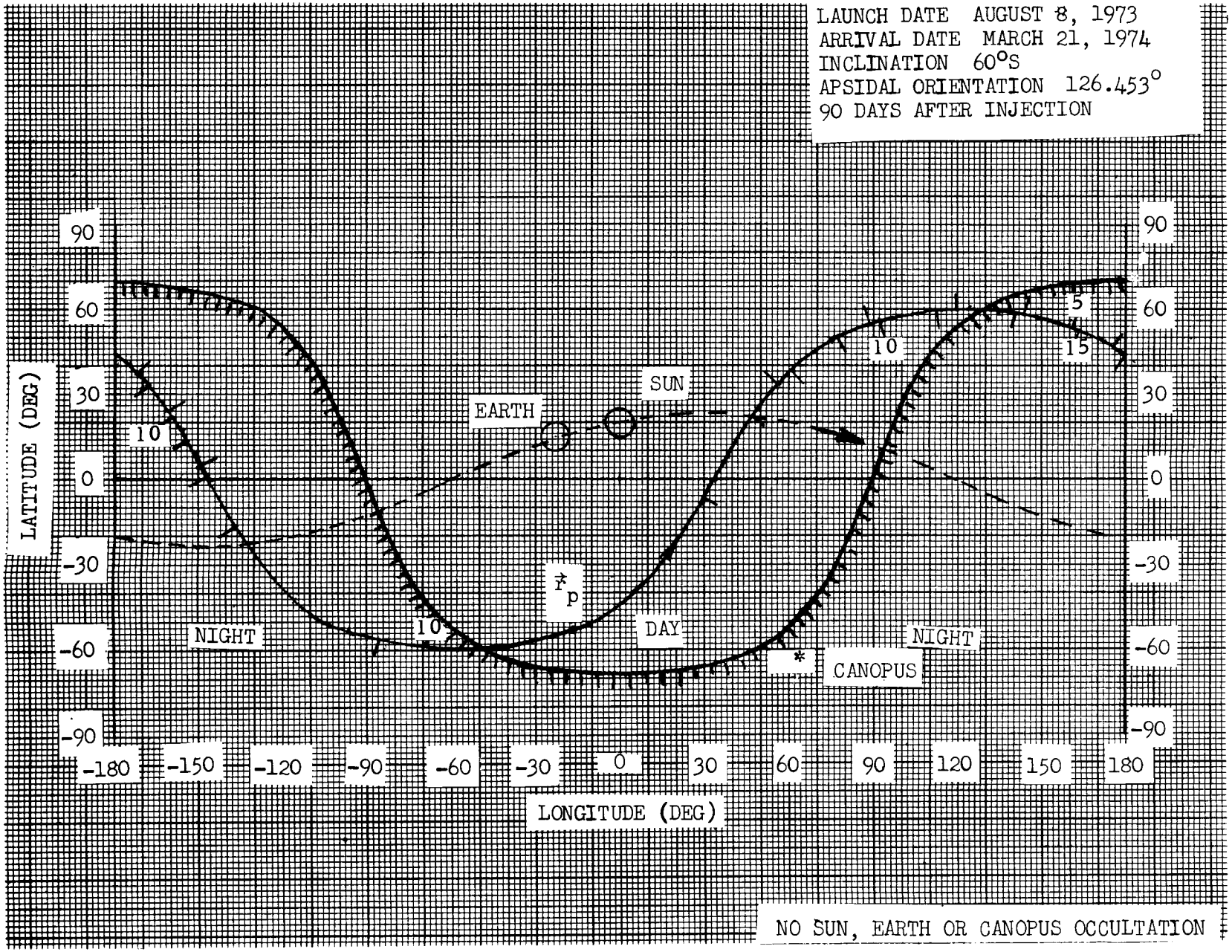
LAUNCH DATE AUGUST 8, 1973
ARRIVAL DATE MARCH 21, 1974
INCLINATION 60°S
APSIDAL ORIENTATION 126.453°
90 DAYS AFTER INJECTION
LATITUDE (DEG)
90
60
30
0
-30
-60
-90
LONGITUDE (DEG)
-180
-150
-120
-90
-60
-30
0
30
60
90
120
150
180
SUN
EARTH
NIGHT
DAY
NIGHT
CANOPUS
10
10
10
5
10
15
NO SUN, EARTH OR CANOPUS OCCULTATION

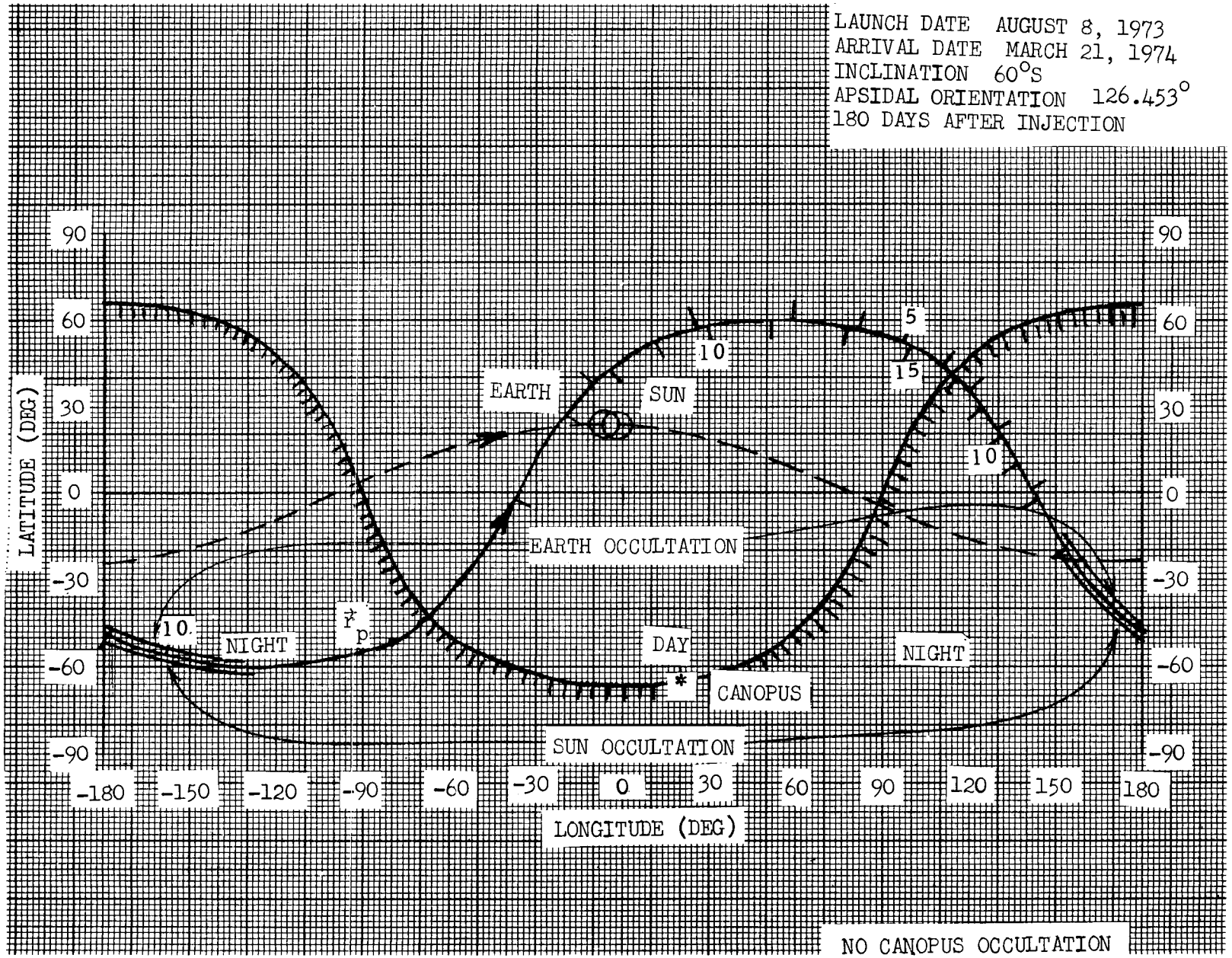
LAUNCH DATE AUGUST 8, 1973
ARRIVAL DATE MARCH 21, 1974
INCLINATION 60°S
APSIDAL ORIENTATION 126.453°
180 DAYS AFTER INJECTION
LATITUDE (DEG)
90
60
30
0
-30
-60
-90
EARTH
SUN
EARTH OCCULTATION
NIGHT
DAY
NIGHT
CANOPUS
SUN OCCULTATION
NO CANOPUS OCCULTATION
-180
-150
-120
-90
-60
-30
0
30
60
90
120
150
180
LONGITUDE (DEG)
10
5
15
10
10

CASE NO. 21

1000 x 15,000 km

$i = 60^{\circ}N$

$\Psi = 126.453$ deg

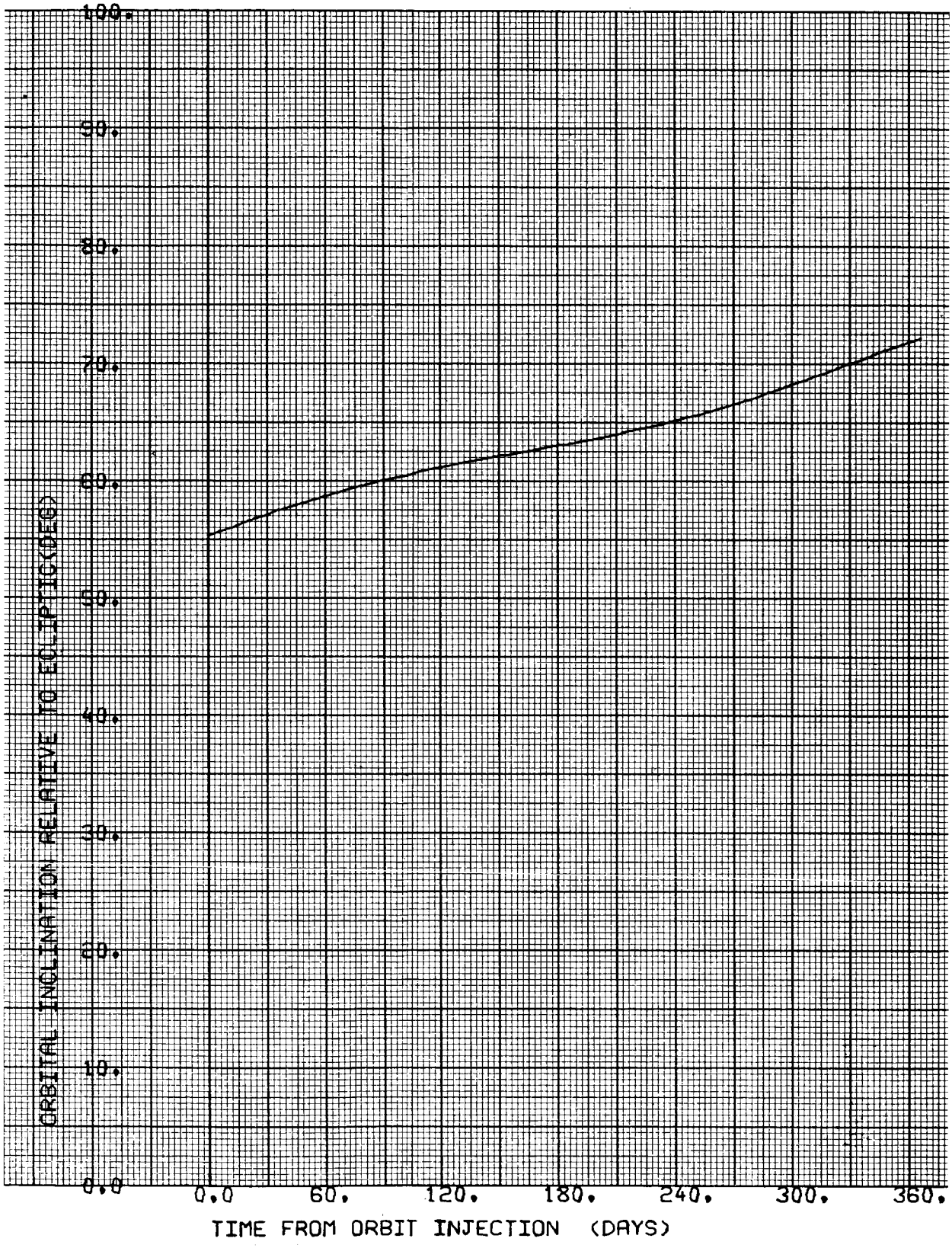
100.
90.
80.
70.
60.
50.
40.
30.
20.
10.
0.0
ORBITAL INCLINATION RELATIVE TO ECLIPTIC(DEG)
0.0
60.
120.
180.
240.
300.
360.
TIME FROM ORBIT INJECTION (DAYS)

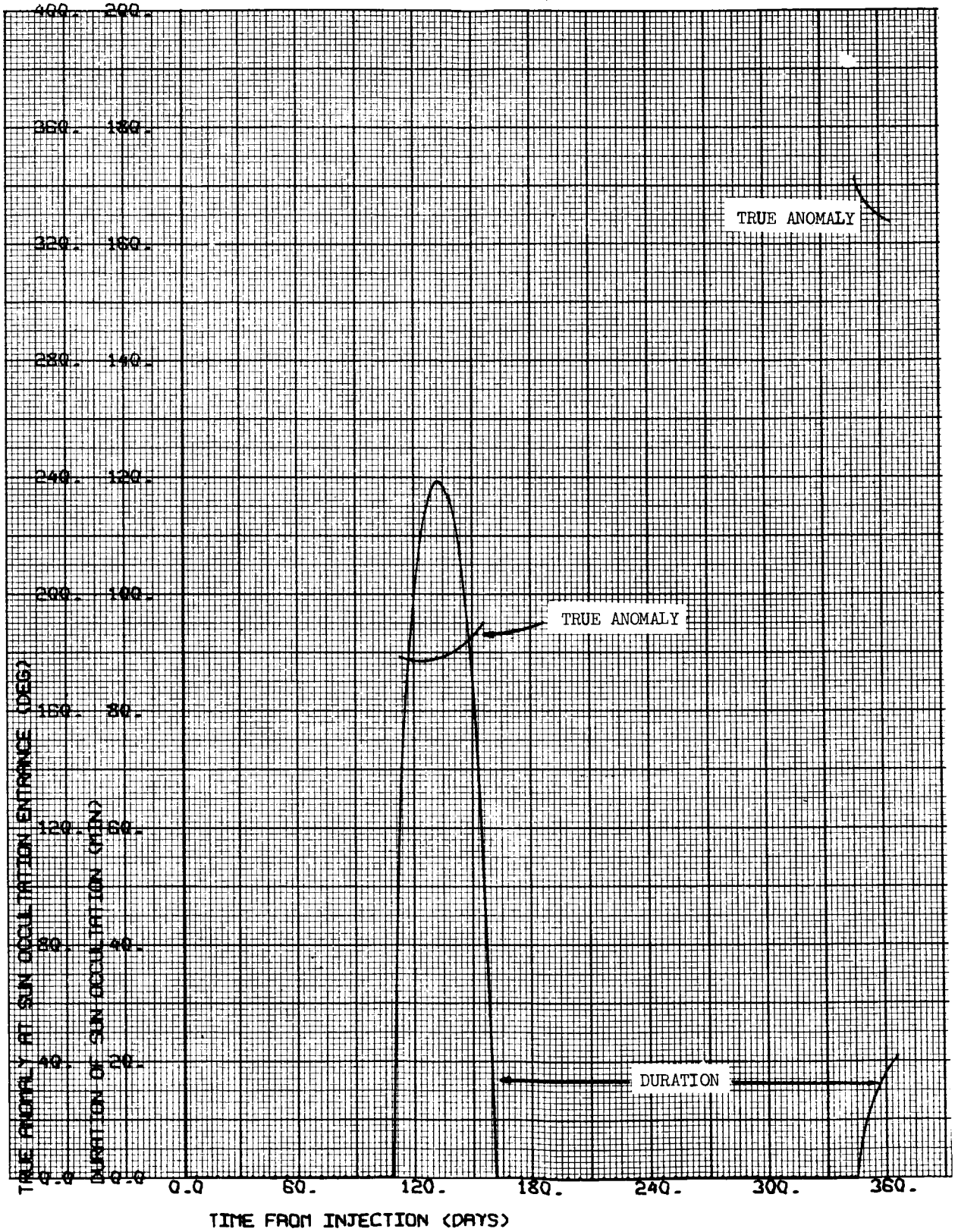
TRUE ANOMALY
TRUE ANOMALY
DURATION
TRUE ANOMALY AT SUN OCCULTATION ENTRANCE (DEG)
DURATION OF SUN OCCULTATION (MIN)
TIME FROM INJECTION (DAYS)
0.0
60.
120.
180.
240.
300.
360.
400.
360.
320.
280.
240.
200.
160.
120.
80.
40.
200.
180.
160.
140.
120.
100.
80.
60.
40.
20.
0.0

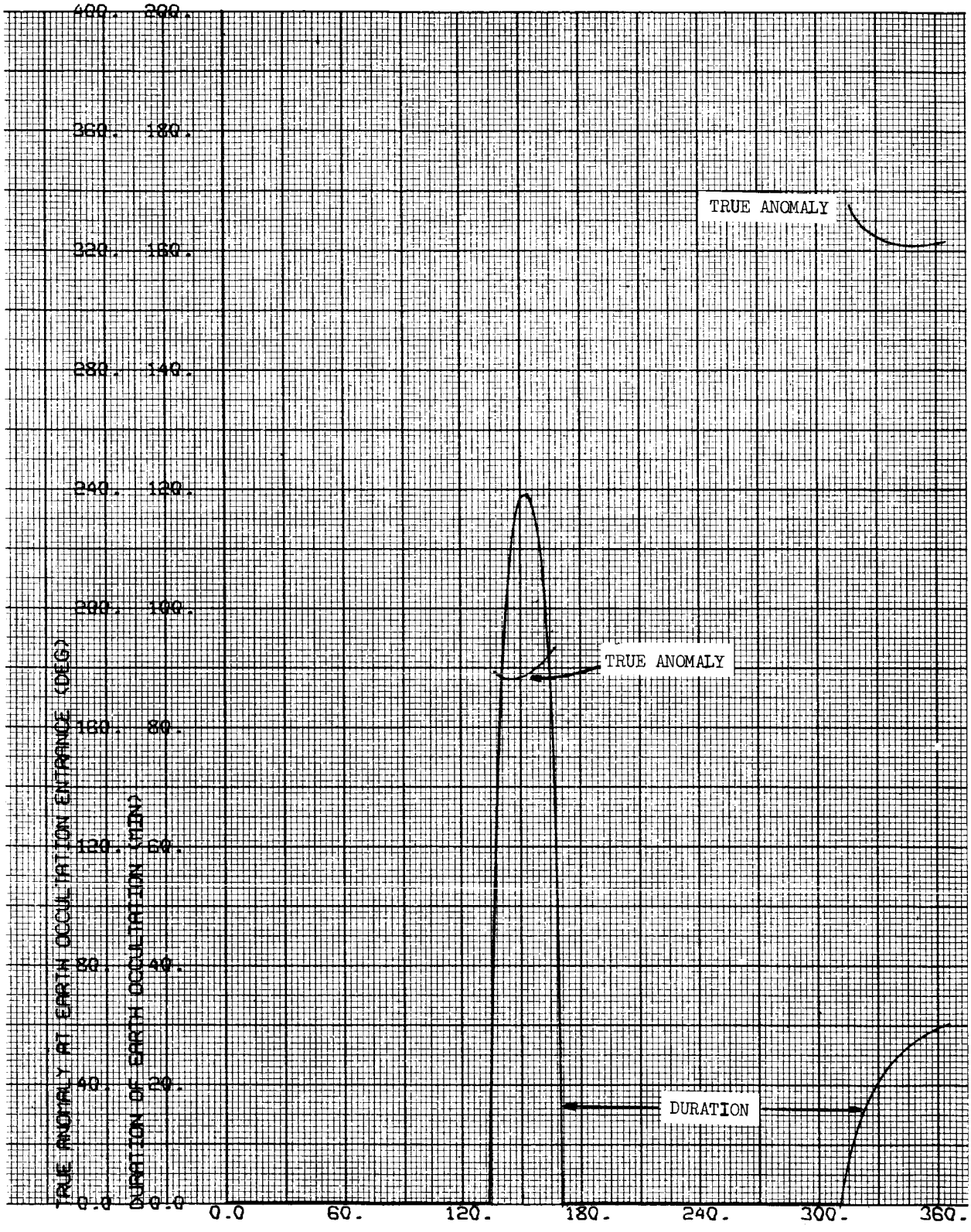
TRUE ANOMALY
TRUE ANOMALY
DURATION
TRUE ANOMALY AT EARTH OCCULTATION ENTRANCE (DEG)
DURATION OF EARTH OCCULTATION (MIN)
TIME FROM INJECTION (DAYS)
0.0
60.
120.
180.
240.
300.
360.
400.
360.
320.
280.
240.
200.
160.
120.
80.
40.
0.0
200.
180.
160.
140.
120.
100.
80.
60.
40.
20.
0.0

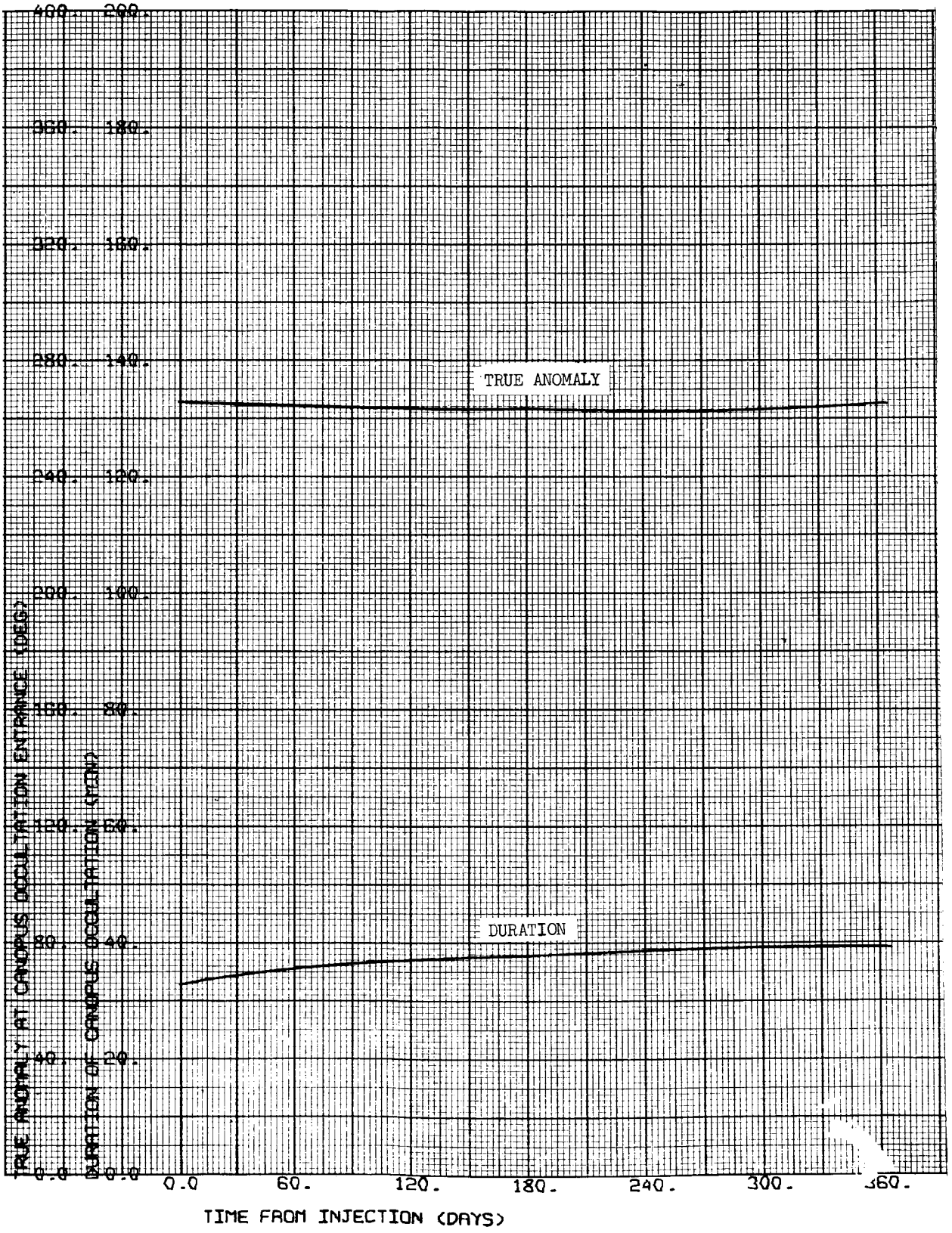
TRUE ANOMALY
DURATION
TRUE ANOMALY AT CANOPUS OCCULTATION ENTRANCE (DEG)
DURATION OF CANOPUS OCCULTATION (MIN)
TIME FROM INJECTION (DAYS)
400.
360.
320.
280.
240.
200.
160.
120.
80.
40.
0.0
200.
180.
160.
140.
120.
100.
80.
60.
40.
20.
0.0
0.0
60.
120.
180.
240.
300.
360.

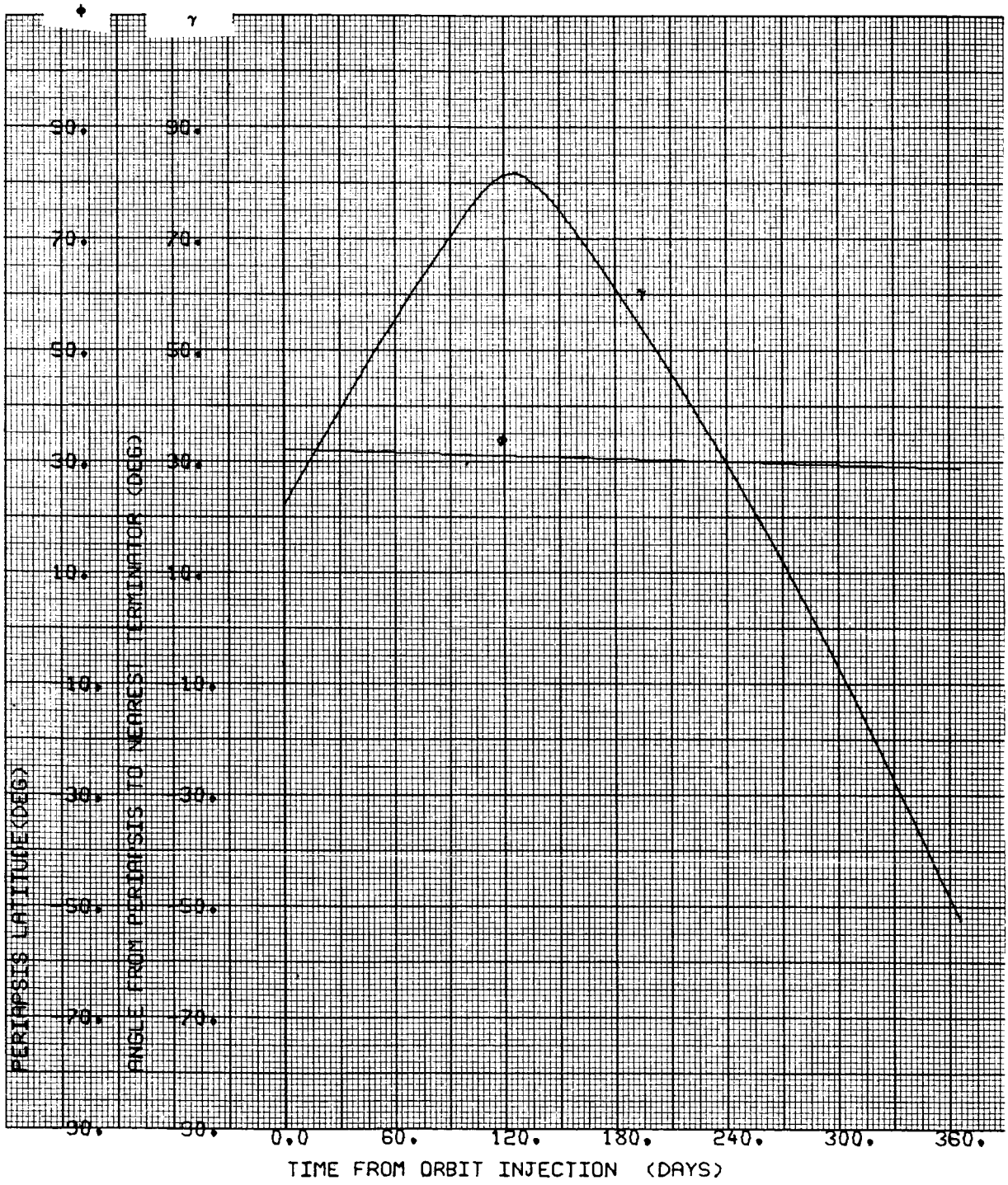
PERIAPSIS LATITUDE (DEG)
ANGLE FROM PERIAPSIS TO NEAREST TERMINATOR (DEG)
90.
70.
50.
30.
10.
-10.
-30.
-50.
-70.
-90.
0.0
60.
120.
180.
240.
300.
360.
TIME FROM ORBIT INJECTION (DAYS)

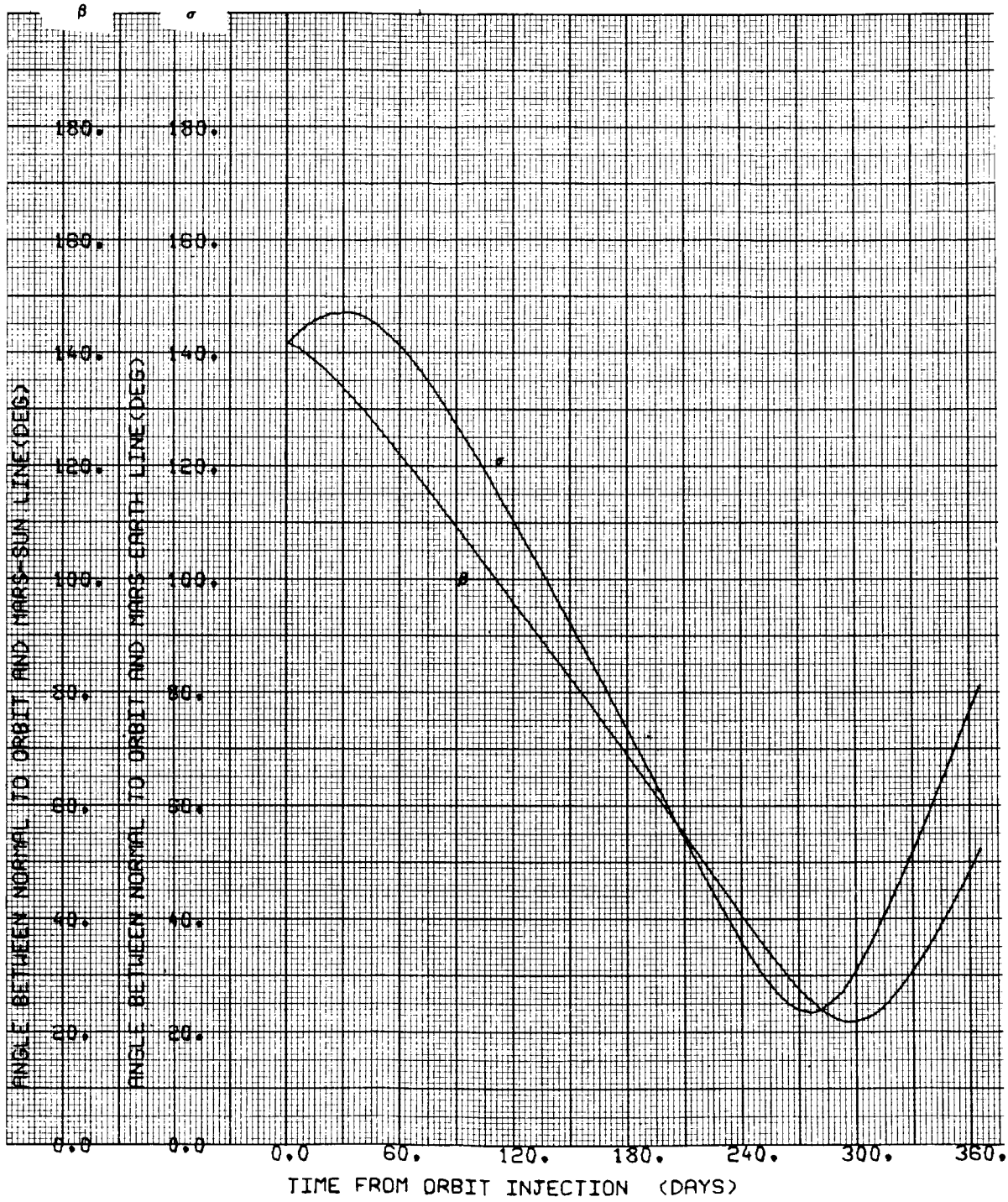
β
σ
180.
160.
140.
120.
100.
80.
60.
40.
20.
0.0
ANGLE BETWEEN NORMAL TO ORBIT AND MARS-SUN LINE(DEG)
ANGLE BETWEEN NORMAL TO ORBIT AND MARS-EARTH LINE(DEG)
0.0
60.
120.
180.
240.
300.
360.
TIME FROM ORBIT INJECTION (DAYS)

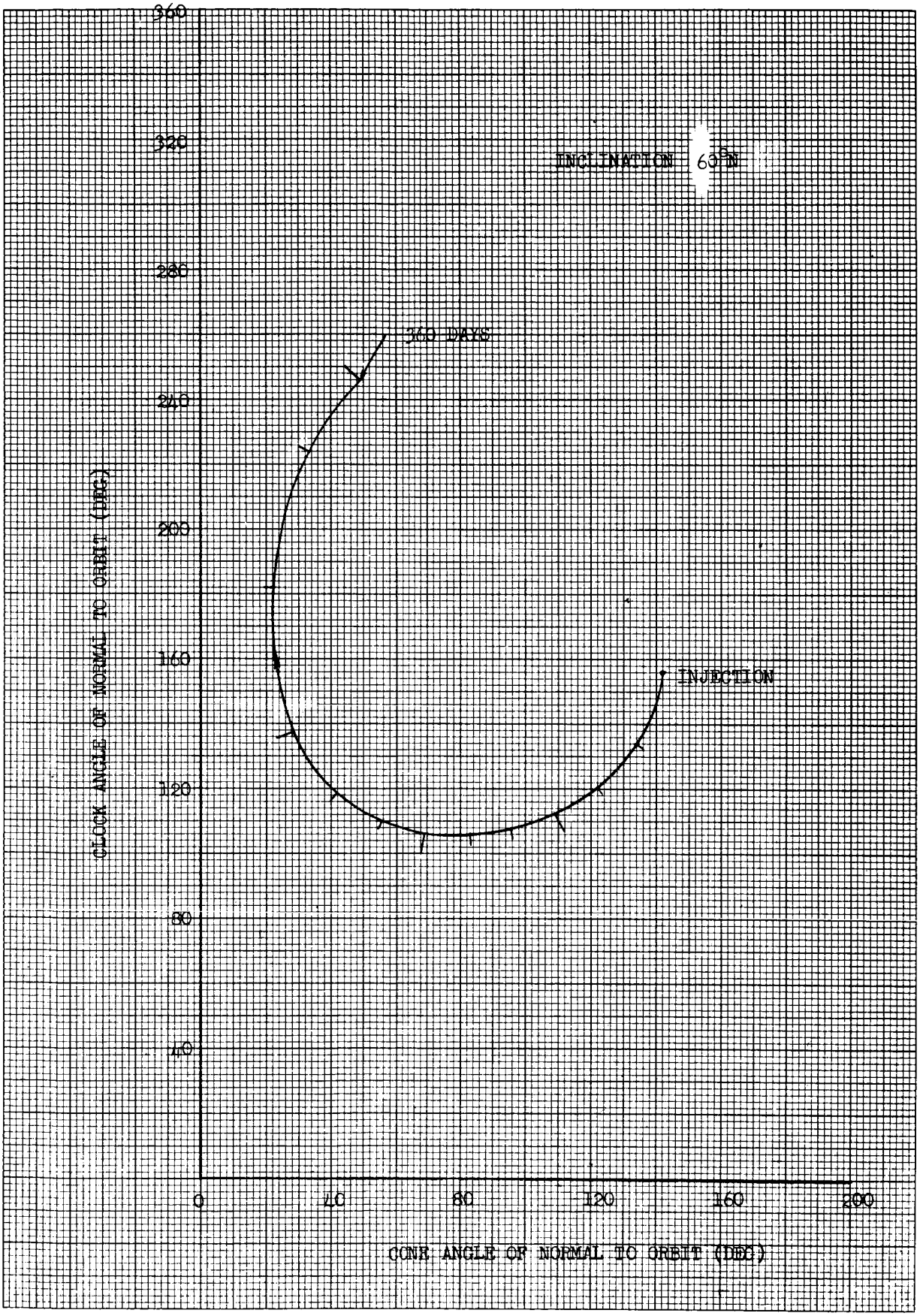
INCLINATION 63°N
360 DAYS
INJECTION
CLOCK ANGLE OF NORMAL TO ORBIT (DEG)
CONE ANGLE OF NORMAL TO ORBIT (DEG)
360
320
280
240
200
160
120
80
40
0
40
80
120
160
200

LAUNCH DATE AUGUST 8, 1973
ARRIVAL DATE MARCH 21, 1974
INCLINATION 60°N
APSIDAL ORIENTATION 126.453°
0 DAYS AFTER INJECTION
CANOPUS OCCULTATION
SUN
EARTH
DAY
CANOPUS NIGHT
NIGHT
NO SUN OR EARTH OCCULTATION
LONGITUDE (DEG)
LATITUDE (DEG)
90
60
30
0
-30
-60
-90
180
150
120
90
60
30
0
-30
-60
-90
-120
-150
-180
10
5
15

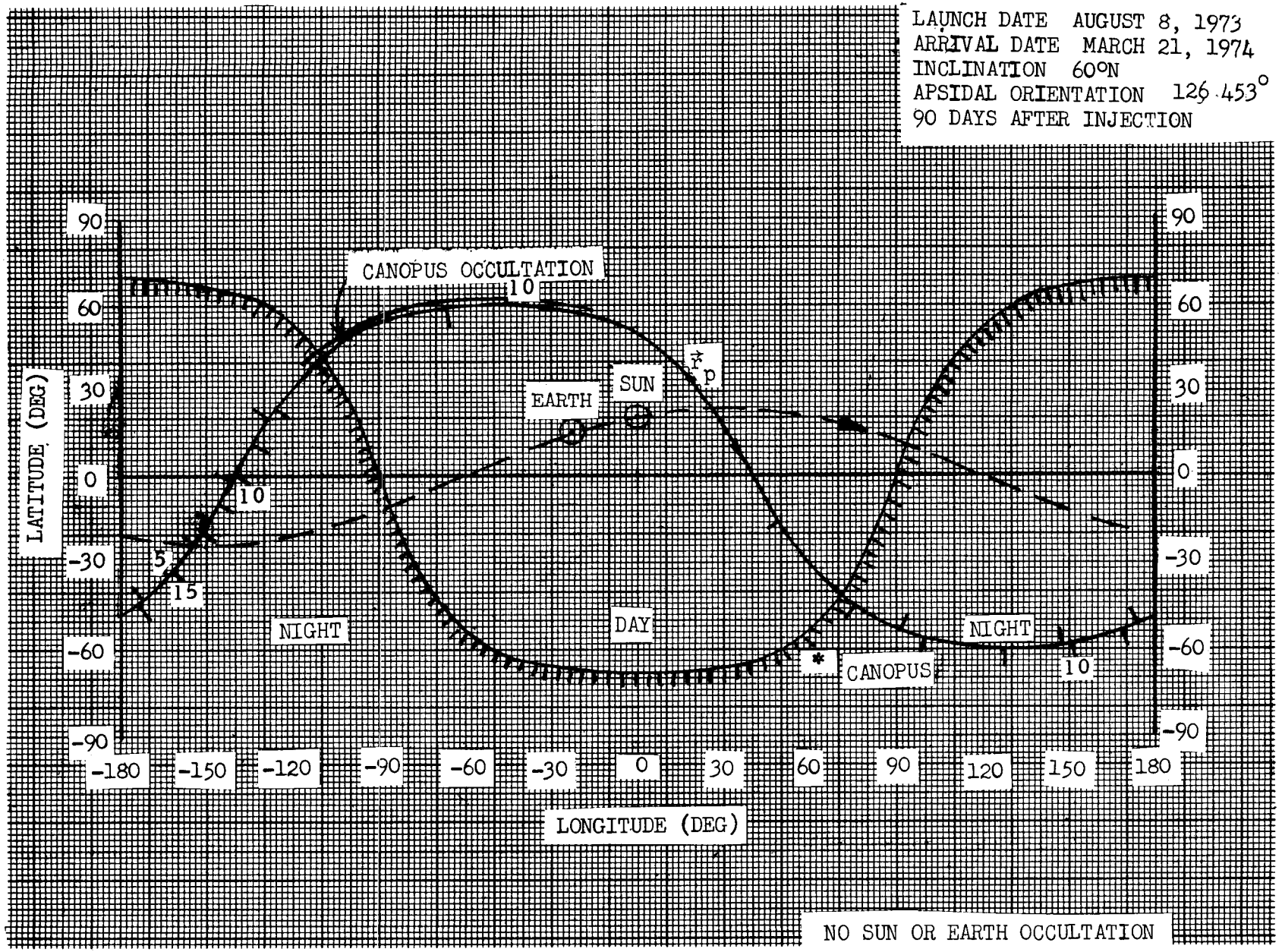
LAUNCH DATE AUGUST 8, 1973
ARRIVAL DATE MARCH 21, 1974
INCLINATION 60°N
APSIDAL ORIENTATION 126.453°
90 DAYS AFTER INJECTION
CANOPUS OCCULTATION
EARTH
SUN
NIGHT
DAY
NIGHT
CANOPUS
LATITUDE (DEG)
LONGITUDE (DEG)
90
60
30
0
-30
-60
-90
-180
-150
-120
-90
-60
-30
0
30
60
90
120
150
180
10
5
15
10
10
NO SUN OR EARTH OCCULTATION

LAUNCH DATE AUGUST 8, 1973
ARRIVAL DATE MARCH 21, 1974
INCLINATION 60°N
APSIDAL ORIENTATION 126.453°
180 DAYS AFTER INJECTION
LATITUDE (DEG)
LONGITUDE (DEG)
90
60
30
0
-30
-60
-90
-120
-150
-180
120
150
180
CANOPUS OCCULTATION
EARTH
SUN
DAY
NIGHT
CANOPUS
NO SUN OR EARTH OCCULTATION
10
15

CASE NO. 22

1000 x 15, 000 km

$i = 40^{\circ}S$

$\Psi = 60$ deg

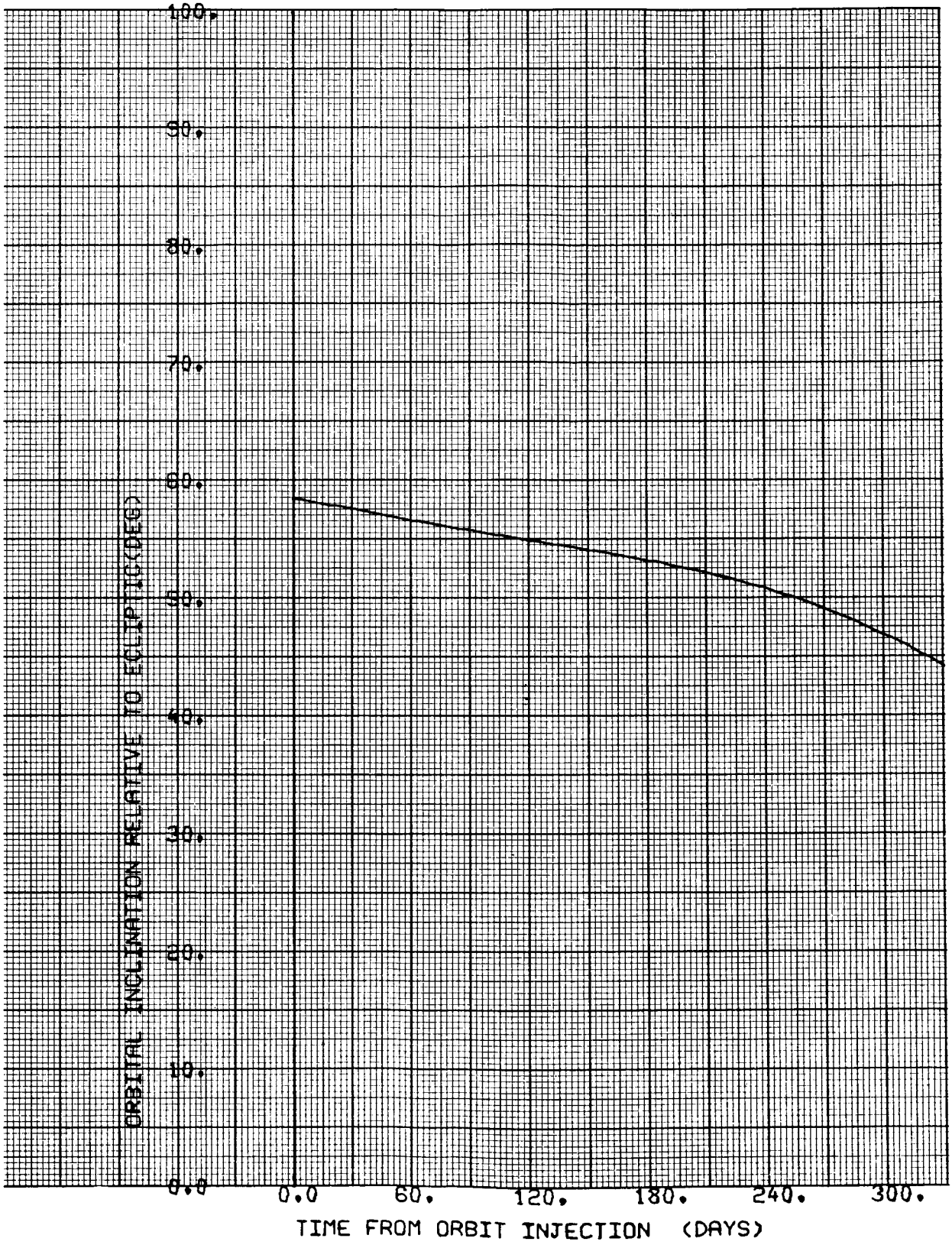
100.
90.
80.
70.
60.
50.
40.
30.
20.
10.
0.0
ORBITAL INCLINATION RELATIVE TO ECLIPTIC(DEG)
0.0
60.
120.
180.
240.
300.
TIME FROM ORBIT INJECTION (DAYS)

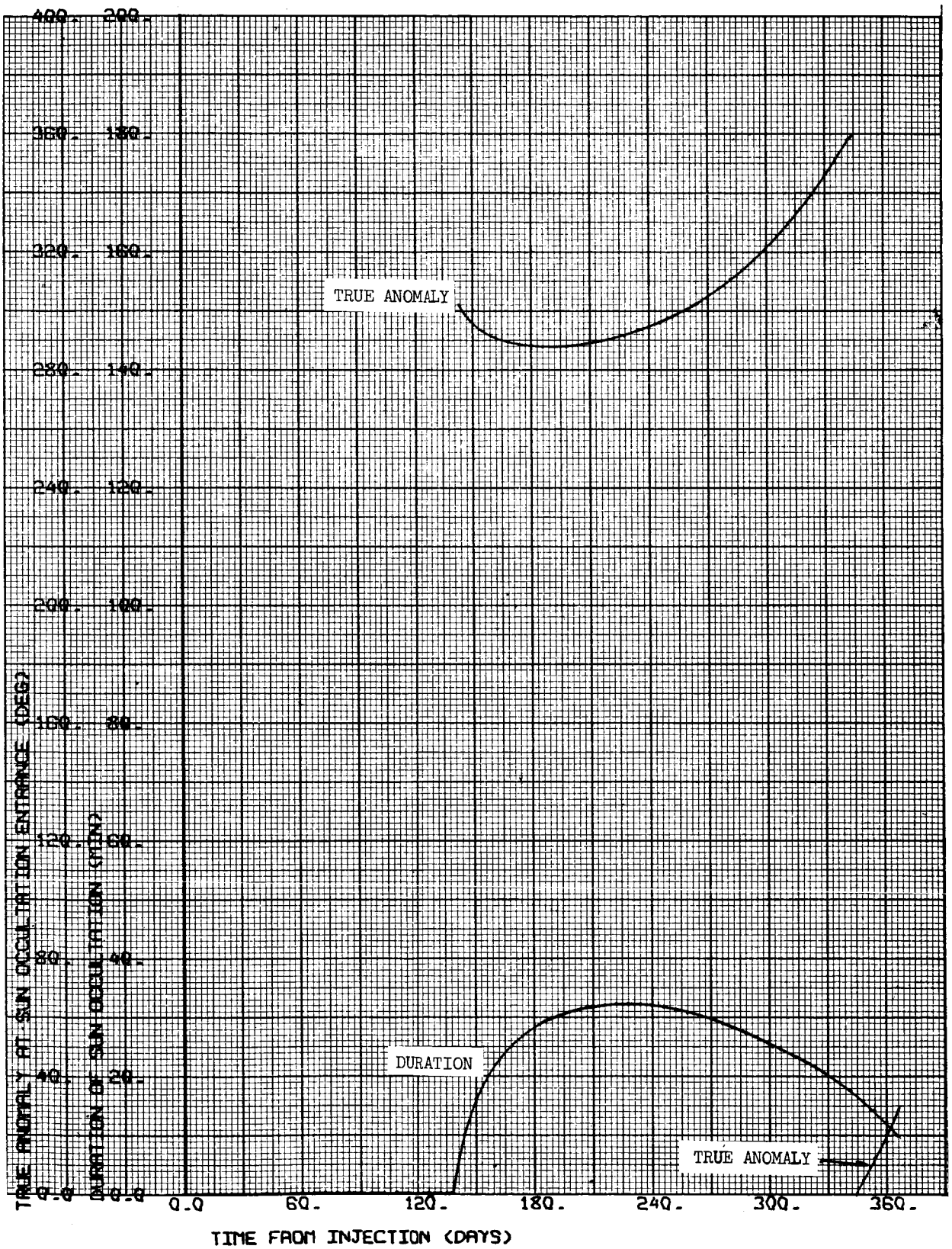
TRUE ANOMALY
DURATION
TRUE ANOMALY
TRUE ANOMALY AT SUN OCCULTATION ENTRANCE (DEG)
DURATION OF SUN OCCULTATION (MIN)
TIME FROM INJECTION (DAYS)
0.0
60.
120.
180.
240.
300.
360.
400.
360.
320.
280.
240.
200.
160.
120.
80.
40.
0.0
200.
180.
160.
140.
120.
100.
80.
60.
40.
20.
0.0

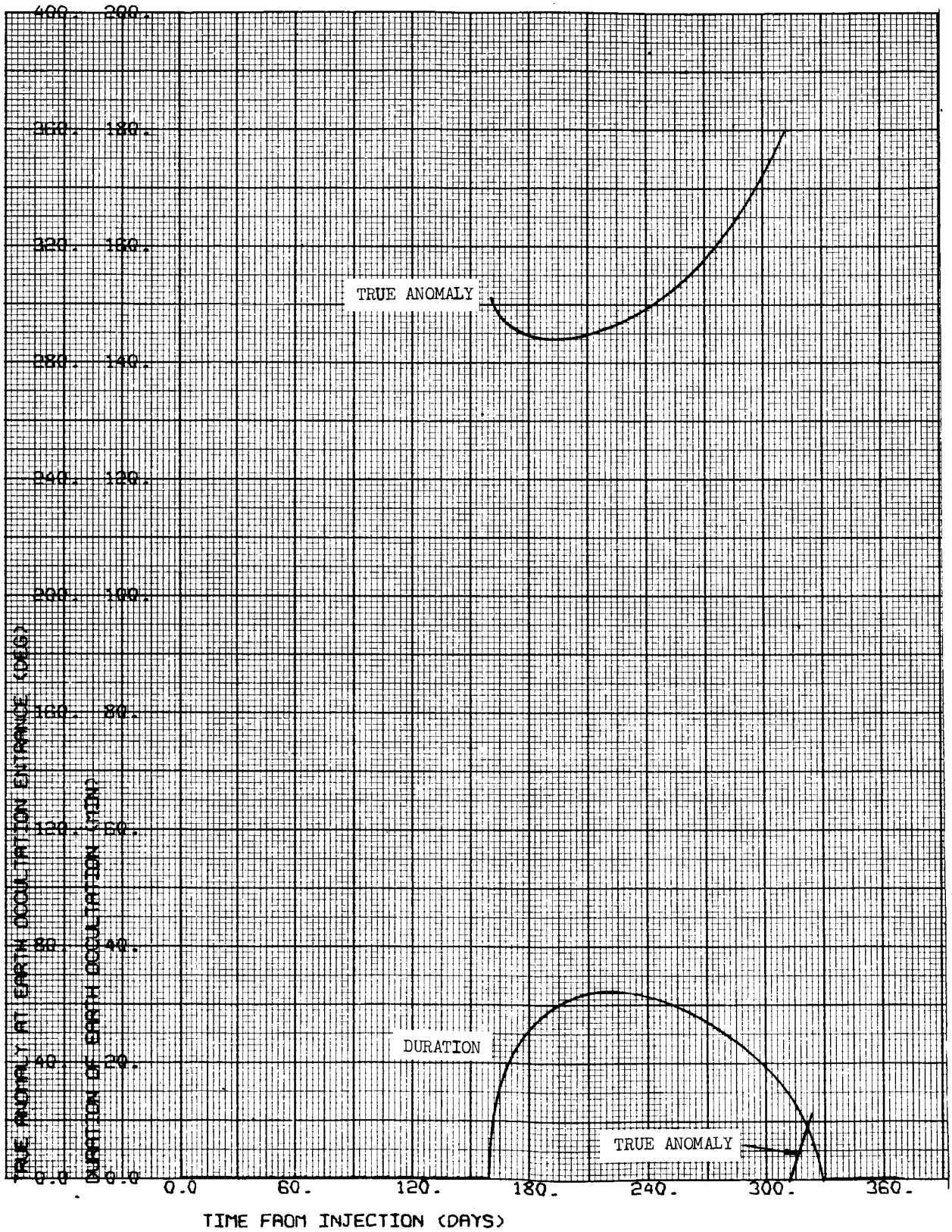
TRUE ANOMALY
DURATION
TRUE ANOMALY
TRUE ANOMALY AT EARTH OCCULTATION ENTRANCE (DEG)
DURATION OF EARTH OCCULTATION (MIN)
TIME FROM INJECTION (DAYS)
0.0
60.
120.
180.
240.
300.
360.
400.
360.
320.
280.
240.
200.
160.
120.
80.
40.
200.
180.
160.
140.
120.
100.
80.
60.
40.
20.
0.0

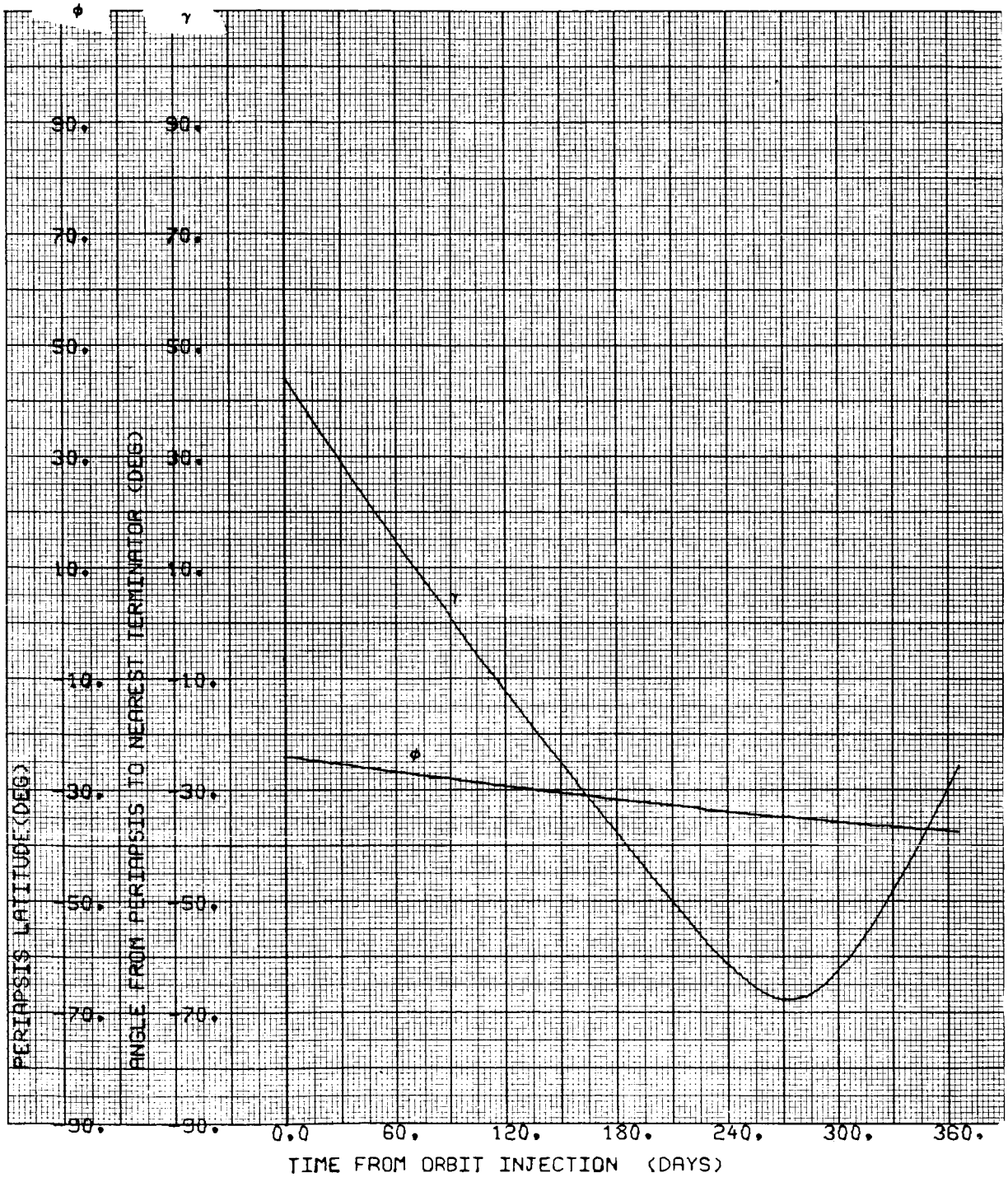
φ
γ
90.
70.
50.
30.
10.
-10.
-30.
-50.
-70.
-90.
PERIAPSIS LATITUDE (DEG)
ANGLE FROM PERIAPSIS TO NEAREST TERMINATOR (DEG)
0.0
60.
120.
180.
240.
300.
360.
TIME FROM ORBIT INJECTION (DAYS)

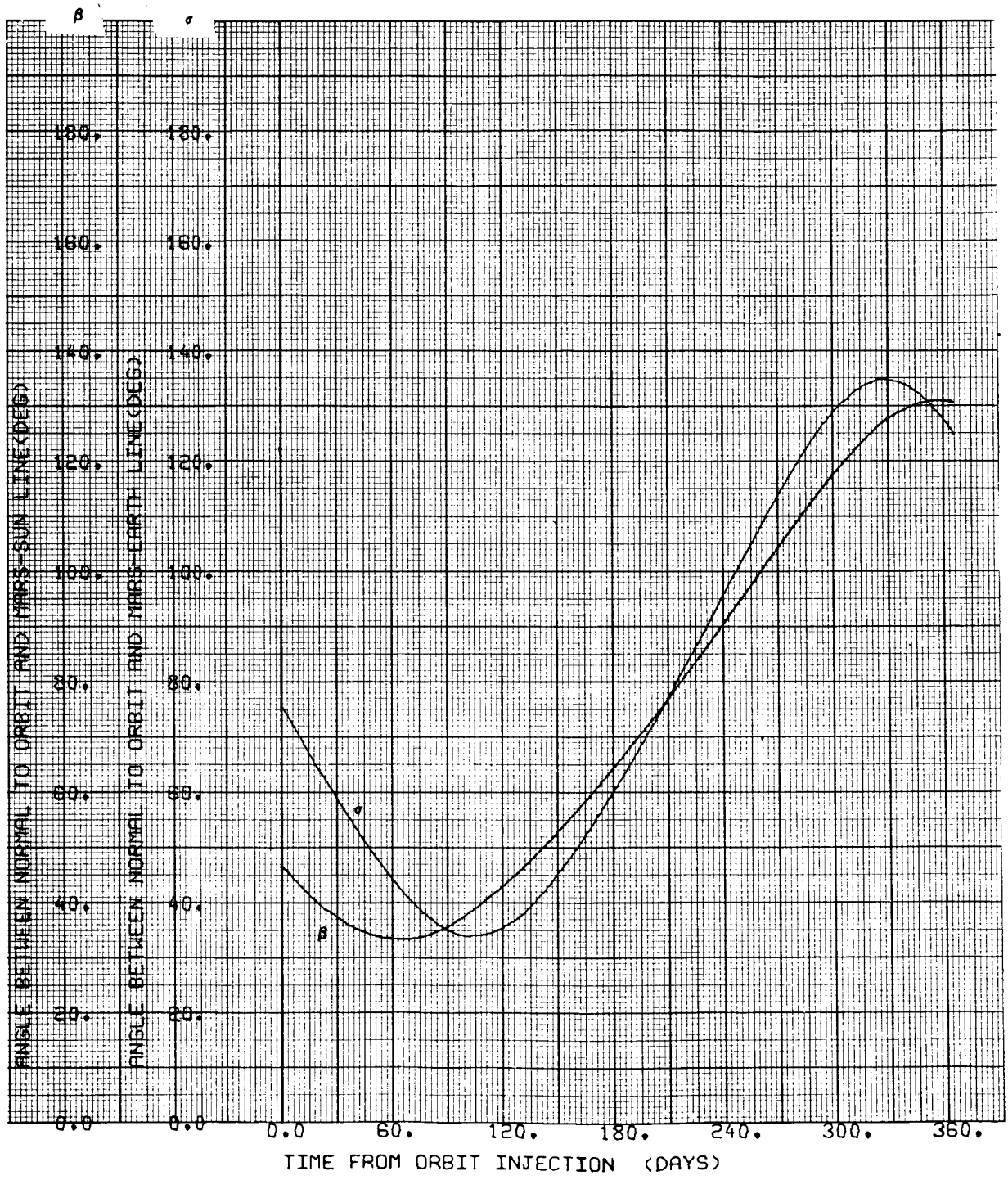
β
σ
180.
160.
140.
120.
100.
80.
60.
40.
20.
0.0
ANGLE BETWEEN NORMAL TO ORBIT AND MARS-SUN LINE (DEG)
ANGLE BETWEEN NORMAL TO ORBIT AND MARS-EARTH LINE (DEG)
0.0
60.
120.
180.
240.
300.
360.
TIME FROM ORBIT INJECTION (DAYS)

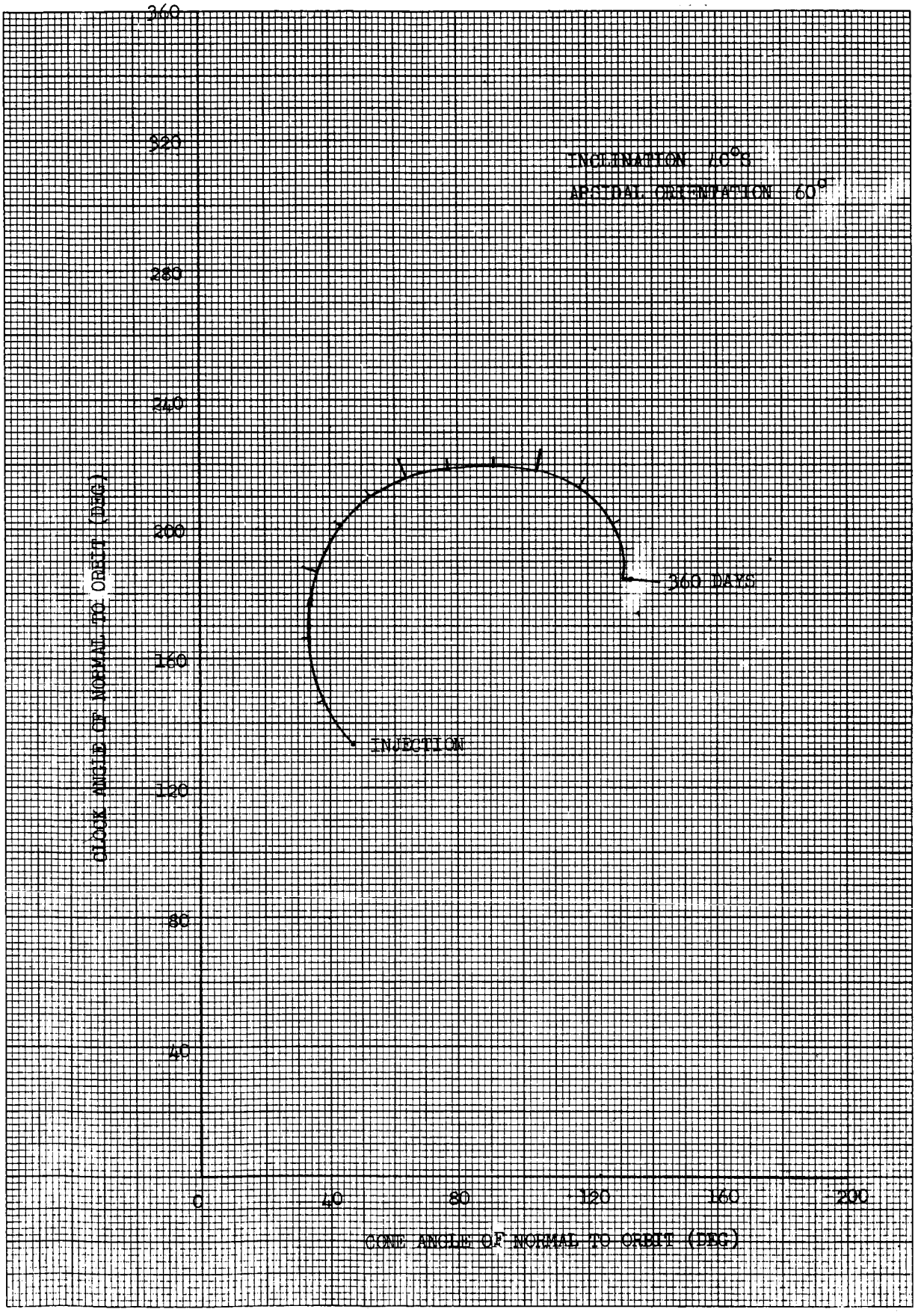
INCLINATION 70°S
ARSTDAL ORIENTATION 60°
360 DAYS
INJECTION
CLOCK ANGLE OF NORMAL TO ORBIT (DEG)
CONE ANGLE OF NORMAL TO ORBIT (DEG)
360
320
280
240
200
160
120
80
40
0
40
80
120
160
200

CASE NO. 23

1000 x 15, 000 km

$i = 40^{o}S$

$\Psi = 90$ deg

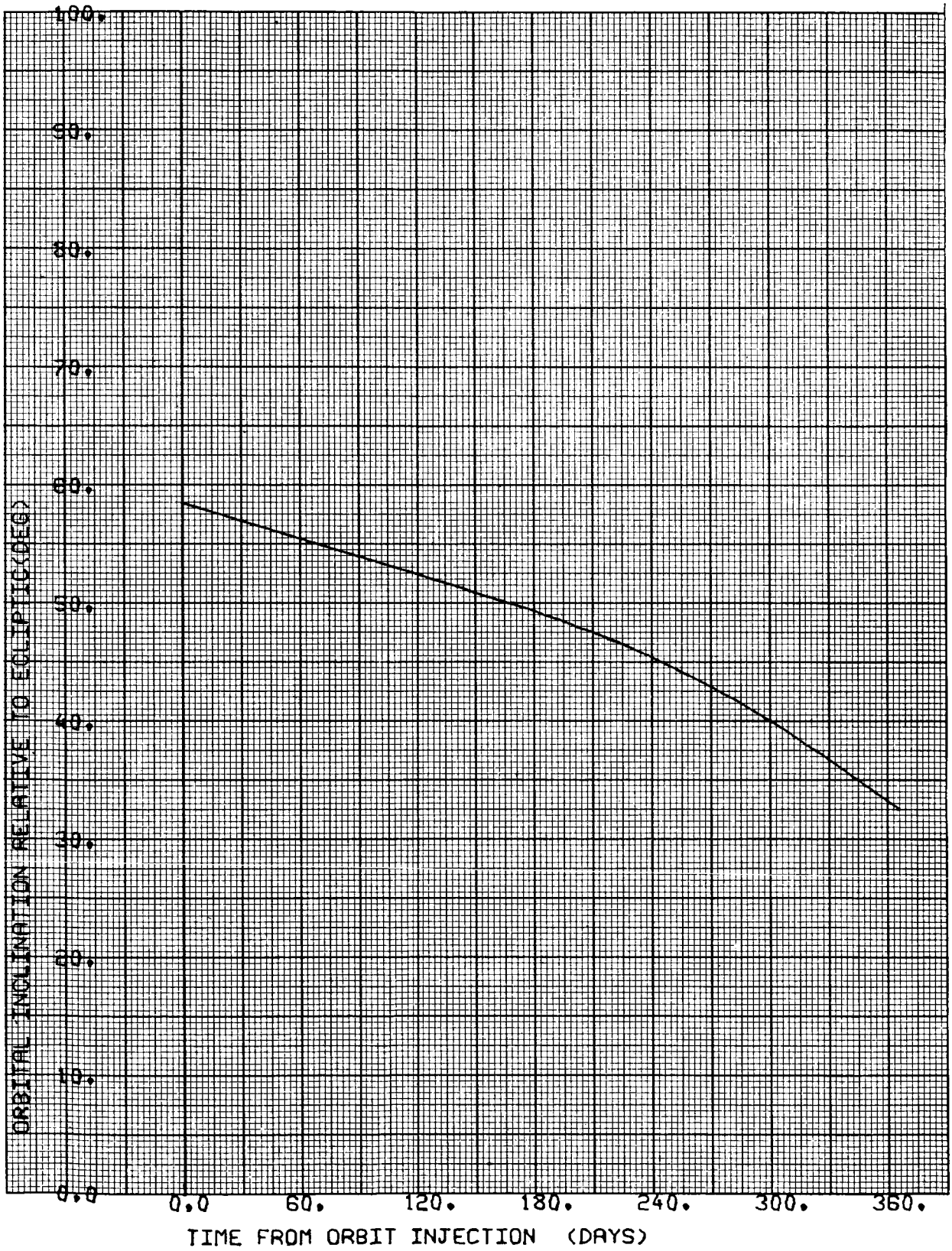
100.
90.
80.
70.
60.
50.
40.
30.
20.
10.
0.0
ORBITAL INCLINATION RELATIVE TO ECLIPTIC(DEG)
0.0
60.
120.
180.
240.
300.
360.
TIME FROM ORBIT INJECTION (DAYS)

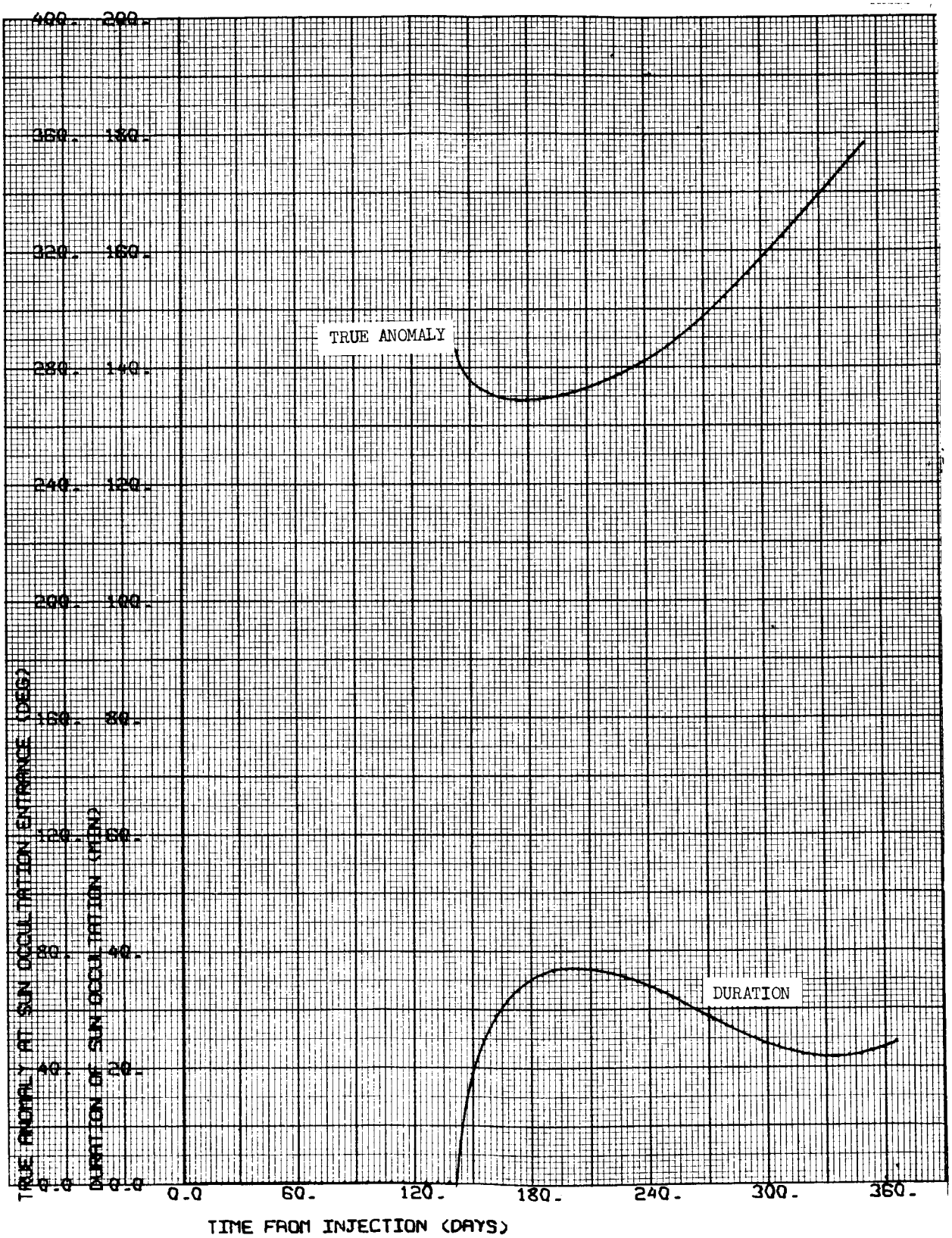
TRUE ANOMALY
DURATION
TRUE ANOMALY AT SUN OCCULTATION ENTRANCE (DEG)
DURATION OF SUN OCCULTATION (MIN)
TIME FROM INJECTION (DAYS)
0.0
60.
120.
180.
240.
300.
360.
400.
360.
320.
280.
240.
200.
160.
120.
80.
40.
0.0
200.
180.
160.
140.
120.
100.
80.
60.
40.
20.
0.0

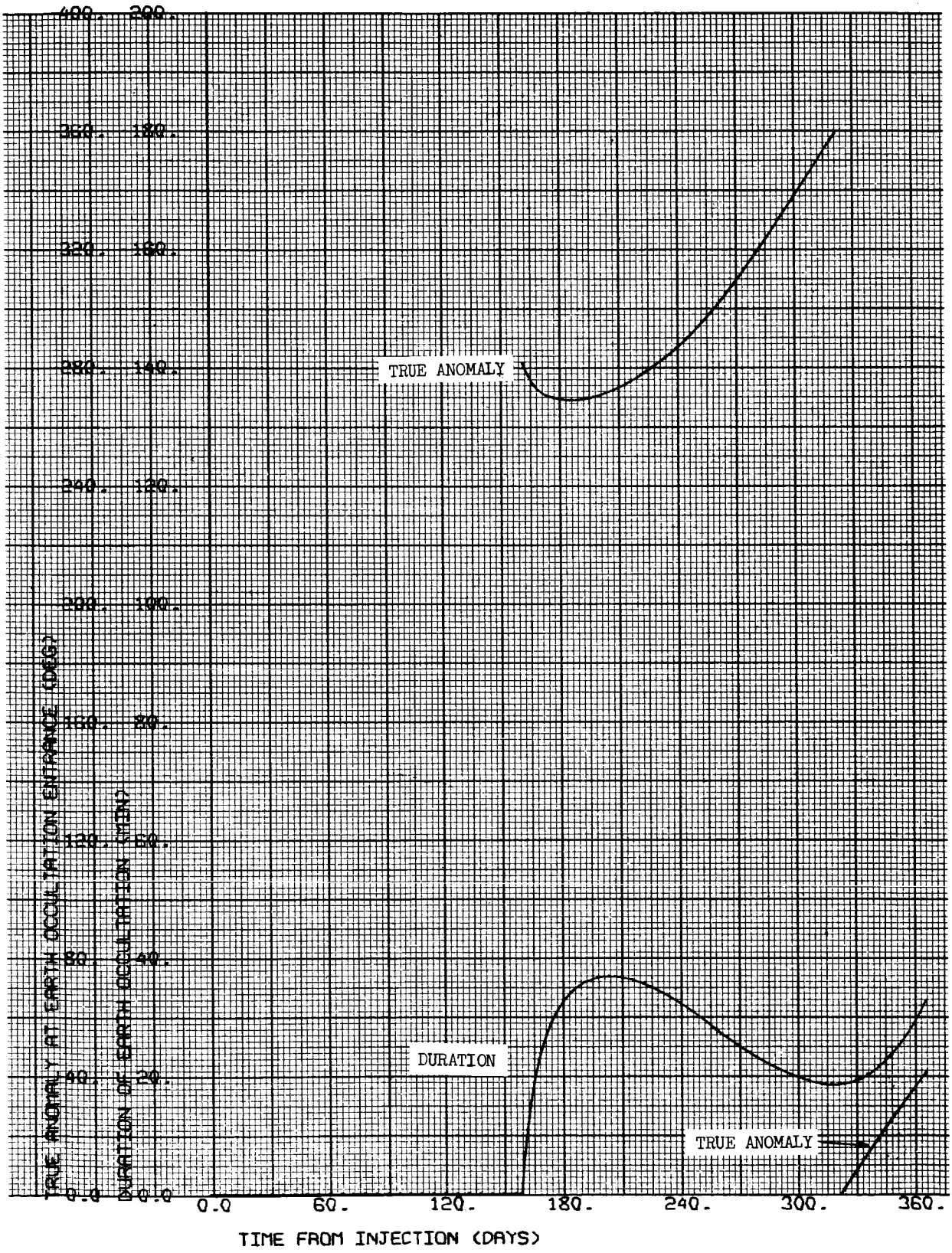
TRUE ANOMALY
DURATION
TRUE ANOMALY
TRUE ANOMALY AT EARTH OCCULTATION ENTRANCE (DEG)
DURATION OF EARTH OCCULTATION (MIN)
TIME FROM INJECTION (DAYS)
0.0
60.
120.
180.
240.
300.
360.
400.
360.
320.
280.
240.
200.
160.
120.
80.
40.
0.0
200.
180.
160.
140.
120.
100.
80.
60.
40.
20.
0.0

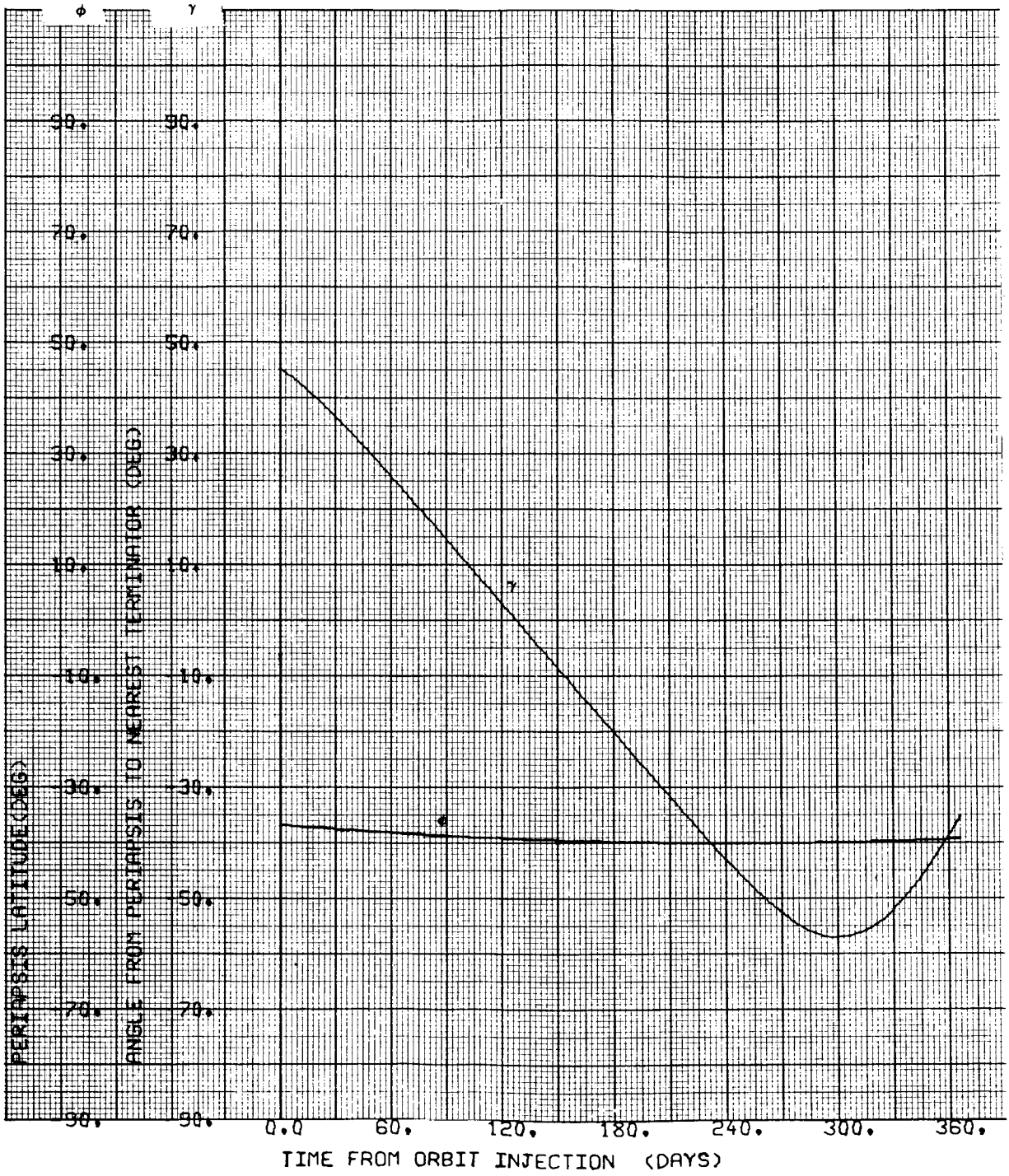
φ
γ
90.
70.
50.
30.
10.
-10.
-30.
-50.
-70.
-90.
0.0
60.
120.
180.
240.
300.
360.
PERIAPSIS LATITUDE (DEG)
ANGLE FROM PERIAPSIS TO NEAREST TERMINATOR (DEG)
TIME FROM ORBIT INJECTION (DAYS)

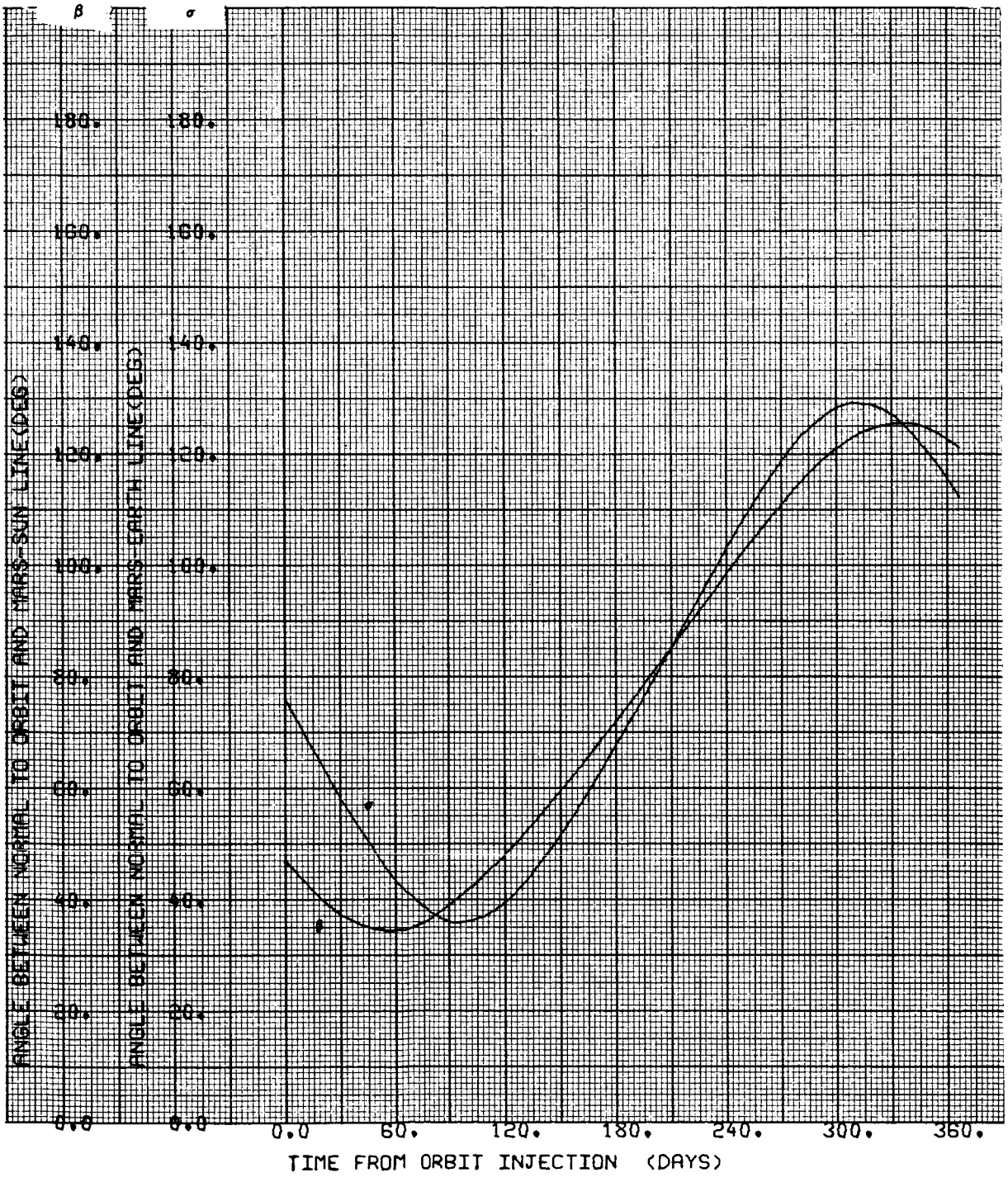
β
σ
180.
160.
140.
120.
100.
80.
60.
40.
20.
0.0
ANGLE BETWEEN NORMAL TO ORBIT AND MARS-SUN LINE(DEG)
ANGLE BETWEEN NORMAL TO ORBIT AND MARS-EARTH LINE(DEG)
0.0
60.
120.
180.
240.
300.
360.
TIME FROM ORBIT INJECTION (DAYS)

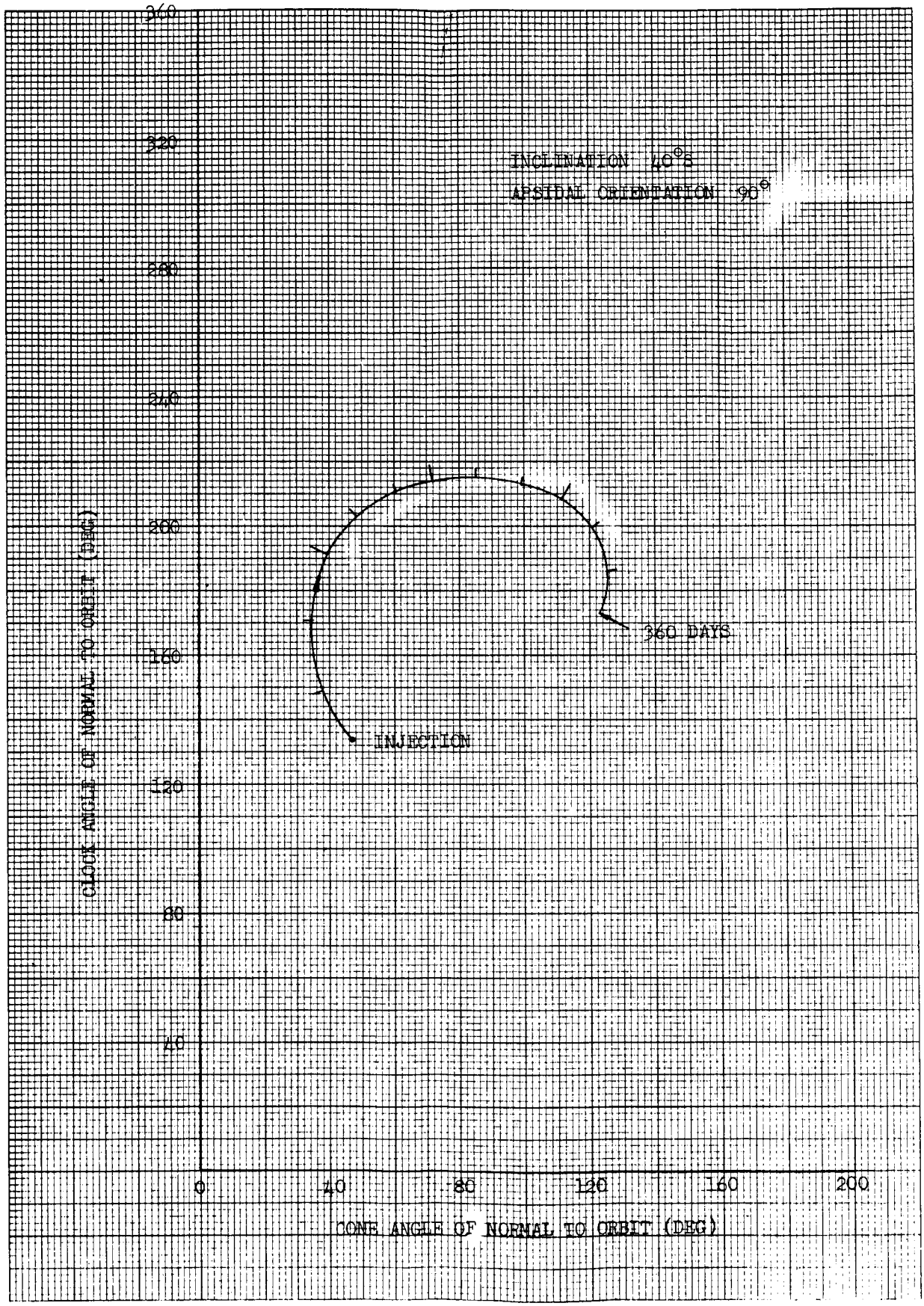
INCLINATION 40°S
APSIDAL ORIENTATION 90°
360 DAYS
INJECTION
CLOCK ANGLE OF NORMAL TO ORBIT (DEG)
CONE ANGLE OF NORMAL TO ORBIT (DEG)
0
40
80
120
160
200
240
280
320
360

CASE NO. 24

1000 x 15, 000 km

$i = 40^{o}S$

$\Psi = 150$ deg

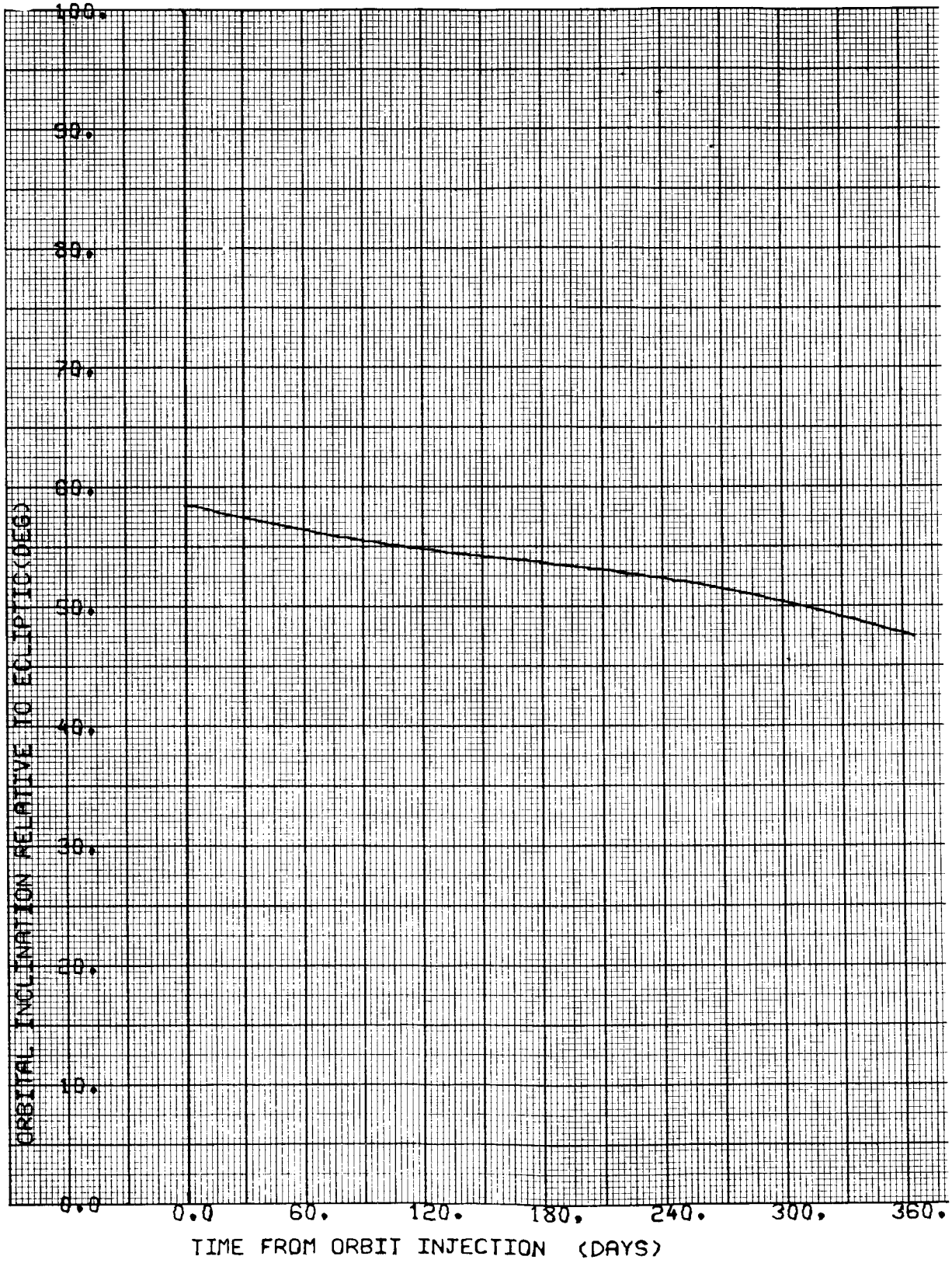
100.
90.
80.
70.
60.
50.
40.
30.
20.
10.
0.0
ORBITAL INCLINATION RELATIVE TO ECLIPTIC(DEG)
0.0
60.
120.
180.
240.
300.
360.
TIME FROM ORBIT INJECTION (DAYS)

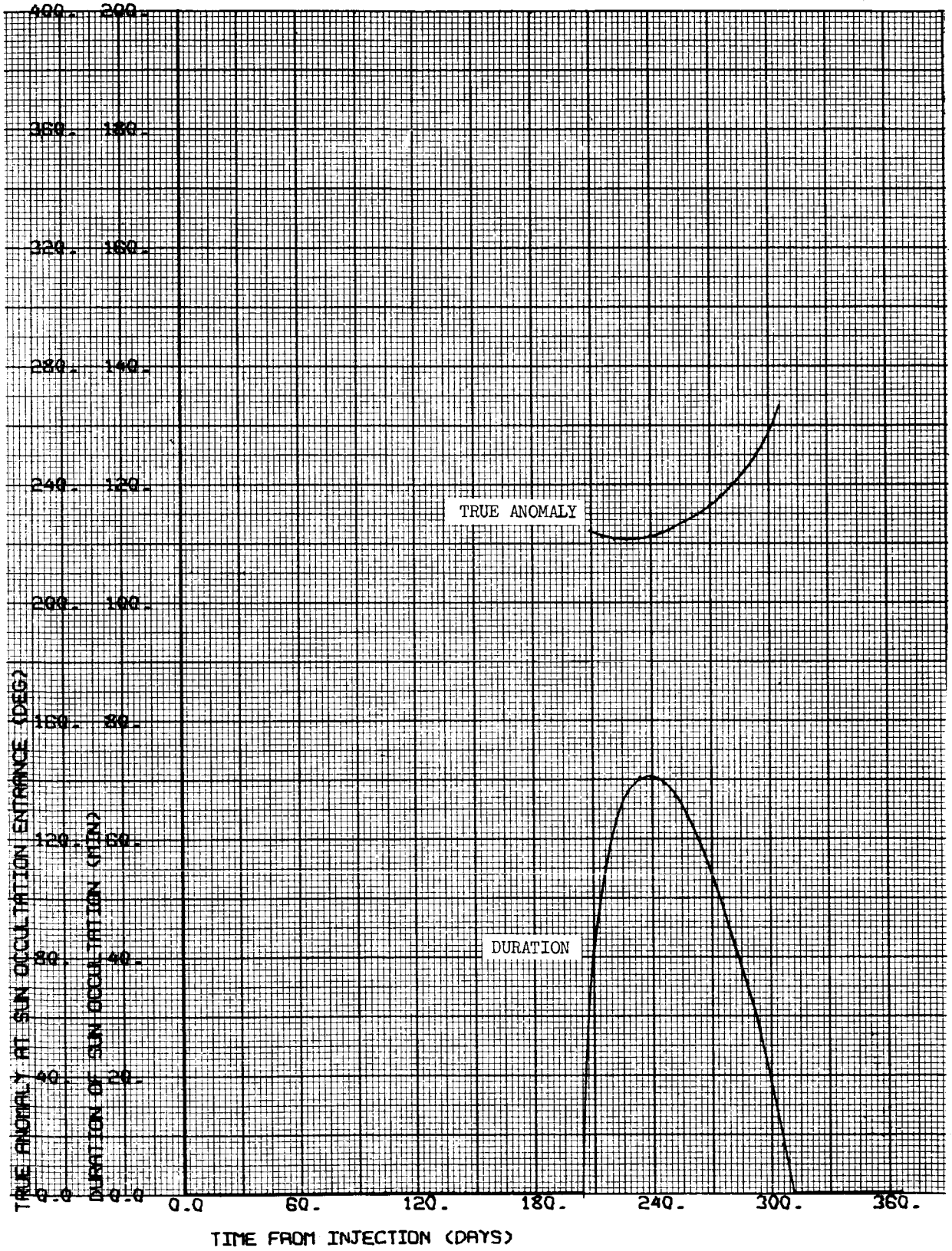
TRUE ANOMALY
DURATION
TRUE ANOMALY AT SUN OCCULTATION ENTRANCE (DEG)
DURATION OF SUN OCCULTATION (MIN)
TIME FROM INJECTION (DAYS)
0.0
60.
120.
180.
240.
300.
360.
400.
360.
320.
280.
240.
200.
160.
120.
80.
40.
200.
180.
160.
140.
120.
100.
80.
60.
40.
20.
0.0

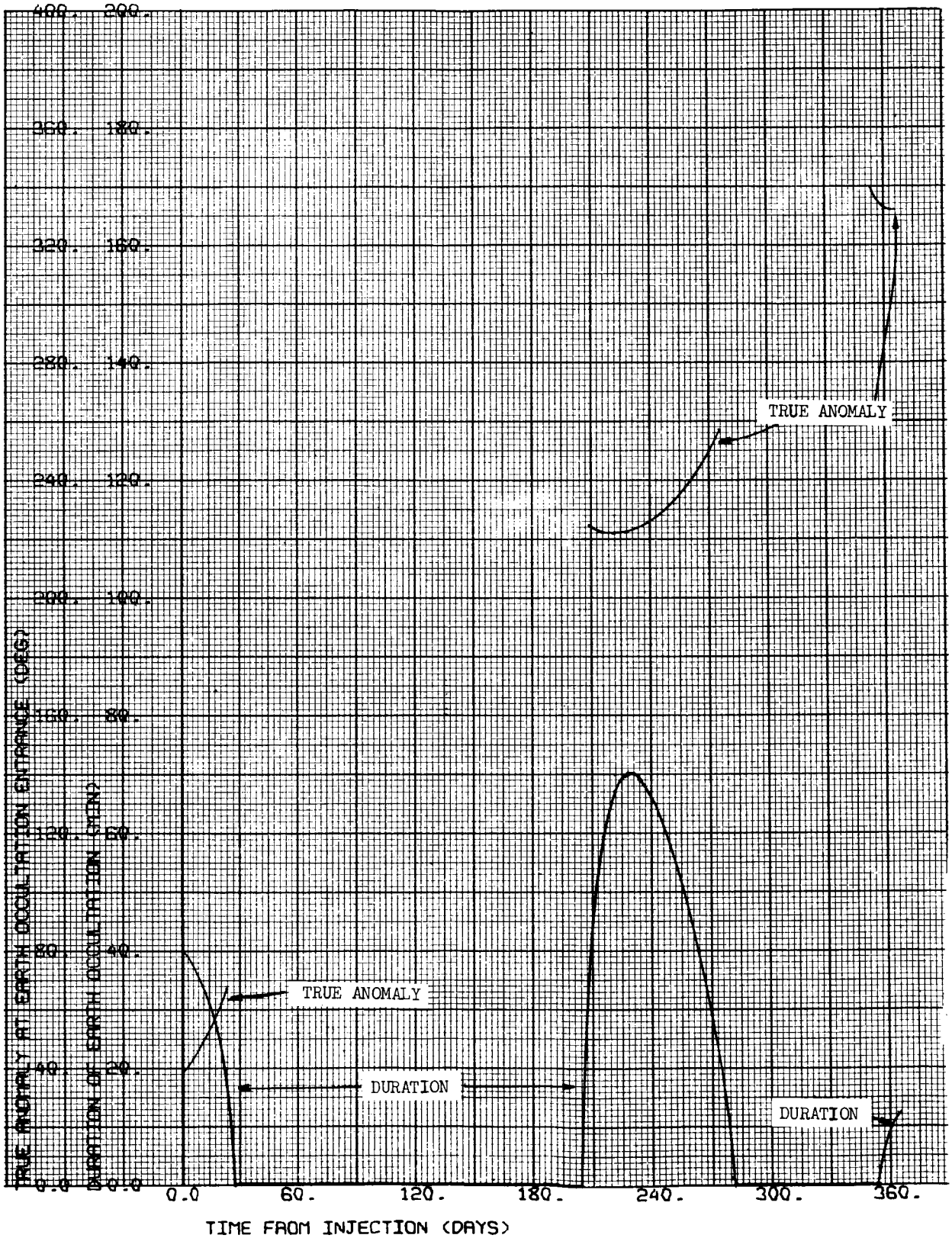
TRUE ANOMALY AT EARTH OCCULTATION ENTRANCE (DEG)
DURATION OF EARTH OCCULTATION (DEG)
400.
360.
320.
280.
240.
200.
160.
120.
80.
40.
0.0
200.
180.
160.
140.
120.
100.
80.
60.
40.
20.
0.0
0.0
60.
120.
180.
240.
300.
360.
TRUE ANOMALY
DURATION
TRUE ANOMALY
DURATION
TIME FROM INJECTION (DAYS)

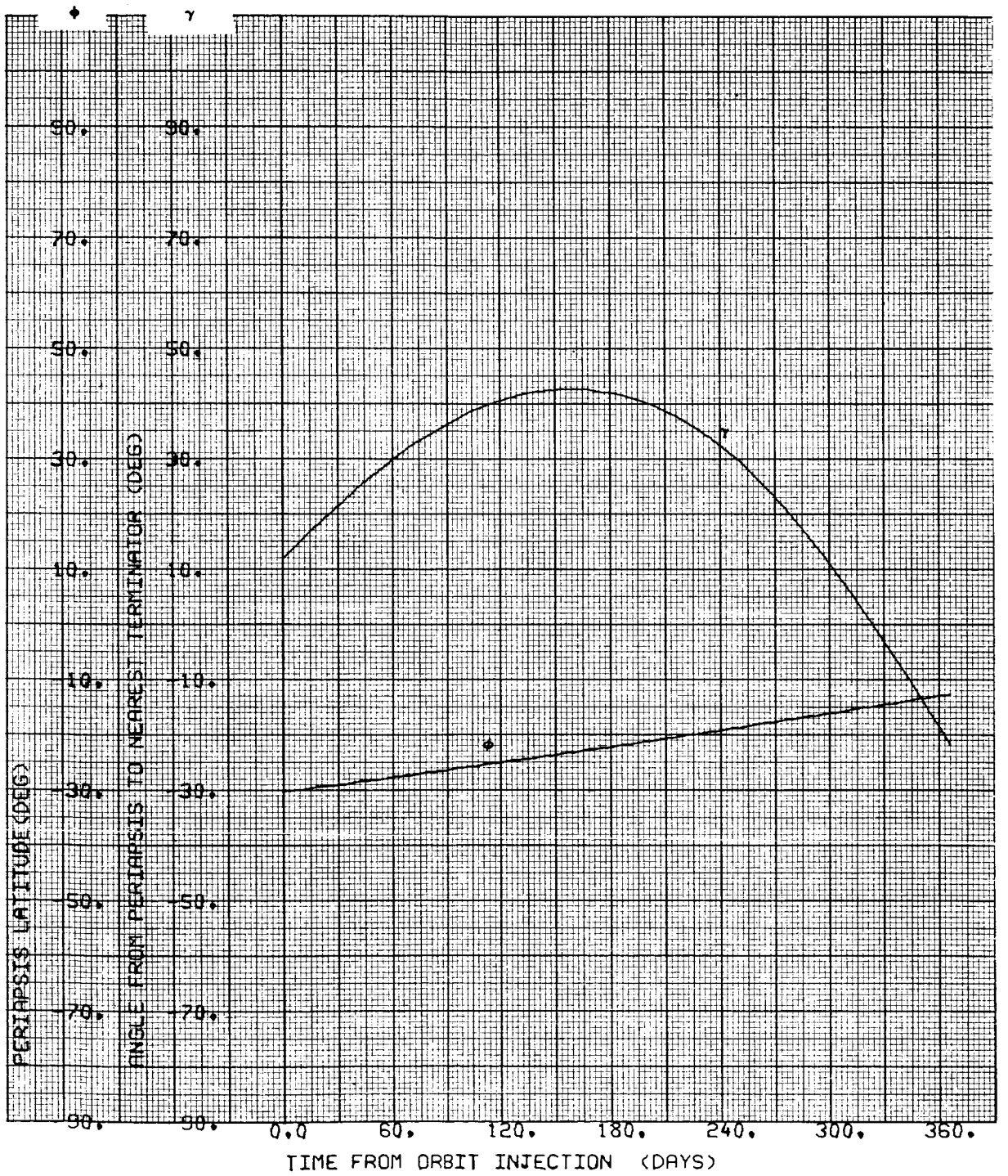
φ
γ
90.
70.
50.
30.
10.
-10.
-30.
-50.
-70.
-90.
0.0
60.
120.
180.
240.
300.
360.
PERIAPSIS LATITUDE (DEG)
ANGLE FROM PERIAPSIS TO NEAREST TERMINATOR (DEG)
TIME FROM ORBIT INJECTION (DAYS)

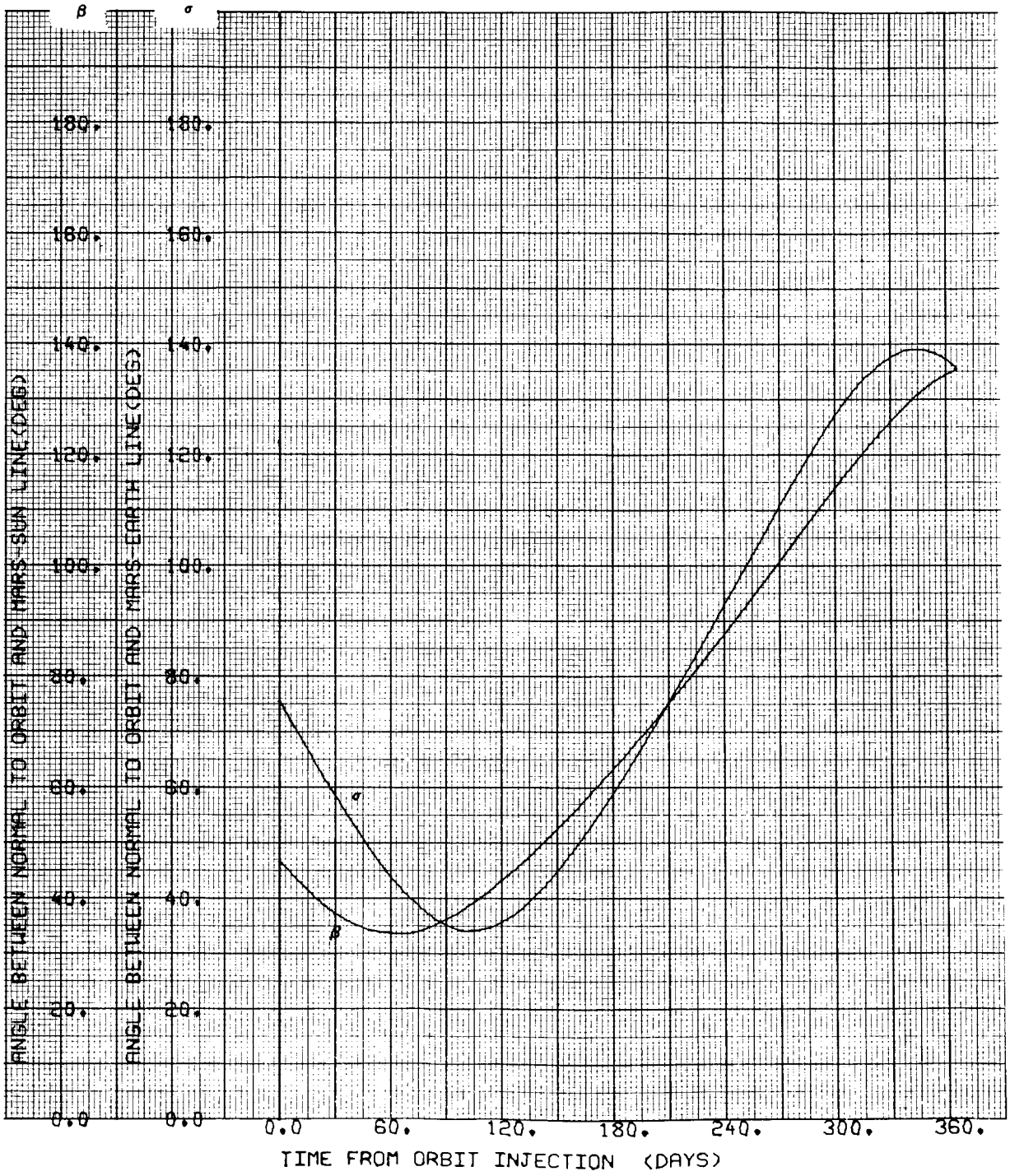
β
σ
180.
160.
140.
120.
100.
80.
60.
40.
20.
0.0
ANGLE BETWEEN NORMAL TO ORBIT AND MARS-SUN LINE (DEG)
ANGLE BETWEEN NORMAL TO ORBIT AND MARS-EARTH LINE (DEG)
0.0
60.
120.
180.
240.
300.
360.
TIME FROM ORBIT INJECTION (DAYS)

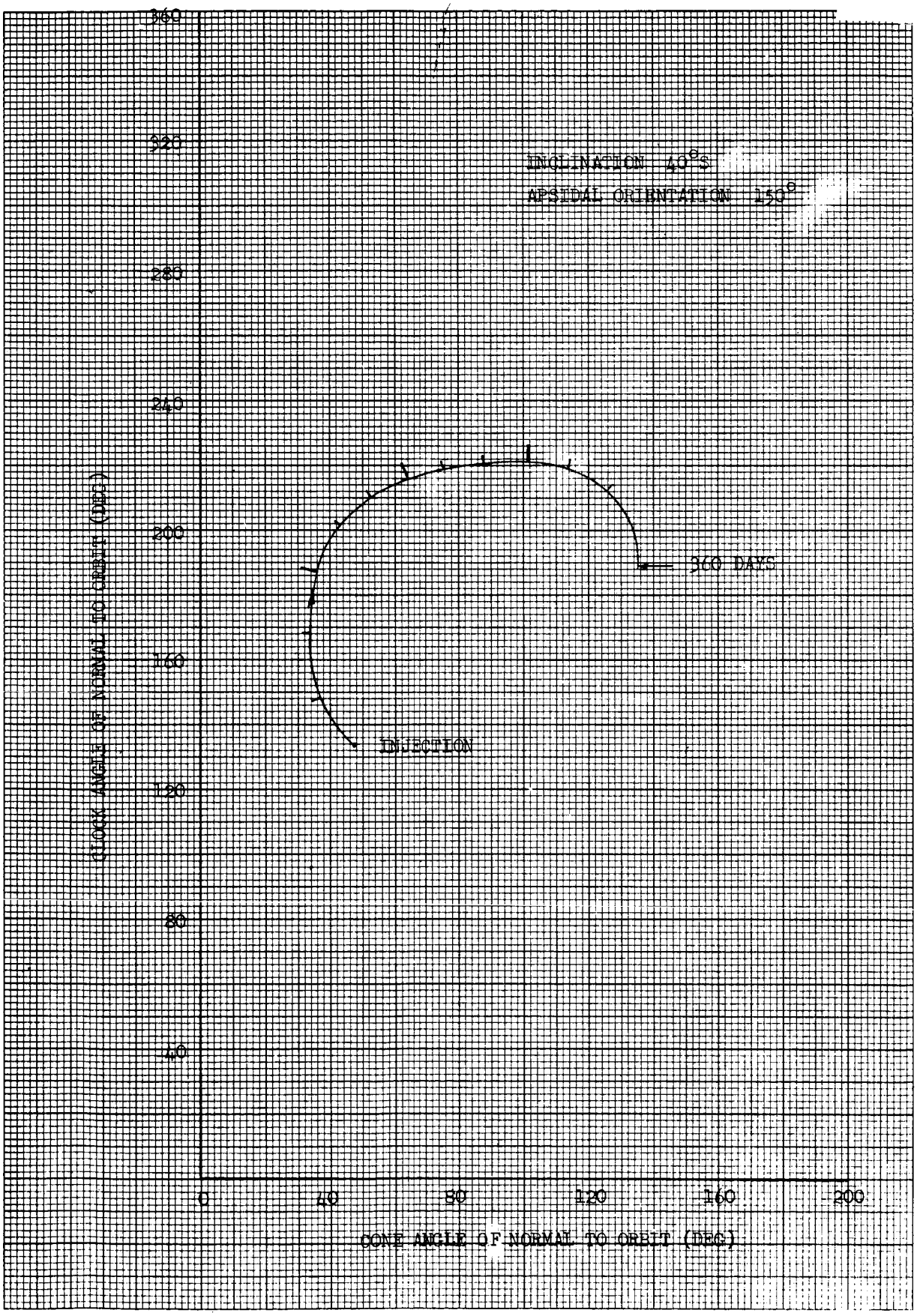
INCLINATION 40°S
APSIDAL ORIENTATION 150°
360 DAYS
INJECTION
CLOCK ANGLE OF NORMAL TO ORBIT (DEG.)
CONE ANGLE OF NORMAL TO ORBIT (DEG.)
360
320
280
240
200
160
120
80
40
0
40
80
120
160
200

CASE NO. 25

1000 x 15,000 km

$i = 40^{\circ}S$

$\Psi = 127.625$ deg

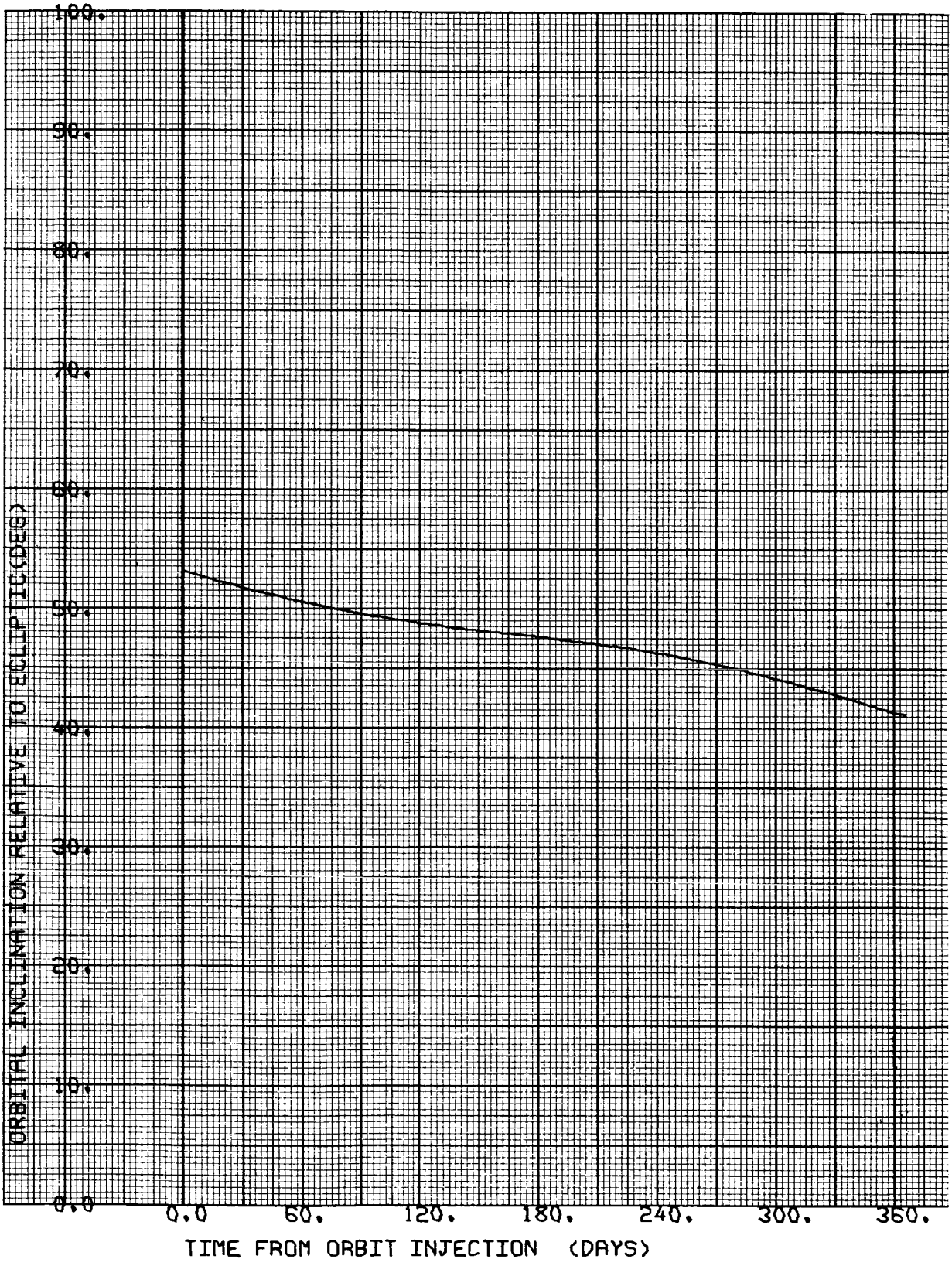
100.
90.
80.
70.
60.
50.
40.
30.
20.
10.
0.0
ORBITAL INCLINATION RELATIVE TO ECLIPTIC(DEG)
0.0
60.
120.
180.
240.
300.
360.
TIME FROM ORBIT INJECTION (DAYS)

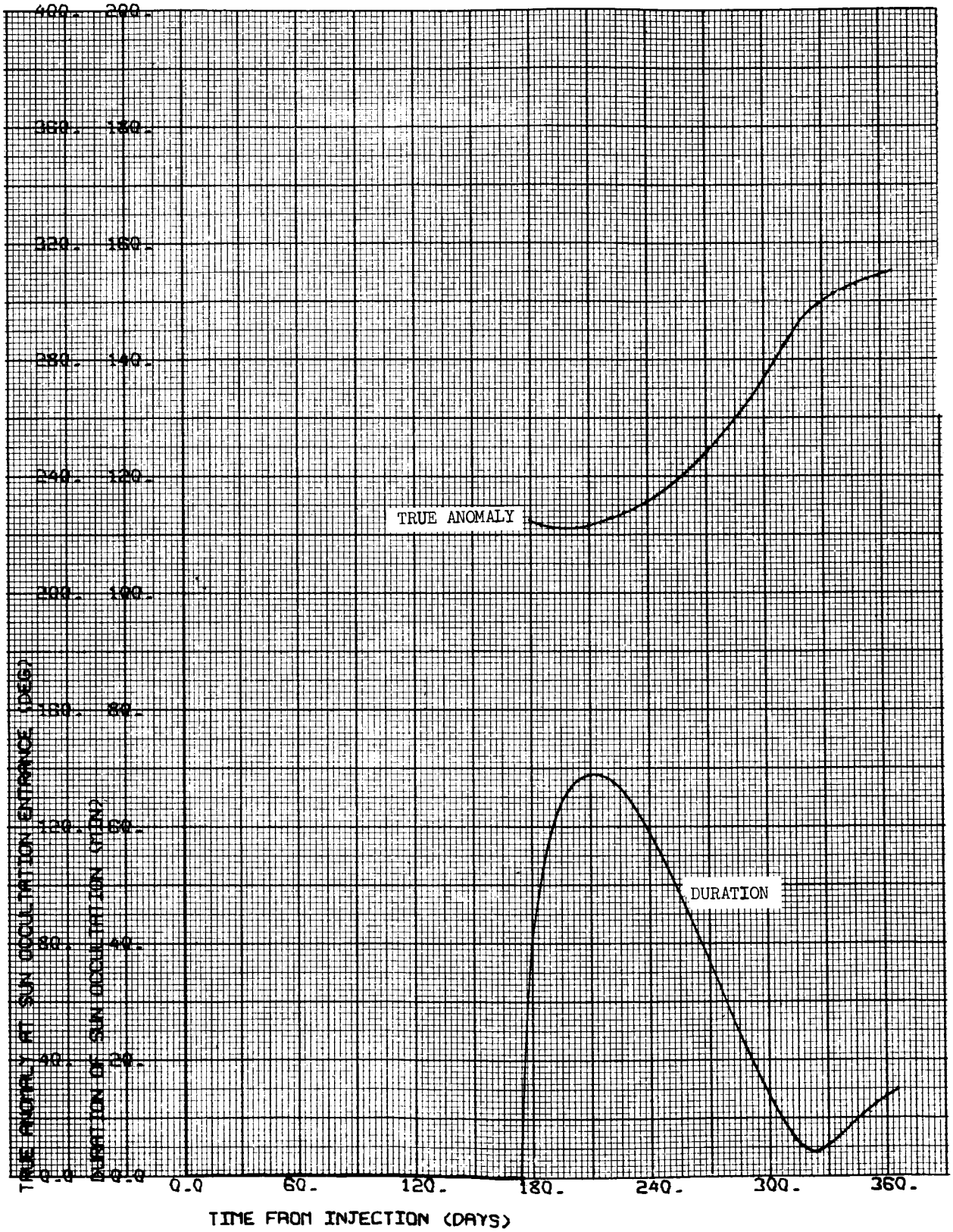
TRUE ANOMALY
DURATION
TRUE ANOMALY AT SUN OCCULTATION ENTRANCE (DEG)
DURATION OF SUN OCCULTATION (MIN)
TIME FROM INJECTION (DAYS)
0.0
60.
120.
180.
240.
300.
360.

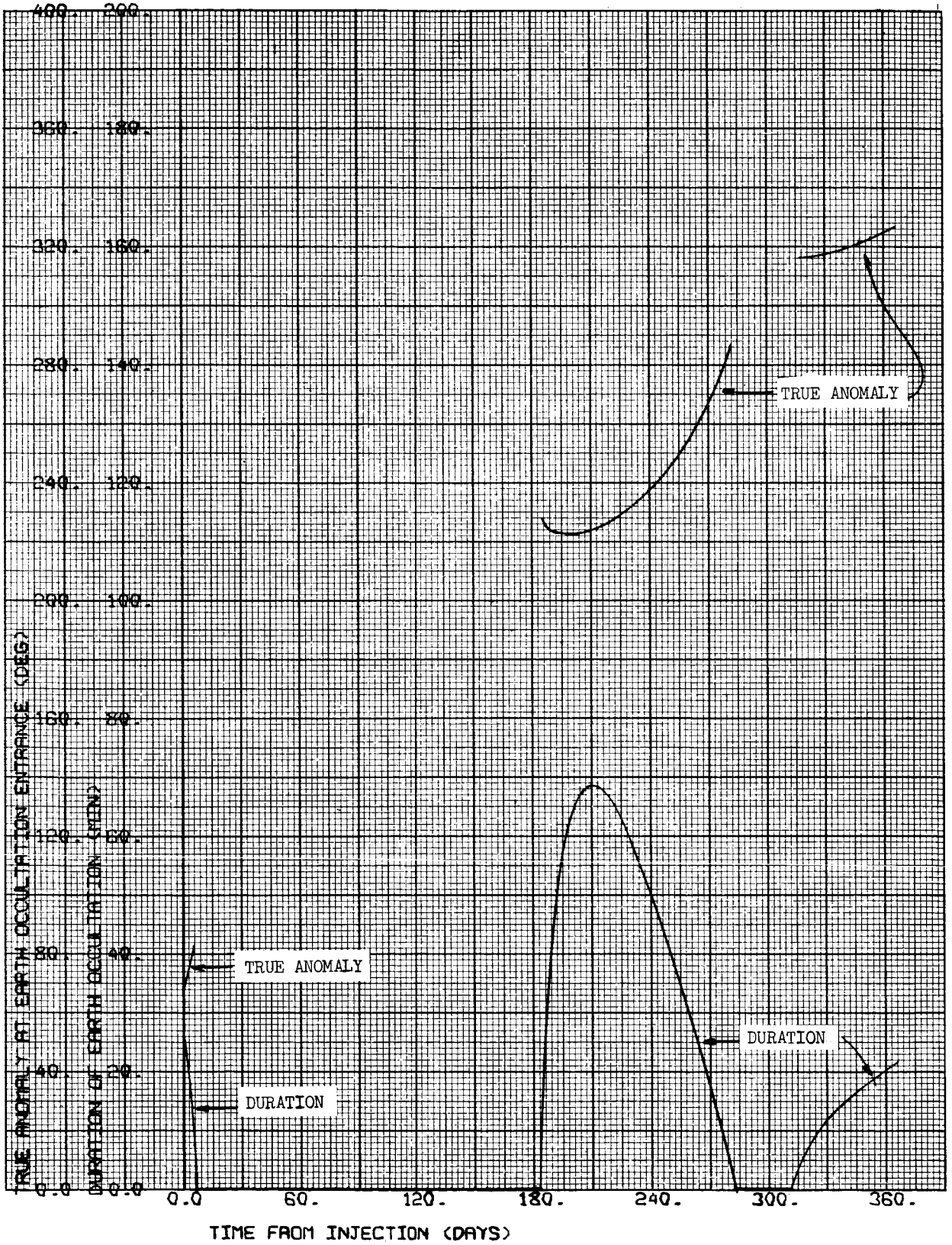
TRUE ANOMALY AT EARTH OCCULTATION ENTRANCE (DEG)
DURATION OF EARTH OCCULTATION (MIN)
TIME FROM INJECTION (DAYS)
TRUE ANOMALY
DURATION
TRUE ANOMALY
DURATION
0.0
60.
120.
180.
240.
300.
360.

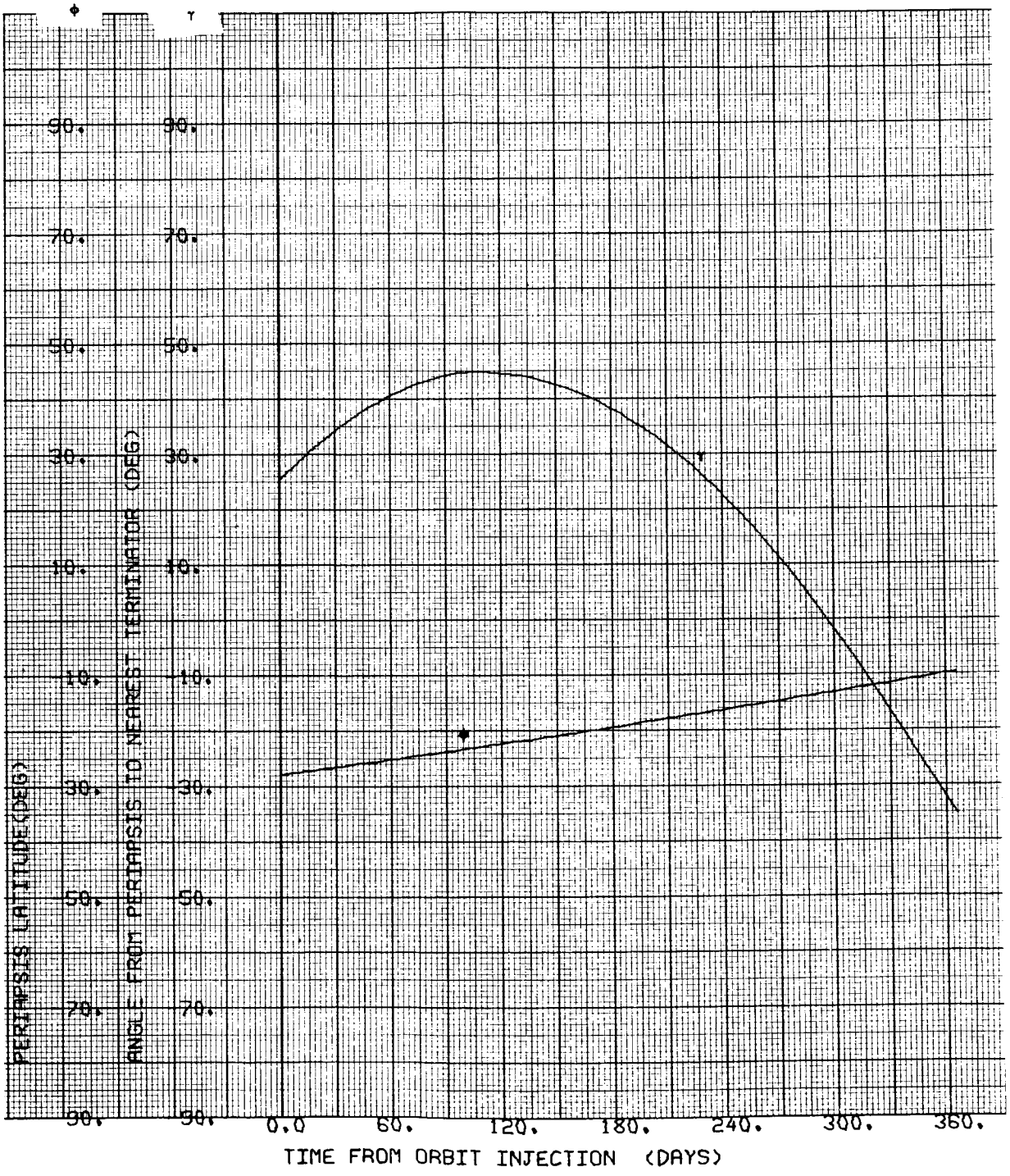
PERIAPSIS LATITUDE(DEG)
ANGLE FROM PERIAPSIS TO NEAREST TERMINATOR (DEG)
90.
70.
50.
30.
10.
-10.
-30.
-50.
-70.
-90.
0.0
60.
120.
180.
240.
300.
360.
TIME FROM ORBIT INJECTION (DAYS)

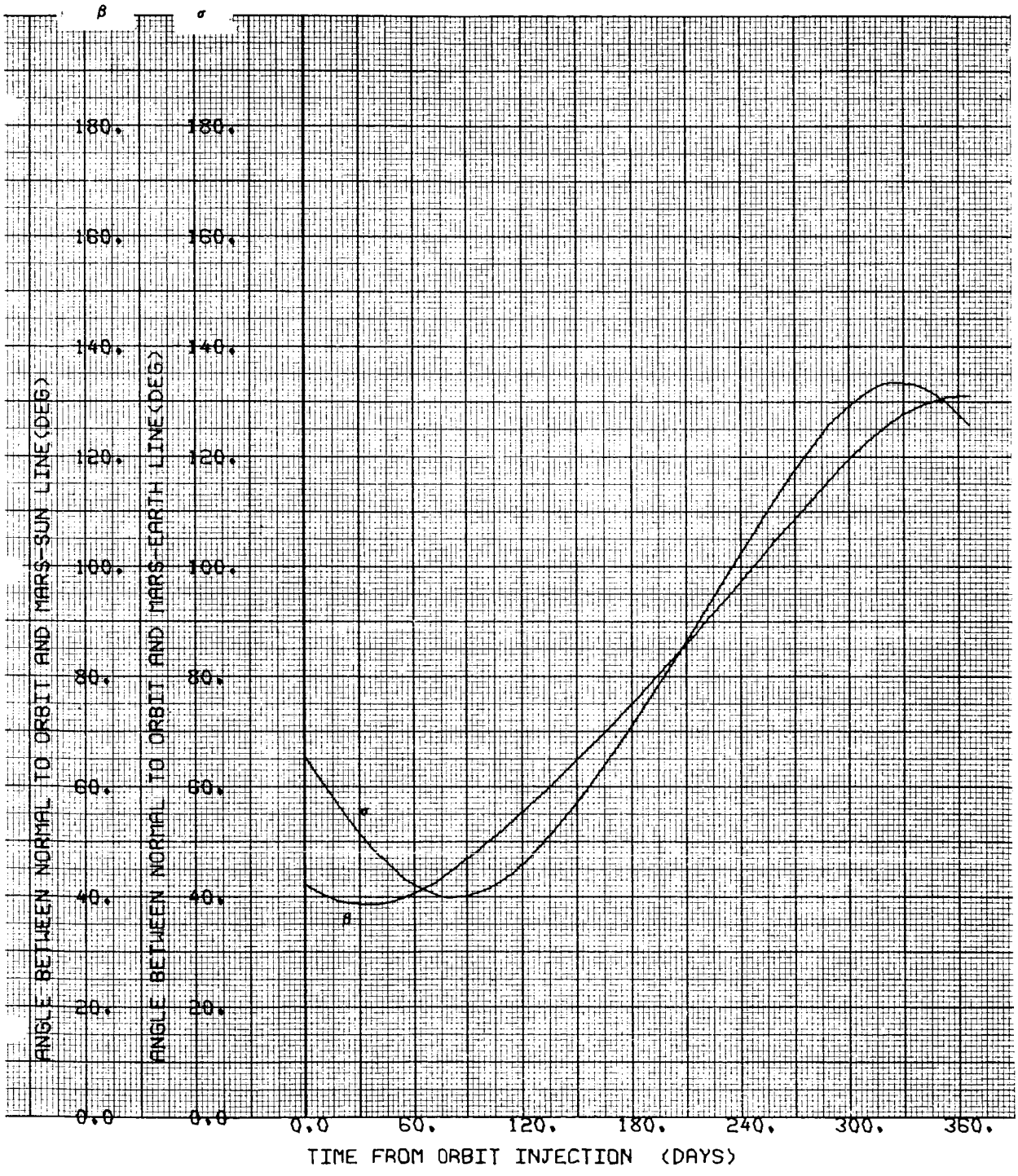
β
σ
180.
160.
140.
120.
100.
80.
60.
40.
20.
0.0
ANGLE BETWEEN NORMAL TO ORBIT AND MARS-SUN LINE(DEG)
ANGLE BETWEEN NORMAL TO ORBIT AND MARS-EARTH LINE(DEG)
σ
β
0.0
60.
120.
180.
240.
300.
360.
TIME FROM ORBIT INJECTION (DAYS)

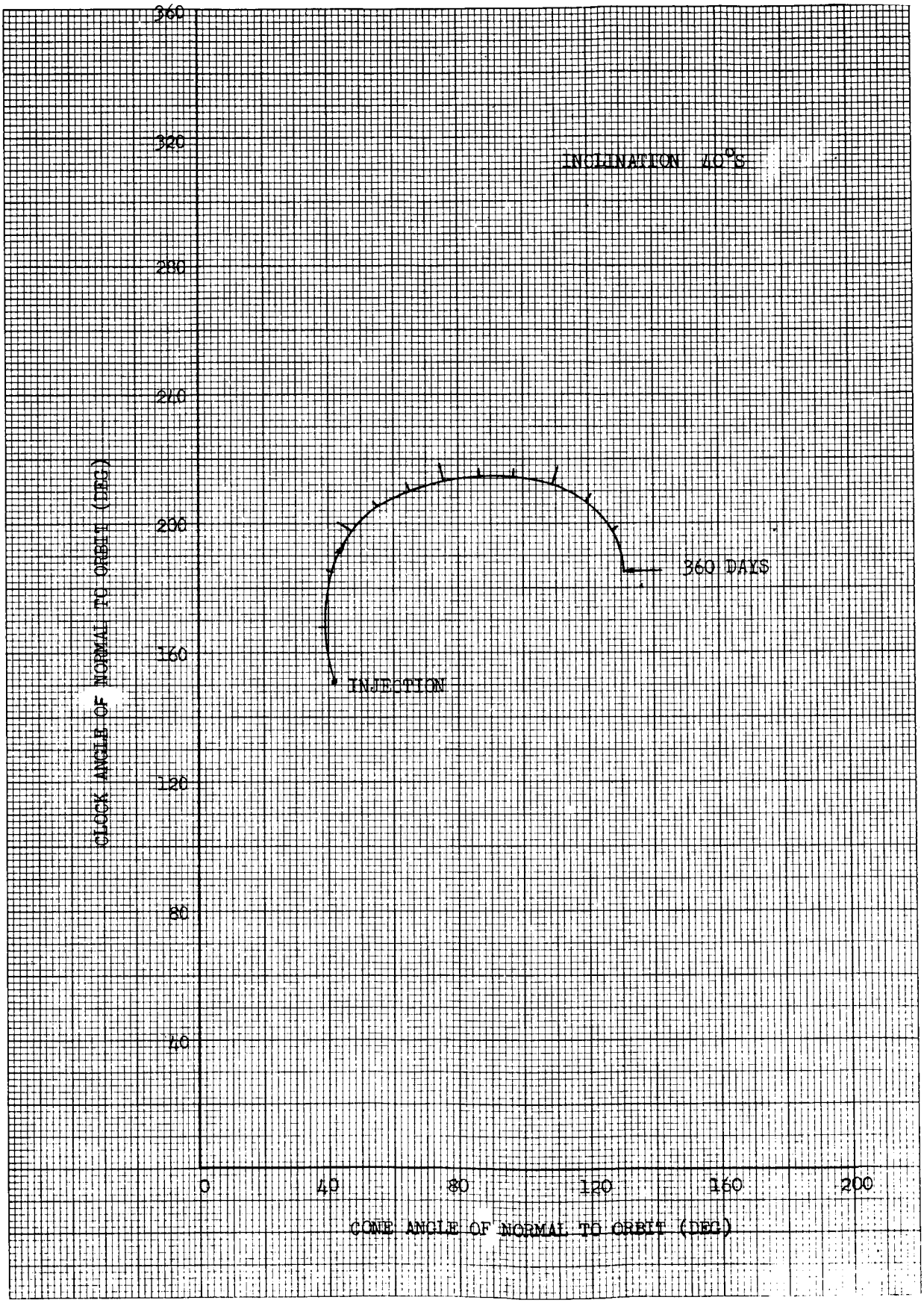
INCLINATION 40°S
360 DAYS
INJECTION
CLOCK ANGLE OF NORMAL TO ORBIT (DEG)
CONE ANGLE OF NORMAL TO ORBIT (DEG)
360
320
280
240
200
160
120
80
40
0
40
80
120
160
200

CASE NO. 26

1000 x 15,000 km

$i = 40^{\circ}N$

$\Psi = 127.625$ deg

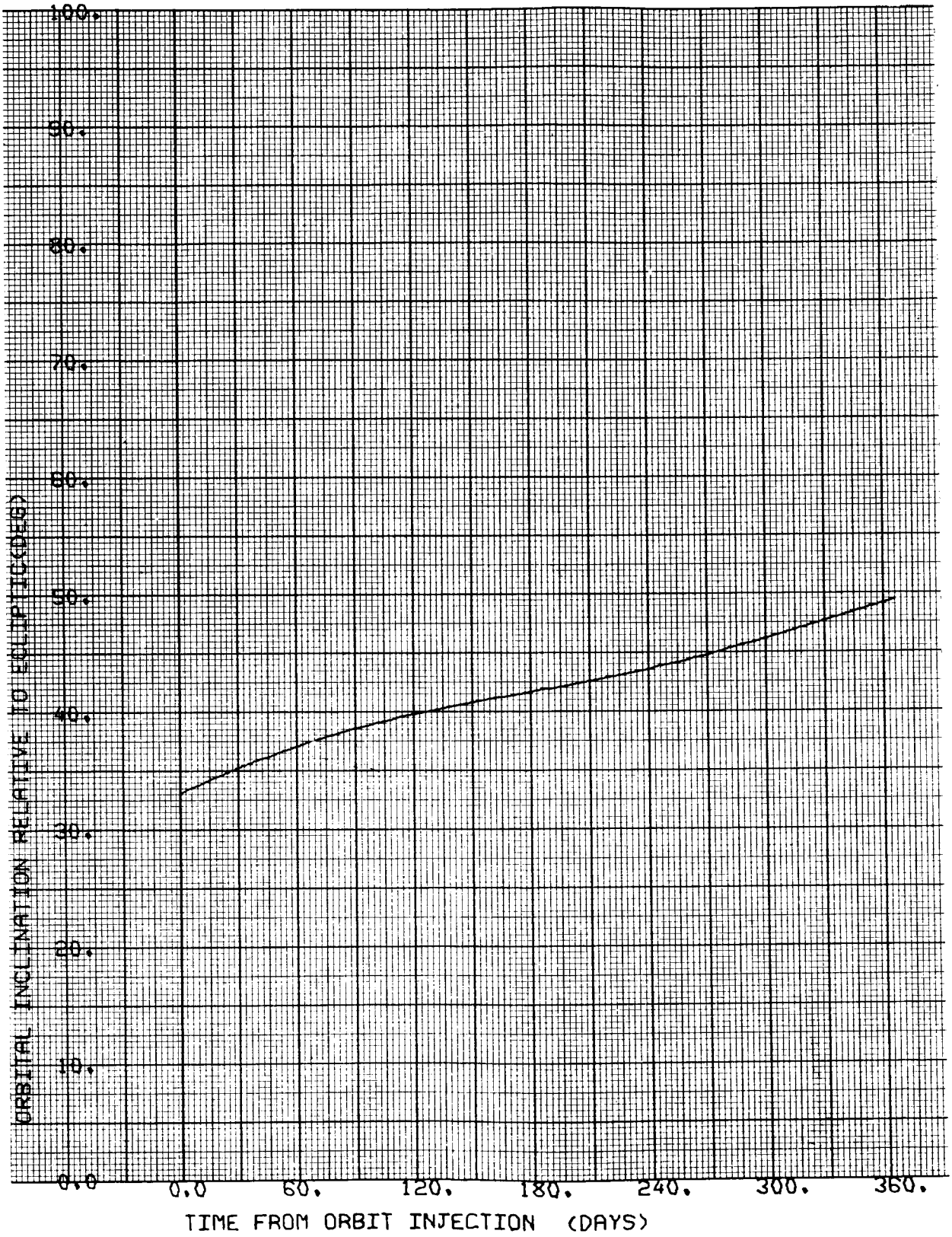
100.
90.
80.
70.
60.
50.
40.
30.
20.
10.
0.0
ORBITAL INCLINATION RELATIVE TO ECLIPTIC(DEG)
0.0
60.
120.
180.
240.
300.
360.
TIME FROM ORBIT INJECTION (DAYS)

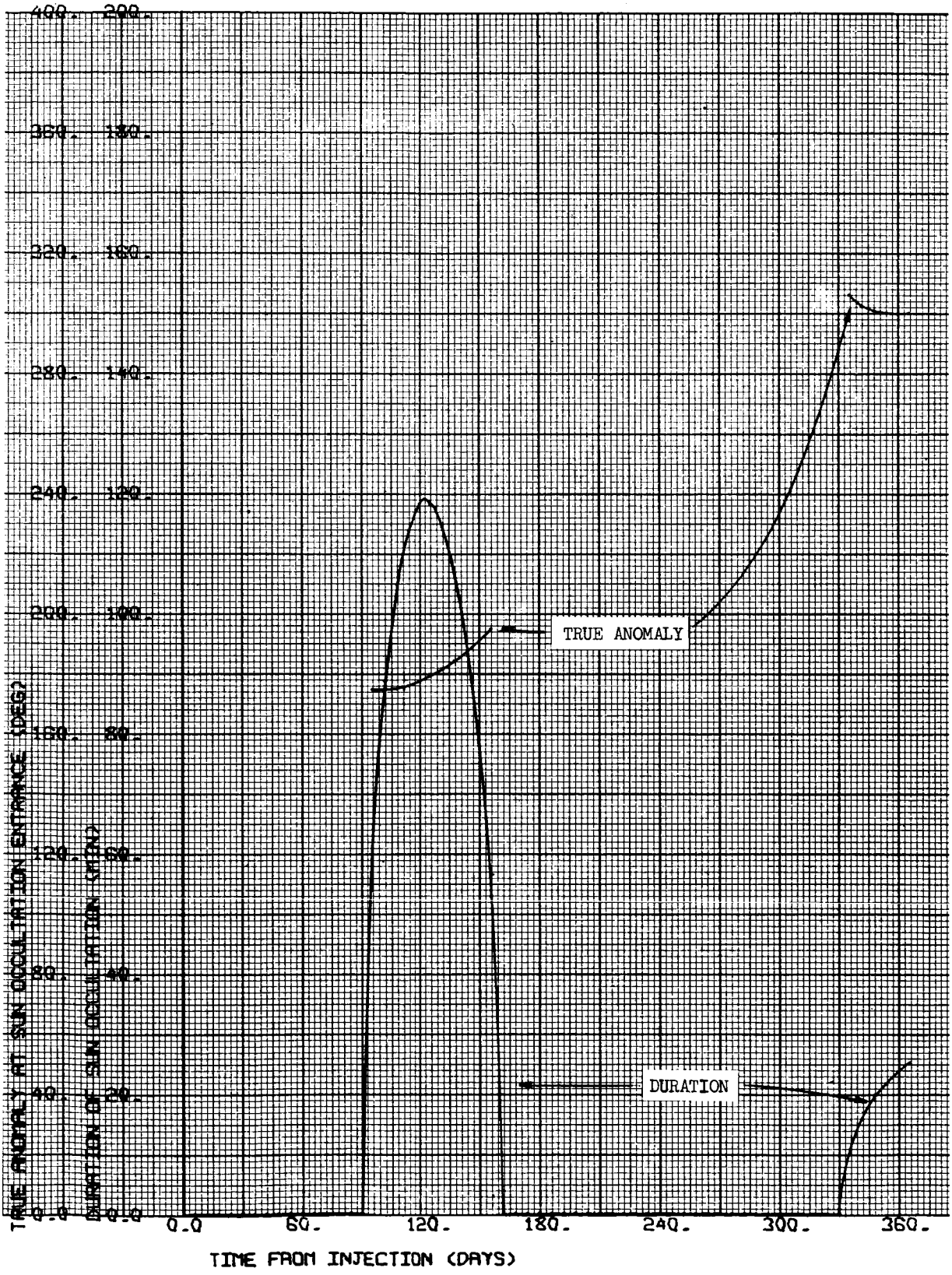
TRUE ANOMALY
DURATION
TRUE ANOMALY AT SUN OCCULTATION ENTRANCE (DEG)
DURATION OF SUN OCCULTATION (MIN)
TIME FROM INJECTION (DAYS)
0.0
60.
120.
180.
240.
300.
360.

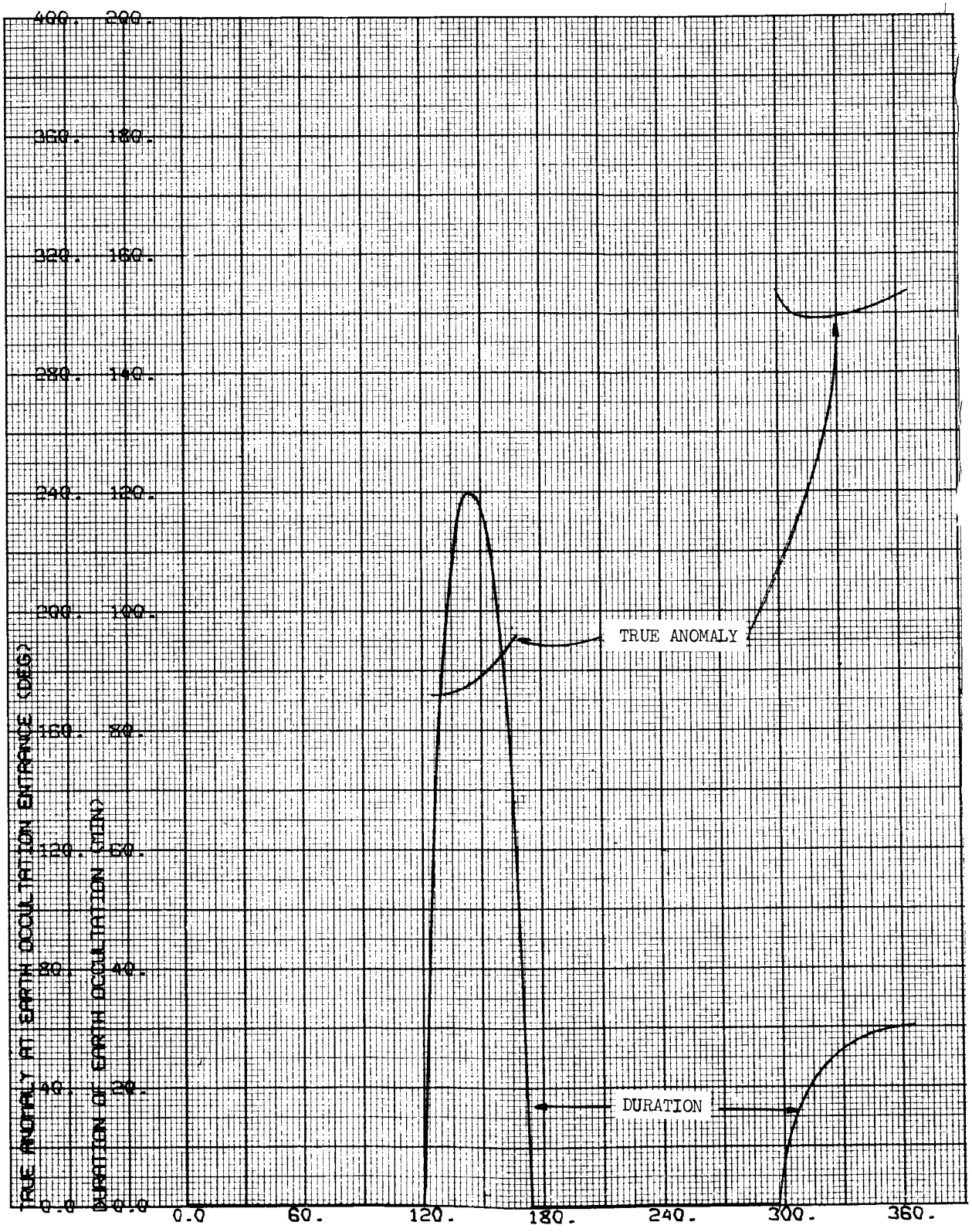
TRUE ANOMALY AT EARTH OCCULTATION ENTRANCE (DEG)
DURATION OF EARTH OCCULTATION (MIN)
TIME FROM INJECTION (DAYS)
TRUE ANOMALY
DURATION
0.0
60.
120.
180.
240.
300.
360.
400.
360.
320.
280.
240.
200.
160.
120.
80.
40.
0.0
200.
180.
160.
140.
120.
100.
80.
60.
40.
20.
0.0

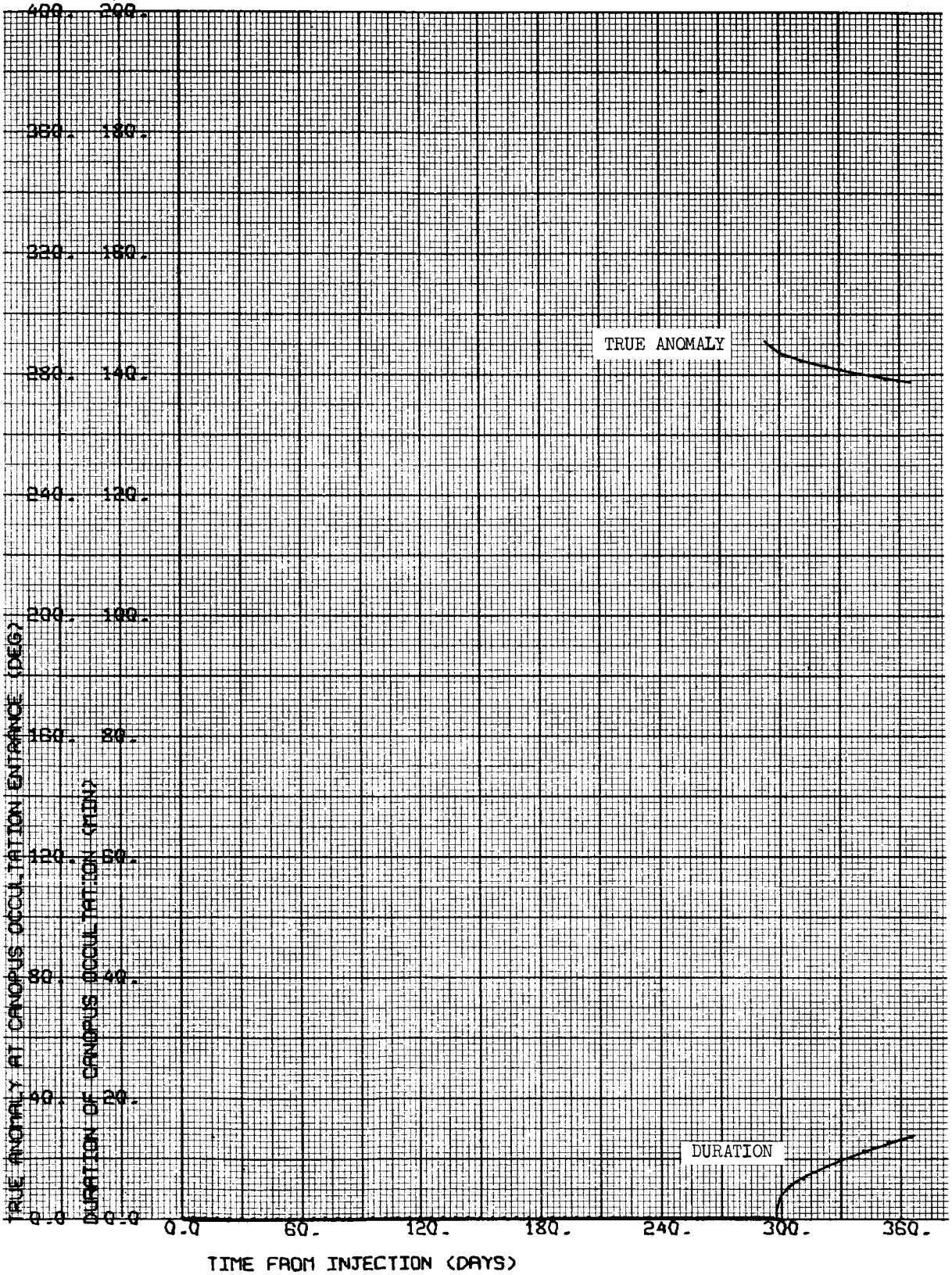
TRUE ANOMALY AT CANOPUS OCCULTATION ENTRANCE (DEG)
DURATION OF CANOPUS OCCULTATION (MIN)
TIME FROM INJECTION (DAYS)
TRUE ANOMALY
DURATION
0.0
60.
120.
180.
240.
300.
360.
400.
360.
320.
280.
240.
200.
160.
120.
80.
40.
0.0
300.
180.
160.
140.
120.
100.
80.
60.
40.
20.
0.0

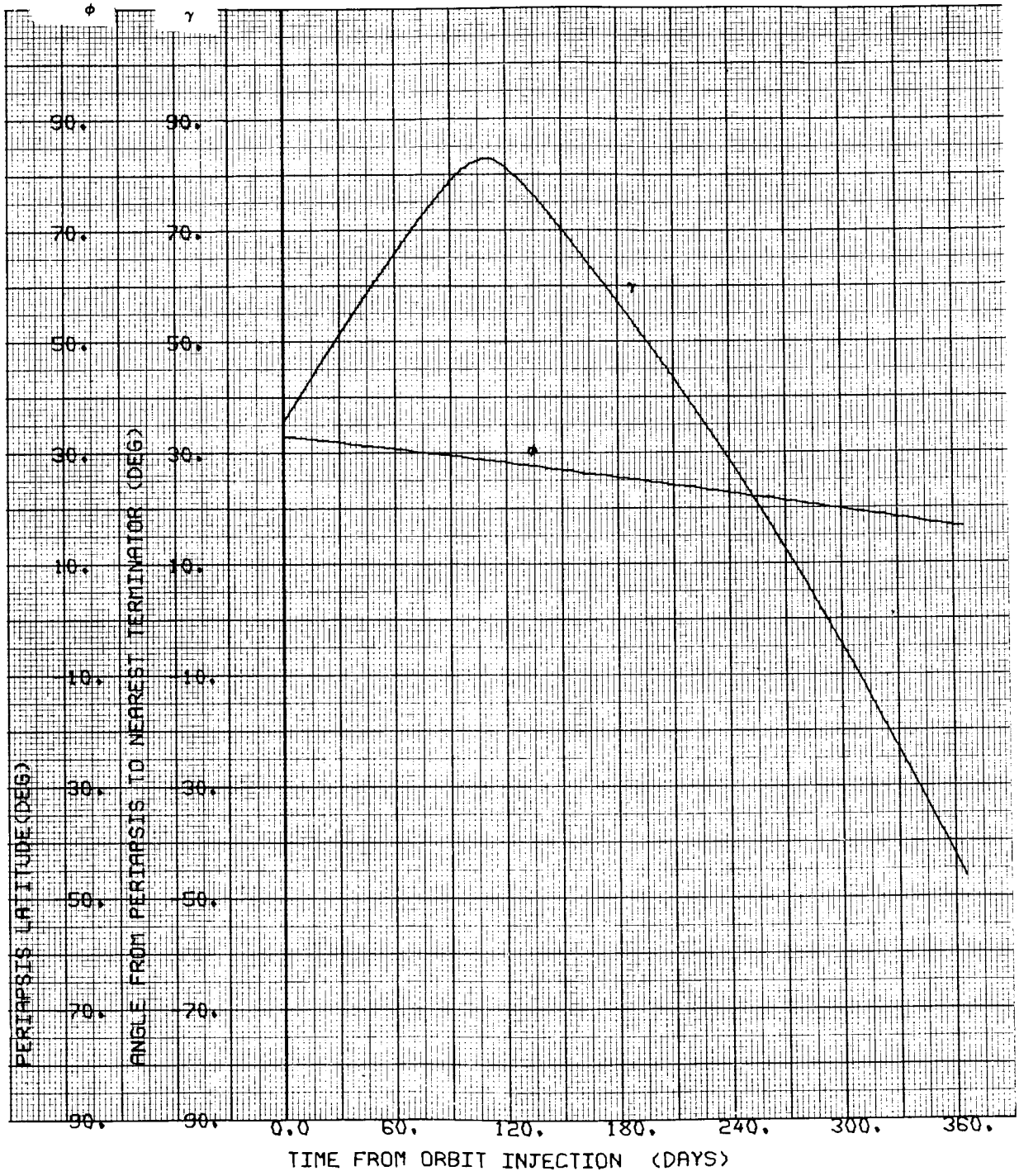
φ
γ
90.
70.
50.
30.
10.
-10.
-30.
-50.
-70.
-90.
γ
φ
PERIAPSIS LATITUDE (DEG)
ANGLE FROM PERIARSIS TO NEAREST TERMINATOR (DEG)
0.0
60.
120.
180.
240.
300.
360.
TIME FROM ORBIT INJECTION (DAYS)

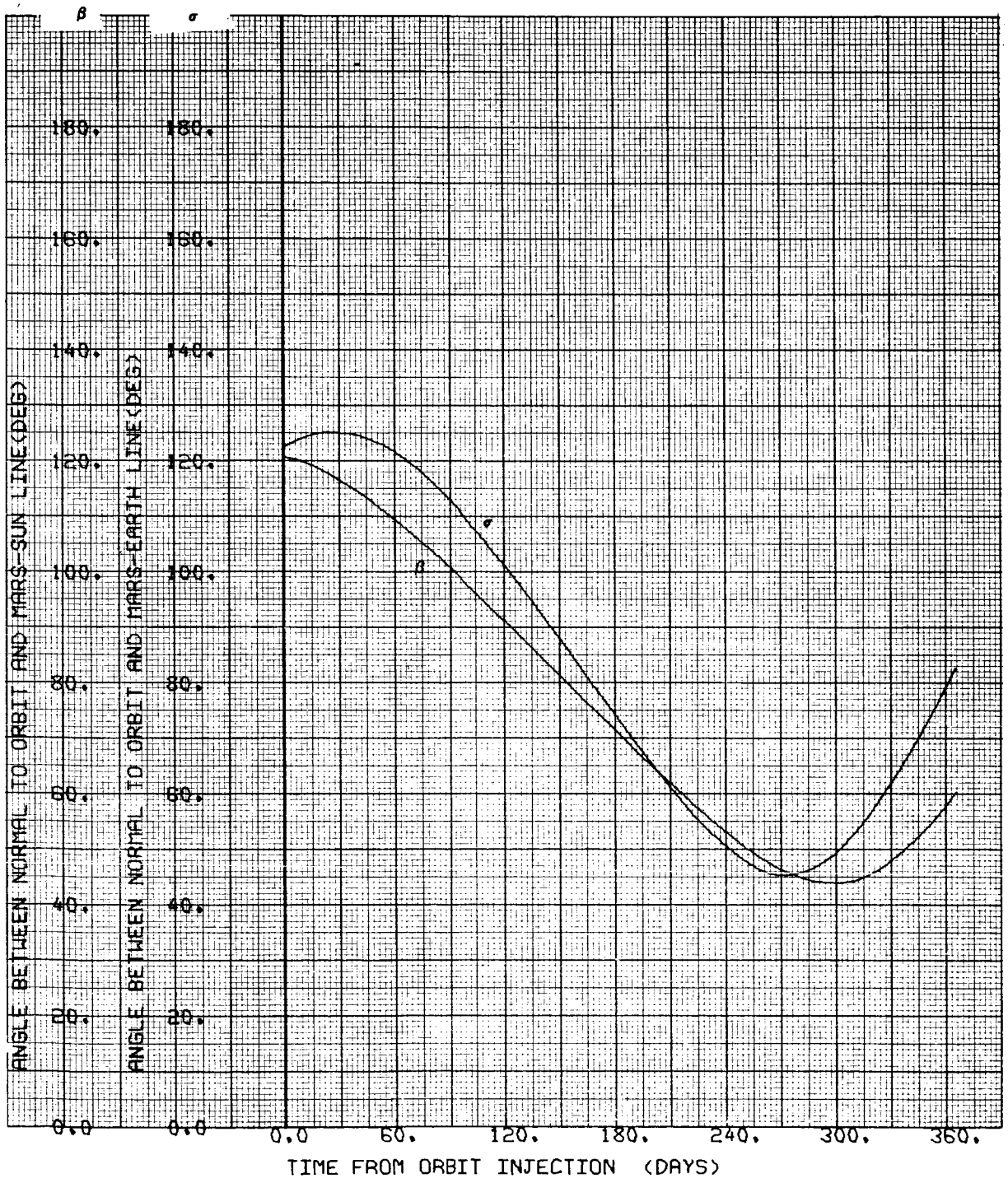
β
σ
180.
160.
140.
120.
100.
80.
60.
40.
20.
0.0
0.0
60.
120.
180.
240.
300.
360.
ANGLE BETWEEN NORMAL TO ORBIT AND MARS-SUN LINE(DEG)
ANGLE BETWEEN NORMAL TO ORBIT AND MARS-EARTH LINE(DEG)
TIME FROM ORBIT INJECTION (DAYS)

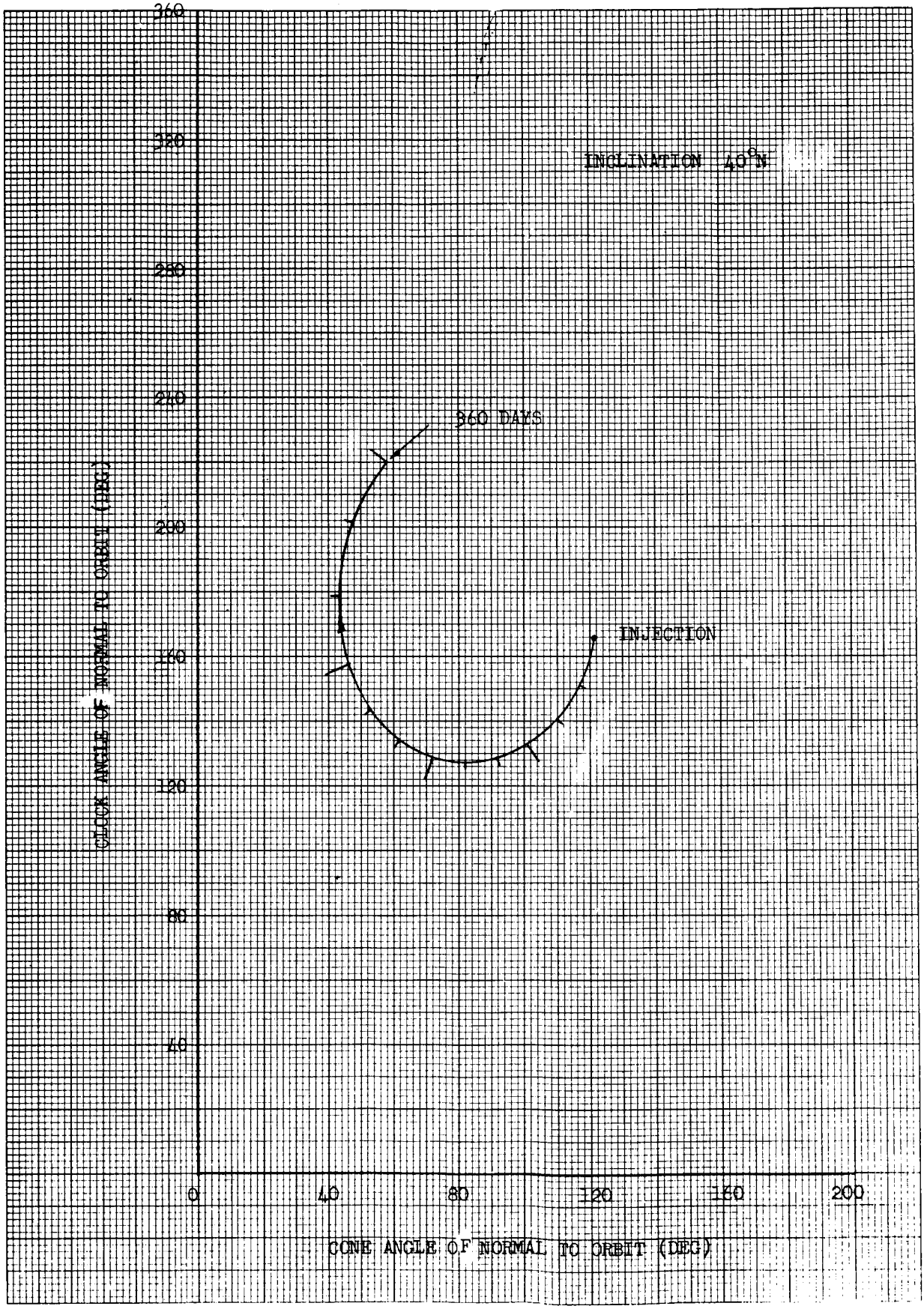
INCLINATION 40°N
360 DAYS
INJECTION
CLOCK ANGLE OF NORMAL TO ORBIT (DEG)
CONE ANGLE OF NORMAL TO ORBIT (DEG)
360
320
280
240
200
160
120
80
40
0
40
80
120
160
200

CASE NO. 27

1000 x 15,000 km

$i = 20^{\circ}S$

$\Psi = 125.289$ deg

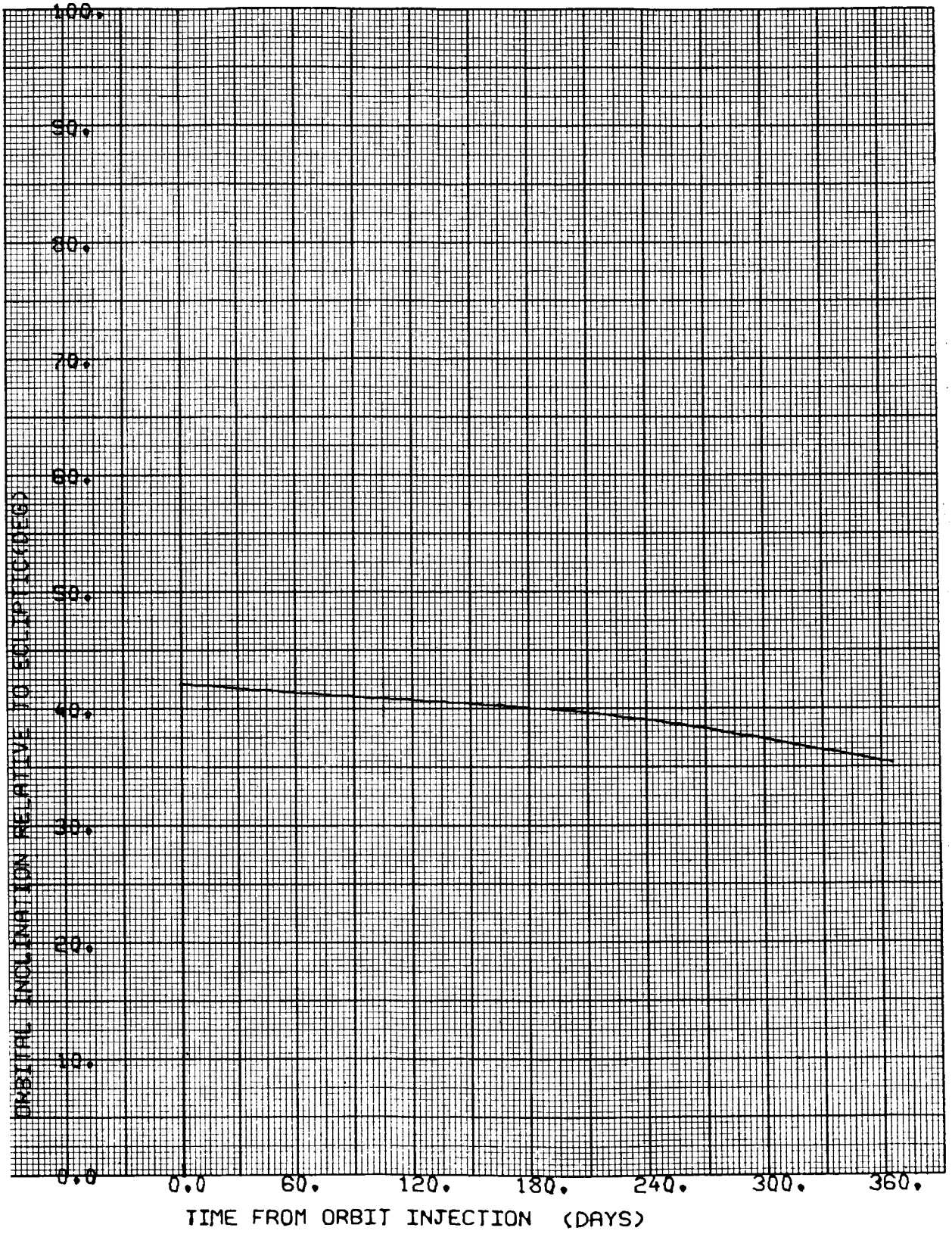
100.
90.
80.
70.
60.
50.
40.
30.
20.
10.
0.0
ORBITAL INCLINATION RELATIVE TO ECLIPTIC(DEG)
0.0
60.
120.
180.
240.
300.
360.
TIME FROM ORBIT INJECTION (DAYS)

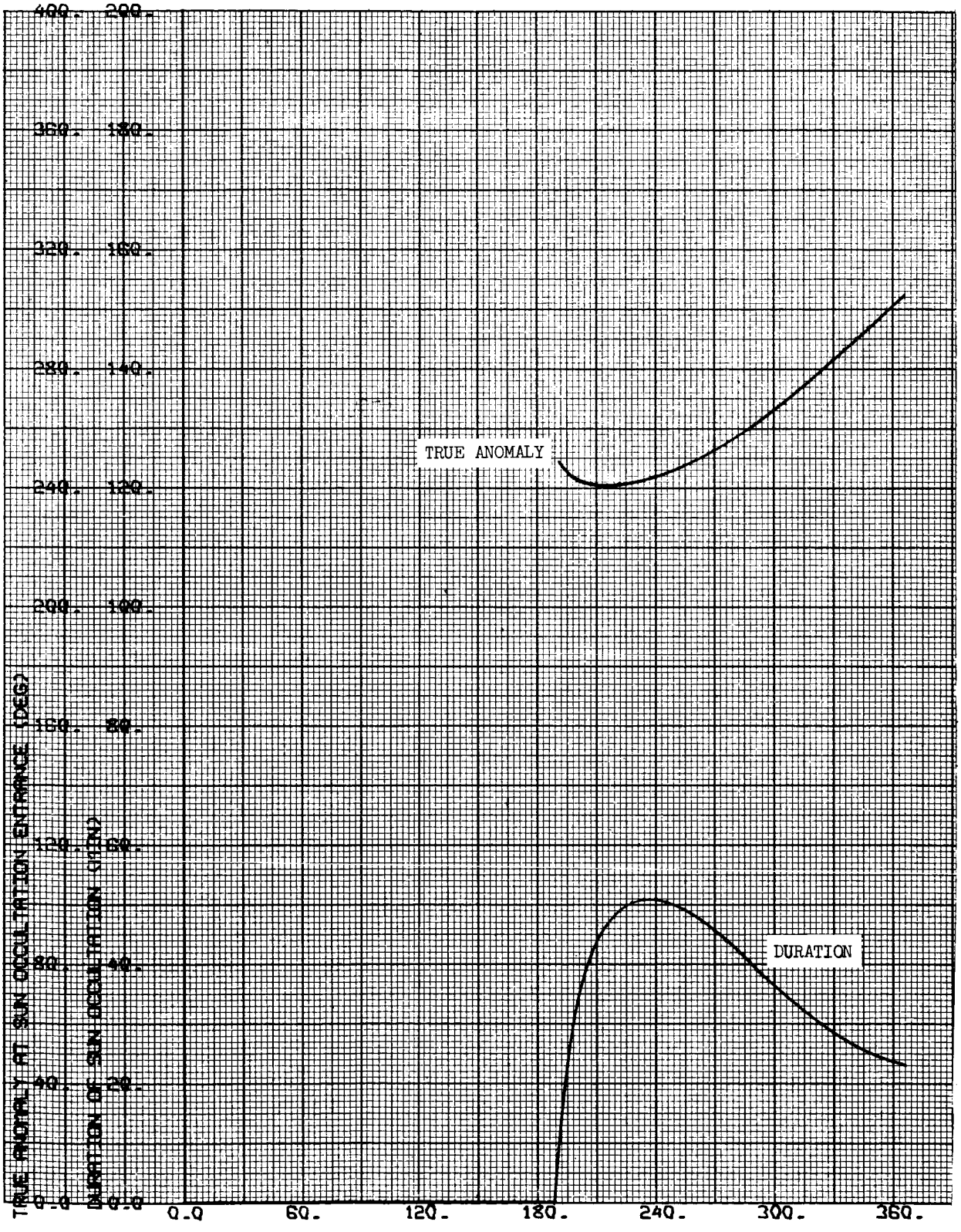
TRUE ANOMALY
DURATION
TRUE ANOMALY AT SUN OCCULTATION ENTRANCE (DEG)
DURATION OF SUN OCCULTATION (DAY)
TIME FROM INJECTION (DAYS)
0.0
60.
120.
180.
240.
300.
360.

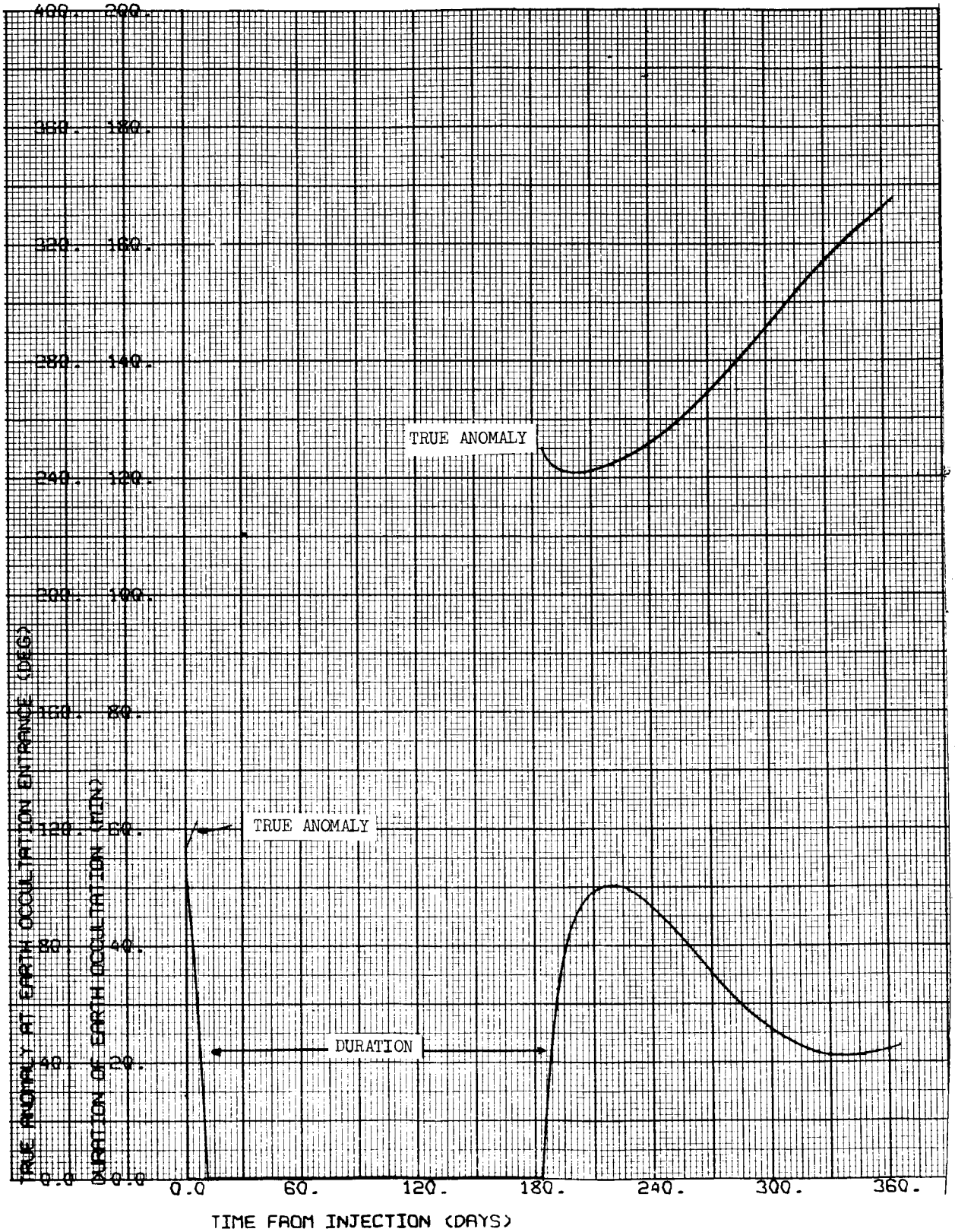
TRUE ANOMALY
TRUE ANOMALY
DURATION
TRUE ANOMALY AT EARTH OCCULTATION ENTRANCE (DEG)
DURATION OF EARTH OCCULTATION (MIN)
TIME FROM INJECTION (DAYS)
0.0
60.
120.
180.
240.
300.
360.
400.
360.
320.
280.
240.
200.
160.
120.
80.
40.
0.0
200.
180.
160.
140.
120.
100.
80.
60.
40.
20.
0.0

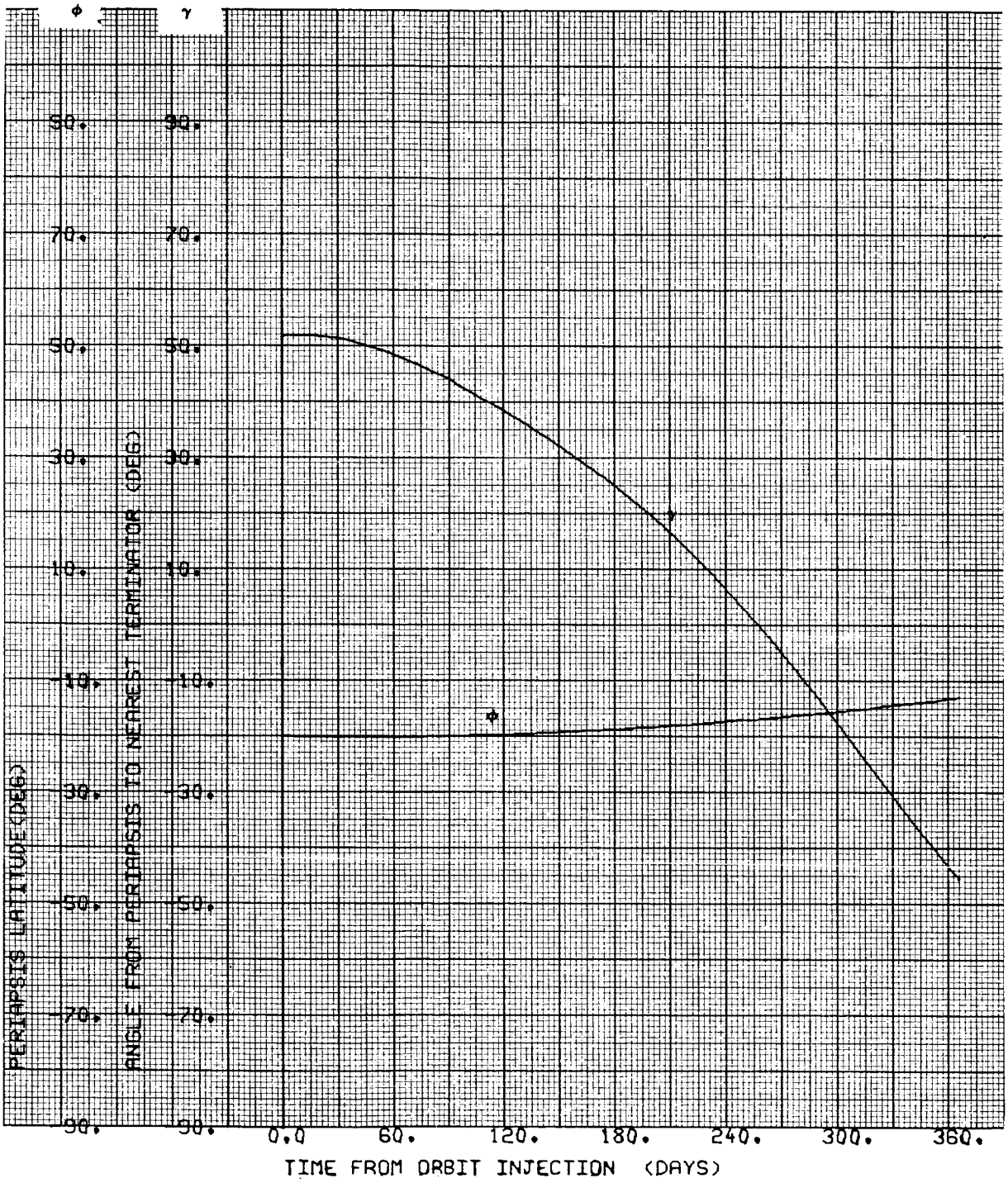
φ
γ
90.
70.
50.
30.
10.
-10.
-30.
-50.
-70.
-90.
0.0
60.
120.
180.
240.
300.
360.
PERIAPSIS LATITUDE (DEG)
ANGLE FROM PERIAPSIS TO NEAREST TERMINATOR (DEG)
TIME FROM ORBIT INJECTION (DAYS)

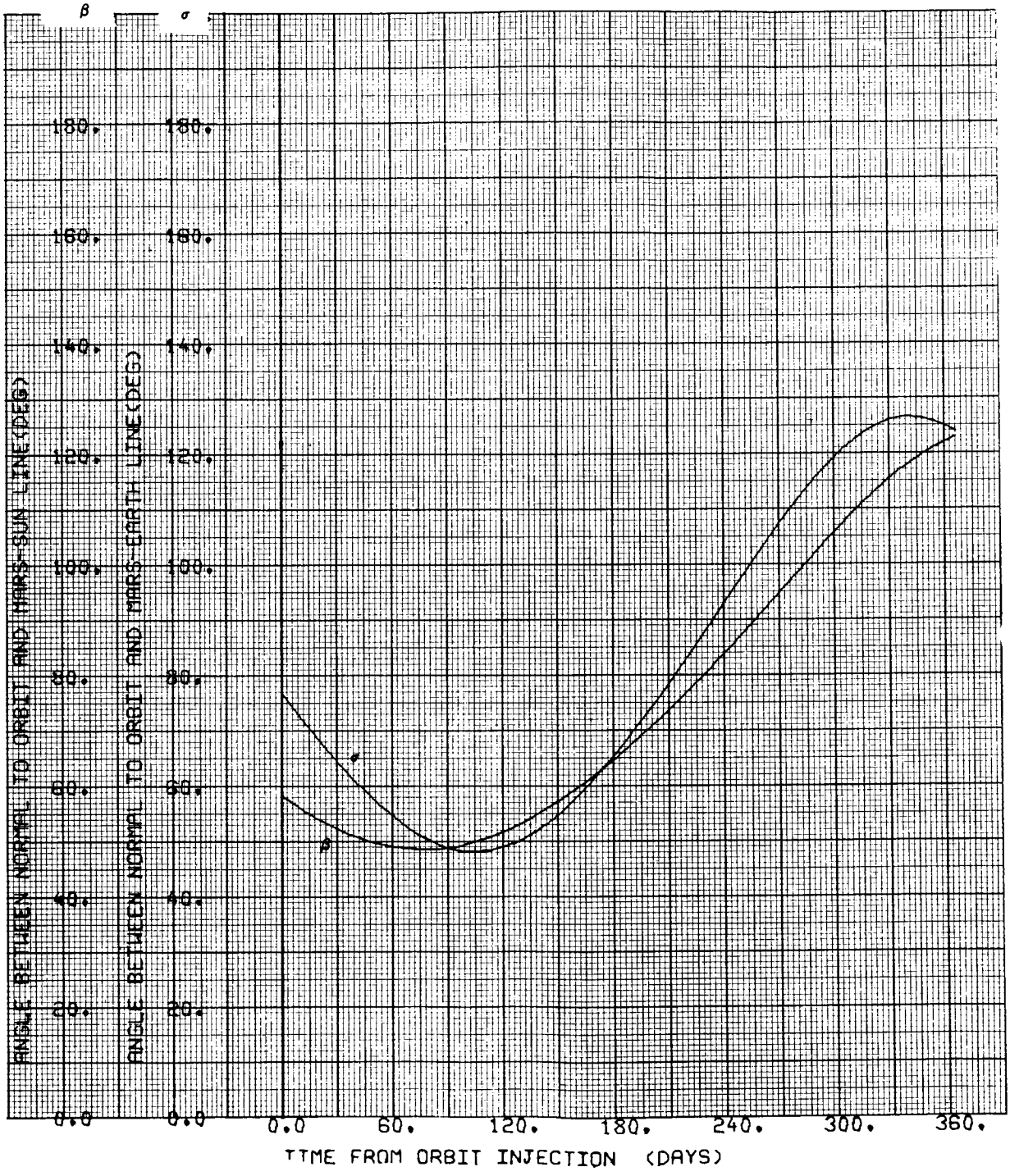
β
σ
180.
160.
140.
120.
100.
80.
60.
40.
20.
0.0
ANGLE BETWEEN NORMAL TO ORBIT AND MARS-SUN LINE(DEG)
ANGLE BETWEEN NORMAL TO ORBIT AND MARS-EARTH LINE(DEG)
0.0
60.
120.
180.
240.
300.
360.
TIME FROM ORBIT INJECTION (DAYS)

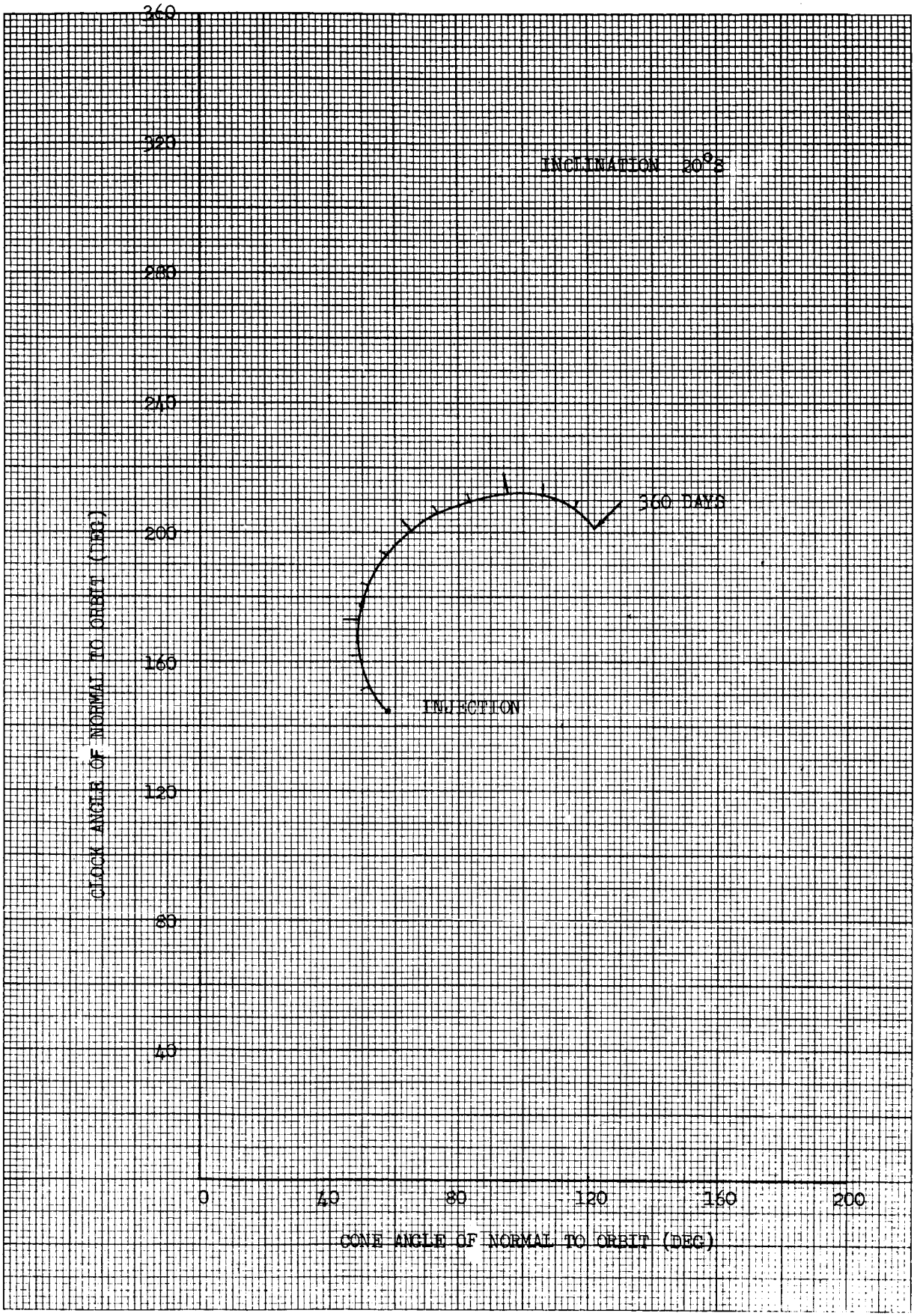
INCLINATION 20°S
360 DAYS
INJECTION
CLOCK ANGLE OF NORMAL TO ORBIT (DEG)
360
320
280
240
200
160
120
80
40
0
40
80
120
160
200
CONE ANGLE OF NORMAL TO ORBIT (DEG)

LAUNCH DATE AUGUST 22, 1973
ARRIVAL DATE APRIL 25, 1974
INCLINATION 20°S
APSIDAL ORIENTATION 125.289°
0 DAYS AFTER INJECTION
LATITUDE (DEG)
LONGITUDE (DEG)
EARTH OCCULTATION
SUN
EARTH
DAY
NIGHT
CANOPUS
NO SUN OR CANOPUS OCCULTATION

LAUNCH DATE AUGUST 22, 1973
ARRIVAL DATE APRIL 25, 1974
INCLINATION 20°S
APSIDAL ORIENTATION 125.289°
90 DAYS AFTER INJECTION
LATITUDE (DEG)
90
60
30
0
-30
-60
-90
-180
-150
-120
-90
-60
-30
0
30
60
90
120
150
180
LONGITUDE (DEG)
NIGHT
DAY
NIGHT
SUN
EARTH
CANOPUS
NO SUN, EARTH OR CANOPUS OCCULTATION

LAUNCH DATE AUGUST 22, 1973
ARRIVAL DATE APRIL 25, 1974
INCLINATION 20°S
APSIDAL ORIENTATION 125.289°
180 DAYS AFTER INJECTION
LATITUDE (DEG)
90
60
30
0
-30
-60
-90
-180
-150
-120
-90
-60
-30
0
30
60
90
120
150
180
LONGITUDE (DEG)
SUN
EARTH
CANOPUS
DAY
NIGHT
NIGHT
NO SUN, EARTH OR CANOPUS OCCULTATION

CASE NO. 28

1000 x 15,000 km

$i = 20^{o}N$

$\Psi = 125.289$ deg

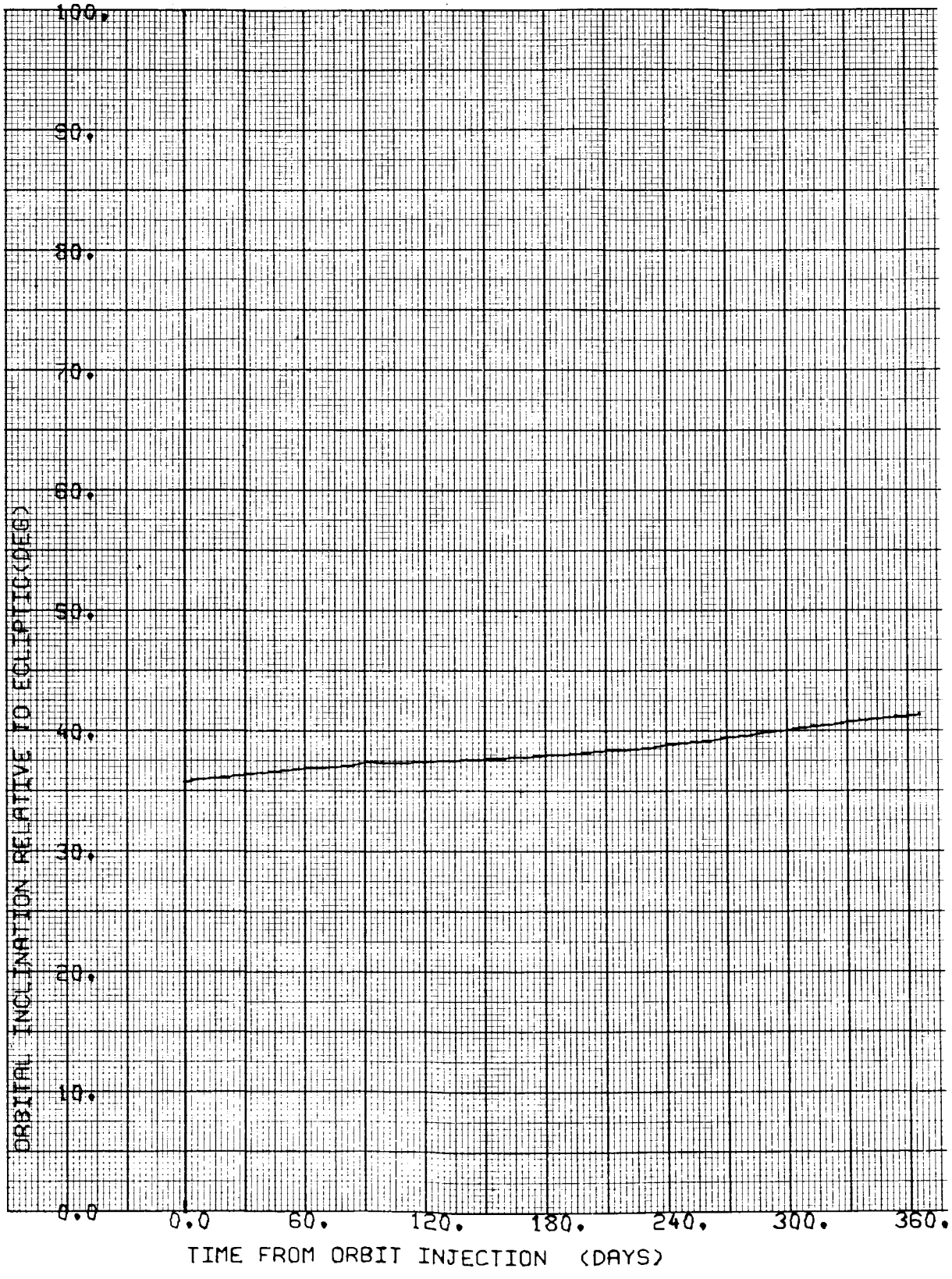
100.
90.
80.
70.
60.
50.
40.
30.
20.
10.
0.0
ORBITAL INCLINATION RELATIVE TO ECLIPTIC(DEG)
0.0
60.
120.
180.
240.
300.
360.
TIME FROM ORBIT INJECTION (DAYS)

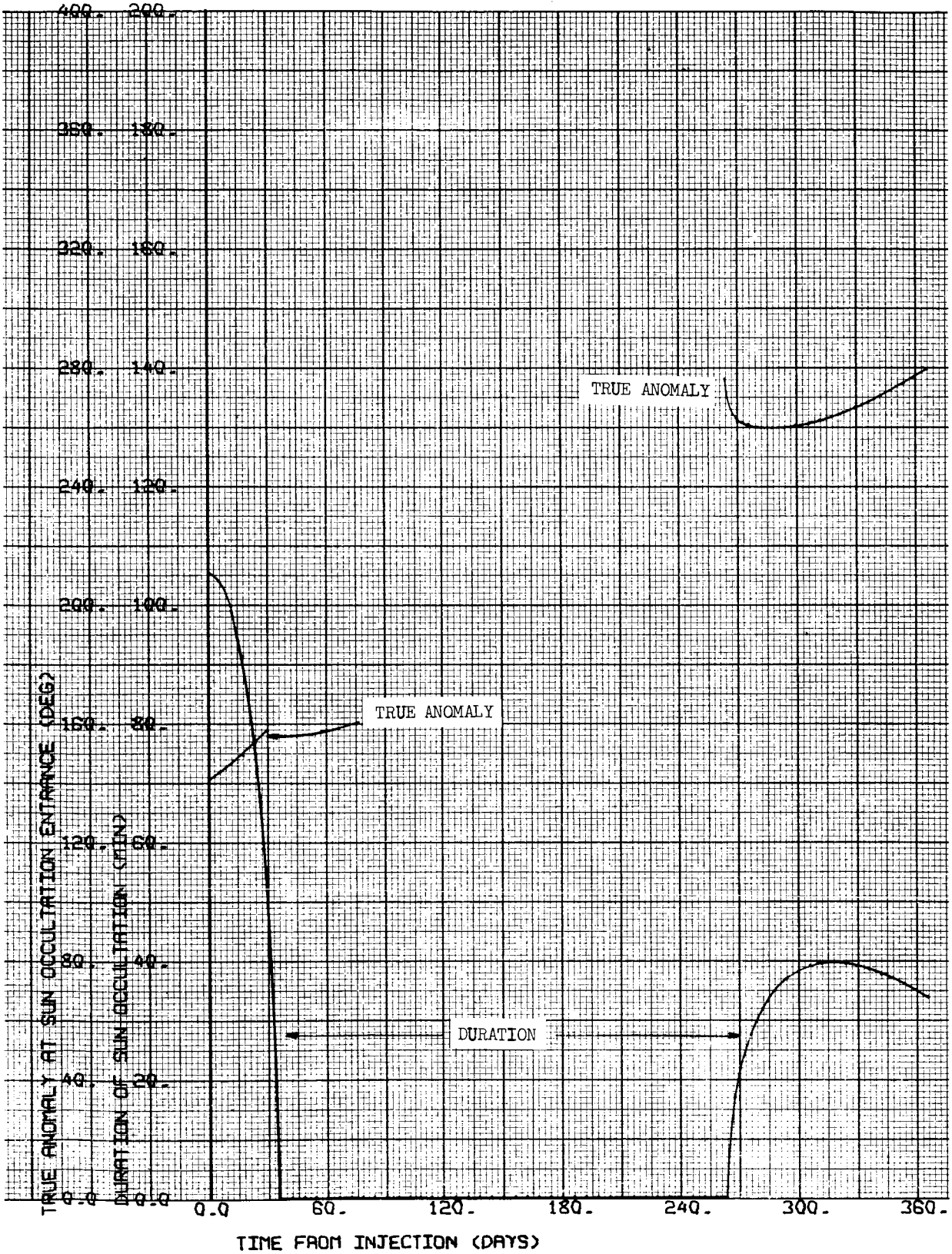
TRUE ANOMALY AT SUN OCCULTATION ENTRANCE (DEG)
DURATION OF SUN OCCULTATION (MIN)
TIME FROM INJECTION (DAYS)
TRUE ANOMALY
TRUE ANOMALY
DURATION
0.0
60.
120.
180.
240.
300.
360.
400.
360.
320.
280.
240.
200.
160.
120.
80.
40.
0.0
200.
180.
160.
140.
120.
100.
80.
60.
40.
20.
0.0

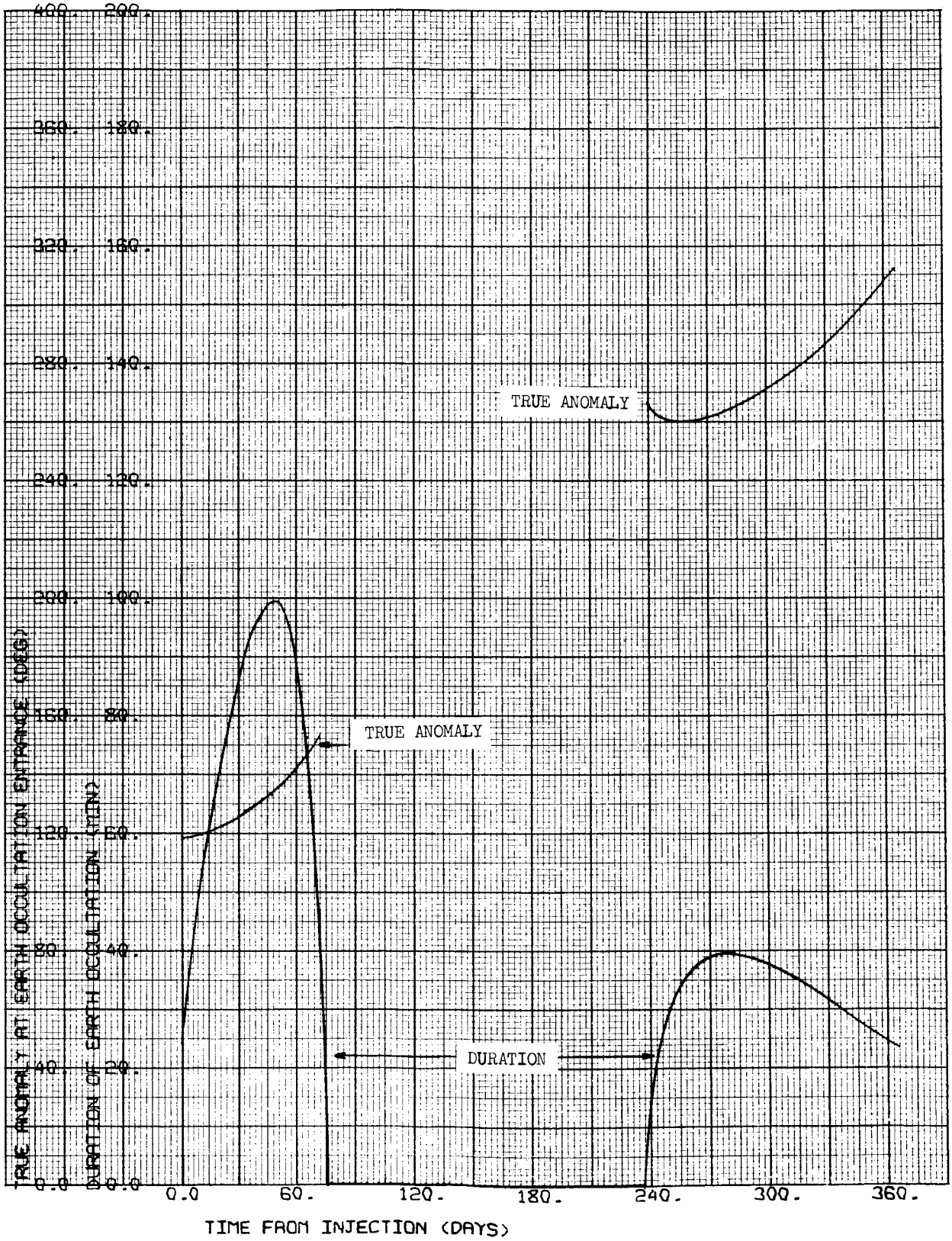
TRUE ANOMALY AT EARTH OCCULTATION ENTRANCE (DEG)
DURATION OF EARTH OCCULTATION (DEG)
TIME FROM INJECTION (DAYS)
TRUE ANOMALY
TRUE ANOMALY
DURATION
0.0
60.
120.
180.
240.
300.
360.
400.
360.
320.
280.
240.
200.
160.
120.
80.
40.
0.0
200.
180.
160.
140.
120.
100.
80.
60.
40.
20.
0.0

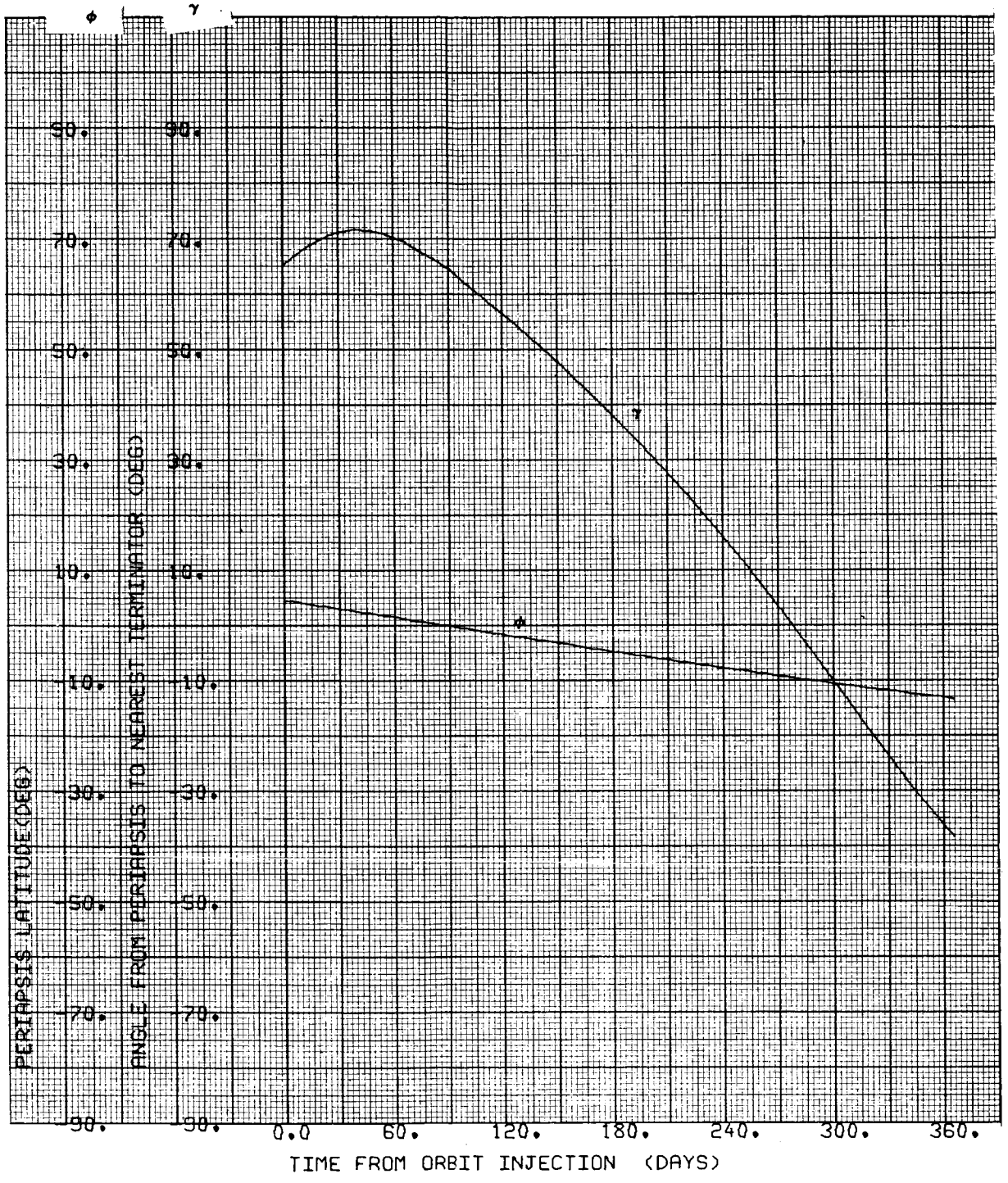
φ
γ
90.
70.
50.
30.
10.
-10.
-30.
-50.
-70.
-90.
PERIAPSIS LATITUDE(DEG)
ANGLE FROM PERIAPSIS TO NEAREST TERMINATOR (DEG)
0.0
60.
120.
180.
240.
300.
360.
TIME FROM ORBIT INJECTION (DAYS)

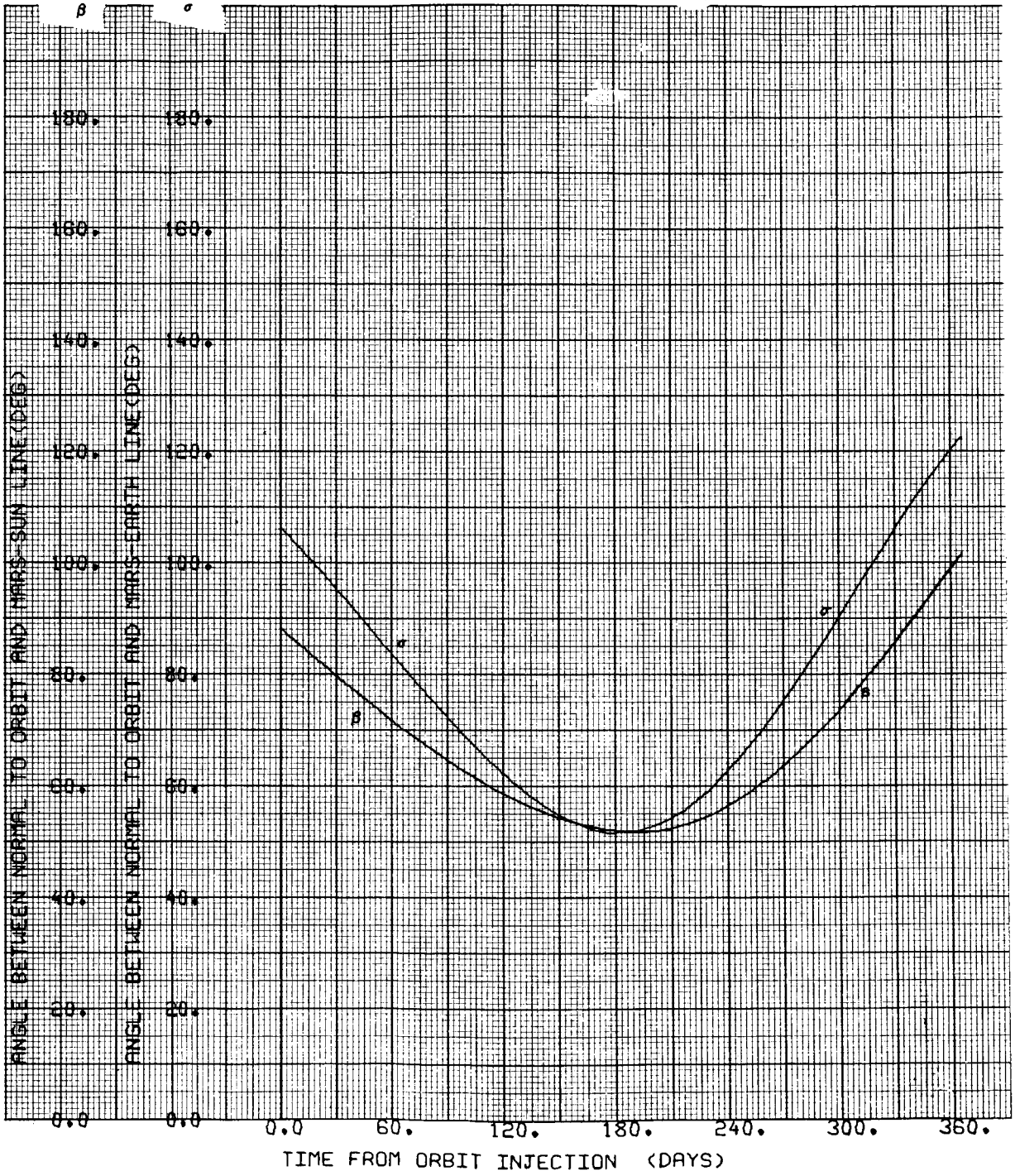
β
σ
180.
160.
140.
120.
100.
80.
60.
40.
20.
0.0
ANGLE BETWEEN NORMAL TO ORBIT AND MARS-SUN LINE(DEG)
ANGLE BETWEEN NORMAL TO ORBIT AND MARS-EARTH LINE(DEG)
0.0
60.
120.
180.
240.
300.
360.
TIME FROM ORBIT INJECTION (DAYS)

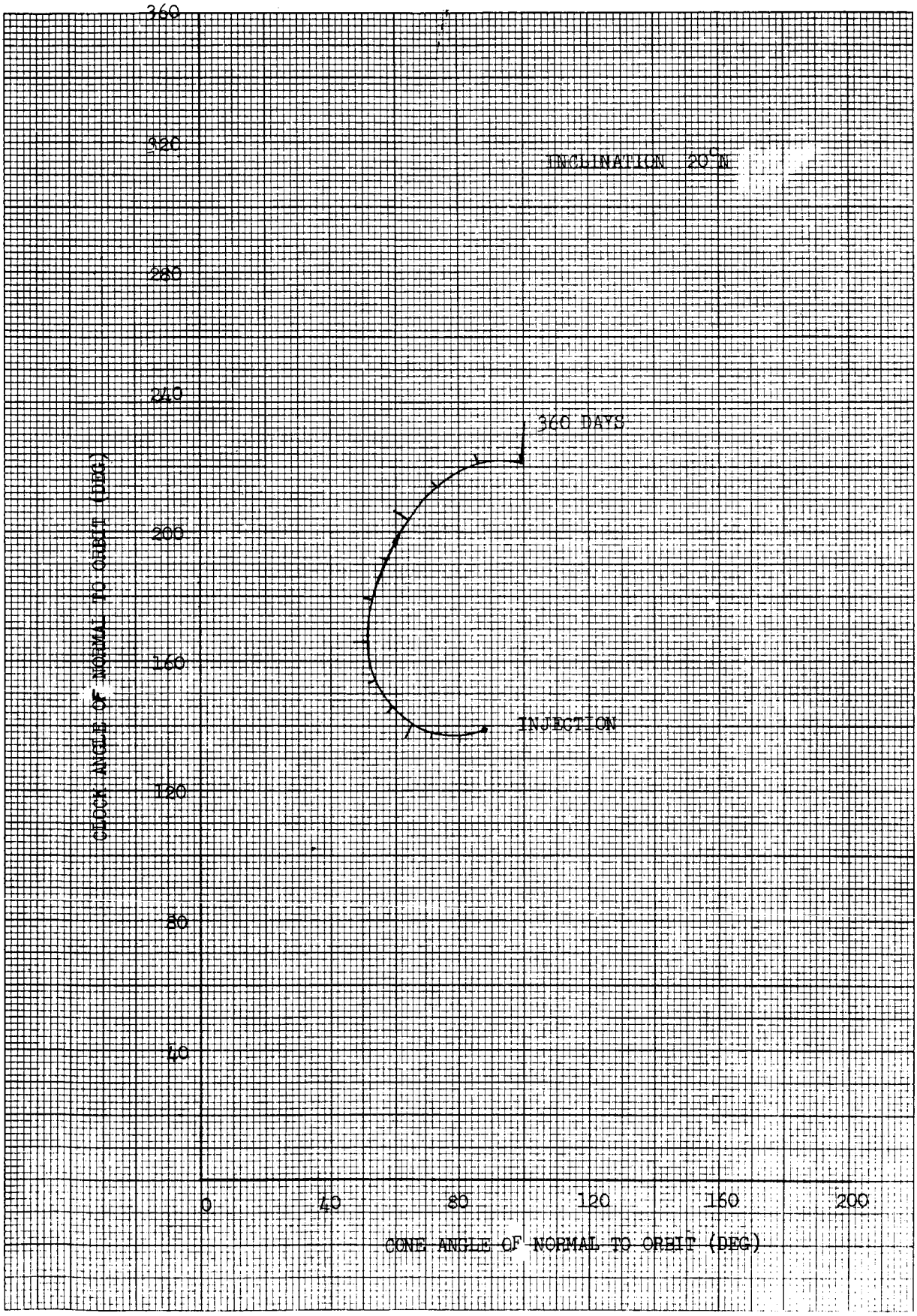
INCLINATION 20° N
360 DAYS
INJECTION
CLOCK ANGLE OF NORMAL TO ORBIT (DEG)
360
320
280
240
200
160
120
80
40
0
40
80
120
160
200
CONE ANGLE OF NORMAL TO ORBIT (DEG)

LAUNCH DATE AUGUST 22, 1973
ARRIVAL DATE APRIL 25, 1974
INCLINATION 20°N
APSIDAL ORIENTATION 125.289°
0 DAYS AFTER INJECTION
LATITUDE (DEG)
LONGITUDE (DEG)
EARTH OCCULTATION
SUN
EARTH
SUN OCCULTATION
NIGHT
DAY
CANOPUS
NO CANOPUS OCCULTATION

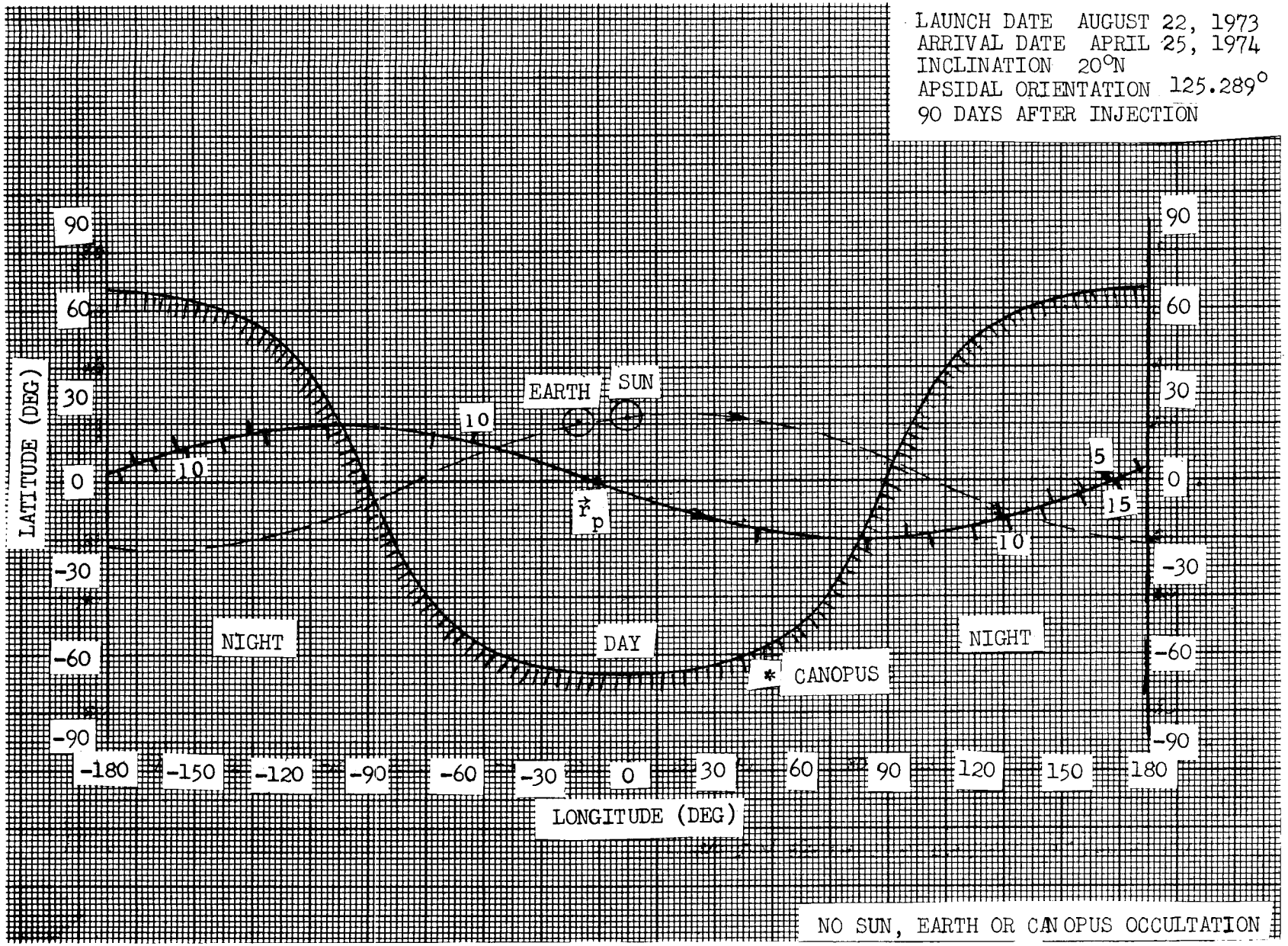
LAUNCH DATE AUGUST 22, 1973
ARRIVAL DATE APRIL 25, 1974
INCLINATION 20°N
APSIDAL ORIENTATION 125.289°
90 DAYS AFTER INJECTION
LATITUDE (DEG)
90
60
30
0
-30
-60
-90
EARTH
SUN
10
10
5
15
10
NIGHT
DAY
NIGHT
CANOPUS
-180
-150
-120
-90
-60
-30
0
30
60
90
120
150
180
LONGITUDE (DEG)
NO SUN, EARTH OR CANOPUS OCCULTATION

LAUNCH DATE AUGUST 22, 1973
ARRIVAL DATE APRIL 25, 1974
INCLINATION 20°N
APSIDAL ORIENTATION 125.289°
180 DAYS AFTER INJECTION
LATITUDE (DEG)
LONGITUDE (DEG)
90
60
30
0
-30
-60
-90
-180
-150
-120
-90
-60
-30
0
30
60
90
120
150
180
10
5
15
10
10
r_p
SUN
EARTH
CANOPUS
DAY
NIGHT
NIGHT
NO SUN, EARTH OR CANOPUS OCCULTATION

CASE NO. 29

1000 x 15, 000 km

$i = 40^{o}S$

$\Psi = 125.289$ deg

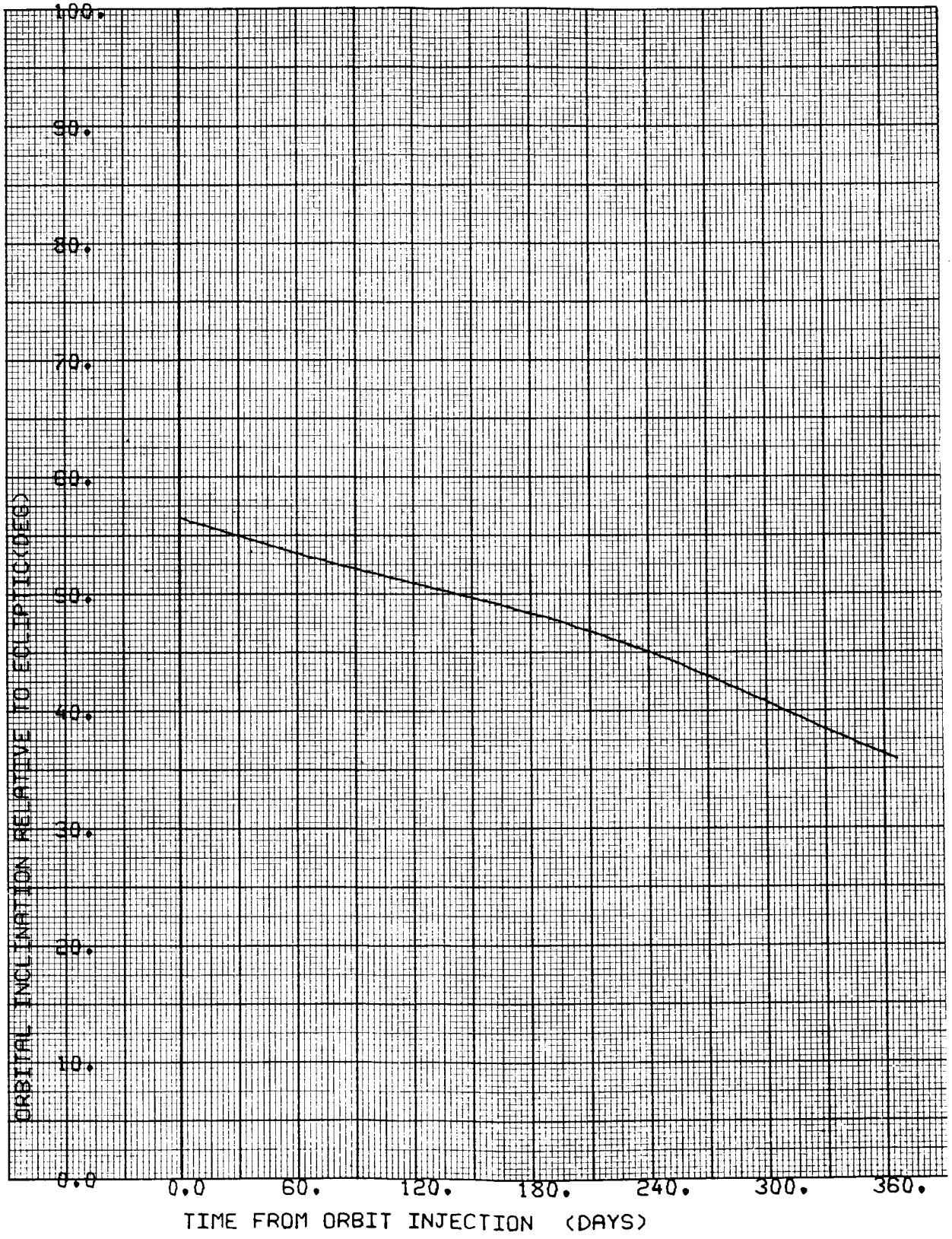
100.
90.
80.
70.
60.
50.
40.
30.
20.
10.
0.0
ORBITAL INCLINATION RELATIVE TO ECLIPTIC(DEG)
0.0
60.
120.
180.
240.
300.
360.
TIME FROM ORBIT INJECTION (DAYS)

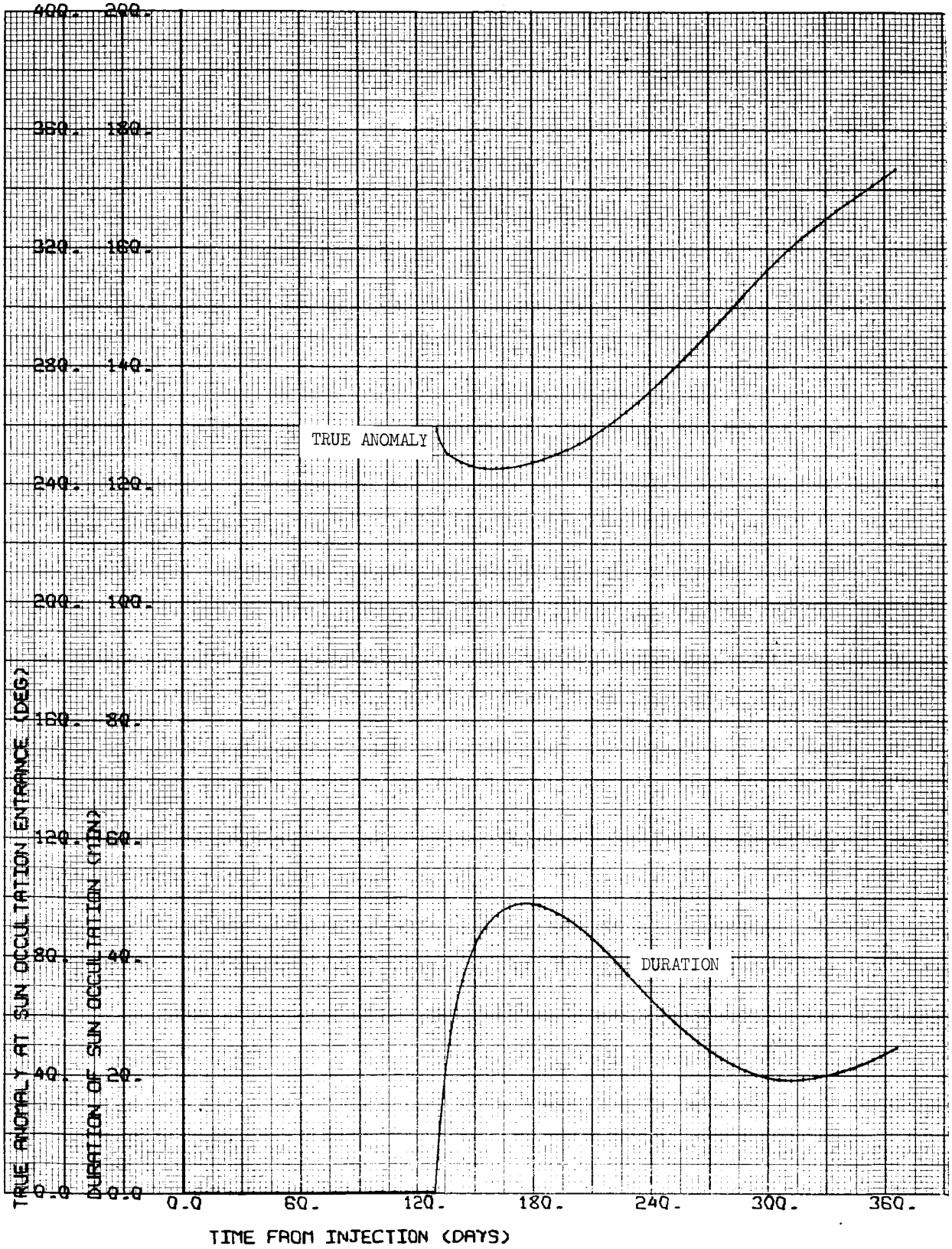
TRUE ANOMALY
DURATION
TRUE ANOMALY AT SUN OCCULTATION ENTRANCE (DEG)
DURATION OF SUN OCCULTATION (MIN)
TIME FROM INJECTION (DAYS)
0.0
60.
120.
180.
240.
300.
360.
400.
360.
320.
280.
240.
200.
160.
120.
80.
40.
0.0
200.
180.
160.
140.
120.
100.
80.
60.
40.
20.
0.0

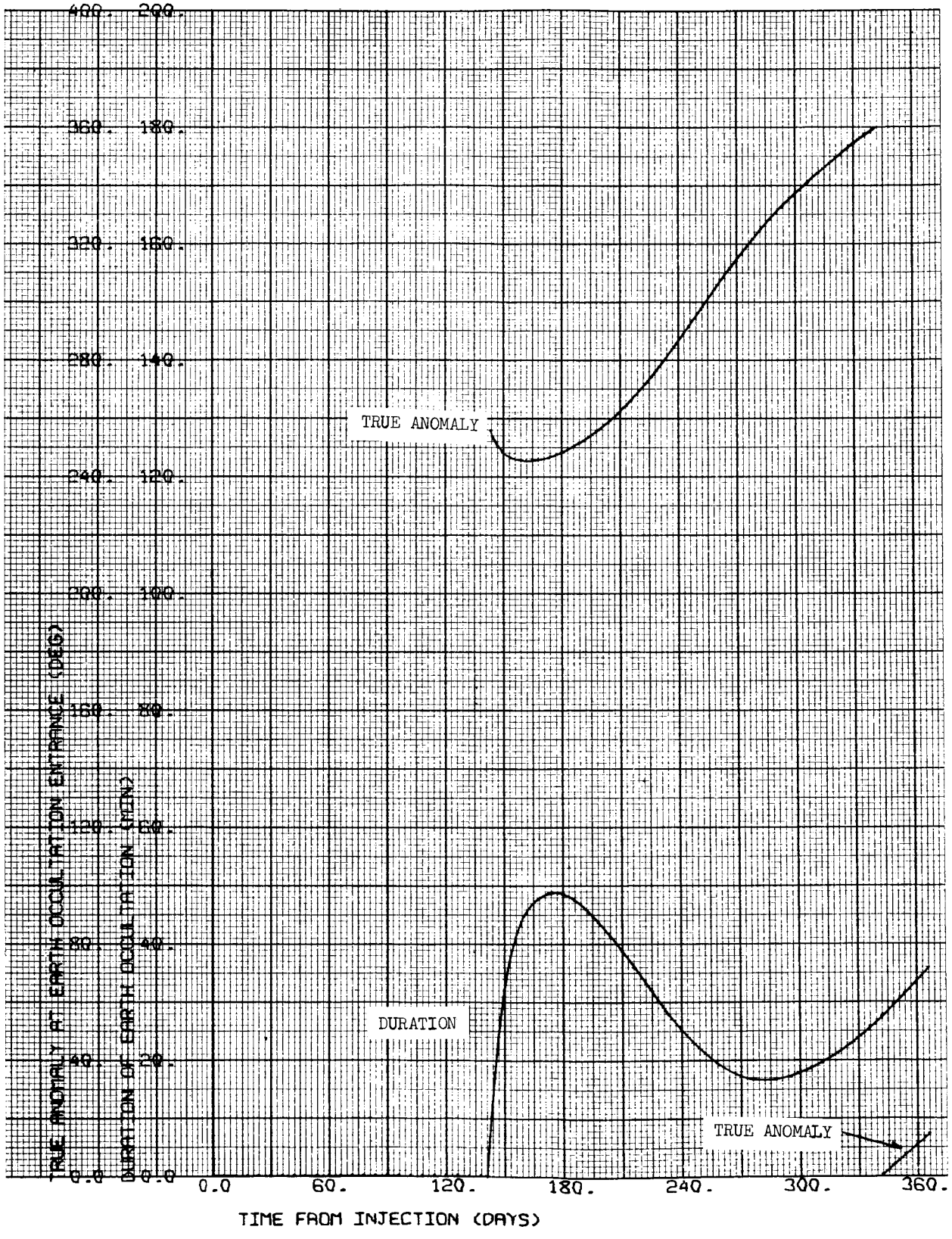
TRUE ANOMALY
DURATION
TRUE ANOMALY
TRUE ANOMALY AT EARTH OCCULTATION ENTRANCE (DEG)
DURATION OF EARTH OCCULTATION (DEG)
TIME FROM INJECTION (DAYS)
0.0
60.
120.
180.
240.
300.
360.
400.
360.
320.
280.
240.
200.
160.
120.
80.
40.
0.0
200.
180.
160.
140.
120.
100.
80.
60.
40.
20.
0.0

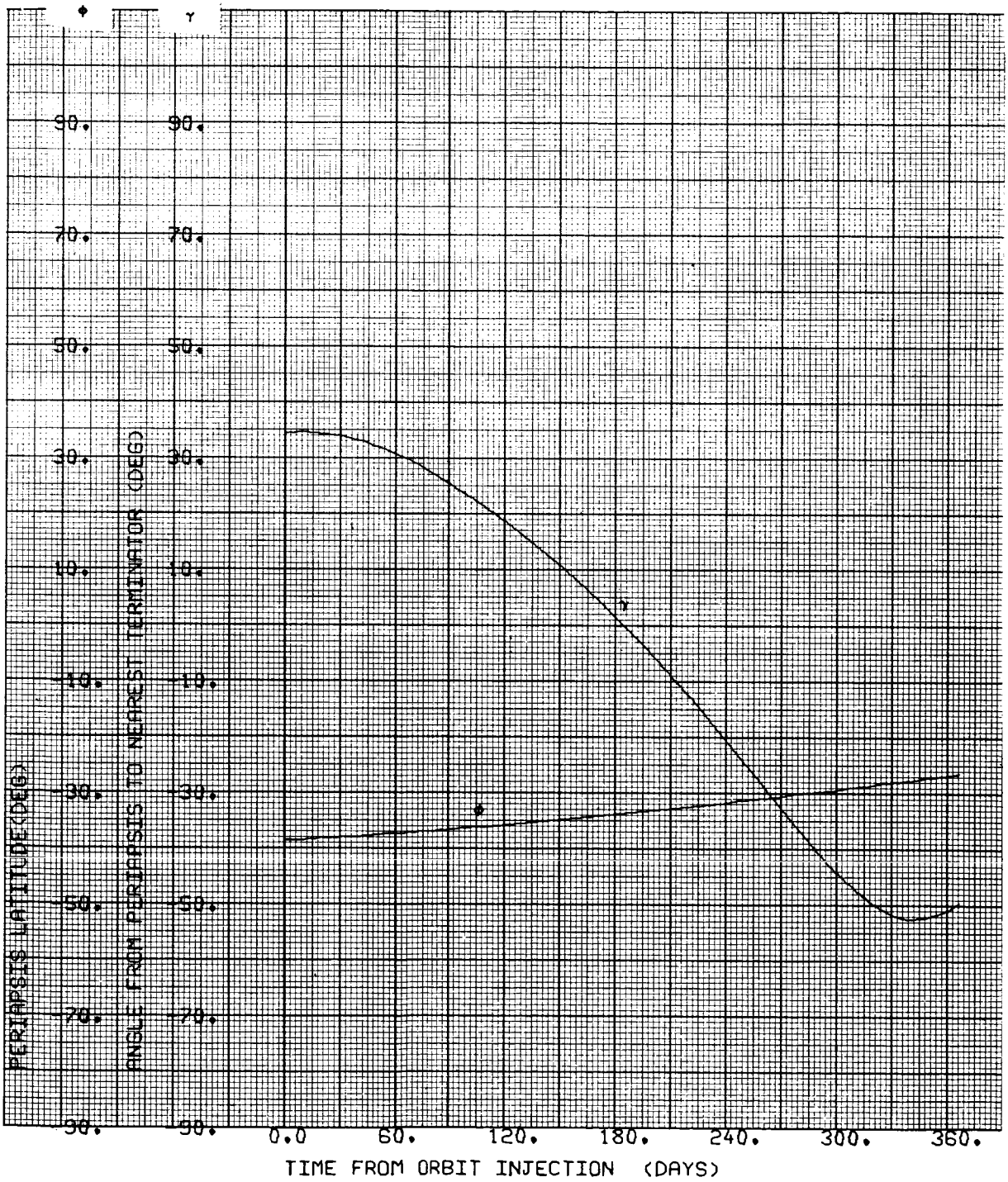
Φ
γ
90.
70.
50.
30.
10.
-10.
-30.
-50.
-70.
-90.
PERIAPSIS LATITUDE (DEG)
ANGLE FROM PERIAPSIS TO NEAREST TERMINATOR (DEG)
0.0
60.
120.
180.
240.
300.
360.
TIME FROM ORBIT INJECTION (DAYS)

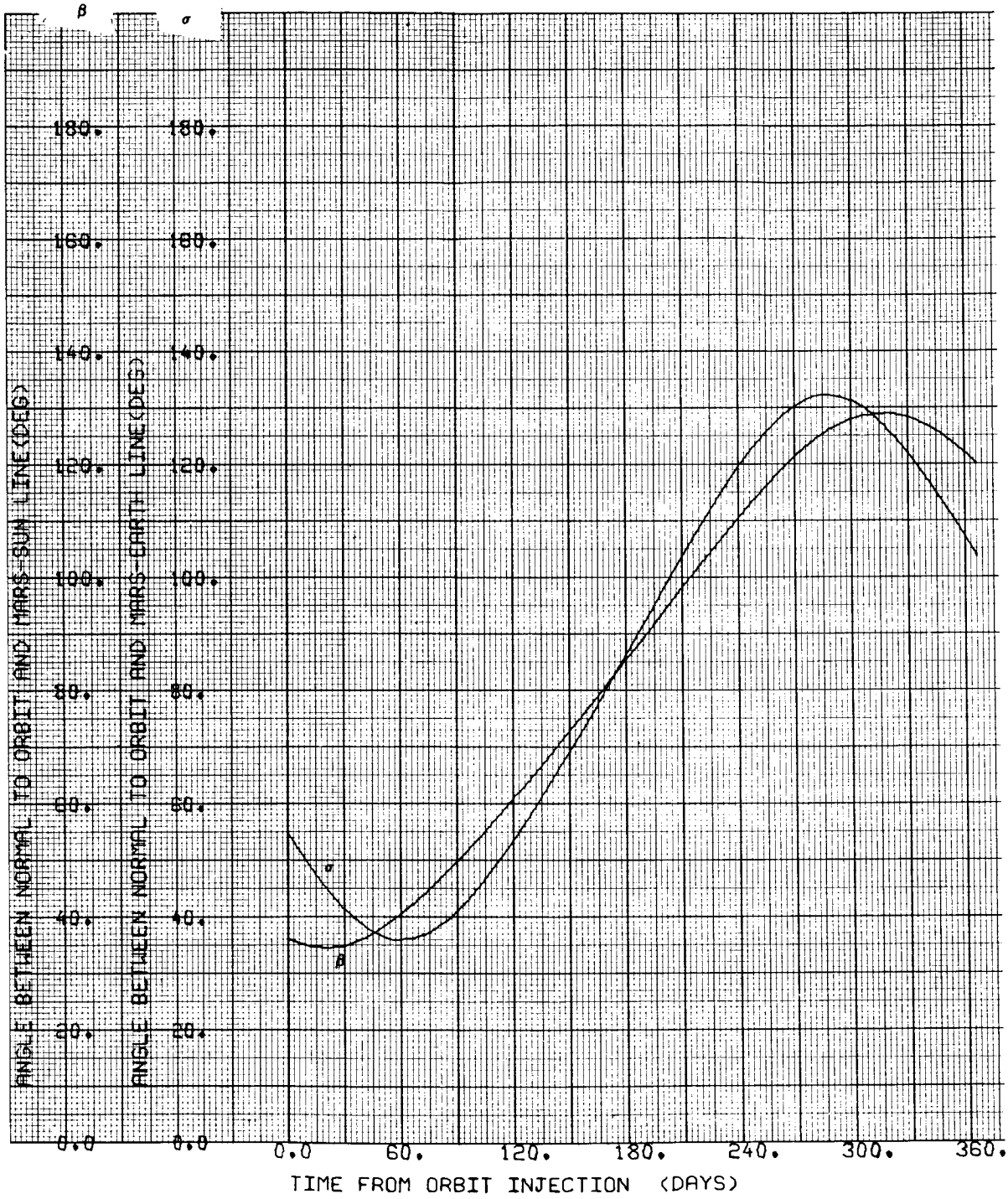
β
σ
180.
160.
140.
120.
100.
80.
60.
40.
20.
0.0
ANGLE BETWEEN NORMAL TO ORBIT AND MARS-SUN LINE (DEG)
ANGLE BETWEEN NORMAL TO ORBIT AND MARS-EARTH LINE (DEG)
0.0
60.
120.
180.
240.
300.
360.
TIME FROM ORBIT INJECTION (DAYS)

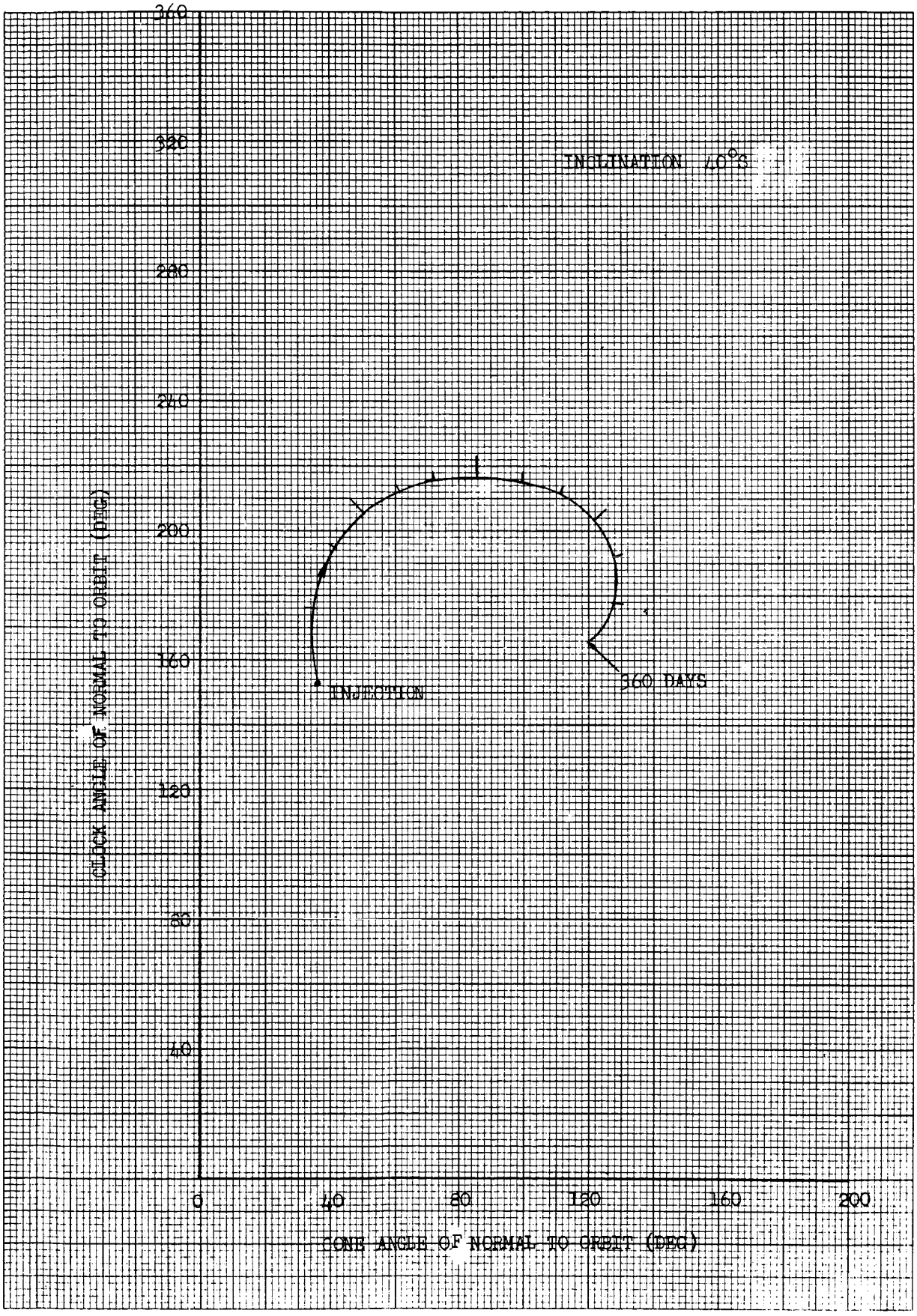
INCLINATION 40°S
INJECTION
360 DAYS
CLOCK ANGLE OF NORMAL TO ORBIT (DEG)
CONE ANGLE OF NORMAL TO ORBIT (DEG)
360
320
280
240
200
160
120
80
40
0
40
80
120
160
200

LAUNCH DATE AUGUST 22, 1973
ARRIVAL DATE APRIL 25, 1974
INCLINATION 40°S
APSIDAL ORIENTATION 125.289°
0 DAYS AFTER INJECTION
LATITUDE (DEG)
LONGITUDE (DEG)
90
60
30
0
-30
-60
-90
-180
-150
-120
-90
-60
-30
0
30
60
90
120
150
180
5
10
15
10
10
SUN
EARTH
DAY
NIGHT
NIGHT
CANOPUS
NO SUN, EARTH OR CANOPUS OCCULTATION

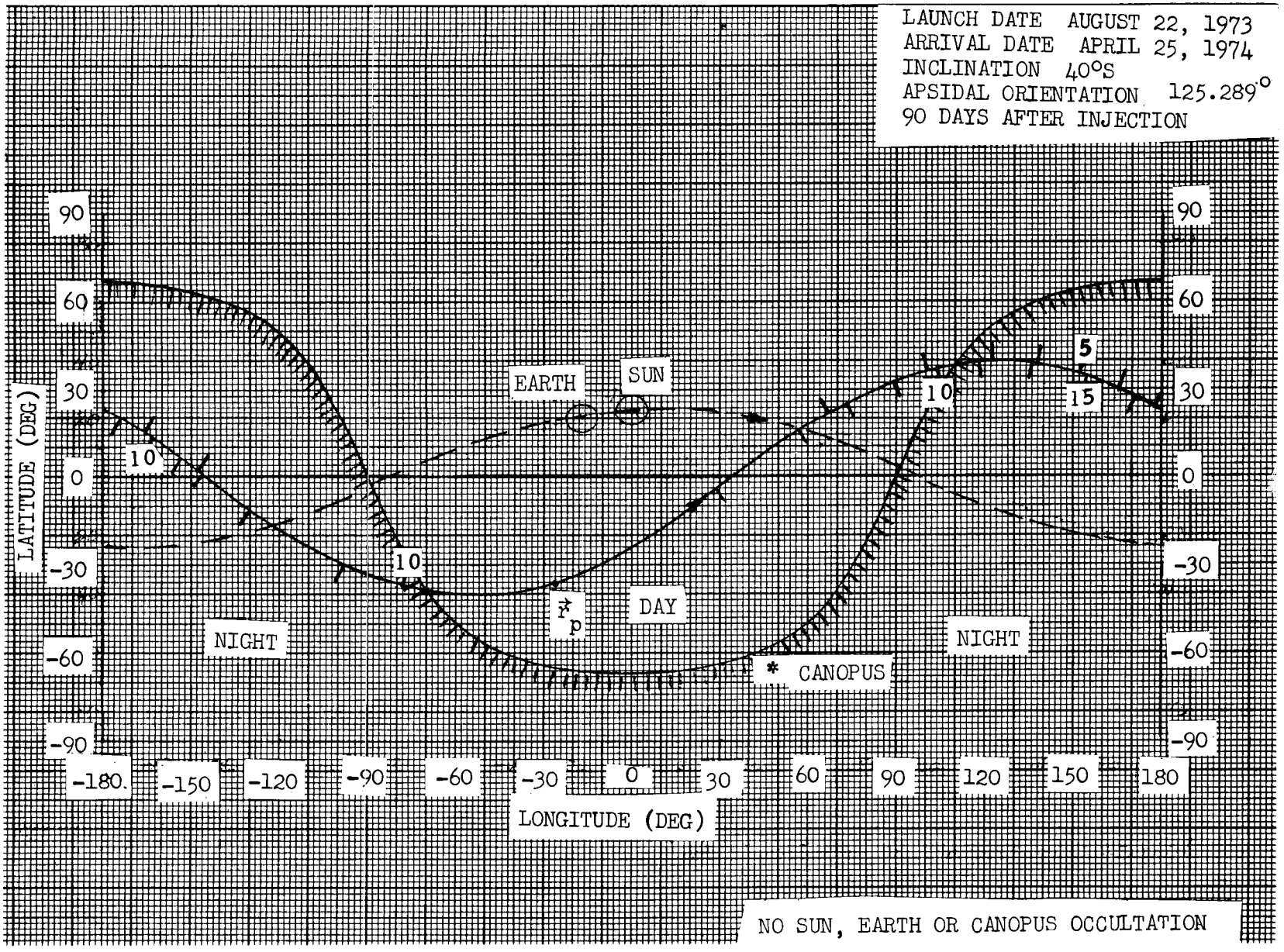
LAUNCH DATE AUGUST 22, 1973
ARRIVAL DATE APRIL 25, 1974
INCLINATION 40°S
APSIDAL ORIENTATION 125.289°
90 DAYS AFTER INJECTION
LATITUDE (DEG)
90
60
30
0
-30
-60
-90
EARTH
SUN
DAY
NIGHT
NIGHT
CANOPUS
10
10
10
5
15
-180
-150
-120
-90
-60
-30
0
30
60
90
120
150
180
LONGITUDE (DEG)
NO SUN, EARTH OR CANOPUS OCCULTATION

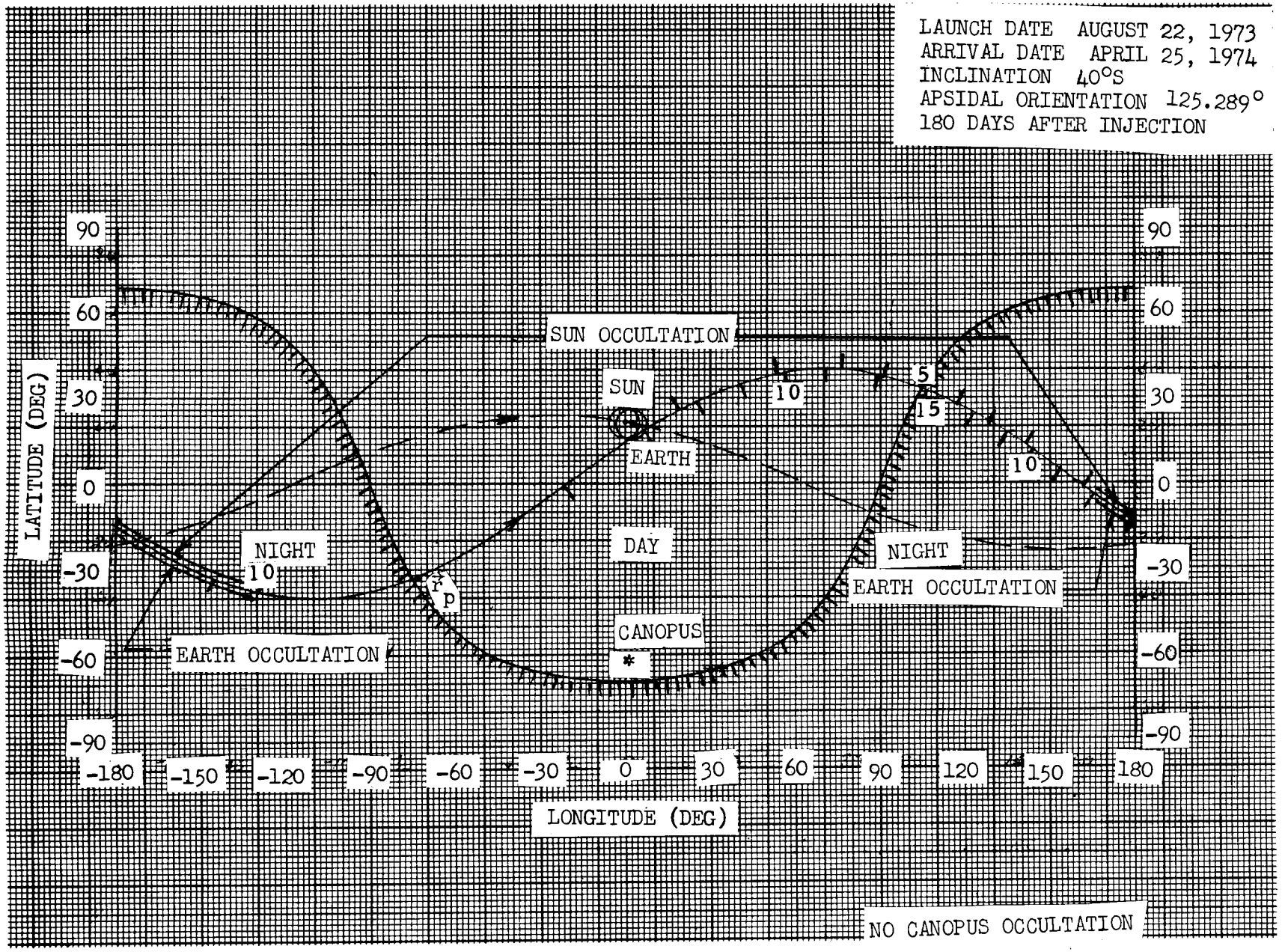
LAUNCH DATE AUGUST 22, 1973
ARRIVAL DATE APRIL 25, 1974
INCLINATION 40°S
APSIDAL ORIENTATION 125.289°
180 DAYS AFTER INJECTION
LATITUDE (DEG)
90
60
30
0
-30
-60
-90
-180
-150
-120
-90
-60
-30
0
30
60
90
120
150
180
LONGITUDE (DEG)
SUN OCCULTATION
SUN
EARTH
NIGHT
DAY
NIGHT
EARTH OCCULTATION
CANOPUS
EARTH OCCULTATION
NO CANOPUS OCCULTATION
5
10
15
10
10
rp

CASE NO. 30

1000 x 15, 000 km

$i = 40^{\circ}N$

$\Psi = 125.289$ deg

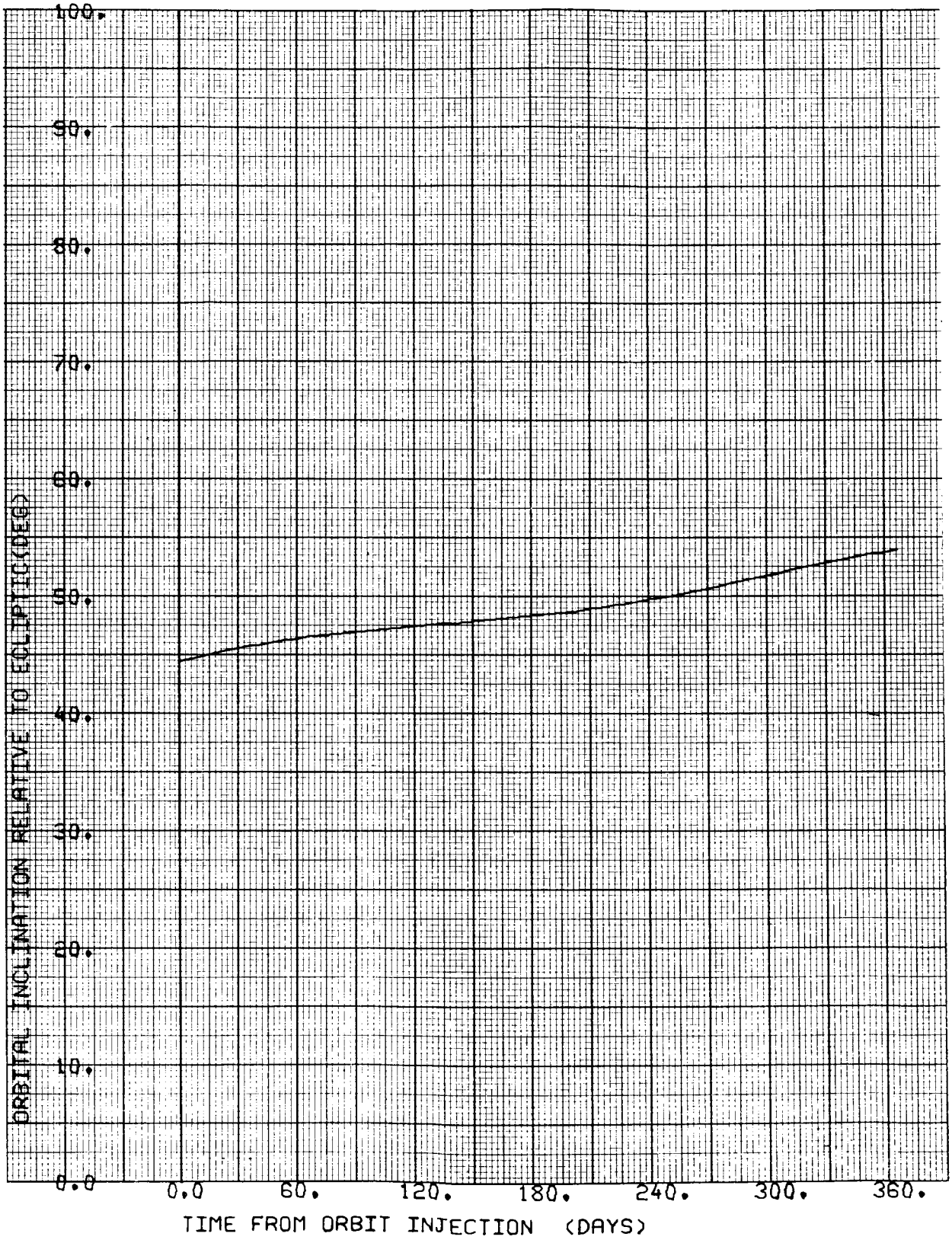
100.
90.
80.
70.
60.
50.
40.
30.
20.
10.
0.0
ORBITAL INCLINATION RELATIVE TO ECLIPTIC(DEG)
0.0
60.
120.
180.
240.
300.
360.
TIME FROM ORBIT INJECTION (DAYS)

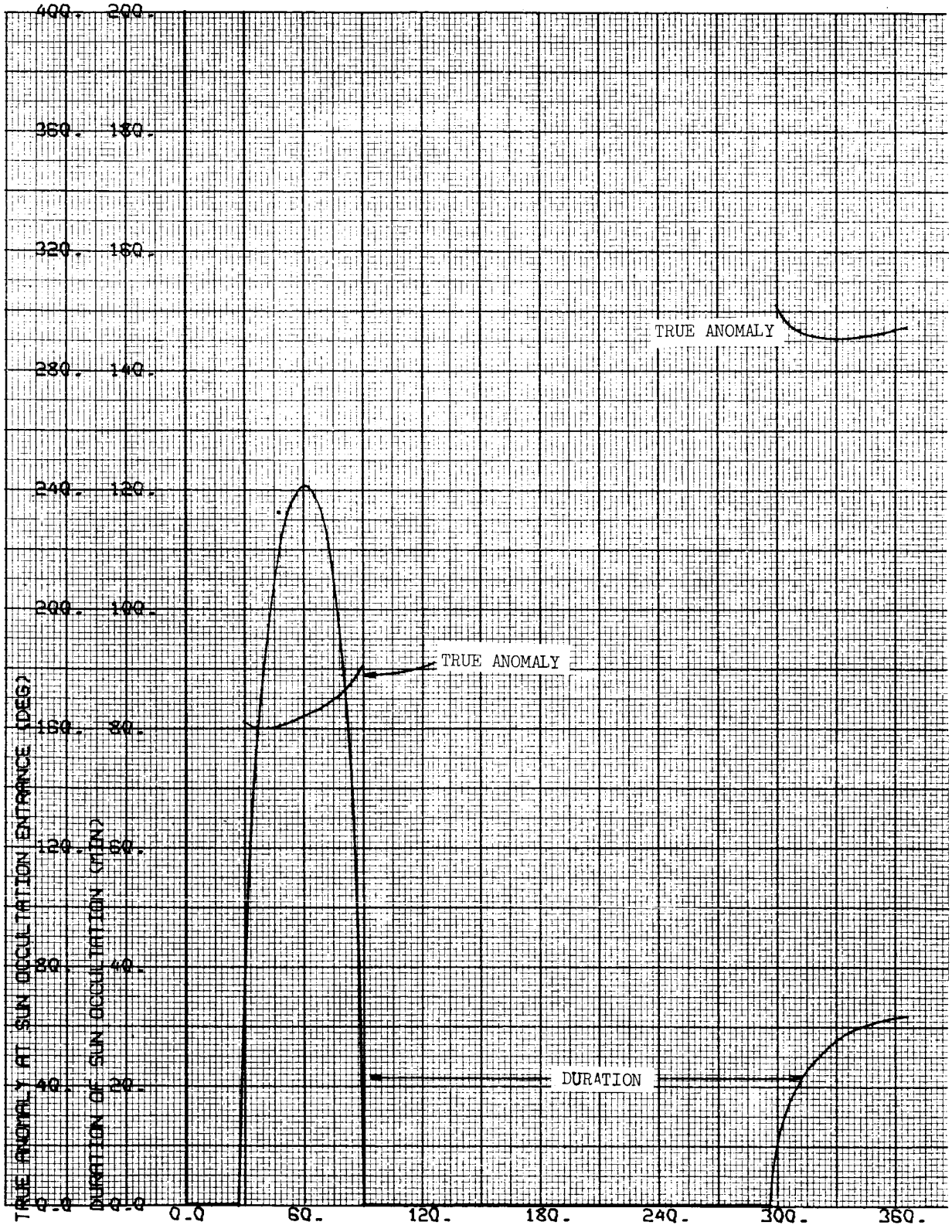
TRUE ANOMALY
TRUE ANOMALY
DURATION
TRUE ANOMALY AT SUN OCCULTATION ENTRANCE (DEG)
DURATION OF SUN OCCULTATION (MIN)
400.
360.
320.
280.
240.
200.
160.
120.
80.
40.
0.0
200.
180.
160.
140.
120.
100.
80.
60.
40.
20.
0.0
0.0
60.
120.
180.
240.
300.
360.
TIME FROM INJECTION (DAYS)

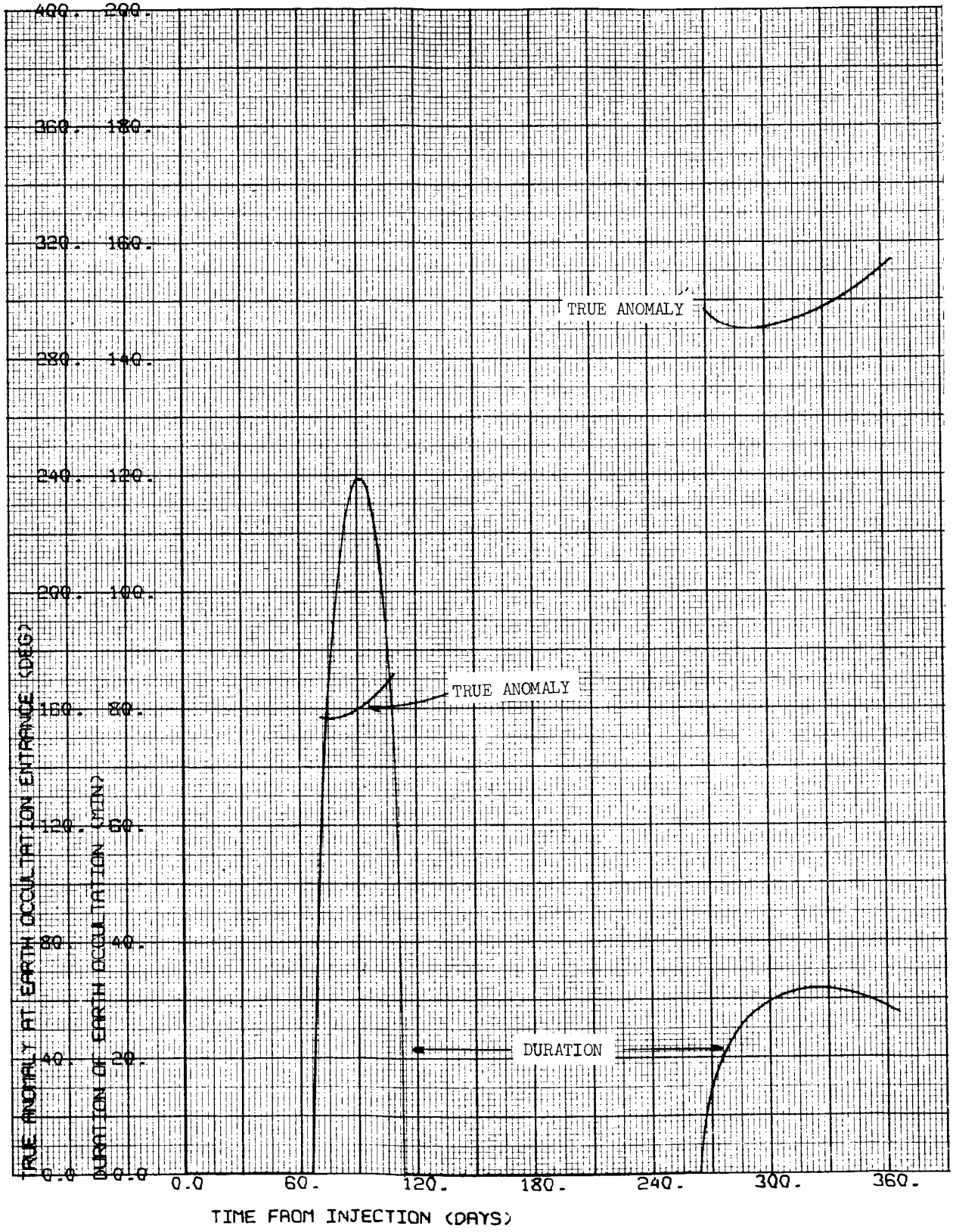
TRUE ANOMALY
TRUE ANOMALY
DURATION
TRUE ANOMALY AT EARTH OCCULTATION ENTRANCE (DEG)
DURATION OF EARTH OCCULTATION (MIN)
TIME FROM INJECTION (DAYS)
0.0
60.
120.
180.
240.
300.
360.
400.
360.
320.
280.
240.
200.
160.
120.
80.
40.
0.0
200.
180.
160.
140.
120.
100.
80.
60.
40.
20.
0.0

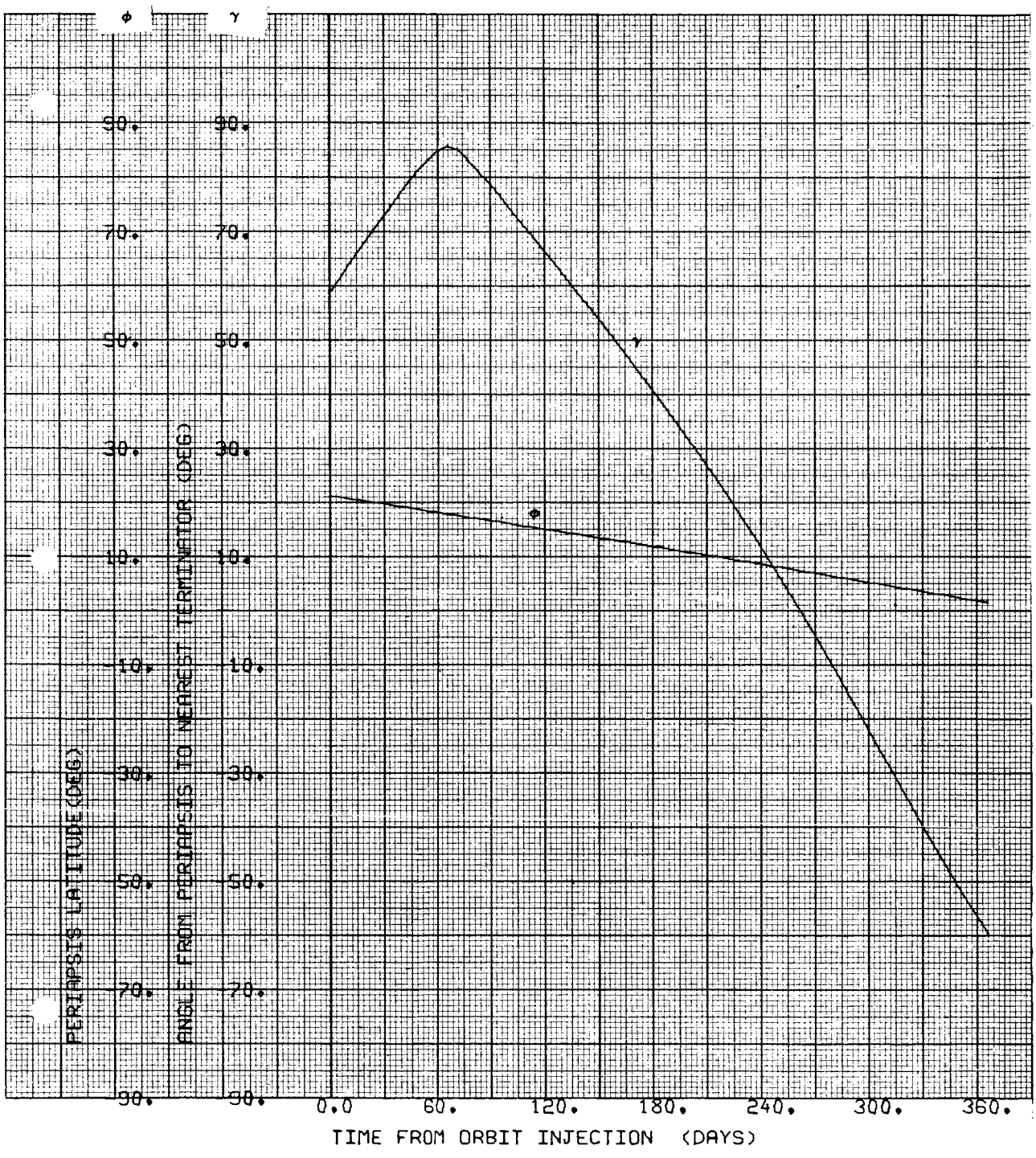
Φ
γ
90.
70.
50.
30.
10.
-10.
-30.
-50.
-70.
-90.
PERIAPSIS LATITUDE (DEG.)
ANGLE FROM PERIAPSIS TO NEAREST TERMINATOR (DEG.)
0.0
60.
120.
180.
240.
300.
360.
TIME FROM ORBIT INJECTION (DAYS)

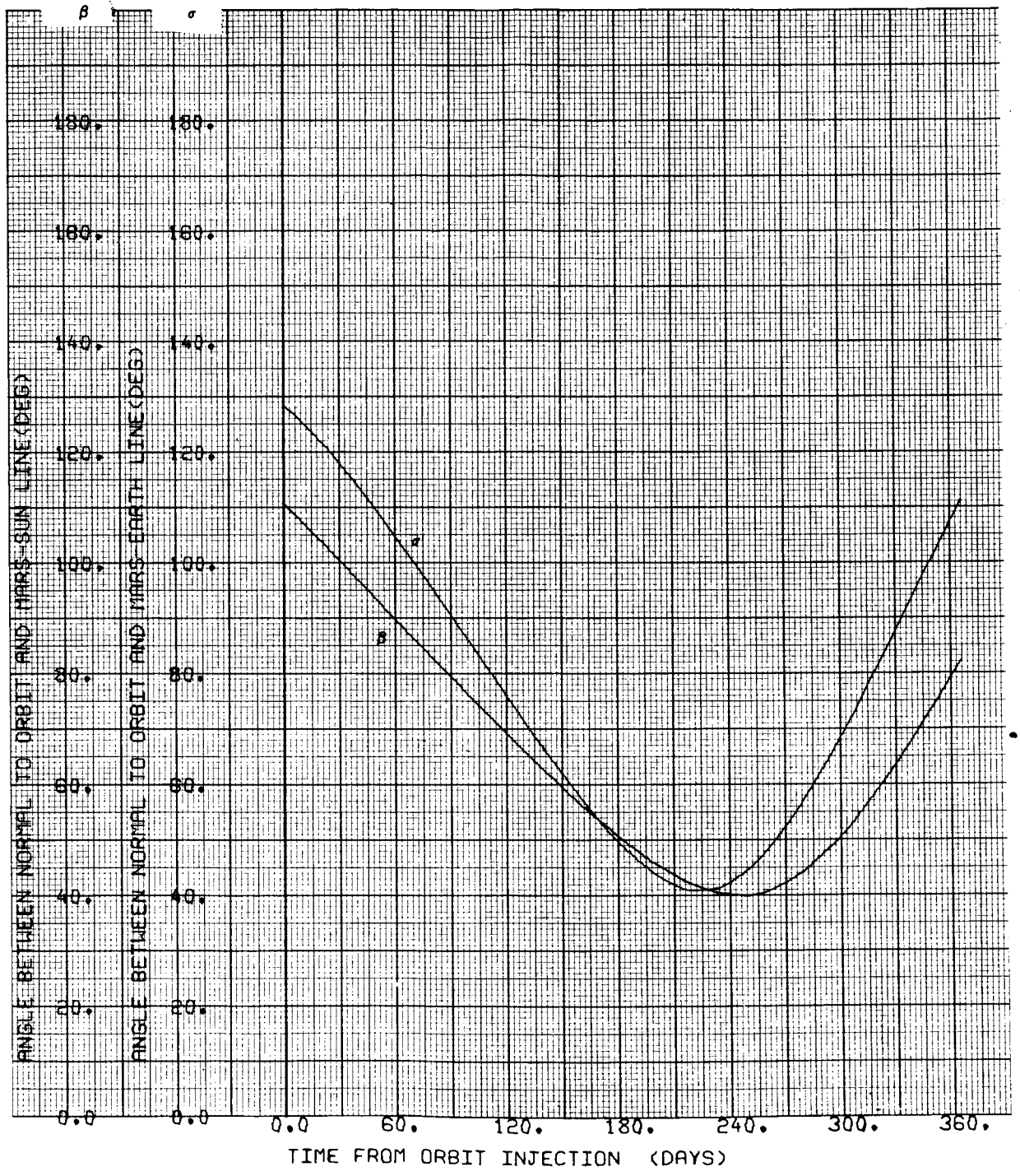
β
σ
180.
160.
140.
120.
100.
80.
60.
40.
20.
0.0
ANGLE BETWEEN NORMAL TO ORBIT AND MARS-SUN LINE(DEG)
ANGLE BETWEEN NORMAL TO ORBIT AND MARS-EARTH LINE(DEG)
0.0
60.
120.
180.
240.
300.
360.
TIME FROM ORBIT INJECTION (DAYS)

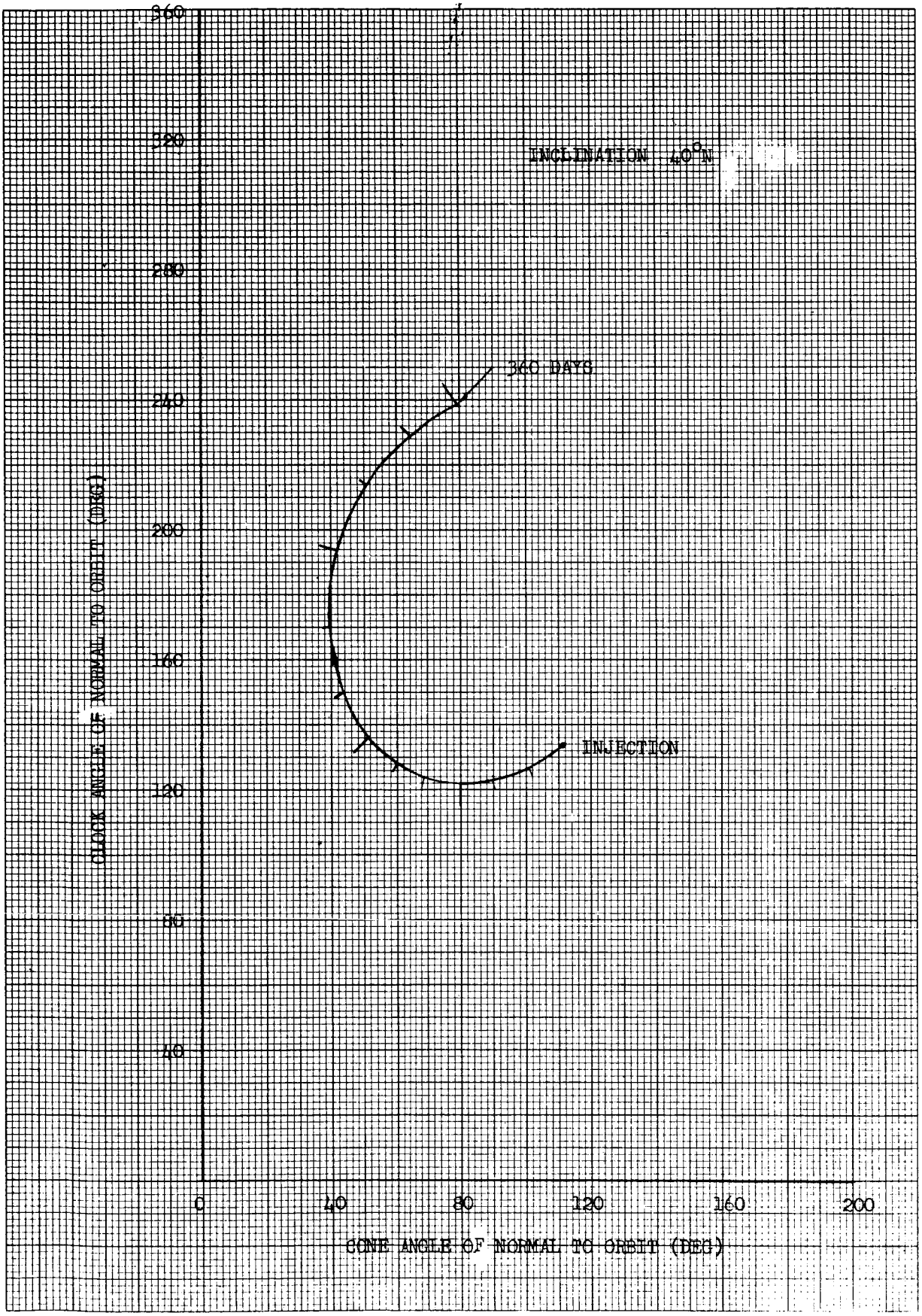
INCLINATION 40°N
360 DAYS
INJECTION
CLOCK ANGLE OF NORMAL TO ORBIT (DEG)
CONE ANGLE OF NORMAL TO ORBIT (DEG)
360
320
280
240
200
160
120
80
40
0
40
80
120
160
200

LAUNCH DATE AUGUST 22, 1973
ARRIVAL DATE APRIL 25, 1974
INCLINATION 40°N
APSIDAL ORIENTATION 125.289°
0 DAYS AFTER INJECTION
LATITUDE (DEG)
LONGITUDE (DEG)
90
60
30
0
-30
-60
-90
-180
-150
-120
-90
-60
-30
0
30
60
90
120
150
180
10
5
15
NIGHT
DAY
NIGHT
SUN
EARTH
CANOPUS
NO SUN, EARTH AND CANOPUS OCCULTATION

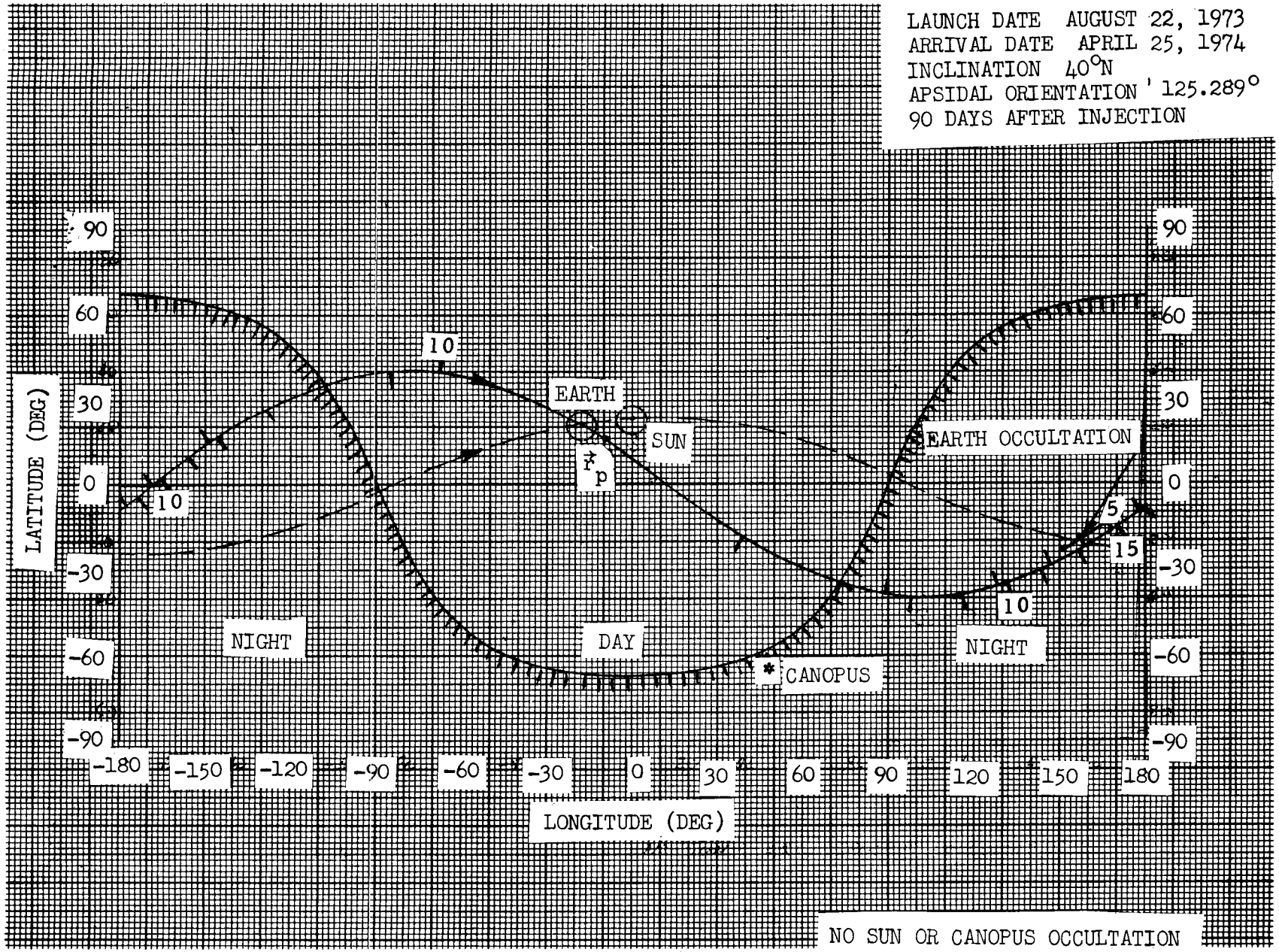
LAUNCH DATE AUGUST 22, 1973
ARRIVAL DATE APRIL 25, 1974
INCLINATION 40°N
APSIDAL ORIENTATION 125.289°
90 DAYS AFTER INJECTION
LATITUDE (DEG)
90
60
30
0
-30
-60
-90
10
10
EARTH
SUN
r_p
NIGHT
DAY
CANOPUS
EARTH OCCULTATION
5
15
10
NIGHT
-180
-150
-120
-90
-60
-30
0
30
60
90
120
150
180
LONGITUDE (DEG)
NO SUN OR CANOPUS OCCULTATION

LAUNCH DATE AUGUST 22, 1973
ARRIVAL DATE APRIL 25, 1974
INCLINATION 40°N
APSIDAL ORIENTATION 125.289°
180 DAYS AFTER INJECTION
LATITUDE (DEG)
LONGITUDE (DEG)
90
60
30
0
-30
-60
-90
-180
-150
-120
150
120
180
SUN
EARTH
CANOPUS
DAY
NIGHT
NIGHT
NO SUN, EARTH OR CANOPUS OCCULTATION

CASE NO. 31

1000 x 15,000 km

$i = 60^{\circ}S$

$\Psi = 125.289$ deg

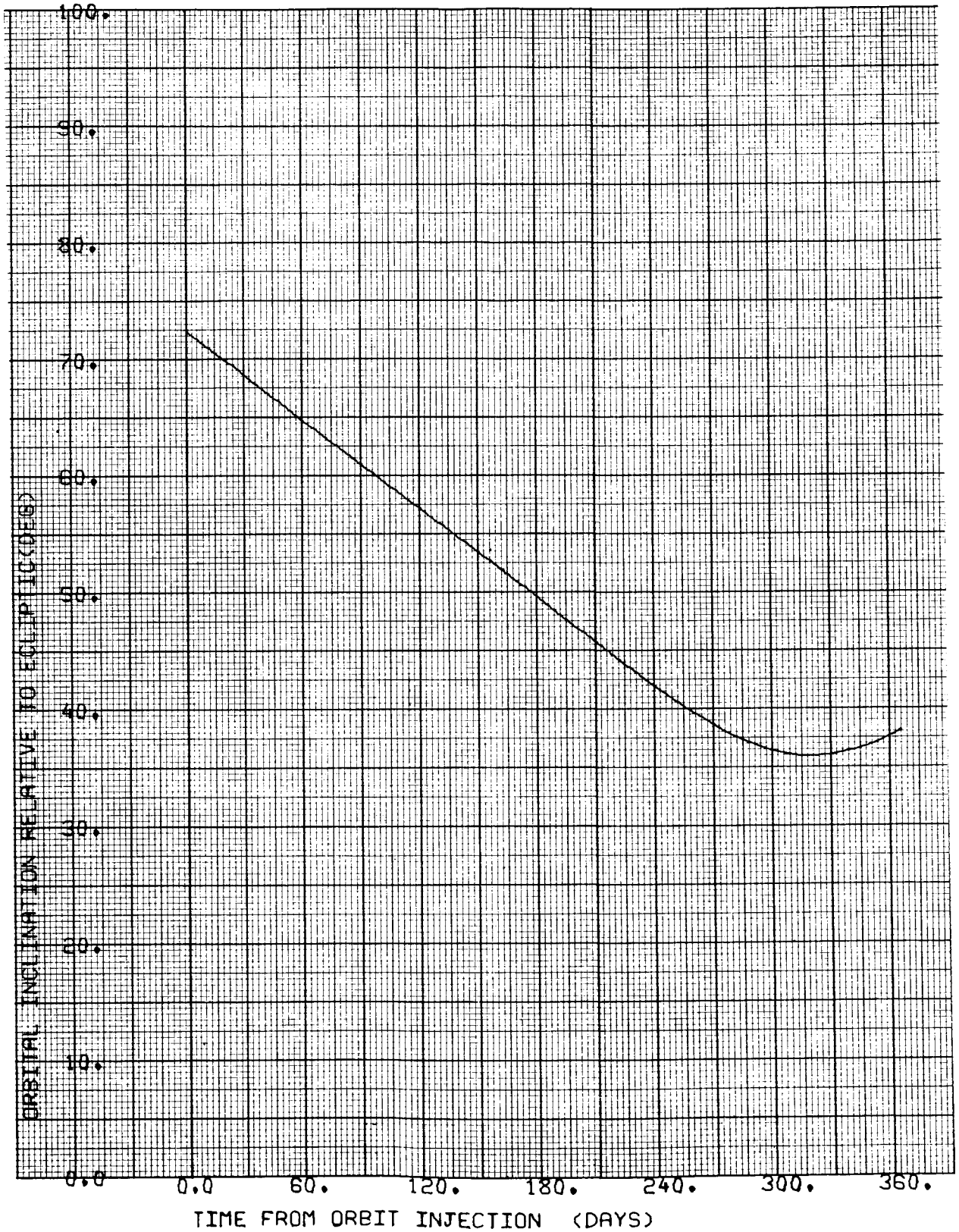
100.
90.
80.
70.
60.
50.
40.
30.
20.
10.
0.0
ORBITAL INCLINATION RELATIVE TO ECLIPTIC(DEG)
0.0
60.
120.
180.
240.
300.
360.
TIME FROM ORBIT INJECTION (DAYS)

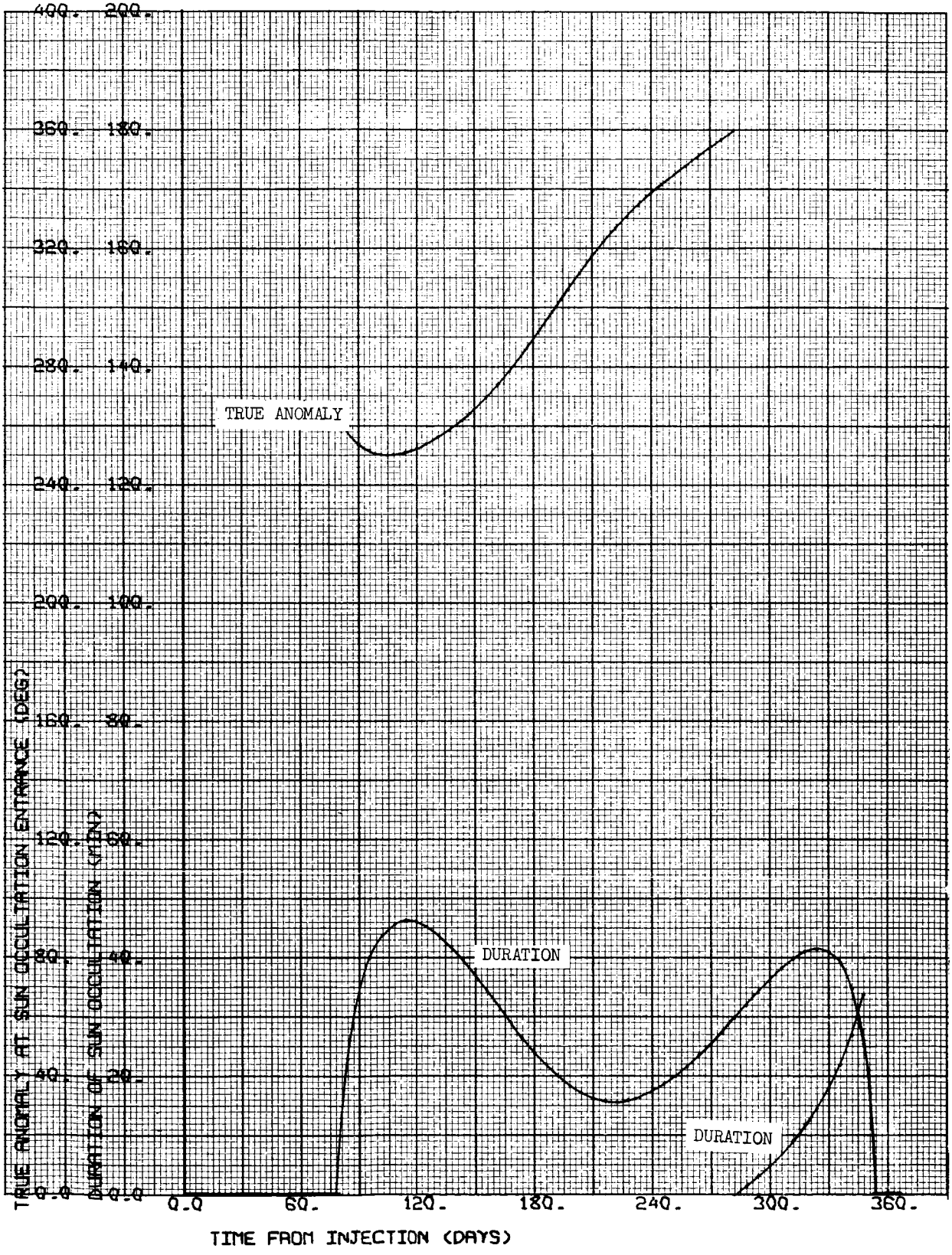
TRUE ANOMALY
DURATION
DURATION
TRUE ANOMALY AT SUN OCCULTATION ENTRANCE (DEG)
DURATION OF SUN OCCULTATION (MIN)
TIME FROM INJECTION (DAYS)
0.0
60.
120.
180.
240.
300.
360.
400.
360.
320.
280.
240.
200.
160.
120.
80.
40.
200.
180.
160.
140.
120.
100.
80.
60.
40.
20.
0.0

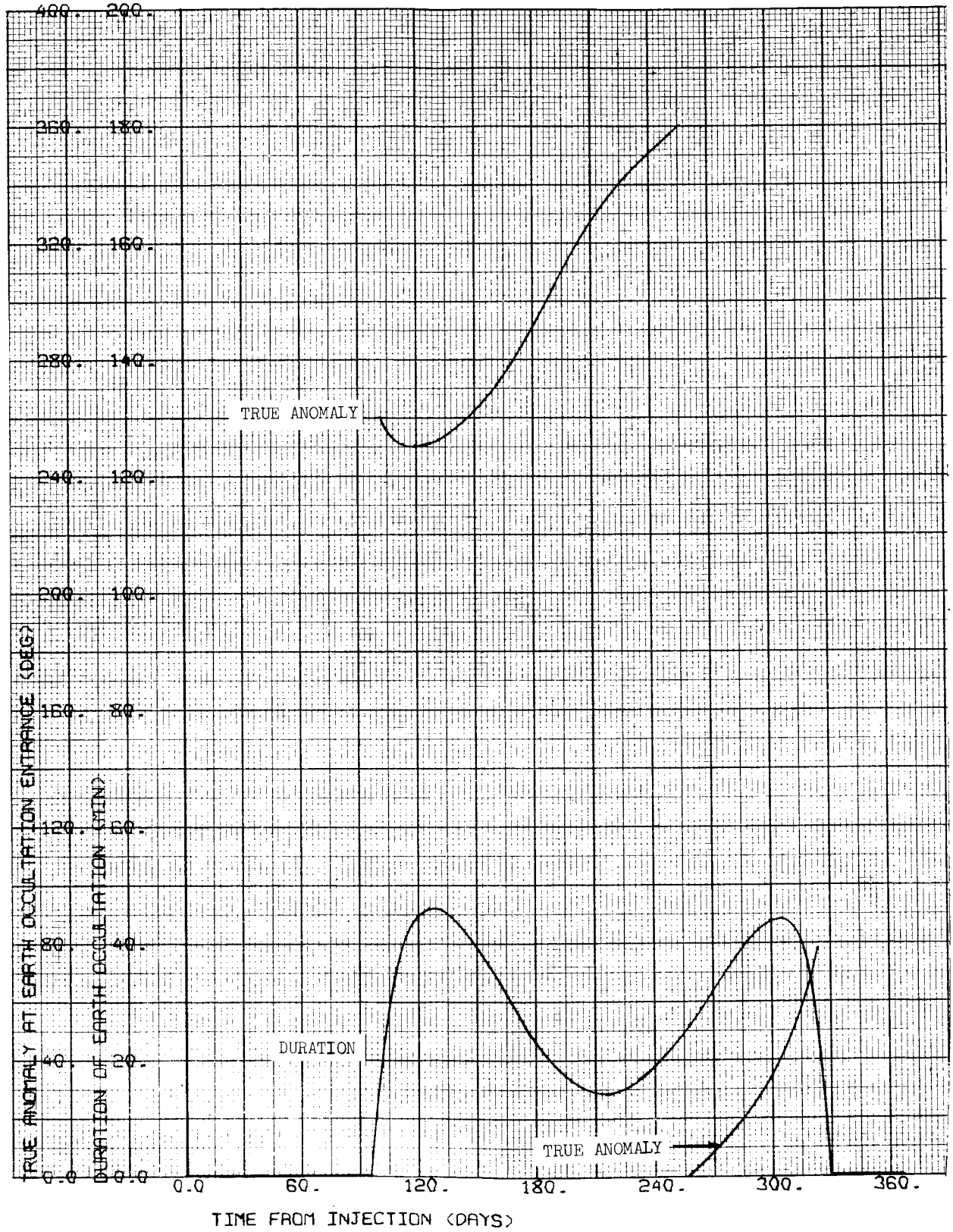
TRUE ANOMALY
DURATION
TRUE ANOMALY
TRUE ANOMALY AT EARTH OCCULTATION ENTRANCE (DEG)
DURATION OF EARTH OCCULTATION (MIN)
TIME FROM INJECTION (DAYS)
0.0
60.
120.
180.
240.
300.
360.
400.
360.
320.
280.
240.
200.
160.
120.
80.
40.
0.0
200.
180.
160.
140.
120.
100.
80.
60.
40.
20.
0.0

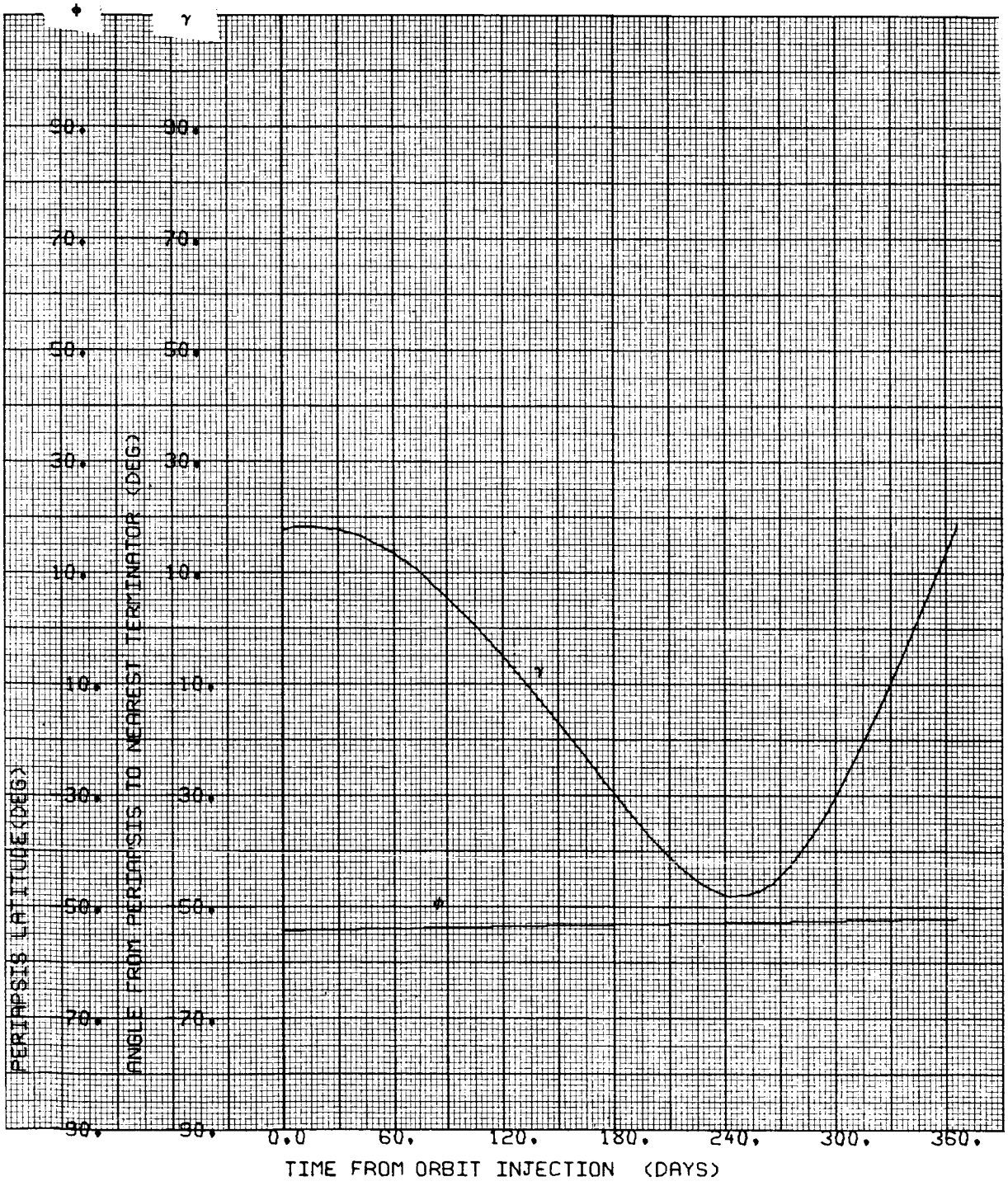
φ
γ
90.
70.
50.
30.
10.
10.
30.
50.
70.
90.
ANGLE FROM PERIAPSIS TO NEAREST TERMINATOR (DEG)
PERIAPSIS LATITUDE (DEG)
0.0
60.
120.
180.
240.
300.
360.
TIME FROM ORBIT INJECTION (DAYS)

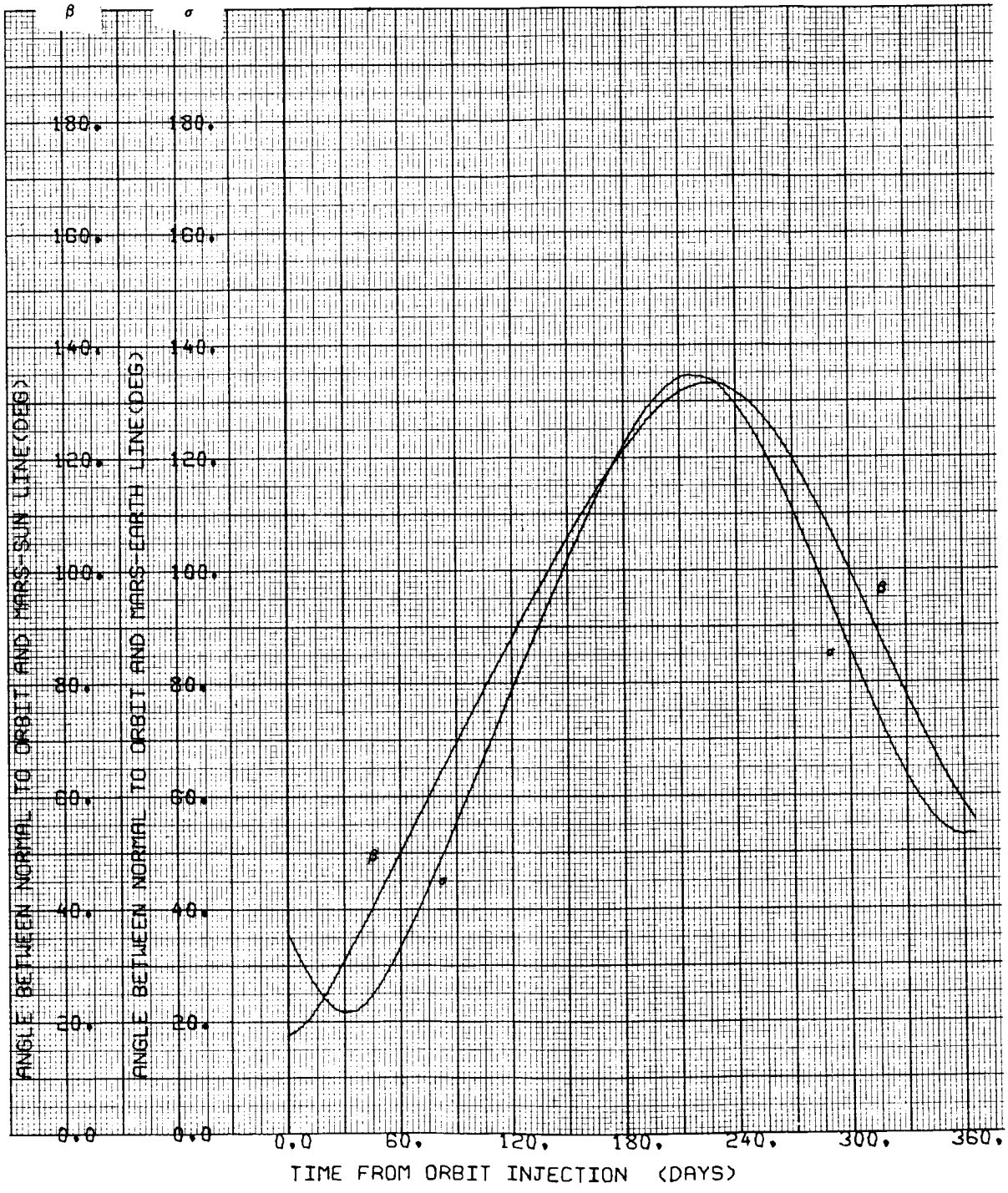
β
σ
180.
160.
140.
120.
100.
80.
60.
40.
20.
0.0
ANGLE BETWEEN NORMAL TO ORBIT AND MARS-SUN LINE(DEG)
ANGLE BETWEEN NORMAL TO ORBIT AND MARS-EARTH LINE(DEG)
0.0
60.
120.
180.
240.
300.
360.
TIME FROM ORBIT INJECTION (DAYS)

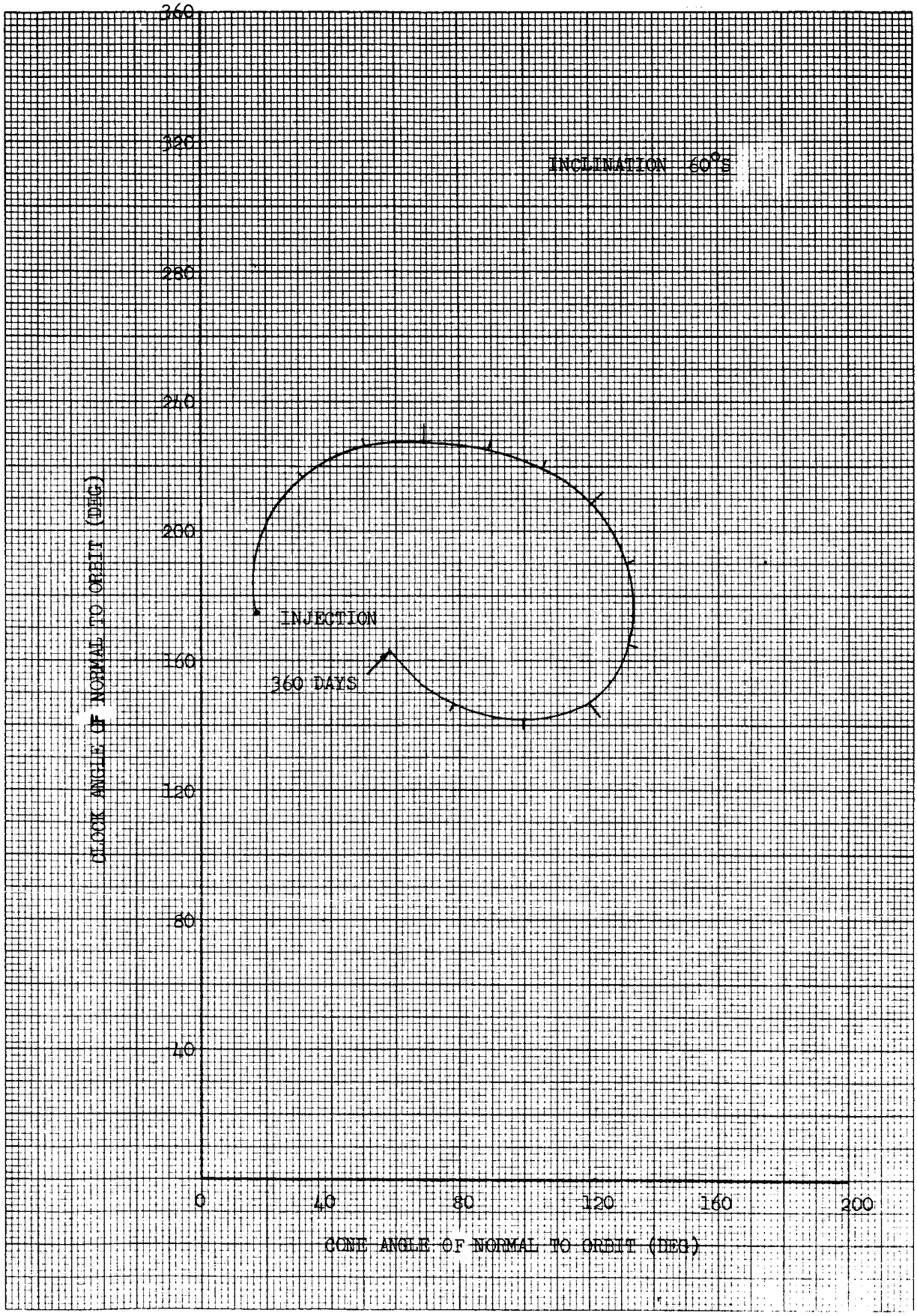
INCLINATION 60°S
INJECTION
360 DAYS
CLOCK ANGLE OF NORMAL TO ORBIT (DEG)
CONE ANGLE OF NORMAL TO ORBIT (DEG)
360
320
280
240
200
160
120
80
40
0
40
80
120
160
200

LAUNCH DATE AUGUST 22, 1973
ARRIVAL DATE APRIL 25, 1974
INCLINATION 60°S
APSIDAL ORIENTATION 125.289°
0 DAYS AFTER INJECTION
LATITUDE (DEG)
LONGITUDE (DEG)
90
60
30
0
-30
-60
-90
-120
-150
-180
120
150
180
SUN
EARTH
DAY
NIGHT
NIGHT
* CANOPUS
NO SUN, EARTH OR CANOPUS OCCULTATION

LAUNCH DATE AUGUST 22, 1973
ARRIVAL DATE APRIL 25, 1974
INCLINATION 60°S
APSIDAL ORIENTATION 125.289°
90 DAYS AFTER INJECTION
LATITUDE (DEG)
90
60
30
0
-30
-60
-90
-180
-150
-120
-90
-60
-30
0
30
60
90
120
150
180
LONGITUDE (DEG)
SUN OCCULTATION
EARTH
SUN
DAY
NIGHT
CANOPUS
NIGHT
NO EARTH OR CANOPUS OCCULTATION

LAUNCH DATE AUGUST 22, 1973
ARRIVAL DATE APRIL 25, 1974
INCLINATION 60°S
APSIDAL ORIENTATION 125.289°
180 DAYS AFTER INJECTION
LATITUDE (DEG)
LONGITUDE (DEG)
90
60
30
0
-30
-60
-90
-180
-150
-120
-90
-60
-30
0
30
60
90
120
150
180
5
10
15
SUN
EARTH
DAY
CANOPUS
SUN OCCULTATION
EARTH OCCULTATION
NIGHT
EARTH
NIGHT
OCCULTATION
NO CANOPUS OCCULTATION

CASE NO. 32

1000 x 15,000 km

$i = 60^{\circ}N$

$\Psi = 125.289$ deg

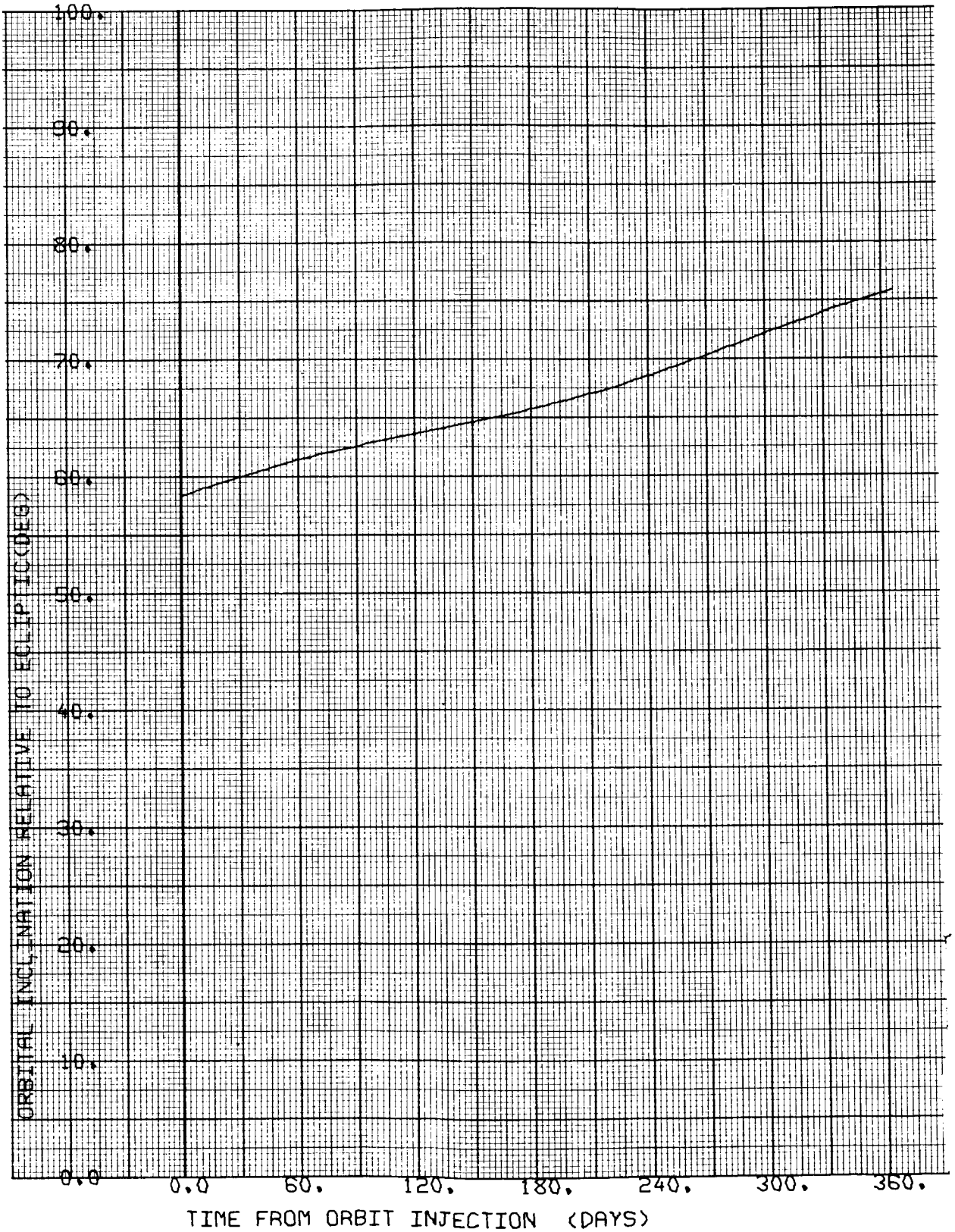
100.
90.
80.
70.
60.
50.
40.
30.
20.
10.
0.0
ORBITAL INCLINATION RELATIVE TO ECLIPTIC(DEG)
0.0
60.
120.
180.
240.
300.
360.
TIME FROM ORBIT INJECTION (DAYS)

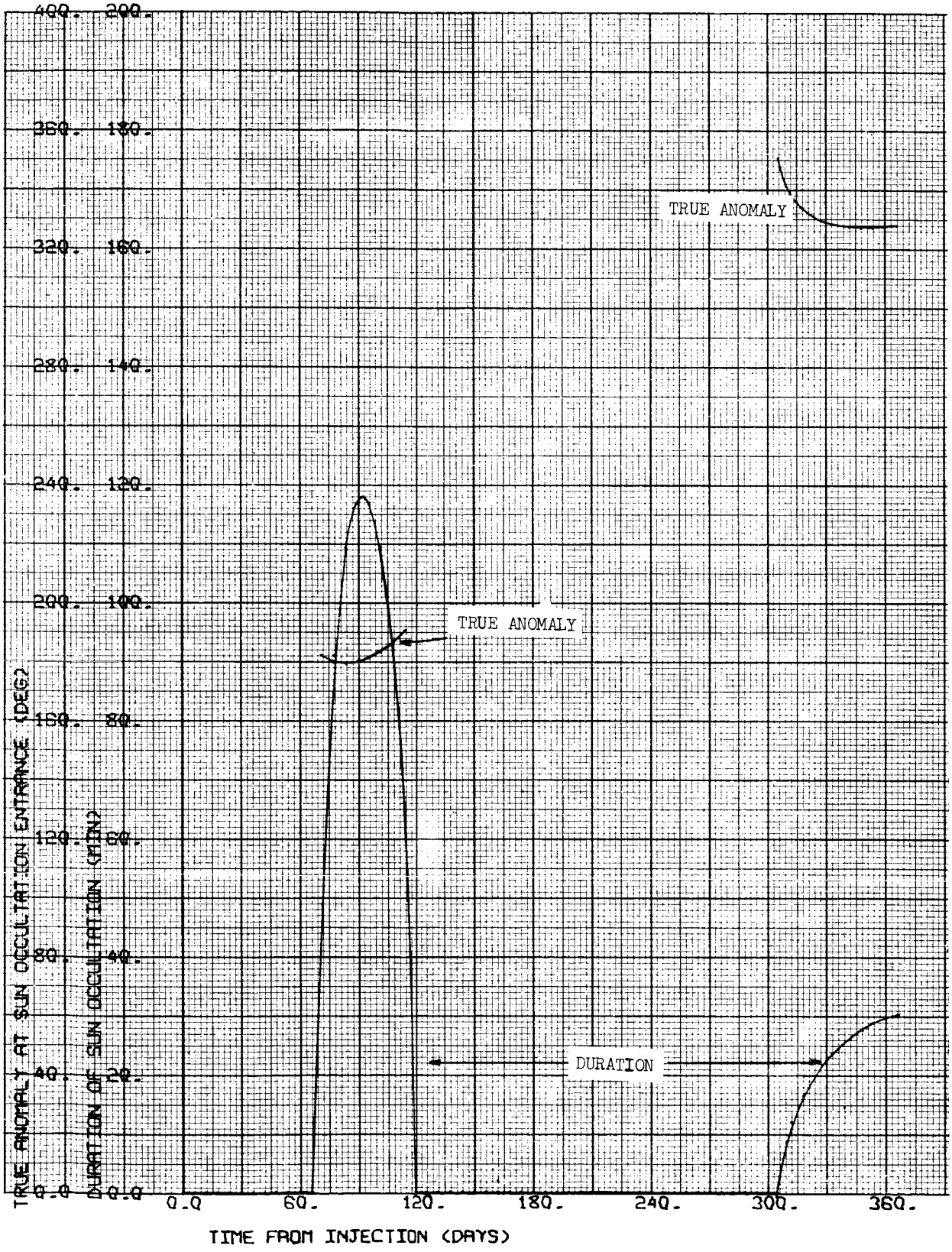
TRUE ANOMALY
TRUE ANOMALY
DURATION
TRUE ANOMALY AT SUN OCCULTATION ENTRANCE (DEG)
DURATION OF SUN OCCULTATION (MIN)
TIME FROM INJECTION (DAYS)
0.0
60.
120.
180.
240.
300.
360.
400.
360.
320.
280.
240.
200.
160.
120.
80.
40.
200.
180.
160.
140.
120.
100.
80.
60.
40.
20.
0.0

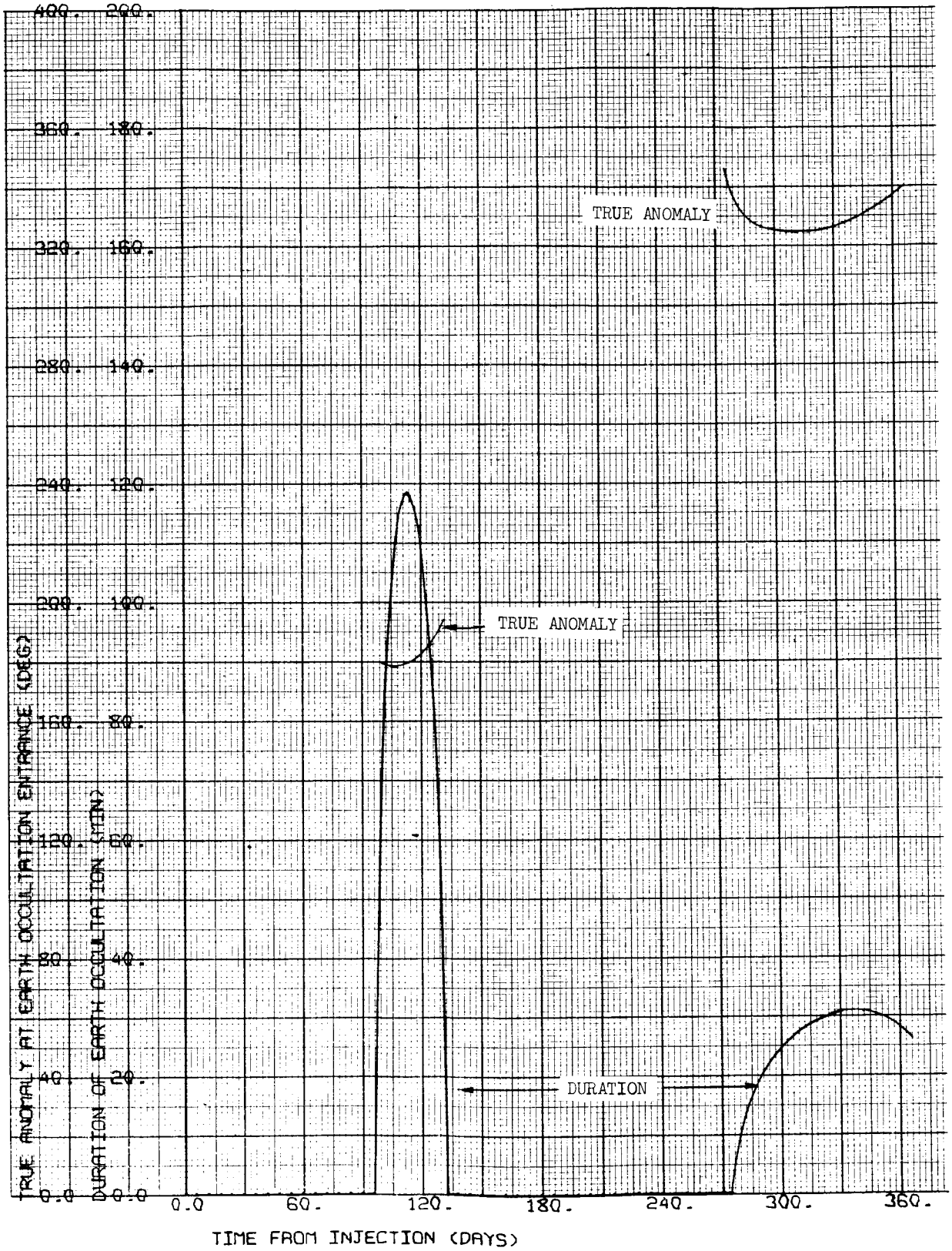
TRUE ANOMALY
TRUE ANOMALY
DURATION
TRUE ANOMALY AT EARTH OCCULTATION ENTRANCE (DEG)
DURATION OF EARTH OCCULTATION (MIN)
400.
360.
320.
280.
240.
200.
160.
120.
80.
40.
0.0
200.
180.
160.
140.
120.
100.
80.
60.
40.
20.
0.0
0.0
60.
120.
180.
240.
300.
360.
TIME FROM INJECTION (DAYS)

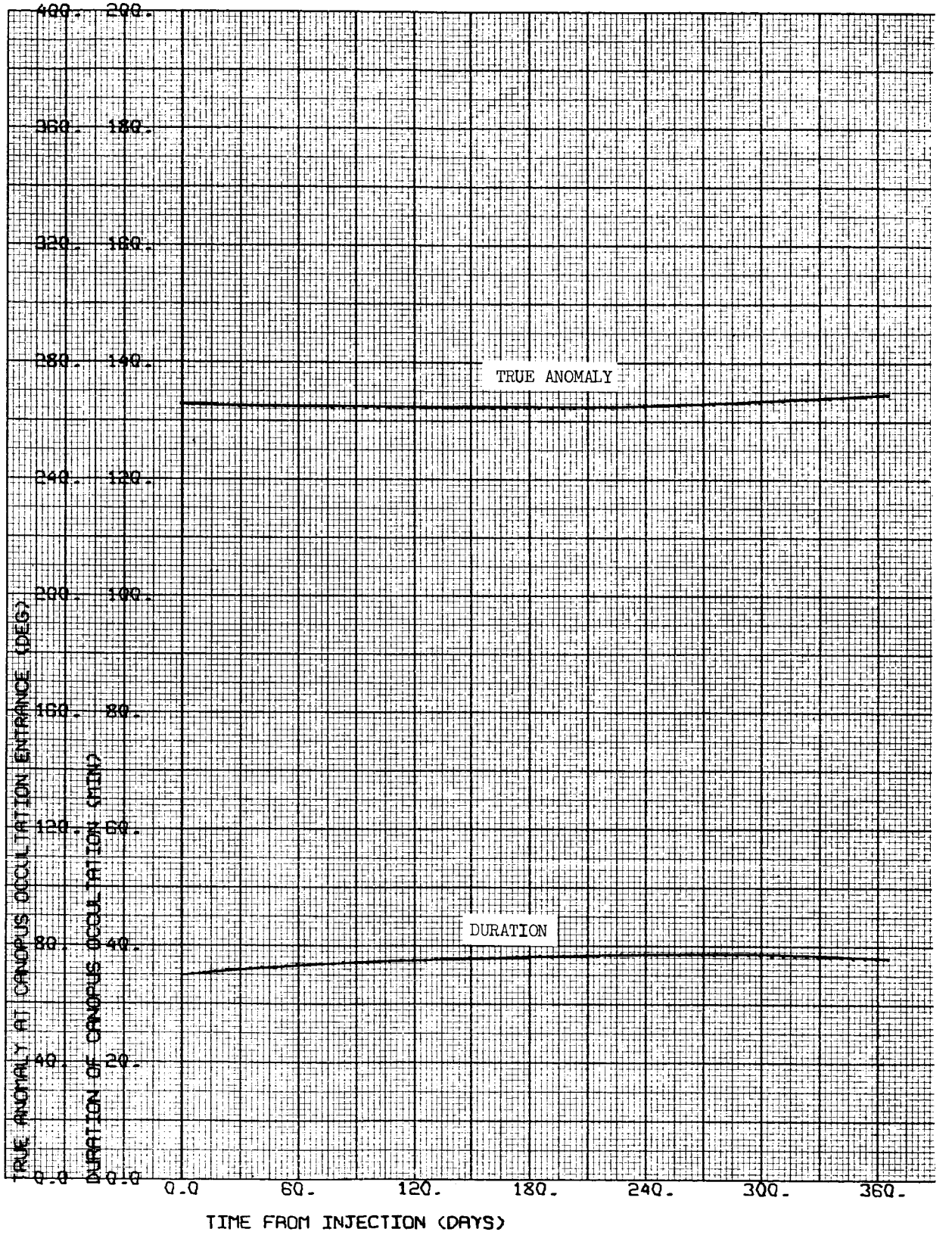
TRUE ANOMALY AT CANOPUS OCCULTATION ENTRANCE (DEG)
DURATION OF CANOPUS OCCULTATION (MIN)
TIME FROM INJECTION (DAYS)
TRUE ANOMALY
DURATION
400.
360.
320.
280.
240.
200.
160.
120.
80.
40.
0.0
200.
180.
160.
140.
120.
100.
80.
60.
40.
20.
0.0
0.0
60.
120.
180.
240.
300.
360.

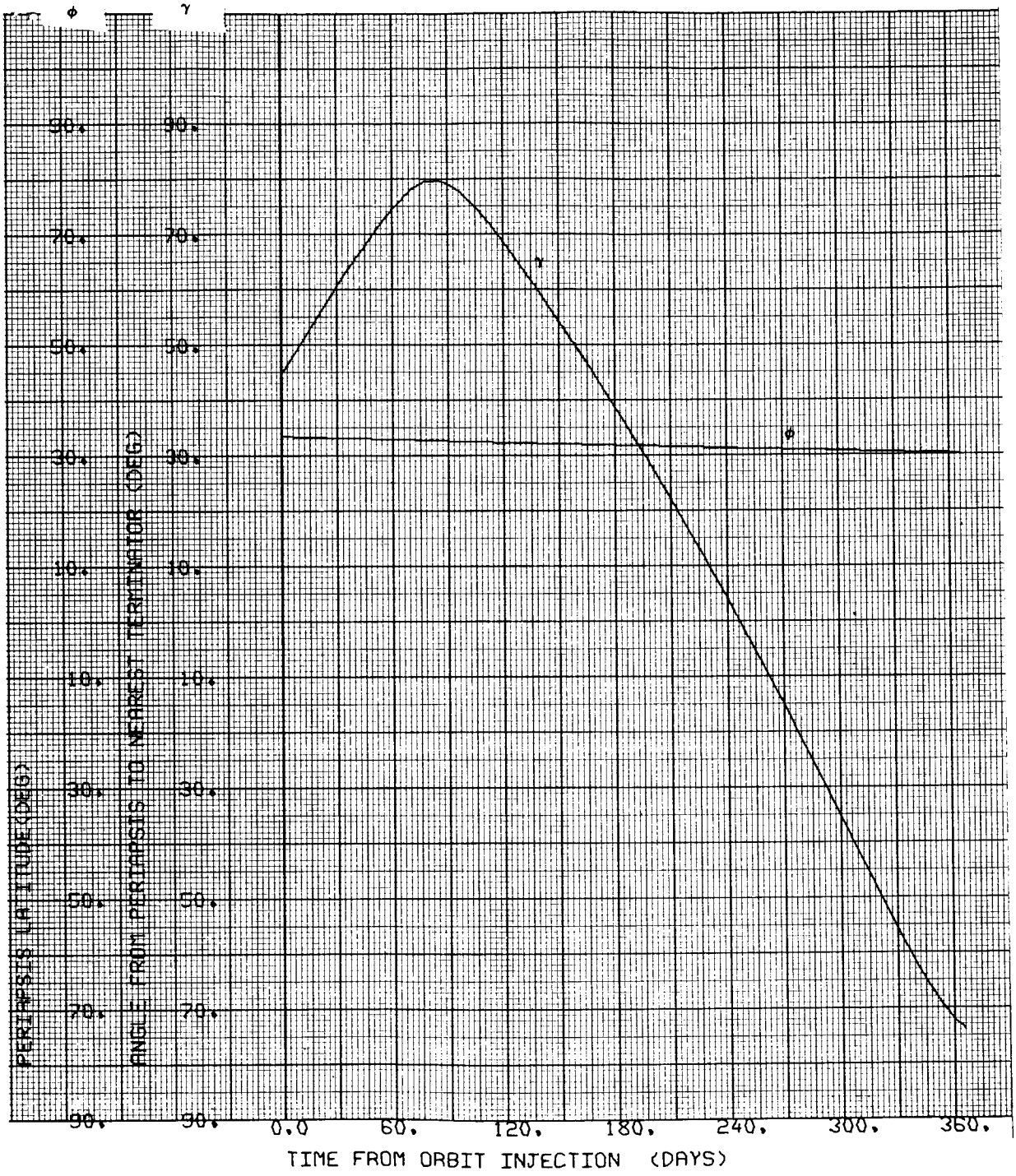
φ
γ
90.
70.
50.
30.
10.
10.
30.
50.
70.
90.
90.
70.
50.
30.
10.
10.
30.
50.
70.
90.
0.0
60.
120.
180.
240.
300.
360.
PERIAPSIS LATITUDE (DEG)
ANGLE FROM PERIAPSIS TO NEAREST TERMINATOR (DEG)
TIME FROM ORBIT INJECTION (DAYS)

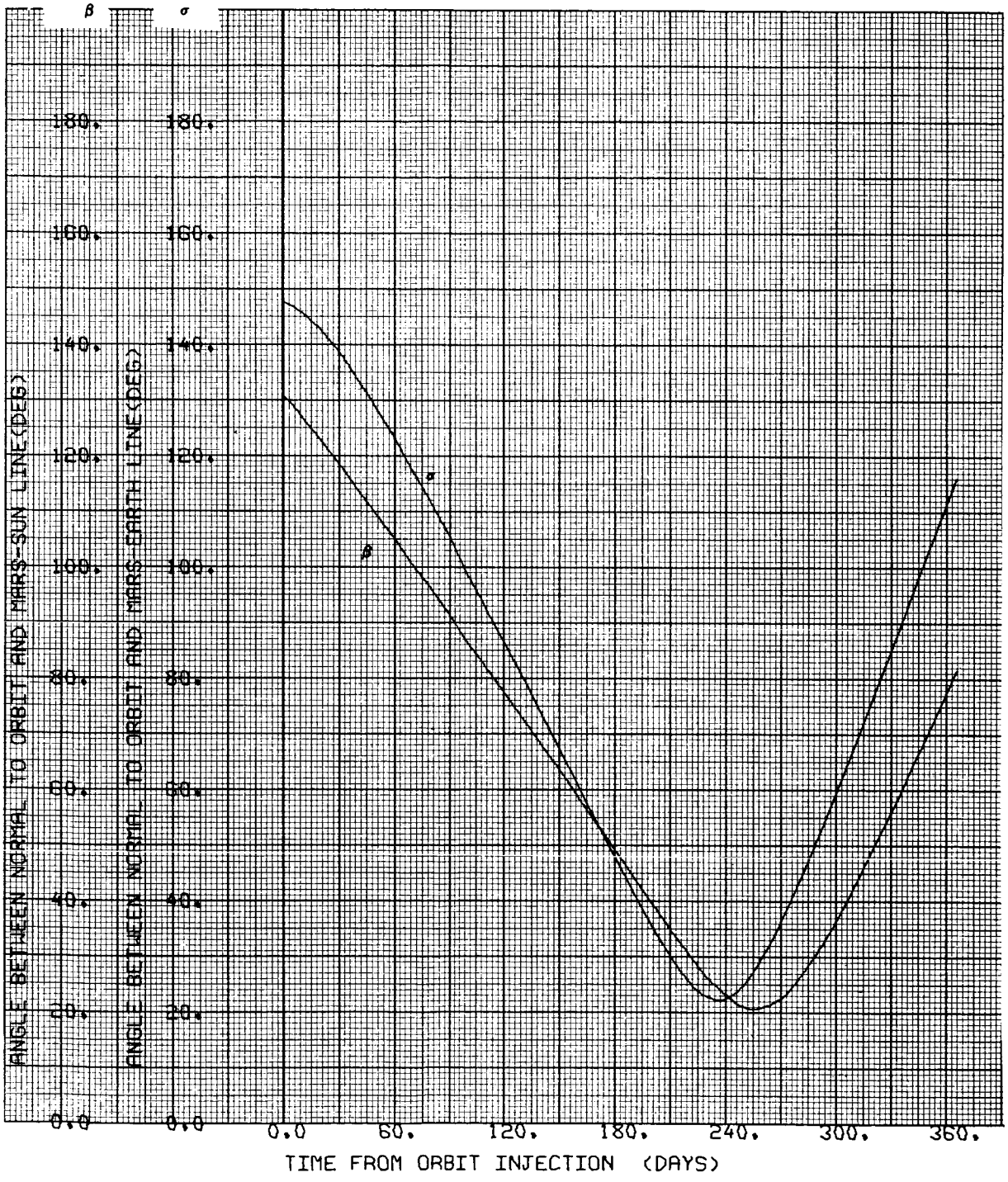
β
σ
180.
160.
140.
120.
100.
80.
60.
40.
20.
0.0
ANGLE BETWEEN NORMAL TO ORBIT AND MARS-SUN LINE(DEG)
ANGLE BETWEEN NORMAL TO ORBIT AND MARS-EARTH LINE(DEG)
0.0
60.
120.
180.
240.
300.
360.
TIME FROM ORBIT INJECTION (DAYS)

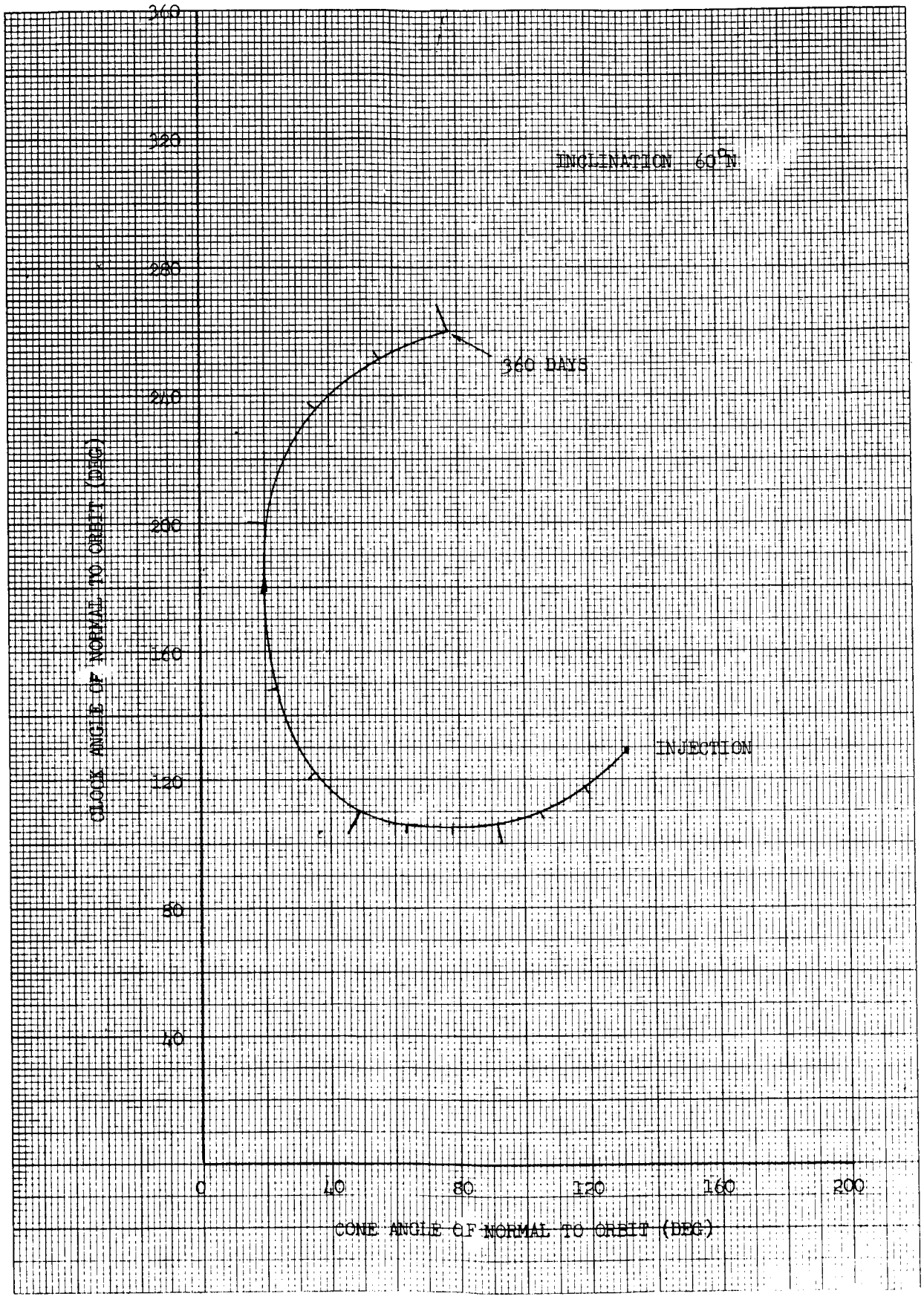
INCLINATION 60°N
360 DAYS
INJECTION
CLOCK ANGLE OF NORMAL TO ORBIT (DEG)
CONE ANGLE OF NORMAL TO ORBIT (DEG)
360
320
280
240
200
160
120
80
40
0
40
80
120
160
200

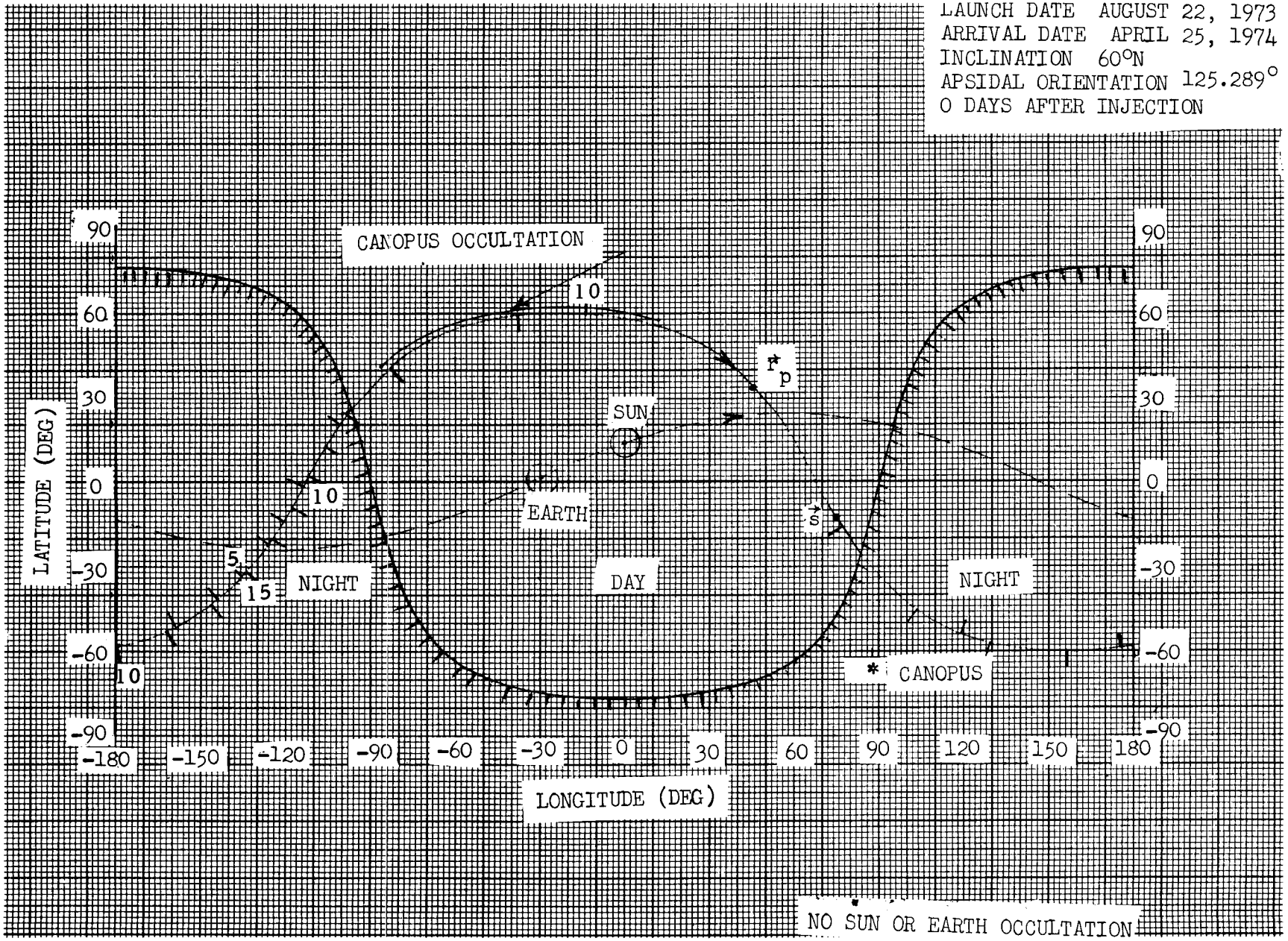
LAUNCH DATE AUGUST 22, 1973
ARRIVAL DATE APRIL 25, 1974
INCLINATION 60°N
APSIDAL ORIENTATION 125.289°
0 DAYS AFTER INJECTION
CANOPUS OCCULTATION
SUN
EARTH
NIGHT
DAY
NIGHT
CANOPUS
NO SUN OR EARTH OCCULTATION
LATITUDE (DEG)
LONGITUDE (DEG)
90
60
30
0
-30
-60
-90
-180
-150
-120
-90
-60
-30
0
30
60
90
120
150
180
10
10
5
15
10

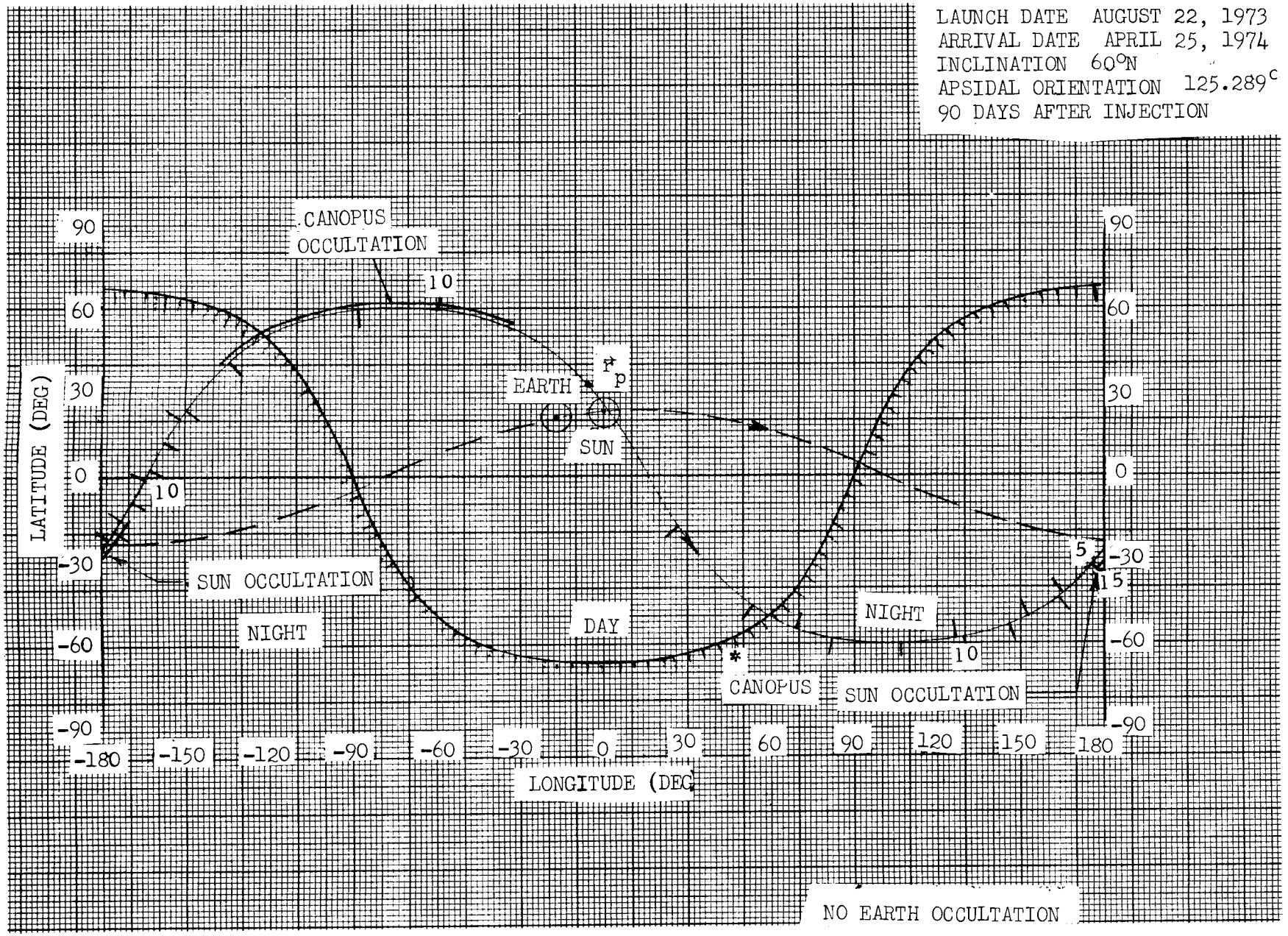
LAUNCH DATE AUGUST 22, 1973
ARRIVAL DATE APRIL 25, 1974
INCLINATION 60°N
APSIDAL ORIENTATION 125.289°
90 DAYS AFTER INJECTION
CANOPUS OCCULTATION
EARTH
SUN
SUN OCCULTATION
NIGHT
DAY
NIGHT
CANOPUS
SUN OCCULTATION
NO EARTH OCCULTATION
LATITUDE (DEG)
LONGITUDE (DEG)
90
60
30
0
-30
-60
-90
-180
-150
-120
-90
-60
-30
0
30
60
90
120
150
180
10
10
10
5
15

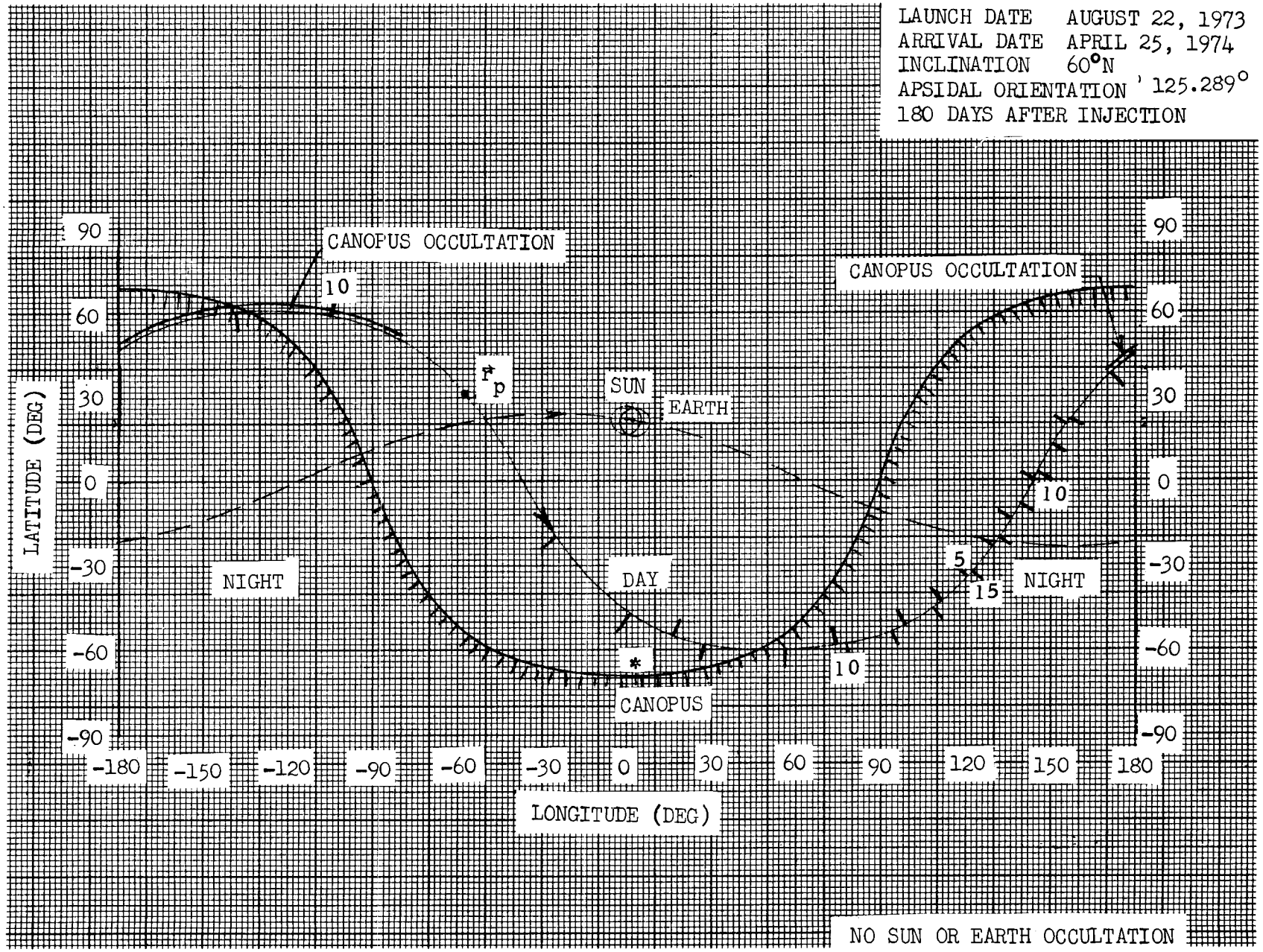
LAUNCH DATE AUGUST 22, 1973
ARRIVAL DATE APRIL 25, 1974
INCLINATION 60°N
APSIDAL ORIENTATION 125.289°
180 DAYS AFTER INJECTION
CANOPUS OCCULTATION
CANOPUS OCCULTATION
SUN
EARTH
DAY
NIGHT
NIGHT
CANOPUS
LATITUDE (DEG)
LONGITUDE (DEG)
NO SUN OR EARTH OCCULTATION
90
60
30
0
-30
-60
-90
-180
-150
-120
-90
-60
-30
0
30
60
90
120
150
180
10
10
10
5
15

CASE NO. 33

1000 x 15,000 km

$i = 40^{\circ}S$

$\Psi = 60$ deg

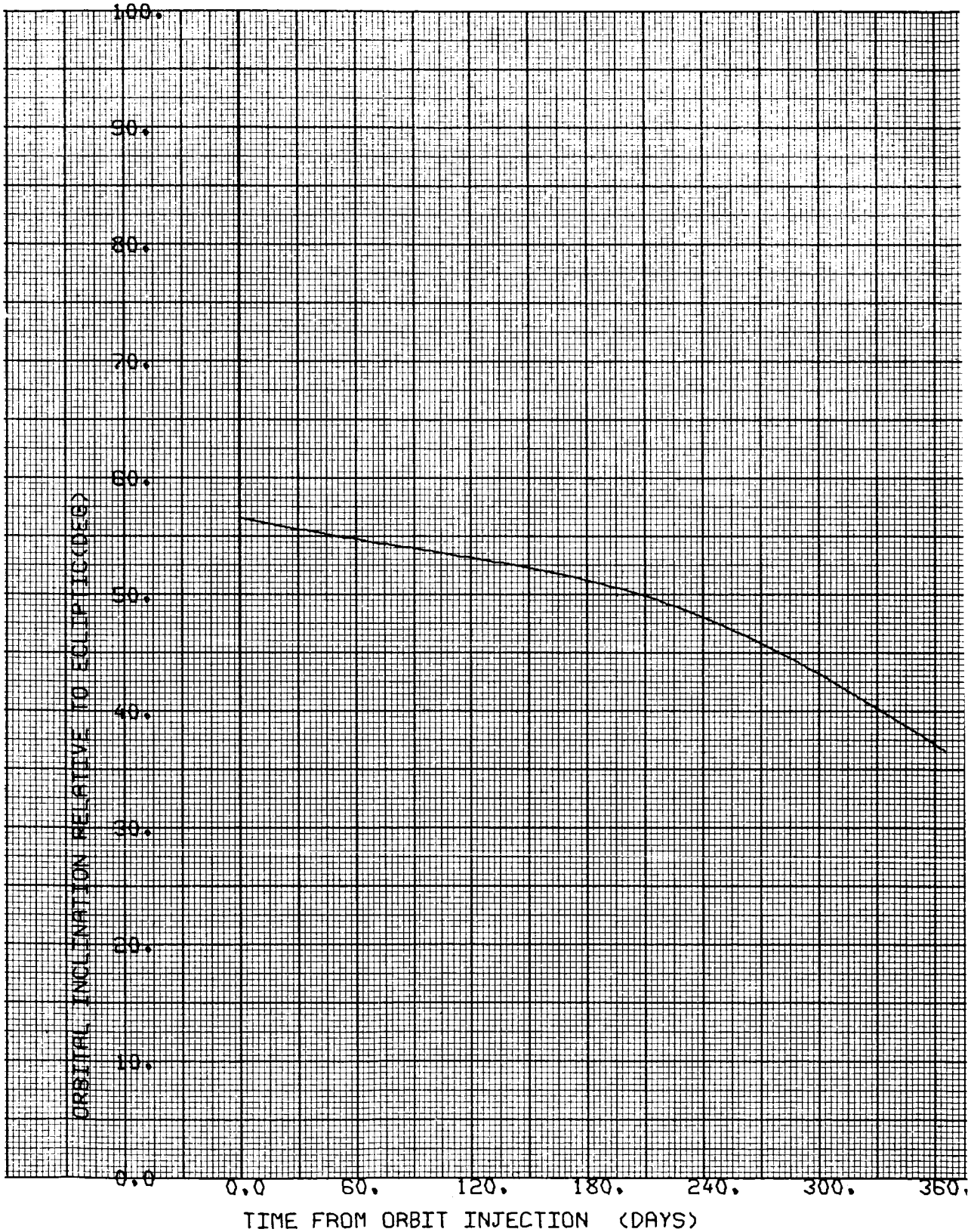
100.
90.
80.
70.
60.
50.
40.
30.
20.
10.
0.0
ORBITAL INCLINATION RELATIVE TO ECLIPTIC(DEG)
0.0
60.
120.
180.
240.
300.
360.
TIME FROM ORBIT INJECTION (DAYS)

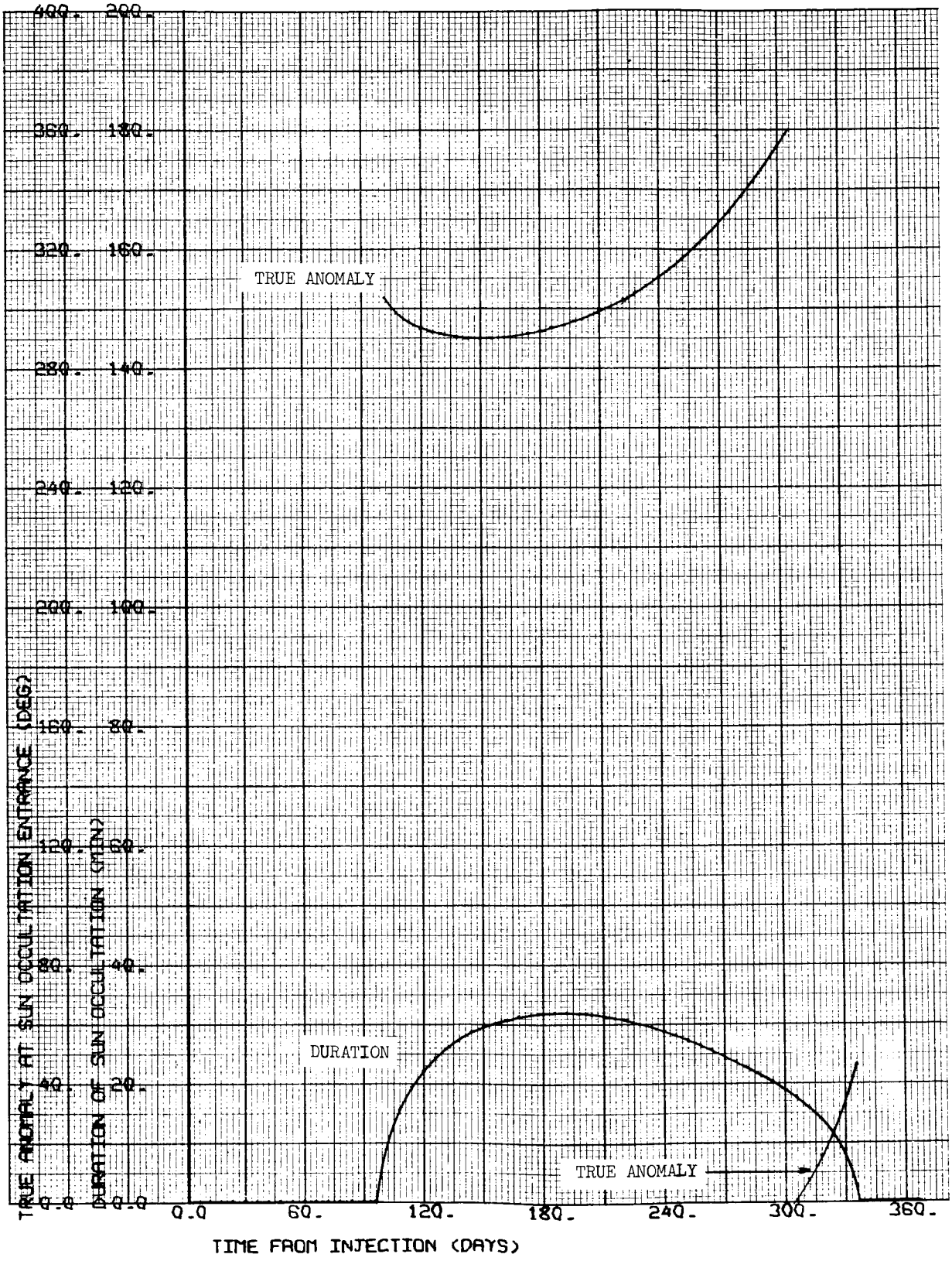
TRUE ANOMALY
DURATION
TRUE ANOMALY
TRUE ANOMALY AT SUN OCCULTATION ENTRANCE (DEG)
DURATION OF SUN OCCULTATION (MIN)
TIME FROM INJECTION (DAYS)
0.0
60.
120.
180.
240.
300.
360.
400.
360.
320.
280.
240.
200.
160.
120.
80.
40.
0.0
200.
180.
160.
140.
120.
100.
80.
60.
40.
20.
0.0

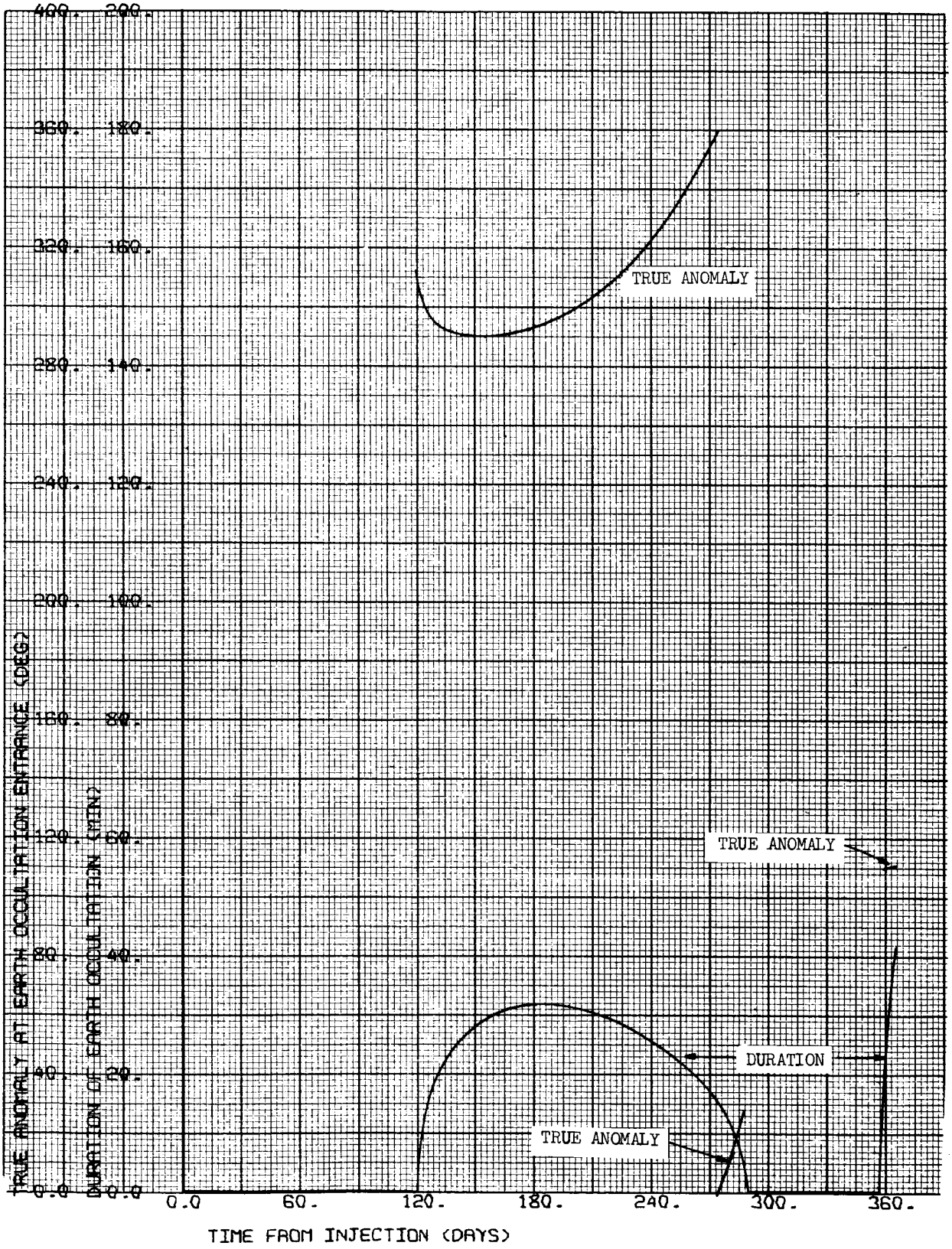
TRUE ANOMALY AT EARTH OCCULTATION ENTRANCE (DEG)
DURATION OF EARTH OCCULTATION (MIN)
TIME FROM INJECTION (DAYS)
TRUE ANOMALY
TRUE ANOMALY
DURATION
TRUE ANOMALY
0.0
60.
120.
180.
240.
300.
360.
20.
40.
60.
80.
100.
120.
140.
160.
180.
200.
220.
240.
260.
280.
300.
320.
340.
360.
380.
400.

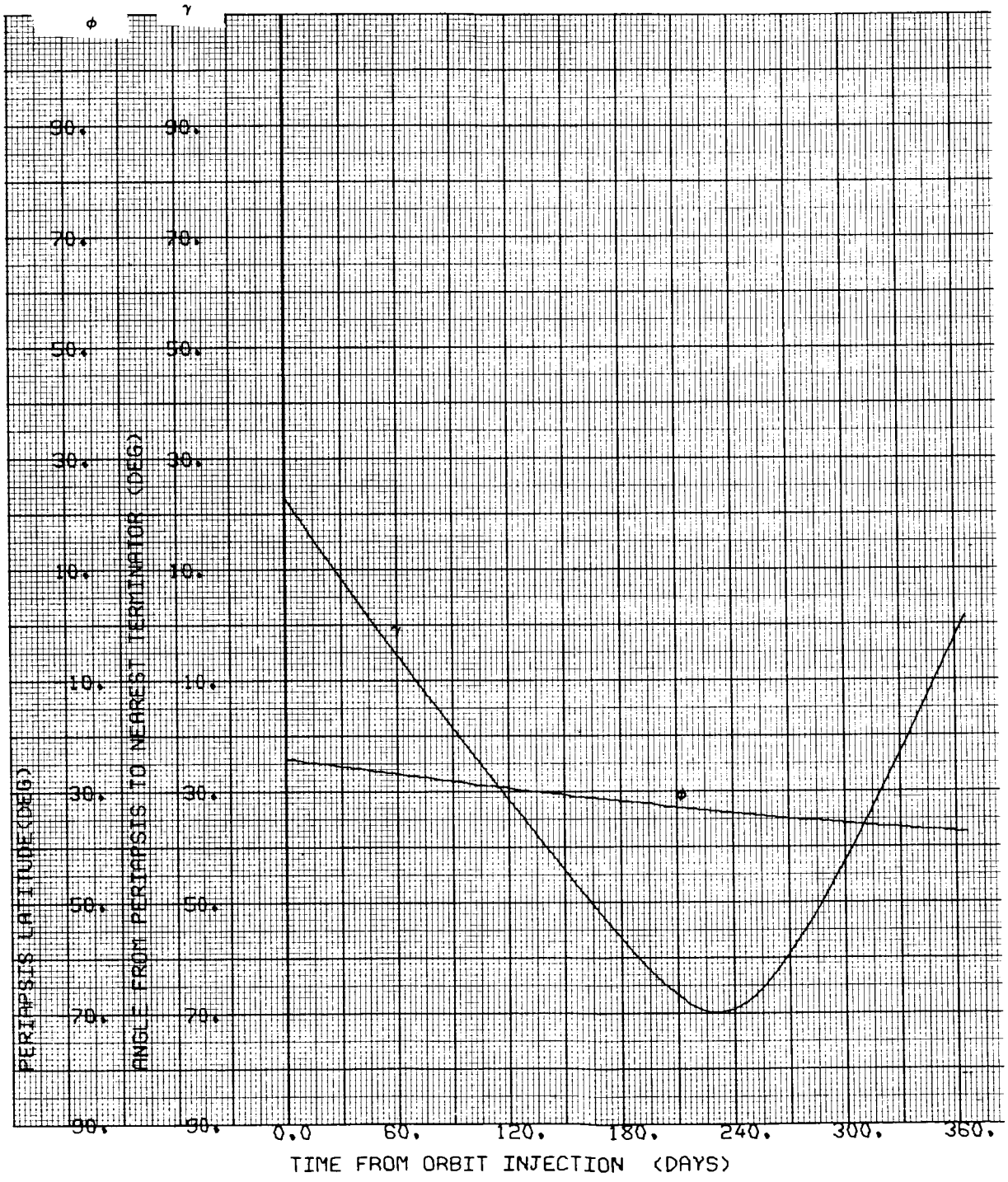
φ
γ
90.
70.
50.
30.
10.
10.
30.
50.
70.
90.
PERIAPSIS LATITUDE(DEG)
ANGLE FROM PERIAPSIS TO NEAREST TERMINATOR (DEG)
0.0
60.
120.
180.
240.
300.
360.
TIME FROM ORBIT INJECTION (DAYS)

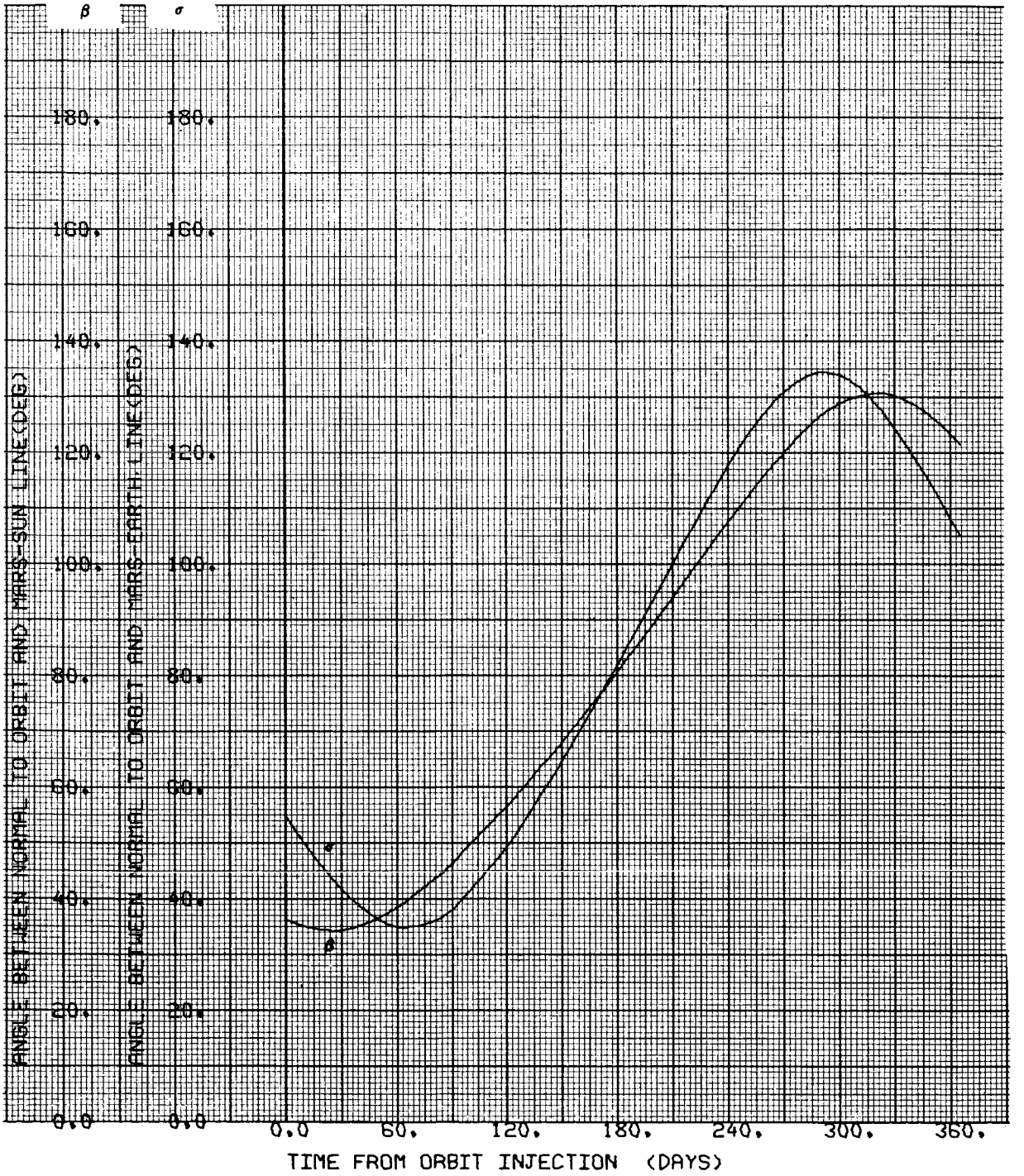
β
σ
180.
160.
140.
120.
100.
80.
60.
40.
20.
0.0
ANGLE BETWEEN NORMAL TO ORBIT AND MARS-SUN LINE(DEG)
ANGLE BETWEEN NORMAL TO ORBIT AND MARS-EARTH LINE(DEG)
0.0
60.
120.
180.
240.
300.
360.
TIME FROM ORBIT INJECTION (DAYS)

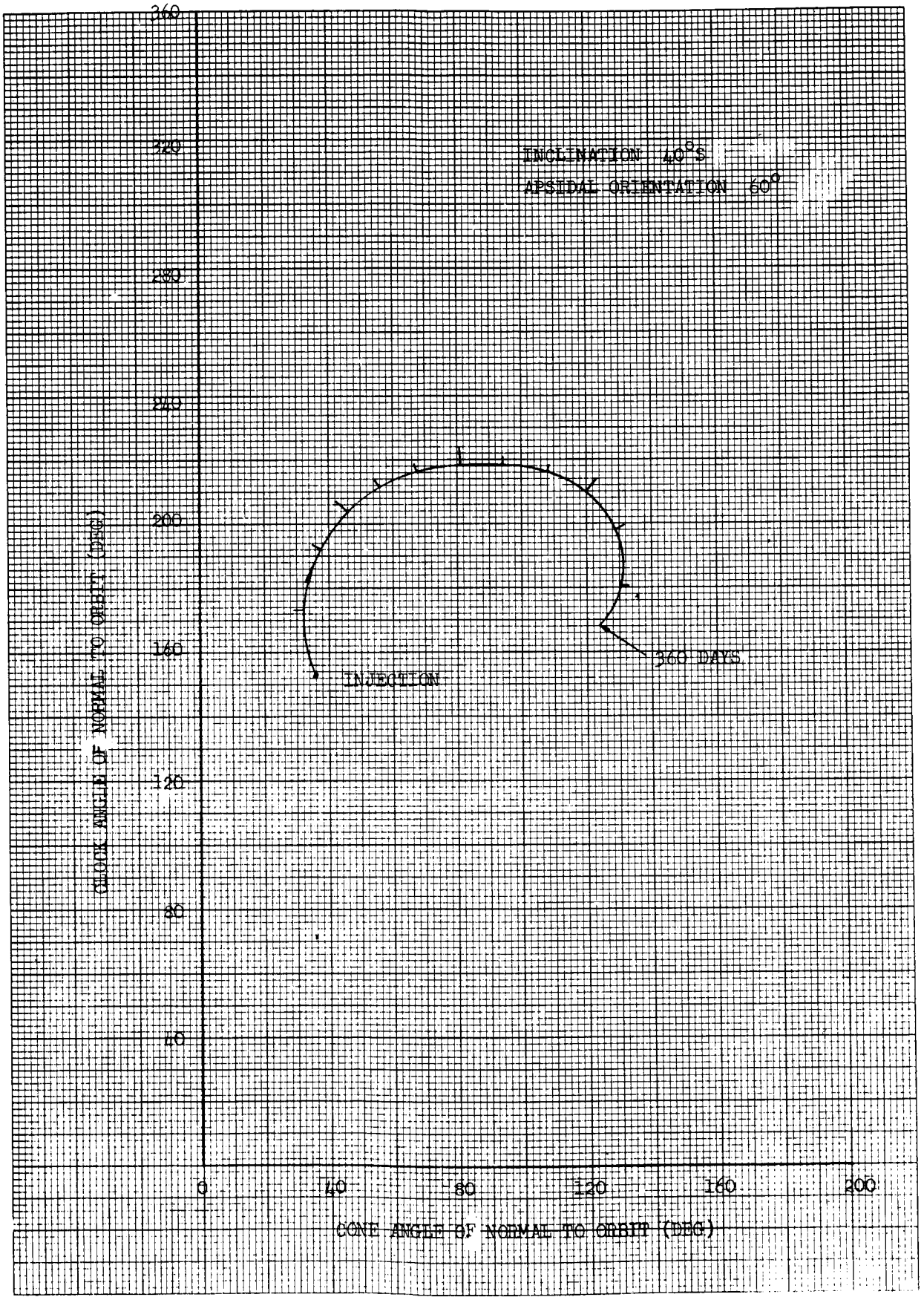
INCLINATION 40°S
APSIDAL ORIENTATION 60°
INJECTION
360 DAYS
CLOCK ANGLE OF NORMAL TO ORBIT (DEG)
CONE ANGLE OF NORMAL TO ORBIT (DEG)
360
320
280
240
200
160
120
80
40
0
40
80
120
160
200

CASE NO. 34

1000 x 15, 000 km

$i = 40^{\circ}S$

$\Psi = 90$ deg

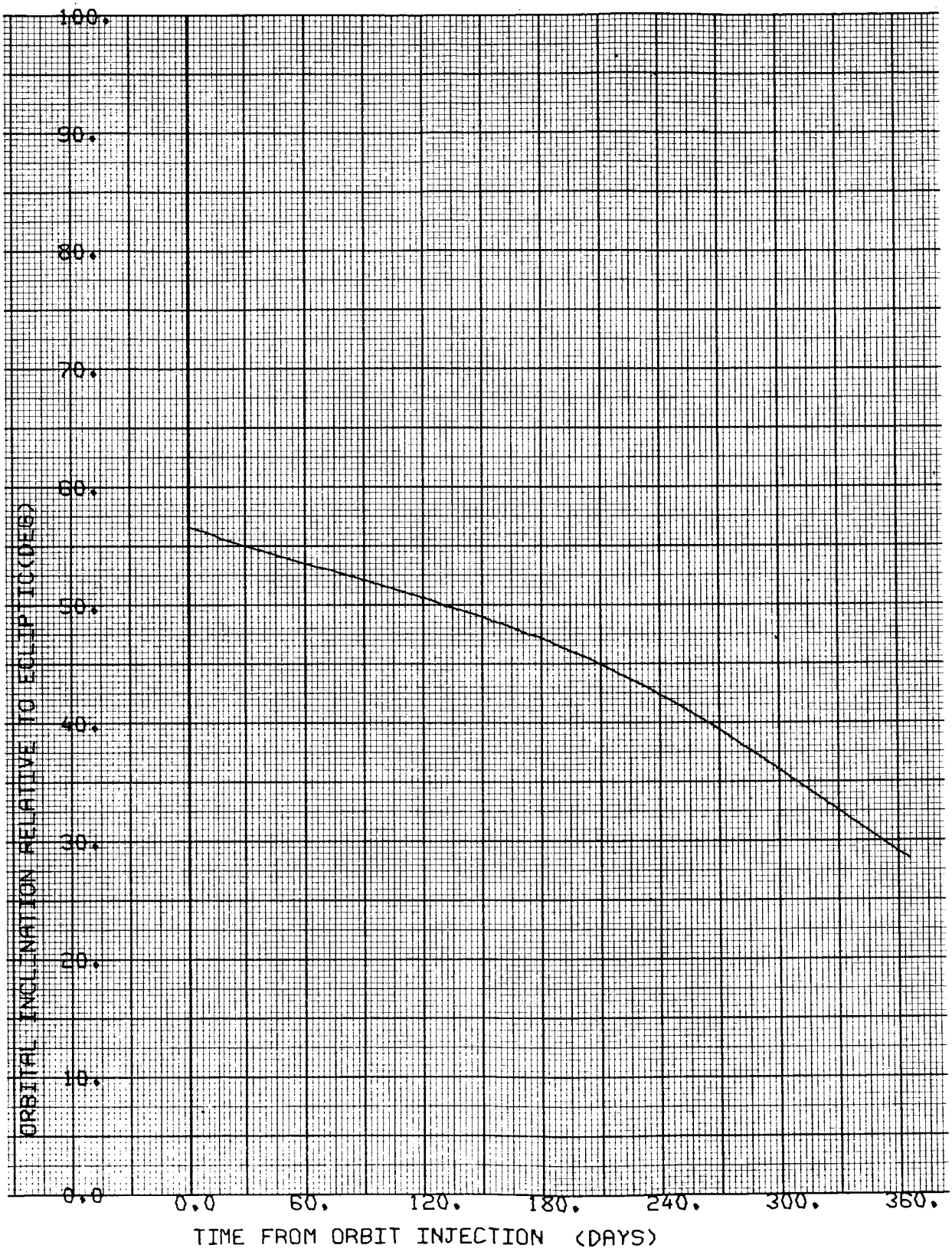
100.
90.
80.
70.
60.
50.
40.
30.
20.
10.
0.0
ORBITAL INCLINATION RELATIVE TO ECLIPTIC(DEG)
0.0
60.
120.
180.
240.
300.
360.
TIME FROM ORBIT INJECTION (DAYS)

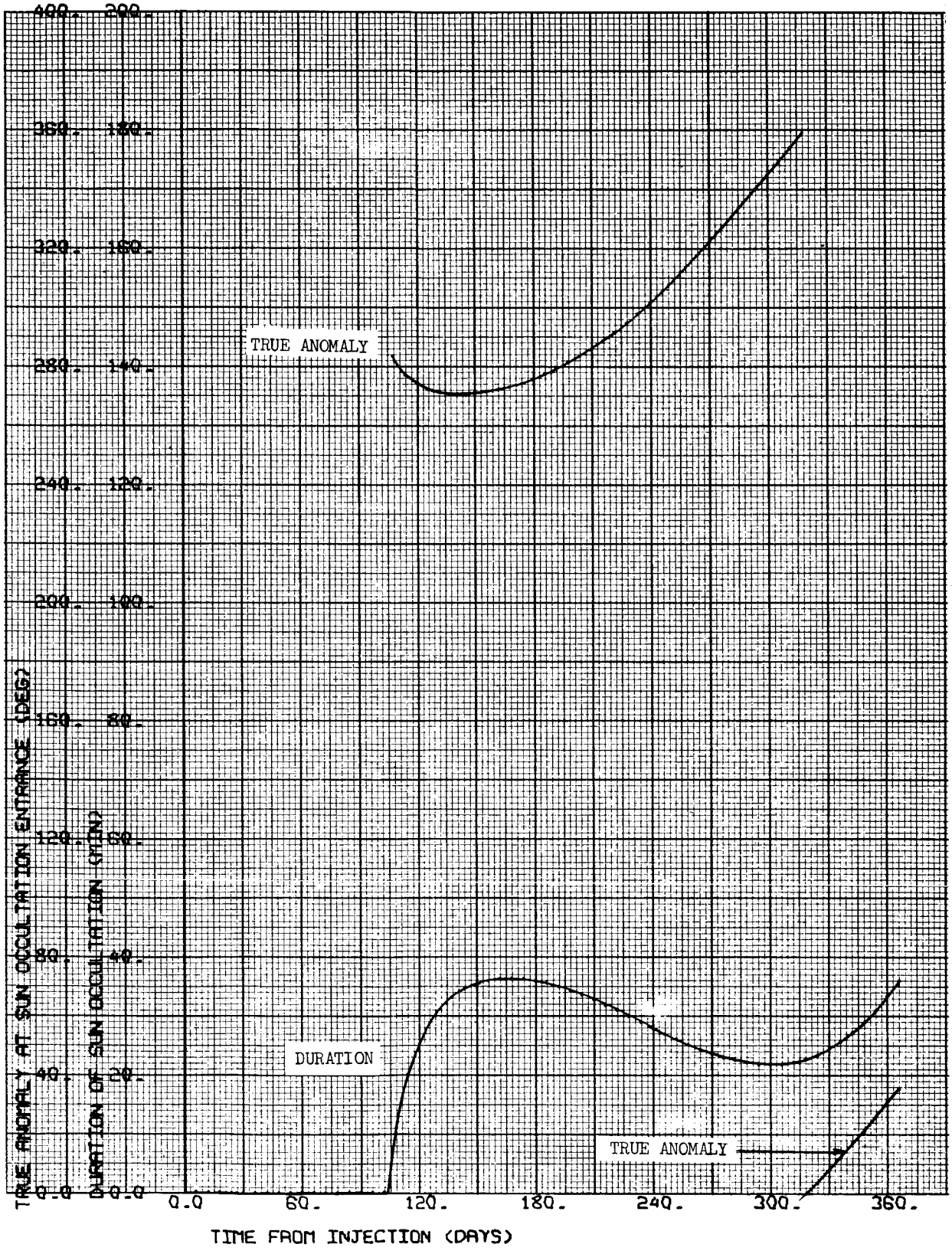
TRUE ANOMALY
DURATION
TRUE ANOMALY
TRUE ANOMALY AT SUN OCCULTATION ENTRANCE (DEG)
DURATION OF SUN OCCULTATION (MIN)
TIME FROM INJECTION (DAYS)
0.0
60.
120.
180.
240.
300.
360.
400.
360.
320.
280.
240.
200.
160.
120.
80.
40.
0.0
200.
180.
160.
140.
120.
100.
80.
60.
40.
20.
0.0

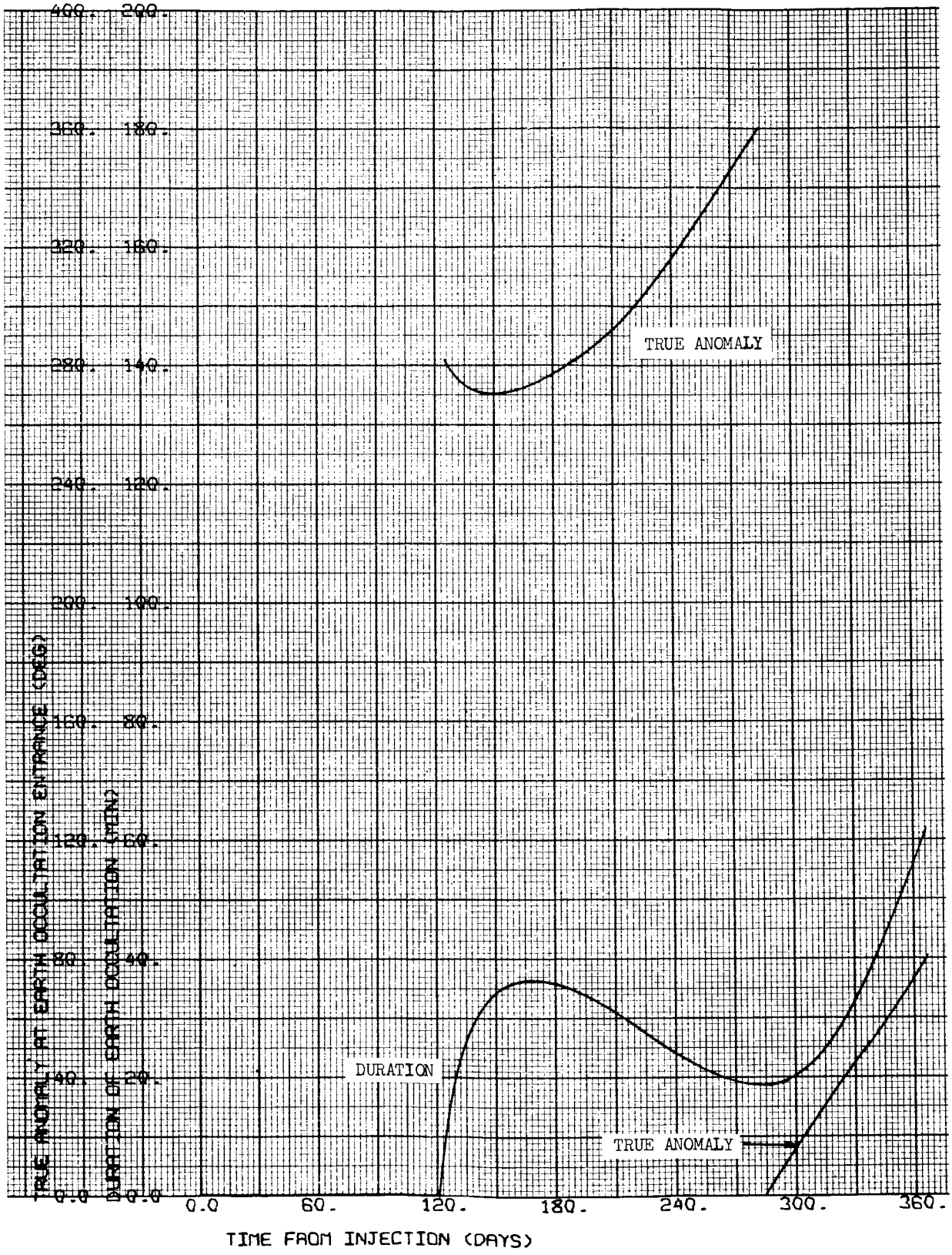
TRUE ANOMALY
DURATION
TRUE ANOMALY
TRUE ANOMALY AT EARTH OCCULTATION ENTRANCE (DEG)
DURATION OF EARTH OCCULTATION (MIN)
TIME FROM INJECTION (DAYS)
0.0
60.
120.
180.
240.
300.
360.
400.
360.
320.
280.
240.
200.
160.
120.
80.
40.
0.0
200.
180.
160.
140.
120.
100.
80.
60.
40.
20.
0.0

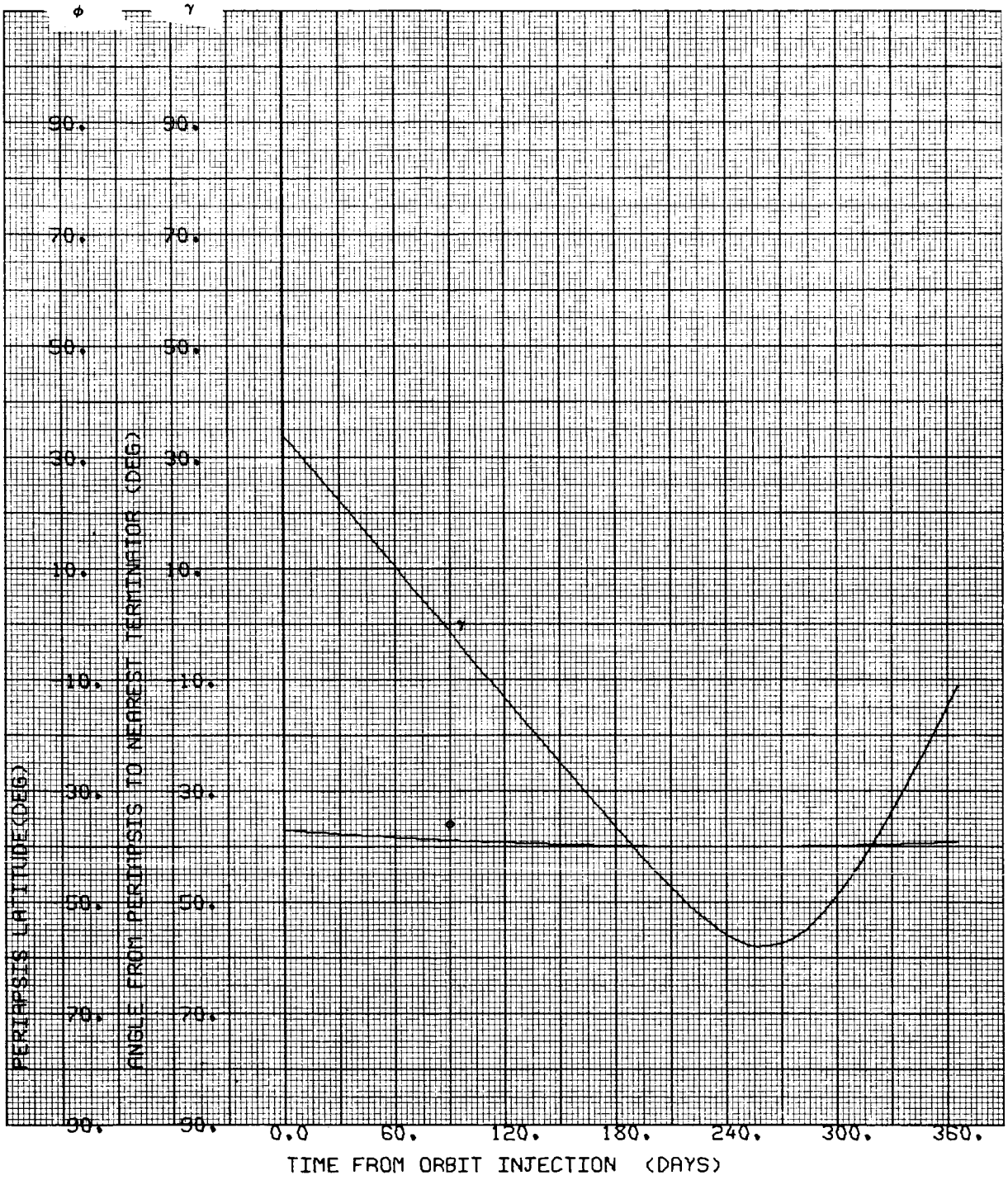
φ
γ
90.
70.
50.
30.
10.
-10.
-30.
-50.
-70.
-90.
PERIAPSIS LATITUDE (DEG)
ANGLE FROM PERIAPSIS TO NEAREST TERMINATOR (DEG)
0.0
60.
120.
180.
240.
300.
360.
TIME FROM ORBIT INJECTION (DAYS)

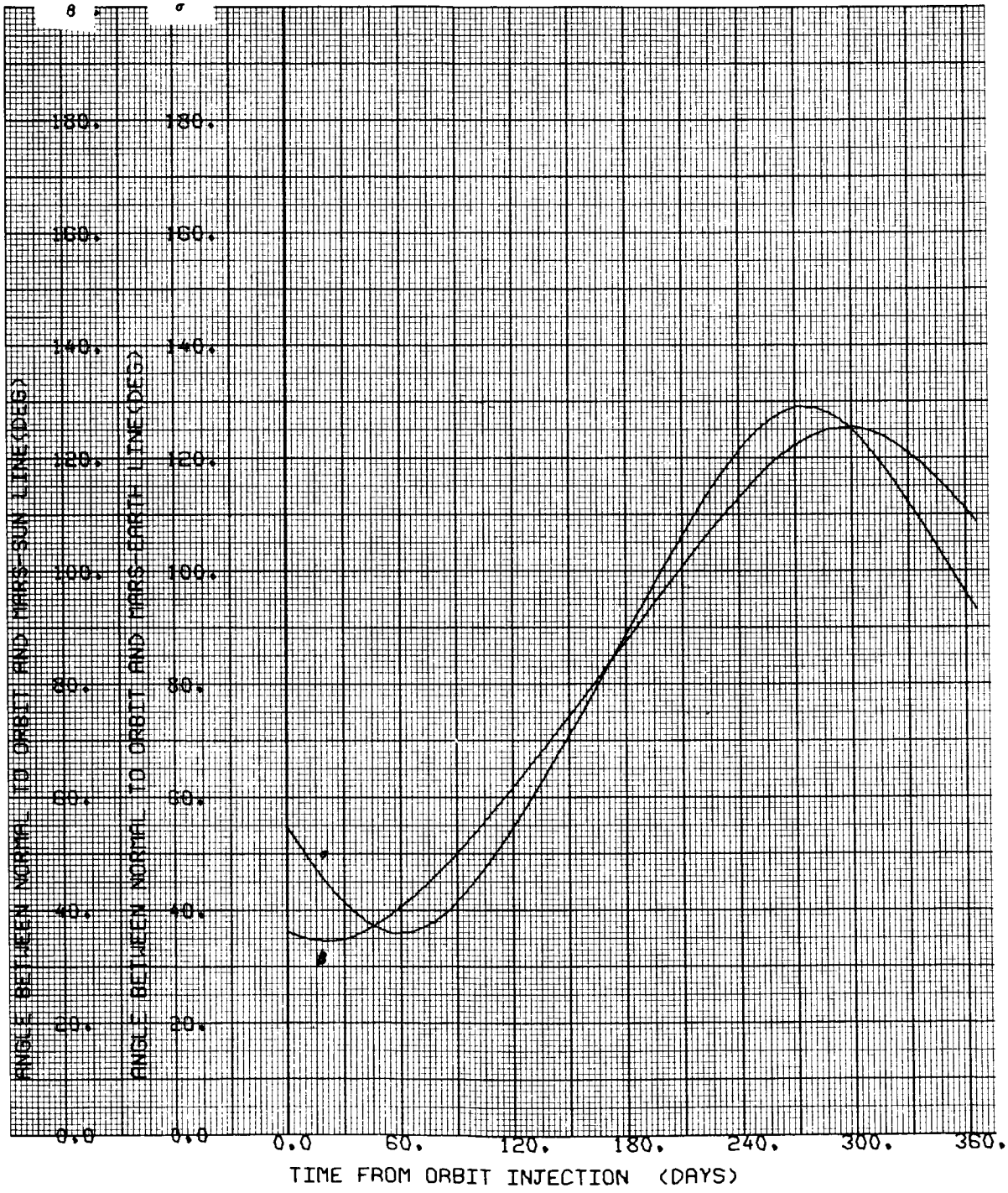
β
σ
180.
160.
140.
120.
100.
80.
60.
40.
20.
0.0
0.0
60.
120.
180.
240.
300.
360.
ANGLE BETWEEN NORMAL TO ORBIT AND MARS-SUN LINE (DEG)
ANGLE BETWEEN NORMAL TO ORBIT AND MARS-EARTH LINE (DEG)
TIME FROM ORBIT INJECTION (DAYS)

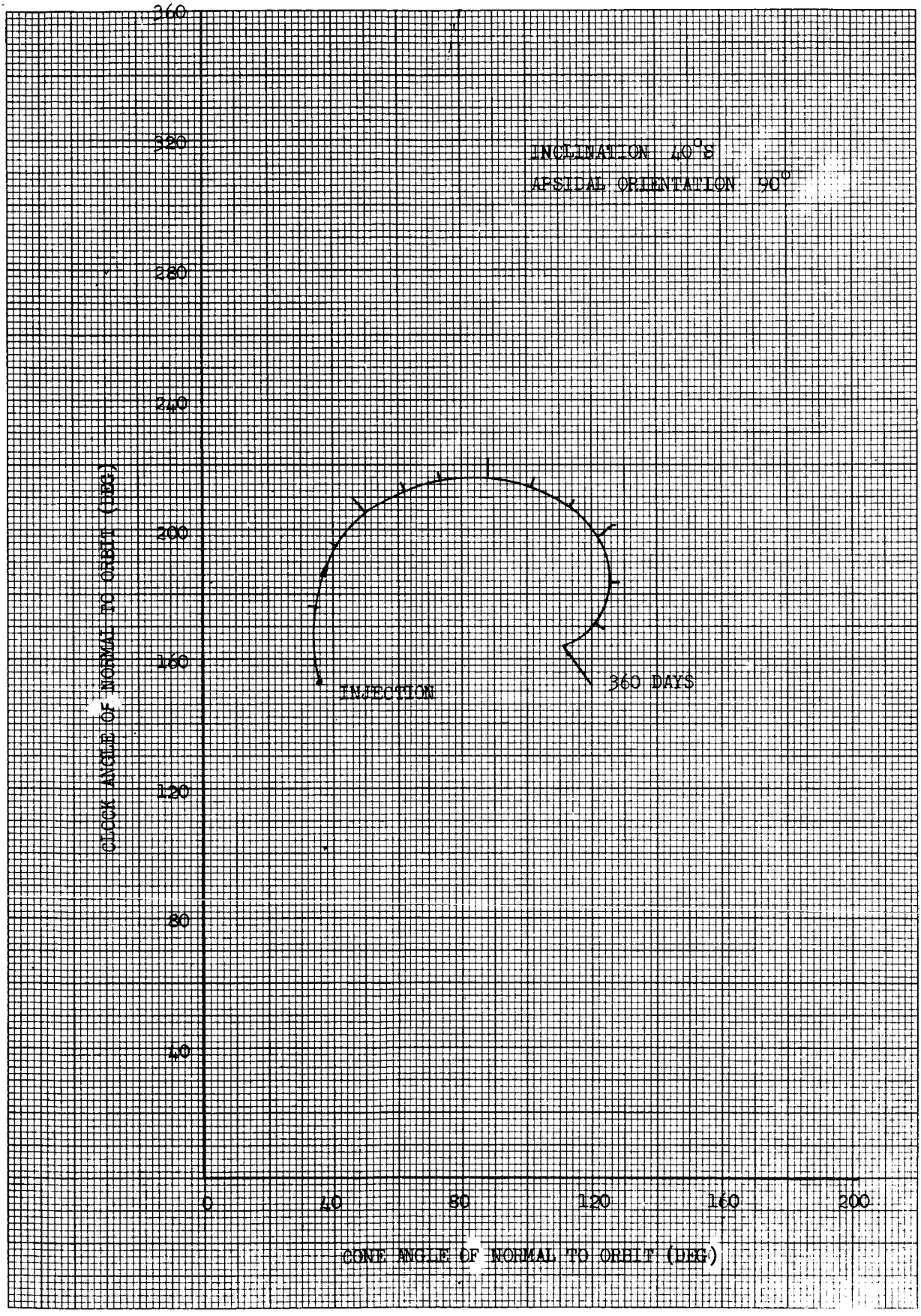
INCLINATION 40°S
APSIDAL ORIENTATION 90°
INJECTION
360 DAYS
CLOCK ANGLE OF NORMAL TO ORBIT (DEG)
CONE ANGLE OF NORMAL TO ORBIT (DEG)
360
320
280
240
200
160
120
80
40
0
40
80
120
160
200

CASE NO. 35

1000 x 15, 000 km

$i = 40^{\circ}S$

$\Psi = 150$ deg

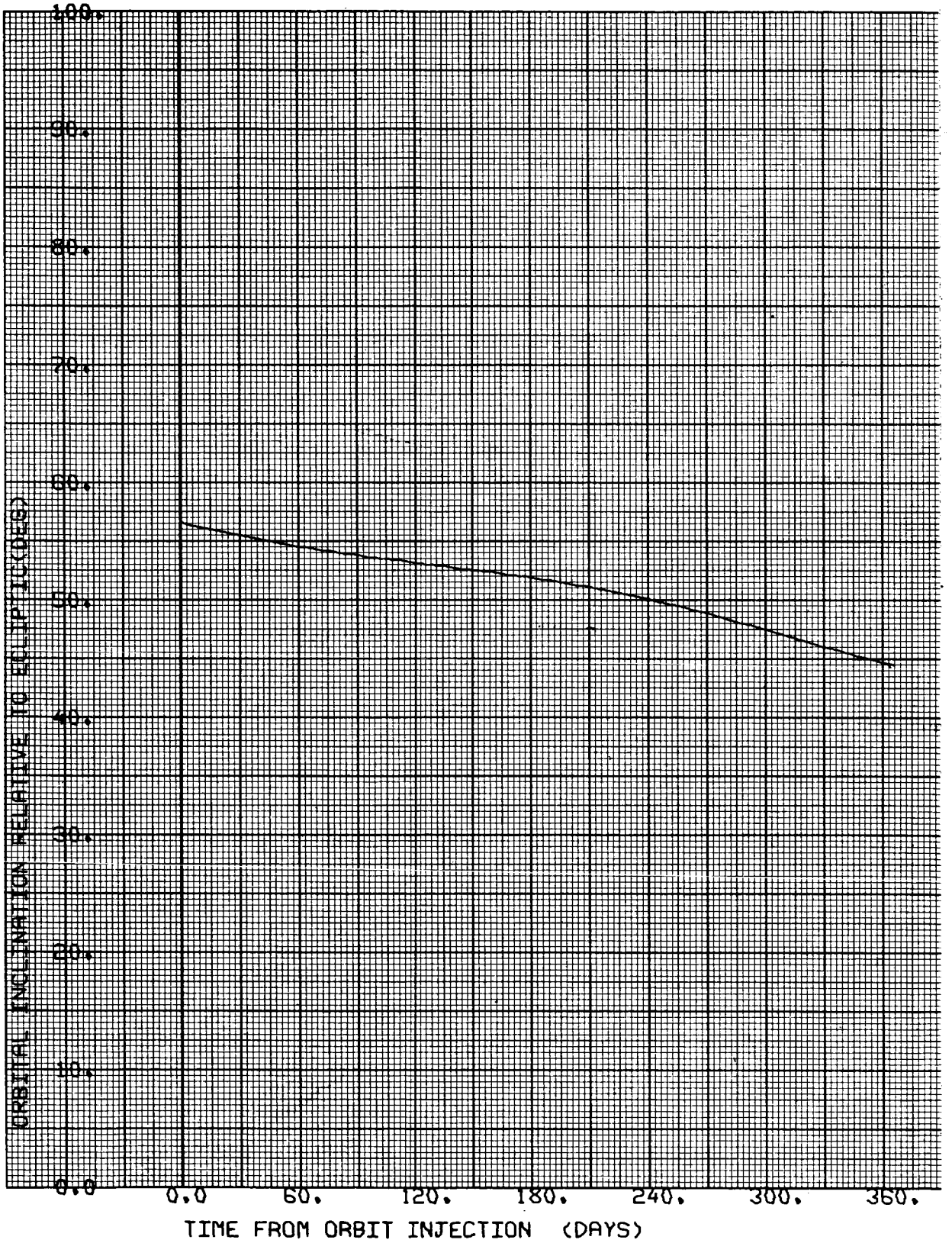
100.
90.
80.
70.
60.
50.
40.
30.
20.
10.
0.0
ORBITAL INCLINATION RELATIVE TO ECLIPTIC (DEG)
0.0
60.
120.
180.
240.
300.
360.
TIME FROM ORBIT INJECTION (DAYS)

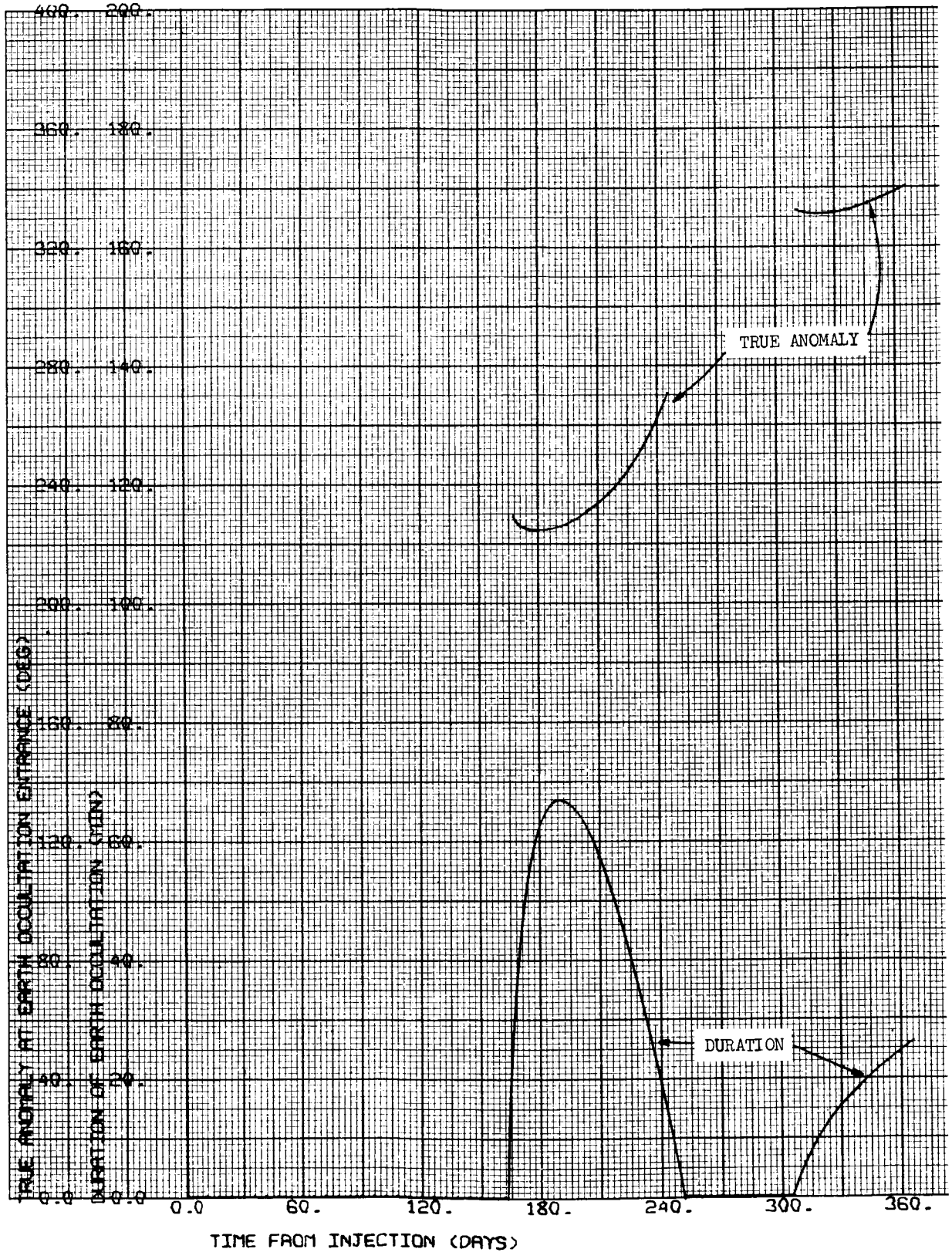
TRUE ANOMALY
DURATION
TRUE ANOMALY AT EARTH OCCULTATION ENTRANCE (DEG)
DURATION OF EARTH OCCULTATION (MIN)
TIME FROM INJECTION (DAYS)
0.0
60.
120.
180.
240.
300.
360.
40.
80.
120.
160.
200.
240.
280.
320.
360.
400.

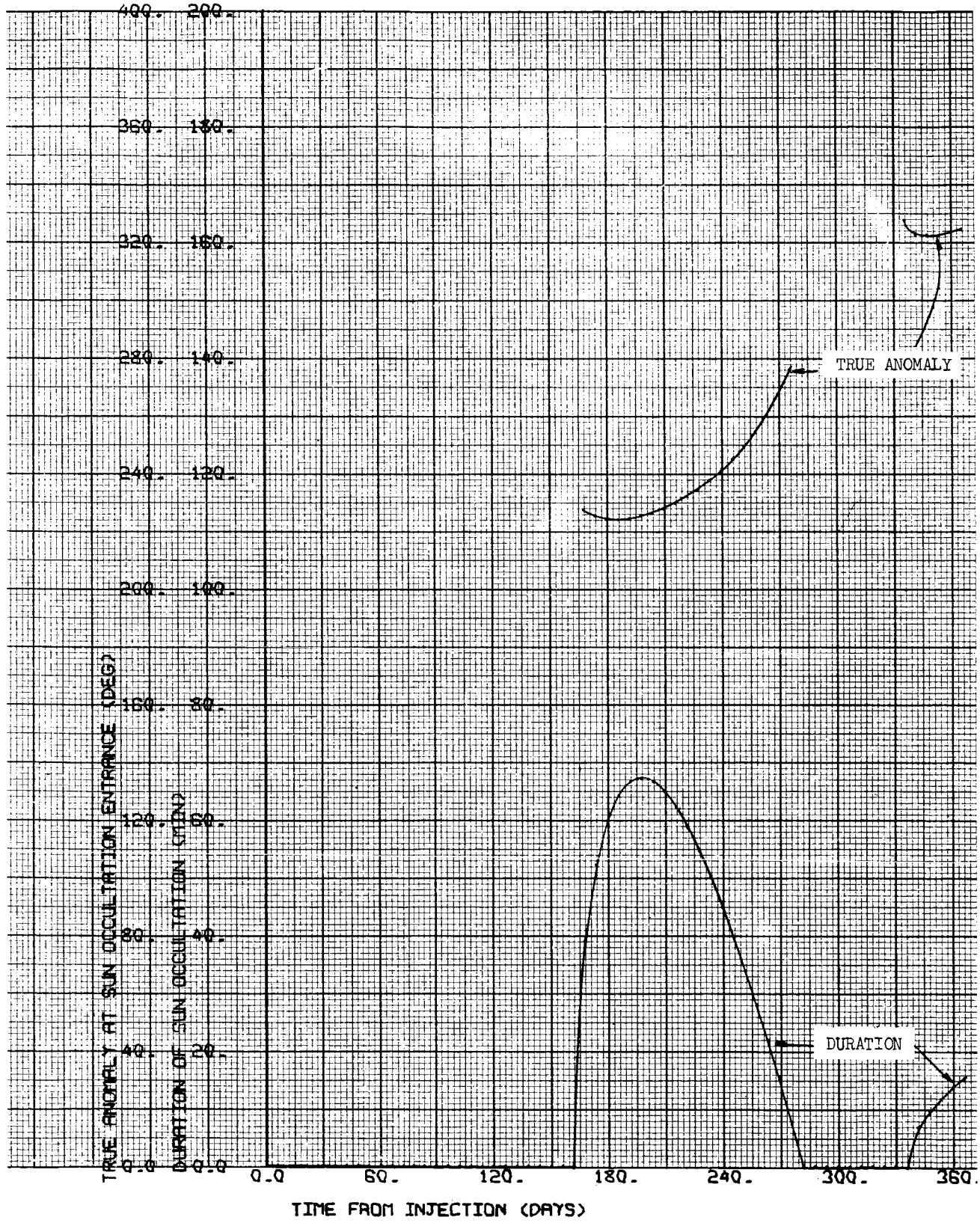
TRUE ANOMALY
DURATION
TRUE ANOMALY AT SUN OCCULTATION ENTRANCE (DEG)
DURATION OF SUN OCCULTATION (MIN)
TIME FROM INJECTION (DAYS)
0.0
60.
120.
180.
240.
300.
360.
200.
180.
160.
140.
120.
100.
80.
60.
40.
20.
0.0

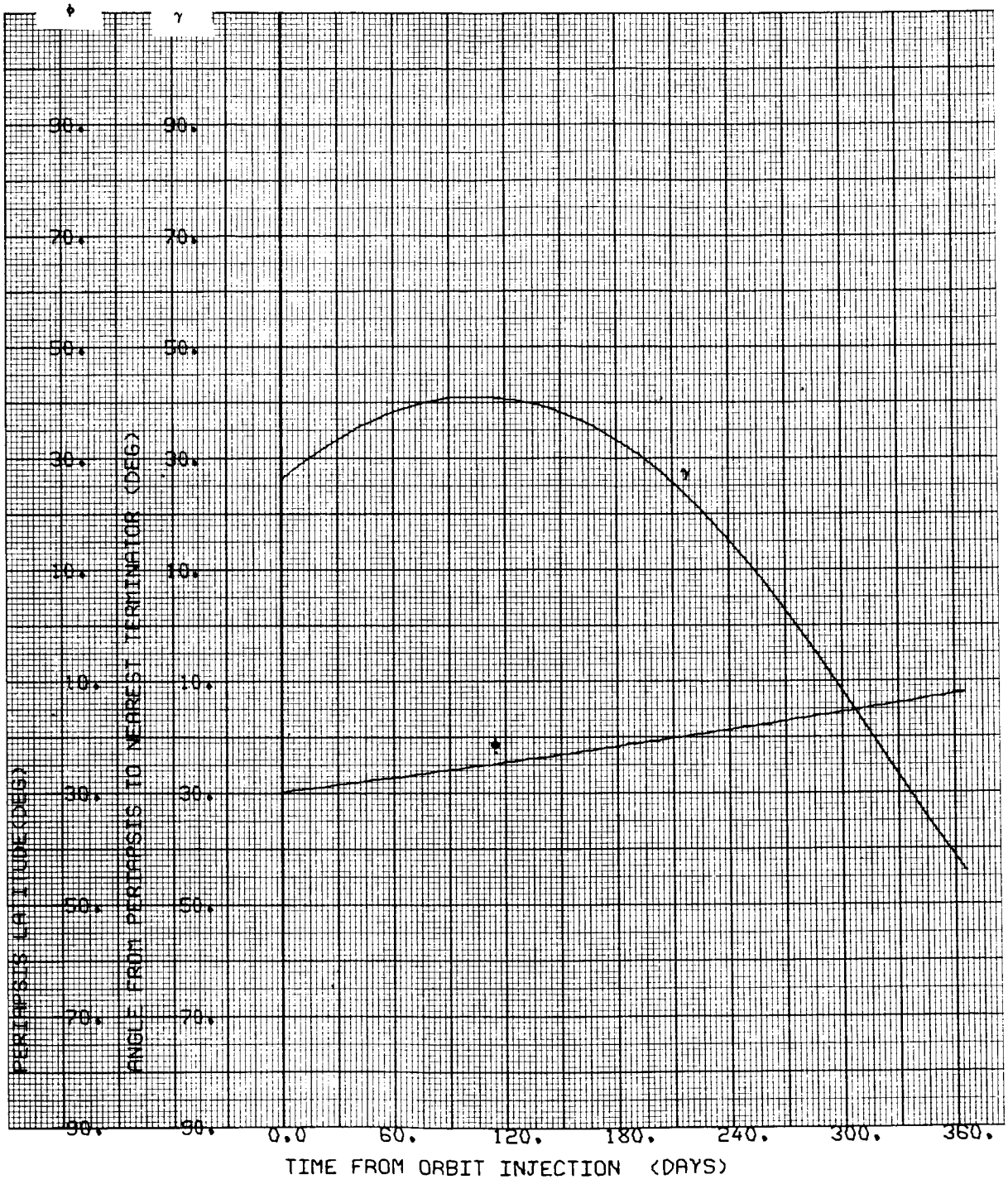
ϕ
γ
90.
70.
50.
30.
10.
10.
30.
50.
70.
90.
PERIAPSIS LATITUDE (DEG)
ANGLE FROM PERIAPSIS TO NEAREST TERMINATOR (DEG)
0.0
60.
120.
180.
240.
300.
360.
TIME FROM ORBIT INJECTION (DAYS)

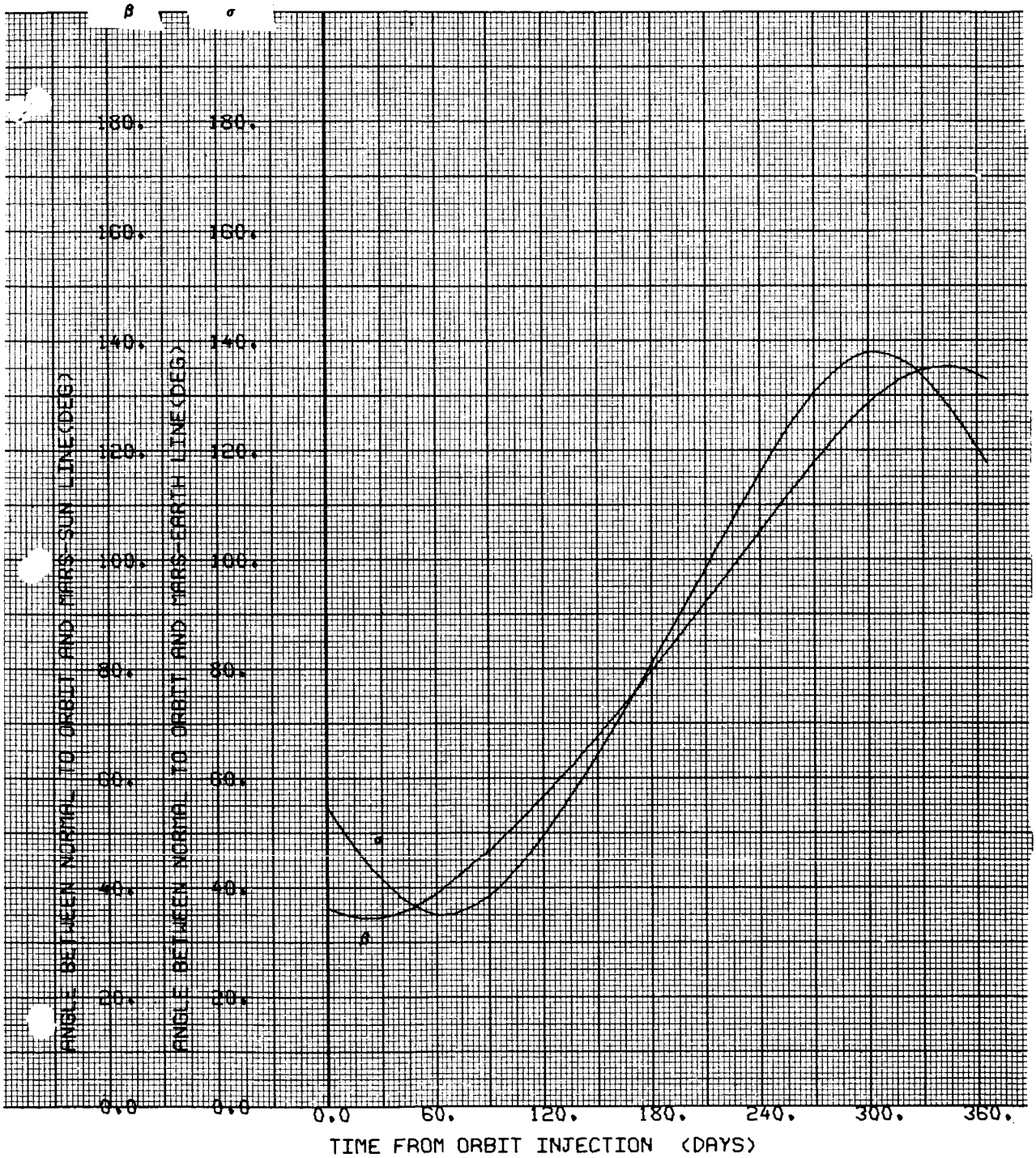
β
σ
180.
160.
140.
120.
100.
80.
60.
40.
20.
0.0
ANGLE BETWEEN NORMAL TO ORBIT AND MARS SUN LINE(DEG)
ANGLE BETWEEN NORMAL TO ORBIT AND MARS-EARTH LINE(DEG)
0.0
60.
120.
180.
240.
300.
360.
TIME FROM ORBIT INJECTION (DAYS)

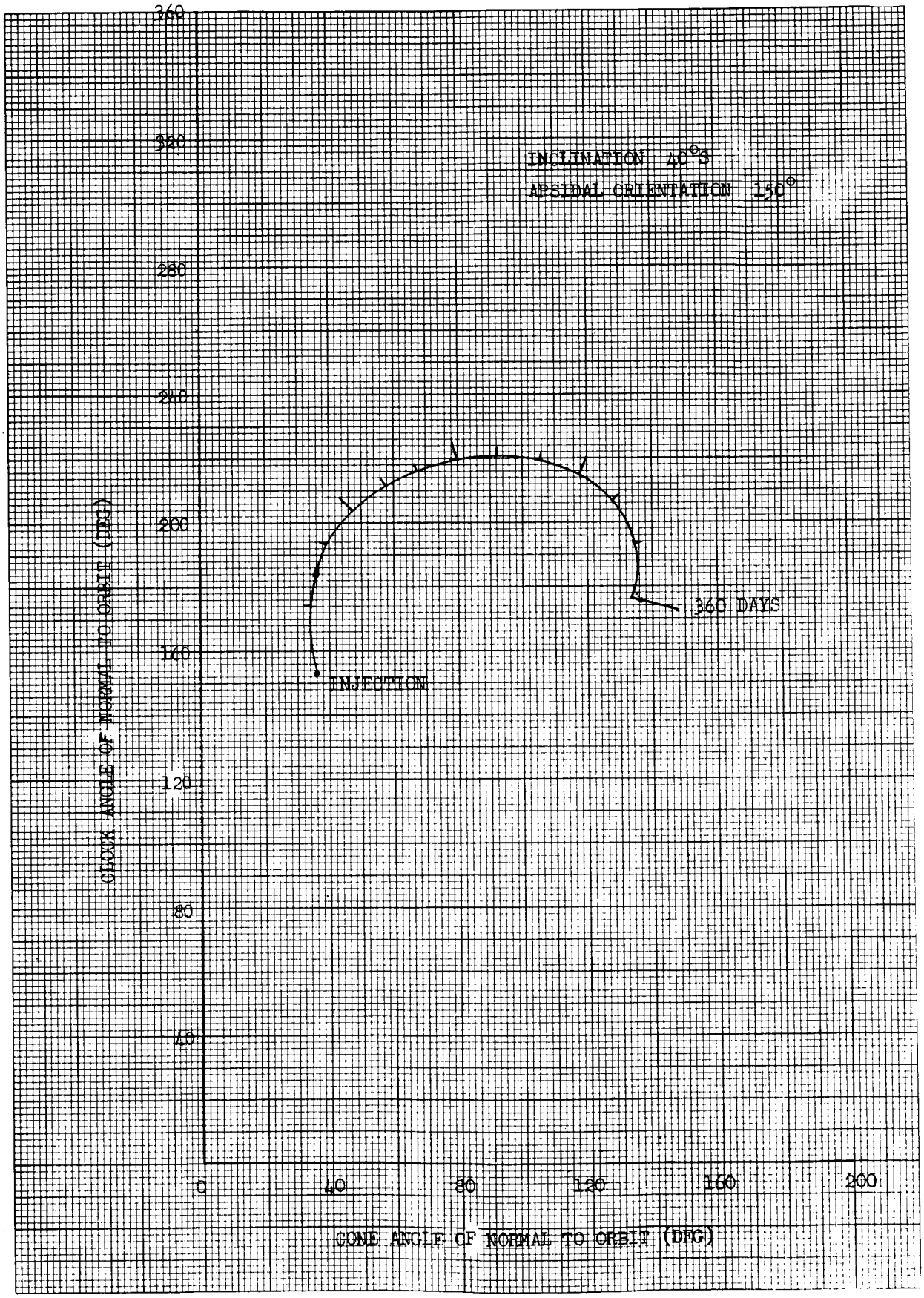
INCLINATION 40°S
APSIDAL ORIENTATION 150°
360 DAYS
INJECTION
CLOCK ANGLE OF NORMAL TO ORBIT (DEG)
CONE ANGLE OF NORMAL TO ORBIT (DEG)
360
320
280
240
200
160
120
80
40
0
40
80
120
160
200

CASE NO. 36

1000 x 15, 000 km

$i = 40^{\circ}S$

$\Psi = 126.375$ deg

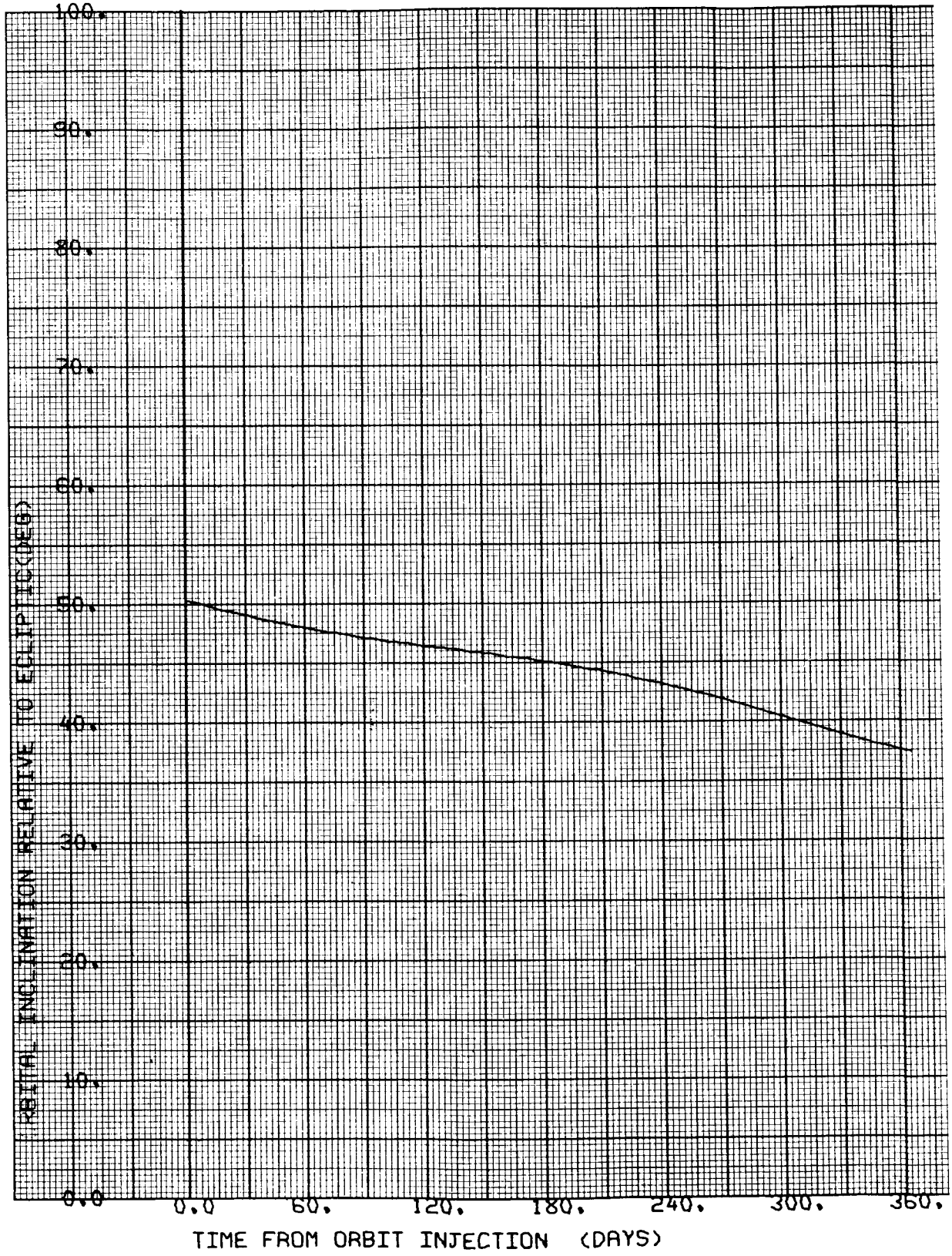
100.
90.
80.
70.
60.
50.
40.
30.
20.
10.
0.0
HELIO. INCLINATION RELATIVE TO ECLIPTIC(DEG)
0.0
60.
120.
180.
240.
300.
360.
TIME FROM ORBIT INJECTION (DAYS)

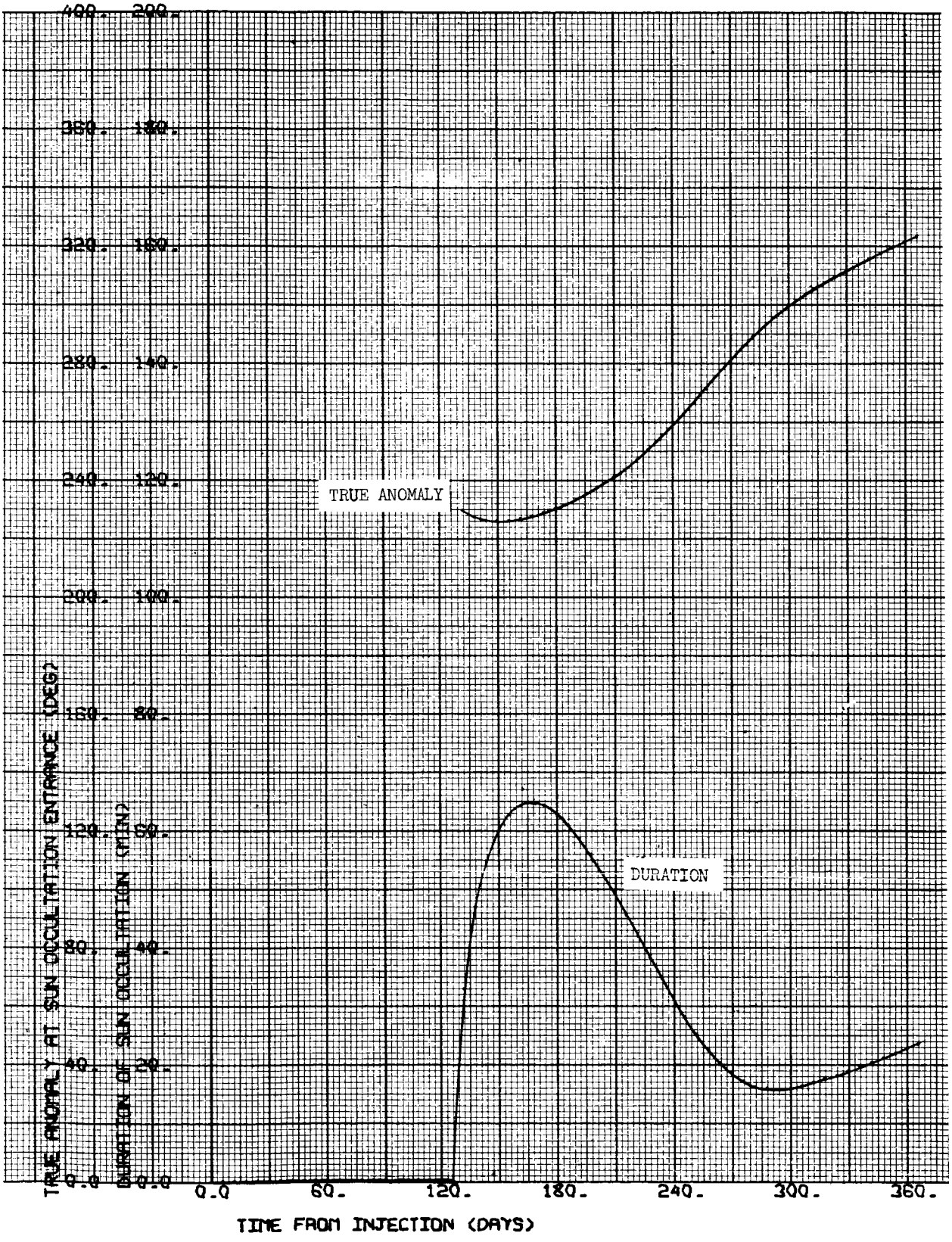
TRUE ANOMALY
DURATION
TRUE ANOMALY AT SUN OCCULTATION ENTRANCE (DEG)
DURATION OF SUN OCCULTATION (MIN)
TIME FROM INJECTION (DAYS)
0.0
60.
120.
180.
240.
300.
360.
400.
380.
320.
280.
240.
200.
160.
120.
80.
40.
200.
180.
160.
140.
120.
100.
80.
60.
40.
20.
0.0

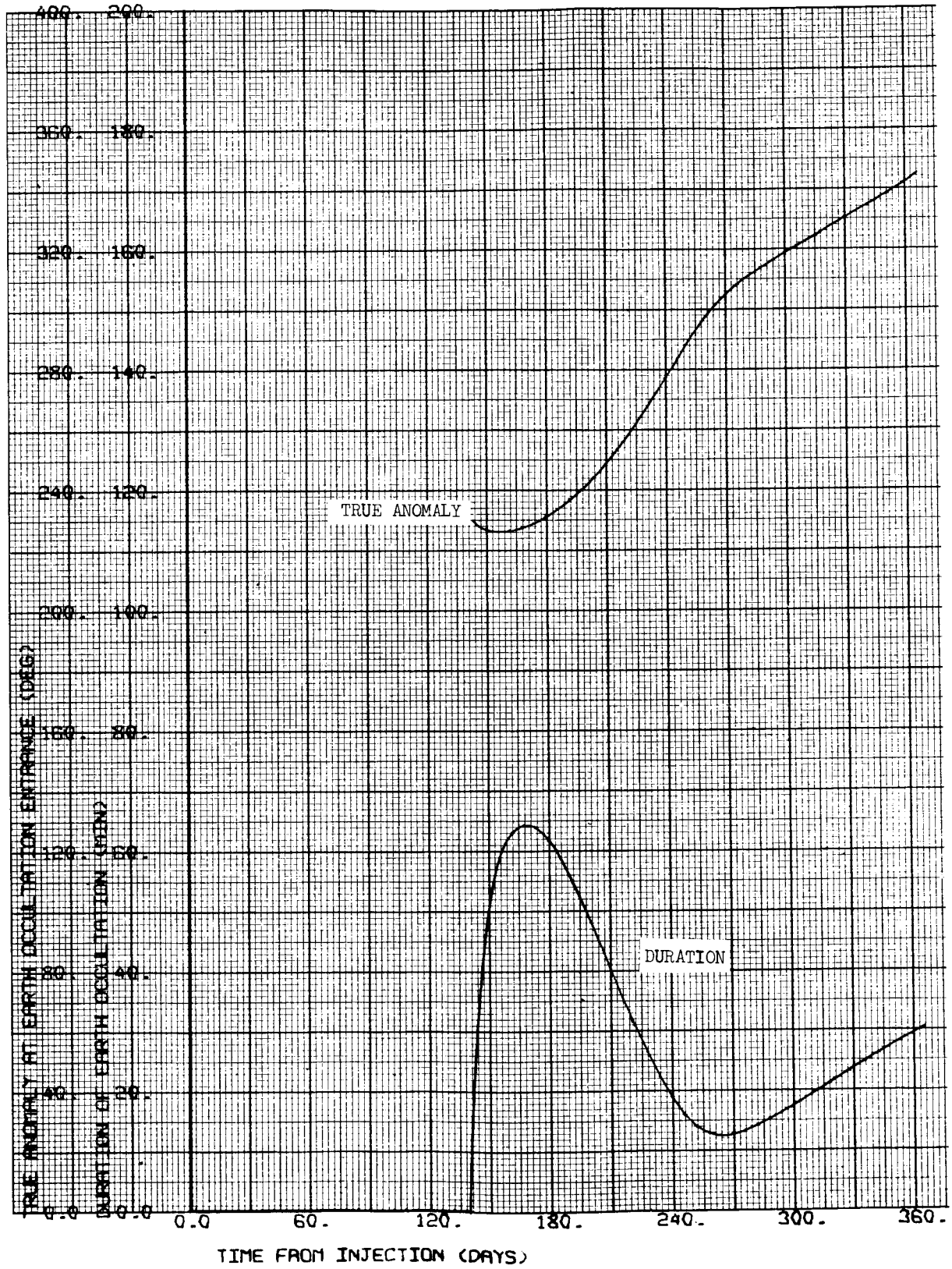
TRUE ANOMALY
DURATION
TRUE ANOMALY AT EARTH OCCULTATION ENTRANCE (DEG)
DURATION OF EARTH OCCULTATION (DEG)
TIME FROM INJECTION (DAYS)
400.
360.
320.
280.
240.
200.
160.
120.
80.
40.
0.0
200.
180.
160.
140.
120.
100.
80.
60.
40.
20.
0.0
0.0
60.
120.
180.
240.
300.
360.

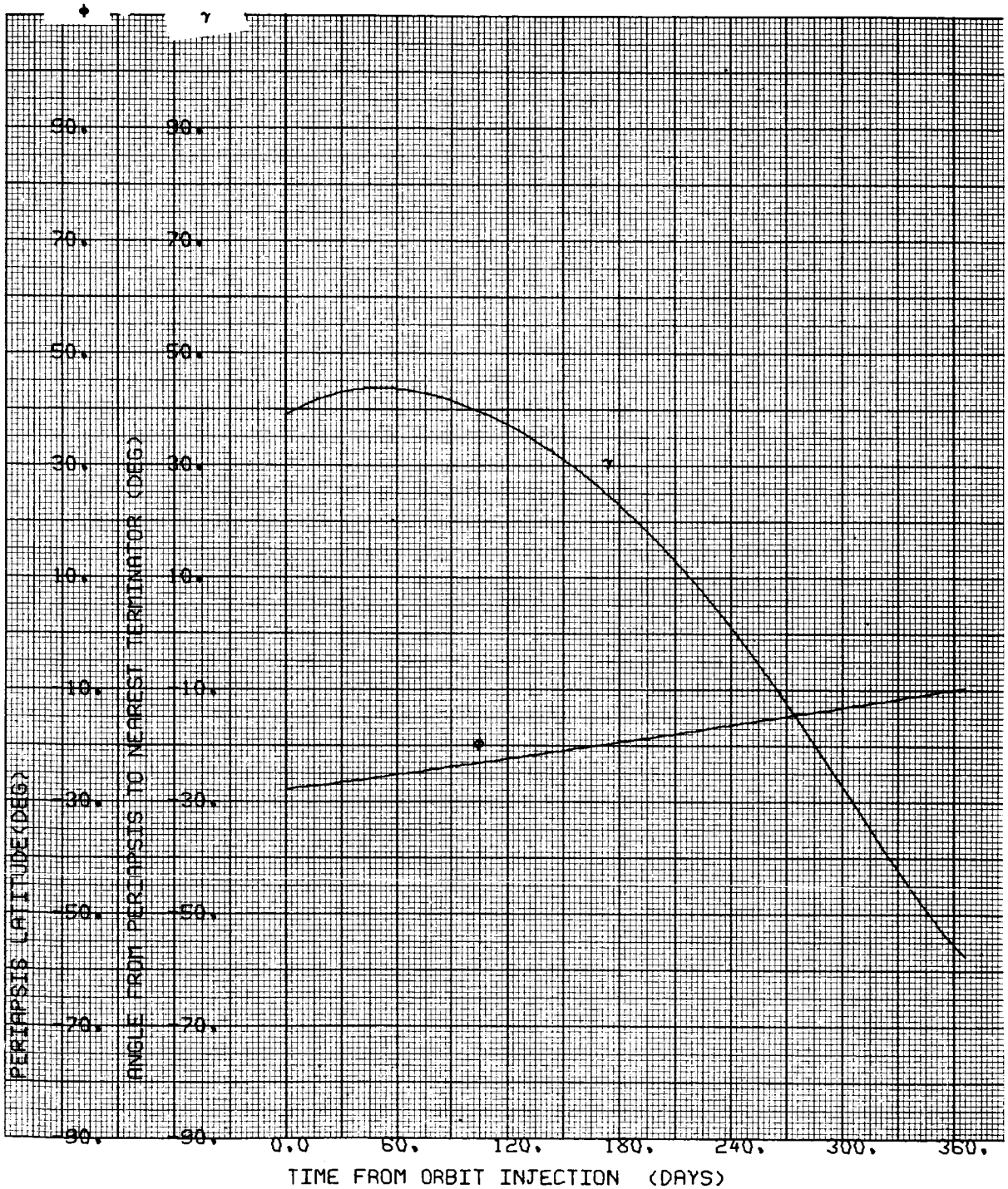
ϕ
γ
90.
70.
50.
30.
10.
-10.
-30.
-50.
-70.
-90.
0.0
60.
120.
180.
240.
300.
360.
PERIAPSIS LATITUDE (DEG)
ANGLE FROM PERIAPSIS TO NEAREST TERMINATOR (DEG)
TIME FROM ORBIT INJECTION (DAYS)

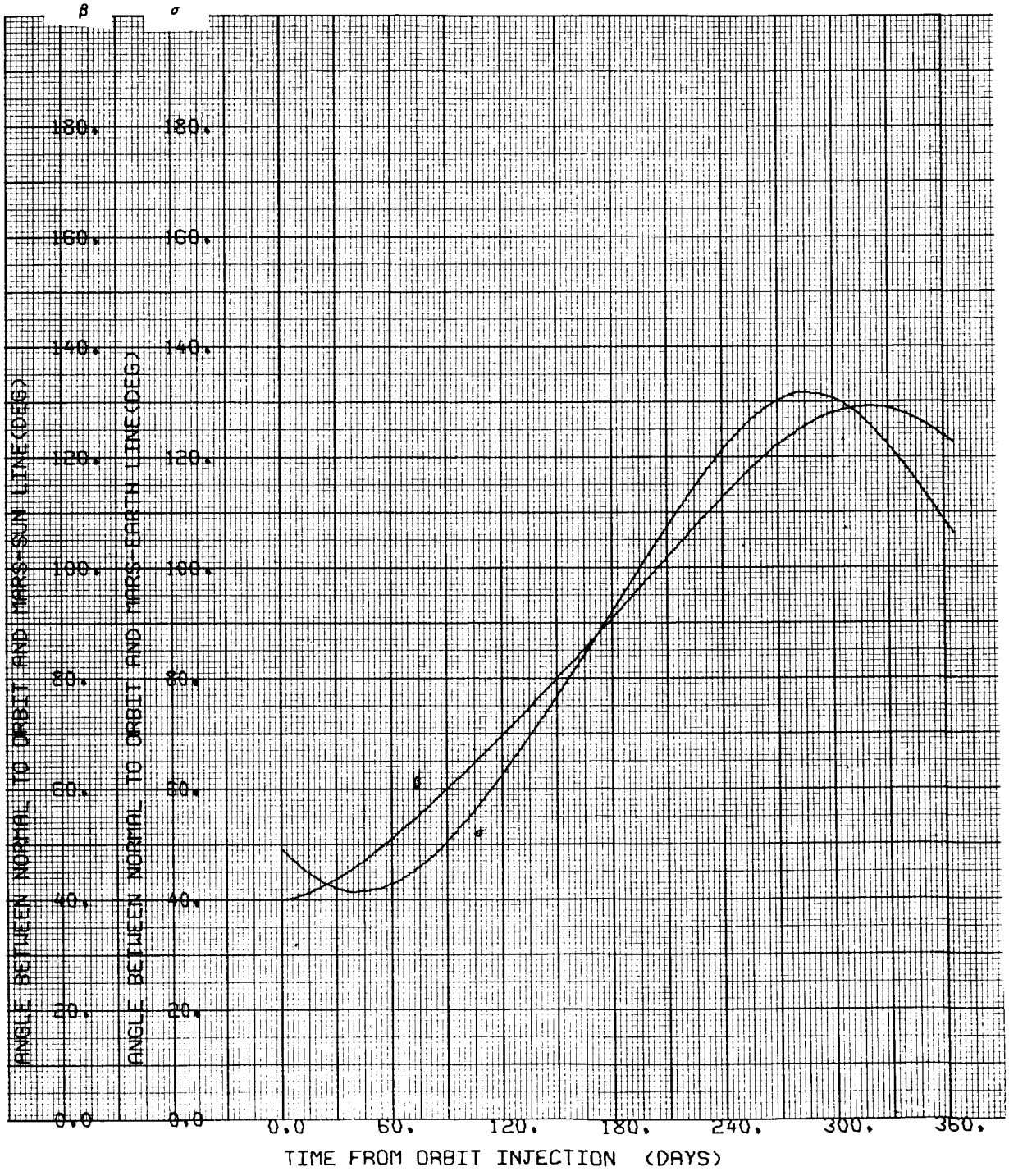
β
σ
180.
160.
140.
120.
100.
80.
60.
40.
20.
0.0
ANGLE BETWEEN NORMAL TO ORBIT AND MARS-SUN LINE(DEG)
ANGLE BETWEEN NORMAL TO ORBIT AND MARS-EARTH LINE(DEG)
0.0
60.
120.
180.
240.
300.
360.
TIME FROM ORBIT INJECTION (DAYS)

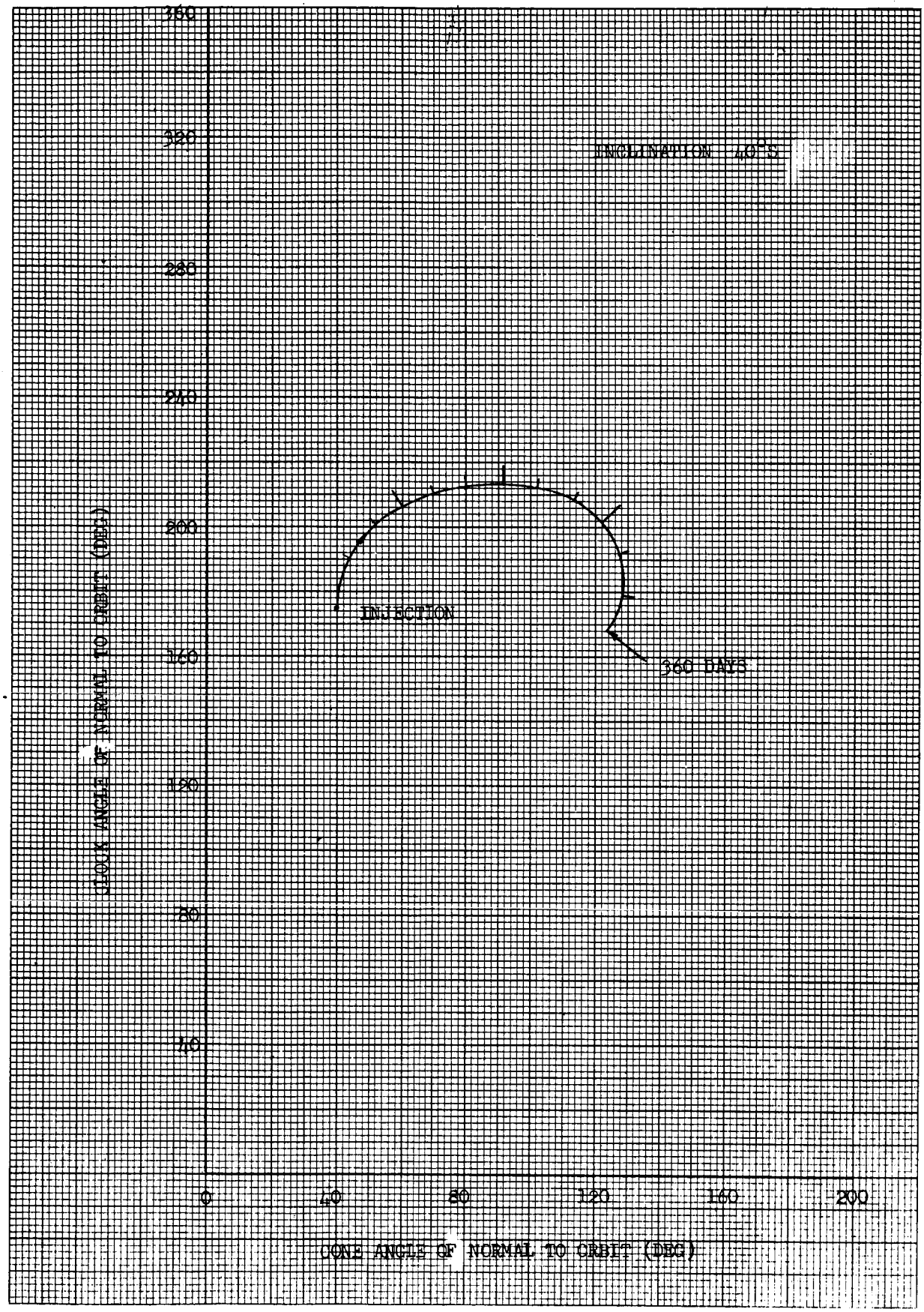
INCLINATION 40°S
INJECTION
360 DAYS
CLOCK ANGLE OF NORMAL TO ORBIT (DEG)
CONE ANGLE OF NORMAL TO ORBIT (DEG)
360
320
280
240
200
160
120
80
40
0
40
80
120
160
200

CASE NO. 37

1000 x 15, 000 km

$i = 40^{o}N$

$\Psi = 126.375$ deg

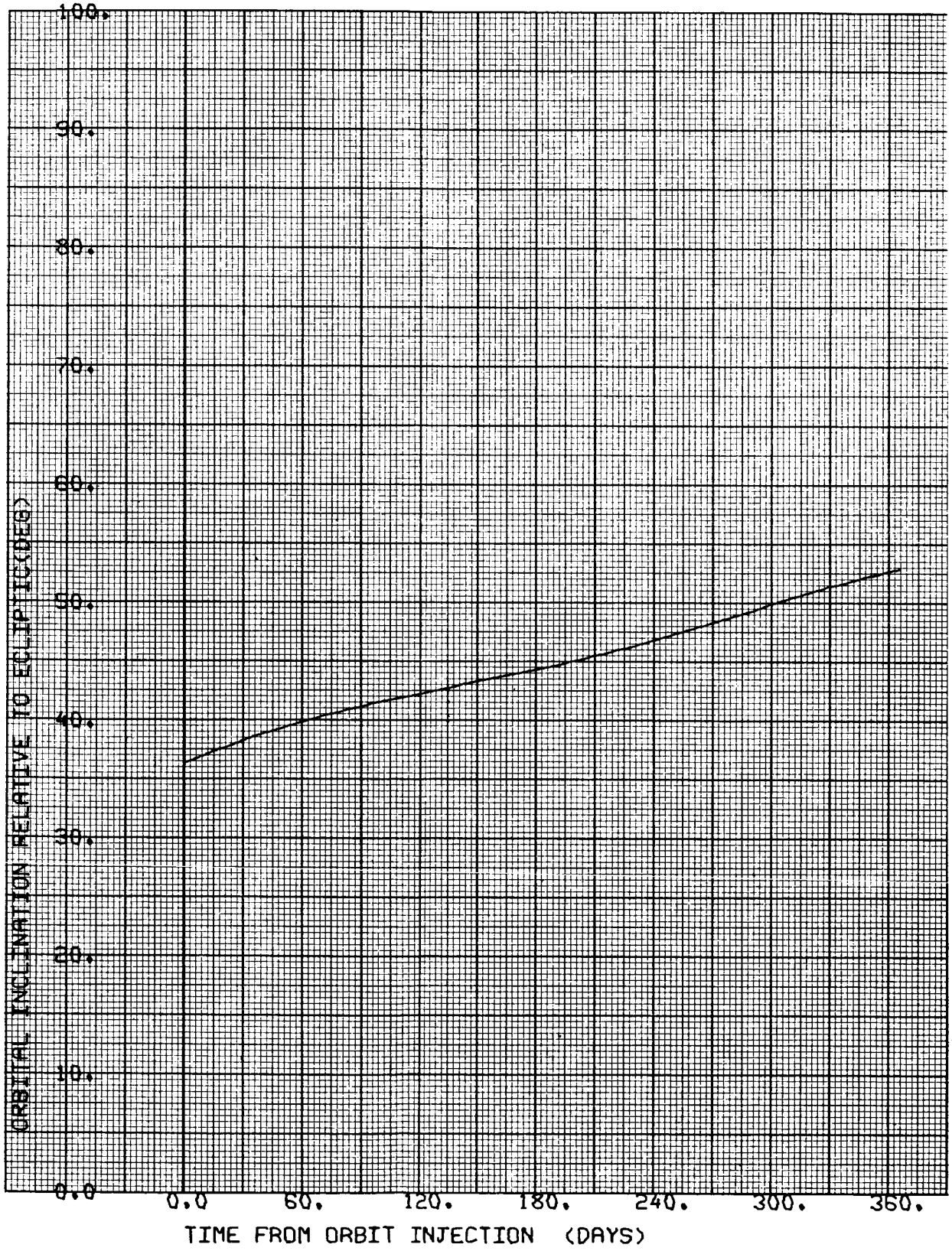
100.
90.
80.
70.
60.
50.
40.
30.
20.
10.
0.0
ORBITAL INCLINATION RELATIVE TO ECLIPTIC(DEG)
0.0
60.
120.
180.
240.
300.
360.
TIME FROM ORBIT INJECTION (DAYS)

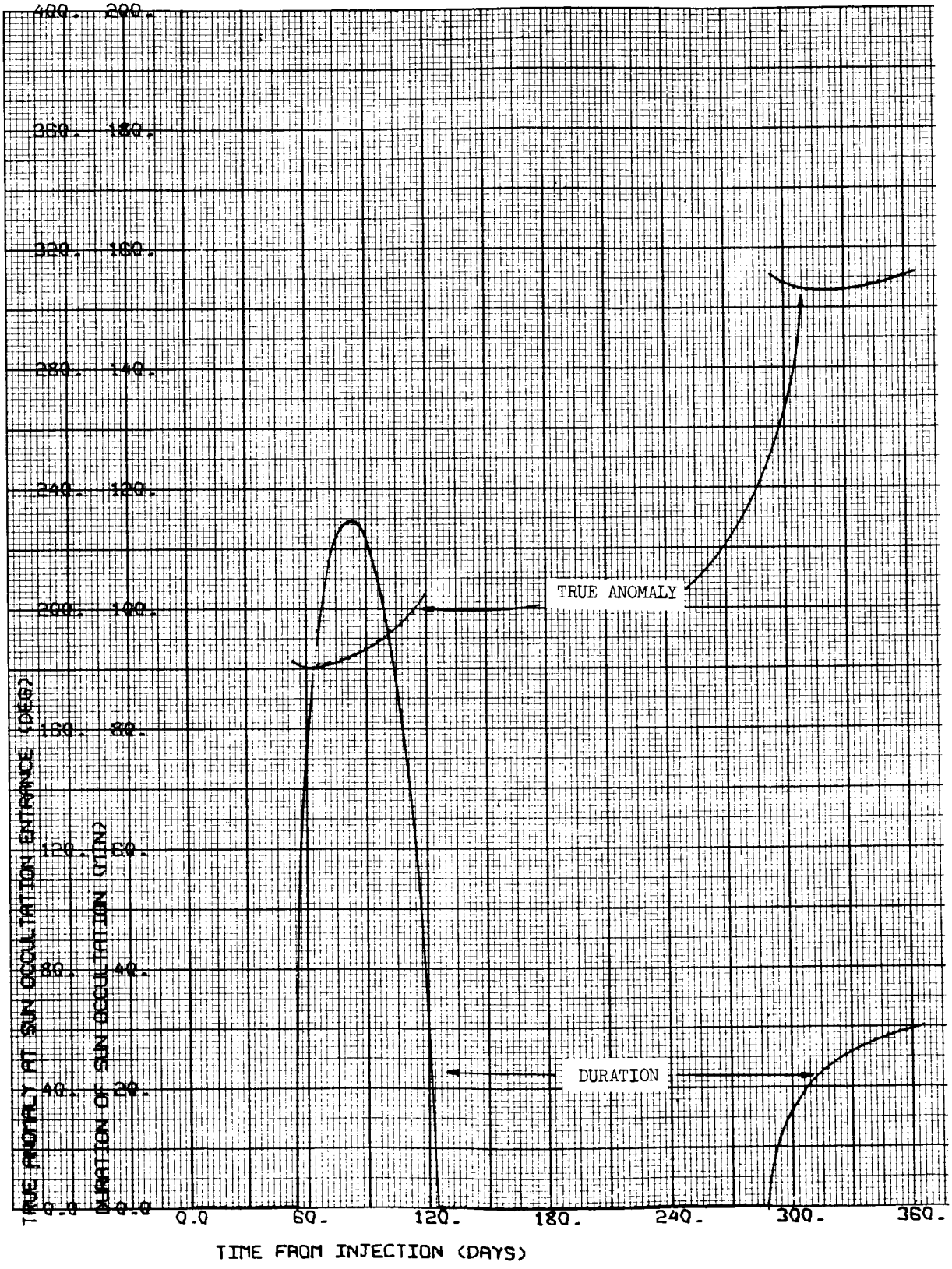
TRUE ANOMALY
DURATION
TRUE ANOMALY AT SUN OCCULTATION ENTRANCE (DEG)
DURATION OF SUN OCCULTATION (MIN)
TIME FROM INJECTION (DAYS)
0.0
60.
120.
180.
240.
300.
360.
400.
360.
320.
280.
240.
200.
160.
120.
80.
40.
0.0
200.
180.
160.
140.
120.
100.
80.
60.
40.
20.
0.0

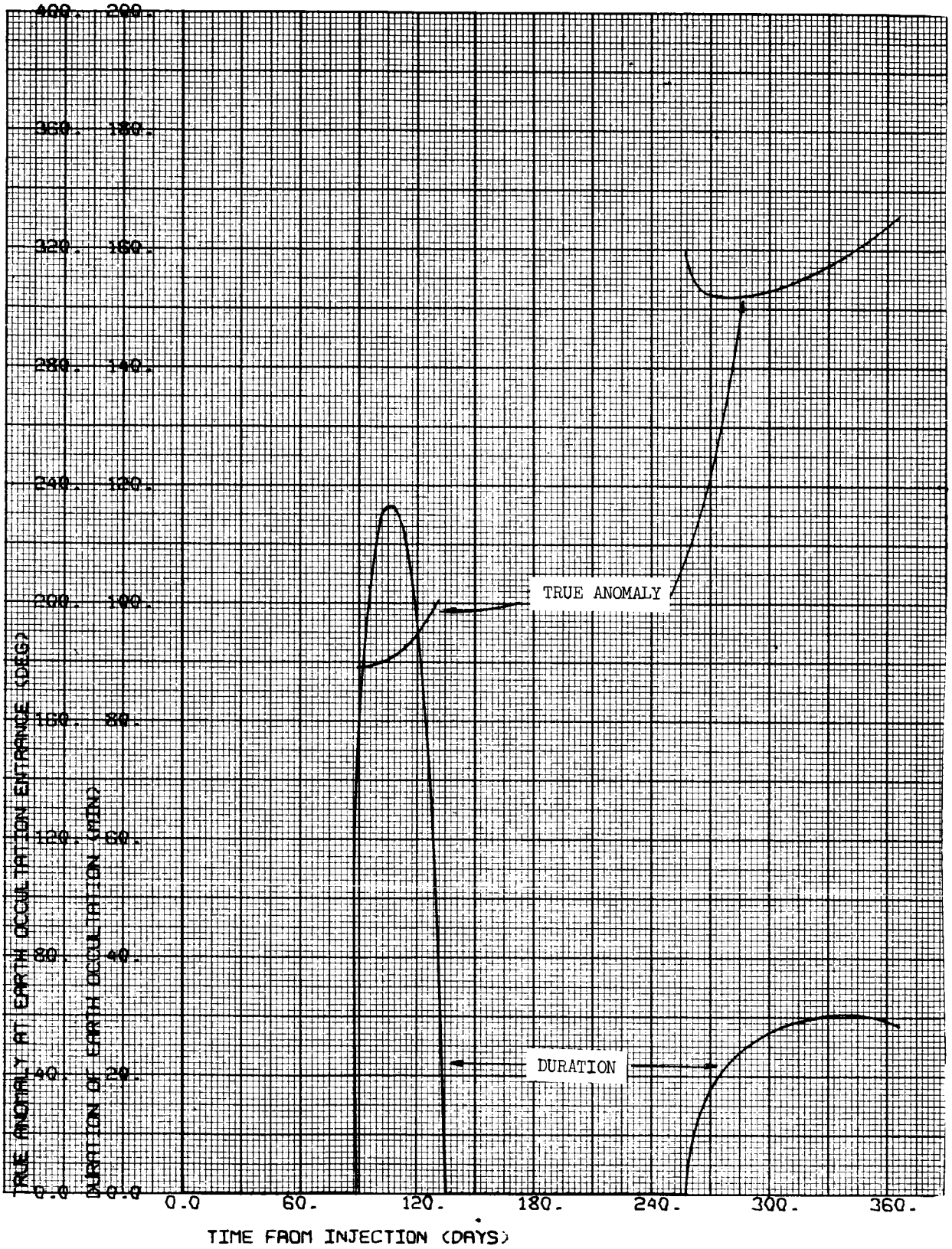
TRUE ANOMALY
DURATION
TRUE ANOMALY AT EARTH OCCULTATION ENTRANCE (DEG)
DURATION OF EARTH OCCULTATION (MIN)
TIME FROM INJECTION (DAYS)
0.0
60.
120.
180.
240.
300.
360.
400.
360.
320.
280.
240.
200.
160.
120.
80.
40.
200.
180.
160.
140.
120.
100.
80.
60.
40.
20.
0.0

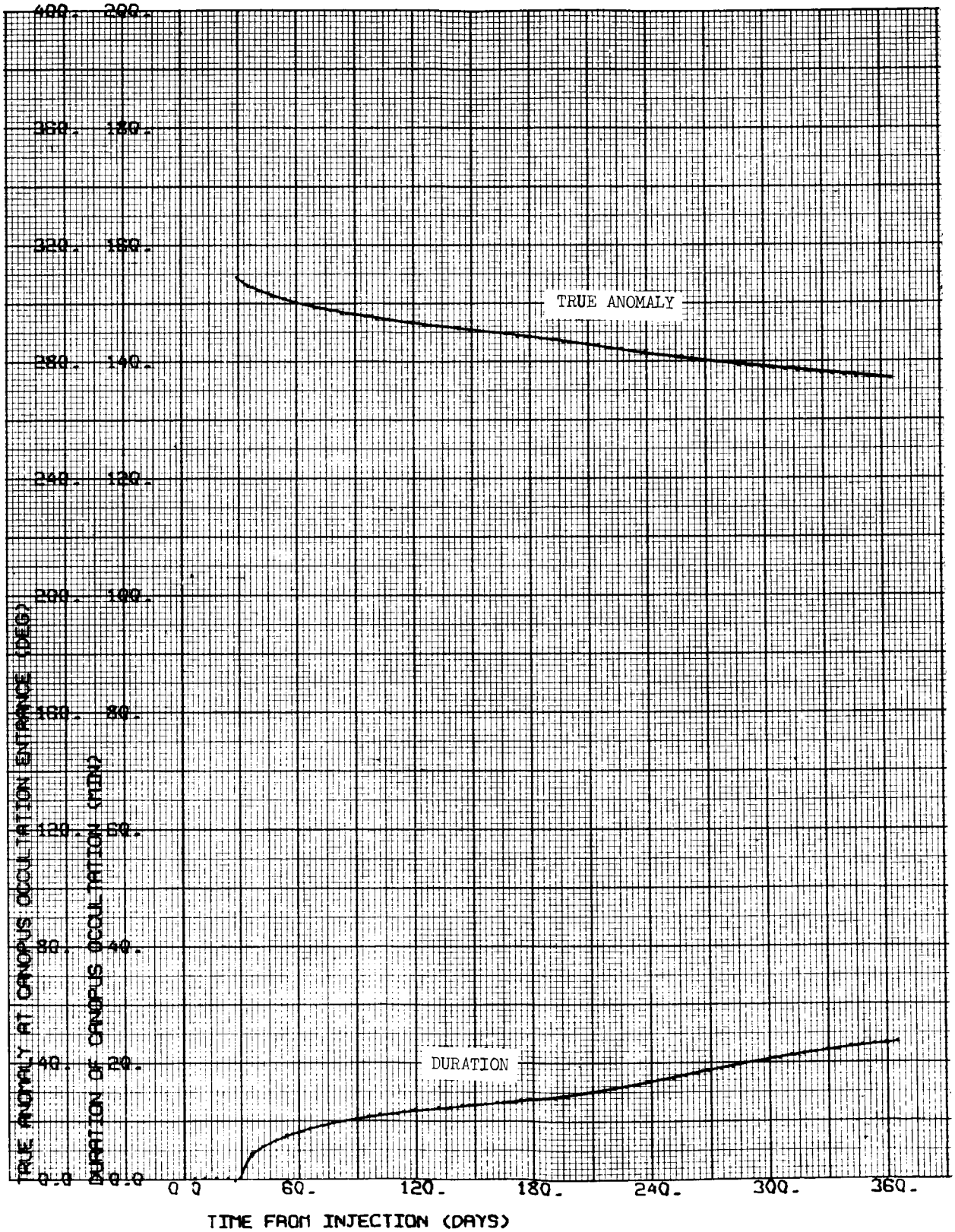
TRUE ANOMALY
DURATION
TRUE ANOMALY AT CANOPUS OCCULTATION ENTRANCE (DEG)
DURATION OF CANOPUS OCCULTATION (MIN)
TIME FROM INJECTION (DAYS)
0.0
0.0
0
0
60.
120.
180.
240.
300.
360.
400.
200.
360.
180.
320.
160.
280.
140.
240.
120.
200.
100.
160.
80.
120.
60.
80.
40.
40.
20.

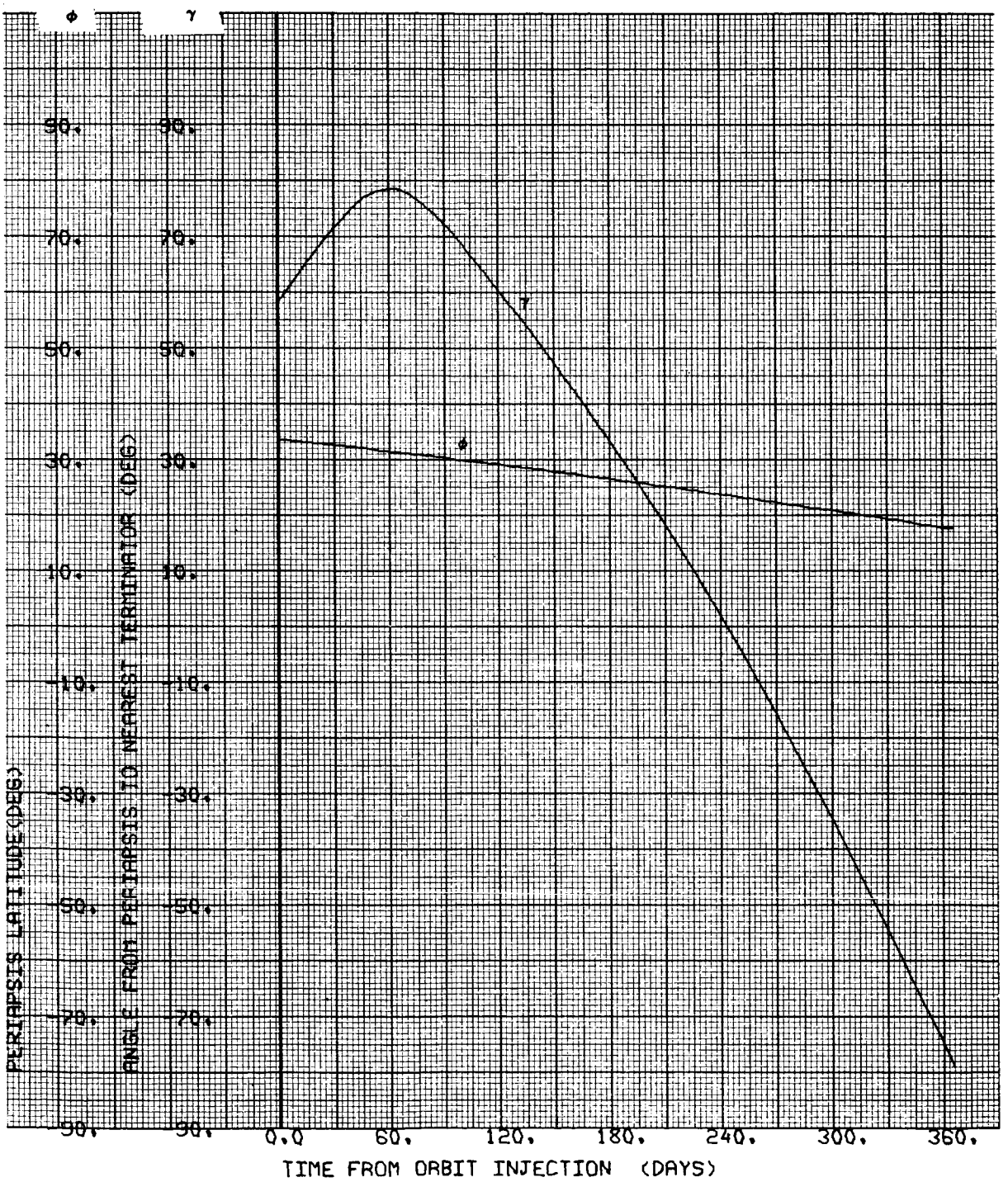
φ
γ
90.
70.
50.
30.
10.
-10.
-30.
-50.
-70.
-90.
γ
φ
PERIAPSIS LATITUDE (DEG)
ANGLE FROM PERIAPSIS TO NEAREST TERMINATOR (DEG)
0.0
60.
120.
180.
240.
300.
360.
TIME FROM ORBIT INJECTION (DAYS)

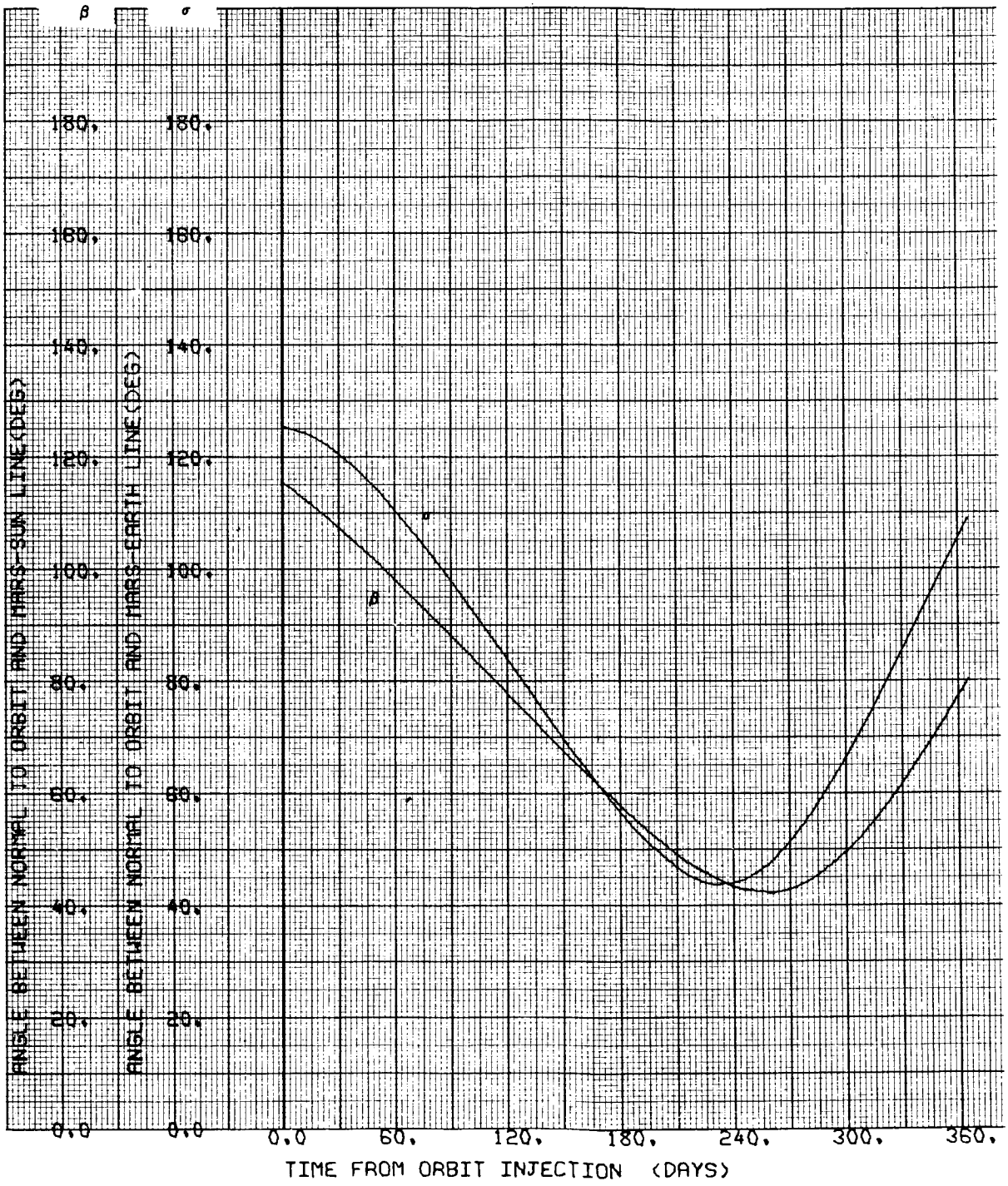
β
σ
180.
160.
140.
120.
100.
80.
60.
40.
20.
0.0
ANGLE BETWEEN NORMAL TO ORBIT AND MARS-SUN LINE(DEG)
ANGLE BETWEEN NORMAL TO ORBIT AND MARS-EARTH LINE(DEG)
0.0
60.
120.
180.
240.
300.
360.
TIME FROM ORBIT INJECTION (DAYS)

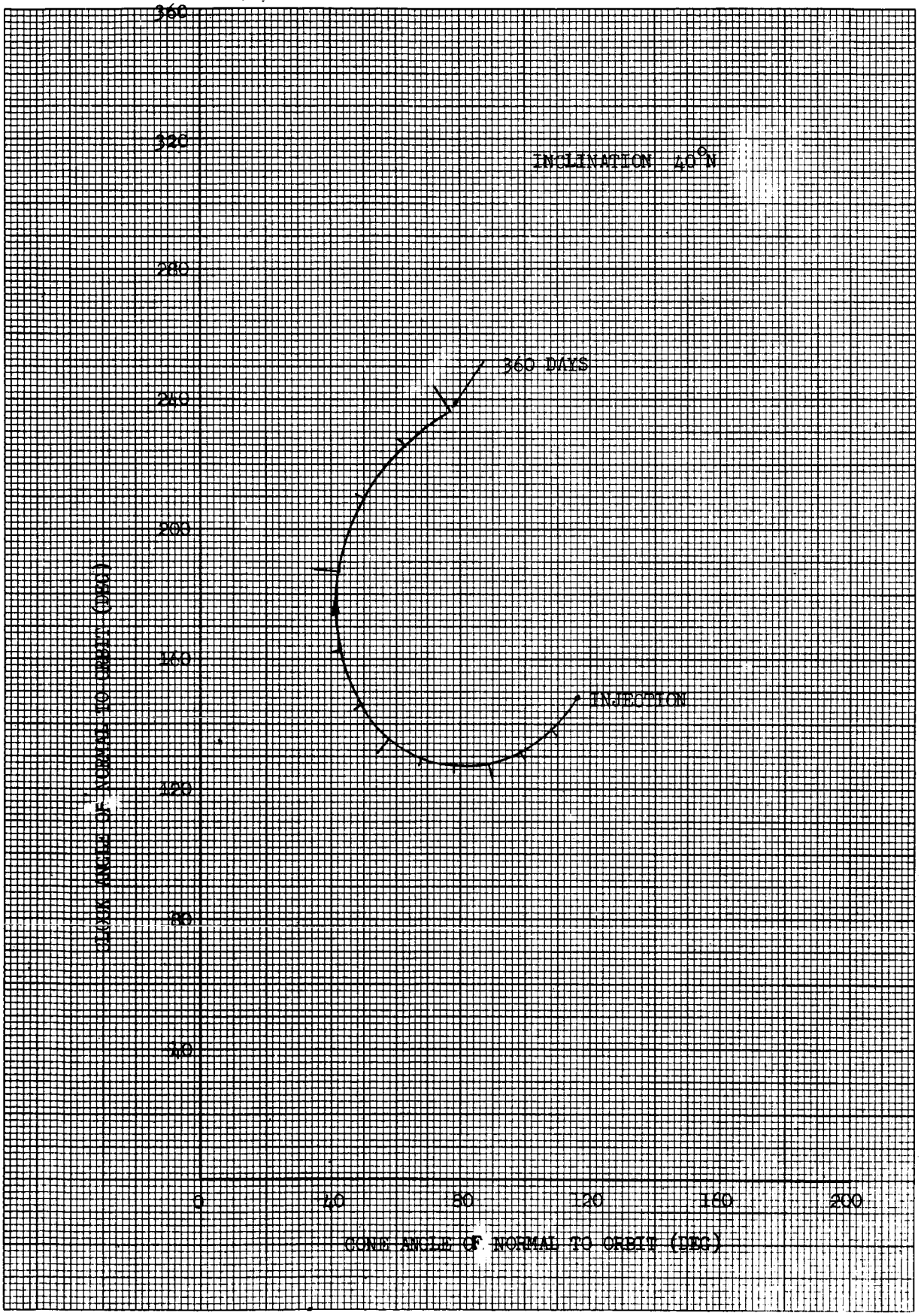
INCLINATION 40°N
360 DAYS
INJECTION
CONE ANGLE OF ECLIPTIC NORMAL TO ORBIT (DEG)
CONE ANGLE OF SUN NORMAL TO ORBIT (DEG)
360
320
280
240
200
160
120
80
40
0
40
80
120
160
200

TRAJECTORY ACCURACY ANALYSIS

CONTENTS

APPENDIX D

TRAJECTORY ACCURACY ANALYSIS

This appendix discusses several topics in support of the trajectory accuracy analysis discussed in Section 3.4.

1. COORDINATE SYSTEM FOR TERMINAL PARAMETERS

The terminal parameters were computed in a B · T, B · R coordinate system. The impact parameter, B, is defined as a vector originating at the center of the target and perpendicular to the incoming asymptote, V_∞. We define a unit vector $\vec{T}$ lying in a plane parallel to the ecliptic according to

$$\vec{T} = \frac{\vec{V}_\infty \times \vec{k}}{|\vec{V}_\infty \times \vec{k}|}$$

where $\vec{k}$ is a unit vector normal to the ecliptic plane and pointing towards the north. The $\vec{R}$ axis is defined by

$$\vec{R} = \frac{\vec{V}_\infty \times \vec{T}}{|\vec{V}_\infty \times \vec{T}|}$$

The impact parameter, B, lies in the R-T plane and has components B · T and B · R.

2. INJECTION ERRORS

The injection errors were computed in a u, v, w coordinate system. This right hand inertial coordinate system has its origin at the nominal injection point; the u axis points radially out from the center of the earth, the v axis points downrange and the w axis is parallel to the angular momentum vector. Position and velocity injection errors in the u, v, w coordinate system may be expressed as position and velocity errors in the x, y, z coordinate system by the following matrix equation

$$\delta X = U^T \delta u$$

where U is a 6 x 6 matrix that rotates the x, y, z coordinate system into the u, v, w coordinate system, and $u = (u, v, w, \dot{u}, \dot{v}, \dot{w})^T$.

The assumed injection error covariance matrix in the u, v, w coordinate system, Σ_u, is shown in Table D-1. The diagonal elements of the symmetric injection covariance matrix are $\sigma_{u_i}^2$, the square of the 1σ injection errors. The off diagonal elements of Σ_u are $\rho_{ij}\sigma_i\sigma_j$, where ρ_{ij} is the correlation coefficient. σ_i is independent of σ_j when ρ_{ij} is zero while, conversely, σ_i is a multiple of σ_j when the absolute value of ρ_{ij} is unity.

The assumed injection error covariance matrix shown in Table D-1 is extrapolated from an early analysis of an Apollo launch of the Saturn V. The injection error covariance matrix in the x, y, z coordinate system is then

$$\Sigma_x = E(\delta X \delta X^T) = U^T \Sigma_u U$$

The uncorrected miss at Mars due to injection errors in the u, v, w coordinate system is obtained from

$$\delta TC = S\,\delta X = SU^T\,\delta u$$

where S is the 3 x 6 midcourse sensitivity matrix at injection. The elements of S are $\partial TC/\partial X$, the partial derivative of the terminal conditions with respect to the components of the spacecraft position and velocity vectors at time t. The terminal conditions are $B \cdot T$, $B \cdot R$, and flight time.

The covariance matrix of uncorrected miss due to injection errors is then

$$\Sigma_s = E\,(\delta TC)(\delta TC)^T = S\,\Sigma_x S^T$$

where Σ_s is a 3 x 3 matrix, but we will only consider the upper left 2 x 2 matrix, Σ'_s,

Table D-1. Injection Error Covariance Matrix, Σ_u (Units are $(\text{meters})^2$ and $(\text{m/sec})^2$)

	u	v	w	$\dot{u}$	$\dot{v}$	$\dot{w}$
u	0.44858537 07	-0.12587177 07	-0.55236324 04	0.42701974 05	-0.90709136 04	-0.39996235 02
v		0.49817037 06	-0.15844877 05	-0.12033856 05	0.36919042 04	-0.14809601 03
w			0.45554530 07	0.11508062 03	0.40518285 03	0.41611285 05
$\dot{u}$				0.40688044 03	-0.86728085 02	0.83102950 00
$\dot{v}$					0.27521334 02	0.37866344 01
$\dot{w}$						0.38193275 03

$$\Sigma_s' = \begin{bmatrix} \sigma_1^2 & \rho_1\sigma_1\sigma_2 \\ \rho_1\sigma_1\sigma_2 & \sigma_2^2 \end{bmatrix}$$

where σ_1 is $\sigma(B \cdot T)$ and σ_2 is $\sigma(B \cdot R)$. The 1σ miss ellipse will be in a rectangle of size $2\sigma_1$, and $2\sigma_2$ centered at the aim point in $B \cdot T$ and $B \cdot R$ coordinates. The square roots of the two eigenvalues of Σ's are the lengths of the semimajor and semiminor axes of the 1σ uncorrected miss ellipse. The eigenvectors associated with each eigenvalue are the direction cosines of the semimajor and semiminor axes.

The semimajor and semiminor axes of the 1σ uncorrected miss ellipse are 399, 149 and 66, 316 km, respectively. Figure D-1 shows the orientation of the 1σ uncorrected miss ellipse.

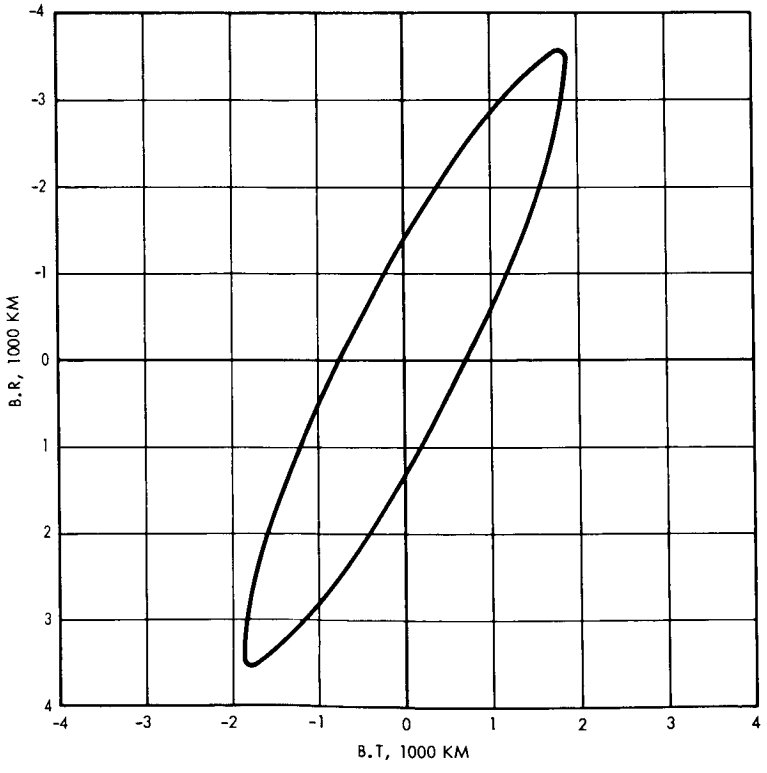

Figure D-1 Uncorrected Miss Ellipse

3. VELOCITY EXECUTION ERRORS

The covariance matrix of velocity execution errors was computed in a u', v', w' coordinate system. The v' axis points in the direction of the velocity correction, the w' axis points in the direction of the $\vec{R} \times \vec{\Delta V}$ vector, and the u' axis completes the right-handed set.

Thus, the 3σ velocity execution error covariance matrix in the u', v', w' coordinate system is

$$\Sigma_{EX} = \begin{bmatrix} \left[(0.014)(\Delta V)\right]^2 & 0 & 0 \\ 0 & \left[(0.001)(\Delta V)\right]^2 + (0.024)^2 & 0 \\ 0 & 0 & \left[(0.014)(\Delta V)\right]^2 \end{bmatrix}$$

4. TRACKING

The simulation of the Voyager mission requires three ground updates of the spacecraft. The updates are required before the separation maneuver and each of the two midcourse corrections. An update is the process of using recently acquired tracking data and considering the effects of systematic errors to obtain a new and revised estimate of the vehicle's state vector. The modeling of these updates will be described below.

4.1 First Ground Update

The spacecraft is assumed to be under surveillance from insertion to 5 days by stations at Goldstone, Madrid, and Woomera. At 5 days, a ground computer would perform a weighted least squares fit to form an estimate of the state vector. This estimated state vector is then propagated to the R-T plane and the estimate used to compute the separation maneuver. Systematic errors (uncertainties in data biases, station locations) were solved for in this update.

4.2 Second Ground Update

The second ground update used the tracking information from 5 to 30 days. The systematic errors were solved for in this update. The

estimated state vector was propagated to the impact parameter plane and was used to compute the first midcourse maneuver. This covariance matrix was compared with unpublished JPL data and the agreement was excellent.

4.3 Third Ground Update

The third ground update used the information from the second ground update plus tracking from 30 to 191 days. The three ground stations tracked continuously from 30 to 40 days and from 186 to 191 days. Only Goldstone tracked the spacecraft between 40 and 186 days and the coverage during this period was 12 hours of tracking every two days. The estimated state vector was propagated to the impact parameter plane and was used to compute the second midcourse maneuver.

In addition to solving for the systematic errors, the effects of state noise were considered in this update.

State noise may be considered as random forces which act upon the spacecraft and thus slightly alter the trajectory. Venting (unbalanced attitude control pulses or very slow leaks) was considered but was found to be of such small magnitude that it did not affect the trajectory. Solar winds and radiation pressure may also be considered a state noise as well as computer roundoff. It was decided that the state noise would produce a total velocity uncertainty of 0.0375 m/sec during the flight time along each axis.

The JPL specification (Ref. D-1) limits unpredictable trajectory perturbations due to the spacecraft to 0.6×10^{-7} cm/sec^2 averaged over one hour. The 0.0375 m/sec^2 figure assumed for the entire transit phase is 250 times as great as the specification, assuming the noise to be completely uncorrelated from one hour to another. It is four times as great, even if the noise were completely time-correlated over the entire mission. In fact, such noises are probably partially time-correlated; thus the noise estimate used appears reasonably conservative.

The combined estimate of the state vector was obtained by adding the state noise covariance matrix to the tracking covariance matrix at

regular intervals (30 days). Thus, at 150 days the combined estimate Λ_{150}, is given by

$$\Lambda_{150} = \left\{ \Lambda_{120}^{-1} + \left[(S) \underset{120-150}{(A^T W A)^{-1}} (S)^T \right]^{-1} \right\}^{-1} + SQS^T$$

where

Λ_{120} is the covariance matrix of the combined estimate at 120 days in the R-T coordinate system

$\underset{120-150}{(A^T W A)^{-1}}$ is the tracking normal matrix in xyz coordinates resulting from tracking from 120 to 150 days

Q is the covariance matrix of state noise in the xyz coordinate system. The matrix Q was assumed to be diagonal. A diagonal element of Q would be $\left(\frac{30}{201}\right)(0.0375)^2 \text{ m}^2/\text{sec}^2$.

5. MONTE CARLO SIMULATION OF THE VOYAGER MIDCOURSE MANEUVERS

5.1 General

The Monte Carlo method relies on the ability to repeat the system simulation a sufficient number of times so that distribution functions of output variables are faithful reproductions of the true but unknown distributions. Thus, there is a basic compromise, which must be made in any substantial simulation, between the accuracy of the simulation and the running time of the problem. The system may be very accurately modeled so that all the possible details are included and a small statistical sample taken or approximation can be made in the less critical phases, substantially decreasing the running time and allowing a statistically more complete representation of the distributions. The only generalization that can be made is that run times should not be greater than 90 minutes because of machine (i.e., digital computer) mean-time-to-failure, assuming that cost and machine availability are not constraints. Apart from this general rule, the compromise made in any particular problem will depend on the needs of the user and the skill of the analyst in separating what is fundamental to the proper representation from what can be ignored or less perfectly simulated.

When one uses the results of a Monte Carlo study it often occurs that the largest values of some quantity computed in the study are as important as the mean value and variance of that particular quantity. The statistical interpretation of the largest samples leads directly to the question of the number of Monte Carlo runs that should be made in conducting the study and the statistical confidence that can be placed on the results. The number of Monte Carlo runs which are to be made can be determined by selecting γ and P such that one is 100γ percent sure that at least 100P percent of the population lies below (above) the largest (smallest) value of the random sample from that population. For example, with 528 samples the confidence level is 0.995 that at least 99 percent of the population lies below the largest value of the random variable under consideration; a confidence level of 0.999 would require 688 samples. In this study, 1001 samples were taken.

5.2 Description of the TAPP VI Error Analysis Program and the Statistical Processor Program

The TAPP VI program may be visualized by referring to Figure D-2, which is a flow chart of the main program. In the diagram, the K loop

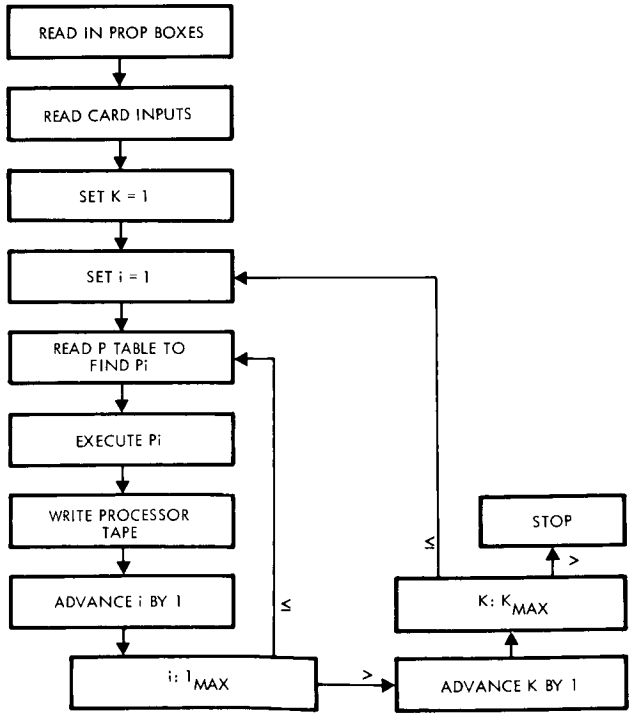

Figure D-2 TAPP VI Main Program

refers to the Monte Carlo cycle being processed and the i loop determines the phase of the mission which is being processed. Each phase has an associated PROP box which simulates the activities of the phase.

The output of the TAPP VI simulation is a tape containing the samples from the Monte Carlo simulation. The tape is used by the Statistical Processor Program to generate means, variances, and cumulative distribution functions of variables which statistically describe the results of the Monte Carlo simulation (Ref. D-2). For purposes of completeness a brief description of what statistics are available in the processor program follows below.

In essence, the statistical processor can compute sample means, sample covariance matrices of scalars and vectors, cumulative distribution functions of scalars or of the individual components of vectors, cross variance matrices, and multiple mean squared correlation coefficients. The sample mean is computed in the obvious manner, namely

$$\text{sample mean} = \frac{1}{N} \sum_{j=1}^{N} \underline{y}_j$$

$\underline{y}$ represents a specified vector produced by the simulation, the subscript j indexes the number of the Monte Carlo run, and N is the total number of runs. The sample covariance matrix is computed using the following equation:

$$\text{sample covariance matrix} = \frac{1}{N-1} \left[\Sigma y_j y_j^T - \frac{1}{N} \left(\Sigma y_j \right) \left(\Sigma y_j \right)^T \right]$$

The processor also computes the sample correlation matrix, which is the above matrix modified by dividing the i, j^{th} element by $(\sigma_i \sigma_j)$ where σ_i is the square root of (i, i)th element of the sample covariance matrix.

The cumulative distribution routine first orders all of the samples in increasing numerical order and then produces a graph of the number of samples less than a specified number. This is done by plotting, say, every 10th sample versus the numerical value of every 10th sample. By simply noting that each sample increases the cumulative distribution function by (1/N), the routine has the capability of changing the increment

of the distribution function between points so that one can study the tails of the distribution without having to print out an excessive number of points in the middle.

Quite often in the statistical results of an error analysis it is desirable to determine how a variable in one phase is related to a different variable in a different phase. For example, in terms of the Voyager mission, the following question could be asked, "How do the conditions at the end of injection affect the separation maneuver?" The purpose of the statistic involving the multiple correlation coefficients is to answer questions similar to this and provide the analyst additional insight into the relationship between variables of interest.

To answer this type of question let X denote the variable from one phase whose effect on a second variable Y is to be determined. The multiple correlation statistic assumes that Y is linearly related to X by a matrix A and uses the samples of X and Y from the Monte Carlo simulation to compute the matrix A. The details of computing the A matrix are as follows.

It has been assumed that the variables are linearly related and also that there is an (unknown) component of X which does not contribute to Y. (In the case where Y is completely uncorrelated with X, this component of X would be the complete X vector.) Thus, the relationship between X and Y can be written as

$$Y = AX + N$$

N is that part of X which does not contribute to Y. The matrix A can be computed by multiplying the above equation by X^T and then taking the expected value of both sides of the resulting equation. This gives

$$\Sigma_{YX} = A\Sigma_{XX}$$

or

$$A = \Sigma_{YX}\left(\Sigma_{XX}\right)^{-1}$$

Now, the A matrix computed in this manner is very dependent upon the units of both X and Y and at times is difficult to interpret. To this end

the covariance matrix that the variable Y would have if X were the only variable that affected Y is computed. If this covariance is denoted by Σ'_{YY} then Σ'_{YY} is computed using the following equation:

$$\Sigma'_{YY} = A \Sigma_{XX} A^T$$

Lastly, the multiple squared correlation coefficients are computed by taking the ratios of the diagonal terms of Σ'_{YY} to the diagonal terms of Σ_{YY}. This ratio is a measure of the contribution of X to the total variation of Y, and indicates the degree of correlation between X and Y.

The information flow of the Monte Carlo simulation of the Voyager mission (from injection to second midcourse maneuver) is shown in Figure D-3 and is self-explanatory.

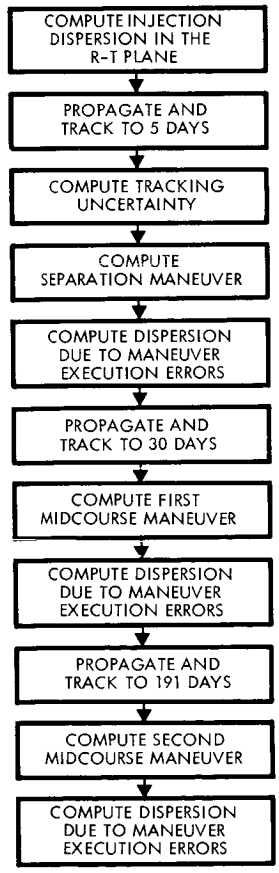

Figure D-3. Information Flow of the Monte Carlo Simulation of the Voyager Mission

Figures D-4 through D-6 show the cumulative distributions of the separation maneuver, first midcourse maneuver, and second midcourse maneuver, respectively. Figures D-7 through D-15 show the cumulative distributions of the dispersions after injection, separation maneuver, and first midcourse maneuver. Table D-2 summarizes the data in table form.

6. ACCURACY ANALYSIS OF MARS ORBIT DETERMINATION

This appendix presents the theoretical basis of a study to determine the accuracy of estimates of elements of a vehicle's orbit about Mars. The numerical results were obtained using a TRW precision orbit determination program.

The matrix equation expressing the tracking residuals is given by

$$\delta R = A\delta X_A + B\delta Z_A + N \qquad (1)$$

where δR is a column matrix (nx1) of actual observations minus the reference observations; A is an nx6 matrix, the elements of which are the partial derivatives of the observations (range, azimuth, etc.) with respect to the reference state vector at some epoch; B is an nxm matrix, the elements of which are the partial derivatives of the observations with respect to the systematic errors (uncertainties in radar station locations, biases in the observational data, and uncertainties in physical constants); δX_A is a column matrix (6x1) of deviations between the actual state vector at epoch and the reference state vector at epoch ($\delta X_A = X_A - X_R$); and where δZ_A is a column matrix (mx1) of systematic errors and N is a column matrix (nx1) of random noise with zero mean and known variance.

First assume that $\delta Z_A = 0$, the Equation (1) reduces to

$$\delta R = A\delta X_A + N \qquad (2)$$

If W is a diagonal matrix whose elements are the reciprocals of the variances of the radar observations, then the weighted least-squares estimate of the deviation from the reference (without a priori information) is

$$\delta X_E = (A^T W A)^{-1} A^T W \delta R \qquad (3)$$

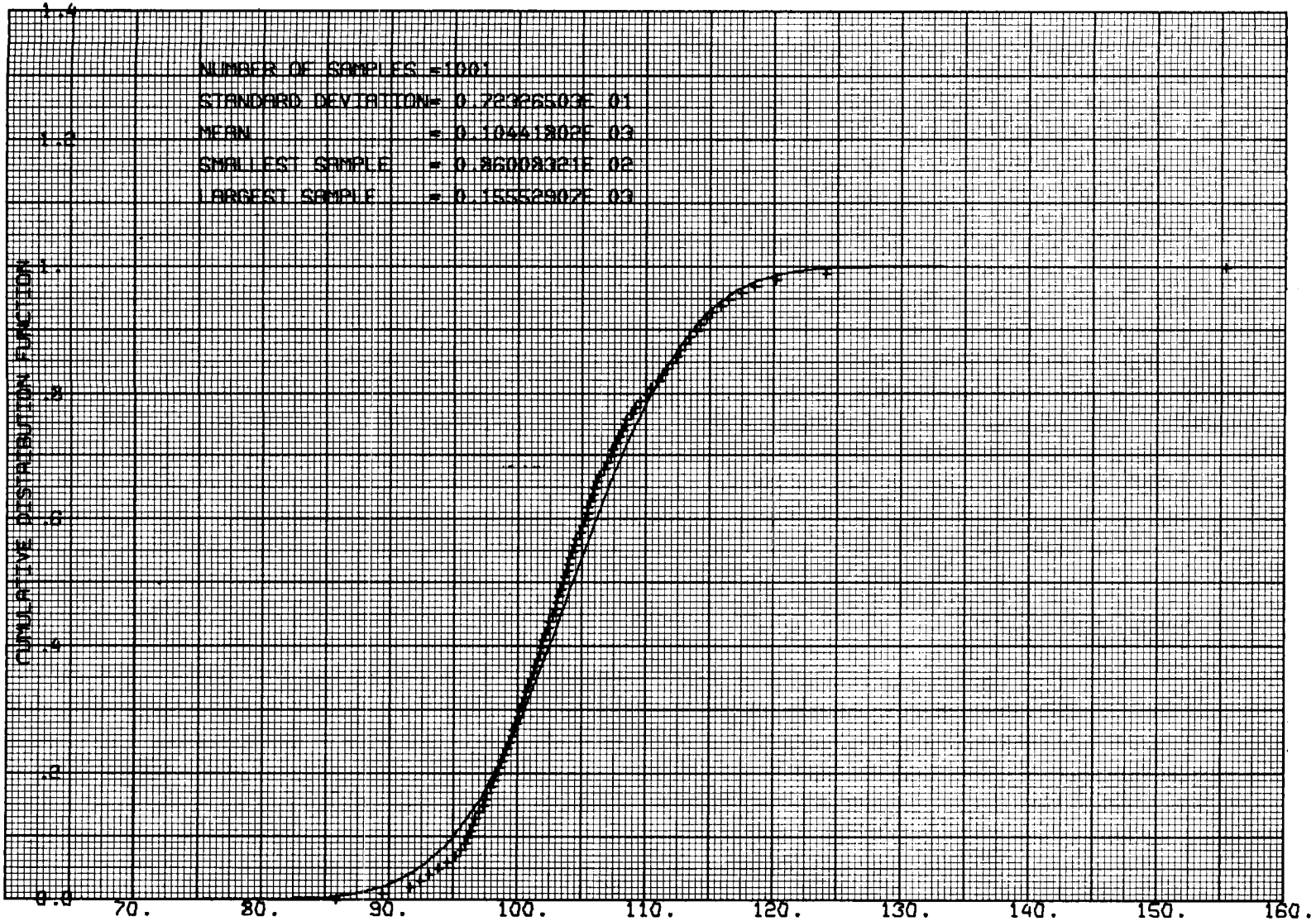

Figure D-4 Cumulative Distribution of Magnitude of the Actual Separation Maneuver (Meters/Sec)

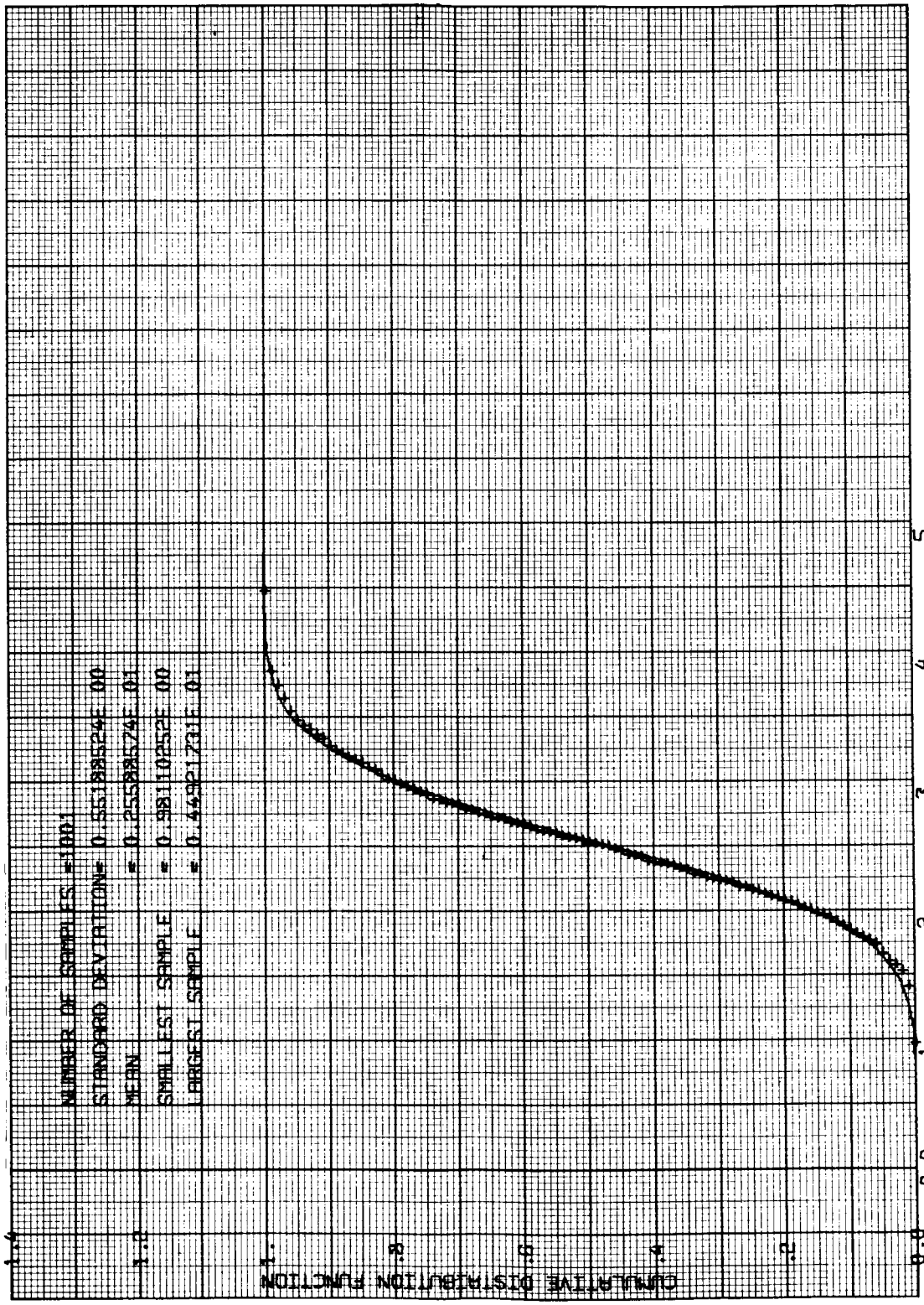

Figure D-5 Cumulative Distribution of Magnitude of the Actual First Midcourse Maneuver (Meters/Sec)

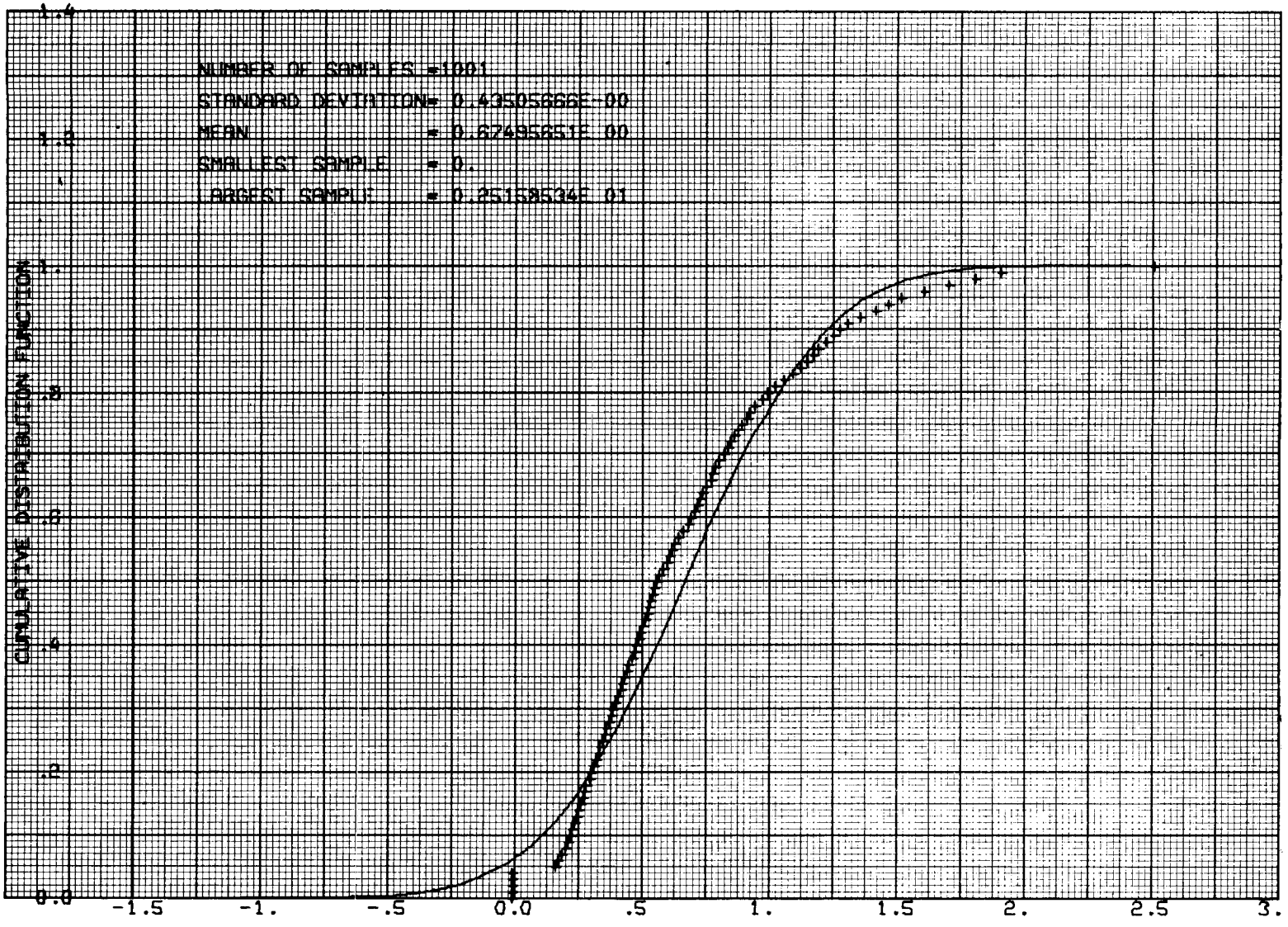

Figure D-6 Cumulative Distribution of Magnitude of the Actual Second Midcourse Maneuver (Meters/Sec)

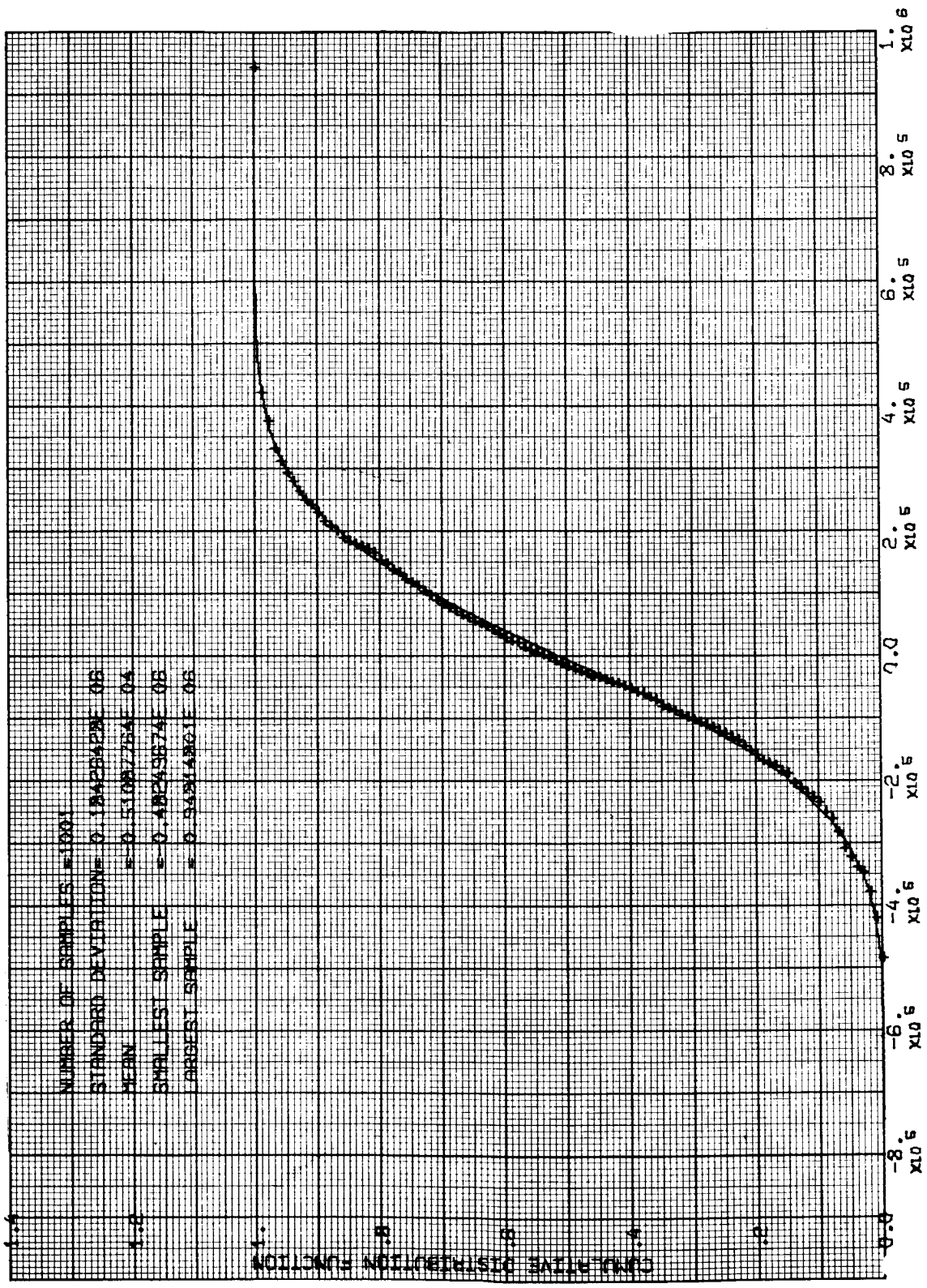

Figure D-7 Cumulative Distribution of Dispersion in B·T After Injection (Km)

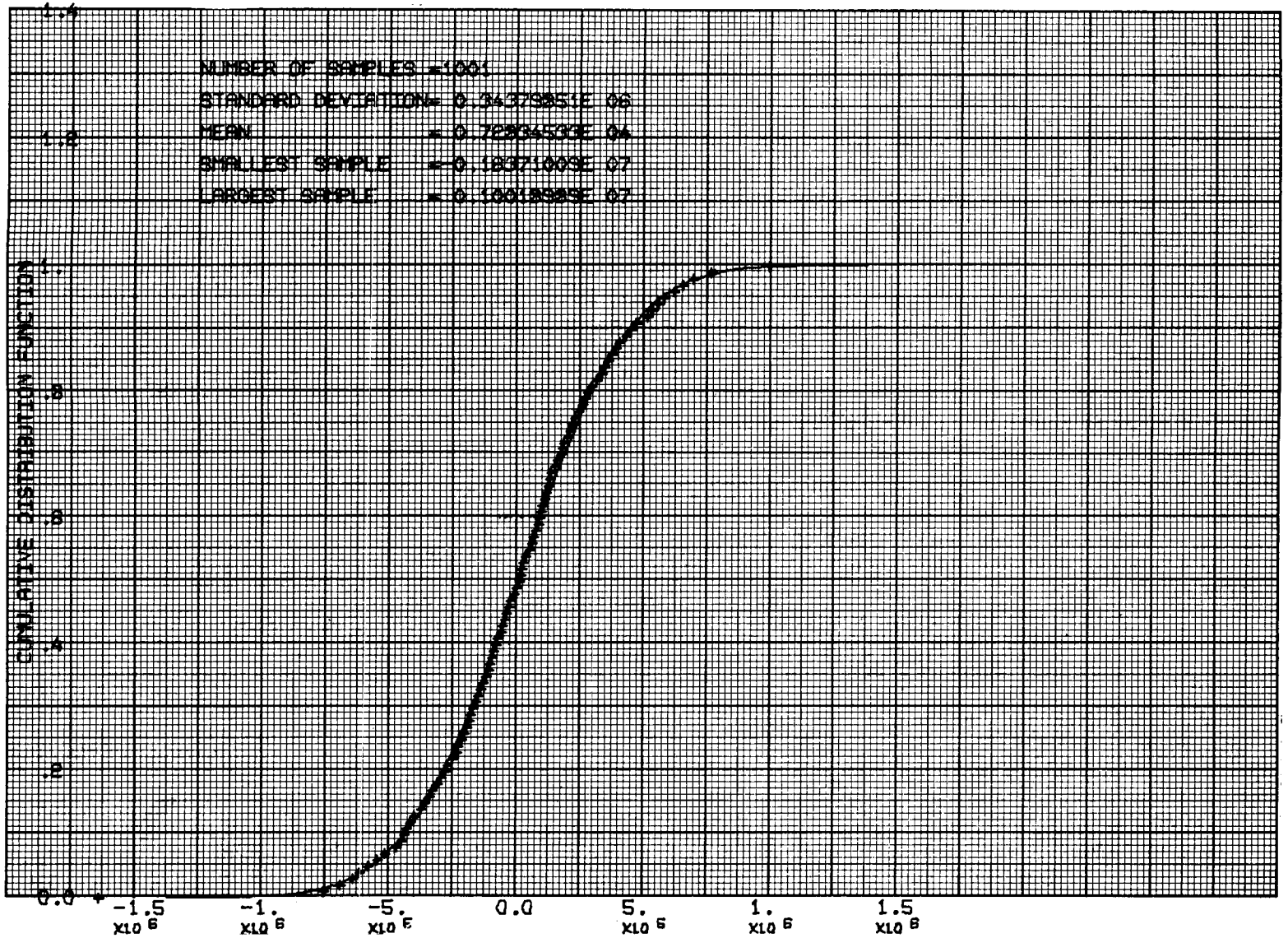

Figure D-8 Cumulative Distribution of Dispersion in B· R After Injection (Km)

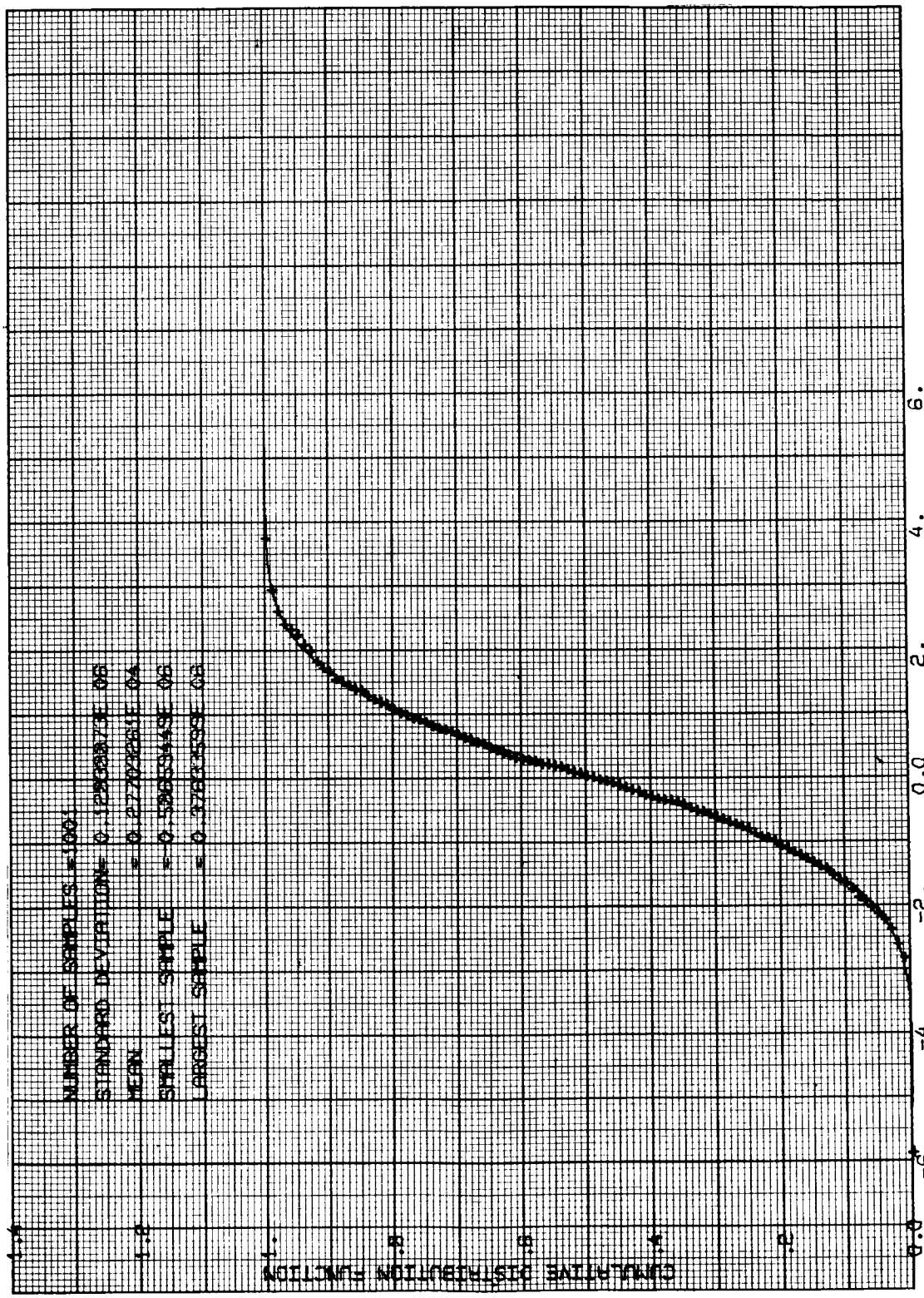

Figure D-9 Cumulative Distribution of Dispersion in Time of Flight After Injection (Sec)

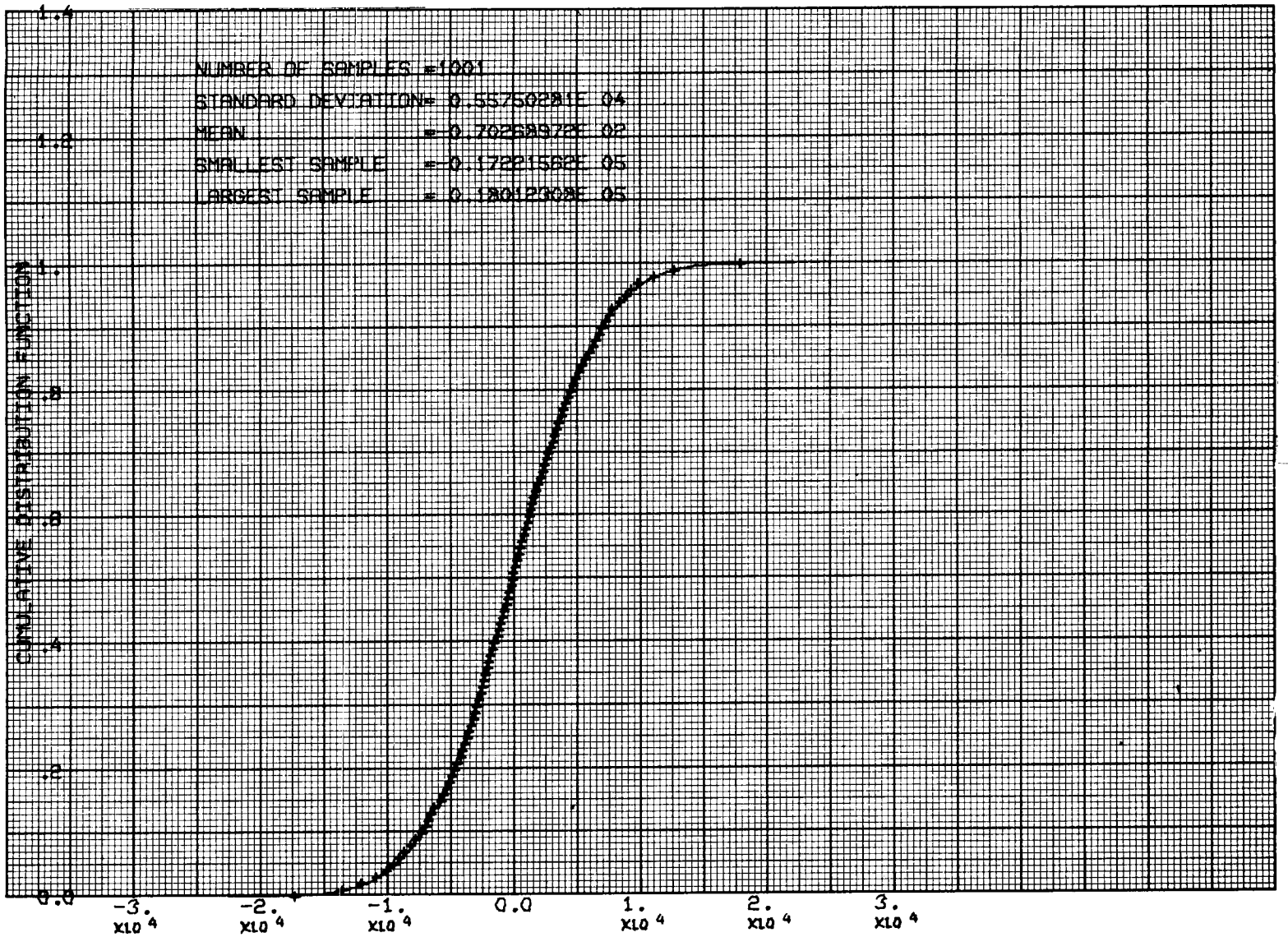

Figure D-10 Cumulative Distribution of Dispersion in B·T After Separation Maneuver (Km)

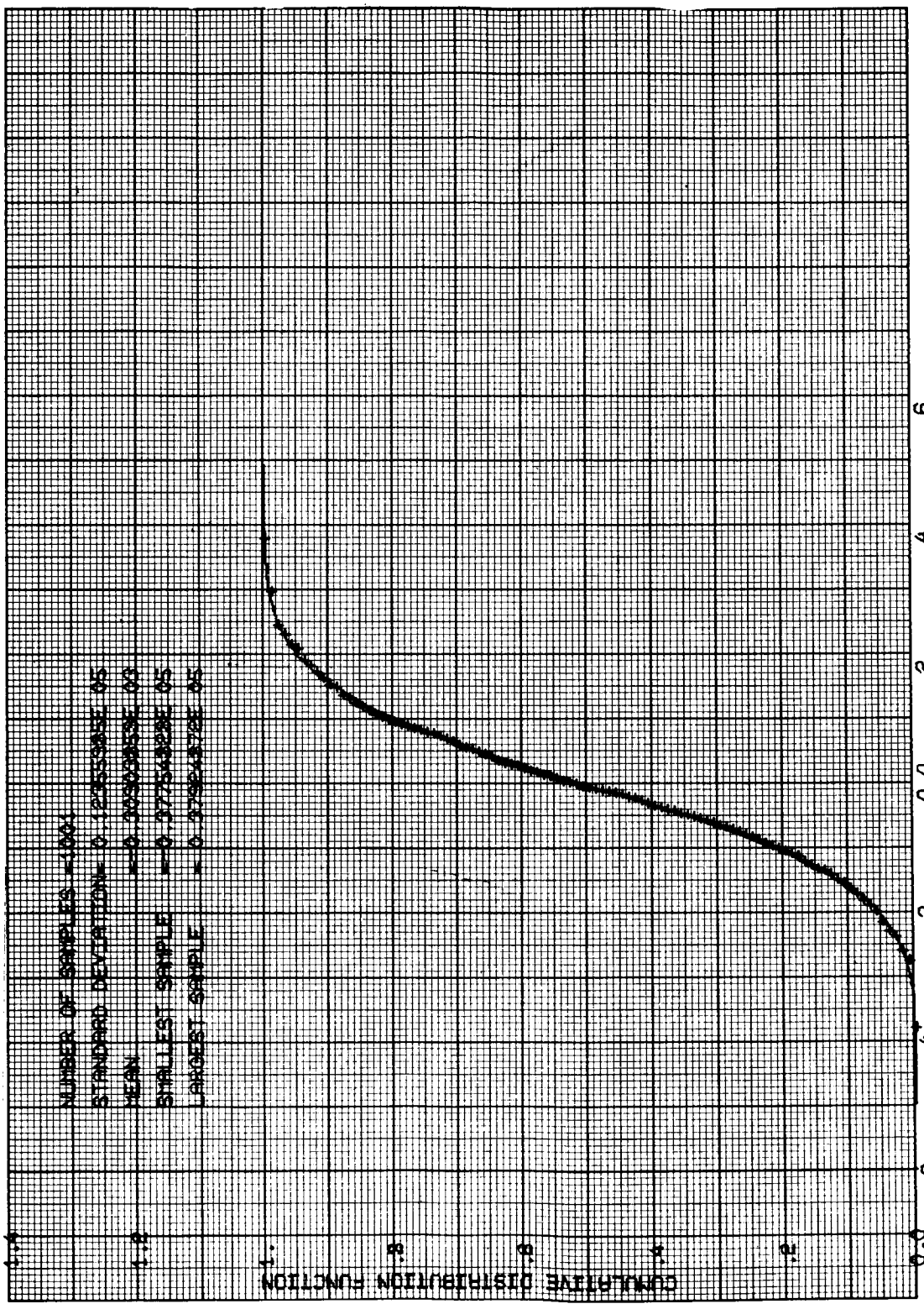

Figure D-11 Cumulative Distribution of Dispersion in B·R After Separation Maneuver (Km)

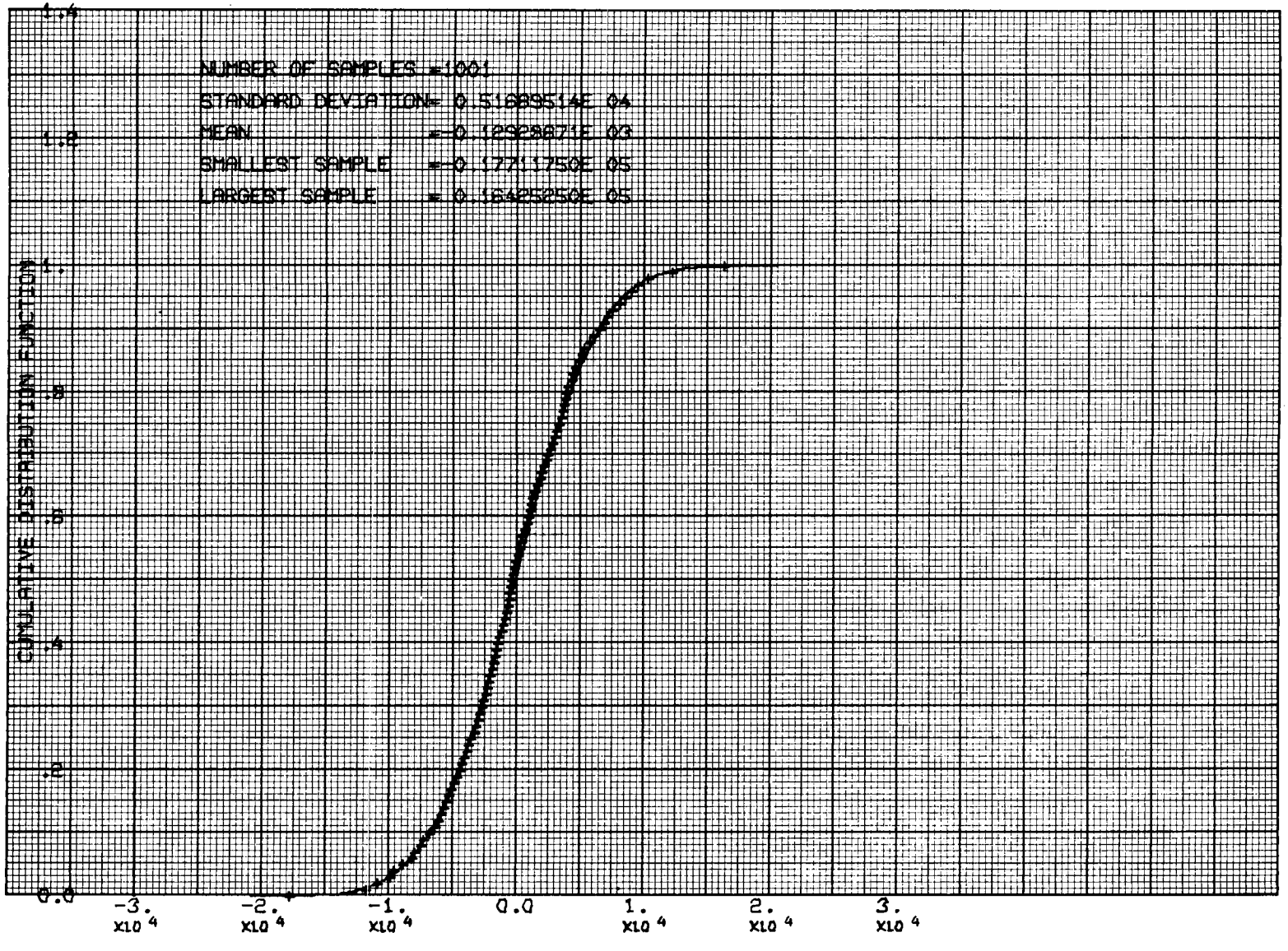

Figure D-12 Cumulative Distribution of Dispersion in Time of Flight After Separation Maneuver (Sec)

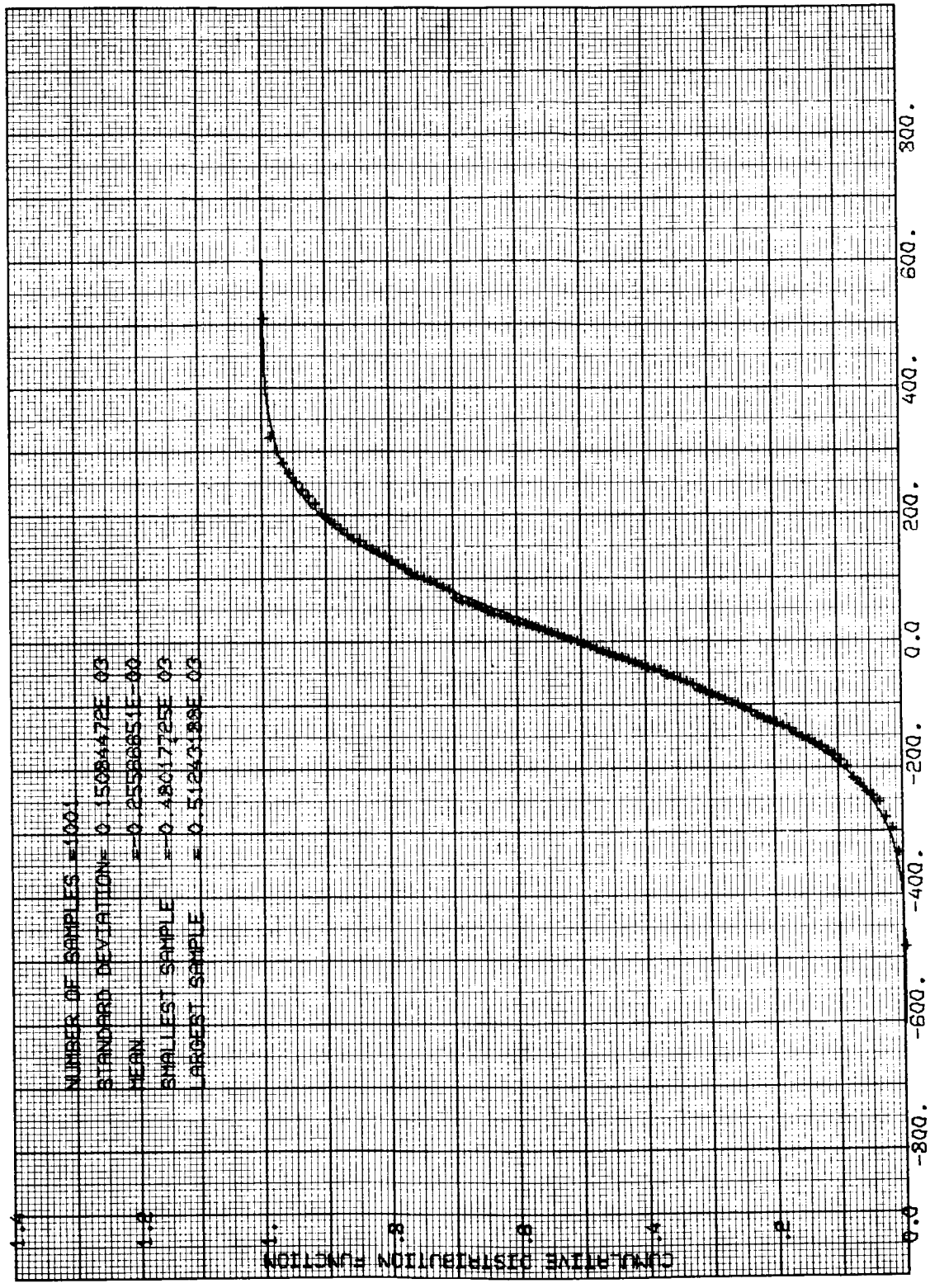

Figure D-13 Cumulative Distribution of Dispersion in B·T After First Midcourse (Km)

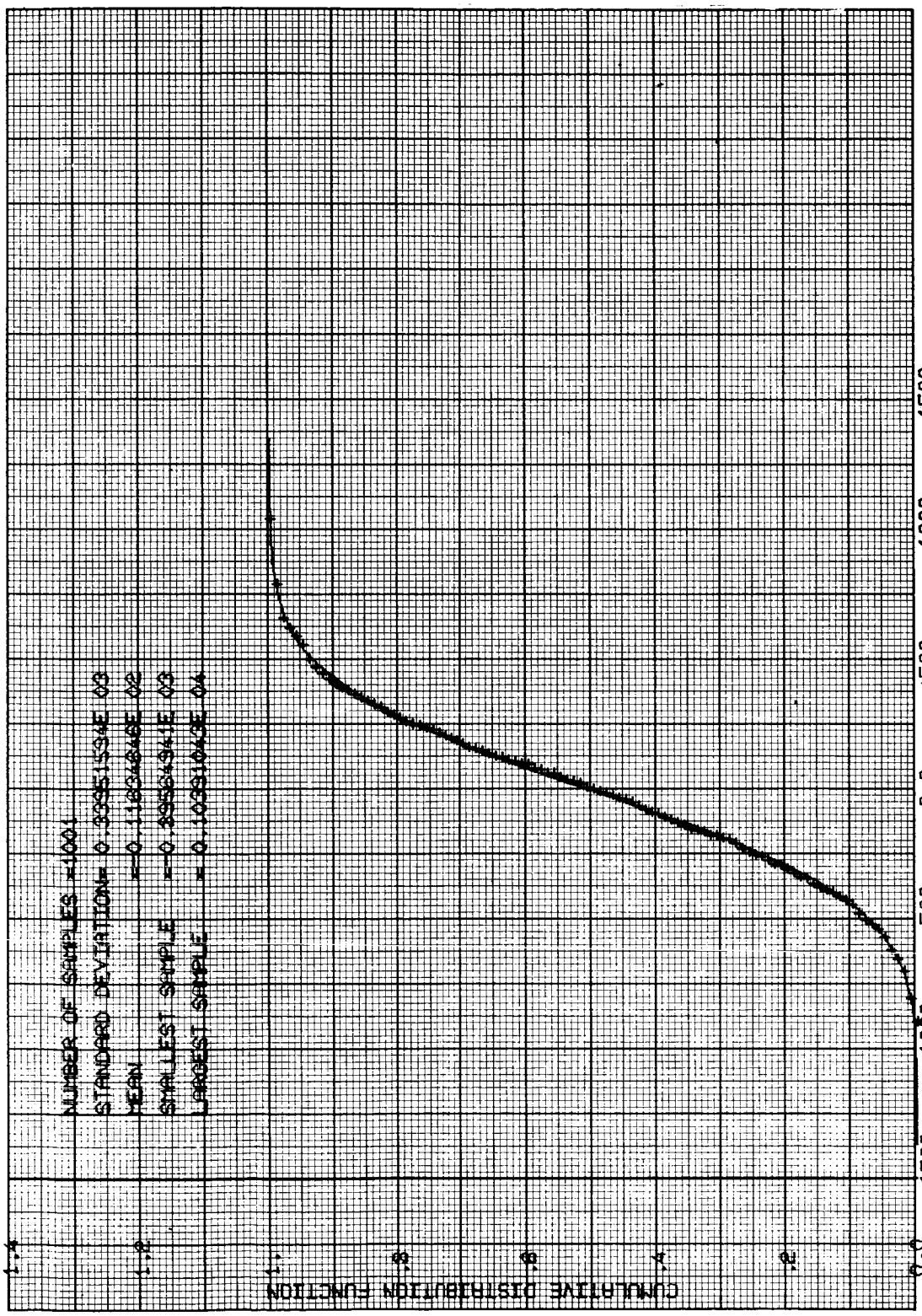

Figure D-14 Cumulative Distribution of Dispersion in B·R After First Midcourse (Km)

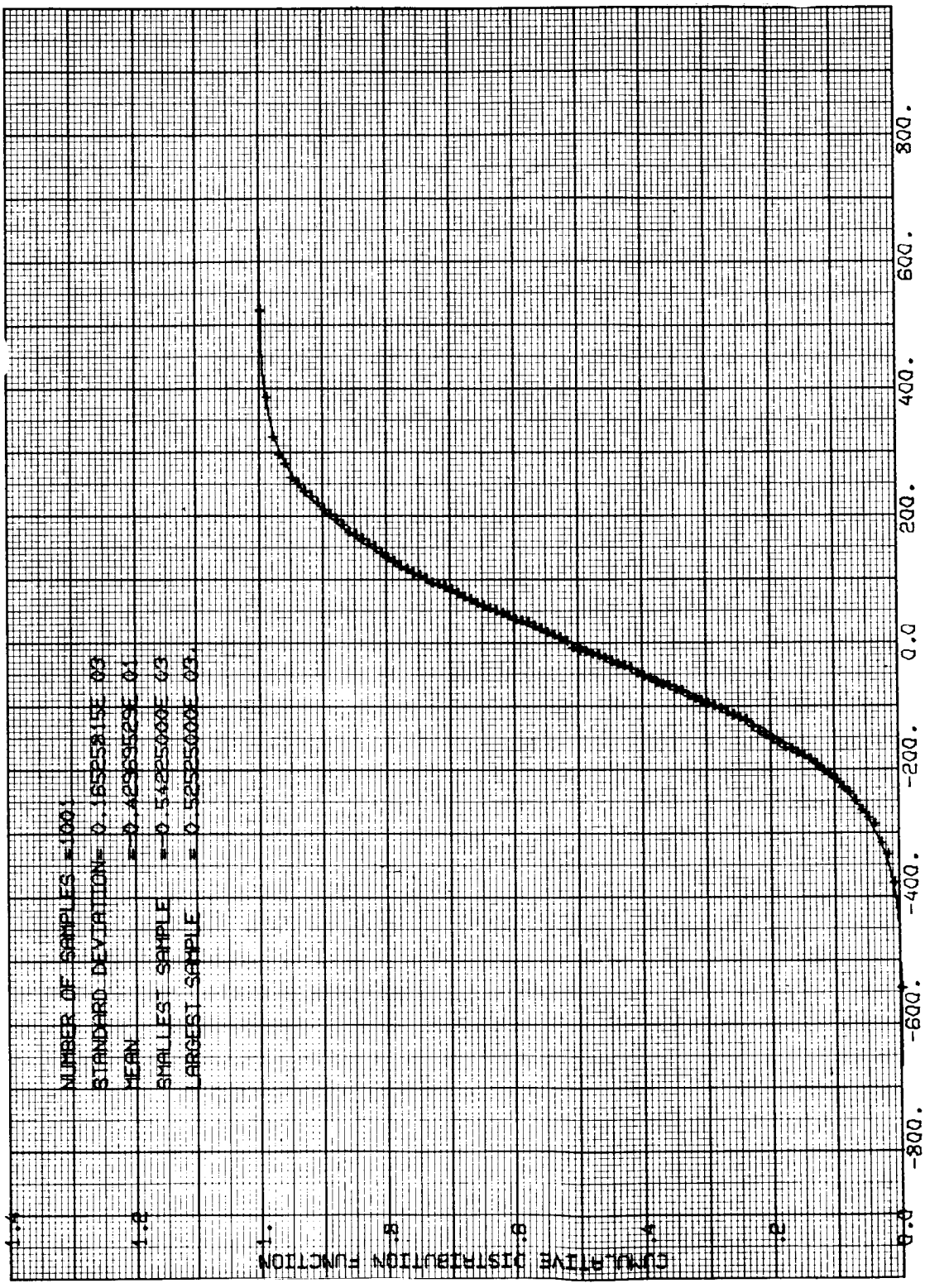

Figure D-15 Cumulative Distribution of Dispersion in Time of Flight After First Midcourse (Sec)

Table D-2. Summary of Statistical Results

MAGNITUDE OF THE ACTUAL SEPARATION MANEUVER - METERS/SEC		
MEAN	=	1.0441802D 02
STANDARD DEVIATION	=	7.2326504D 00
SMALLEST SAMPLE	=	8.6008321E 01
5TH PERCENTILE SAMPLE	=	9.3985945E 01
10TH PERCENTILE SAMPLE	=	9.6278299E 01
90TH PERCENTILE SAMPLE	=	1.1411383E 02
95TH PERCENTILE SAMPLE	=	1.1662488E 02
LARGEST SAMPLE	=	1.5552907E 02

MAGNITUDE OF THE ACTUAL FIRST MIDCOURSE MANEUVER - METERS/SEC		
MEAN	=	2.5588575D 00
STANDARD DEVIATION	=	5.5188524D-01
SMALLEST SAMPLE	=	9.8110251E-01
5TH PERCENTILE SAMPLE	=	1.6756492E 00
10TH PERCENTILE SAMPLE	=	1.8620695E 00
90TH PERCENTILE SAMPLE	=	3.2937802E 00
95TH PERCENTILE SAMPLE	=	3.4930044E 00
LARGEST SAMPLE	=	4.4921732E 00

MAGNITUDE OF THE ACTUAL SECOND MIDCOURSE MANEUVER - METERS/SEC		
MEAN	=	6.7495651D-01
STANDARD DEVIATION	=	4.3505666D-01
SMALLEST SAMPLE	=	0.
5TH PERCENTILE SAMPLE	=	1.6890080E-01
10TH PERCENTILE SAMPLE	=	2.2769952E-01
90TH PERCENTILE SAMPLE	=	1.2863307E 00
95TH PERCENTILE SAMPLE	=	1.5231875E 00
LARGEST SAMPLE	=	2.5158535E 00

Table D-2. Summary of Statistical Results (Continued)

DISPERSION IN B DOT T AFTER INJECTION - KM

MEAN	=	-5.1087765D 03
STANDARD DEVIATION	=	1.8426429D 05
SMALLEST SAMPLE	=	-4.8249674E 05
5TH PERCENTILE SAMPLE	=	-3.2005183E 05
10TH PERCENTILE SAMPLE	=	-2.3195662E 05
90TH PERCENTILE SAMPLE	=	2.3103453E 05
95TH PERCENTILE SAMPLE	=	2.9507820E 05
LARGEST SAMPLE	=	5.4814801E 05

DISPERSION IN B DOT T AFTER SEPARATION MANEUVER - KM

MEAN	=	-7.0268973D 01
STANDARD DEVIATION	=	5.5750281D 03
SMALLEST SAMPLE	=	-1.7221562E 04
5TH PERCENTILE SAMPLE	=	-9.4200836E 03
10TH PERCENTILE SAMPLE	=	-7.1756924E 03
90TH PERCENTILE SAMPLE	=	7.1008477E 03
95TH PERCENTILE SAMPLE	=	8.9630039E 03
LARGEST SAMPLE	=	1.8012309E 04

DISPERSION IN B DOT T AFTER FIRST MIDCOURSE - KM

MEAN	=	-2.5566651D-01
STANDARD DEVIATION	=	1.5084473D 02
SMALLEST SAMPLE	=	-4.8017724E 02
5TH PERCENTILE SAMPLE	=	-2.4208008E 02
10TH PERCENTILE SAMPLE	=	-1.8522412E 02
90TH PERCENTILE SAMPLE	=	1.9545239E 02
95TH PERCENTILE SAMPLE	=	2.5344751E 02
LARGEST SAMPLE	=	5.1243188E 02

Table D-2. Summary of Statistical Results (Continued)

DISPERSION IN B DOT T AFTER SECOND MIDCOURSE - KM

MEAN	=	-1.8586351D-01
STANDARD DEVIATION	=	1.7911520D 01
SMALLEST SAMPLE	=	-1.3037866E 02
5TH PERCENTILE SAMPLE	=	-2.2221679E 01
10TH PERCENTILE SAMPLE	=	-1.7117737E 01
90TH PERCENTILE SAMPLE	=	1.7546814E 01
95TH PERCENTILE SAMPLE	=	2.3252075E 01
LARGEST SAMPLE	=	9.9246581E 01

DISPERSION IN B DOT R AFTER INJECTION - KM

MEAN	=	7.2834534D 03
STANDARD DEVIATION	=	3.4379852D 05
SMALLEST SAMPLE	=	-1.6371009E 06
5TH PERCENTILE SAMPLE	=	-5.7623162E 05
10TH PERCENTILE SAMPLE	=	-4.3528503E 05
90TH PERCENTILE SAMPLE	=	4.5387838E 05
95TH PERCENTILE SAMPLE	=	5.8272311E 05
LARGEST SAMPLE	=	1.0018990E 06

DISPERSION IN B DOT R AFTER SEPARATION MANEUVER - KM

MEAN	=	-3.0903859D 02
STANDARD DEVIATION	=	1.2355986D 04
SMALLEST SAMPLE	=	-3.7754828E 04
5TH PERCENTILE SAMPLE	=	-2.1359484E 04
10TH PERCENTILE SAMPLE	=	-1.6257607E 04
90TH PERCENTILE SAMPLE	=	1.5438960E 04
95TH PERCENTILE SAMPLE	=	2.0986328E 04
LARGEST SAMPLE	=	3.7924873E 04

Table D-2. Summary of Statistical Results (Continued)

DISPERSION IN B DOT R AFTER FIRST MIDCOURSE - KM		
MEAN	=	-1.1634646D 01
STANDARD DEVIATION	=	3.3951595D 02
SMALLEST SAMPLE	=	-8.9564941E 02
5TH PERCENTILE SAMPLE	=	-5.6900616E 02
10TH PERCENTILE SAMPLE	=	-4.4554712E 02
90TH PERCENTILE SAMPLE	=	4.0290649E 02
95TH PERCENTILE SAMPLE	=	5.5685876E 02
LARGEST SAMPLE	=	1.0391044E 03

DISPERSION IN B DOT R AFTER SECOND MIDCOURSE - KM		
MEAN	=	1.6811539D-01
STANDARD DEVIATION	=	2.0582645D 01
SMALLEST SAMPLE	=	-1.1429431E 02
5TH PERCENTILE SAMPLE	=	-2.8801880E 01
10TH PERCENTILE SAMPLE	=	-2.1660583E 01
90TH PERCENTILE SAMPLE	=	2.2877502E 01
95TH PERCENTILE SAMPLE	=	2.9290222E 01
LARGEST SAMPLE	=	1.0314111E 02

DISPERSION IN TIME OF FLIGHT AFTER INJECTION - SEC		
MEAN	=	2.7703262D 03
STANDARD DEVIATION	=	1.2838874D 05
SMALLEST SAMPLE	=	-5.8659450E 05
5TH PERCENTILE SAMPLE	=	-2.1165050E 05
10TH PERCENTILE SAMPLE	=	-1.6445325E 05
90TH PERCENTILE SAMPLE	=	1.6866475E 05
95TH PERCENTILE SAMPLE	=	2.2615325E 05
LARGEST SAMPLE	=	3.7633600E 05

Table D-2. Summary of Statistical Results (Continued)

DISPERSION IN TIME OF FLIGHT AFTER SEPARATION MANEUVER - SEC		
MEAN	=	-1.2928671D 02
STANDARD DEVIATION	=	5.1669515D 03
SMALLEST SAMPLE	=	-1.7711750E 04
5TH PERCENTILE SAMPLE	=	-8.8367500E 03
10TH PERCENTILE SAMPLE	=	-6.7097500E 03
50TH PERCENTILE SAMPLE	=	6.6427500E 03
95TH PERCENTILE SAMPLE	=	8.6090000E 03
LARGEST SAMPLE	=	1.6425250E 04
DISPERSION IN TIME OF FLIGHT AFTER FIRST MIDCOURSE - SEC		
MEAN	=	-4.2969530D 00
STANDARD DEVIATION	=	1.6525816D 02
SMALLEST SAMPLE	=	-5.4225000E 02
5TH PERCENTILE SAMPLE	=	-2.7375000E 02
10TH PERCENTILE SAMPLE	=	-2.1425000E 02
50TH PERCENTILE SAMPLE	=	2.1225000E 02
95TH PERCENTILE SAMPLE	=	2.6125000E 02
LARGEST SAMPLE	=	5.2525000E 02
DISPERSION IN TIME OF FLIGHT AFTER SECOND MIDCOURSE - SEC		
MEAN	=	2.3501499D-01
STANDARD DEVIATION	=	6.7243234D 00
SMALLEST SAMPLE	=	-3.4750000E 01
5TH PERCENTILE SAMPLE	=	-9.2500000E 00
10TH PERCENTILE SAMPLE	=	-6.5000000E 00
50TH PERCENTILE SAMPLE	=	6.7500000E 00
95TH PERCENTILE SAMPLE	=	8.5000000E 00
LARGEST SAMPLE	=	4.6750000E 01

Table D-2. Summary of Statistical Results (Continued)

TOTAL VELOCITY USED DURING THE THREE MANEUVERS - METERS/SEC

MEAN	=	1.0765183D 02
STANDARD DEVIATION	=	7.2740568D 00
SMALLEST SAMPLE	=	8.9649957E 01
5TH PERCENTILE SAMPLE	=	9.7297781E 01
10TH PERCENTILE SAMPLE	=	9.9333644E 01
90TH PERCENTILE SAMPLE	=	1.1722216E 02
95TH PERCENTILE SAMPLE	=	1.2002124E 02
LARGEST SAMPLE	=	1.5986888E 02

Table D-2. Summary of Statistical Results (Continued)

MEAN OF MAGNITUDE OF THE ACTUAL SEPARATION MANEUVER - METERS/SEC
1.04418C2D C2

STANDARD DEVIATION OF MAGNITUDE OF THE ACTUAL SEPARATION MANEUVER - METERS/SEC
7.2326504D CC

MEAN OF MAGNITUDE OF THE ACTUAL FIRST MIDCOURSE MANEUVER - METERS/SEC
2.5588575D CC

STANDARD DEVIATION OF MAGNITUDE OF THE ACTUAL FIRST MIDCOURSE MANEUVER - METERS/SEC
5.5188524D-C1

MEAN OF MAGNITUDE OF THE ACTUAL SECOND MIDCOURSE MANEUVER - METERS/SEC
6.7495651D-01

STANDARD DEVIATION OF MAGNITUDE OF THE ACTUAL SECOND MIDCOURSE MANEUVER - METERS/SEC
4.35C5666D-C1

MEAN OF DISPERSION AFTER INJECTION - R-T PLANE
-5.1C877659D C3 7.2834534D C3 2.7703262D 03

COVARIANCE MATRIX OF DISPERSION AFTER INJECTION - R-T PLANE

	1	2	3
1	3.3953327D 1C	-5.7866056D 1C	-2.0770223D 1C
2	-5.7866C56D 1C	1.1819742D 11	4.3849206D 10
3	-2.077C223D 1C	4.3849206D 10	1.6483668D 1C

CORRESPONDING CORRELATION MATRIX

	1	2	3
1	1.8426429D C5	-9.1343724D-01	-8.7795661D-01
2	-9.1343724D-01	3.4379852D 05	9.9341521D-01
3	-8.7795661D-01	9.9341521D-01	1.2838874D 05

MEAN OF UNCERTAINTY BEFORE SEPARATION MANEUVER R-T PLANE
3.8966794D-C1 1.8603467D 0C 9.005994CD-01

Table D-2. Summary of Statistical Results (Continued)

COVARIANCE MATRIX OF UNCERTAINTY BEFORE SEPARATION MANEUVER R-T PLANE

	1	2	3
1	2.9405792D 02	1.0869483D 02	1.1617796D 02
2	1.0869483D 02	3.2966042D 03	1.4714425D 03
3	1.1617796D 02	1.4714425D 03	6.7453586D 02

CORRESPONDING CORRELATION MATRIX

	1	2	3
1	1.7148117D 01	1.1039745D-01	2.6085837D-01
2	1.1039745D-01	5.7416062D 01	9.8675051D-01
3	2.6085837D-01	9.8675051D-01	2.5971828D 01

MEAN OF DISPERSION AFTER SEPARATION MANEUVER R-T PLANE

-7.0268973D 01	-3.0903859D 02	-1.2928671D 02

COVARIANCE MATRIX OF DISPERSION AFTER SEPARATION MANEUVER R-T PLANE

	1	2	3
1	3.1086938D 07	-3.8639221D 07	-1.5496394D 07
2	-3.8639221D 07	1.5267038D 08	6.3758169D 07
3	-1.5496394D 07	6.3758169D 07	2.6697388D 07

CORRESPONDING CORRELATION MATRIX

	1	2	3
1	5.5750281D 03	-5.6092385D-01	-5.3795903D-01
2	-5.6092385D-01	1.2355986D 04	9.9867472D-01
3	-5.3795903D-01	9.9867472D-01	5.1669515D 03

MEAN OF UNCERTAINTY BEFORE FIRST M.C. R-T PLANE

2.3495021D 00	6.0545231D 00	3.8606394D 00

COVARIANCE MATRIX OF UNCERTAINTY BEFORE FIRST M.C. R-T PLANE

	1	2	3
1	1.6563379D 04	-9.2359875D 03	-2.1785101D 03
2	-9.2359875D 03	7.2482567D 04	3.1037194D 04
3	-2.1785101D 03	3.1037194D 04	1.6725176D 04

Table D-2. Summary of Statistical Results (Continued)

CORRESPONDING CORRELATION MATRIX

	1	2	3
1	1.28698790 02	-2.66558220-01	-1.30887980-01
2	-2.66558220-01	2.69225870 02	8.91415790-01
3	-1.30887980-01	8.91415790-01	1.29325850 02

MEAN OF DISPERSION AFTER FIRST M.C. R-T PLANE

-2.55666510-01	-1.16346460 01	-4.29695300 00

COVARIANCE MATRIX OF DISPERSION AFTER FIRST M.C. R-T PLANE

	1	2	3
1	2.27541320 04	-8.38121210 03	-1.46170700 03
2	-8.38121210 03	1.15271080 05	4.98156000 04
3	-1.46170700 03	4.98156000 04	2.73102580 04

CORRESPONDING CORRELATION MATRIX

	1	2	3
1	1.50844730 02	-1.63650190-01	-5.86363990-02
2	-1.63650190-01	3.39515950 02	8.87855480-01
3	-5.86363990-02	8.87855480-01	1.65258160 02

MEAN OF UNCERTAINTY BEFORE SECOND M.C. R-T PLANE

-2.27363330-01	-1.00390270-01	-2.82967030-01

COVARIANCE MATRIX OF UNCERTAINTY BEFORE SECOND M.C. R-T PLANE

	1	2	3
1	1.40131840 02	-6.98489210 01	-4.63889970 00
2	-6.98489210 01	2.48328230 02	2.22593810 01
3	-4.63889970 00	2.22593810 01	2.00387870 01

CORRESPONDING CORRELATION MATRIX

	1	2	3
1	1.18377290 01	-3.74436560-01	-8.75408710-02
2	-3.74436560-01	1.57584340 01	3.15547200-01
3	-8.75408710-02	3.15547200-01	4.47647040 00

MEAN OF DISPERSION AFTER SECOND M.C R-T PLANE

-1.85663510-01	1.68115390-01	2.35014990-01

Table D-2. Summary of Statistical Results (Continued)

COVARIANCE MATRIX OF DISPERSION AFTER SECOND M.C. B-T PLANE

	1	2	3
1	3.2082256D 02	-1.1250423D 02	-1.0717560D 00
2	-1.1250423D 02	4.2364528D 02	1.1404597D 01
3	-1.0717560D 00	1.1404597D 01	4.5216525D 01

CORRESPONDING CORRELATION MATRIX

	1	2	3
1	1.7911520D 01	-3.0516535D-01	-8.8984608D-03
2	-3.0516535D-01	2.0582645D 01	8.2400557D-02
3	-8.8984608D-03	8.2400557D-02	6.7243234D 00

MEAN OF UNCERTAINTY IN THE SEPARATION MANEUVER - UNITS OF (KM/SEC)SQUARED

-7.1929984D-06 -1.0495331D-05 -1.5667922D-05

COVARIANCE MATRIX OF UNCERTAINTY IN THE SEPARATION MANEUVER - UNITS OF (KM/SEC)SQUARED

	1	2	3
1	2.2746993D-07	-2.0102002D-08	2.1060156D-08
2	-2.0102002D-08	1.0879788D-07	1.1108590D-07
3	2.1060156D-08	1.1108590D-07	1.3765473D-07

CORRESPONDING CORRELATION MATRIX

	1	2	3
1	4.7693807D-04	-1.2778124D-01	1.1901564D-01
2	-1.2778124D-01	3.2984524D-04	9.0772259D-01
3	1.1901564D-01	9.0772259D-01	3.7101850D-04

MEAN OF UNCERTAINTY IN THE FIRST M.C. MANEUVER - UNITS OF (KM/SEC)SQUARED

-2.1072888D-07 3.1446749D-07 -4.4017090D-07

COVARIANCE MATRIX OF UNCERTAINTY IN THE FIRST M.C. MANEUVER - UNITS OF (KM/SEC)SQUARED

	1	2	3
1	1.0804221D-10	3.5373751D-11	9.7634975D-13
2	3.5373751D-11	9.6397507D-11	-8.7824062D-12
3	9.7634975D-13	-8.7824062D-12	1.4159573D-10

Table D-2. Summary of Statistical Results (Continued)

CORRESPONDING CORRELATION MATRIX

	1	2	3
1	1.0394335D-05	3.4661830D-01	7.8937544D-03
2	3.4661830D-01	9.8182232D-06	-7.5171902D-02
3	7.8937544D-03	-7.5171902D-02	1.1899400D-05

MEAN OF UNCERTAINTY IN THE SECOND M.C. MANEUVER - UNITS OF (KM/SEC)SQUARED

2.5850612D-07 2.4518459D-07 2.7778315D-07

COVARIANCE MATRIX OF UNCERTAINTY IN THE SECOND M.C. MANEUVER - UNITS OF (KM/SEC)SQUARED

	1	2	3
1	3.7413222D-11	1.2352457D-11	6.7160775D-12
2	1.2352457D-11	2.8225489D-11	5.8645406D-12
3	6.7160775D-12	5.8645406D-12	2.1954243D-11

CORRESPONDING CORRELATION MATRIX

	1	2	3
1	6.1166349D-06	3.8011941D-01	2.3433864D-01
2	3.8011941D-01	5.3127666D-06	2.3558847D-01
3	2.3433864D-01	2.3558847D-01	4.6855355D-06

MEAN OF DISPERSION IN B DOT T AFTER INJECTION - KM

-5.1087765D 03

STANDARD DEVIATION OF DISPERSION IN B DOT T AFTER INJECTION - KM

1.8426429D 05

MEAN OF DISPERSION IN B DOT T AFTER SEPARATION MANEUVER - KM

-7.0268973D 01

STANDARD DEVIATION OF DISPERSION IN B DOT T AFTER SEPARATION MANEUVER - KM

5.5750281D 03

MEAN OF DISPERSION IN B DOT T AFTER FIRST MIDCOURSE - KM

-2.5566651D-01

STANDARD DEVIATION OF DISPERSION IN B DOT T AFTER FIRST MIDCOURSE - KM

1.5084473D 02

Table D-2. Summary of Statistical Results (Continued)

MEAN OF DISPERSION IN B DOT T AFTER SECOND MIDCOURSE - KM
-1.8586351D-C1

STANDARD DEVIATION OF DISPERSION IN B DOT T AFTER SECOND MIDCOURSE - KM
1.791152CD C1

MEAN OF DISPERSION IN B DOT R AFTER INJECTION - KM
7.2834534D C3

STANDARD DEVIATION OF DISPERSION IN B DOT R AFTER INJECTION - KM
3.4379852D C5

MEAN OF DISPERSION IN B DOT R AFTER SEPARATION MANEUVER - KM
-3.09C3859D C2

STANDARD DEVIATION OF DISPERSION IN B DOT R AFTER SEPARATION MANEUVER - KM
1.2355986D C4

MEAN OF DISPERSION IN B DOT R AFTER FIRST MIDCOURSE - KM
-1.1634646D C1

STANDARD DEVIATION OF DISPERSION IN B DOT R AFTER FIRST MIDCOURSE - KM
3.3951595D C2

MEAN OF DISPERSION IN B DOT R AFTER SECOND MIDCOURSE - KM
1.6811539D-01

STANDARD DEVIATION OF DISPERSION IN B DOT R AFTER SECOND MIDCOURSE - KM
2.0582645D 01

MEAN OF DISPERSION IN TIME OF FLIGHT AFTER INJECTION - SEC
2.77C3262D C3

STANDARD DEVIATION OF DISPERSION IN TIME OF FLIGHT AFTER INJECTION - SEC
1.2838874D C5

MEAN OF DISPERSION IN TIME OF FLIGHT AFTER SEPARATION MANEUVER - SEC
-1.2928671D 02

Table D-2. Summary of Statistical Results (Continued)

STANDARD DEVIATION OF DISPERSION IN TIME OF FLIGHT AFTER SEPARATION MANEUVER - SEC 5.1669515D 03
MEAN OF DISPERSION IN TIME OF FLIGHT AFTER FIRST MIDCOURSE - SEC -4.2969530D 00
STANDARD DEVIATION OF DISPERSION IN TIME OF FLIGHT AFTER FIRST MIDCOURSE - SEC 1.6525816D 02
MEAN OF DISPERSION IN TIME OF FLIGHT AFTER SECOND MIDCOURSE - SEC 2.3501499D-01
STANDARD DEVIATION OF DISPERSION IN TIME OF FLIGHT AFTER SECOND MIDCOURSE - SEC 6.7242234D 00
MEAN OF TOTAL VELOCITY USED DURING THE THREE MANEUVERS - METERS/SEC 4.8295587D 13
STANDARD DEVIATION OF TOTAL VELOCITY USED DURING THE THREE MANEUVERS - METERS/SEC 3.2292936D 12

Substitution for δR from Equation (2) yields

$$\delta X_E - \delta X_A = (A^T W A)^{-1} A^T W N \tag{4}$$

The covariance matrix of the error in the estimated state vector due to tracking is

$$\Lambda_T = E\left[(\delta X_E - \delta X_A)(\delta X_E - \delta X_A)^T\right] \tag{5}$$

Substituting Equation (1) into (5) and making the assumption that $E(NN^T) = W^{-1}$, yields

$$\Lambda_T = (A^T W A)^{-1} \tag{6}$$

The tracking covariance matrix is of order 6x6 when $\delta Z_A = 0$; the square root of the diagonal elements yields the standard deviations of the six components of the state vector.

If systematic errors are to be estimated along with the orbit parameters, Equation (1) should be rewritten as

$$\delta R = \left[A\ B\right] \begin{bmatrix} \delta X_A \\ \\ \delta Z_A \end{bmatrix} + N \tag{7}$$

or

$$\delta R = C\,\delta Y_A + N \tag{8}$$

Since Equation (8) has the same form as Equation (2), the estimate will have the same form; namely,

$$\delta Y_E = (C^T W C)^{-1} C^T W \delta R \tag{9}$$

The covariance matrix of the error in the estimate is given by

$$\Lambda_S = (C^T W C)^{-1} \tag{10}$$

and is similar in form to the covariance matrix for orbit parameters only, except it has larger dimensions. The square root of the diagonal elements of Λ_S are the standard deviations of the six components of the state vector and of the systematic errors.

If systematic errors are neglected in forming the least-squares estimate but are considered in the analysis of the estimate, the residuals can be written in the form of Equation (1). Since $B\delta Z_A$ is neglected in the curve fit

$$\delta X_E = \delta X_A + (A^T W A)^{-1} A^T W (B\delta Z_A + N) \tag{11}$$

the error in the estimate is

$$(\delta X_E - \delta X_A) = (A^T W A)^{-1} A^T W (B\delta Z_A + N) \tag{12}$$

The covariance matrix of the error in the estimate state vector is

$$\Lambda_C = E\left[(\delta X_E - \delta X_A)(\delta X_E - \delta X_A)^T\right] \tag{13}$$

or

$$\Lambda_C = (A^T W A)^{-1} + (A^T W A)^{-1} (A^T W B) \Lambda_Z (B^T W A) (A^T W A)^{-1} \tag{14}$$

where

$$\Lambda_Z = E\left[(\delta Z_A)(\delta Z_A)^T\right] \tag{15}$$

and

$$E(NN^T) = W^{-1} \tag{16}$$

Λ_C is a 6x6 matrix. Since the systematic errors cause an error in the curve fit which is uncorrelated with the errors caused by noise, the square root of the diagonal elements of the covariance matrix are larger when systematic errors are considered than when only noise is considered.

REFERENCES

D-1. "Performance and Design Requirements for the 1973 Voyager Mission, General Specification for," January 1, 1967, Jet Propulsion Laboratory.

D-2. F. J. Mullin, J. J. Goldman, and P. A. Brinkman, "Description of PROC Statistical Processor Program," TRW Report 05959-6085-R000, 20 February 1966.

RELIABILITY ANALYSIS AND DATA

CONTENTS

APPENDIX E

RELIABILITY ANALYSES AND DATA

This appendix collects Voyager spacecraft reliability data, such as structural reliability analyses and failure rates.

Section 1 presents the structural reliability analysis, including adapter separation. Propulsion system firing and vent sequences appear in Section 2. Detailed temperature control reliability calculations appear in Section 3.

Failure rates and probability of success are listed for Voyager subsystem equipment in Tables E-1 through E-16.

1. STRUCTURAL RELIABILITY ANALYSIS FOR VOYAGER

1.1 Stress-Strength Approach

An estimate of the structural reliability may be obtained from the values used for the factor of safety and the margin of safety in the design of the spacecraft structure.

Each of the structural members in the Voyager is subjected to one or more stresses of varying magnitude during the mission. Of the stresses which are applied to an individual member, often one stress is predominant and when failure occurs, it is almost always due to this stress. This critical stress is used in the sizing of each member. The second factor which determines the reliability of a member is its strength or ability to withstand stress. A part will fail only if the applied stress or stresses exceed its strength. The probability that this occurs is defined as the unreliability of the part.

Let X be the strength of the part and Y be the maximum stress placed on the part during the mission where X and Y are independent random variables. Then reliability is defined as

$$R = P(X > Y) \qquad \text{(E-1)}$$

Assuming that the probability densities of X and Y are reasonably approximated by independent normal distributions; i.e., X is normal with mean μ_X and standard deviation σ_X, Y is normal with mean μ_Y and standard deviation σ_Y, we may let

$$D = X - Y \tag{E-2}$$

and write $R = P(X > Y) = P(D > 0)$. By the addition theorem for normal variables, D has a normal distribution with

$$\text{Mean of } D = \mu_D = \mu_X - \mu_Y \tag{E-3}$$

$$\text{Standard Deviation of } D = \sigma_D = \sqrt{\sigma_X^2 + \sigma_Y^2} \tag{E-4}$$

Note that distributional assumptions of normality which may not be precisely satisfied for X and Y will tend to be more satisfied for D since by the central limit theorem, the difference of two variables will be more normal than either of the two.

Thus,

$$R = P(D > 0) = \int_0^\infty \frac{1}{\sigma_D \sqrt{2\pi}} \exp - \frac{1}{2} \left(\frac{D-\mu_D}{\sigma_D}\right)^2 dD \tag{E-5}$$

Letting

$$t = \frac{D-\mu_D}{\sigma_D}$$

$$dt = \frac{dD}{\sigma_D}$$

$$R = \int_{-\mu_D/\sigma_D}^{\infty} \frac{1}{\sqrt{2\pi}} \exp - \frac{t^2}{2} dt = \int_{\infty}^{\mu_D/\sigma_D} \frac{1}{\sqrt{2\pi}} \exp - \frac{t^2}{2} dt$$

by symmetry of the integrand

$$R = \Phi\left(\frac{\mu_D}{\sigma_D}\right) = \Phi\left(\frac{\mu_X - \mu_Y}{\sqrt{\sigma_X^2 + \sigma_Y^2}}\right) = \Phi(z) \tag{E-6}$$

where Φ is the cumulative distribution function of the standardized normal variable.

This procedure can be used as the basis for estimating the reliability of structural members. In stress analysis, it is customary to

design in terms of a factor of safety, F. S., margin of safety, M. S., and the stresses or loads. These are related by the equation

$$\text{F. S. (M. S. + 1)} = \frac{\text{Allowable Stress}}{\text{Limit Load}} \qquad \text{(E-7)}$$

The allowables are determined based upon material properties found in MIL-HDBK-5A. Both 99 or 90 percent guaranteed values (95 percent confidence) are used. Similarly, the limit load is usually taken as some value above the expected maximum stress. Thus, employing normal distribution notation:

$$\text{F. S. (M. S. + 1)} = \frac{\mu_X - \eta\sigma_X}{\mu_Y + m\sigma_Y} \qquad \text{(E-8)}$$

For the Voyager a safety factor of 1.25 is used. A margin of safety as close to zero on the positive side as possible is desired. Substituting these values in the above, one has

$$\frac{\mu_X - n\sigma_X}{\mu_Y + m\sigma_Y} = 1.25$$

or

$$\left(\frac{\mu_X}{\mu_Y}\right)\left(\frac{1 - n(\sigma_X/\mu_X)}{1 + m(\sigma_Y/\mu_Y)}\right) = 1.25 \qquad \text{(E-9)}$$

The quantity $\nu = \sigma/\mu$ is called the coefficient of variation and measures the spread of the distribution relative to the mean.

If the four quantities, n, m, ν_X, ν_Y were known, they could be substituted and the ratio between the means determined from Equation (9).

Rewriting the quantity

$$Z = \left(\mu_X - \mu_Y\right)\Big/\sqrt{\sigma_X^2 + \sigma_Y^2}$$

$$Z = \frac{\left(\frac{\mu_X}{\mu_Y}\right) - 1}{\sqrt{\left(\frac{\sigma_X}{\mu_X}\right)^2 \left(\frac{\mu_X}{\mu_Y}\right)^2 + \left(\frac{\sigma_Y}{\mu_Y}\right)^2}} \qquad \text{(E-10)}$$

$$Z = \frac{\left(\frac{\mu_X}{\mu_Y}\right) - 1}{\sqrt{\nu_X^2 \left(\frac{\mu_X}{\mu_Y}\right)^2 + \nu_Y^2}}$$

Thus, reliability can be determined as in Equation (E-6)

$$R = \Phi(Z) \qquad \text{(E-11)}$$

provided n, m, ν_X, and ν_Y are known.

1.1.1 Estimation of n, m, ν_X and ν_Y in Voyager Design

The allowable and limit stresses are not known with complete precision in any given situation. Materials vary from batch to batch, loads vary from vehicle to vehicle. Thus the quantities, allowable and limit stresses, in Equation (E-7) can be considered as variables with probability distributions, again approximable by the normal. The needed quantities are estimated in the following sections.

1.1.1.1 Estimation of n

For the Voyager, 99 percent guaranteed values were used in determining allowables. Thus,

$$\mu_X - n\sigma_X = \text{allowable stress}$$

is such that 99 percent of samples chosen will withstand the tabulated value of stress without breaking, cracking, or otherwise failing catastrophically in any way. As may be determined from a normal table, the number of standard deviations below the mean corresponding to 99 percent probability is 2.33. Thus, n is estimated as 2.33.

1.1.1.2 Estimation of ν_X

Two tabulated values are given in the Handbook of Material Properties,* one 90 percent guaranteed, the other 99 percent. For 7075-T6 aluminum (heat treated and aged) which makes up the large majority of Voyager structural items, these two values are 78 and 76 ksi, respectively. Thus,

$$P(X < 76) = 0.01$$

$$P(X < 78) = 0.10$$

or

$$P\left(\frac{X - \mu_X}{\sigma_X} < \frac{76 - \mu_X}{\sigma_X}\right) = 0.01$$

$$P\left(\frac{X - \mu_X}{\sigma_X} < \frac{78 - \mu_X}{\sigma_X}\right) = 0.10$$

Again consulting a normal table shows that the 0.01 and 0.10 lower values are -2.33 and -1.28. Thus,

$$\frac{76 - \mu_X}{\sigma_X} = -2.33$$

$$\frac{78 - \mu_X}{\sigma_X} = -1.28$$

Solving these equations for μ_X and σ_X:

$$\sigma_X = 1.905 \text{ ksi}$$

$$\mu_X = 80.4387 \text{ ksi}$$

so that

$$\frac{\sigma_X}{\mu_X} = \nu_X = \frac{1.905}{80.4387} = 0.0237$$

* MIL-HDBK-5, February 8, 1966; Table 3.2.7.0(b), p. 334

1.1.1.3 Estimation of m

In the case of estimating m, it is difficult to assess the degree of conservatism exhibited in determination of the loads. A rough estimate was obtained in discussions with TRW personnel that actual loads would be less than those specified with a probability of 90 percent. In terms of m, this percentage corresponds to

90 percent: m = 1.282 best estimate

1.1.1.4 Estimation of ν_Y

In order to obtain some feeling regarding possible load variability, the following question was asked of several structures people. "Assuming that actual load data is available from previous payloads which are similar enough to be meaningful to the Voyager structure, what do you estimate as the probability that actual limit loads will fall within ±25 percent of conscientiously obtained best estimates of limit loads?" Note that the question was phrased not in terms of possible conservatism of specified loads, but predicated upon the assumption that these loads were best estimates. Thus, answers reflect estimates of the uncertainty associated with load prediction with possible conservatism being accounted for in the estimation of m.

Answers to this question ranged over a considerable spread although most felt that the past actual load information would greatly improve the accuracy of present load estimates. A best answer to the question is felt to be 95 percent. The computation of ν_Y for a value of 95 percent is used in this analysis as follows:

Assuming a 95 percent probability that the actual loads will be within ±25 percent of the predicted implies that 95 percent of the probability distribution will lie between $\mu_Y + 0.25$ and $\mu_Y - 0.25\,\mu_Y$. This implies, from the normal table that

$$1.25\,\mu_Y = \mu_Y + 1.96\,\sigma_Y$$

$$0.25\,\mu_Y = 1.96\,\sigma_Y$$

$$0.128 = \frac{0.25}{1.96} = \frac{\sigma_Y}{\mu_Y} = \nu_Y$$

1.1.2 Computation of Reliability for One Structural Member

Since all structural members are being designed with the same general design guidelines, it is a good first approximation to assume that all have equal reliability.

Computation of the reliability estimate is done through the use of Equations (E-9), (E-10), and (E-11). Values of n, m, ν_X, ν_Y are substituted into Equation (E-10), which results in a value for Z. The reliability is then obtained from

$$R = \Phi(Z)$$

by consulting a normal table.

In this case, $\frac{\mu_X}{\mu_Y} = 1.5402$, $Z = 4.0586$ and $R = 0.9_4753$

1.1.3 Spacecraft Structure and Booster Adapter Structure Reliability Estimates

R_{ss}, the spacecraft structure reliability estimate, is derived assuming 100 independent structural members, i.e.

$$R_{ss} = (0.9_4753)^{100} = 0.99753$$

R_A, the booster adapter structure reliability, is derived assuming 116 independent structural members, i.e.

$$R_A = (0.9_4753)^{116} = 0.99714$$

1.2 Separation Reliability Analyses

Details of the squib, cable assembly, and coil spring reliability analyses are shown in Tables E-1, E-2, E-3 and E-4.

Separation Nut:

$q = 48,000 \times 10^{-9}$/cycle (based on TRW test history)

Dual redundant, therefore,

$q = \lambda^2 = 2304 \times 10^{-12}$

Since there are 12 sets of nuts required for separation

$Q = Nq = 12 \times 2304 \times 10^{-12} = 27,\ 648 \times 10^{-12}$

$R = 1 - Q = 0.9_7724$

Separation Reliability

$$R_{separation} = R_{squib} \times R_{cable\ assembly} \times R_{coil\ spring} \times R_{separation\ nut}$$

$$R_{separation} = (0.9_5892)\ (0.9_6793)\ (0.9_3604)\ (0.9_7724)$$

$$R_{separation} = 0.9_3603$$

2. PROPULSION SYSTEM

2.1 Firing and Vent Sequences (Figure E-1)

2.1.1 Gas Pressurized High-Thrust Firing*

There is one of this type (Mars Orbit Insertion) and one gas pressurized low thrust firing (Orbit Trim).

2.1.1.1 System Pressurization (Prior to Zero "g" Start)

1) Fire open one (of one) normally closed explosive valve in one (of two) branches of each of explosive valve units (A), (B), and (C). Open redundant pre-valve unit (M).

   a) Actuation of units (A) and (M) in conjunction with power to the pintle actuator (D) solenoid valve allows regulated gas to drive the pintle actuator to the high thrust position (it is spring loaded to a normally low thrust position) and also pressurizes the valve actuator (E) of the shutoff valve (F).

   b) Actuation of units (B) and (C) allows regulated gas to pressurize the propellant tanks.

2.1.1.2 Zero "g" Start

1) Open redundant solenoid valve units (G) and (G) and redundant shutoff valve (F).

---

* The only difference between the gas pressurized high thrust firing described here and the gas pressurized low thrust firing is that the pintle actuator solenoid valve is not actuated and the pintle actuator thus remains at the low thrust level.

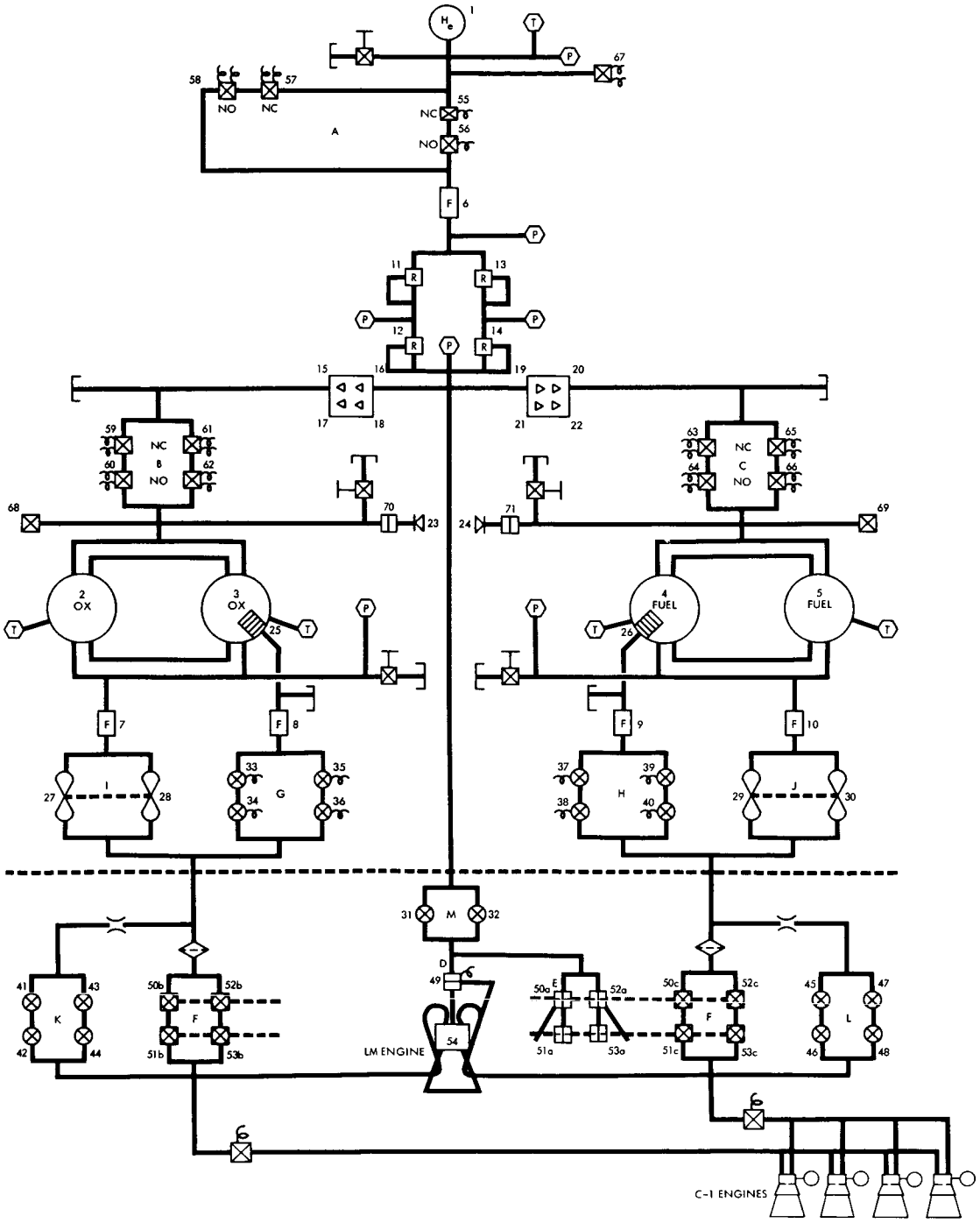

Figure E-1. Voyager Propulsion Subsystem Schematic

a) Actuation of solenoid valve units (G) and (H) allows propellant from the start tanks to flow to the shutoff valve (F). Actuation of shutoff valve unit (F) results in zero "g" engine start.

2.1.1.3 Engine Firing

1) Open redundant pre-valve units (I) and (J) (motor driven poppet valves) and close redundant solenoid valve units (G) and (H).

a) Actuation of units (I) and (J) allows propellant flow from the propellant tanks. De-activation of units (G) and (H) stops propellant flow from the start tanks.

2.1.1.4 Engine Shutdown

1) Close redundant shutoff valve unit (F), redundant pre-valve units (I), (J), and (M) and fire close one (of one) normally open explosive valve in each of the branches of units (A), (B) and (C) previously opened.

a) All propellant and gas flow is stopped.

2.1.2 Blowdown Mode Low Thrust Firings (Interplanetary Trajectory Corrections)

2.1.2.1 Zero "g" Start

1) Open redundant solenoid valve units (G) and (H) and redundant solenoid shutoff valve units (K) and (L).

a) Actuation of solenoid valve units (G) and (H) allows propellant from the start tanks to flow to the solenoid shutoff valve units (K) and (L). Actuation of solenoid shutoff valve units (K) and (L) results in zero "g" engine start.

2.1.2.2 Engine Firing

1) Open redundant pre-valve units (I) and (J) (motor driven poppet valves) and close redundant solenoid valve units (G) and (H).

a) Actuation of units (I) and (J) allows propellant flow from the propellant tanks. De-activation of units (G) and (H) stops propellant flow from the start tanks.

2.1.2.3 Engine Shutdown

1) Close redundant solenoid shutoff valve units (K) and (L), and redundant pre-valve units (I) and (J).

2.2 Vent

1) System venting is accomplished after the last orbit trim firing.

a) Fire open normally closed explosive valves numbered 67, 68, and 69 to vent the oxidizer and fuel pressurant.

3. DETAILED TEMPERATURE CONTROL RELIABILITY CALCULATIONS

3.1 Heaters

Of the 12 Type I heaters, eight of these are located in the equipment module, and four are located in the propulsion module. For purposes of this analysis, the equipment module heaters are called Type I, and the propulsion module heaters are called Type III. The four Type II heaters are located on the deployed booms. Mission heater success is defined as no more than one failure of Type I heaters (that is seven of the eight heaters in the equipment module must work), and no failures of the Type II heaters (that is, four of the four boom heaters must work), and no more than one failure of the Type III heaters (that is, three of the four propulsion module heaters must work). Mathematically this is expressed as follows:

$$R_{Heaters} = R\ (7/8,\ Type\ I) \times R\ (4/4,\ Type\ II) \times R\ (3/4,\ Type\ III)$$

$$\lambda_{Heater} = 20 \times 10^{-9} \text{ per hour}$$

$$\lambda_{Thermoswitch} = 500 \times 10^{-9} \text{ per hour}$$

$$\lambda_{Relay,\ 4\ Contact} = 350 \times 10^{-9} \text{ per hour}$$

Therefore

$$\lambda\ (\text{heater-thermoswitch}) = 520 \times 10^{-9} \text{ hour}$$

$$\lambda\ (\text{heater-relay} = 370 \times 10^{-9} \text{ per hour}$$

$$t\ (\text{mission}) = 6800 \text{ hours @ 50 percent duty cycle}$$

$\therefore$ Probability (0 failure Type I, or Type III) = Probability (0 failure, heater on) + Probability (0 failure, heater off)

Probability (0 failure, Type I, Type III) = $520 \times 10^{-9} \times 0.50 \times 6800 \left[1 + 0.10\right] = 0.0019448$

Similarly,

Probability (0 failure, Type II) = $370 \times 10^{-9} \times 0.50 \times 6800 \left[1 + 0.10\right] = 0.0013838$

Using the binomial equation (1),

Probability (no more than k failures occur in n trials)

$$= \sum_{i=o}^{k} Cn,i\, p^{i}\, (1-p)^{n-i} \qquad (1)$$

Where $Cn,i = \frac{n!}{i!\,(n-i)!}$

Probability (7/8, Type I Survive) = $0.9^{3}895$

Probability (4/4, Type II Survive) = $0.9944^{6}5$

Probability (3/4, Type III Survive) = $0.9^{4}774$

$R_{Heaters} = 0.9^{3}895 \times 0.994465 \times 0.9^{4}774$

Therefore,

$R_{Heaters} = 0.994338$

3.2 Louvers

λ (Spring) = 1.21×10^{-6} per cycle based on OGO temperature control louver tests

t (Mission) = 2500 cycles

Probability of one louver failure occurring = $1.21 \times 10^{-6} \times 2500 = 0.00302$

Using the binomial theorem:

Type I louvers - Prob (≤ 3 of 8 louvers fail) = $R_{\text{Type I}} = 0.9_6755$

Type II louvers - Prob (≤ 5 of 30 louvers fail) = $R_{\text{Type II}} = 0.9_9585$

$$\therefore R_{\text{Louvers}} = (R_{\text{Type I}})^2 \ (R_{\text{Type II}})^9$$

$$R_{\text{Louvers}} = 0.9_6507$$

Table E-1. Reliability Analysis, Squib

Description	Reliability Analysis
Operational modes One-shot device	1) Failure rate (λ) = $300,000 \times 10^{-9}$ failures/cycle 2) Source: TRW experience, 200 squib firing with no failures is equivalent to probability of failure = 3×10^{-4} @ 50 percent confidence
Environmental modes Failure could occur as a result of boost environment or faulty workmanship	3) Details Probability of premature fire = 1/50 total failure probability based on TRW Bruceton test history Therefore, Prob (premature fire) = $\frac{300,000 \times 10^{-9}}{50}$ = $6,000 \times 10^{-9}$ Prob (no fire) = $300,000 - 6,000 = 294,000 \times 10^{-9}$
Primary failure modes • Premature fire • No fire	
Possible Causes • Poor workmanship • Faulty design	
Effect on mission Failure to separate spacecraft properly	4) Mission time (c) = 1 cycle 5) $q = \lambda c = 300,000 \times 10^{-9} \times 1 = 3 \times 10^{-4}$ 6) Dual redundant squibs $q = (\lambda c)^2 = (3 \times 10^{-4}) = 9 \times 10^{-8}$

Table E-1. Reliability Analysis, Squib (Continued)

Description	Reliability Analysis
Back-up provisions • Redundant squib cartridges • Separate power source for each squib • Considerable test programs to verify item design and fabrication	7) Number of items used = 12. Therefore, $Q = 12 \times 9 \times 10^{-8} = 108 \times 10^{-8}$ 8) $R = 1 - Q = 0.9^{5}892$

Table E-2. Reliability Analysis, Cable Assembly

Description	Reliability Analysis
Operational modes A 2-pin connector, two solder joints and two wires were considered for each cable assembly	1) Failure rate (λ) = 438×10^{-9} f/hr (two wires) 2) Source: Farada, dated 3/1/65, Source 138, and Martin Company Report M63-3 3) Details Connector: 200/pin x 2 pins = 400×10^{-9}/hr Wire: 15 x 2 = 30×10^{-9} Solder joint: 4 x 2 = 8×10^{-9} 438×10^{-9}/hr
Environmental modes Failure could occur as a result of vibration during boost	4) Environment application factor (K_E) = 1000 5) Mission time (t) = 0.3 hr
Primary failure mode Failure to supply electrical ignition	6) Number of assemblies used: 12, dual redundant
Possible causes • Poor pin contact • Broken wire	7) $K_E \lambda t = 1000 \times 0.3 \times 438 \times 10^{-9} = 131.4 \times 10^{-6}$
Effect on mission Possibly catastrophic	8) Since the assembly is dual redundant, $q = (\lambda t)^2 = (131.4 \times 10^{-6})^2 = 17266 \times 10^{-12}$ and $Q = 12q = 12 \times 17266 \times 10^{-12} = 207,192 \times 10^{-12}$
Backup provisions Dual redundant squibs (and bridgewires)	9) $R = 1 - Q = 0.9^6 793$

Table E-3. Reliability Analysis, Coil Spring

Description	Reliability Analysis
Operational modes After release of bolt tension, the spring ejects the pin from the assembly	1) Failure rate (λ) - 110×10^{-9} failures/hr 2) Source: Farada, dated 3/1/65, Source 138 p. 2.374
Environmental modes Failure could occur as a result of the boost environment	3) Environment application factor (K_E) = 1000 4) Mission time (t) = 0.3 hr
Primary failure mode Failure to eject bolt	5) Number of items used: 12 6) $NK_E\lambda t = 12 \times 1000 \times 110 \times 10^{-9} \times 0.3 = 396 \times 10^{-6} = Q$
Possible causes • Vacuum weld of coils • Loss of spring tension	7) $R = 1 - Q = 0.9^3604$
Backup provisions • Considerable TRW experience with similar design application • Test program to verify item design and fabrication	
Effect on mission Either misalignment or no separation	

Table E-4. Reliability Analysis, Release Device

Description	Reliability Analysis
Operational modes Gas retaining, no fragmentation, pin-pulling device to release spacecraft appendages	1) Failure Rate (λ) = 0.001 failures/cycle
Environmental modes Failure could occur as a result of the boost environment	2) Source: Farada Failure rate data has been recently generally substantiated based on Hi-Shear Corp. TAT/Reliability test program reported in Hi-Shear document 2-204 (295 tests, 0 failures)
Primary failure mode Failure to release pin when proper force is available	3) Environment application factor (K_E) = 1 4) Mission time (c) = 1 cycle 5) $q = (K_E)\,\lambda\, c = 0.001 \times 1 = 0.001$
Possible causes • Jammed pin • Broken pin	6) Number of items used = 6 = N 7) Therefore, $Q = Nq = 6 \times 0.001 = 0.006$
Effect on the mission Failure to deploy appendages can result in total mission failure	8) $R = 1 - Q = 0.994$
Backup provisions • Considerable TRW experience with similar design application • Test program to verify item design and fabrication	

Table E-5. Propulsion Component Data

Component Number	Component	Failure Mode		Total Component Failure Rate	Source	Percent of Component Failures by Mode	Failure Rate/Mode
1-5	Tank	A	Leak or rupture	0.026×10^{-6} failures/hr	(1)	100	0.026×10^{-6} failures/hr
6-10	Filter	A	Loss of filter function	0.032×10^{-6}	(1)	100	0.032×10^{-6} failures/hr
11-14	Regulator	A	Leak to space	0.400×10^{-6}	(1)	4	0.016×10^{-6} failures/hr
		B	Fail closed			15	0.060×10^{-6} failures/hr
		C	Leak downstream (including loss of regulation function)			81	0.324×10^{-6} failures/hr
15-22	Check valve	A	Leak downstream	0.045×10^{-6} failures/hr	(1)	100	0.045×10^{-6} failures/hr
		B	Fail closed			Negligible	Negligible
23-24	Relief Valve	A	Leak to space	0.250×10^{-6} failures/hr	(1)	100	0.250×10^{-6} failures/hr
		B	Fail closed			Negligible	Negligible
25-26	Start tank (bellows)	A	Leak	$0.016 \times 10\text{-}6$ failures/hr 0.010×10^{-6} failures/cycle	(1)	100	0.016×10^{-6} failures/hr and 0.010×10^{-6} failures/cycle
27-30	Pre-valve (motor-driven poppet valve)	A	Leak to space	1.319×10^{-6} failures/hr 0.004×10^{-6} failures/cycle	(1, 2)	1	0.007×10^{-6} failures/hr 0.0
		B	Leak downstream			23	0.300×10^{-6} failures/hr and 0.002×10^{-6} failures/cycle
		C	Fail closed (inoperative motor)			76	1.012×10^{-6} failures/hr and 0.002×10^{-6} failures/cycle
31-48	Solenoid valve	A	Leak to space	0.365×10^{-6} failures/hr 0.004×11^{-6} failures/cycle	(1) (1)	2	0.007×10^{-6} failures/hr 0.0
		B	Fail closed			16	0.058×10^{-6} failures/hr and 0.002×10^{-6} failures/cycle
		C	Leak downstream			82	0.300×10^{-6} failures/hr and 0.002×10^{-6} failures/cycle
49	Pintle actuator (solenoid valve-bellows)	A	Leak to space	0.390×10^{-6} failures/hr 0.014×10^{-6} failures/cycle	(1, 2)	6	0.023×10^{-6} failures/hr and 0.010×10^{-6} failures/cycle
		B	Fail closed			15	0.058×10^{-6} failures/hr and 0.002×10^{-6} failures/cycle
		C	Leak downstream			79	0.309×10^{-6} failures/hr and 0.002×10^{-6} failures/cycle
50-53	Valve actuator, propellant ball valves units (a, b, c)	A	Leak to space	4.332×10^{-6} failures/hr 0.004×10^{-6} failures/cycle	(2)	1	0.021×10^{-6} failures/hr 0.0
		B	Fail closed			23	0.994×10^{-6} failures/hr and 0.002×10^{-6} failures/cycle
		C	Leak downstream			76	3.317×10^{-6} failures/hr and 0.002×10^{-6} failures/cycle
54	Thruster (injector-combustion chamber)	A	Structural failure, leak, burnthrough	48×10^{-6} failures/sec	(3)	100	48×10^{-6} failures/sec $172,800 \times 10^{-6}$ failures/hr
55-69	Explosive valve	A	Premature fire	Probability of explosive valve failure = 0.0019	(4)	10	Probability of premature fire = 0.00019
		B	Fail to fire			90	Probability does not fire = 0.00171
70-71	Burst disc	A	Premature burst	Probability of burst disc failure = 0.0005	(2)	50	Probability of premature burst = 0.00025
		B	Fail to burst			50	Probability does not burst = 0.00025

Data Source

(1) FARADA (Bureau of Naval Weapons, U. S. Naval Fleet Missile Systems Analysis and Evaluation Group, Corona, California) adjusted to reflect TRW failure rate experience on satellite systems.

(2) TRW estimated.

(3) TRW test data: LMDE (Injector: 91,274 firing seconds with 0 failures = a failure rate $\leq 10 \times 10^{-6}$ failures/second: Chamber: 24,135 firing seconds with 0 failures = a failure rate $\leq 38 \times 10^{-6}$ failures/second @ 60 percent level of confidence).

(4) Vendor reliability prediction based on applicable test results.

Table E-6. Voyager Standard Level Failure Rates

Part Type	Failure Rate (Failures/10^9 hr)
Resistor	
Carbon composition	12
Metal film	8
Carbon film	8
Wire-wound accurate	40
Wire-wound power	50
Wire-wound variable	60
Carbon variable	40
Diode	
Analog	30
Zener	73
Rectifier	30
Digital	14
Tunnel	100
Varactor	65
μ wave mixer	50
μ wave detector	50
Germanium	50
SCR	150
Pin	50
Capacitor	
Ceramic	14
Ceramic feed-through	24
Glass	6
Mica dipped	8
Mica button	8
Paper	25
Plastic	25
Paper plastic	25

Table E-6. Voyager Standard Level Failure Rates (Continued)

Part Type	Failure Rate (Failures/10^9 hr)
Tantalum foil	80
Tantalum solid	40
Tantalum wet slug	80
Miscellaneous variable	39
Connector	
Coaxial	60
General	10
Multilayer	5
Transistor	
Silicon general	100
Silicon switching	40
Field effect	60
Germanium	150
Transformer	
IF, 4 term	30
RF, 4 term	30
General, 4 term	30
General, 5 term	40
General, 6 term	50
Pulse	45
Magnetic amplifier	
2 winding	30
3 winding	40
Thermistor	10
Crystal	76
Memory Cores/hundred	1
Relay	
General, 2 contact sets	300

Table E-6. Voyager Standard Level Failure Rates (Continued)

Part Type	Failure Rate (Failures/10^9 hr)
General, 4 contact sets	350
Latching 1 winding	450
Latching 2 winding	500
Sense	400
Coaxial	475
Coil	
General	10
RF	4
Integrated Circuits	
Digital	50
Analog	150
Crystal Filer	200
Tube	
Rectifier	1,250
Klystron (LP)	10,000
Klystron (HP)	25,000
TWT	10,000
Waveguide	
Switch (LP)	1,000
Switch (HP)	5,000
Section	10
Coupling	100
Cavity filter	100
Resistive termination	10
Battery cell	150
Connection	1
Wire-wrap	3
Fuse	200
LC filter	73

Table E-6. Voyager Standard Level Failure Rates (Continued)

Part Type	Failure Rate (Failures/10^9 hr)
Meter	500
Switch, toggle DPDT	100
Lamp	1,000
Video amplifier	5,000
Operational amplifier (not IC)	800
Shaft encoder	2,000
Indicator	0
Mixer	1,100
Crystal oscillator	850
Cavity	100
Circulator	100
Step recovery diode	200
Resolvers	6,000
Circuit breaker	500
Nixie	1,000
Brush	40
Solar cell	10
Thermal switch	500
Motor	300
FEB, encoder	135
FSU	4,900
Gyro	10,000
Sun sensor	685
Engine actuator	100
Drive actuator assembly	100
Array drive	100
Resistor network	30
1/2 Integrated circuit gate	25
Pressure tank	26
Cold gas filter	32
Regulator	400

Table E-6. Voyager Standard Level Failure Rates (Continued)

Part Type	Failure Rate (Failures/10^9 hr)
Pintle actuator	404
Check valve	45
Start tank	26
Relief valve	250
Propellant ball valve actuators	4336
Propellant tank	26
Propellant filter	32
Bipropellant valve motor driven poppet valve	1323
Bearing	500
Cable	438
Gear	77
Hinge	662
Motor	230
Pulley	154
Roller	423
Spring	110
Track	123
Latching mechanism	125
Heater	20
Temperature transducer	335
Pressure transducer	1400
Fill valve	21
Diffuser	32
Bellows	26
Solenoid valve	3619

Table E-7. Voyager Cyclic Failure Probabilities

Component	Failure Probability
Explosive valves (N/O)	0.0003
Explosive valves (N/C)	0.0003
Start valves (N/C)	0.0003
Burst disc	0.0005
Bimetallic spring	0.00000121
Solenoid valve per cycle	0.000001

Table E-8. Environmental Factors

Mission Condition	Factor
Boost	100
Interplanetary cruise	1
Midcourse corrections	10
Orbital insertion	50
Orbit cruise	1
Orbit trim	10

Table E-9. Guidance and Control Component Reliability

Component	Failure Rate (10^9 hr) (Failures per 10^9 hr)	Probability of Success	Probability of Success (Redundant Conf.)
Canopus sensor	6494	0.9570	0.9993
Coarse sun sensor	980	0.9933	0.9999
Fine sun sensor	790	0.9947	0.9999
Gyro control assembly	9640	0.9350	0.9960
Control electronics	5000	0.9666	-
Reaction control	6727	0.9552	0.9980
Thrust vector control	1000	0.9932	0.9999
Accelerometer	350	0.9976	-
Total		0.958	

Table E-10. Command Unit Component Reliability

Component	Failure Rate (10^9 hr) (Failures per 10^9 hr)	Probability of Success
Bit synchronizer detector	9417	0.938
Detector selector	300	0.998
Input decoder	2250	0.985
Output decoder	3900	0.974
Output drivers	2100	0.986
Total (Redundant Configuration)		0.995

Table E-11. Command and Sequencer Unit Component Reliability

Component	Failure Rate (10^9 hr) (Failures per 10^9 hr)	Probability of Success (Redundant Conf.)
Decoder and drivers	10,890	0.929
Memory and timers	18,965	0.879
Accelerometer counter	1,200	0.992
Counter backup	500	0.997
Function generator	1,500	0.990
Antenna pointing backup	500	0.997
Command events register		
Total (Redundant Configuration)	0.981	

Table E-12. S-Band Radio Subsystem Component Reliability

Component	Failure Rate (10^9 hr) (Failures per 10^9 hr)	Probability of Success (Redundant Conf.)
Baseband assembly	4,000	0.9732
Exciter and TWT	20,350	0.8708
Transmitter selector	2,342	0.9841
Receiver selector	1,219	0.9917
High-gain antenna and diplexer	42,760	0.7477
High-gain receiver	17,200	0.8894
Circulator switch	250	0.9983
Medium-gain antenna and diplexer	21,150	0.8639
Medium-gain receiver	17,200	0.8894
Circulator switch and selector	1,500	0.9898
Low-gain antenna and receiver	17,400	0.8894
Total (Redundant Configuration)	0.916	

Table E-13. Telemetry and Data Storage Component Reliability

Component	Failure Rate (Failures per 10^9 hr)	Probability of Success
Hard-wired programmer (subcarrier)	330	0.9978
Hard-wired programmer (main-carrier)	240	0.9983
Flexible format generator	6,067	0.9595
Bit rate generator and sync generators	2,730	0.9816
Subcarrier and main carrier multiplexers	4,035	0.9730
Engineering data direct output	910	0.9938
Engineering data tape recorder	12,000	0.9210
Science data direct output	60	0.9999
Science data tape recorder	12,000	0.9210
Video data tape selector	150	0.9990
Video data tape recorders	12,000	0.9210
Data output coder and switch	150	0.9990
Total (Redundant Configuration)		0.921

Table E-14. Electrical Power Subsystem Component Reliability

Component	Failure Rate (10^9 hr) (Failures per 10^9 hr)	Probability of Success: Single Component	Probability of Success: Redundant Configuration
Solar array and shunts			0.9985
Boost regular	4000	0.9732	0.9997
Synchronizer	3800	0.9745	0.9996
400-Hz inverter	7100	0.9529	0.9989
Load control	7500	0.9503	0.9988
Battery and control	7000	0.9535	0.9937
Telemetry	600	0.9959	-
Total (Redundant Configuration)			0.985

Table E-15. Electrical Distribution Subsystem Component Reliability

Component	Failure Rate (10^9 hr) (Failures per 10^9 hr)	Probability of Success: Single Component	Probability of Success: Redundant Configuration
Electrical distribution unit	1650	0.9888	0.9999
Pyro-Group 1: One safe/arm unit and seven pyro control units	5850	0.9986	0.9999
Pyro-Group 2: One safe/arm unit and three pyro control units	3450	0.9975	0.9999
Pyro-Group 3: Two safe/arm units and nine pyro control units	8700	0.9544	0.9999
Total (Redundant Configuration)			0.999

Table E-16. Planetary Scan Platform Component Reliability

Component	Failure Rate (10^9 hr) (Failures per 10^9 hr)	Probability of Success For Mission
PSP drive and electronics	3583	0.9740
Mars sensor electronics	2585	0.9826
Mars sensor	2454	0.9986
Total (Redundant Configuration)		0.955

MASS PROPERTIES DATA

CONTENTS

APPENDIX F

MASS PROPERTIES DATA

The weight and mass properties of the recommended spacecraft are presented in this appendix. Data is displayed in tabular and graphic form, together with a discussion of supporting data.

The weights of the planetary vehicle are 20, 107, 22, 166, and 24, 097 pounds including capsule weights of 5000, 6000, and 7000 pounds respectively. These planetary vehicle weight estimates include a propulsive capability of 1.95 km/sec and weight allocations of 400 pounds for the spacecraft science and 50 pounds for the capsule radio link (as per the requirements and guidelines of References F-1 and F-2). The configuration incorporating the 5000 pound capsule of Case A for the study (Reference F-2) meets the maximum weight requirement of Reference F-1, i.e., that the gross weight of the planetary vehicle including adapter must not exceed 22, 000 pounds.

The spacecraft also meets other basic criteria established during the course of the study:

- Powered flight slosh stability requirements are met with a reasonable margin.
- Adequate main engine gimbal moment arm for control purposes is provided throughout all phases of the mission.

1. WEIGHT DATA

Tables F-1 and F-2 give summary and detailed weight estimates for the planetary vehicle, utilizing the guideline format supplied by MSFC. This data is also given in Tables F-3, F-4, and F-5 in terms of a format based on the breakdown of the spacecraft into two major modules. Table F-6 gives a mission weight history for the reference velocity profile given in Section 3.15 and for capsule weights of 5000, 6000, and 7000 pounds.

The weight estimates shown are predicated upon the use of a 5 percent weight contingency as per the MSFC guideline of Reference F-2. This is considered to be an optimistic assumption for the present state of configuration definition.

Table F-1. Summary Weight Estimates—Recommended Configuration (Guideline Format)

Item	Weight (lb) Case A	Case B	
Structure	913.0	913.0	913.0
Basic shell	211.4	211.4	211.4
Meteoroid protection	562.6	562.6	562.6
Supports	110.4	110.4	110.4
Separation mechanism	28.6	28.6	28.6
Propulsion	1,568.7	1,568.7	1,568.7
Engine (main)	408.5	408.5	408.5
Fuel system	232.1	232.1	232.1
Oxidizer system	237.1	237.1	237.1
Pressurization	348.8	348.8	348.8
Supports	308.2	308.2	308.2
Secondary engine installation	34.0	34.0	34.0
Equipment and Instrumentation	2,276.0	2,340.6	2,340.6
Structure	180.0	180.0	180.0
Guidance, control and navigation	168.2	168.2	168.2
Instrumentation	397.7	397.7	397.7
Electric power	443.5	443.5	443.5
Electric networks	298.0	298.0	298.0
Temperature control system	238.5	238.5	238.5
Attitude control system	150.1	214.7	214.7
Science equipment	400.0*	400.0*	400.0*
Balance Weights	15.0	15.0	15.0
Contingency	216.1	217.7	217.7
Total Dry Spacecraft	4,988.8	5,055.0	5,055.0
Unusable Fluids	455.1	458.2	461.2
Propellant residuals	412.9	416.0	419.0
Pressurant residuals	42.2	42.2	42.2
Total Inert Spacecraft	5,443.9	5,513.2	5,516.2
Usable Propellant	9,663.1	10,652.5	11,580.5
Total Spacecraft at Liftoff	15,107.0	16,165.7	17,096.7
Capsule	5,000.0	6,000.0	7,000.0
Total Planetary Vehicle at Liftoff	20,107.0	22,165.7	24,096.7

* JPL specification payload weight allocation. See Volume 5, Appendix G, for weight estimates of science payloads described in that volume.

Table F-2. Planetary Vehicle Weight Estimate (5000-lb Capsule) (Guideline Format)

Item		Weight (lb)		
Structure				913.0
Basic shell			211.4	
Rings and frames		77.0		
Stringers and longerons		96.6		
Longerons	75.6			
Radial members	21.0			
Miscellaneous		37.8		
Attachments—equipment module	23.5			
Attachments—propulsion module	14.3			
Meteoroid protection			562.6	
Panels—equipment module		510.0		
Panels—propulsion module		52.6		
Supports			110.4	
Supports—antenna		36.9		
Support—medium-gain antenna	12.5			
Support—low-gain antenna	2.0			
Support—high-gain antenna	22.4			
Support—planetary scan platform		38.5		
Supports—solar array		35.0		
Separation mechanism			28.6	
Propulsion				1,568.7
Engine (main)			408.5	
Fuel system			232.1	
Tanks and supports		193.0		
Tanks	146.0			
Start tank	25.0			
Tank supports	22.0			
Plumbing		34.1		
Fill/drain coupling	0.9			
Pre-valve	10.0			
Quad solenoid valve	5.0			
Filter	2.3			
Pressure transducer	0.3			
Temperature transducer	0.5			
Hardware	2.1			
Fuel lines	13.0			
Miscellaneous		5.0		
Electrical harness	2.5			
Electrical junction box	2.5			

Table F-2. Planetary Vehicle Weight Estimate (5000-lb Capsule) (Guideline Format) (Continued)

Item		Weight (lb)	
Oxidizer system			237.1
Tanks and supports		193.0	
Tanks	146.0		
Start tank	25.0		
Tank supports	22.0		
Plumbing		39.1	
Fill/drain	0.9		
Pre-valve	10.0		
Quad solenoid valve	5.0		
Filter	2.3		
Pressure transducer	0.3		
Temperature transducer	0.5		
Hardware	2.1		
Oxidizer lines	18.0		
Miscellaneous		5.0	
Electrical harness	2.5		
Electrical junction box	2.5		
Pressurization			348.8
Bottles and supports		300.0	
Pressurant tanks	264.0		
Pressurant tank supports	36.0		
Plumbing		48.8	
Fill/vent coupling—helium	0.3		
Fill/vent coupling—propellant	0.9		
Explosive valves	12.0		
Filter	0.9		
Quad pressure regulator	12.0		
Quad check valve	1.8		
Burst disc and relief valve	1.6		
Pressure transducer	0.8		
Temperature transducer	0.5		
Hardware	3.0		
Lines	15.0		
Supports			308.2
Engine supports		31.8	
System supports		276.4	
Main cross beams	72.0		
End beams	48.0		
Center beams	20.0		
Base panel	136.4		
Secondary engine installation			34.0
Engines (4)		29.2	
Valves (2)		1.0	
Plumbing		1.8	
Supports		2.0	

Table F-2. Planetary Vehicle Weight Estimate (5000-lb Capsule) (Guideline Format) (Continued)

Item		Weight (lb)		
Equipment and Instrumentation				2,276.0
Structure			180.0	
Equipment mounting panels		180.0		
Guidance, control and navigation			168.2	
Sensors		34.2		
Canopus sensor (2)	30.2			
Coarse sun sensor (4)	2.4			
Fine sun sensor (2)	0.4			
Limb and terminator crossing detector (2)	1.2			
Computer/sequencer		34.0		
Primary computer and sequencer	18.0			
Backup computer and sequencer	16.0			
Control computer		63.0		
Inertial reference assembly (2)	50.0			
Guidance and control electronics	13.0			
Servo actuators		37.0		
TVC actuators	37.0			
Instrumentation			397.7	
Radio		118.6		
S-band radio	68.6			
Baseband assembly	1.0			
Modulator exciter (2)	6.0			
1-watt transmitter	3.0			
Power amplifier and power supply (2)	15.6			
Transmitter selector	1.0			
Receiver (4)	14.0			
Receiver selector	1.0			
Low-gain antenna selector	0.5			
Circulator switch assembly	7.5			
Diplexer (4)	4.0			
Preamplifier (4)	2.0			
Interconnecting cables	8.0			
Antenna drive electronics	5.0			
Capsule radio link	50.0			

Table F-2. Planetary Vehicle Weight Estimate (5000-lb Capsule) (Guideline Format) (Continued)

Item		Weight (lb)	
Command		12.5	
Command unit	10.5		
PSP remote decoder	2.0		
Telemetry		15.0	
Telemetry data handling unit	11.0		
PSP video remote multiplexer	2.0		
PSP remote multiplexer	2.0		
Data system		116.0	
Video tape recorder (4)	80.0		
Engineering and science tape recorder (2)	36.0		
Antennas		135.6	
Low-gain antenna (2)	6.0		
Low-gain antenna feed (2)	6.5		
High-gain antenna	52.1		
High-gain antenna feed	6.4		
High-gain antenna drive	30.0		
Medium-gain antenna	12.4		
Medium-gain antenna feed	5.2		
Medium-gain antenna drive	17.0		
Electrical power			443.5
Solar panels		217.5	
Batteries (3)		150.0	
Power control		76.0	
Inverter	10.0		
Converter (8)	40.0		
Power control unit	20.0		
Shunt element assembly (1)	6.0		
Electrical networks			298.0
Networks		273.0	
Cabling and connectors — equipment module	207.0		
propulsion module	5.0		
Junction box—propulsion module	5.0		
Junction box (6)	44.0		
Distribution control unit	12.0		
Pyrotechnics		25.0	
Pyrotechnic control assembly	25.0		
Temperature control system			238.5
Insulation—equipment module		127.6	
Insulation—propulsion module		31.9	
Louvers and mechanisms		36.3	
Other devices		13.4	
Insulation—engine		29.3	

Table F-2. Planetary Vehicle Weight Estimate (5000-lb Capsule) (Guideline Format) (Continued)

Item		Weight (lb)		
Attitude control system			150.1	
Bottles (2)		56.0		
Plumbing		2.0		
Thruster assembly (4)		2.4		
Mounts		11.0		
Controls		16.2		
Regulator—low pressure	2.4			
Regulator—high pressure	5.0			
Solenoid valve	7.2			
Selector valve	1.2			
Fill valve	0.4			
Miscellaneous		1.4		
Transducer—low pressure	0.2			
Transducer—high pressure	0.2			
Transducer—outlet	0.1			
Nitrogen gas		61.1		
Usable N_2	56.3			
Residual N_2	4.8			
Science equipment			400.0*	
Scan platform		145.0		
Science instruments		255.0		
Balance Weights				15.0
Contingency				216.1
Total Dry Spacecraft				4,988.8
Residuals				455.1
Propellants			412.9	
Tanks		359.8		
Lines and engine		53.1		
Pressurant			42.2	
Total Inert Spacecraft				5,443.9
Usable Propellants				9,663.1
Fuel			3,716.6	
Oxidizer			5,946.5	
Total Spacecraft at Liftoff				15,107.0
Capsule				5,000.0
Total Planetary Vehicle at Liftoff				20,107.0

* JPL Specification payload weight allocation. See Volume 5, Appendix G, for weight estimates of science payloads described in that volume.

Table F-3. Recommended Planetary Vehicle Weight Summary (Format Based on Modularity)

(5000-lb Capsule)

Item	Weight (lb)
Capsule	5,000.0
Spacecraft Science Subsystem	400.0
Capsule Radio Link	50.0
Spacecraft Equipment Module	2,677.8
Structure	1,008.5
Thermal control	177.3
Electrical power	443.5
Electrical distribution and pyrotechnic control	288.0
Guidance and control	236.3
S-Band radio	204.2
Telemetry and data storage	131.0
Command and sequencer	46.5
Balance weights	15.0
Contingency (5 percent)	127.5
Spacecraft Propulsion Module	11,979.2
Structure	483.7
Thermal control	61.2
Electrical distribution and pyrotechnic control	10.0
Thrust vector control actuators	37.0
Engine	408.5
C-1 engine installation	34.0
Propellant feed	425.2
Pressurization system	312.8
Residuals (propellant and helium)	455.1
Contingency (5 percent)	88.6
Impulse propellant	9,663.1
Planetary Vehicle Gross Weight	20,107.0
Planetary Vehicle Adapter	685.5
Structure	474.2
Electrical distribution and pyrotechnic control	8.0
Shroud modification	134.7
Separation system	36.0
Contingency	32.6
Planetary Vehicle Gross Weight + Adapter	20,792.5

Table F-4. Detailed Weight Estimate – Equipment Module

Item	Weight (lb)
Structure	1,008.5
Equipment panels (6)	180.0
Meteoroid protection panels (27)	510.0
Longerons (8)	75.6
Rings (5)	77.0
Diagonal members (8)	21.0
Medium-gain antenna supports and deployment mechanism	12.5
Low-gain antenna deployment mechanism	2.0
High-gain antenna supports and deployment mechanism	22.4
PSP supports and deployment mechanism	38.5
Solar array supports	35.0
Nitrogen bottle supports	11.0
Attachments and miscellaneous	23.5
Thermal Control	177.3
Insulation	127.6
Louvers	36.3
Heaters and thermostats	4.0
Attachments and miscellaneous	9.4
Electrical Power	443.5
Solar array	217.5
Battery (3)	150.0
Inverter, 400 H_z (1)	10.0
Converter, DC/DC (8)	40.0
Power control unit (1)	20.0
Shunt element assembly (2)	6.0
Electrical Distribution and Pyrotechnic Control	288.0
Cabling and connectors	207.0
Junction box (6)	44.0
Pyrotechnic control assembly (1)	25.0
Distribution control unit (1)	12.0
Guidance and Control	236.3
Inertial reference assembly (2)	50.0
Guidance and control electronics (1)	13.0
Canopus sensor (2)	14.0
Canopus sensor shield (2)	16.2
Coarse sun sensor (4)	2.4
Fine sun sensor (2)	0.4

Table F-4. Detailed Weight Estimate—Equipment Module (Continued)

Item	Weight (lb)
Limb and terminator crossing detector (2)	1.3
Pressure vessel (2)	56.0
Regulator, low pressure (2)	2.4
Regulator, high pressure (2)	5.0
Solenoid valve (12)	7.2
Selector valve (2)	1.2
Transducer, low pressure (2)	0.2
Transducer, high pressure (2)	0.2
Transducer outlet (12)	1.0
Fill valve (2)	0.4
Plumbing set (2)	2.0
Thruster assembly (4)	2.4
Residual nitrogen	4.8
Usable nitrogen	56.3
S-Band Radio	204.2
Baseband assembly (1)	1.0
Modulator exciter (2)	6.0
1-watt transmitter (1)	3.0
Power amplifier and power supply (2)	15.6
Transmitter selector (1)	1.0
Receiver (4)	14.0
Receiver selector (1)	1.0
Low-gain antenna selector (1)	0.5
Circulator switch assembly (1)	7.5
Diplexer (4)	4.0
Preamplifier (4)	2.0
Low-gain antenna (2)	6.0
Low-gain antenna feed (2)	6.5
High-gain antenna (1)	52.1
High-gain antenna feed (1)	6.4
High-gain antenna drive (1)	30.0
Medium-gain antenna (1)	12.4
Medium-gain antenna feed (1)	5.2
Medium-gain antenna drive (1)	17.0
Interconnecting cables (15)	8.0
Antenna drive electronics (1)	5.0
Telemetry and Data Storage	131.0
Video tape recorder (4)	80.0
Engineering and science recorder (2)	36.0
Telemetry, data handling unit (1)	11.0
PSP video remote multiplexer (1)	2.0
PSP remote multiplexer (1)	2.0

Table F-4. Detailed Weight Estimate—Equipment Module (Continued)

Item	Weight (lb)
Command and Sequencer	46.5
Command unit (1)	10.5
Primary computer and sequencer (1)	18.0
Backup computer and sequencer (1)	16.0
PSP remote decoder (1)	2.0
Balance Weights	15.0
Contingency	127.5
Spacecraft Equipment Module	2,677.8

Table F-5. Detailed Weight Estimate—Propulsion Module

Item	Weight (lb)
Structure	483.7
Main cross beams (4)	72.0
End beams (8)	48.0
Center beams (4)	20.0
Base panel (1)	136.4
Meteoroid protection panels (5)	52.6
Separation system	28.6
Propellant tank supports	44.0
Pressurant tank supports	36.0
Engine supports	31.8
Attachments and miscellaneous	14.3
Temperature Control	61.2
Insulation, base panel	31.9
Insulation, engine	29.3
Electrical Distribution and Pyrotechnic Control	10.0
Cabling and connectors	5.0
Junction box	5.0

Table F-5. Detailed Weight Estimate—Propulsion Module (Continued)

Item	Weight (lb)
Thrust Vector Control Actuators	37.0
Thrust vector control actuators (2)	37.0
Engine and Valves	408.5
Combustion chamber assembly	202.5
Chamber heat shield	8.0
Seal	2.0
Nozzle extension	36.0
Nozzle insulation	26.5
Hardware	5.0
Injector	29.3
Pintle actuator	4.0
Propellant lines and ducts	13.0
Shut-off valve, high thrust	17.0
Shut-off valve, low thrust	13.8
Pre-valve	3.5
Hardware	0.8
Trim orifices	0.5
Electrical harness	6.0
Junction box	4.0
Hardware, junction box	2.0
Instrumentation	3.0
Gimbal assembly	26.1
Hardware	5.5
C-1 Engine Installation	34.0
Engines (4)	20.0
Nozzle extension (4)	5.2
Nozzle insulation (4)	4.0
Isolation valve (2)	1.0
Plumbing	1.8
Hardware	2.0
Propellant Feed System	425.2
Tanks (4)	292.0
Start tanks (2)	50.0
Fill-drain coupling (4)	1.8
Pre-valve (4)	20.0
Quad solenoid valve (2)	10.0
Filter (2)	4.6
Pressure transducer (2)	0.5
Temperature transducer (4)	1.0
Electrical harness	5.0
Electrical junction box	5.0

Table F-5. Detailed Weight Estimate – Propulsion Module (Continued)

Item	Weight (lb)
Hardware	4.3
Fuel lines	13.0
Oxidizer lines	18.0
Pressurization System	312.8
Tanks (2)	264.0
Fill/vent coupling, helium (1)	0.3
Fill/vent coupling, propellant (2)	0.9
Explosive valves (15)	12.0
Filter (3)	0.9
Quad pressure regulator (1)	12.0
Quad check valve (2)	1.8
Burst disc and relief valve (2)	1.6
Pressure transducer (3)	0.8
Temperature transducer (2)	0.5
Hardware	3.0
Plumbing	15.0
Residuals	455.1
Fuel	31.7
Fuel, tanks	126.2
Oxidizer, tanks	201.9
Fuel, lines	20.4
Oxidizer, Lines	32.7
Helium, tanks	42.2
Contingency (5 percent)	88.6
Impulse Propellant	9,663.1
Fuel	3,716.6
Oxidizer	5,946.5
Spacecraft Propulsion Module	11,979.2

Table F-6. Planetary Vehicle Weight Histories

Condition	Capsule Weight (lb)		
	5,000	6,000	7,000
Gross Injected Weight	20,793	22,852	24,783
Less planetary vehicle adapter	-686	-686	-686
Net Injected Weight	20,107	22,166	24,097
Less midcourse correction propellant	-1,393	-1,536	-1,670
Less 50 percent usable nitrogen (assumed)	-28	-44	-44
Planetary Vehicle at Begin Mars Orbit Insertion	18,686	20,586	22,383
Less Mars orbit insertion propellant	-7,706	-8,490	-9,231
Planetary Vehicle in Mars Orbit	10,980	12,096	13,152
Less capsule	-5,000	-6,000	-7,000
Spacecraft in Mars Orbit	5,980	6,096	6,152
Less available orbit correction propellant	-564	-627	-680
Less remainder of usable nitrogen	-28	-44	-44
Spacecraft at End-of-Life	5,388	5,425	5,428

2. MASS DISTRIBUTION PROPERTIES

Center of mass and moment of inertia data for the planetary vehicle and the spacecraft are presented in Table F-7. The corresponding information showing the orientation of the principal axes is given in Table F-8. The system of coordinate axes and principal axis orientation angles for the planetary vehicle are shown in Figure F-1.

Table F-7. Inertial Properties Summary (5000-lb Capsule)

Condition	Planetary Vehicle (5000-lb Capsule)					Spacecraft				
	Weight (lb)	$\bar{Z}$ (in.)	Inertia—slug ft^2			Weight (lb)	$\bar{Z}$ (in.)	Inertia—slug ft^2		
			I_x	I_y	I_z			I_x	I_y	I_z
Ignition—appendages stowed	20,107	135.7	24,412	24,930	14,723	15,107	103.9	6,885	7,403	10,222
Ignition—appendages deployed	20,107	137.0	26,197	25,034	16,492	15,107	107.7	8,812	7,654	11,987
End midcourse corrections	18,686	139.4	25,700	24,400	15,800	13,686	107.8	8,650	7,250	11,300
End Mars orbit insertion	10,980	169.4	19,462	17,300	11,927	5,980	122.6	6,779	4,640	7,404
Spacecraft in Mars orbit	5,980	122.6	6,779	4,640	7,404	5,980	122.6	6,779	4,640	7,404
Spacecraft at end-of-life	5,388	126.4	6,309	4,077	6,892	5,388	126.4	6,309	4,077	6,892
Dry spacecraft—appendages stowed	--	--	--	--	--	4,928	121.1	4,245	3,618	4,960
Dry spacecraft—appendages deployed	--	--	--	--	--	4,928	130.6	6,046	3,782	6,685

See Figure F-9 for planetary vehicle coordinate axis system

Table F-8. Principal Axis Data
(5000-lb Capsule)

Condition	Planetary Vehicle		Spacecraft	
	ϕ_1 (deg)	ϕ_2 (deg)	ϕ_1 (deg)	ϕ_2 (deg)
Ignition—appendages stowed	+0.6	+8.6	-1.1	-8.7
Ignition—appendages deployed	-3.3	-5.2	+9.6	-4.3
End Mars orbit insertion	-2.4	-2.6	+12.9	-6.3
Spacecraft in Mars orbit	+12.9	-6.3	+12.9	-6.3
Spacecraft at end of life	+13.4	-6.4	+13.4	-6.4
Dry spacecraft—appendages stowed	--	--	-3.6	-7.7
Dry spacecraft—appendages deployed	--	--	+12.3	-5.9

See Figure F-9 for explanation of ϕ_1 and ϕ_2

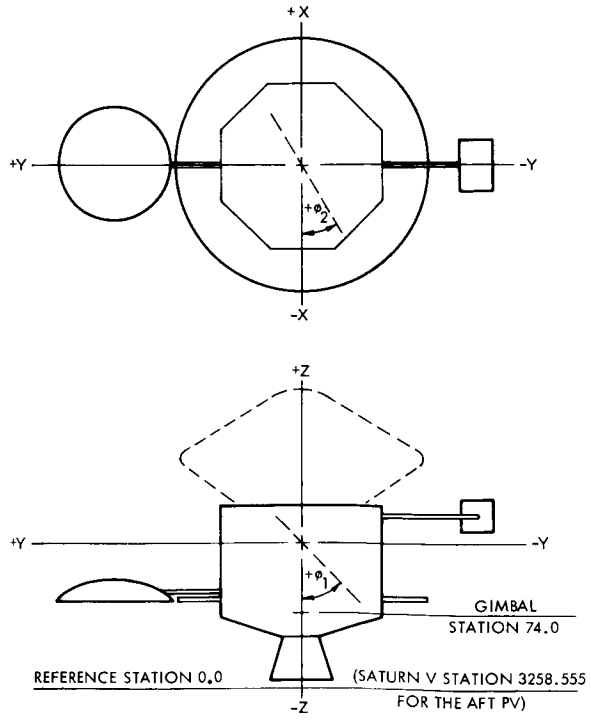

Figure F-1. Planetary Vehicle Coordinate Axis System

Figure F-2 shows center of mass variation with weight for the spacecraft alone, and Figure F-3 shows this for the planetary vehicle with a 5000-pound capsule. Figure F-4 shows the variation of the center of mass (for the initial case of no capsule) as propellant is utilized, in relation to slosh stability. The powered flight slosh stability criteria and main engine gimbal moment arm requirements have a significant effect on the recommended configuration. In particular all equipment was placed as far forward and the engine as far aft as possible within the constraints of the planetary vehicle envelope. In satisfying the center of mass requirement as shown in Figure F-4, the PSP must be deployed to the far forward position.

Minimum c.g. travel is a desirable feature and speaking in terms of longitudinal travel has been achieved as far as possible with this configuration. Better capsule information will be required before refinements can be made. The desired radial c.g. offset limit of 0.5 inch at

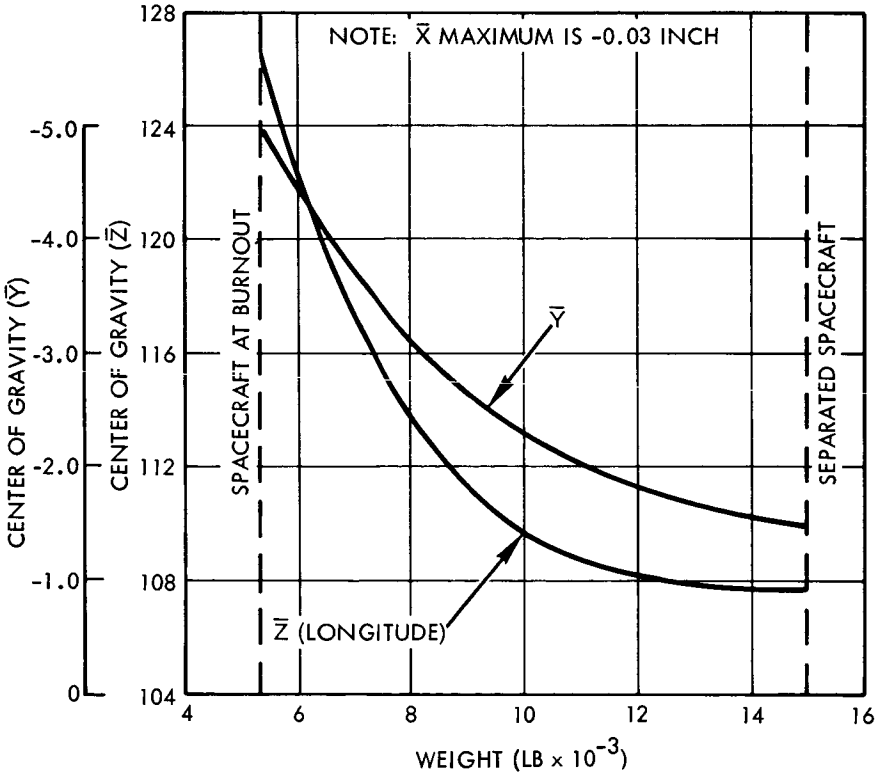

Figure F-2. Center of Mass vs. Weight—Spacecraft with No Capsule

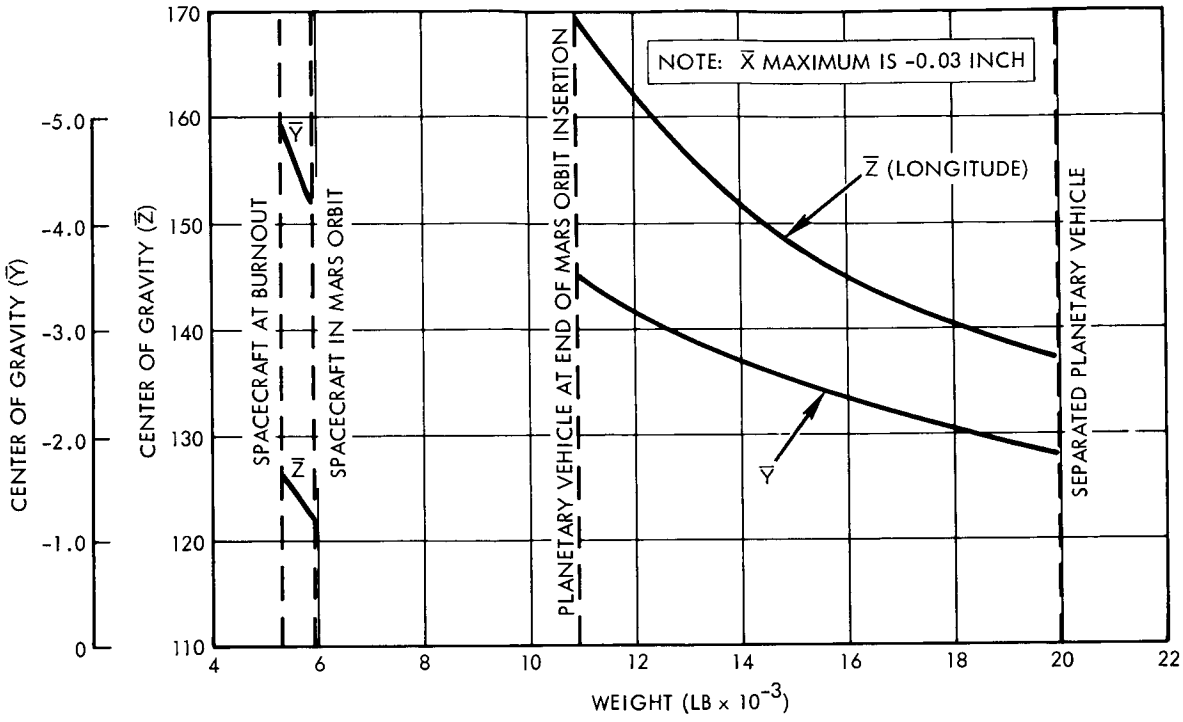

Figure F-3. Center of Mass vs. Weight—Planetary Vehicle (5000-lb Capsule)

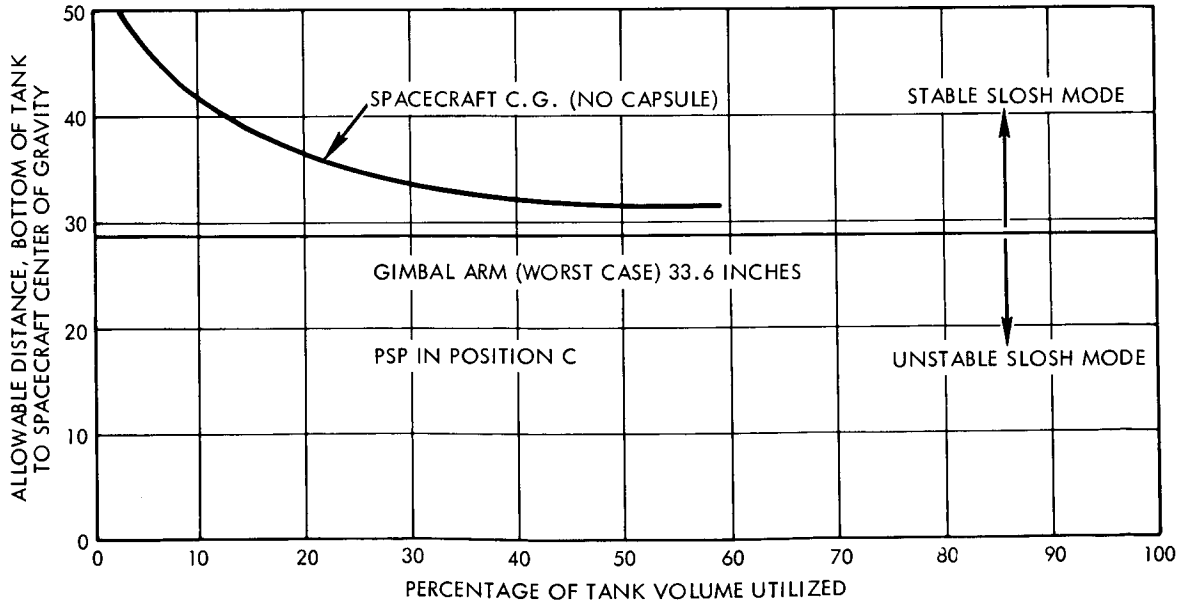

Figure F-4. Powered Flight Slosh Stability

Mars orbit insertion burnout is a difficult value to achieve due to the large offset mass of the PSP. Efforts have been made to distribute equipment weight to obtain this value with the spacecraft alone, and so far the best figure that has been achieved is about 4.9 inches. This represents an engine gimbal angle of 5.3 degrees, which is just within the maximum allowable of $\pm$ 6 degrees.

Estimates of moments of inertia and principal axis angles are plotted versus weight for the spacecraft alone in Figures F-5 and F-6. Estimated moments of inertia of the capsule versus weight are given in Figure 5-7, and this data has been used to estimate moments of inertia and principal axis angles as shown in Figure F-8 and F-9.

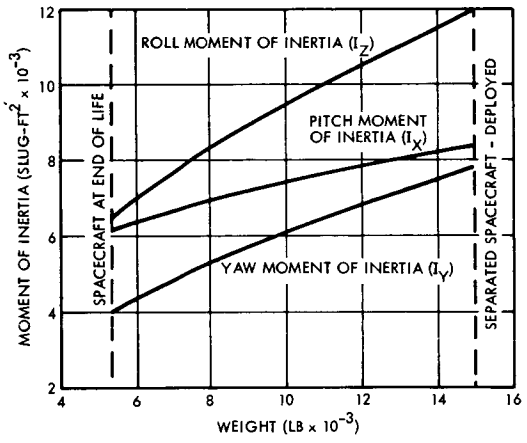

Figure F-5. Spacecraft Moments of Inertia vs. Weight (no Capsule)

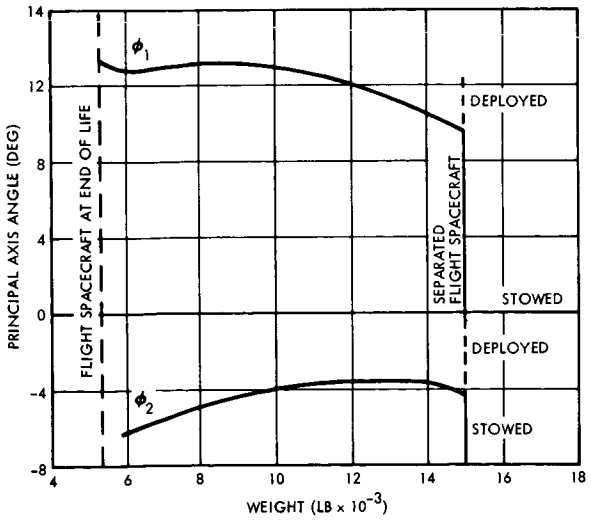

Figure F-6. Spacecraft Principal Axis Angles vs. Weight

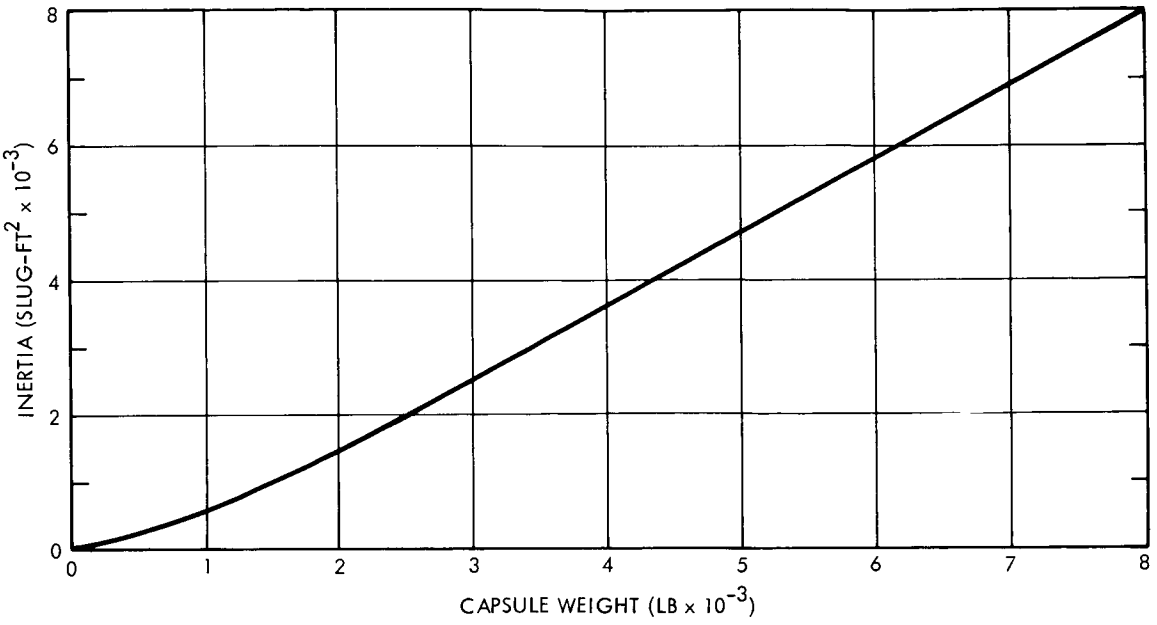

Figure F-7. Estimated Capsule Moments of Inertia ($I_x = I_y = I_z$)

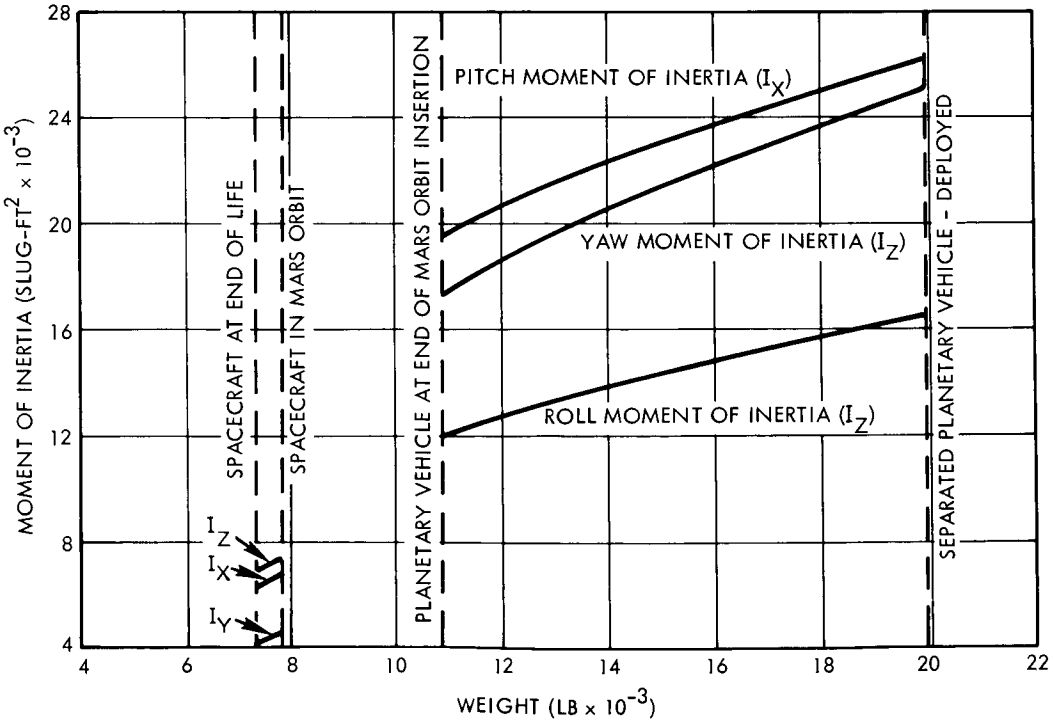

Figure F-8. Planetary Vehicle Moments of Inertia vs. Weight (5000-lb Capsule)

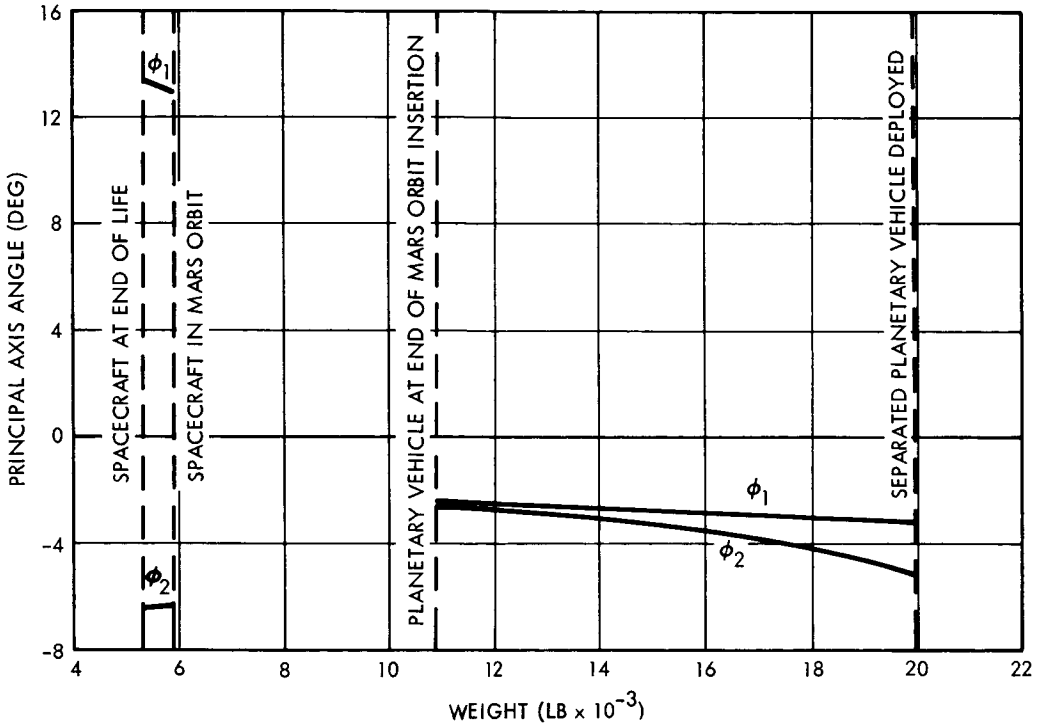

Figure F-9. Planetary Vehicle Principal Axis Angles vs. Weight (5000-lb Capsule)

It is desirable for the spacecraft axis through the high-gain antenna and the PSP (y axis) to coincide with a principal axis, and also to minimize any movement of the principal axis in order to lessen cross coupling effects when the attitude control system is activated or when the PSP or antenna is rotated. Also it is desirable to install the attitude control system nozzles on the principal axes of the spacecraft. Initial estimates indicate a maximum movement (transverse) of 3.8 degrees, with the principal axis being up to 6.4 degrees away from the PSP axis. Balancing the transverse inertias allows a single level thruster for attitude control in pitch and yaw.

3. SUPPORTING DATA AND DISCUSSION

3.1 Capsule

No attempt was made to estimate subsystem weights within the capsule system. The capsule was therefore assumed to be a homogeneous mass, with center of mass at its geometric center. Specific information concerning the capsule c.m. was obtained from Reference F-1, which

indicated a possible wide tolerance both longitudinally and transversely. Simplified inertia values were computed for a range of capsule weights during the Phase 1A Task B study. This curve is reproduced here (see Figure F-7) and formed the basis for inputs to the moments of inertia and principal axis angle calculations.

3.2 Science Subsystem

In sizing the spacecraft a total science subsystem weight allocation of 400 pounds has been assumed. This weight is consistent with the minimum value quoted in Reference F-1. More recent payloads are discussed in Volume 5 with comparative weight estimates summarized in Appendix G of that volume. For the performance of mass properties configuration analyses, a weight breakdown, as shown below, has been established. This differs from weights shown in Volume 5, where instrument weights are selected based on desired performance, rather than by allocation of the specified weight constraint of 400 pounds.

	Weight, (lb)	
PSP Mounted Instruments		255
Photo-imaging system	155	
High resolution IR spectrometry	30	
Broadband IR spectrometer	20	
IR radiometer	20	
UV spectrometer	30	
PSP		145
Platform structure	58	
Platform support structure	10	
Cryogenic control	10	
Thermal control	16	
Control electronics	5	
Mars sensors	12	
Drive mechanisms	14	
Electrical harness	10	
Attachments	10	
		400

3.3 Capsule Radio Link

The subsystem elements of the capsule radio link are two UHF receivers, two demodulators, a preamplifier, tape recorder, and a UHF antenna which is a quad-spiral array occupying a volume 27 x 27 x 10 inches. A conservative weight allowance of 50 pounds has been allocated for this subsystem (Ref. F-1). Fourteen pounds has been allowed for the antenna, 7 pounds for each of two preamplifier, receiver, demodulator units, and 12 pounds for the data recorder. The remaining 10 pounds includes the weight of transformers incorporated into the feed transmission line, three integrated hybrid rings, and feed coax and connectors.

3.4 Structure

The spacecraft structure consists of two main elements, an octagonal equipment module section weighing 1008.5 pounds, and a propulsion module structural assembly that weighs 483.7 pounds.

The equipment module structure consists of six side-mounted equipment panels, a total of 19 meteoroid panels, longerons, rings and supports, and deployment mechanism for the various appendages.

Equipment panels are constructed of aluminum honeycomb hex-core 1.5-inch thick and 2.3 lb/ft^3 density bonded between 0.035-inch aluminum alloy face sheets. The specific weight is 1.52 lb/ft^2 including allowances for bond and mechanical inserts.

The remaining side and top panels were sized to provide adequate meteoroid protection to the interior of the spacecraft. Based upon an estimated probability of zero penetration of 0.87, the panels were constructed from a 2.0 lb/ft^3 foam core, 1.5 inches thick, bonded between aluminum alloy face sheets 0.010 and 0.030 inch thick for the outer and inner, respectively. The specific weight was estimated to be 1.04 lb/ft^2.

The meteoroid panels account for over 50 percent of the equipment module structural weight and so far as the planetary vehicle is concerned constitute a weight penalty of almost 1085 pounds, assuming the reference

velocity profile (see Section 3.15). Any improvement in meteoroid protection hazard prediction could therefore be of great benefit to the planetary vehicle.

Other equipment module structural items were computed on the basis of strength and stiffness requirements and reflect the results of a detailed structural analysis.

The propulsion module structure consists of a double cruciform beam assembly upon which is mounted an aluminum honeycomb core panel. The panel core is 1.5 inches thick and 2.0 lb/ft^3 density, and face sheets of 0.020 inch aluminum alloy, with a total installed specific weight of 0.97 lb/ft^2. Beams are constructed mainly from 0.040-inch aluminum alloy webs with Tee section caps ranging in center section area from 0.19 to 0.27 in^2.

Meteoroid protection for the engine and tanks is provided by the base-mounted solar array panels supplemented with additional aluminum alloy bumper panels.

The weight estimates include supports for propellant and pressurant tanks and engine mounting.

3.5 Thermal Control

Thermal protection is provided by an external aluminized Mylar insulating blanket that surrounds the top, sides, base panel and PSP, antennas and solar array support struts of the spacecraft. This blanket, which is installed by means of Velcro tape, is made up of two outer layers, 3 mils thick, sandwiched between which are 70 layers, 1/4 mil thick. The installed weight per square foot is 0.25 pounds.

Thermal control of the equipment is provided by means of heat sinks and louver assemblies, together with heaters and thermostats. Louver assemblies (approximately 43 ft^2) which are mounted on the equipment panels consist of OGO type louvers operated by Pioneer type bimetallic actuators. The estimated weight per square foot is 0.855 pound.

Protection is provided the solar array from engine heat by means of a spun aluminum/Refrasil shell that surrounds the engine, plus a

0.005 titanium cover around the nozzle extension. The aluminum/ Refrasil shell is made up of a 0.5 inch of 4.8 lb/ft^3 Refrasil core bonded between two 0.010 aluminum face sheets. Specific weight is 0.49 lb/ft^2.

3.6 Electrical Power Subsystem

The spacecraft electrical power subsystem consists of a solar array, secondary batteries, a 400 Hz inverter, DC to DC converters, a shunt element assembly, and a power control unit.

Solar array power is provided by an uninsulated annular array and three insulated rectangular panels which mount on the aft surface of the spacecraft. The annular array has the following characteristics:

Power output at 1.67 AU	582 watts
Cells in series	110
Cells in parallel	288
Total cells	31,680
Total area	165 ft^2
Packing factor	84%

The total weight of the annular array, including the substrate, is 168.9 pounds. Electrical portions of the array, including P on N, 2 by 2 cm solar cells, cover glass, cells interconnects, diodes, wiring, and electrical insulation have a combined weight of 0.23 lb/ft^2. The substrate which is aluminum platerib construction weighs 0.83 lb/ft^2.

The characteristics of the aft array are as follows:

Power output at 1.67 AU	205 watts
Cells in series	120
Cells in parallel	108
Total cells	12,960
Total area	62.5 ft
Packing factor	91%

Each of the three panels which make up the aft array is 50 by 60 inches in size. The electrical portion of the array weighs 0.23 lb/ft^2, the same as the annular segment. The substrates, which are aluminum honeycomb, weigh 0.57 lb/ft^2 and are made from 0.010 face sheets and

2.3-pound per cubic foot core. FM 1000 film bond adhesive weighing 0.04 lb/ft^2 is used to bond the face sheets to the core.

Electrical power required during vehicle acquisition, maneuvering, and Mars eclipse is provided by three nickel-cadium secondary batteries which have the following characteristics:

Nominal capacity	16 ampere-hours
Average discharge current	3.5 amperes
Nominal discharge voltage	41 volts
Number of cells	33 series connected
Maximum depth of discharge	50%

The estimated weight for each of the batteries is 50 pounds.

Weight and size data on each of the remaining units in the electrical power subsystem has been estimated using Intelsat packaging concepts as a basis. These units are the inverter, converters, shunt element assembly, and the power control unit.

3.7 Electrical Distribution and Pyrotechnic Control

Unit weight for items within this subsystem have been estimated, for the most part, using OGO spacecraft components as a basis. The distribution control unit and J-boxes are all similar in design to OGO units. Spacecraft harness weight estimates were established employing the following considerations: spacecraft size, harness function, wire size, current requirements, shielding requirements, spacecraft system complexity, and redundancy requirements.

3.8 Guidance and Control

Weights and sizes of units in the subsystem have been generally estimated on the basis of similarity to units on other spacecraft. The Canopus sensors are similar to those used on Lunar Orbiter, and the sun sensors to those of OGO and Pioneer spacecraft.

The dual mode, triple redundant attitude control system was sized to the following performance requirements:

Cruise impulse at low thrust	307 lb-sec
Acquisition and maneuver impulse at high thrust	739 lb-sec
Powered flight roll control impulse at high thrust	130 lb-sec

Low thrust specific impulse is 120 seconds, and high thrust specific impulse is 60 seconds. Tank sizes and weights were calculated using titanium as a material with 160,000 psi allowable tensile strength, a storage pressure of 3,000 psia and a safety factor of 1.5. Weights of other components in the attitude control system were estimated from the design or derived from vendor-furnished information.

3.9 S-Band Communications

S-band electrical component mass property characteristics have been estimated largely from similar units on other spacecraft. The modulator exciters, low power transmitter, and receivers are similar to MOL units, the baseband assembly is similar to an SGLS unit, and the circulator switch assembly, and diplexers are similar to Pioneer units. The remaining units in the subsystem will be designed specifically for Voyager, with weights and sizes having been estimated on the basis of function and part count using current state of the art packaging concepts.

The two low-gain antennas, which are located on opposite sides of the spacecraft to obtain omnidirectional receiving capability, are identical, each consisting of a four-arm conical spiral element at the end of a six-foot deployable boom. The antenna elements are estimated to weigh 0.5 pound each and each antenna boom 2.5 pounds. The coax feed for the low-gain antennas is 0.5-inch diameter foamflex cable weighing 0.152 lb/ft.

The medium-gain antenna consists of an elliptical reflector, feed horn with supports, and mounting and supporting structure. The reflector is 0.5-inch thick aluminum honeycomb with 0.007-inch face sheets and 1 lb/ft^3 core. Bonding material between the face sheets and core is estimated to weigh 0.04 lb/ft^2. The total reflector has a calculated weight of 8 pounds. Weights of remaining components have been estimated as follows:

Feed horn with	1.5
Reflector mounting structure	1.0
Support tube	1.9

Solid jacketed 0.5-inch diameter foamflex cable is used for the coax feed. This is the same coax as is used with the low-gain antennas.

The spacecraft high-gain antenna has a 9.5-foot diameter parabolic reflector constructed of 3/4-inch aluminum honeycomb. A weight of 29.5 pounds has been calculated for the reflector assuming 0.005 inch thick face sheets, 1 lb/ft^3 core, and 0.04 lb/ft^2 bonding material. Peripheral and intermediate rings weighing 5.3 pounds are provided for structural stiffness. Weight estimates of the other items are as follows:

Feed horn and support structure	7.0
Reflector support arm	5.3

As with the other antennas, 0.5-inch diameter foamflex coax weighing 0.152 lb/ft is used for the feed.

3.10 Telemetry and Data Storage Subsystem

With the exception of remote multiplexers, which are similar to SGLS units, items within this subsystem cannot be compared directly in terms of mass property characteristics with existing units on other spacecraft; therefore, component weights as shown on the table represent the best judgment based on design detail.

Although the multiplexers are located in the planetary scan platform, and are not mounted on an equipment panel with the other subsystem units, they are considered to be a part of the subsystem because of function and functional responsibility.

3.11 Command and Sequencing System

For the most part, units and components in this subsystem, except for bit synchronizers in the command unit, are not comparable with existing units. Weights and unit sizes used in moment of inertia calculations have been estimated on the basis of unit complexity.

The PSP remote decoder is packaged in the PSP but is considered to be a part of the command and sequencing subsystem.

3.12 Engine and Valves

The component weights of the modified LMDE for the Voyager were based on data based on LMDE Project experience. The total weight for the engine is 408.5 pounds and is approximately 20 pounds heavier than the basic LMDE that weighs 390 pounds. The modifications include a redesigned head and propellant throttling valve changes to provide a two-point thrust arrangement rather than a continuously variable thrust installation.

Four Thiokol C-1 engines are mounted at the base of the cross beam structure for use as a back-up engine system. The engine weights (5.0 pounds each) were based on specification data and include bipropellant valves. The total system installation weighs 34.0 pounds.

3.13 Propellant Feed System

The propellant feed system, consisting of four propellant tanks, two start tanks, propellant feed lines, and valves, has a total estimated weight of 425.2 pounds. This does not include the pressurization system, which is treated separately.

The four equivolume sperical propellant storage tanks, were sized to contain 16,000 pounds of usable A-50/N_2O_4 propellant. Tank sizing criteria were as follows:

A-50 density	56.3 lb/ft^3 at 70°F
N_2O_4 density	90.1 lb/ft^3 at 70°F
Mixture ratio	1.6
Bulk density	73.2 lb/ft^3 at 70°F
Allowance for ullage	2% of the usable propellant weight
Allowance for trapped and residual propellant	412 lb
Nominal tank pressure	235 psi
Maximum tank pressure	280 psi

Tank material	6 Al-4V titanium alloy, 0.16 lb/in^3
σ_u	160,000 psi
Factor of safety	1.5
Non-optimum factor	1.1

Based upon the above criteria the four propellant tanks were computed to weigh 292 pounds and were each 57.4 inches in outside diameter, with a wall thickness of 0.04 inch.

The stainless steel propellant feed line weights were computed on the basis of being 2.0 inches and 1.75 inches outside diameter x 0.020 inch walls for the oxidizer and fuel lines, respectively.

3.14 Pressurization System

Pressurization for the propellant tanks is provided by means of helium gas stored under pressure in two spherical titanium alloy bottles mounted over the oxidizer propellant tanks. The system is estimated to weigh 355.0 pounds, including 42.2 pounds of helium. Helium weight was computed on the basis of the following data:

Supply pressure	235 psi
Initial helium storage pressrue	4000 psi
Final pressure in H_e tank	335 psi
Compressibility factor	1.105
Effective ratio of specific heats	1.14
Volume to be pressurized	228 ft^3

The helium tanks were estimated to be 29.6 outside diameter with a wall thickness of 0.272 inch and a weight of 32.0 pounds each. Design criteria in this case being:

Material	6 Al 4 V titanium alloy
Density	0.16 lb/in.^{3}
σ_u	160,000 psi
Factor of safety	1.5
Non-optimum factor	1.1
Tank pressure	4,000 psi

3.15 Propellant

The propellant requirements are based upon the nominal operating parameters for the modified LMDE and the reference velocity profile totalling to a requirement of 1.95 km/sec (Ref. F-2). This reference velocity profile is:

Maneuver	ΔV		I_{sp} (sec)	$\frac{W_p}{W_o}$
	m/sec	ft/sec		
Midcourse corrections	210	689	298	0.0693
Mars orbit insertion	1,590	5,217	305	0.4124
Orbit trim*	150	493	298	0.0502

* Capability with capsule not separated.

The integrated propellant fraction was computed to be 0.4806 from which the required usable propellants were determined.

As described in Volume 6, propellant tanks were sized to contain 16,000 pounds of usable propellant, this being approximately optimum so far as Saturn V booster capability and contemplated missions are concerned.

Propellants selected are A-50 (50/50 mix of N_2H_4 and UDMH) and nitrogen tetroxide (N_2O_4). Densities assumed were 56.3 lb/ft^3 for the A-50 and 90.1 lb/ft^3 for the N_2O_4. Combined with a mixture of 1.6 resulted in identically required volumes, considered a desirable feature in terms of design, cost, tooling, etc.

The propellant residuals were computed on the basis of Reference F-3, as follows:

	Fuel	Oxidizer
Trapped in propellant lines	19.8	33.4
Residuals in tanks	23.3	65.2
Stop and start transients (8)	28.3	34.2
Outage (valve operation, etc.)	69.5	107.2
	140.8 lb	240.0 lb

Fuel bias was derived from the same reference to be $0.0032\ W_{P_{use}} + 1.2$. The overall equation for unusable propellant weight was therefore $382 + 0.0032\ W_{P_{use}}$.

Two bellows type start tanks are incorporated into the feed system and are installed in one of the fuel and oxidizer tanks, respectively. They are sized to provide the capability for eight starts, and are loaded separate to the main tanks. Preliminary estimates indicate a weight of 50 pounds for the total installation.

3.16 Balance Weights

Although equipment has been placed to minimize the center of mass offset, an allowance of 15 pounds for balance weights has been included in the spacecraft weight. This allowance is made to account for possible design changes after equipment locations are fixed, and to reduce the center of mass travel when appendages are moved from the stowed to the deployed position during space flight.

3.17 Planetary Vehicle Adapter

The planetary vehicle is supported at 12 points on a tubular truss adapter, sized to strength and stiffness requirements. It was calculated to weigh 510.2 pounds, including a spring-type separation system weighing 36 pounds.

The shroud modifications required to mount the adapter assembly consist of rings and longerons that weigh 134.7 pounds. An electrical distribution and pyrotechnic control system of 8.0 pounds was included, together with a weight contingency of 5 percent. The total weight of the planetary vehicle adapter installation is therefore 685.5 pounds.

REFERENCES

F-1. JPL Document No. SE 002 BB001-1B21, "Performance and Design Requirements for the 1973 Voyager Mission General Specification For," dated January 7, 1967.

F-2. Letter from J. A. Belew to T. Wiggins dated July 7, 1967, Ref. R-AS-A-67-101, containing guidelines.

F-3. "Voyager Support Study, LM Descent Stage Applications, Final Report. Volume I: Propulsion Studies," TRW Report 04480-6004-R000, February 1967.

EQUIPMENT LIST AND DESIGN PARAMETERS

APPENDIX G

EQUIPMENT LIST AND DESIGN PARAMETERS

Contained in Table G-1 is a listing of the Voyager spacecraft flight equipment, including the planetary vehicle adapter. Also given is a tabulation of associated power, temperature limits, weight, and size parameters.

Dashed lines will be found in lieu of numbers in those cases where parameters are not particularly meaningful as related to the item of equipment. For example, size is not listed for items of irregular shape, such as wiring harnesses, or power is not listed when it is negligible or not consumed by the equipment item. Temperatures contained in Table G-1 are the allowable extremes for the equipment, not the actual working extremes.

Table G-1. Equipment List and Design Parameters

Component	Number Required per Spacecraft	Weight (each) (lb)	Dimensions (in.) Length	Width	Height	Volume (each) (cu in.)	Maximum Electrical Power (watts) and Sources Average	Peak	Power Bus	Allowable Operating Temperature (°F) Max.	Min.	Allowable Nonoperating Temperature (°F) Max.	Min.
EQUIPMENT MODULE													
Electric Power Subsystem													
Solar array panel (annular)	8	21.4	area = 3000 sq in.			6000	-	-	-	250	-260	250	-260
Solar array panel (rectangular)	3	16.2	50	60	1	3000	-	-	-	250	-260	250	-260
Power control unit	1	20	10	10	5	500	100	120	Array	120	-20	200	-50
Shunt element assembly	1	6	25	6	3	450	100	110	Array	150	-20	200	-50
Battery	3	59	13.3	8.5	7.5	850	70	70	Array	90	-50	90	-50
400 Hz inverter	1	10	7	7	5	245	0.5	12	Main	120	-20	200	-50
DC-DC converter, S-band radio	1	5	6	6	3.5	126	30	40	Main	120	-20	200	-50
DC-DC converter, guidance and control	1	5	6	6	3.5	126	10	20	Main	120	-20	200	-50
DC-DC converter, temperature control	1	5	6	6	3.5	126	10	20	Main	120	-20	200	-50
DC-DC converter, capsule supply	1	5	6	6	3.5	126	30	40	Main	120	-20	200	-50
DC-DC converter, PSP assembly	1	5	6	6	3.5	126	20	30	Main	120	-20	200	-50
DC-DC converter, telemetry and data storage	1	5	6	6	3.5	126	15	20	Main	120	-20	200	-50
DC-DC converter, command and sequencing	1	5	6	6	3.5	126	10	20	Main	120	-20	200	-50
DC-DC converter	1	5	6	6	3.5	126	10	20	Main	120	-20	200	-50
S-Band Radio Subsystem													
Low-gain antenna (+x location)	1	3	-	-	-	-	-	-	-	360	-350	360	-350
Low-gain antenna (-x location)	1	3	-	-	-	-	-	-	-	360	-350	360	-350
High-gain antenna assembly													
High-gain antenna support structure	1	22.4	-	-	-	-	-	-	-	360	-350	360	-350
Reflector and associated structure	1	52.1	9.5 ft-dia.			-	-	-	-	250	-250	250	-250
Feed assembly	1	6.4	-	-	-	-	-	-	-	250	-250	250	-250
High-gain antenna drive	1	30.0	16	12	20	3840	4	33	400 Hz	250	-250	250	-250
Antenna drive electronics assembly	1	5.0	6	7	5	210	6	8	Main	130	-20	130	-20
Medium-gain antenna assembly													
Medium-gain antenna support structure	1	12.5	-	-	-	-	-	-	-	360	-350	360	-350
Reflector and associated structure	1	12.4	-	-	-	-	-	-	-	360	-350	360	-350
Feed assembly	1	5.2	-	-	-	-	-	-	-	250	-250	250	-250
Medium-gain antenna drive	1	17.0	16	12	12	2302	0.3	7	400 Hz	250	-250	250	-250

Table G-1. Equipment List and Design Parameters (Continued)

Component	Number Required per Spacecraft	Weight (each) (lb)	Dimensions (in.) Length	Width	Height	Volume (each) (cu in.)	Maximum Electrical Power (watts) and Sources Average	Peak	Power Bus	Allowable Operating Temperature (°F) Max.	Min.	Allowable Nonoperating Temperature (°F) Max.	Min.
S-band electronics													
S-band receiver	4	3.5	7.25	5	3	109	2	2	Main	110	30	175	-25
Receiver selector	1	1.0	3.5	5	1.62	28.4	0.9	0.9	Main	110	30	175	-25
Low-gain antenna selector	1	0.5	3.5	5	1.62	28.4	0.3	0.3	Main	110	30	175	-25
One-watt transmitter and power monitor	1	3.0	7.25	5	1.62	58.7	15	15	Main	110	30	175	-25
Modulator exciter	2	3.0	7.25	5	1.62	58.7	2.1	2.1	Main	110	30	175	-25
Power amplifier, power monitor, and power supply	2	7.8	12	4.2	3.0	151	165	165	Main	210	-20	250	-25
Transmitter selector	1	1.0	3.5	5	1.62	28.4	0.9	0.9	Main	110	30	175	-25
Circulator switch assembly and control unit	1	7.5	10	6	6	360	-	1 amp 50 ms	Main	110	30	175	-25
Diplexer	4	1.0	7.5	4.0	2.5	75	-	-	Main	110	30	175	-25
Baseband assembly	1	1.0	3.5	5	2.5	43.8	1.0	1.0	Main	110	30	175	-25
Preamplifier	4	0.5	2	2	1	4	0.25	0.25	Main	110	30	175	-25
Relay Link (GFE)													
Relay link antenna	1	8.0	27	27	10	-	-	-	-	360	-350	360	-350
Relay link receiver	2	2	7	6	1	42	1.5	3.0	400 Hz	110	30	175	-25
Relay link demodulator	2	0.4	7	6	1	42	1.0	1.0	400 Hz	110	30	175	-25
Command and Sequencing Subsystem													
Command unit	1	10.5	7	7	7	343	6.5	6.5	Main	110	30	175	-25
Primary computer and sequencer	1	20	8	8	7.5	480	20	20	Main	110	30	175	-25
Backup computer and sequencer	1	18	8	8	6.5	415	20	20	Main	110	30	175	-25
PSP remote decoder unit	1	2.0	4	5	0.5	10	0.5	0.5	Main	110	30	175	-25
Telemetry and Data Storage Subsystem													
Spacecraft and capsule TV recorder	4	20	12	10	8	650	20	30	Main	110	30	170	-25
Engineering and science recorder	2	18	12	10	8	600	15	22	Main	110	30	175	-25
Telemetry data processor	1	11	10	8	6	580	6	12	Main	110	30	175	-25
PSP remote multiplexer	1	2	4	5	0.5	10	0.5	1.0	Main	110	30	175	-125
PSP remote photo-imaging multiplexer	1	2	4	5	1.0	20	2.0	3.0	Main	110	30	175	-125

Table G-1. Equipment List and Design Parameters (Continued)

Component	Number Required per Spacecraft	Weight (each)	Dimensions (in.)			Volume (each)	Maximum Electrical Power (watts) and Sources			Allowable Operating Temperature (°F)		Allowable Nonoperating Temperature (°F)	
		(lb)	Length	Width	Height	(cu in.)	Average	Peak	Power Bus	Max.	Min.	Max.	Min.
Guidance and Control Subsystem													
Inertial reference assembly	2	25	12	8	7	672	40	54.1	Main	130	30	180	-22
Guidance and control electronics assembly	1	13	7	11	6	462	25	38	Main	130	-30	200	-30
Canopus sensor	2	7	4	12	4	192	6	6	Main	130	-30	160	-30
Coarse sun sensor	4	3	1.5	1	1	1.5	0.3	0.3	Main	130	30	160	-20
Fine sun sensor	2	0.2	2	3	2	12	0.7	0.7	Main	130	30	160	-20
Limb crossing detector	2	0.3	1.5	2.5	1.25	4.7	0.1	0.1	Main	130	30	160	-20
Terminator crossing detector	2	0.3	1.5	2.5	1.25	4.7	0.1	0.1	Main	130	30	160	-20
Pressure vessel	2	35.7	19.1 dia. sphere			3600	-	-	-	120	-30	150	0
Solenoid valve	12	0.6	1.13 dia. x 3.14 lg.			-	-	25	Battery	250	-65	250	-65
Pressure regulators and selector valve	2	4.3	8.5 dia. x 6.7 lg.			380	-	15	Battery	140	0	200	0
High pressure transducer	2	0.1	1.08 dia. x 2.08 lg.			1.6	-	0.2	Battery	140	0	200	0
Low pressure transducer	2	0.1	1.0 dia. x 1.6 lg.			1.25	-	0.2	Battery	140	0	200	0
Pressure switch	12	0.08	0.88 dia. x 3.24 lg.			2	-	-	-	140	0	200	0
Fill valve	2	0.2	0.65 dia. x 3 lg.			1	-	-	-	250	-65	250	-65
Plumbing set	2	2.0	-	-	-	-	-	-	-	250	-200	250	-200
Dual axis thruster	2	0.6	1.5 dia. x 4.0 lg.			7	-	-	-	250	-200	250	-200
Single axis thruster	2	0.6	1.5 dia. x 4.0 lg.			-	-	-	-	250	-200	250	-200
Nitrogen tank	2	23.5	23.1 dia. sphere			5730	-	-	-	120	-30	150	0
Nitrogen tank support	2	5.5	-	-	-	-	-	-	-	250	-250	250	-250
Electrical Distribution Subsystem													
Pyro control assembly	1	25	15	7	7	490	2	500 w 50 μs	Main	150	10	160	-10
Equipment module main harness	1	69	-	-	-	-	-	-	-	160	10	160	-10
Equipment module science harness	1	45	-	-	-	-	-	-	-	160	10	160	-10
Panel I harness	1	15	-	-	-	-	-	-	-	160	10	160	-10
Panel III harness	1	15	-	-	-	-	-	-	-	160	10	160	-10
Panel IV harness	1	15	-	-	-	-	-	-	-	160	10	160	-10
Panel VII harness	1	15	-	-	-	-	-	-	-	160	10	160	-10
Panel VIII harness	1	15	-	-	-	-	-	-	-	160	10	160	-10
J-box, Panel I	1	7	9	6	6	324	-	-	-	160	10	160	-10

Table G-1. Equipment List and Design Parameters (Continued)

Component	Number Required per Spacecraft	Weight (each)	Dimensions (in.)			Volume (each)	Maximum Electrical Power (watts) and Sources			Allowable Operating Temperature (°F)		Allowable Nonoperating Temperature (°F)	
		(lb)	Length	Width	Height	(cu in.)	Average	Peak	Power Bus	Max.	Min.	Max.	Min.
J-box, Panel III	1	7	9	6	6	324	-	-	-	160	10	160	-10
J-box, Panel IV	1	3	4	5	6	120	-	-	-	160	10	160	-10
J-box, Panel V	1	3	4	5	6	120	-	-	-	160	10	160	-10
J-box, Panel VII	1	7	9	6	6	324	-	-	-	160	10	160	-10
J-box, Panel VIII	1	7	9	6	6	324	-	-	-	160	10	160	-10
In-flight jumper	1	1.0	2	2	2	8	-	-	-	160	10	160	-10
Distribution control unit	1	12	10	7	7	490	5	5	Main	150	10	160	-10
Ordnance harness and test connector	1	5	-	-	-	-	-	-	-	160	10	160	-10
Structure and Mechanical Subsystem													
Equipment panel structure	6	26.5	62	36	1	2232	-	-	-	250	-250	250	-250
Equipment module primary structure assembly	1	161.2	-	-	-	-	-	-	-	250	-250	250	-250
Tiedown assembly, PSP	1	1.0	-	-	-	-	-	-	-	250	-250	250	-250
Tiedown assembly, low-gain antenna	1	1.0	-	-	-	-	-	-	-	250	-250	250	-250
Tiedown assembly, medium-gain antenna	1	2.0	-	-	-	-	-	-	-	250	-250	250	-250
Tiedown assembly, high-gain antenna	1	2.0	-	-	-	-	-	-	-	250	-250	250	-250
Low-gain antenna boom	2	2.5	-	-	-	-	-	-	-	250	-250	250	-250
Low-gain antenna deployment mechanism	2	2.0	-	-	-	-	-	525	Battery	250	-250	250	-250
Solar array support	8	4.4	-	-	-	-	-	-	-	250	-250	250	-250
Micrometeoroid protection Panel II, side forward	1	19.4	36	64	1.5	3460	-	-	-	250	-250	250	-250
Micrometeoroid protection Panel VI, side forward	1	19.4	36	64	1.5	3460	-	-	-	250	-250	250	-250
Micrometeoroid protection panel, side aft (Panel I, II, III, V, VI, VII)	6	33.5	65	64	1.5	6240	-	-	-	250	-250	250	-250
Micrometeoroid protection panel, side aft (Panel IV and VIII)	2	33.5	65	64	1.5	6240	-	-	-	250	-250	250	-250
Micrometeoroid protection panel, forward outboard	8	10.4	Irregular		1.5	-	-	-	-	250	-250	250	-250
Micrometeoroid protection panel, forward conical	8	12.4	Irregular		1.5	-	-	-	-	250	-250	250	-250
Micrometeoroid protection panel, forward inboard	1	6.4	30 dia.		1.5	-	-	-	-	250	-250	250	-250

Table G-1. Equipment List and Design Parameters (Continued)

Component	Number Required per Spacecraft	Weight (each) (lb)	Dimensions (in.) Length	Width	Height	Volume (each) (cu in.)	Maximum Electrical Power (watts) and Sources Average	Peak	Power Bus	Allowable Operating Temperature (°F) Max.	Min.	Allowable Nonoperating Temperature (°F) Max.	Min.
Planetary Scan Platform Assembly													
Planetary scan platform structure	1	100	-	-	-	-	-	-	-	250	-250	250	-250
Planetary scan platform support structure	1	32.0	-	-	-	-	-	-	-	250	-250	250	-250
PSP drive assembly - yoke	1	7.0	-	-	-	-	-	-	-	250	-250	250	-250
PSP drive assembly - main shaft	1	7.0	-	-	-	-	-	-	-	250	-250	250	-250
PSP drive electronics assembly	1	8.75	7	6	10	468	88	112	400 Hz	250	-250	250	-250
PSP deployment mechanism	1	5.0	-	-	-	-	-	525	Battery	250	-250	250	-250
Mars sensor	2	12	-	-	-	200	10	12	Main	130	30	160	20
Protective shutter group	1	16	-	-	-	-	-	-	-	120	0	120	0
Broadband IR spectrometer	1	20	14	12	11	1848	5.5	20	Main	105	-20	105	-20
High resolution IR spectrometer	1	16	12	11	12	1590	5.5	20	Main	105	-20	105	-20
Infrared radiometry unit	1	20	10	7	7	490	5.5	20	Main	120	0	120	0
UV spectrometry unit	1	30	24	8	8	1536	5.5	20	Main	105	32	105	32
PSP electrical harness	1	7.0	-	-	-	-	-	-	-	160	10	160	-10
PSP remote science switching unit	1	13.0	9	4	12	432	-	30	Main	160	10	160	-10
PSP boom harness and gimbal crossover assembly	1	5.0	-	-	-	-	-	-	-	160	10	160	-10
Photo-imaging system													
Medium resolution camera	1	50	12	6	6	432	50	-	Main	105	32	105	32
High resolution camera	1	50	15	7	7	735	20	-	Main	105	32	105	32
Temperature Control Equipment													
Louver assembly	8	18	60	36	1	216	-	-	-	250	-200	250	-200
Strip heater, 1-watt	6	2	-	-	-	-	-	1	Main	250	-200	250	-200
Strip heater, 2-watt	8	2	-	-	-	-	-	2	Main	250	-200	250	-200
Thermostat assembly	14	-	-	-	-	-	-	-	-	250	-200	250	-200
Temperature sensor	20	-	-	-	-	-	-	-	-	250	-200	250	-200
PROPULSION MODULE													
Thrust vector control actuator	1	37	-	-	-	-	-	800	Battery	160	-65	160	-65
Pressure transducer	6	0.25	-	-	-	-	-	-	-	-	-	-	-
Temperature transducer	12	0.25	-	-	-	-	-	-	-	-	-	-	-

Table G-1. Equipment List and Design Parameters (Continued)

Component	Number Required per Spacecraft	Weight (each) (lb)	Dimensions (in.) Length	Width	Height	Volume (each) (cu in.)	Maximum Electrical Power (watts) and Sources Average	Peak	Power Bus	Allowable Operating Temperature (°F) Max.	Min.	Allowable Nonoperating Temperature (°F) Max.	Min.
High temperature insulation, refrasil	2	24.3	-	-	-	-	-	-	-	-	-	-	-
Engine nozzle insulation	1	26.5	-	-	-	-	-	-	-	-	-	-	-
Micrometeoroid panel, side	8	1.53	-	-	-	-	-	-	-	-	-	-	-
Micrometeoroid panel, aft, triangular	4	3.0	-	-	-	-	-	-	-	-	-	-	-
Micrometeoroid panel, aft, rectangular	1	6.0	-	-	-	-	-	-	-	-	-	-	-
Micrometeoroid panel, tank protection	4	2.65	-	-	-	-	-	-	-	-	-	-	-
C-1 engine with bipropellant valving	4	7.25	17.29	6.75 max. dia.		-	-	-	-	-	-	-	-
C-1 engine mounting bracket and strut set	4	0.5	-	-	-	-	-	-	-	-	-	-	-
Plumbing set	4	0.45	-	-	-	-	-	-	-	-	-	-	-
C-1 engine isolation valve	2	0.5	-	-	-	-	-	-	-	-	-	-	-
C-1 engine pressure transducer	4	0.25	-	-	-	-	-	-	-	-	-	-	-
Engine Subsystem													
Thrust chamber and gimbal assembly	1	307	92.9	59 max. dia.		-	-	-	-	-	-	-	-
Quad bipropellant ball valve assembly	2	4.0	-	-	-	-	-	35	Battery	-	-	-	-
Injector actuator assembly	1	4.0	-	-	-	-	-	-	-	-	-	-	-
Injector	1	-	-	-	-	-	-	-	-	-	-	-	-
Quad solenoid valve	2	1.7	4.75	2.8	4.1	-	-	35	Battery	-	-	-	-
Electrical harness and J-box	1	12	-	-	-	-	-	-	-	-	-	-	-
Nozzle extension	1	-	-	-	-	-	-	-	-	-	-	-	-
Propellant Feed Assembly													
Cross-beam structure and engine beams	1	171.8	-	-	-	-	-	-	-	-	-	-	-
Separation assembly	12	28.6	-	-	-	-	-	-	-	-	-	-	-
Base panel	1	136.4	-	-	-	-	-	-	-	-	-	-	-
Start tank	2	25	19.25	16.5 dia.	-	-	-	-	-	-	-	-	-
Isolation valve	4	0.25	-	-	-	-	-	-	-	-	-	-	-
Quad regulator	1	6	-	-	-	-	-	-	-	-	-	-	-
Quad solenoid valve	2	5	-	-	-	-	-	-	-	-	-	-	-
Helium tank	2	132	29.6 dia. sphere			-	-	-	-	-	-	-	-
Helium tank support	2	18	-	-	-	-	-	-	-	-	-	-	-

Table G-1. Equipment List and Design Parameters (Continued)

Component	Number Required per Spacecraft	Weight (each) (lb)	Dimensions (in.) Length	Width	Height	Volume (each) (cu in.)	Maximum Electrical Power (watts) and Sources Average	Peak	Power Bus	Allowable Operating Temperature (°F) Max.	Min.	Allowable Nonoperating Temperature (°F) Max.	Min.
Electrical harness	1	5	-	-	-	-	-	-	-	-	-	-	-
J-box	1	5	-	-	-	-	-	-	-	-	-	-	-
Propellant tank	4	73	57.4 dia. sphere			-	-	-	-	-	-	-	-
Propellant tank support	4	11	-	-	-	-	-	-	-	-	-	-	-
Pressure transducer	9	0.25	-	-	-	-	-	-	-	-	-	-	-
Temperature transducer	8	0.25	-	-	-	-	-	-	-	-	-	-	-
Explosive valve	24	0.8	-	-	-	-	-	-	-	-	-	-	-
Helium tank fill vent valve	1	0.3	-	-	-	-	-	-	-	-	-	-	-
Propellant tank fill vent valve	2	0.45	-	-	-	-	-	-	-	-	-	-	-
Propellant tank fill drain valve	4	0.45	-	-	-	-	-	-	-	-	-	-	-
Relief valve	2	0.8	-	-	-	-	-	-	-	-	-	-	-
Burst disk	2	0.8	-	-	-	-	-	-	-	-	-	-	-
Filter	5	0.9	-	-	-	-	-	-	-	-	-	-	-
Quad check valve	2	0.9	-	-	-	-	-	-	-	-	-	-	-
Prevalve	4	5	12.7	2.5	2.06	-	-	-	-	-	-	-	-
SPACECRAFT TEMPERATURE CONTROL EQUIPMENT													
Thermal blanket, side	7	11.5	-	-	-	3.8	-	-	-	300	-400	300	-400
Thermal blanket, side	1	11.5	-	-	-	3.8	-	-	-	300	-400	300	-400
Thermal blanket, trapezoidal, forward	8	5.8	-	-	-	1.9	-	-	-	300	-400	300	-400
Thermal blanket, forward, square	1	2.8	-	-	-	0.94	-	-	-	300	-400	300	-400
Thermal closeout corner, longitudinal	8	0.8	-	-	-	0.26	-	-	-	300	-400	300	-400
Thermal closeout trapezoidal, edge	8	0.4	-	-	-	0.13	-	-	-	300	-400	300	-400
Thermal closeout square	1	0.42	-	-	-	0.14	-	-	-	300	-400	300	-400
Thermal closeout forward transverse	1	0.5	-	-	-	0.17	-	-	-	300	-400	300	-400
Thermal closeout aft transverse	1	0.5	-	-	-	0.17	-	-	-	300	-400	300	-400
Blanket aluminized Mylar, PSP	1	2.5	-	-	-	0.8	-	-	-	300	-400	300	-400
Blanket aluminized Mylar, equipment	1	3.0	-	-	-	1.0	-	-	-	300	-400	300	-400
Solar array support strut, insulation	8	0.6	-	-	-	1.7	-	-	-	300	-400	300	-400
PSP deployment arm insulation	1	3.7	-	-	-	1.2	-	-	-	300	-400	300	-400
High-gain antenna drive insulation	1	2.8	-	-	-	0.94	-	-	-	300	-400	300	-400
Medium-gain antenna drive insulation	1	2.3	-	-	-	0.77	-	-	-	-	-	-	-

Table G-1. Equipment List and Design Parameters (Continued)

Component	Number Required per Spacecraft	Weight (each)	Dimensions (in.)			Volume (each)	Maximum Electrical Power (watts) and Sources			Allowable Operating Temperature (°F)		Allowable Nonoperating Temperature (°F)	
		(lb)	Length	Width	Height	(cu in.)	Average	Peak	Power Bus	Max.	Min.	Max.	Min.
PLANETARY VEHICLE ADAPTER													
Planetary vehicle adapter ordnance electrical harness and remote disconnect	1	8.0	-	-	-	-	-	-	-	-	-	-	-
Primary structure assembly	1	374	-	-	-	-	-	-	-	-	-	-	-
Shroud support assembly	1	134.7	-	-	-	-	-	-	-	-	-	-	-
Ejector assembly	1	77	-	-	-	-	-	-	-	-	-	-	-